# THE MORPHOLOGY AND RELATIONSHIPS OF THE HYBODONT SHARK *TRIBODUS LIMAE*, WITH A PHYLOGENETIC ANALYSIS OF HYBODONT SHARKS (CHONDRICHTHYES, HYBODONTIFORMES)

By

JENNIFER A. LANE

VOLUME I

A dissertation submitted to the Graduate Faculty in Biology in partial fulfillment of the requirements for the degree of Doctor of Philosophy, The City University of New York

2010

UMI Number: 3411361

All rights reserved

INFORMATION TO ALL USERS
The quality of this reproduction is dependent upon the quality of the copy submitted.

In the unlikely event that the author did not send a complete manuscript
and there are missing pages, these will be noted. Also, if material had to be removed,
a note will indicate the deletion.




UMI 3411361
Copyright 2010 by ProQuest LLC.
All rights reserved. This edition of the work is protected against
unauthorized copying under Title 17, United States Code.




ProQuest LLC
789 East Eisenhower Parkway
P.O. Box 1346
Ann Arbor, MI 48106-1346

© 2010

JENNIFER ALEXANDRA LANE

All Rights Reserved

This manuscript has been read and accepted for the Graduate Faculty in Biology in satisfaction of the dissertation requirement for the degree of Doctor of Philosophy.

| | |
|---|---|
| _____ | Dr. John G. Maisey, AMNH_____ |
| Date | Chair of Examining Committee |
| _____ | Dr.Laurel A. Eckhardt_____ |
| Date | Executive Officer |

Dr. John H. Wahlert, Baruch College_____

Dr. Valerie Schawaroch, Baruch College_____

Dr. Scott A. Schaefer, AMNH_____

Dr. Robert K. Carr, Ohio University_____

Supervising Committee

The City University of New York

Abstract

THE MORPHOLOGY AND RELATIONSHIPS OF THE HYBODONT SHARK *TRIBODUS LIMAE*, WITH A PHYLOGENETIC ANALYSIS OF HYBODONT SHARKS (CHONDRICHTHYES, HYBODONTIFORMES)

by

Jennifer A. Lane

Adviser: Dr. John G. Maisey

'Hybodonts' (Hybodontiformes Maisey, 1989) have been proposed to represent the monophyletic sister group to Neoselachii (extant sharks and rays). Hybodontiformes have been considered to include the suborder Hybodontoidei, as well as two problematic taxa, *Tristychius* and *Onychoselache*. However, classifications of Hybodontiformes have been traditionally based on isolated dermal elements, and skeletal material is known from only 17 hybodontiform species and 11 genera (out of a total of over 44 species previously described).

New, exceptionally well preserved fossil material of the atypical hybodontiform *Tribodus limae*, from the Lower Cretaceous of Brazil, provides the first detailed description of skeletal morphology in this genus, shedding new light on hybodontiform diversity. Morphology of the cranial and postcranial skeleton and dermal elements are

described. A three-dimensional braincase of *Tribodus* is examined and described using CT scanning and 3-D digital imaging, and cranial anatomy of another hybodont (*Egertonodus basanus*) is also examined for comparison. Reconstructions of cranial arterial circulation and the embryonic cranial cartilages in *Tribodus* are presented. The visceral skeleton of *Tribodus* is also described, and the first reconstruction of jaw musculature in a hybodont is presented. CT scanning reveals the presence of supportive endochondral "struts" in force-bearing regions of the jaws, similar to those found in extant batoids. A revised reconstruction of the pectoral fin skeleton of *Tribodus* is presented based on the new material.

Skeletal morphological data from *Tribodus* are then combined with that from 19 other hybodontiform taxa and 13 outgroup taxa to produce a matrix of 33 total taxa and 129 characters. A phylogenetic analysis is performed using the software programs PAUP* and T.N.T., testing the monophyly of Hybodontiformes, their proposed sister-group relationship with neoselachians, their interrelationships, and the phylogenetic position of *Tribodus*. Most-parsimonious trees are summarized using strict consensus, and Bremer support and bootstrap are used to test node strength.

Results of phylogenetic analysis support the monophyly of Hybodontiformes above *Tristychius* and their sister-group relationship with neoselachians, but suggest that Hybodontiformes including *Tristychius* is paraphyletic unless Neoselachii is included. Results of this analysis support monophyly of Hybodontoidei, Hybodontidae, and Hybodontinae. The position of *Tribodus* as sister to *Asteracanthus* is supported.

## PREFACE

This dissertation contains several chapters and chapter sections, which Jennifer A. Lane prepared as part of her own independent work for this PhD project, that have subsequently been published in peer-reviewed scientific journals during the writing of this dissertation, or are soon to be submitted for publication in similar journals. All of the work presented herein (including all chapters submitted for publication as single-authored papers, or as co-authored papers with Jennifer as first author) represents original work by Jennifer A. Lane. Chapters that have been accepted for publication or are soon to be submitted as single-authored or co-authored research papers are indicated in the appropriate chapter headings.

## ACKNOWLEDGMENTS

I am grateful to numerous people who helped to make this project a reality. I especially thank my advisor, Dr. John Maisey, for his generosity in accepting me to work with him as his first PhD advisee, and supporting my research over the past few years, without which this work would not have been possible. I am also very grateful to the other members of my PhD Committee, Valerie Schawaroch, John Wahlert, Robert Carr, and Scott Schaefer, for all their helpful guidance and suggestions over the past few years.

Special thanks also go to the following people, for providing much-needed assistance with collections access and specimen loans for this project: the staff of the Natural History Museum (NHM), London (especially Zerina Johanson, Alison Longbottom, and Martha Richter); Paulo Brito and his research group at the Universidade do Estado do Rio de Janeiro (UERJ); Alex Kellner and Deise Henriques at the Universidade Federal do Rio de Janeiro (UFRJ); Matthew Lowe and Matthew Riley at the University of Cambridge; Michael Taylor and his staff at the National Museums of Scotland, Edinburgh; Jeffrey Liston and Neil Clark (Hunterian Museum, Glasgow); Paul Jeffery (Oxford University Museum); Ronald Böttcher (Staatliches Museum für Naturkunde, Stuttgart, Germany); Rolf Hauff (Hauff Museum, Holzmaden, Germany); Michael Maisch (Institut und Museum für Geologie und Paläontologie, Universität Tübingen, Germany); Oliver Rauhut (Paläontologische Sammlung, München); and Charles Schaaf (Museum of Comparative Zoology, Harvard). R. J. Zakrzewski and M. Everhart (Fort Hays State Museum, Fort Hays, Kansas) provided loans of fossil ctenacanth material discussed in the chapter on pectoral fin morphology. I also thank Luciano Crivano (UERJ), for assistance with photographing specimens and helpful advice; and Kim Dennis-Bryan (The Open

University, London, UK) and Lillian Bergqvist (UFRJ), for kindly opening their homes to me during my research trips to London and Rio de Janeiro, respectively.

I am very grateful to Robert Carr (Ohio University) and Philippe Janvier (MNHN) for their helpful reviews of the manuscript based on chapter 5 herein (neurocranial anatomy of *Tribodus*) for publication in AMNH Novitates, which was subsequently accepted by that journal; and Mary Knight (AMNH) for her much-needed editorial assistance. I also thank Kenshu Shimada (DePaul University), Michael Gottfried (Michigan State University), Zerina Johanson (NHM), and an anonymous reviewer, for their useful critiques of my paper on *Tribodus* pectoral fin anatomy (based on chapter 7 of this thesis), which was published in the Journal of Vertebrate Paleontology with John Maisey as co-author.

At AMNH, I thank Melanie Stiassny, Barbara Brown, and Radford Arrindell, for kindly providing access to AMNH Department of Ichthyology specimens; Steve Thurston, Lorraine Meeker, Jackie Beckett, Craig Chesek, Frank Ippolito, and Mick Ellison, for assistance with illustrations and photography; Ivy Rutzky, for help with specimen loans and locating material in the AMNH fossil fish collections; Robert Evander and Jeanne Kelly, for help with fossil preparation; Maria Dickson, for helpful assistance with academic details; Gloria M. P. de Carvalho, for assistance with Brazilian Portuguese translations and for finding me a place to stay during my research trip to Rio de Janeiro last year; and Alejandra Lora and Judy Galkin, for administrative assistance. Over the past few years, I additionally benefited from helpful discussions with Christopher Duffin (Surrey, UK); John Wahlert (Baruch College); Valerie Schawaroch (Baruch College); Robert Carr (Ohio University); Michael Coates (University of

Chicago); Martha Richter (NHM); Zerina Johanson (NHM); Alison Longbottom (NHM); Gilles Cuny (Natural History Museum of Denmark); Jack Conrad (AMNH); Ted Macrini (AMNH); Adriana Aquino (AMNH); Bolortsetseg Minjin (Mongolian Institute for the Study of Dinosaurs); Jonathan Geisler (SUNY Stonybrook); Andres Giallombardo (AMNH); Christian Kammerer (AMNH); Xijun Ni (AMNH); Toby Schuh (AMNH); and Michelle Spaulding (AMNH).

Support for this project was provided in part by an American Museum of Natural History Graduate Science Fellowship; the AMNH Axelrod Fund; a CUNY Graduate Science Fellowship; and a Sigma Xi Grant-In-Aid of Research. Additional funding was provided by an SVP Jackson School of Geosciences Student Travel Grant; a Baermann Award for Student Travel from City College of New York, and a Susan R. Zalk Student Travel Grant from CUNY Graduate Center. The Biology department at CUNY Graduate Center also provided partial funding for travel. Lastly, I wish to express my gratitude to Roger Cuffey (Pennsylvania State University), mentor and friend, for his patience and sage advice in answering my many questions (and for generously lending me the necessary funds for my research trip to England and Scotland in summer 2008); to all who encouraged me during my time here at AMNH and CUNY; and finally, to my parents, Marie-Helene and Kenneth Lane, for their encouragement and support and for always believing I had the ability to do this.

# TABLE OF CONTENTS

VOLUME I

Page

COPYRIGHT PAGE……..…….ii

EXAMINATION COMMITTEE SIGNATURE PAGE.……..…….iii

ABSTRACT……..…….iv

PREFACE…….…..…….vi

ACKNOWLEDGEMENTS……..……...…….vii

TABLE OF CONTENTS…….x

LIST OF FIGURES…….……..xv

**PART I: INTRODUCTION**

OBJECTIVES.....…….……..…….…...1

CHAPTER 1: SIGNIFICANCE OF *TRIBODUS LIMAE*…….....3

OVERVIEW……...…3

MORPHOLOGICAL AND PHYLOGENETIC SIGNIFICANCE…….....9

TAXONOMIC BACKGROUND……..10

CHAPTER 2: GEOLOGIC SETTING……..14

CHAPTER 3: HISTORICAL REVIEW OF HYBODONTS……....28

CHAPTER 4: MATERIALS AND METHODS……...…36

**PART II: DESCRIPTIVE MORPHOLOGY OF *TRIBODUS LIMAE***……...……78

CHAPTER 5: NEUROCRANIAL MORPHOLOGY OF *TRIBODUS LIMAE* AND *EGERTONODUS BASANUS* …….....…...79

Introduction…….....…79

Description…….....…82

Neurocranium: General Features…….....…….83

Rostral and Ethmoidal Regions…….86

Orbitotemporal region……95

Trigemino-facialis Recess……102

Basicranium…….....109

Otico-occipital region……..114

Endocranial Space, Cranial Endocast, and Skeletal Labyrinth…120

Endocranial Morphology of *Egertonodus basanus*…….……126

Discussion……....132

CHAPTER 6: VISCERAL SKELETON OF *TRIBODUS* AND

RECONSTRUCTION OF JAW SUSPENSION….....229

Introduction……..229

Palatoquadrates……233

Meckel's cartilages……..……235

Hyoid arch……237

Branchial arches……...239

Labial cartilages……...240

CT scanning of internal jaw structure……..241

RECONSTRUCTION OF *T. LIMAE* JAW MUSCULATURE…….....242

DISCUSSION OF VISCERAL SKELETON……..250

CHAPTER 7: PECTORAL GIRDLE AND FIN…….323

CHAPTER 8: PELVIC FINS……..377

CHAPTER 9: AXIAL SKELETON……383

RIBS AND VERTEBRAL ELEMENTS…….383

UNPAIRED FINS……387

Dorsal fins……387

Anal and caudal fins…….389

CHAPTER 10: DERMAL SKELETON…….....410

Dentition …….410

Cephalic spines……413

Finspines……..416

Dermal denticles……..418

VOLUME II

**PART III: PHYLOGENETIC ANALYSIS OF HYBODONT SHARKS**……434

CHAPTER 11: TAXON SAMPLING…….....435

CHAPTER 12: PHYLOGENETIC METHODS…….....442

CHAPTER 13: CHARACTER LIST……..444

CHAPTER 14: RESULTS……...503

CHAPTER 15: DISCUSSION……511

CHAPTER 16: CONCLUSIONS …….....522

**APPENDICES**…….....…542

APPENDIX A: List of characters……542

APPENDIX B: Character matrix used for phylogenetic analysis…….....550

APPENDIX C: List of specimens examined.....551

APPENDIX D: List of taxa.....553

APPENDIX E: Apomorphy list.....555

APPENDIX F: Primary trees resulting from phylogenetic analysis in PAUP*..559

**BIBLIOGRAPHY**……...…….....628

LIST OF FIGURES

VOLUME I

**PART I: Introduction**

**Figure 1.** Geological time scale showing the temporal position of the Santana Formation within the Cretaceous period. Modified from Maisey, 1991. ……...52

**Figure 2.** Geological map of the Araripe Plateau. Modified from Maisey, 1991…...…..54

**Figure 3.** Location of the Araripe Basin and other Cretaceous sedimentary basins within northeastern Brazil. Modified from Maisey, 1991…….56

**Figure 4.** Map showing global distribution of *Tribodus* species during the Cretaceous..58

**Figure 5.** General appearance of hybodontiform sharks, as reconstructed by Maisey (1982, 1989)……...60

**Figure 6.** Previous hypotheses of hybodont relationships…….62

**Figure 7.** A, currently hypothesized phylogenetic relationships among hybodontiforms, modified from Coates and Gess, 2007 (based on Maisey et al., 2004); B, phylogeny of hybodontiforms plotted against geologic timescale, after Coates and Gess, 2007……64

**Figure 8.** AMNH specimens of *Tribodus limae* described in this dissertation…….....66

**Figure 9.** Braincase of *Tribodus limae*, AMNH FF 13958, in dorsal, ventral, and lateral views……..68

**Figure 10.** *Tribodus limae*, MN 5807V, overview…….....…….70

**Figure 11.** *Tribodus limae*, MN 5808V, overview……...…….72

**Figure 12.** *Tribodus limae*, UERJ-PMB-40, in A, dorsal, and B, ventral views…..……..74

**Figure 13.** *Tribodus limae*, UERJ-PMB-114, in A, dorsal, and B, ventral views…..……76

**PART II: Descriptive Morphology of *Tribodus limae***

**Figure 14.** Reproduction of original illustrations of the *Tribodus limae* braincase, modified from Brito, 1992..…….153

**Figure 15.** Transverse CT scan slices of the *Tribodus limae* braincase, AMNH 13958. Ethmoidal region……..155

**Figure 16.** Transverse CT scan slices through the *Tribodus limae* braincase. Orbital region……...157

**Figure 17.** Transverse CT scan slices through the *Tribodus limae* braincase. Otic region……...159

**Figure 18.** Transverse CT scan slices through the *Tribodus limae* braincase. Occipital region……...161

**Figure 19.** Dorsal view of the *Tribodus limae* braincase, AMNH FF 13958 (surface rendering)…….163

**Figure 20.** Dorsal view of the *Tribodus limae* braincase, line drawing……...……...165

**Figure 21.** Ventral view of the *Tribodus* braincase (surface rendering)……...……..167

**Figure 22.** Ventral view of the *Tribodus* braincase, line drawing……...169

**Figure 23.** Anterior and posterior views of the *Tribodus* braincase

(surface renderings)…….171

**Figure 24.** Anterior and posterior views of the *Tribodus* braincase, line drawing…....173

**Figure 25.** Lateral view of the *Tribodus* braincase (surface rendering)……...…...175

**Figure 26.** Medial view of the *Tribodus* braincase sliced through the sagittal plane (surface rendering)……...177

**Figure 27.** Dorsal view of the *Tribodus limae* endocast, surface rendering……...……179

**Figure 28.** Ventral view of the *Tribodus limae* endocast, surface rendering…….....181

**Figure 29.** Anterior and posterior views of the *Tribodus* endocast, surface renderings.183

**Figure 30.** Lateral view of the *Tribodus limae* endocast, surface rendering……...……185

**Figure 31.** Dorsal view of the *Tribodus* endocast and skeletal labyrinth, surface rendering……..187

**Figure 32.** Ventral view of the *Tribodus* endocast and skeletal labyrinth, surface rendering……..189

**Figure 33.** A, anterior and B, posterior views of the *Tribodus* endocast and skeletal labyrinth, surface renderings...……...…….……..191

**Figure 34.** Lateral view of the *Tribodus* endocast and skeletal labyrinth, surface rendering……..193

**Figure 35.** Close-up of *Tribodus limae* (UERJ-PMB-40) braincase, ventral view…....195

**Figure 36.** Close-up of posterior basicranial foramina in *Tribodus limae*, UERJ-PMB-40…….197

**Figure 37.** Close-up of lateral basicranial foramina in *Tribodus limae*, UERJ-PMB-40.....199

**Figure 38.** Braincase of *Egertonodus basanus* NHM P60110, which was CT scanned for the present study……..201

**Figure 39.** Transverse CT scan slices of the *Egertonodus* braincase, NHM P60110. Ethmoidal and orbital regions……..203

**Figure 40.** Transverse CT scan slices of the *Egertonodus* braincase, NHM P60110. Orbital and otic regions……205

**Figure 41.** Transverse CT scan slices of the *Egertonodus* braincase, NHM P60110. Otic and occipital regions……207

**Figure 42.** Lateral view of the *Egertonodus* braincase (NHM P60110), surface rendering……..209

**Figure 43.** Medial view of the *Egertonodus* braincase (NHM P60110), sliced through the sagittal plane (surface rendering)…….211

**Figure 44.** A, dorsal, B, ventral, and C, lateral views of the *Egertonodus* endocast (surface renderings)…..……...213

**Figure 45.** Line drawings of the *Egertonodus* endocast in dorsal, ventral, and lateral views……215

**Figure 46.** Skeletal labyrinth of *Egertonodus basanus* (surface renderings) and *Tribodus limae* (reconstructed by Maisey, 2005)……217

**Figure 47.** Skeletal labyrinth structure in other elasmobranchs. After Maisey, 2005….219

**Figure 48.** Reconstructions of the basicranial circulation in *Tribodus limae*……..…..221

**Figure 49.** Oblique medial view of the *Tribodus* braincase showing the foramina for the efferent pseudobranchial and ophthalmic arteries.……...223

**Figure 50.** Basicranial circulation in other elasmobranchs……...……...225

**Figure 51.** Composite reconstructions showing probable extent of embryonic cranial cartilages in *Tribodus limae* and *Egertonodus basanus*……..227

**Figure 52.** Top, reconstruction of *Tribodus* head region in lateral view, showing position of mandibular and hyoid arch elements in relation to the basicranium; Bottom, reconstruction of *Tribodus* head region in ventral view, showing position of mandibular and hyoid arch elements in relation to the basicranium……...263

**Figure 53.** Jaws of *Tribodus limae*, AMNH 13958; articulated upper and lower jaws..265

**Figure 54.** Jaws of *Tribodus limae*, AMNH 13958, overviews……..…...267

**Figure 55.** Left Meckel's cartilage of *Tribodus limae*, AMNH 13961, with partial dentition preserved……...…269

**Figure 56.** Hyoid arch elements of *Tribodus limae*, AMNH 13958……...……271

**Figure 57.** Anterior of *Tribodus limae*, MN 5807V……...…….273

**Figure 58.** Anterior of *Tribodus limae*, MN 5808V……...…….275

**Figure 59.** Closeup of *Tribodus limae*, MN 5807V, showing jaws, hyoid arch, and branchial elements……...277

**Figure 60.** Jaw suspensions of A, *Egertonodus basanus* and B, *Tribodus limae*, modified from Maisey (2008)……...……..279

**Figure 61.** *Tribodus limae* (MN 5808V), closeup showing branchial skeleton……...281

**Figure 62.** *Tribodus limae* (MN 5808V), closeup of pharyngobranchials……..…...283

**Figure 63.** Line drawing of MN 5808V (Fig. 61), and gill arches restored……...….285

**Figure 64.** Gill arches of other hybodonts and extant neoselachians……..287

**Figure 65.** CT scan slices of *Tribodus limae* (AMNH 13958) upper and lower jaws, showing struts of trabecular cartilage……..289

**Figure 66.** Reconstructions of the jaw musculature of *Tribodus limae*……..……...291

**Figure 67.** Evolution of cranial-palatoquadrate ligamentous connections in elasmobranchs, with holocephalans as the outgroup (after Wilga, 2005)……...293

**Figure 68.** Superficial jaw muscles in extant elasmobranchs, after Shirai (1992)……..295

**Figure 69.** Ventral jaw muscles in extant elasmobranchs, after Shirai (1992)……...297

**Figure 70.** Head and jaw muscles of carcharhinoid sharks (Galea)……..….299

**Figure 71.** Upper jaw musculature mapped onto a phylogeny of extant elasmobranchs (after Wilga, 2005)……...301

**Figure 72.** Previous reconstructions of jaw musculature in fossil chondrichthyans, adapted from Maisey (1989B, 2007)……...303

**Figure 73.** Gnathostome phylogeny showing evolution of lower jaw depression mechanisms and function of the coracomandibularis and coracohyoideus muscles (After Wilga et al., 2000)……305

**Figure 74.** Jaws of other hybodontoids, adapted from Maisey, 1982……..……...307

**Figure 75.** Jaw suspension types found in extant elasmobranchs. (After Wilga, 2005)……309

**Figure 76.** Current hypothesis of jaw evolution in chondrichthyans. Adapted from Maisey, 2008……311

**Figure 77.** Endochondral "struts" in the extant batoid Rhinoptera bonasus. Adapted from Summers et al., 1998……313

**Figure 78.** Occurrence of endochondral "struts" in extant myliobatid stingrays, mapped onto their phylogeny. Adapted from Summers, 2000)……315

**Figure 79.** Durophagy in extant chondrichthyans. (Modified from Huber et al., 2008)……317

**Figure 80.** Jaws and dentitions of representative types of durophagous extant elasmobranchs. (After Wilga and Motta, 2000)……...319

**Figure 81.** Teeth of some other durophagous hybodontoids……...…321

**Figure 82.** Close-up of Figure 8B (*Tribodus limae*, AMNH FF 13959) showing articular process of left scapulocoracoid……349

**Figure 83.** *Tribodus limae* (AMNH 13958), right scapulocoracoid (lateral view) with basal cartilages of right pectoral fin in ventral view……..……...351

**Figure 84.** Right scapulocoracoid of *Tribodus limae* (AMNH 13958), in stereophotographic views…….....353

**Figure 85.** Line drawing of right scapulocoracoid (*Tribodus limae*, AMNH FF 13958) seen in Figure 84……..…355

**Figure 86.** *Tribodus limae* Brito and Ferreira, 1989. CT scan images of articular region of right scapulocoracoid (AMNH FF 13958)……...……...357

**Figure 87.** *Orthacanthus texensis* (Cope, 1888), right scapulocoracoid (AMNH FF 20273)……..359

**Figure 88.** Comparison of pectoral fin articulation in *Tribodus* and neoselachians…...361

**Figure 89.** Comparison of previous and revised reconstructions of pectoral endoskeleton in *Tribodus limae*…….363

**Figure 90.** Left scapulocoracoid and pectoral fin of *Tribodus limae*, MN 5807V…….365

**Figure 91.** *Tribodus limae* MN 5807V, closeup showing articular region of left pectoral fin…….367

**Figure 92.** Left scapulocoracoid of *Tribodus limae* MN 5808V…….369

**Figure 93.** *Tribodus limae* MN 5808V, closeup of left pectoral fin……...371

**Figure 94.** *Tribodus limae* Brito and Ferreira, 1989. Composite reconstruction based on the new material and previous knowledge of hybodont skeletal anatomy……..373

**Figure 95.** Phylogenetic relationships among hybodontiform elasmobranchs, showing positions of pectoral skeletal characters on the tree (after Coates and Gess, 2007)……375

**Figure 96.** Posterior of the skeleton of *Tribodus limae*, MN 5807V……..……...379

**Figure 97.** Closeup of *Tribodus limae*, MN 5807V, posterior (Figure 96), showing pelvic fin…….381

**Figure 98.** Closeup of anterior part of *Tribodus limae*, MN 5808V showing anterior vertebrae in relation to other skeletal elements…….390

**Figure 99.** Anterior vertebrae of *Tribodus limae*, MN 5808V……392

**Figure 100.** Morphology of the anterior part of the vertebral column of various extant elasmobranchs. Adapted from Shirai, 1992…….394

**Figure 101.** Trunk region of *Tribodus limae*, MN 5807V……..396

**Figure 102.** Basiventrals of *Tribodus limae*, MN 5807V……...398

**Figure 103.** Closeup of basiventrals of *Tribodus limae*, MN 5807V (Figure 102)…….400

**Figure 104.** *Tribodus limae*, MN 5807V, closeup showing left pectoral fin and ventral vertebral elements, including calcified pleural ribs…….402

**Figure 105.** *Tribodus limae*, MN 5808V, closeup showing left pectoral skeleton and calcified pleural ribs…….404

**Figure 106.** Anterior dorsal fin of *Tribodus limae*, MN 5807V…….406

**Figure 107.** Posterior dorsal fin of *Tribodus limae*, MN 5807V…….408

**Figure 108.** Scanning electron microscope photographs of *Tribodus limae* teeth……..420

**Figure 109.** Close-up of the head region of *Tribodus limae* (AMNH 13959), showing right cephalic spine in-situ, after acid preparation……...422

**Figure 110.** Top, bottom, and lateral views of left cephalic spine of *Tribodus limae* (UERJ-PMB-40)…….....424

**Figure 111.** SEM of *Tribodus limae* cephalic spine, AMNH 13959……..426

**Figure 112.** *Tribodus limae* cephalic spines……428

**Figure 113.** Dorsal fin spines of *Tribodus limae*, AMNH 13958……...430

**Figure 114.** Dermal denticles from the dorsal trunk region of *Tribodus limae*, AMNH 13958……432

VOLUME II

**PART III: Phylogenetic Analysis**

**Figure 115.** Strict consensus of 70 most parsimonious trees generated in PAUP* 4.0. Numbered nodes correspond to the apomorphy list in Appendix E.....528

**Figure 116.** Strict consensus of four most-parsimonious trees generated in T.N.T. using identical search parameters to the PAUP* search, and resulting in the same topology..529

**Figure 117.** Strict consensus tree summarizing search results, with Bremer support values shown above each nod and bootstrap values shown below each node. Unnumbered nodes have bootstrap values less than 50%.....530

**Figure 118.** Results of bootstrap analysis generated in T.N.T. Collapsed nodes have bootstrap values less than 50%.....531

**Figure 119.** Phylogeny of Hybodontiformes proposed by Maisey, 1989.....532

**Figure 120.** Phylogeny of Hybodontoidea proposed by Rees, 2008..... 534

## OBJECTIVES

The overall purpose of this dissertation is to advance scientific understanding of extinct hybodontiform sharks (considered the sister group of extant neoselachians) by providing a complete description of the morphology of the Cretaceous hybodont *Tribodus limae*, on the basis of CT scans, digital reconstructions, and other methods, and by then including this taxon in a comprehensive phylogenetic analysis of hybodontiforms based on skeletal morphology (representing the first application of computer-based phylogenetic methods to study of this group).

This objective will be achieved by pursuing the following more specific goals:

1. To provide the first detailed morphological description of *Tribodus limae*, on the basis of new and exceptionally well preserved fossil material from northeastern Brazil (including a three-dimensionally preserved neurocranium and pectoral girdle). This will include description and reconstruction of its internal and external cranial morphology and cranial endocast through the use of CT scanning and 3-D digital reconstructions. Cranial anatomy of another Cretaceous hybodont, *Egertonodus basanus* (representing the only other three-dimensionally preserved hybodont braincase currently known), is also examined for comparison. This investigation represents the first detailed CT scan-based study of cranial anatomy in any hybodont. In addition to cranial anatomy, all other morphological features that are preserved in available specimens of *Tribodus limae* are examined and described. The visceral skeleton (mandibular, hyoid, and branchial arches) is described and reconstructed, and a reconstruction of the jaw musculature of *Tribodus* is presented. Morphology of the pectoral girdle and fin in *Tribodus* are also described, and a new, revised reconstruction of its pectoral anatomy is presented on the basis of three-

dimensionally preserved fossil material. The pelvic fins, axial skeleton (including the vertebral column, ribs, and unpaired fins), and dermal elements (teeth, fin spines, cephalic spines, and dermal denticles) are also described.

2. To present a phylogenetic analysis of Hybodontiformes based on a matrix of skeletal morphological data from *Tribodus limae* and other hybodontiform and outgroup taxa, with data obtained from firsthand examination of specimens (representing the first computer-based phylogenetic analysis of hybodontiforms) as well as from the literature, in order to test their monophyly and sister-group relationship with neoselachians, their interrelationships, and the phylogenetic position of *Tribodus*. The results of this analysis will then be discussed in comparison with previous hypotheses of hybodontiform phylogeny; and used either to support previous classifications or to propose a new classification of hybodontiforms and related groups, as needed.

# CHAPTER 1: SIGNIFICANCE OF *TRIBODUS LIMAE*

## Overview

New material of the Cretaceous hybodontiform shark *Tribodus limae* Brito & Ferreira, 1989, described in the present study, is significant for several reasons. First, it represents one of the best preserved and most complete fossil chondrichthyans known thus far, and only the second such specimen of a hybodont. Second, as a result of this completeness, portions of the anatomy not normally preserved in fossils (such as the ethmoid region of the braincase, and a nearly complete cranial endocast) are available for study. Third, the three-dimensional preservation of the braincase makes it ideal for study using CT scanning technology. Fourth, the fact that the specimen is articulated means that detailed and accurate reconstructions of the complete head skeleton can be made. Finally, this exceptionally well-preserved fossil shows that the morphology of *Tribodus* is considerably different from that of most other known hybodonts, contributing to knowledge of anatomical diversity among these extinct forms.

*Tribodus limae* is known from the Romualdo Member of the Santana Formation, Chapada do Araripe, northeastern Brazil (Lower Cretaceous, Albian) (Figs. 1–3). Brito & Ferreira (1989) discussed the morphology of the teeth, fin spines, and dermal denticles based on the holotype (a damaged, but fairly complete individual lacking the caudal fin) and two additional specimens (one of which was not figured) showing partial neurocrania, the anterior dorsal fin spine, and associated dermal denticles.

Additional, more complete specimens were later described by Brito (1992), who provided new information on the teeth and dermal denticles, as well as the first description of the braincase in this taxon, based on a partial neurocranium lacking most

of the ethmoid region (which Brito, 1992, reconstructed on the basis of its structure in *Egertonodus basanus*: Maisey, 1983); two incomplete neurocrania included in the original type series; and two additional nearly complete individuals in right profile. Aside from these two initial descriptions (Brito & Ferreira, 1989; Brito, 1992), as well as (1) a comparative study of chondrichthyan endocranial morphology (which included notes on endocranial morphology of *T. limae*) (Maisey, 2004A); (2) a brief description of inner ear morphology of *Tribodus* (Maisey, 2005); and (3) a very brief overview of its external cranial morphology (Maisey & Carvalho, 1997), *Tribodus limae* remains largely undescribed.

*Tribodus limae* has been diagnosed (Brito & Ferreira, 1989:54) on the basis of its teeth ("weakly heterodont dentition, high-crowned teeth under 5 mm in length, crown with strong vascular striae deeper than broad in anterior and postero-lateral teeth and shallower than broad in antero-lateral teeth, and 'hybodontoid' tooth roots"), fin spines ("slender, about 12.5 cm long, lateral faces with 8 to 10 sharp continuous ridges, single anterior ridge forming a keel in the anterior border, posterior denticles in two series"), and dermal denticles ("large, thorn-like, from 2.5–3.0 mm"). In terms of its phylogenetic relationships, Brito (1992) placed *T. limae* in the hybodont subfamily Acrodontinae, based on the single shared character "presence of irregular osteodentine in teeth."

Although only *Tribodus limae* is known from relatively complete skeletal material (all from the Lower Cretaceous Santana Formation of Brazil), three additional species within the genus *Tribodus* have been proposed on the basis of microremains (mostly teeth and fin spines), known from northern Africa and southern France (Fig. 4). These additional species are *Tribodus tunisiensis* Cuny, Ouaja, Srarff, Schmitz, Buffetaut, and Benton,

2004, from the Early Cretaceous (Albian) Ain el Guettar Formation of Tunisia; *Tribodus aschersoni* (Stromer, 1927) (=*Aegyptobatus kuehnei* Werner, 1989) from the Upper Cenomanian of Egypt (Werner, 1994; Capetta et al., 2006); and *Tribodus morlati* (Landemaine, 1991), from the basal Cenomanian of Charente-Maritime, France, originally described by Landemaine (1991) as *Protohypolophites morlati* (Cappetta, 1992; Cappetta and Case, 1999; Vullo et al., 2003; Vullo et al., 2005). In addition, teeth identified as *Tribodus* sp. have been described from the Cenomanian of Morocco (Dutheil, 1999; Cavin et al., 2001). *Tribodus* (=*Distobatus*) has also been described from the Cenomanian Draa Ubari Formation of Libya (Nessov et al., 1998; Rage and Cappetta, 2002). According to Cuny et al. (2004), several authors have suggested (on the basis of similar specimens) that *Tribodus* may also be present elsewhere in Africa, including Congo (Casier, 1961; Maisey, 2000) and Niger (Cappetta and Case, 1999; Dutheil, 1999; and Maisey, 2000). However, *Tribodus limae* has not been observed thus far outside of South America (Cuny et al., 2004).

*Tribodus aschersoni* was erected by Werner (1994) after she compared the pavement dentitions of *Hypolophites* (described by Stromer, 1927) and *Aegyptobatus kuehnei* (described by Werner, 1989), and the dorsal fin spine of *Hybodus aschersoni* (described by Stromer, 1927), to complete skeletons of *Tribodus limae* Brito and Ferreira, 1989. Werner (1994) included these taxa within the genus *Tribodus*, but considered them different enough from the Brazilian material to be distinguished as a separate species. However, there is some room for doubt as to the validity of *Tribodus aschersoni*, firstly because Werner (1994) based this new taxon on isolated teeth and fin spines not certain to be from the same animal, and secondly because the fin spine morphology of *Tribodus*

is very similar to that of a number of other hybodontoid sharks, suggesting that in these taxa, genus (and species) cannot be determined from fin spines alone. Werner's (1994) taxonomic designation also raises the possibility that *Tribodus* might perhaps be considered a junior synonym of *Hypolophites*, which Stromer (1927) based on teeth (as opposed to the more dubious fin spines), and which would have taxonomic priority to the name *Tribodus* (erected by Brito and Ferreira, 1989). Cappetta et al. (2006) used the putative junior synonym *Aegyptobatus* Werner, 1989 rather than *Tribodus aschersoni* when referring to this material (despite the fact that the type species, *Aegyptobatus kuehnei* Werner, 1989, was referred to the latter taxon), indicating that referral of *Aegyptobates* to *Tribodus aschersoni* may still be premature. *Distobatus* Werner, 1989 (originally classified as a myliobatiform) has also been considered a junior synonym of *Tribodus* (Cappetta and Case, 1999; Rage and Cappetta, 2002), but some authors are less certain about this designation (Vullo et al., 2003).

*Tribodus morlati* was originally described as *Protohypolophites morlati* by Landemaine (1991), and subsequently synonymised with *Distobatus* Werner, 1989 (Cappetta, 1992; Rage and Cappetta, 2002), which in turn was synonymised with *Tribodus* and given the species name originally used (Cappetta and Case, 1999; Vullo et al., 2003; Vullo et al., 2005). The species *Tribodus tunisiensis* was erected based on isolated teeth, including the holotype (a complete tooth with preserved root) and over 250 additional tooth specimens (Cuny et al., 2004).

Although *Tribodus limae* exhibits a number of shared hybodont characteristics (such as cephalic spines in males and otic capsules situated between the postorbital processes), it differs from other hybodonts in a number of interesting respects, most notably in terms

of cranial morphology. Unlike many other hybodonts such as *Egertonodus basanus* (Maisey, 1983, 1987), the palatoquadrates in *T. limae* do not reach the ethmoid region, and the braincase lacks an ethmopalatine process and an ethmoidal keel (Maisey, 1983). Additionally, *T. limae* lacks a suborbital shelf, has short jaws not extending below the orbit, and has a ray-like pavement dentition and a basihyal that forms a wide transverse bar. There are also paired, calcified projections from the floor of the otic region not seen in any other fossil or recent shark (Maisey and Carvalho, 1997).

Although these differences would seem to indicate that *Tribodus limae* was a specialized hybodont, some of these characteristics (e.g., the ray-like dentition, short jaws, and basihyal forming a wide transverse bar) also occur in neoselachians and are considered advanced evolutionary features for various members of that group (Maisey & Carvalho, 1997). This is probably due to convergence (Maisey et al., 2004), but could call into question the usefulness of these characters as neoselachian synapomorphies. In any case, *T. limae* sheds new light on the amount of variation present among hybodonts, and may help to further define the characters that unite hybodonts as a group.

New material to be described in the present study includes one specimen (AMNH 13958) in which a nearly complete three-dimensional braincase with jaw and hyoid arch elements is present (described in a short note by Maisey & Carvalho, 1997), as well as a nearly complete pair of three dimensional scapulocoracoids with associated basal cartilages (Lane & Maisey, 2009) and three additional specimens: a crushed neurocranium with jaw elements and the coracoid region of the right scapulocoracoid (AMNH 13959); a nearly complete individual in right profile lacking the caudal fin, with an intact right scapulocoracoid, dorsal fin spine, and scales (AMNH 13957); and a partial

skeleton with an anterior dorsal fin spine (and its basal cartilage, calcified ribs and neural arches) and a complete left scapulocoracoid with partial (coracoid region) of the right scapulocoracoid (AMNH 13961). Additional well-preserved specimens of *Tribodus limae* reposited in Brazil are also examined (see Materials and Methods section, below).

The neurocranium, jaws, and hyoid arch of AMNH 13958 were described very briefly by Maisey & Carvalho (1997), and this is the most complete three-dimensional material known thus far for any hybodont (and quite possibly any extinct chondricthyan). The neurocranium is much more complete than that described by Brito (1992), and as such is invaluable in providing new data for *Tribodus* and for hybodonts in general.

The pectoral girdle and fin of *Tribodus limae* were described for this dissertation and subsequently published (Lane & Maisey, 2009) as part of the morphological description for the present study, and are informative in providing the first evidence of the three-dimensional structure of the pectoral girdle and fin articulation in a hybodont. The results of this research show that the pectoral fin articulated on a diagonal ridge on the posterior surface of the scapulocoracoid, as in many extant neoselachians such as hexanchoids, *Chlamydoselachus*, squaloids, and galeomorphs (but interestingly, not in *Heterodontus*, once thought to be an extant hybodont). This morphology is different from previous reconstructions of hybodont pectoral girdles, which were mainly based on specimens preserved in profile and tend to show a sagittally compressed view of the pectoral articulation.

**Morphological and Phylogenetic Significance**

A complete and thorough study of the morphology of *Tribodus limae* is important for several reasons. Although the morphology of *Tribodus limae* has been briefly described by previous authors (Brito & Ferreira, 1989; Brito, 1992; Maisey & Carvalho, 1997; Maisey, 2004A), a complete, detailed morphological description of *T. limae* has never been presented. Such a description is necessary both for its own sake (contributing to knowledge of hybodont paleobiology and diversity), and also for its potential to provide new morphological character data for studies of hybodontiform phylogeny.

A complete morphological examination of *Tribodus limae* is especially important relative to the braincase and its articulation with the visceral arches, for the following reasons. First, the three-dimensional braincase and elements of the first two visceral arches of AMNH 13958 are exceptionally complete, and can thus provide the most complete morphological data known to date.

Second, the most thorough previous description of the braincase (Brito, 1992) was based on an incomplete specimen (missing much of the ethmoid and otic regions, the orbital wall, the postorbital processes, and much of the jaw and hyoid arch structures), and the resulting reconstruction, largely based on other hybodonts such as *Egertonodus basanus* (Maisey, 1983), differs from the morphology now known in *Tribodus limae*. Notably, Brito (1992:148) shows an "articular process for palatoquadrate articulation" (fig. 1, p. art) in the ethmoid region, corresponding to the ethmopalatine process of *H. basanus* (Maisey, 1983), whereas AMNH 13958 does not have an ethmopalatine articulation with the palatoquadrate (its jaws do not extend forward beyond the posterior of the orbit) and thus clearly lacks such a structure (Maisey & Carvalho, 1997).

Third, although Maisey & Carvalho (1997) give a brief general description of the basic large-scale structures of the *Tribodus limae* braincase, the smaller-scale anatomical features of the neurocranium, including positions of nerve and blood vessel foramina, remain undescribed thus far. Many of these features carry important information for reconstructing cranial nerve and circulatory pathways, and for delimiting boundaries of developmental regions (e.g., the positions of the embryonic cranial cartilages).

A phylogenetic analysis of hybodontiforms including *Tribodus limae* is important because no large-scale phylogenetic analyses of Hybodontiformes based on complete skeletal material and using computerized cladistic methods have yet been presented, and only a few such comprehensive cladistic analyses have even included hybodont skeletal material as an outgroup (e.g., Coates & Sequeira, 2001A, B). The study by Coates and Sequeira (2001A, B) mainly focused on the position of the symmoriiform *Akmonistion*, and included four hybodontiforms (*Hybodus*, *Hamiltonichthys*, *Onychoselache*, *Tristychius*), which resolved as a monophyletic group with *Hybodus* and *Hamiltonichthys* as sister taxa and *Tristychius* as basal. However, no extant neoselachians were included in that analysis, and many hybodont taxa were left out (as shown by the hypothesis of hybodont interrelationships illustrated by Maisey et al., 2004). A computer-based cladistic analysis of hybodonts based on a large array of skeletal characters and including as many taxa as possible would thus be significant as the first study of its kind.

## Taxonomic Background

Chondrichthyan fishes are considered to form a monophyletic clade, united by the presence of prismatic calcified cartilage in the endoskeleton (Maisey, 1984). The two

extant groups (neoselachians and holocephalans) are the surviving members of a formerly much more diverse lineage, which originated in the Early Silurian and is represented by numerous extinct taxa (Janvier, 1998). Early authors considered the terms "chondrichthyan" and "elasmobranch" to be interchangeable; however, Maisey (1984) differentiated the two terms, defining elasmobranchs as a derived clade within chondrichthyans that forms the sister group of holocephalans and contains neoselachians (modern sharks and batoids), hybodonts, ctenacanths, xenacanths, and possibly several other taxa whose relationships remain open to debate.

Hybodonts (Fig. 5), believed to have been extant from the Devonian to the Upper Cretaceous (Maisey, 1989; Werner, 1990; Janvier, 1998), have been considered the sister group of neoselachians on the basis of a number of synapomorphies (described below). They are currently considered monophyletic (Maisey et al., 2004). They were similar in general form and appearance to modern sharks, and were characterized by the presence of cephalic spines in males; elongated, rounded, and often low teeth with ridges and numerous nutrient canals; and fin spines convex posteriorly, with posterior retrorse denticles and an ornament of smooth ridges (Janvier, 1998).

The majority of fossil shark taxa are known from isolated teeth, dermal denticles, and fin spines. The softer, cartilaginous endoskeleton of chondrichthyans typically does not fossilize as readily as these hard parts, making body fossils comparatively rarer. Among chondrichthyans in general, the braincase in particular is fully known in only a handful of specimens, including the taxa *Orthacanthus* (Schaeffer, 1981, Maisey, 1987), *Tamiobatis* (Eastman, 1897; Romer, 1964; Schaeffer, 1981; Williams, 1998), *Akmonistion* (Coates & Sequeira, 1998, 2001A, B), *Cladoselache* (Harris, 1938), *Cobelodus* (Zangerl & Case,

1976; Maisey, 2007), *Cladodoides* (Maisey, 2005), *Pucapampella* (Maisey, 2001B), and a few others, and articulated body fossils are relatively rare.

Hybodont sharks and their relatives are generally no exception, and many taxa are known and defined solely on the basis of teeth and finspines. However, good endoskeletal material of hybodonts does exist, and relatively well preserved cranial and postcranial material is available for study. Complete cranial material is known from a small number of specimens, and has been described in the hybodonts *Egertonodus basanus* (Maisey, 1983, 1987) and *Hybodus reticulatus* (Maisey, 1987). Partial cranial material is known from *Hybodus delabechei* (Charlesworth, 1839; Day, 1864; Woodward, 1889a, 1889b; Maisey, 1982), *Egertonodus fraasi* (Brown, 1900, Maisey, 1982; 1987), *Hybodus hauffianus* (Fraas, 1889, 1896; Brown, 1900; Jaekel, 1906; Koken, 1907; Maisey, 1982), *Lissodus africanus* (Broom, 1909; Brough, 1935), and *Hamiltonichthys mapesi* (Maisey, 1989).

Postcranial material is well known from *Hybodus hauffianus*, *Egertonodus fraasi*, *Hamiltonichthys mapesi, Lissodus cassangensis* (Teixeira, 1954, 1956, 1978; Maisey, 1990), *Lissodus africanus* (Broom, 1909; Brough, 1935), and partial postcrania and/or jaws are additionally known in *Acrodus*, *Asteracanthus*, *Palaeobates*, and a few other hybodontiforms (Maisey, 1982), such as *Onychoselache traquairi* (Dick & Maisey, 1980; Coates and Gess, 2007) and *Tristychius arcuatus* (Dick, 1978). The postcranium in *Egertonodus basanus* is relatively unknown.

Considering that hybodontiform sharks comprise over 16 genera and 57 species (although exact numbers fluctuate as taxa continue to be revised), the fact that there are only 14 species in which the endoskeleton is known (only two of which have reasonably

complete neurocrania) emphasizes the great need for additional hybodont skeletal material to be found and described. New, complete material of the hybodont *Tribodus limae*, including a well-preserved braincase, can therefore contribute significantly to current knowledge of that group.

# CHAPTER 2: GEOLOGIC SETTING

The Chapada do Araripe (Araripe Plateau) is approximately 150 km in length and 50 km in width, and is located several hundred kilometers inland from the Atlantic coast, at the border between the Brazilian states of Ceará, Pernambuco, and Piauí (Brito, 1992; Figs. 2, 3). As described by Maisey (1991), its Mesozoic sedimentary sequence is up to approximately 700 m thick, comprising Jurassic and Cretaceous strata overlying a Paleozoic and Precambrian basement, and contains several unconformities. Unconformities occur between between the basement rock and the bottom of the Jurassic sequence; between the Jurassic and Cretaceous (in the eastern part of the plateau); at two places within the Cretaceous (within the Santana Formation, and between the Santana and Exu Formations); directly between the Cretaceous and the basement rock; and between the Exu Formation and an overlying Cenozoic unit, the Barreiras Formation. The Chapada do Araripe reaches altitudes of approximately 600–900 meters above sea level, and was uplifted in the Cretaceous due to faulting and tilting of the rock strata during a geologically active period following the rifting apart of South America and Africa, which resulted in formation of the southern Atlantic Ocean (Maisey, 1991).

**Brief historical review of the Santana Formation**—Geology and paleogeography of the Santana Formation has been discussed by a number of previous authors (Beurlen, 1963; Silva Santos and Valenca, 1968; Beurlen, 1971; Mabesoone and Tinoco, 1973; Lima, 1979; Silva, 1983, 1986a, b; Maisey, 1991). The geology of the Santana Formation, and particularly its stratigraphy (Fig. 1) and geologic age, have been a source of controversy over the years. Much of this controversy has had to do with identification

of distinct subunits within the Santana, as well as with determining its geologic age. An extensive historical review and discussion of geology of the Santana was presented by Maisey (1991), but a brief summary is provided here. Spix and Martius (1831) were the first to publish on fossil fishes from the region, followed by Gardner and Agassiz (1841). Small (1913) gave the rock sequence its name, referring to it as the "Sant'Ana Limestones." More detailed stratigraphic work was done later in the 20th century: Beurlen (1962; 1963) considered the Santana Formation to consist of three units, a lower member with interbedded shales and laminated limestones, a middle member with evaporate deposits, and an upper member with concretionary limestones, shales, marls (calcareous shale), and siltstones. In his 1963 paper, Beurlen removed the lower member from the Santana Formation, naming it the Crato Formation, but he later returned to the concept of a three-member sequence (lower Crato, middle Ipubi, and Upper Romualdo). Although some researchers agreed with Beurlen's 1971 assessment (e.g., Mabesoone and Tinoco, 1973), others did not, notably Moraes et al (1963), who informally divided the Santana into a lower member (shales, laminated limestones, and gypsum) and an upper member (concretionary marls, clay, and limestone). In a 1968 paper, Silva Santos and Valença agreed with Moraes at al (1963), and argued that the 'Crato' and 'Santana' subdivisions were very similar, and that the "Ipubi member" of Beurlen (1971) was merely a normal carbonate to evaporitic sequence within the 'lower limestone' subdivision. Lima (1979) proposed that Beurlen's (1971) Ipubi and Romualdo Members were invalid because they represented contemporaneous facies rather than distinct temporal depositional phases, but he considered the Crato Member to be a distinct unit. The strongest evidence for recognition of two distinct phases was provided by Silva (1983; 1986a, b), who first

noted the presence of a break in sedimentation between the upper and lower units, indicating a period of uplift and erosion (Maisey, 1991).

**Tectonic history—**An overview of the tectonic history of northeastern Brazilian Cretaceous basins, including the Araripe Basin, was provided by Maisey (2000). The rock strata comprising the Santana Formation were deposited during a tectonically active period in this region, when the previously existing supercontinent of Gondwana was in the process of rifting apart to form the modern continents of South America and Africa, and the southern Atlantic Ocean. Gondwana was a remaining fragment of the much larger and more ancient supercontinent of Pangaea, which formed approximately 250 million years ago (MYA) and began to break up approximately 180 million years ago. By 120 MYA, much of this former supercontinent had already broken apart (with North America, Antarctica and Australia already separated), and on the remaining continent of Gondwana the southern tips of South America and Africa had begun to rift apart. South America and Africa were completely separate by approximately 100 MYA, although northeastern Brazil was still relatively close to western Africa at this time. At 110 MYA (the age of the Santana fossils), then, South America and Africa were still in the process of separating, and the region was still quite active tectonically. The setting was probably comparable to the present-day rift valley in eastern Africa, where the African and Arabian plates are currently separating.

Evidence that eastern South America and western Africa were once joined is still visible today in the ‘puzzle-like’ fit of their respective coastlines, which was one of the many facts used by Alfred Wegener to support his 1929 hypothesis of continental drift. Between South America and Africa, the Mid-Atlantic Ridge follows the shape of the two

coastlines flanking it on either side. The Mid-Atlantic Ridge is a divergent plate boundary separating the African and South American plates. As new ocean floor is produced along the Mid-Atlantic Ridge, the continents on either side of it are gradually pulled apart. The eastern coast of South America, like the western coast of Africa, is presently a passive plate margin, with very little seismic activity.

Perpendicular to the Mid-Atlantic Ridge and parallel to the direction of plate movement are numerous small transform faults, which occur in many parts of the ocean floor, but especially in the equatorial region, and are caused by pressure due to the curvature of the Mid-Ocean Ridge (Maisey, 1991). These transform faults can extend past the ocean floor and into surrounding continents, where they are called lineaments (Maisey, 1991). Movement along lineaments is typically up or down, and if the crust on one side of a lineament moves down, it can create a fault-bounded basin. The Patos lineament in northeastern Brazil defines the northern edge of the Araripe Basin, and this basin may have been connected with the Recôncavo-Tucano-Jatoba Basin to the south (which is south of the Pernambuco lineament), until it was isolated by activity along both faults during the Lower Cretaceous (Maisey, 1991). Minor seismic activity still occurs along these fault lines (Maisey, 1991).

According to Maisey (2000), the East Brazilian Rift System (EBRIS), which was active during the late Jurassic and early Cretaceous, includes six major marginal basins (Pelotas, Santos, Campos, Espirito Santo, Bahia Sul and Sergipe-Alagoas) and three major onshore ones (Reconcavo, Tucano and Jatoba). Rifting within the EBRIS system occurred in three phases, followed by a transitional phase and a marine phase. The entire period from initial rifting to commencement of the final marine phase took approximately

50 million years.

The first rifting phase, referred to as Syn-rift phase I (corresponding to the Dom João stage of Brazilian geological literature), occurred from the Tithonian Stage (Late Jurassic) to the Berriasian Stage (Early Cretaceous), approximately 155-145 MYA. During this phase, rifting began along a southern branch of fault lines (located in southern Gondwana), and sediments began to accumulate in a large Afro-Brazilian depression. The second rift phase, called Syn-rift phase II (Rio da Serra and Aratu Stages of local geology), occurred from the Berriasian to the early or mid-Barremian, between 145–130 Ma. During this main rift phase, extensional deformation occurred along three major axes: the Gabon-Sergipe-Alagoas (GSA) trend, the Reconcavo-Tucano-Jatoba trend (RTJ), and the Cariri-Potiguar (CP) trend (whose axis is NE-SW and includes the Araripe Basin). Extensional deformation began along the GSA trend, forming discrete basins within which sedimentation was confined. In the final rifting phase, Syn-rift phase III (Buracica and Jiquiá Stages), which occurred from middle or late Barremian Stage to earliest Aptian Stage (130–125 Ma), extensional deformation moved westward to affect the Recôncavo-Tucano-Jatoba (RTJ) and Cariri-Potiguar (CP) trends and formed individual basins with continental sedimentary sequences. Later in this phase, the CP trend was abandoned tectonically. The last Syn-rift phase was followed by a Transitional or 'rift-to-drift' phase (Alagoan local stage), from early to mid-Aptian (125–115 Ma), during which the RTJ trend was abandoned tectonically, the GSA trend transitioned from extensional rifting to passive drifting, and abandoned basins began to be infilled with a 'transitional' sequence. Rifting then began along the equatorial branch of fault lines, and in the Benue trough of West Africa. In the last, or Marine, phase, from late Aptian (112

Ma) onwards, a permanent equatorial seaway formed between the southern Atlantic ocean and the western (Caribbean) Tethys sea. The Benue trough was abandoned tectonically later in the Cretaceous, but was briefly the site of a seaway linking the southern Atlantic ocean with the eastern (Mediterranean) Tethys.

The Araripe Basin, which contains the Santana Formation, was part of the Cariri-Potiguar (CP) rift axis, which was tectonically active for approximately 20 million years during the Berriasian and early Barremian Stages (Syn-rift phase II). Its tectonic activity ceased during the late Barremian, when rifting began along the equatorial branch farther north. Like the Araripe Basin, CP basins tend to be small (only a few tens of kilometers wide), and many are located near the Patos and Pernambuco lineaments. .

**Structure and Geomorphology—**The Araripe Basin is one of only a few Cretaceous inland basins in Brazil (although there are numerous marginal basins of Cretaceous age located in Brazil). It formed within a half-graben (rift valley) between the Patos and Pernambuco lineaments in northeastern Brazil, and its structural development and sedimentation were largely controlled by a fault system associated with the Patos lineament. The Araripe Basin was formed within an active rift trend (the Cariri-Potiguar, or CP, trend), and contains continental, transitional and marine sequences. The Mesozoic sedimentary sequence of the Araripe Basin comprises a lower conglomerate unit (the possibly Upper Jurassic Brejo-Santo Formation); above which is a succession of fine-grained, lacustrine clays, marls, and limestones; evaporates; and lastly, fluviatile sandstones of the Albian Exu Formation (Maisey, 1991). It has been suggested (Silva Santos, 1991) that several of the Cretaceous basins of northeastern Brazil may have been joined, including the Araripe Basin, to form a series of interconnected basins. A

paleogeographic relationship has been proposed between the Araripe Basin and the Parnaiba Basin to the northwest; and with the Reconcavo-Tucano-Jatoba Basin to the southeast, which was in turn connected with the Sergipe-Alagoas Basin to its northeast. These proposed interconnections are largely based on similarities in ichthyofauna between the basins, with certain fish taxa (such as the actinopterygian *Vinctifer*) appearing across several basins and linking them biogeographically (Silva Santos, 1991).

**Stratigraphy**—The Mesozoic sequence within the Araripe Basin can be subdivided into several parts (Maisey, 1991). The lowest part has been referred to as the Brotas Group, of Jurassic or Lower Cretaceous age, which rests unconformably atop the ancient Paleozoic and Precambrian basement rock and comprises interbedded shales and sandstones. The Brotas Group is further subdivided into the (lower) Aliança Formation and the (upper) Sergi Formation. Above the Brotas Group is the Santana Formation (Fig. 1), comprising a mostly calcareous succession and believed to represent a later Syn-rift or early post-rift sequence. It has been subdivided into three members, regarded by some authors (Silva, 1986a; Martill, 1993) as three separate formations: the Crato (inferior), Ipubi (middle), and Santana or Romualdo (superior). According to Maisey (1991), the Crato Member lies unconformably atop the Brotas group. The Crato largely comprises shallow-water laminated carbonates and black shales (Maisey, 2000). Fine ripples are occasionally preserved, indicating very shallow, wind-blown water (only a few centimeters in depth). Palynological data indicates an age of upper Aptian-lower Albian for the Crato unit.

Above the Crato unit is the Ipubi, an evaporitic sequence of recrystallized gypsum considered to be early-middle Albian in age (Maisey, 2000). Bituminous shales occur

periodically between gypsum layers, occasionally containing fossils of the actinopterygian fishes *Dastilbe* and *Vinctifer* as well as conchostracans and small gastropods. The Ipubi Member has sometimes been included within the overlying unit (Santana or Romualdo).

Overlying the Ipubi Member is a unit that has been referred to as the Santana Formation (more strictly) or the Romualdo Member. At the base of this formation are dark, well-foliated bituminous shales, containing ostracods and palynological data that indicate an age of middle Albian (Maisey, 2000). A marine influence has been suggested based on levels of hydrogen and organic carbon in these strata (Baudin et al., 1990; Maisey, 2000). Above these strata are oil shales containing fossil-bearing carbonate concretions. Numerous fossil fish have been found within concretions from this layer, and it is the source of the *Tribodus limae* fossils. An age of middle-late Albian has been suggested for the Santana concretions (Maisey, 2000). Above the concretion-bearing zone is a 1.5 m thick laminated clay containing foraminiferans, above which is a carbonate bank containing cassiopiid gastropods, believed to suggest an intertidal high-energy littoral environment (Maisey, 2000). This layer has also yielded fragmentary fish fossils (Maisey, 2000).

Above the Santana Formation is the Exu Formation, which comprises fluviatile sands and conglomerates (Martill et al., 2007) with no fossils except palynomorphs (which suggest a mid- to late Albian age), and is believed to represent near-shore marine or estuarine conditions.

*Tribodus* material reposited at AMNH and used in the present study comes from the BRA-01 locality (Santana Formation/Romualdo Member, Chapada do Araripe [Araripe

Plateau], Ceará province, northeastern Brazil). It comes from the fossiliferous concretion-bearing layer of this formation.

**Geologic age**—The age of the Santana fossils was assessed by several important discoveries. Early on, Agassiz (1841) concluded that the fossil-bearing strata were of the same age as the "Chalk Formation" (Cretaceous) of Europe based on the occurrence of ganoid, ctenoid, and cycloid fishes together. Gardner (1849) linked the Santana to the "Chalk Formation," but his reasoning based on presence of septarian concretions was erroneous (Maisey, 1991). Later, Woodward dated the Santana fossils to the Upper Cretaceous based on similarities with fish fossils from the Cenomanian of Lebanon and Syria. In 1968, Silva Santos and Valença specified the age of the Santana fishes as Aptian, as a result of their extensive comparison of the fossils with fish faunas from elsewhere in the world (they found them most closely similar to the Benevento fauna of Italy, which was Aptian-Albian in age). An Aptian age has been confirmed by studies of ostracods (Braun, 1966), and is consistent with some palynological studies (Maisey, 1991). However, other palynological work (Lima, 1979b) has suggested an Albian age for the Santana Formation, and some authors (e.g., Schobbenhaus and Campos, 1984; Martill, 1988) consider the formation to be an undifferentiated Aptian-Albian age (Brito, 1992). Pons et al. (1990) attributed an age of uppermost Aptian/basal Albian to the Crato Member, and an age of middle-upper Albian to the Romualdo Member (Brito, 1992), although the Crato Member has been estimated by various other studies to be anywhere from Lower Barremian to Aptian in age (Maisey, 1991). Based on the results of the previous studies mentioned above (many of which are contradictory), it seems that the consensus of opinion gives an age of Aptian-Albian for the Romualdo Member

concretions, the most precise age estimate currently available on which a majority of authors are in agreement. An age of 110 Ma has been attributed to the Romualdo Member.

**Paleoecology**—According to Maisey (2000), the paleoenvironmental sequence within the Araripe Basin Cretaceous series progressed from an early fluvial and lacustrine phase (the Missao Velha and Camadas Batateiras units), to a later lacustrine or lagoonal phase with increasing salinity (the Crato Member), then an evaporate-producing hypersaline lake or shoreline (the Ipubi Member), followed by a semi-enclosed lagoon varying from fresh to brackish waters (the Santana Formation), and finally a near-shore marine or estuarine environment (the Exu Formation). This succession of environments reflects the gradual transition in this region from an inland continental rift valley to a near-shore or marine location, as South America and Africa continued to separate and marine incursions from the newly forming South Atlantic Ocean occurred within rift-produced basins such as the Araripe.

Within the Cretaceous of the Araripe Basin, the Crato unit (considered by some authors as the lowest unit in a three-unit Santana Formation, or as an independent formation) is believed to represent freshwater lacustrine or lagoonal conditions increasing in salinity. That the Crato paleoenvironment was fresh water is indicated by conchostracans, freshwater algae, and halophobic aquatic insects, whereas presence of terrestrial plants, insects, and numerous land vertebrates also indicate a close proximity to land (Maisey, 2000). Periodic elevations in salinity may have been caused by influx of waters from a nearby seaway, or alternatively by overturn of a stratified column of lake water (indicated by black shales). The Crato unit has produced many fossils including the

actinopterygian fish *Dastilbe*, tetrapods including frogs and birds, and numerous well-preserved fossil insects (discussed below). However, the species diversity of the Crato is relatively low (Maisey, 2000).

Above the Crato Member, the evaporitic Ipubi Member is believed to indicate the end of the lacustrine cycle, although there is no evidence of a clear transition between the two (Maisey, 2000). It is considered to be late-transitional (post-rift), representing a mainly hypersaline environment. Although fishes such as *Dastilbe* and *Vinctifer* are found in bituminous shales of the Ipubi Member, its species diversity, like that of the Crato, is relatively low.

Above the Ipubi Member is the Santana Formation (or the Romualdo Member of the Santana Formation), from which the *Tribodus limae* fossils derive. Based on analysis of clay minerals, ostracods, dinoflagellates and palynomorphs, this formation has been interpreted as representing a semi-enclosed, freshwater to brackish lagoon, which eventually became an estuary (Maisey, 2000). The paleoenvironment of the concretion-bearing layers of the Santana unit has been interpreted as saline to hypersaline (based on analysis of organic matter in the concretions and surrounding sediment), and occasional sharp increases in salinity may have been what killed many of the fish preserved in the concretions (Maisey, 2000). The concretion-bearing layer of the Santana reflects a high species diversity. Above the concretion-bearing zone is a 1.5 m thick laminated clay containing foraminiferans, followed by a carbonate bank containing cassiopiid gastropods, believed to suggest an intertidal high-energy littoral environment (Maisey, 2000). The presence of fish fragments in this layer supports the conclusion that this was a high-energy shoreline (Maisey, 2000).

Above the Santana or Romualdo unit are the fluviatile sands and conglomerates of the Exu Formation, which have no fossils except palynomorphs (suggesting a mid- to late Albian age) and are believed to represent near-shore marine or estuarine conditions (Maisey, 2000).

**Faunal and floral diversity of the Santana Formation—**In addition to *Tribodus*, the Santana Formation has yielded numerous other fish taxa, mainly osteichthyans (e.g., the actinopterygians *Vinctifer*, *Dastilbe*, and *Tharrhias*; and the coelacanth *Axelrodichthys*; Jordan, 1919; Silva Santos, 1947; Silva Santos and Valenca, 1968; Maisey, 1986). These taxa differ in distribution between the different subdivisions of the Santana; for example, *Vinctifer* and *Tharrhias* are common in Romualdo Member concretions, whereas *Dastilbe* is most common in the Crato Member. The Santana Formation has also produced fossil tetrapods: the Crato member has yielded frogs and birds (Kellner and Campos, 1986; Martins-Neto and Kellner, 1988); and the concretion-bearing strata has produced crocodilians (Price, 1959; Kellner, 1987); turtles (Gaffney et al., 2001); dinosaurs (Sues et al., 2004), and pterosaurs (Kellner and Campos, 2002; Kellner, 2004). Invertebrate and plant fossils are also known from the Santana Formation: invertebrate fossils include pelecypods, gastropods, conchostracans, ostracods, the oldest copepods known, and more rarely, decapods and echinoids, as well as insects and arachnids from the Crato Member (Cressey and Patterson, 1973; Mabesoone and Tinoco, 1973; Lima, 1979; Maisey, 1991; Grimaldi, 2003); plants are found in both the Romualdo and Crato Members (Duarte, 1969; Fanton et al., 2006).

**Other occurrences of *Tribodus*—**Complete skeletal material of *Tribodus limae* is currently known only from the Romualdo Member of the Santana Formation (Lower

Cretaceous, Aptian/Albian) of the Chapada do Araripe, State of Ceará, northeastern Brazil (Brito and Ferreira, 1989; Brito; 1992). All complete skeletal fossils of *Tribodus* known to date are from this site (including all new and previously described specimens included in the present work). However, isolated tooth specimens identified as *Tribodus* have also been described from the Middle-Late Cretaceous (Albian-Cenomanian) of Brazil (Alcântara Formation; teeth originally described as *Myliobatis*: Brito and Ferreira, 1989; Dutra and Malabarba, 2001). In addition to the Brazilian material, microremains (teeth and finspines) of *Tribodus* have been reported from the Early Cretaceous (?Valanginian-Barremian, Loia Series) of Congo (Maisey, 2000; described as ?Hylaeobatis by Casier, 1961); the Early Cretaceous (Albian) of Tunisia (Chenini Formation; teeth assigned to *Tribodus limae*, *Tribodus tunisiensis*, *Tribodus aschersoni*: Cuny et al., 2004; Martill, 2007) and Algeria (Tiout Formation; Landemaine, 1991); from the Late Cretaceous (Cenomanian) of southwestern France (Charentes; teeth assigned to *Tribodus morlati*; Landemaine, 1991; Vullo et al., 2003; Vullo et al., 2005; Vullo et al., 2007; Vullo and Néraudeau, 2008), southeastern Morocco (Kem Kem Beds; Dutheil, 1999; Cavin et al., 2001), Libya (Draa Ubari Formation; Nessov et al., 1998; Rage and Cappetta, 2002), Egypt (Bahariya Formation; identified as *Tribodus aschersoni*; Werner, 1989); and from the Late Cretaceous (possibly Cenomanian) of Niger (In Abangharit Beds; Dutheil, 2001) and Sudan (Wadi Milk Formation; Werner, 1994: described as *Asteracanthus aegyptiacus*). For a paleogeographic map of *Tribodus* localities, see Figure 4. *Tribodus* occurrences therefore span a period of approximately 36 to 46 Ma (from Valanginian-Barremian to Cenomanian), with a paleogeographic distribution that was apparently mainly confined to western and northern Gondwana (i.e., South America,

West and North Africa), with a few scattered occurrences on nearby landmasses (such as France, which was an island situated close to northern Africa during the middle to late Cretaceous).

**Taphonomy and preservation—**Fossils of *Tribodus limae*, like most of fossils from the Romualdo Member of the Santana Formation, are typically preserved within calcareous concretions. The Santana Formation is considered a type of Lagerstätten (a sedimentary deposit exhibiting extraordinary fossil richness or completeness), and many of its fossils (including *Tribodus*) are extraordinarily well preserved, articulated and nearly complete, some even with soft parts occasionally preserved. Concretions generally form within a surrounding softer sediment. The fossils they contain usually have not been flattened or crushed, because the concretions form relatively quickly on or near the surface, before they are compacted by overlying sediments (Maisey, 1991, p. 59). In brief, concretions form when substances produced by a decaying organism (such as a fish) and by decompository bacteria interact with pore water in the surrounding sediment, causing formation of hard mineral precipitates. Martill (1988) suggested that the periodic mass mortalities of Santana fishes may have been caused by fluctuations in salinity.

# CHAPTER 3: HISTORICAL REVIEW OF HYBODONTS

The majority of hybodont shark taxa are based on isolated teeth, fin spines and dermal denticles. Agassiz (1837) described the type species of *Hybodus*, *H. reticulatus*, on the basis of tooth characteristics, and created the higher taxon "Hybodontes" to include *Hybodus*, *Cladodus*, *Sphenonchus*, and *Diplodus*. Hybodontes was considered by Agassiz to represent an intermediate group between the "ancient" Cestraciontes and the more "modern" Squalides (Agassiz, 1837), and was united on the basis of rounded, protruding teeth ("dents saillantes, plus ou moins arrondies," p. 83). Hybodontes was divided into two groups based on differing tooth morphology: one including *Hybodus* and *Cladodus* (which have teeth with acuminate, or pointed, cusps and without a principal pulp cavity, later referred to as osteodont teeth); and the other including *Diplodus* and *Sphenonchus* and having a principal pulp cavity present and differing cusp morphology, later called orthodont teeth (Maisey, 1982). *Sphenonchus* was subsequently synonymized with *Hybodus* (Charlesworth, 1845; Day, 1854; Fraas, 1889; Maisey, 1982).

The taxon Cestraciontes of Agassiz (1837) included the hybodont genera *Acrodus* and *Ptychodus* along with *Helodus* (a holocephalan), *Ceratodus* (a lungfish), and *Cestracion* (the extant shark *Heterodontus*), and was based on tooth characteristics including a continuous pavement of flattened, non-cutting teeth, and structures of the tooth crown and root. Both Cestraciontes and Hybodes were distinguished from Squalides on the basis that the latter group has sharper, cutting teeth (Agassiz, 1837). Cestraciontes, Hybodontes and Squalides were the three subdivisions of the larger taxon Squales (sharks; Agassiz, 1837).

Though Agassiz (1837) placed *Hybodus* and *Acrodus* in different taxa, Owen (1840) noted that teeth of the two taxa had histological similarities. Day (1864) was the first author to emphasize the similarities of the two taxa in aspects other than teeth, on the basis that teeth of *Acrodus anningiae* were found associated with fin spines similar to those of *Hybodus* (Day, 1864; Maisey, 1982). Subsequent authors still included *Acrodus* (and now *Hybodus*) with *Cestracion* (*Heterodontus*). Woodward (1889a) included the hybodonts *Hybodus*, *Acrodus*, *Asteracanthus*, and *Tristychius* in his family Cestraciontidae, along with *Heterodontus* (*Cestracion*), *Synechodus*, *Palaeospinax*, *Sphenacanthus*, and *Orodus*, thus grouping hybodonts with numerous extant sharks (except squaloids, *Squatina* and batoids) under the suborder Asterospondyli. Although Woodward based the suborder on vertebral characteristics, hybodonts lack calcified vertebral centra (however, *Palaeospinax* and *Synechodus*, which Woodward identified as hybodonts based on their teeth, do have Asterospondylous vertebrae) (Maisey, 1982). Woodward also thought hexanchoids and *Chlamydoselachus* were descendants of *Hybodus* (Woodward, 1886).

Brown (1900) was one of the first authors to suggest that *Hybodus* and *Heterodontus* were unrelated, on the basis that the jaw suspension of *Hybodus* was more similar to hexanchoids than *Heterodontus*. He considered hexanchoids to be the sister group of *Hybodus* and extant sharks + batoids, and regarded *Palaeospinax* as closer to squaloids and *Heterodontus* than to *Hybodus* (Maisey, 1982) on the basis of fin spine morphology (he designated forms with ornamented, denticulate fin spines and male cephalic spines as Hybodontidae, and distinguished them from those with smooth, non-denticulate fin spines and no cephalic spines such as *Palaeospinax*). Goodrich (1909, 1930) supported

this grouping, but placed *Heterodontus* with *Hybodus* rather than with other recent sharks (Maisey, 1982). Regan (1906) considered batoids to be the sister group of *Hybodus* + other recent sharks, a view later echoed by White (1937) and Romer (1945). Berg (1955) and Patterson (1967) gave a similar grouping, except that these authors placed *Heterodontus* with *Hybodus* as the sister group of other sharks (Maisey 1982).

Zittel (1911) was first to suggest that hybodonts should be separated from extant sharks and from cestracionts (which included *Palaeospinax* and *Synechodus*). Brough (1935) held similar views, and listed a number of characters shared by hybodonts (fusiform body of "normal" shape with moderately-sized fins; posteriorly placed anal fin; tribasal pectoral fin, non-fused teeth; dorsal fins dissimilar to each other; finspines with longitudinal furrows and posteriorly located denticles; massive jaws that were either amphistylic or early hyostylic; and *Sphenonchus*-like head spines present in males). Maisey (1982) discussed the relative importance of these characters as hybodont synapomorphies.

Moy-Thomas (1939A, 1939B) supported this view, but created the order Protoselachii comprising Hybodontidae and Tristychiidae. Young (1962) upheld this grouping, but placed *Heterodontus* with *Hybodus* (in the order Protoselachii) as the sister group of other recent sharks + batoids (Euselachii). Patterson (1967) placed the Hybodontidae within Heterodontiformes. Blot (1969) constructed a phenetic classification of hybodonts based on the mosaic of shared derived and primitive characters described by Schaeffer (1967), in which the clade Hybodontiformes included hybodonts with *Heterodontus*, *Chlamydoselachus*, hexanchoids, *Palaeospinax*, *Synechodus*, and several other extinct forms, while the clade Euselachiformes comprised other extant sharks and batoids.

However, this classification is based mainly on plesiomorphic characters. Glikman (1964) suggested a sister group relationship between *Hybodus* and extant lamnoid sharks, and considered this clade as sister to other recent sharks and batoids.

In summary, the hypotheses of hybodont relationships described above have differed in their arrangement of taxa, but there have been essentially four hypotheses: 1) that batoids are the sister group of hybodonts + recent sharks; 2) that hybodonts form the sister group to batoids and recent sharks; 3) that hexanchoids are the sister group to hybodonts, batoids, and remaining extant sharks; 4) that hybodonts are nested within recent sharks, either as sister to lamnoids (Glickman, 1964) or sister to *Heterodontus*, galeomorphs, and hexanchoids (Woodward, 1889a). A diagram showing these and other earlier hypotheses of hybodont relationships is provided in Figure 6.

Maisey (1982) listed six shared apparently derived characters linking *Heterodontus* with other recent sharks, and noted that none of the synapomorphies uniting hybodonts were shared by *Heterodontus*. Maisey (1982) thus concluded that *Heterodontus* is unrelated to hybodonts, and rejected the hypotheses of Woodward (1889a); Goodrich (1909, 1930); Young (1962) and Patterson (1967) that held that hybodonts are more closely related to *Heterodontus* than to other recent elasmobranchs. Lane & Maisey (2009) further noted that *Heterodontus* and hybodonts differ in the structure of the pectoral fin articulation (the articulation in *Heterodontus* has a ball-and-cup arrangement, whereas in *Tribodus limae* and apparently other hybodonts the fin articulates along a protruding ridge on the scapulocoracoid).

Maisey (1982) also rejected the hypotheses that batoids are the sister group of hybodonts and recent sharks (Regan, 1906; White, 1937; Romer, 1945; Berg, 1955;

Patterson, 1967) and that hexanchoids are the sister group of hybodonts + other recent elasmobranchs (Brown, 1900; Goodrich, 1909, 1930). Maisey (1982) proposed that the most parsimonious solution placed hybodonts as the monophyletic sister group of all extant elasmobranchs (sharks + batoids), the hypothesis propounded by Brough (1935) and Moy-Thomas (1939A, B), on the basis of several shared characters (an ectethmoid process on the postnasal wall, a continuous puboischiadic bar, and a unique arrangement of basibranchials and hypobranchials).

It is now generally accepted that hybodonts are the sister group of neoselachians (modern sharks and batoids). Various authors have proposed characters supporting their relationship as a monophyletic group, including the presence of a puboischiadic bar (Compagno, 1973), presence of non-growing (synchronomorial) denticles (Reif, 1978), presence of an ectethmoid process, and presence of an occipital arch not projecting behind the otic capsules (Schaeffer, 1981).

The Paleozoic forms *Tristychius* and *Onychoselache* have been considered problematic in terms of their relationship to other hybodontiforms (Maisey et al., 2004). Maisey (1989) listed four characters (shoulder joint with strong propterygial support, pectoral articulation rotated, enlarged pelvic "propterygium", and presence of a glossopharyngeal canal) uniting neoselachians and hybodonts with *Tristychius* and *Onychoselache*. Other characters proposed to unite *Tristychius*, hybodonts and neoselachians (to the exclusion of “Paleozoic sharks,” e.g., xenacanths, ctenacanths, symmoriiforms, and *Cladoselache*) have included: dorsal otic ridge lacking horizontal crest; presence of perilymphatic openings; otico-occipital fissure closed behind endolymphatic fossa; embryonic metotic fissure closed apart from glossopharyngeal-

vagus canal; ventral otic fissure absent in adult; anterior ampulla located between or in front of postorbital process; and shoulder joint narrowed with increased propterygial participation (Maisey et al., 2004).

Maisey et al. (2004) further listed four characters uniting hybodonts with neoselachians, but unknown in *Tristychius*: pre-ampullary part of posterior semicircular canal extends dorsally to perilymphatic fenestra; separation of utricular and saccular regions; posterior canal duct present; and medial chondrified otic capsular wall present. *Tristychius* and *Onychoselache* have long, *Hybodus*-like ribs, but have an unfused pelvic girdle (puboischiadic bar), which according to outgroup comparison with other gnathostomes may be a primitive state; the most parsimonious conclusion is that pleural ribs are primitive and that *Tristychius* and *Onychoselache* are sister groups to *Hybodus* + neoselachians (Maisey, 1982).

In terms of hybodont interrelationships, Maisey et al. (2004) distinguished between classification schemes based on the use of dental characters (usually phenetic) and those using other morphologic characteristics (considered putative synapomorphies). Capetta (1987) used the former approach to distinguish five families of hybodont sharks: Hybodontidae (*Hybodus, Priohybodus*, and *Pororhiza*); Acrodontidae (*Acrodus, Asteracanthus* and *Bdellodus*); Polyacrodontidae (*Lissodus, Lonchidion, Palaeobates*, and *Polyacrodus*); Ptychodontidae (*Hylaeobatis* and *Ptychodus*); and Steinbachodontidae (*Steinbachodus*).

Maisey (1989) employed the latter approach, combining dental and skeletal characteristics, and found two characters supporting Mesozoic hybodonts (*Lissodus, Polyacrodus, Palaeobates, Asteracanthus, Acrodus, Egertonodus*, and *Hybodus*): unequal

scapulocoracoid proportions, and presence of a puboischiadic bar in females. Maisey (1989) linked *Egertonodus* and *Hybodus* on the basis of their high-crowned, multicuspid teeth, and recognized a sister relationship between *Asteracanthus* and *Acrodus* based on two characters (teeth with columnar osteodentine, and adjacent tooth rows). Maisey (1989) listed three characters (involving teeth, cephalic spines and labial cartilages) linking *Asteracanthus* + *Acrodus* and *Egertonodus* + *Hybodus* in a monophyletic group, which with its sister taxon *Palaeobates* comprised the family Hybodontidae (encompassing most of Capetta's 1987 families Acrodontidae and Hybodontidae as seperate subfamilies). Ten characters were cited linking *Hamiltonichthys* with Mesozoic hybodonts (Hybodontoidei, Maisey, 1989). This group plus *Tristychius* and *Onychoselache* comprised the Hybodontiformes (Maisey, 1989).

Maisey et al. (2004) proposed an emended phylogeny (also adapted by Coates and Gess, 2007; Fig. 7) with *Polyacrodus* removed (on the basis that it remains poorly diagnosed), and the additional taxa *Lonchidion, Bdellodus*, and *Tribodus* included. Although *Lonchidion* was considered synonymous with *Lissodus* by Duffin (1985), Maisey et al. (2004) suggest that the two groups should remain seperate despite dental similarities. In the phylogeny of Maisey et al. (2004), *Asteracanthus* and *Tribodus* are united by transversely oriented palatoquadrates lacking an ethmoidal buttress; this group is joined with *Acrodus* (and possibly *Bdellodus*) by teeth with columnar osteodentine; and *Hybodus* and *Egertonodus* form a monophyletic group (unchanged from Maisey, 1989), united with the above-named taxa by the presence of osteodont teeth. *Palaeobates* is sister to this monophyletic group based on denticle, head spine, and fin spine characters. *Lissodus* and *Lonchidion* are linked by "convict-arrow" cephalic spine shape, and this

clade is joined to the above taxa by further cephalic spine characters. The phylogeny presented in Maisey et al. (2004) leaves out several of Maisey's original (1989) characters linking *Hamiltonichthys* with Mesozoic hybodonts, notably his characters 9 (elongate lateral teeth); 11 (inflated and elongate jugular canal); and 13 (puboischiadic bar in males). Maisey (1986) proposed a close similarity between *Egertonodus fraasi* and *E. basanus* on the basis of cranial anatomy, and suggested that these two taxa differ from other hybodonts such as *Hybodus reticulatus* in lacking compound "growing" denticles, and having certain features of the ethmopalatine and otico-occipital region.

Orthodont teeth have been used to unite *Lissodus*, *Polyacrodus* and *Palaeobates* (Glikman, 1964; Cappetta, 1987), but Maisey et al. (2004) pointed out that these also occur in *Hamiltonichthys* and are probably plesiomorphic. Fin spine ornamentation and cephalic spine structure in *Palaeobates* suggest a closer relationship with hybodonts having osteodont teeth (*Hybodus, Egertonodus, Acrodus, Asteracanthus*, and *Tribodus*).

Many of the hybodont taxa recognized by Cappetta (1987) remain questionable. Of these, *Ptychodus* is probably closer to neoselachians and has none of the characters uniting hybodonts (Maisey et al., 2004). Several of Cappetta's other taxa (*Priohybodus, Pororhiza, Bdellodus, Hylaeobatis, Steinbachodus*) are based solely on teeth or other isolated dermal features, which can be problematic as Jaekel (1889) showed in finding ten hybodont tooth "species" in a single jaw of *Acrodus* (Maisey, 1986). It is likely that the large number of hybodont taxa now recognized is a result of oversplitting.

# CHAPTER 4: MATERIALS AND METHODS

All specimens of *Tribodus limae* described here are from the upper (Romualdo) Member of the Lower Cretaceous (Aptian–Albian) Santana Formation, Chapada do Araripe, Ceará state, northeastern Brazil, and come from the fossiliferous concretion-bearing layers of that formation. This is the only locality yielding complete specimens of *Tribodus* known thus far (Brito and Ferreira, 1989; Brito, 1992; Maisey and Carvalho, 1997). In the present thesis, all references to *Tribodus* (except where specifically stated otherwise) indicate the type species, which is the only species of *Tribodus* for which articulated skeletal material is preserved. The holotype of *Tribodus limae*, as well as several paratypes and additional specimens, are reposited in Brazilian museum collections (Brito and Ferreira, 1989; Brito, 1992).

Of the four AMNH specimens of *Tribodus limae* included in the present study (Figs. 8, 9), two (AMNH FF 13957 and 13959) are acid-prepared specimens; the rest were prepared mechanically. Specimens of *Tribodus limae* examined for the present study include AMNH 13957 (articulated specimen with right upper and lower jaws, Fig. 8A), 13958 (complete, exceptionally preserved braincase, Figure 9; upper and lower jaws, hyoid arch elements, and pectoral girdle), 13959 (crushed endocranium with right palatoquadrate, left and right Meckel's cartilages, possible labial cartilages, and left and right hyomandibulae, Fig. 8B), and 13961 (partial braincase with left and right palatoquadrates, left Meckel's cartilage, and right Meckel's cartilage including partial dentition, Fig. 8C, D); MN 5807-V (formerly CD-P-105), an articulated specimen in left lateral view (Fig. 10); 5808-V (formerly CD- P-106), also an articulated specimen in left

lateral view (Fig. 11); and UERJ-PMB-40 (Fig. 12), PMB-114 (Fig. 13), and PMB-119 (not shown), all partial specimens showing the anterior part of the fish (including the braincase and parts of the visceral skeleton). AMNH 13958 includes a three-dimensionally preserved braincase, originally reported by Maisey and Carvalho (1997) and described in further detail in the present thesis. Additionally, the right scapulocoracoid of AMNH 13958 has been prepared out of the matrix and is also exceptionally well preserved three-dimensionally, showing a ridge on its posterolateral surface for articulation of the basal fin elements. A complete list of specimens of *Tribodus limae* examined is provided below and in Appendix D.

The braincase of AMNH FF 13958 (*Tribodus limae*) was CT scanned and digitally reconstructed for the present study. This specimen is three-dimensional and almost perfectly preserved, with an infilling of carbonate matrix that gives a low-density contrast, with the exception of localized pyritization and small areas lacking matrix. This specimen was scanned and briefly discussed by Maisey (2004a). CT scanning of this specimen was performed by R. Ketcham and M. Colbert (UT Austin), 3/16/1999. Scanning parameters include: 8bit and 16bit: RLS, 420 kV, 1.8 mA, 2 brass filters, air wedge, 160% offset, gain of 4, integration time 128 ms, slice thickness 0.25 mm, source object distance 630 mm, 2000 views, 4 rays per view, 1 sample per view, scan position 141 mm, interslice spacing 0.25 mm, field of reconstruction 94 mm, reconstruction offset 400, reconstruction scale 500. 8-bit export parameters 2400/1000.

One braincase of *Egertonodus basanus* (NHM P. 60110) was also scanned and briefly discussed (but not figured) by Maisey (2004a). This specimen is three-dimensional, but partially crushed. Its preservation is in an ironstone matrix giving a good density contrast

with the prismatic calcification of the specimen. CT scanning was performed by R. Ketcham and M. Colbert (UT Austin), 1/26-27/2001. Scanning parameters include: 16bit: RLS, 420 kV, 4.7 mA, on brass filter, empty mount wedge, offset 130%, gain 4, integration time 64 ms, slice thickness 0.25 mm, S.O.D 595 mm, 1000 views, 5 rays averaged per view, 1 sample per view, inter-slice spacing 0.25 mm, field of reconstruction 77 mm, reconstruction offset 630, reconstruction scale 448. Detector running average width 5 pixels (skip 1).

Scan data for both *Tribodus* and *Egertonodus* was originally exported as TIFF images, and cropped and reprocessed in ImageJ version 1.34s. Contour-based surface reconstruction of both fossils was generated in Imaris X64 version 5.0.2. Three-dimensional images of the braincase of *Tribodus* and *Egertonodus* were constructed through contour-based surface rendering of CT slices using Imaris/Surpass software. Illustrations of soft anatomical features were prepared using the computer program Adobe Photoshop Elements version 4.0.

Several additional skeletal elements of *Tribodus* were also CT scanned for the present thesis. For the section on the visceral skeleton of *Tribodus*, the palatoquadrate and Meckel's cartilage of AMNH 13958 were also scanned using computed tomography (CT), by M. Colbert (UT Austin, 23 February 2007). Scan data: 210 kV; .11 mA; slice thickness 2 lines (= 0.139 mm); field of reconstruction 65 mm (maximum field of view 66.31449 mm). Scan data originally exported as TIFF images. CT scan slices were then examined in Imaris X64 version 6.0.1. For the section on pectoral fin morphology, the scapulocoracoid of AMNH 13958 was CT scanned perpendicular to its long axis by M. Colbert (University of Texas at Austin, 23 February 2007). Scan data: 210 kV; 0.11 mA;

slice thickness 2 lines (= 0.139 mm); field of reconstruction 65 mm (maximum field of view 66.31449 mm). Scan data was originally exported as TIFF images, and cropped and reprocessed in ImageJ version 1.34s. Contour-based surface reconstruction was generated in Imaris X64 version 5.0.2. 3-D images of the scapulocoracoid were constructed through contour-based surface rendering of CT slices using Imaris/Surpass software.

Teeth of *Tribodus limae* (AMNH 13961) were examined using scanning electron microscopy (SEM), after being etched with 2 *N* HCl for 10 seconds, rinsed in a water bath, and dried overnight. Cephalic spines and dermal denticles of *Tribodus limae* (AMNH 13958, 13959) were also examined under SEM.

In addition to *Tribodus*, other hybodontiform taxa for which complete or partial skeletal material is known (as opposed to isolated dermal elements) were examined firsthand for comparison, including specimens of *Hybodus hauffianus*, *Hybodus reticulatus*, *Hybodus delabechei*, *Hybodus medius*, *Acrodus anningiae*, *Acrodus nobilis*, *Asteracanthus ornatissimus*, *Egertonodus fraasi*, *Egertonodus basanus*, *Lissodus africanus*, *Lissodus cassangensis*, *Hamiltonichthys mapesi*, and two problematic hybodontiform taxa, *Onychoselache traquairi* and *Tristychius arcuatus*. All of these taxa were also coded for inclusion in the character/taxon matrix for phylogenetic analysis. A complete list of hybodontiform specimens examined, and the institutions in which they are reposited, is provided in Appendix D (List of Specimens Examined). Further details regarding choice of ingroup (hybodontiform) taxa is provided in the section on taxon sampling in part III of this thesis (Phylogenetic Analysis).

In addition to specimens of *Tribodus* and other hybodonts, numerous wet- and dry-preserved specimens of extant chondrichthyans from the AMNH Ichthyology collections

were examined for comparison with *Tribodus*. The following specimens were examined. Cleared-and-stained specimens: *Heterodontus francisci* (AMNH 38182SW, 47912SW), *Carcharhinus leucas* (AMNH 55610, 97541SW), *Negaprion brevirostris* (AMNH 56003SW), *Galeocerdo cuvier* (AMNH 55041SW), and *Squatina californica* ( AMNH 38184SW). Alcohol-preserved specimens: *Heterodontus francisci* (AMNH 96795SW, 225820SW), *Carcharhinus obscurus* (AMNH 59037), *Sphyrna tiburo* (AMNH 222468SW), *Negaprion brevirostris* (AMNH 47932SW, 222829SW), *Squalus acanthias* (AMNH 225783), *Heptranchias perlo* (AMNH 226011SW), *Chlamydoselachus* (AMNH Vertebrate Paleontology Teaching Collection no. K 3–9), *Squatina californica* (AMNH 55686SW), and *Squatina australis* (AMNH 98468SW), and *Hydrolagus collei* (AMNH 58237SW). Dried specimens: *Sphyrna tiburo* (AMNH 93843SD, 218154SD), *Galeocerdo cuvier* (AMNH 218207SD), *Carcharhinus brevipinna* (AMNH 93845SD, 93846SD, 218152SD), *Carcharhinus acronotus* (AMNH 218150SD), and *Dasyatis americana* (AMNH 218289SD). Uncatalogued wax-preserved neurocrania and latex and plastic endocasts of *Squalus acanthias* and *Notorynchus cepedianus* from the AMNH Division of Paleontology collections were also examined. An uncatalogued specimen of *Squalus acanthias* was additionally dissected to examine its soft anatomy in comparison with *Tribodus*. Taxonomic authorities are given only for fossil taxa. Taxonomic authorities for extant taxa can be found in the online database FishBase (www.fishbase.org).

For the chapter on pectoral girdle and fin morphology of *Tribodus*, scapulocoracoids of the xenacanth *Orthacanthus texensis* (Cope, 1884), from the Permian of Texas (MCZ 13915, 13916, 13384; AMNH FF 20273; Fig. 7), and of an undescribed Permian

ctenacanth (FHSM VP-15012), were additionally examined for comparison with *Tribodus* and other hybodonts. Additional specimens of *Orthacanthus texensis* and several other Paleozoic chondrichthyan taxa (*Akmonistion zangerli*, *Diplodoselache woodi*, *Tamiobatis* sp., *Cladoselache* sp.), were also examined and coded for use in the phylogenetic analysis part of this study, as were numerous hybodontiform taxa and six extant chondrichthyan taxa (the neoselachians *Squalus acanthias*, *Notorynchus cepedianus*, *Carcharhinus brevipinna*, *Heterodontus francisci*, and *Dasyatis americana*, and the chimaeroid *Hydrolagus collei*). The ingroup and outgroup taxa and specimens chosen for use in the phylogenetic analysis are discussed in further detail in the section on taxon sampling in part III of this dissertation (Phylogenetic Analysis), and a complete list of specimens examined is provided in Appendix D.

A detailed description of the methodology used for the phylogenetic analysis portion of this project is provided in part III of this dissertation, under the headings "Taxon Sampling" and "Methods for Phylogenetic Analysis."

Figures listed and described in the text are included at the end of their appropriate chapters in the thesis, and a list of figures and their page numbers is provided in the List of Figures at the beginning of this section.

**MATERIAL OF *TRIBODUS LIMAE*:**

**HOLOTYPE: GP/2T-2 IG-USP.** Complete fish lacking the caudal fin, figured by Brito and Ferreira (1989: fig. 1A).

**PARATYPE: DGM-DNPM 1296-P.** Skull with first fin spine and associated dermal elements, figured by Brito and Ferreira (1989: fig. 2B).

**OTHER MATERIAL OF *TRIBODUS LIMAE* EXAMINED:**

**AMNH FF 13957.** Acid-prepared, nearly complete fish lacking the caudal fin, figured by Lane and Maisey (2009: fig. 1A).

**AMNH 13958.** Mechanically prepared, three-dimensionally preserved braincase with mandibular and hyoid arch elements, figured by Maisey and Carvalho (1997: fig.1); pectoral endoskeleton, figured by Lane and Maisey (2009: figs. 3, 4).

**AMNH 13959.** Acid-prepared, crushed neurocranium with mandibular and hyoid arch elements and partial pectoral girdle (figured by Lane and Maisey, 2009: figs. 1B, 2).

**AMNH 13961.** Mechanically prepared partial braincase, anterior dorsal fin, and pectoral girdles, figured by Lane and Maisey (2009: fig. 1C, D).

**UERJ-PMB-40.** Articulated partial specimen with three-dimensionally preserved head, visceral arch elements, and anterior dorsal fin spine.

**UERJ-PMB-114.** Articulated partial specimen with braincase and partial visceral skeleton.

**UERJ-PMB–119.** Articulated partial specimen with braincase, visceral arch elements, dorsal fin spine and fragmentary pectoral girdles.

**MN 5808-V (formerly CD-P-106).** Nearly complete fish lacking the caudal fin, figured by Brito (1992: fig. 2).

**MN 5807-V (formerly CD-P-105).** Nearly complete fish lacking the caudal fin, figured by Brito (1992: fig. 1).

## ABBREVIATIONS

**Institutional**

| | |
|---|---|
| **AMNH** | American Museum of Natural History, New York |
| **BSPGM** | Bayerische Staatssammlung fur Geologie und Palaontology, Munich, Germany |
| **DGM-DNPM** | Divisao de Geologia e Mineralogia, Departamento Nacional de Producao Mineral, Rio de Janeiro, Brazil |
| **FHSM** | Sternberg Museum of Natural History, Fort Hays State University, Hays, Kansas |
| **GPIT** | Palaontologische Sammlung Institut fur Geowissenschaften, Universitat Tubingen, Tubingen, Germany |
| **HMV** | Hunterian Museum (fossil vertebrate collection), Glasgow, UK |
| **IG-USP** | Instituto de Geosciencias, Universidade de Sao Paulo, Sao Paulo, Brazil |
| **MCZ** | Museum of Comparative Zoology, Harvard University, Cambridge, Massachussetts |
| **MN** | Museu Nacional, Rio de Janeiro, Brazil |
| **NHM** | The Natural History Museum, London, UK |
| **OUM** | Oxford University Museum, Oxford, UK |
| **RSM** | Royal Scottish Museum/National Museums of Scotland, Edinburgh, UK |
| **SMNS** | Staatliches Museum für Naturkunde, Stuttgart, Germany |
| **UCMZ** | University of Cambridge Museum of Zoology, Cambridge, UK |

**UERJ** Universidade do Estado do Rio de Janeiro, Rio de Janeiro, Brazil.

**Anatomical**

| | |
|---|---|
| **aa** | anterior ampulla |
| **acv** | anterior cerebral vein |
| **adfs** | anterior dorsal fin spine |
| **adll** | anterodorsal lateral line nerve |
| **af** | adductor fossa |
| **am** | adductor mandibularis muscle |
| **ams** | adductor mandibularis superficialis muscle |
| **ars** | articular surface of pectoral fin |
| **art** | articular process for pectoral fin |
| **art cot** | articular cotylus of Meckel's cartilage |
| **art k** | articular knob of palatoquadrate |
| **ash** | coracoid anterodorsal shoulder |
| **asc** | anterior semicircular canal |
| **at** | accessory terminal cartilage of pelvic fin |
| **b** | basal segment of pelvic metapterygium |
| **ba** | barb on cephalic spine |
| **bas pr** | basicranial process |
| **bbr** | basibranchial |
| **bd** | basidorsal |
| **bh** | basihyal |

| | |
|---|---|
| **bp** | basal plate of dorsal fin spine |
| **bpt** | basipterygium |
| **bv** | basiventral |
| **c** | crown of cephalic spine |
| **cbr** | ceratobranchial |
| **ceph** | cephalic spine |
| **cephb** | cephalic spine base |
| **cer** | cerebellar region |
| **cf** | foramen for caudal blood vessels |
| **ch** | ceratohyal |
| **cik** | caudal internasal keel |
| **cl** | lateral cusp of cephalic spine |
| **coa** | coracoarcualis muscle |
| **coh** | coracohyoideus muscle |
| **com** | coracomandibularis muscle |
| **cor** | coracoid process of scapulocoracoid |
| **cost** | columnar osteodentine of tooth |
| **cr** | tooth crown |
| **crd** | dorsal crest of cephalic spine |
| **crl** | lateral crest of cephalic spine |
| **crm** | mesial crest of cephalic spine |
| **crp** | posterior crest of cephalic spine |
| **da** | dorsal aorta |

| | |
|---|---|
| **ddf** | dorsal diazonal foramen |
| **den gr** | dental groove |
| **dnr** | dorsal spinal nerve root |
| **dnt** | dermal denticles |
| **ds** | dorsum sellae |
| **dt** | dorsal terminal cartilage of pelvic fin |
| **ea** | external ampulla |
| **eart** | ethmoidal articulation |
| **ebr** | epibranchial |
| **ect p** | ectethmoid process |
| **eha** | efferent hyoidean artery |
| **end f** | endolymphatic foramen |
| **ep** | epaxial muscles |
| **epsa** | efferent pseudobranchial artery |
| **esc** | external semicircular canal |
| **ethp pr** | ethmopalatine process |
| **ethr** | ethmoid region of braincase |
| **fm** | foramen magnum |
| **gf** | glenoid fossa |
| **hbr** | hypobranchials |
| **hl** | hyoid ligament |
| **hm** | hyomandibula |
| **hym art** | hyomandibular articulation |

| | |
|---|---|
| **hyp f** | hypophyseal foramen |
| **i** | intermediate segment of pelvic metapterygium |
| **ica** | internal carotid artery |
| **id** | interdorsal |
| **ih** | interhyoideus muscle |
| **im** | intermandibularis muscle |
| **jc** | jugular canal |
| **jj** | jaw joint |
| **lab** | labial cartilage(s) |
| **lda** | lateral dorsal aorta |
| **lh** | hyoid levator muscle |
| **lhr** | lateral hypophyseal ridge |
| **ll** | lateral lobe of cephalic spine |
| **lm** | mesial lobe of cephalic spine |
| **lop** | lateral otic process |
| **lpa** | levator palatoquadrati muscle |
| **lp** | posterior lobe of cephalic spine |
| **lr** | foramen for lateral ramule of buccal + maxillary ramus (="buccal branch of facial nerve"). |
| **mc** | Meckel's Cartilage |
| **mdf** | medial diazonal foramen |
| **med** | medullary region |

| | |
|---|---|
| **mes** | mesencephalic region |
| **mil** | lateral marginal indentation of cephalic spine |
| **mim** | mesial marginal indentation of cephalic spine |
| **mk** | mandibular knob |
| **mpt** | mixipterygium (clasper cartilage) |
| **mpvdf** | medial opening of posteroventral diazonal foramen |
| **mtf** | articular facet for metapterygium |
| **mvpr** | median ventral process of basicranium |
| **nc** | neurocranium |
| **not can** | notochordal canal |
| **oc** | otic capsule |
| **occ** | occlusal surface of tooth |
| **oc a** | occipital arch |
| **oc cot** | occipital cotylus |
| **olf** | olfactory tract |
| **olf can** | olfactory canal |
| **olfc** | olfactory (nasal) capsule |
| **onv** | orbitonasal vein |
| **opa** | optic artery |
| **opha** | ophthalmic artery |
| **or** | orbit |
| **ora** | orbital artery |
| **pa** | posterior ampulla |

| | |
|---|---|
| **pac** | preampullary canal |
| **palp** | palatine process of palatoquadrate |
| **palpr?** | Palatobasal process |
| **pbr** | pharyngobranchial |
| **pdfs** | posterior dorsal fin spine |
| **ped** | location of optic pedicel |
| **pelvg** | pelvic girdle |
| **p fen** | perilymphatic fenestra |
| **pit v** | pituitary vein |
| **pla** | posterolateral angle |
| **pnw** | postnasal wall |
| **po** | preorbitalis muscle |
| **popr** | postorbital process |
| **pq** | palatoquadrate |
| **prcf** | precerebral fontanelle |
| **prf** | articular facet for propterygium |
| **prof** | profundus nerve |
| **psc** | posterior semicircular canal |
| **pvdf** | posteroventral diazonal foramen |
| **q con** | quadrate condyle |
| **qfl** | quadrate flange of palatoquadrate |
| **r** | radials |
| **rb** | rostral bar |

| | |
|---|---|
| **rbs** | ribs |
| **re** | insertion of external rectus muscle |
| **rt** | tooth root |
| **s** | striae (cephalic spine) |
| **sac** | sacculus |
| **sb** | scapular buttress |
| **sc** | scapulocoracoid |
| **scap** | scapular process of scapulocoracoid |
| **sce** | single crystallite enameloid of tooth |
| **soc** | spinooccipital nerves |
| **soph** | course of superficial ophthalmic complex (trigeminal + anterodorsal lateral line nerves) |
| **supc** | supraorbital crest |
| **t** | teeth |
| **tel** | telencephalic region |
| **tfr** | trigemino-facialis recess |
| **ur** | utricular recess |
| **vdf** | ventral diazonal foramen |
| **vlc** | vestibulolateral (auricular) region |
| **vlr** | ventrolateral ridge |
| **vnr** | ventral root of spinal nerve |
| **vt** | ventral terminal cartilage of pelvic fin |
| **II** | optic nerve |

| | |
|---|---|
| **III** | oculomotor nerve |
| **IV** | trochlear nerve |
| **V** | trigeminal nerve |
| **VI** | abducens nerve |
| **VII** | facial nerve |
| **VII hm** | hyomandibular ramus of facial nerve |
| **VII pal** | palatine ramus of facial nerve |
| **VIII** | octaval (acousticovestibular) nerve |
| **IX** | glossopharyngeal nerve |
| **X** | vagus nerve |

FIGURE 1. Geological time scale showing the temporal position of the Santana Formation within the Cretaceous Period (Modified from Maisey, 1991). Fossils of *Tribodus limae* are found in the Romualdo Member, and are Lower Cretaceous (Aptian-Albian) in age (approximately 110 MYA).

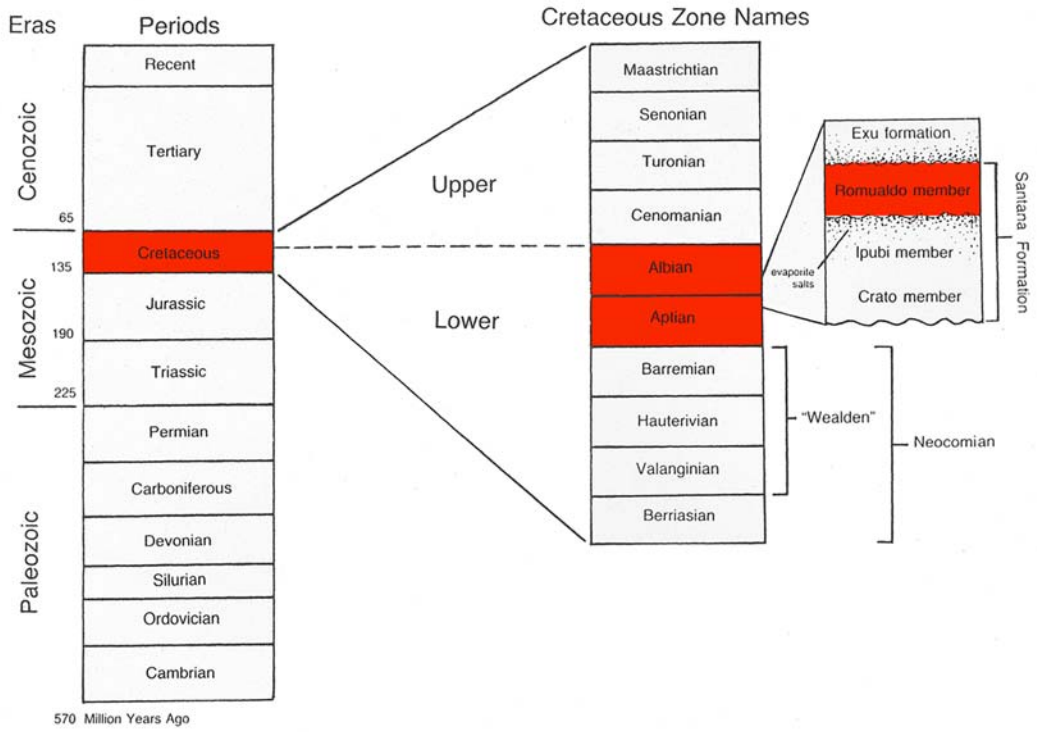

Eras
Periods
Cretaceous Zone Names
Recent
Tertiary
Cretaceous
Jurassic
Triassic
Permian
Carboniferous
Devonian
Silurian
Ordovician
Cambrian
Cenozoic
Mesozoic
Paleozoic
65
135
190
225
570 Million Years Ago
Upper
Lower
Maastrichtian
Senonian
Turonian
Cenomanian
Albian
Aptian
Barremian
Hauterivian
Valanginian
Berriasian
"Wealden"
Neocomian
Exu formation
Romualdo member
Ipubi member
Crato member
evaporite salts
Santana Formation

FIGURE 2. Geological map of the Araripe Plateau, Ceará province, northeastern Brazil, showing main roads and towns, including those nearest to classic collecting sites (Santana do Cariri, Jardim, and Missão Velha). Modified from Maisey, 1991.

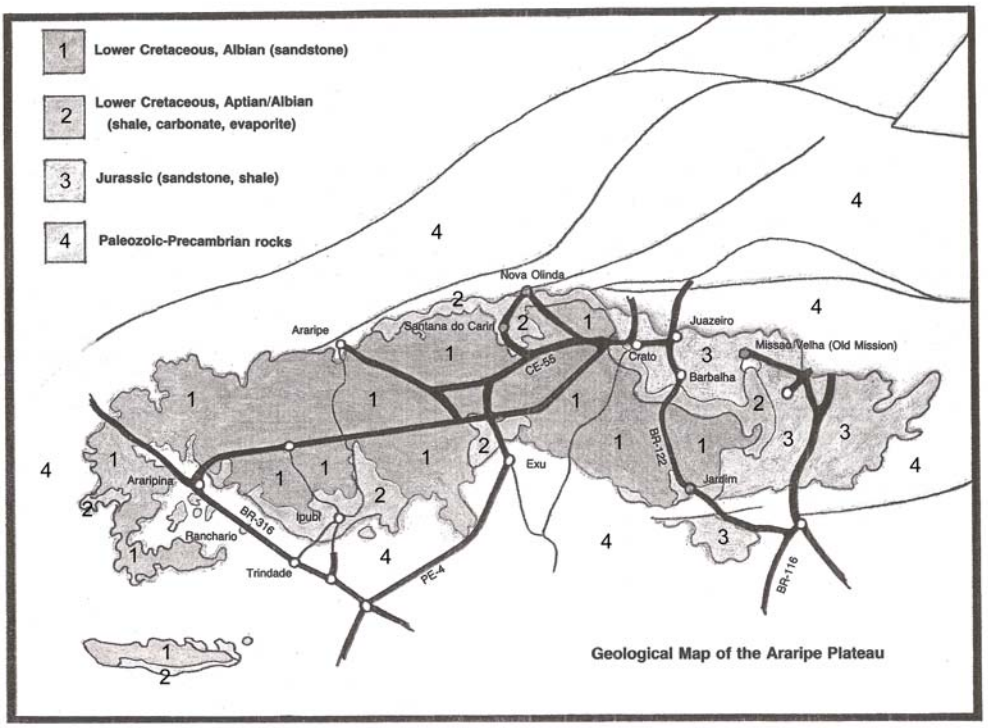

1 Lower Cretaceous, Albian (sandstone)
2 Lower Cretaceous, Aptian/Albian (shale, carbonate, evaporite)
3 Jurassic (sandstone, shale)
4 Paleozoic-Precambrian rocks
Nova Olinda
Araripe
Santana do Cariri
Juazeiro
Crato
Barbalha
Missão Velha (Old Mission)
CE-55
BR-122
Exu
Jardim
Araripina
Ipubi
Ranchario
Trindade
BR-316
PE-4
BR-116
Geological Map of the Araripe Plateau

FIGURE 3. Location of the Araripe Basin and other Cretaceous sedimentary basins within northeastern Brazil. Box highlights Araripe Basin. Modified from Maisey, 1991.

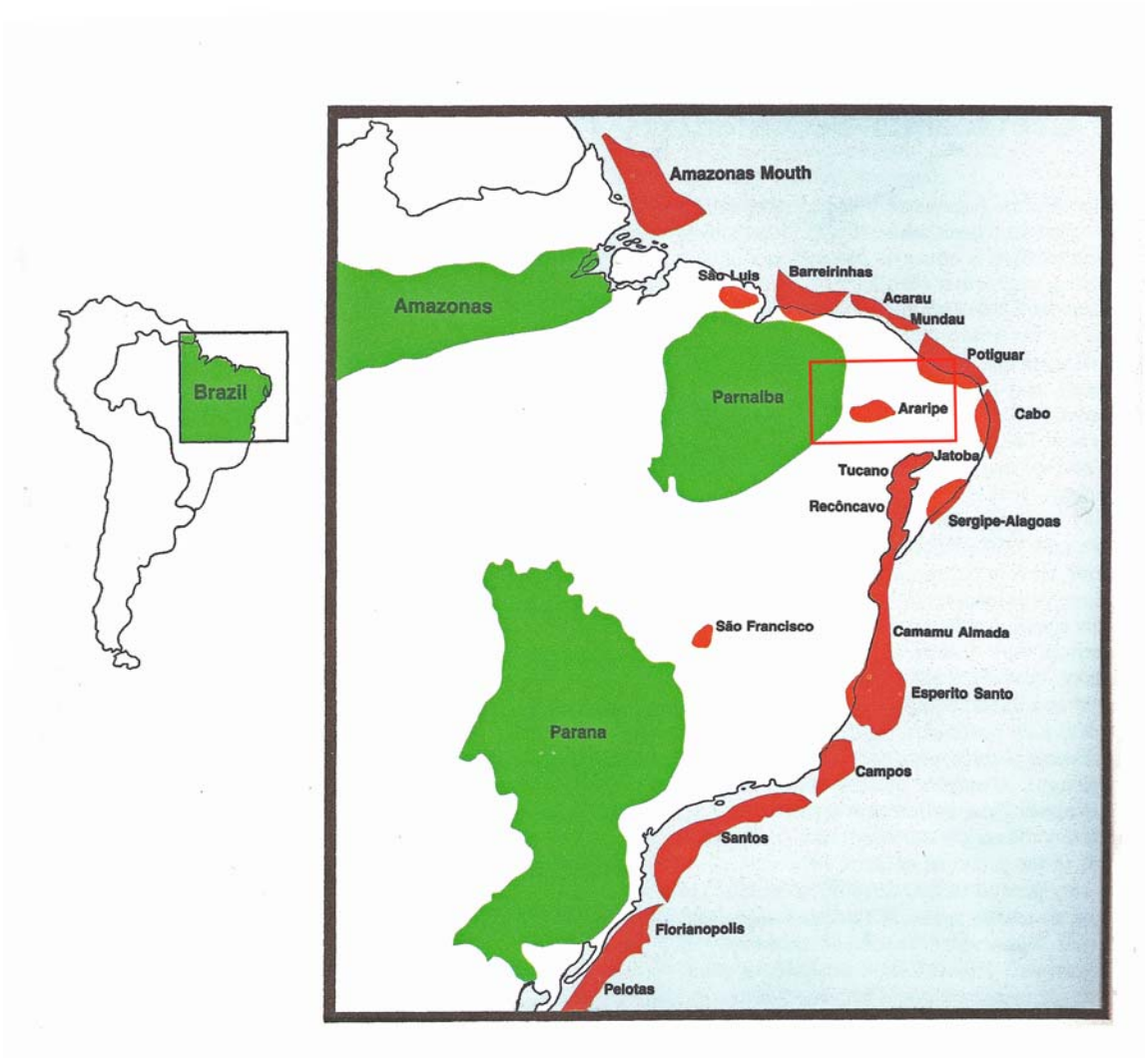

Brazil
Amazonas Mouth
Amazonas
São Luis
Barreirinhas
Acarau
Mundau
Potiguar
Parnaiba
Araripe
Cabo
Tucano
Jatoba
Recôncavo
Sergipe-Alagoas
São Francisco
Camamu Almada
Esperito Santo
Parana
Campos
Santos
Florianopolis
Pelotas

FIGURE 4. Map showing global distribution of *Tribodus* species during the Cretaceous (paleogeographic map modified from Ron Blakey, http://jan.ucc.nau.edu/~rcb7, showing arrangements of continents at approximately 105 MYA; *Tribodus* localities based on Vullo and Neraudeau, 2008). Green star: Valanginian-Barremian; yellow star: Aptian-Albian; red star: Cenomanian; orange star: Albian-Cenomanian. **1**–Aptian-Albian (Santana Formation), Brazil (Brito & Ferreira, 1989; Brito, 1992; and the present paper); **2**–Albian-Cenomanian (Alcântara Formation), Brazil (Dutra and Malabarba, 2001); **3**–?Cenomanian (In Abangharit Beds), Niger (Dutheil, 2001); **4**–Cenomanian (Kem Kem Beds), Morocco (Dutheil, 1999); **5**–Albian (Tiout Formation), Algeria (Landemaine, 1991); **6**–Albian (Chenini Formation), Tunisia (Cuny et al., 2004); **7**–Cenomanian (Draa Ubari Formation), Libya (Nessov et al., 1998; Rage and Cappetta, 2002); **8**–Cenomanian (Bahariya Formation), Egypt (Werner, 1989); **9**–?Cenomanian (Wadi Milk Formation), Sudan (Werner, 1994); **10**–Cenomanian (Charentes), France (Landemaine, 1991; Vullo et al., 2007; Vullo and Néraudeau, 2008); **11**–?Valanginian-Barremian (Loia Series), Congo (Casier, 1961; Maisey, 2000).

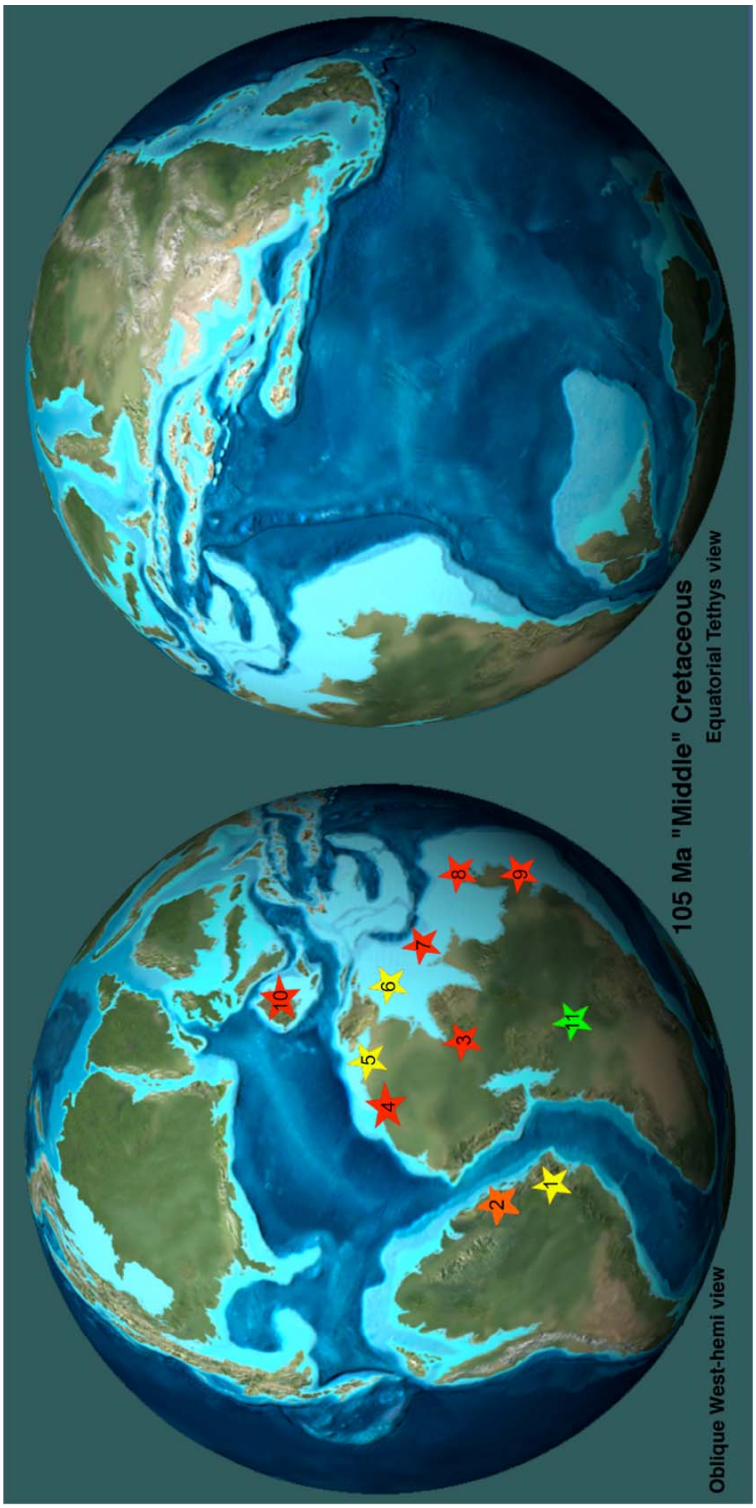

105 Ma "Middle" Cretaceous
Equatorial Tethys view
Oblique West-hemi view
1
2
3
4
5
6
7
8
9
10
11

FIGURE 5. General appearance of hybodontiform sharks, as reconstructed by Maisey (1982, 1989).

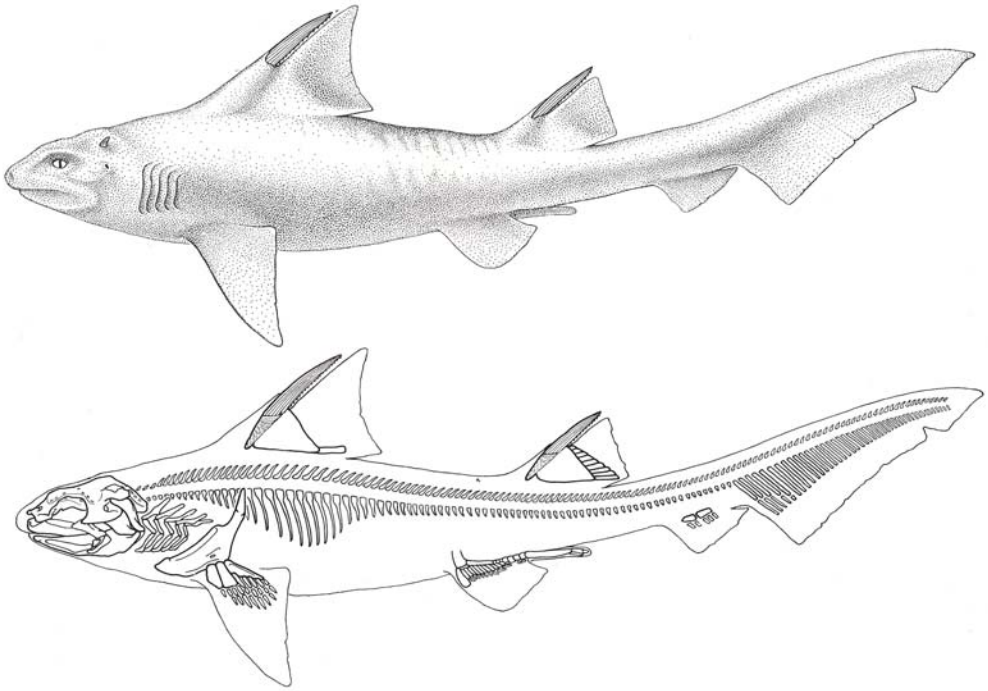


FIGURE 6. Previous hypotheses of hybodont relationships.

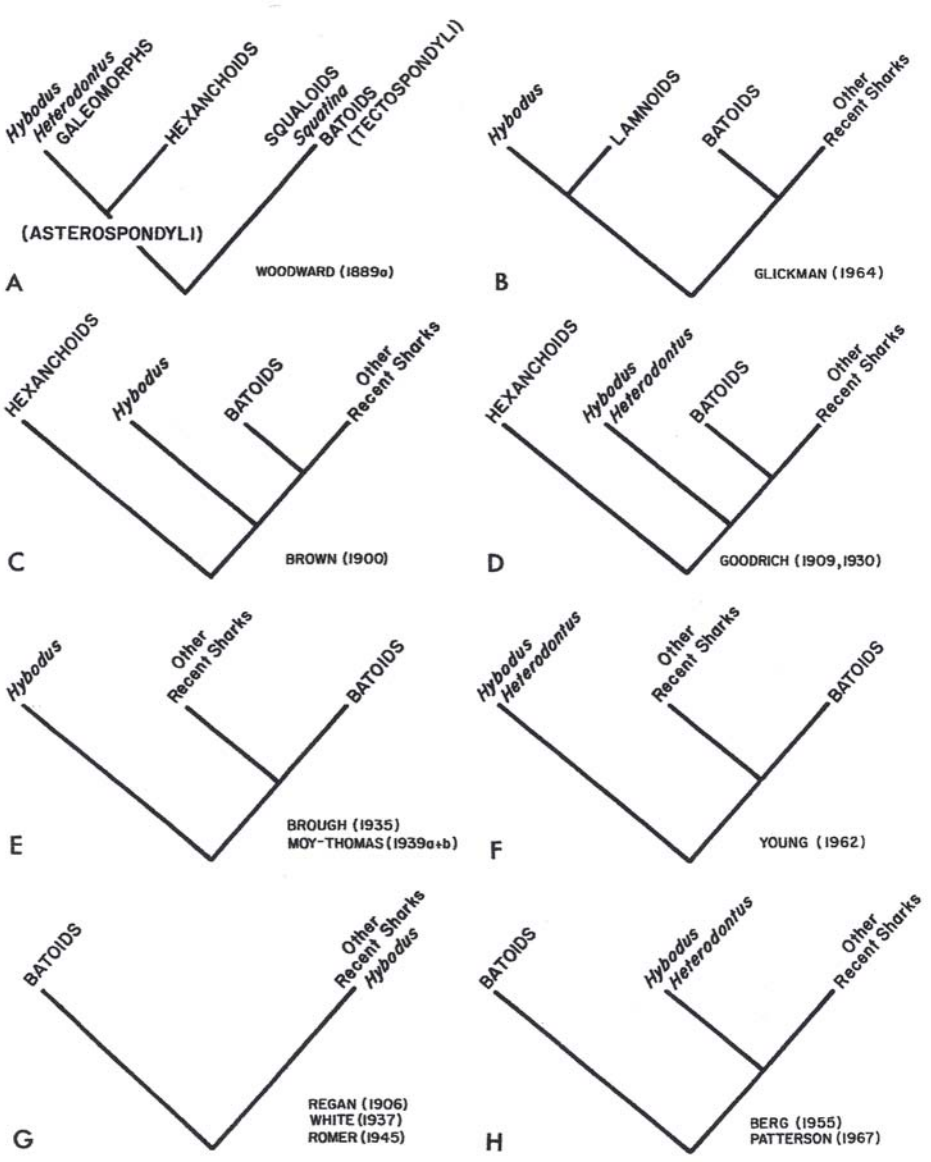

Hybodus
Heterodontus
GALEOMORPHS
HEXANCHOIDS
SQUALOIDS
Squatina
BATOIDS
(TECTOSPONDYLI)
(ASTEROSPONDYLI)
A
WOODWARD (1889a)
Hybodus
LAMNOIDS
BATOIDS
Other
Recent Sharks
B
GLICKMAN (1964)
HEXANCHOIDS
Hybodus
BATOIDS
Other
Recent Sharks
C
BROWN (1900)
HEXANCHOIDS
Hybodus
Heterodontus
BATOIDS
Other
Recent Sharks
D
GOODRICH (1909, 1930)
Hybodus
Other
Recent Sharks
BATOIDS
E
BROUGH (1935)
MOY-THOMAS (1939a+b)
Hybodus
Heterodontus
Other
Recent Sharks
BATOIDS
F
YOUNG (1962)
BATOIDS
Other
Recent Sharks
Hybodus
G
REGAN (1906)
WHITE (1937)
ROMER (1945)
BATOIDS
Hybodus
Heterodontus
Other
Recent Sharks
H
BERG (1955)
PATTERSON (1967)

FIGURE 7. A, currently hypothesized phylogenetic relationships among hybodontiforms. Modified from Coates and Gess, 2007 (based on Maisey et al., 2004; B, phylogeny of hybodontiforms plotted against geologic timescale. Modified from Coates and Gess, 2007.

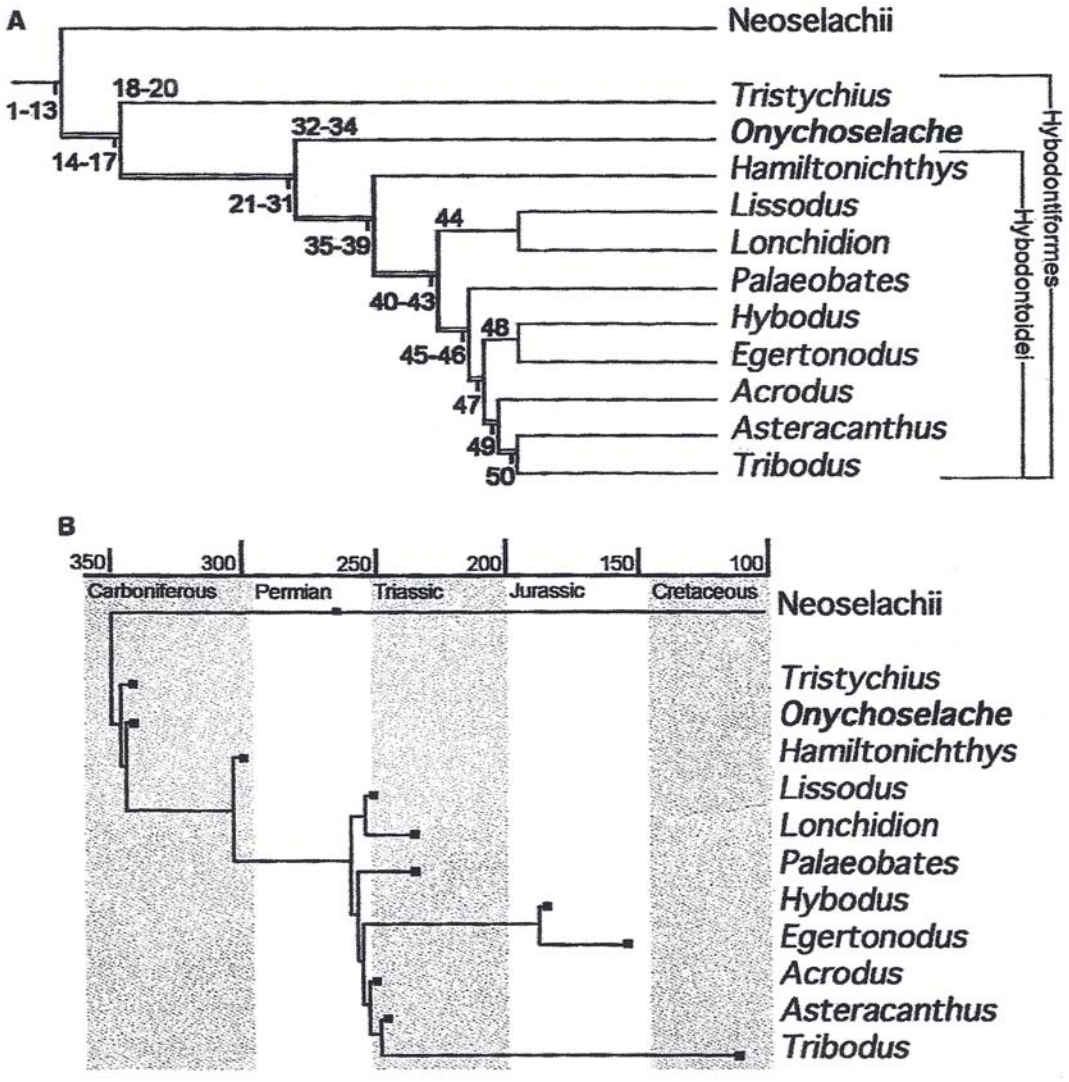

A
Neoselachii
1-13
18-20
32-34
14-17
21-31
35-39
44
40-43
48
45-46
47
49
50
Tristychius
Onychoselache
Hamiltonichthys
Lissodus
Lonchidion
Palaeobates
Hybodus
Egertonodus
Acrodus
Asteracanthus
Tribodus
Hybodontiformes
Hybodontoidei
B
350
300
250
200
150
100
Carboniferous
Permian
Triassic
Jurassic
Cretaceous
Neoselachii
Tristychius
Onychoselache
Hamiltonichthys
Lissodus
Lonchidion
Palaeobates
Hybodus
Egertonodus
Acrodus
Asteracanthus
Tribodus

FIGURE 8. AMNH specimens of *Tribodus limae* Brito and Ferreira, 1989 described in this study. A, AMNH FF 13957, nearly complete individual, anterior to the right; B, AMNH FF 13959, crushed neurocranium with jaw elements and coracoid region of left scapulocoracoid showing articular ridge; C, AMNH FF 13961, shoulder girdle region showing anterior dorsal fin spine and basal plate, calcified ribs and neural arches, and complete left and partial right scapulocoracoid, anterior to the left; D, reverse of AMNH FF 13961 showing articular ridge of right scapulocoracoid, anterior to the right. Scale bar equals 2 cm.

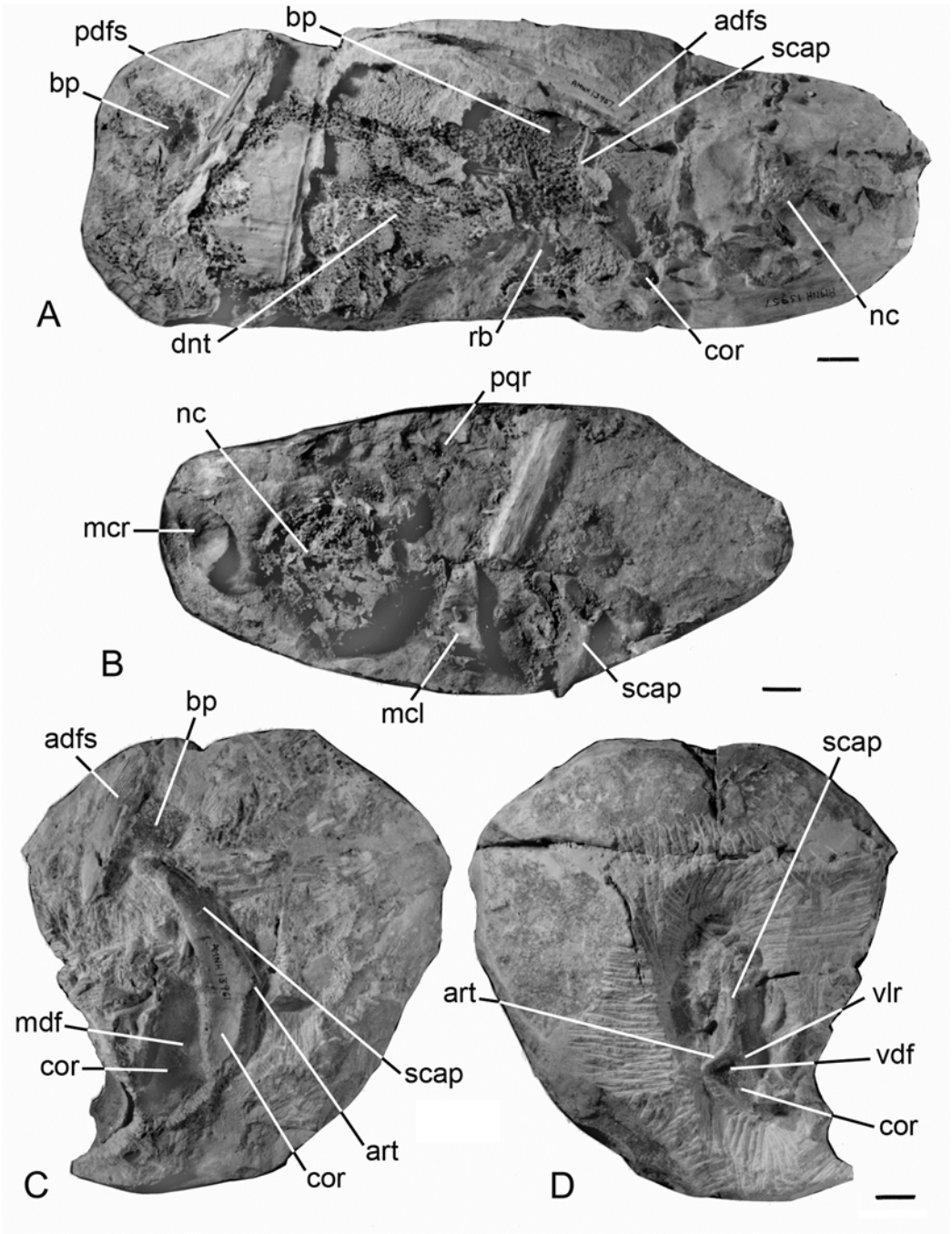

pdfs
bp
bp
adfs
scap
A
dnt
rb
cor
nc
pqr
nc
mcr
B
mcl
scap
bp
adfs
mdf
cor
scap
art
cor
C
scap
art
vlr
vdf
cor
D

FIGURE 9. Braincase of *Tribodus limae*, AMNH FF 13958. A, dorsal view; B, ventral view; C, lateral view. Scale bar is 2 cm.

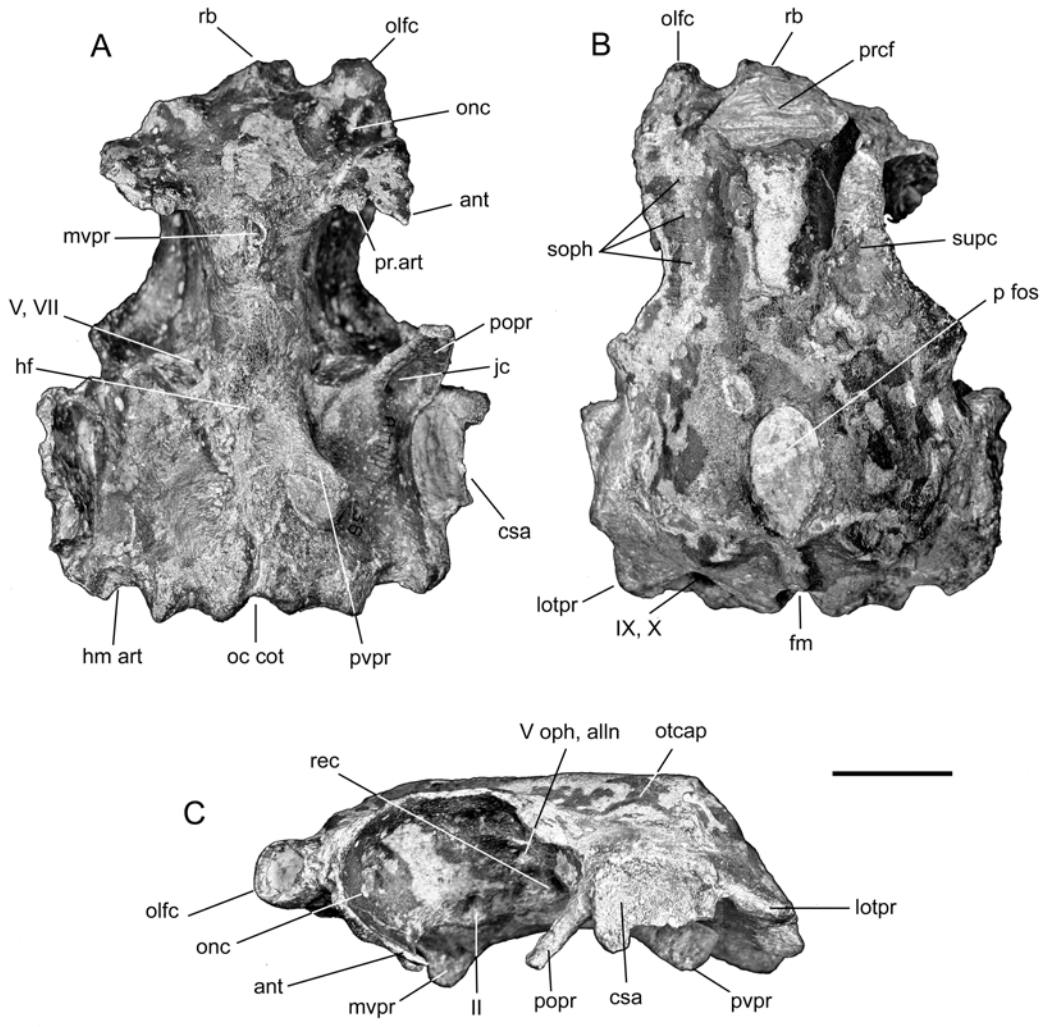

A
rb
olfc
onc
ant
mvpr
pr.art
V, VII
popr
hf
jc
csa
hm art
oc cot
pvpr
B
olfc
rb
prcf
soph
supc
p fos
lotpr
IX, X
fm
C
V oph, alln
otcap
rec
olfc
onc
ant
mvpr
II
popr
csa
pvpr
lotpr

FIGURE 10. *Tribodus limae*, MN 5807V, overview. Scale bar equals 5 cm. Anterior to the left.



FIGURE 11. *Tribodus limae*, MN 5808V, overview. Scale bar equals 5 cm. Anterior to the left.



FIGURE 12. *Tribodus limae*, UERJ-PMB-40. A, dorsal; B, ventral views. Scale bar is 2 cm.

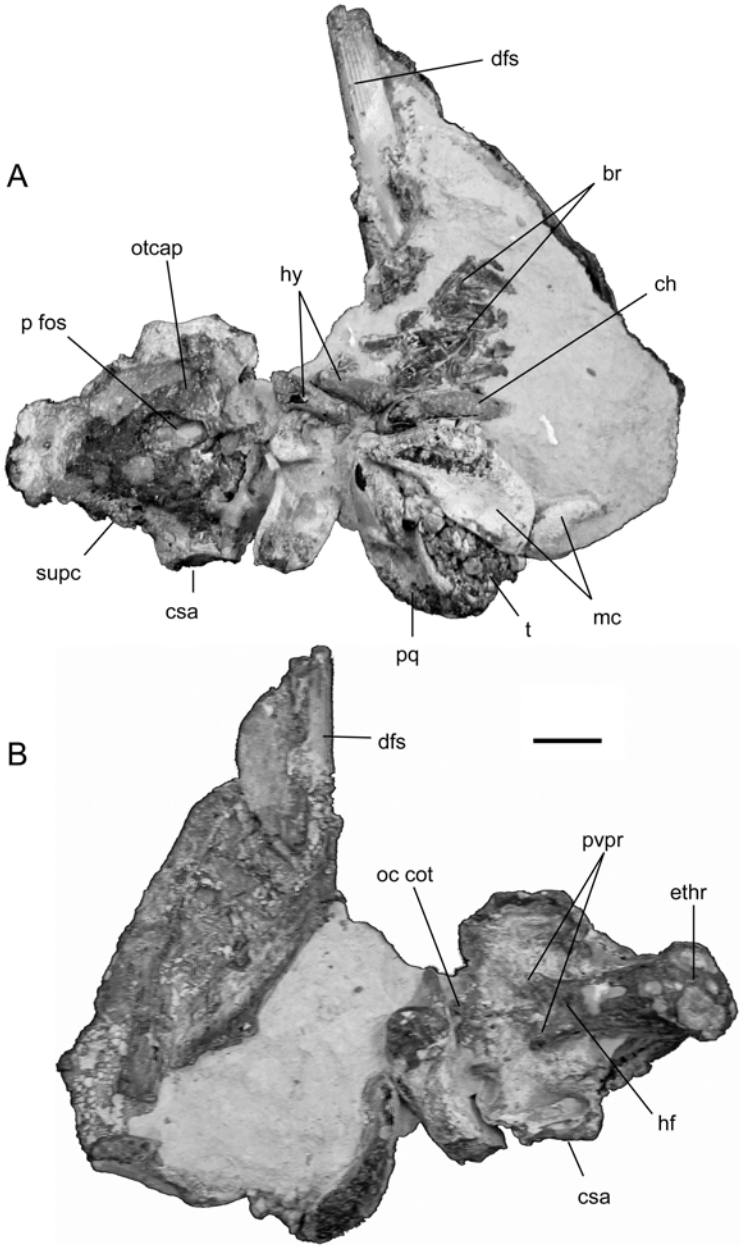
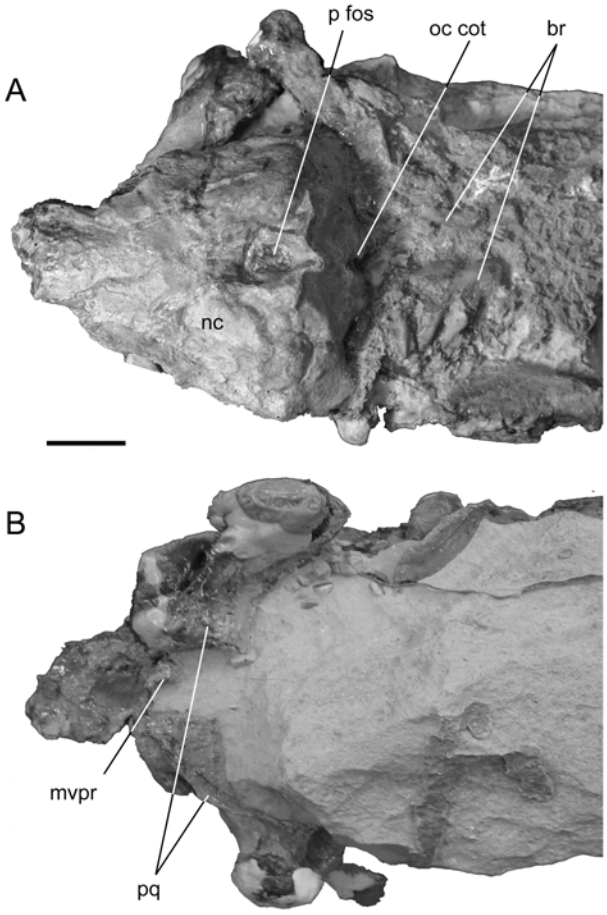

A
dfs
br
otcap
hy
ch
p fos
supc
csa
pq
t
mc
B
dfs
pvpr
oc cot
ethr
hf
csa

FIGURE 13. *Tribodus limae*, UERJ-PMB-114. A, dorsal; B, ventral views. Scale bar is 2 cm.


A
p fos
oc cot
br
nc
B
mvpr
pq

# PART II: DESCRIPTIVE MORPHOLOGY OF *TRIBODUS LIMAE*

# CHAPTER 5: NEUROCRANIAL MORPHOLOGY OF *TRIBODUS*

[Adapted from: Lane, J. In Press. Morphology of the Braincase in the Cretaceous Hybodont Shark *Tribodus limae* (Chondrichthyes: Elasmobranchii), Based on CT Scanning. American Museum Novitates.]

## INTRODUCTION

Interrelationships of extinct chondrichthyans have only recently begun to be understood with clarity. Knowledge of fossil chondrichthyan cranial morphology, in particular, was impeded until recently by a lack of well-preserved material as well as the means to examine that which did exist without destroying the specimens in the process. Serial grinding/sectioning techniques (e.g., Stensiö, 1927; Poplin and de Ricqlès, 1970; Jarvik, 1980) were once the methods of choice for examining fossil shark braincases, and were still widely used until fairly recently (e.g., Schaeffer, 1981). These methods resulted in numerous slabs or slices that make it difficult to reconstruct the original three-dimensional fossil, although they provided the best view of internal structures then available.

It is only in the past decade that CT scanning technology has provided a breakthrough in paleontological studies, allowing intact fossil neurocrania to be examined without damage to the specimens. Fossil chondrichthyan braincases recently investigated with the aid of CT scanning now include *Cladodoides wildungensis* (Maisey, 2005) and

symmoriiforms (e.g., "*Cobelodus*": Maisey, 2007). Moreover, the extant shark *Notorynchus cepedianus* has also been examined using CT scanning (Maisey, 2004b), providing valuable information on the relationship of soft anatomical cranial features to skeletal morphology, as well as a control for interpreting the reliability of CT scanning of fossil taxa. In addition, non-CT scan-based studies of well-preserved fossil chondrichthyan braincases (e.g., *Pucapampella*: Maisey, 2001b; Maisey and Anderson, 2001; *Orthacanthus* and *Tamiobatis*: Schaeffer, 1981; *Egertonodus basanus*: Maisey, 1983; *Hybodus reticulatus*: Maisey, 1987; *Synechodus*: Maisey, 1985; *Akmonistion*: Coates and Sequeira, 1998) have provided additional information of value for comparative studies. However, CT scanning of fossil chondrichthyan braincases is a relatively new field of study, and due to a number of factors (e.g., cost, time, effort involved in CT-scan based studies, and rarity of appropriate specimens), many taxa have yet to be examined. Hybodont sharks, considered the extinct sister group of extant elasmobranchs (neoselachians), are one such group.

Among hybodonts, relatively complete neurocrania are known in only a few taxa, including *Hybodus reticulatus* (Maisey, 1987), *Egertonodus basanus* (Woodward, 1889, 1916; Maisey, 1983, 1987), and *Tribodus limae* (Brito and Ferreira, 1989; Brito, 1992; Maisey and Carvalho, 1997). Thus far, only the latter two taxa include specimens that are well enough preserved for CT scanning. However, despite the existence of these potential candidates for CT scanning, no in-depth descriptive studies of these specimens based on CT scanning have yet been carried out, although brief descriptions (mainly in the context of comparative studies of which other taxa were the focus) have been provided (i.e., Maisey, 2004a; Maisey, 2005). *Egertonodus basanus*, from the Lower Cretaceous

(Valanginian-Lower Aptian) of southeastern England, is considered to belong to Hybodontinae, the sister-group of Acrodontinae, which also contains *Hybodus* (e.g., Maisey et al., 2004), again on the basis of tooth structure.

Endocranial morphology in *Tribodus limae* was briefly described by Maisey (2004a) in a comparative study of fossil and extant chondrichthyan endocrania based on CT scans. A braincase of *Egertonodus basanus* was also mentioned in that paper, but was not figured or described in great detail. Maisey (2005) did describe the inner ear of *Tribodus* in considerable detail, and found a number of interesting features of potential phylogenetic significance, including several characters of the skeletal labyrinth associated with semi-directional low-frequency phonoreception in extant neoselachians (e.g., presence of a medial chondrified capsular wall separating the skeletal labyrinth and main endocranial cavity; absence of a crus commune and sinus superior; isolation of the posterior semicircular canal and its pre-ampullary extension to describe an almost complete circuit; presence of perilymphatic fenestrae; out-of-plane orientation of the external canal; and presence of a complete parietal fossa). These may represent further synapomorphies supporting the putative sister-group relationship between hybodonts and neoselachians (Maisey, 2004a).

However, a full description of internal cranial morphology in *Tribodus* and *Egertonodus* has not yet been provided, the interior of the braincase of *Egertonodus* has never been figured in a publication, and the cranial endocast has never been reconstructed in these or any other hybodont. The aim of this chapter is to provide the first detailed description of external and internal cranial morphology in hybodont sharks (*Tribodus* and *Egertonodus*) based on CT scanning and digital imaging technologies. This information

will then be used to reconstruct soft anatomical features of *Tribodus* (including the cranial nerves and vascularization) for the first time, and to compare cranial morphology in hybodonts to that of other fossil and extant chondrichthyans.

# DESCRIPTION

## SYSTEMATIC PALEONTOLOGY

Class CHONDRICHTHYES Huxley, 1880

Subclass ELASMOBRANCHII Bonaparte, 1832

Plesion HYBODONTIFORMES Maisey, 1987

Suborder HYBODONTOIDEI Maisey, 1989

Family HYBODONTIDAE Owen, 1846

Subfamily ACRODONTINAE Maisey, 1989

Genus *TRIBODUS* Brito and Ferreira, 1989

*Tribodus limae* Brito and Ferreira, 1989

Type species: *Tribodus limae* Brito and Ferreira, 1989

Diagnosis: As for the type species, Brito and Ferreira, 1989:

> Hybodont shark, weakly heterodont. Teeth high-crowned not exceeding 5 mm in length, crown with strong vascular striae, deeper than broad in anterior and postero-lateral teeth, shallower than broad in antero-lateral teeth, root hybodontoid; fin spines slender reaching about 12.5 cm, lateral faces with 8 to 10

> sharp continuous ridges, single anterior ridge forming a keel in the anterior border, posterior denticles in two series; large dermal denticles with thorn-like shape measuring approximately 2.5 to 3.0 mm.

An emended diagnosis for *Tribodus limae* was provided by Brito (1991), in agreement with that of Brito and Ferreira (1989) except for the following change:

> Hybodont shark of approximately 700 mm total length; teeth weakly heterodont [heterodonty is monognathic; possibly also dignathic], higher than broad…tooth crown with striae, deeper than broad in postero-lateral teeth and shallower than broad in anterior and antero-lateral teeth; root much more developed than the crown, showing in labial view a central foramen.

## NEUROCRANIUM

GENERAL FEATURES: The neurocranium of *Tribodus limae* was first described by Brito (1992), who reconstructed it as generally similar in overall morphology to that of *Egertonodus basanus* and other previously described hybodonts. However, that description was based on an incomplete specimen (lacking much of the ethmoid region and postorbital processes), the only material then available (Fig. 14). Later, Maisey and Carvalho (1997) announced the discovery of a more complete specimen, AMNH 13958. Although this specimen (Fig. 9) was mentioned in several later papers, revealing a selection of intriguing morphological details (Maisey, 2004a, 2005, 2007), a complete description of its morphology has not been presented until now. Additional specimens of *Tribodus limae* neurocrania have since been discovered and are included in the present description (Figs. 12, 13). CT scans of the braincase of AMNH 13958 were examined for

the present study (Figs. 15–18), and were used to produce digitally rendered images of the braincase (Figs. 19–26), cranial endocast (Figs. 27–30), and skeletal labyrinth (Figs. 31–34), described below.

*Tribodus limae* has a platybasic braincase (Figs. 19, 20), wedge-shaped to trapezoidal in lateral view (Fig. 25), in which the dorsal surfaces of the occipital and ethmoid regions slope downward to form obtuse angles with the top of the orbitotemporal region. When viewed under a light microscope, the pattern of prismatic calcified cartilage is visible on the surface of the neurocranium as a thin layer composed of dark brown tesserae, which appear rounded to polygonal in shape. The prismatic cartilage is particularly visible on the ventral surface of the braincase, and in the area surrounding the parietal (= endolymphatic) fossa dorsally. This prismatic pattern is also visible in many of the other cartilaginous skeletal elements in the AMNH specimens of *Tribodus*, except those in which the surface was abraded during preparation (e.g., the jaws of AMNH FF 13958). As in other hybodonts and neoselachians (and unlike many Paleozoic sharks), most of the skeleton is covered with only a single layer of prismatic cartilage, which wraps around to cover both outer and inner surfaces including that of the endocranial space.

In dorsal view (Fig. 19) the braincase is weakly triangular, with the otico-occipital region approximately 1.5 times wider than the ethmoid region. Although the distal parts of the postorbital processes (Figs. 19–25: popr) are broken off, their lateral extent can be extrapolated based on the shape of the preserved portion of each process. Based on this, it can be concluded that the widest part of the braincase was across the otic region, rather than between the postorbital processes as in *Egertonodus* (Maisey, 1983). The maximum width of the braincase in *Tribodus* is 88.5 mm, 78% of its total length of 113 mm. As in

*Egertonodus* (Maisey, 1983), the width of the neurocranium is only slightly less than its length.

The margins of the orbits form a more complete oval than in *Egertonodus basanus* (Maisey, 1983), in which the broad forward-pointed postorbital processes give the orbits a more anteriorly directed appearance. A major difference between *Tribodus* and *Egertonodus* is the lack in *Tribodus* of an anteroposterior ventral ethmoidal keel (the "caudal internasal keel"; Maisey, 1983: figs. 9B–D: cik; this paper, Figs. 38B, 42, 43: cik). Instead, the ventral surface of the ethmoid region in *Tribodus* is smooth and very slightly convex both anteroposteriorly and transversely, and slopes posteroventrally before joining with a median ventral process (Figs. 21, 22: mvpr), located between and directly posterior to the antorbital processes. *Tribodus* also lacks the inflated ethmopalatine processes of *Egertonodus*. A raised supraorbital crest is present above the orbits in *Tribodus*. At the widest part of the neurocranium (at the level of the otic capsules) are paired, rectangular, laterally concave structures, which are fibrous and lack prismatic calcification (Fig. 9, csa). These have been identified as the points of articulation for the cephalic spines (Maisey & Carvalho, 1997). The convexly curved cephalic spine bases fit neatly within these concave, bowl-shaped platforms, with the curved distal cusps of the spines directed posteriorly. Elevated ridges on the cranial roof immediately anterior and posterior to the parietal fossa correspond to the positions of the anterior and posterior semicircular canals (cf. *Notorynchus*; Maisey, 2004b). As in *Egertonodus basanus* (Maisey, 1983) and many other hybodonts, the otico-occipital region is ‘telescoped’ forward between the postorbital processes so that the otic capsules are situated between these processes (unlike many Paleozoic sharks, in which the otic

capsules are located behind the postorbital processes). However, in *Egertonodus* the occiput projects somewhat farther posteriorly than it does in *Tribodus* and most neoselachians (cf. Maisey, 1983).

## ROSTRAL AND ETHMOIDAL REGIONS

PROPORTIONS OF THE ETHMOID REGION: The ethmoid region of *Tribodus limae* is proportionally wider across than it is in *Egertonodus basanus*, and the olfactory capsules are more widely spaced. The left olfactory chamber of AMNH 13958 is well preserved, and although its interior is filled with matrix, it can be observed via CT scanning (Fig. 15A). The right olfactory chamber is not preserved. The ethmoid region of *Tribodus* comprises about one-third of the entire length of the braincase, unlike *Egertonodus basanus* and *Hybodus reticulatus*, in which the ethmoid region constitutes only one-quarter of its length (Maisey, 1983, 1987). Maisey (1983) describes the ethmoid region in *Egertonodus* as shorter than in most living sharks, but similar in length to that of *Tristychius*, while in *Cobelodus*, *Tamiobatis*, and *Xenacanthus*, the proportion is even lower (Maisey, 2005, 2007). In the extant shark *Notorynchus* (Maisey, 2004b), the ethmoid region comprises approximately one-third of the total braincase length, resembling the condition in *Tribodus*. The proportional length of the ethmoid region in *Tribodus* thus more closely resembles that of some extant neoselachians than that of other hybodonts and outgroup chondrichthyan taxa.

PRECEREBRAL FONTANELLE, ROSTRAL BAR, AND BASICRANIAL PROCESS: The precerebral fontanelle of *Tribodus limae* is oval in cross-section, and is slightly wider across than in *Egertonodus basanus* (Fig. 9B, 15A–D). At the anteroventral tip of the

precerebral fontanelle, the base of a forward-directed process is visible, although its anterior portion is missing (Fig. 9B, rb). This is interpreted as a rostral bar, as in *Egertonodus* (Maisey, 1983). On the ventral medial surface of the rostral bar (Figs. 21, 22) there is a small ventrally directed process, which appears V-shaped in anterior view. Posterior to this, the ventral surface of the internasal septum is broad and smooth, without a caudal internasal keel medially or paired ethmopalatine processes laterally such as those described in *Egertonodus* by Maisey (1983: fig.9: cik, ethppr).

Farther posteriorly, a large, medial, ventrally directed process is present on the ventral surface of the basicranium, originating anteriorly directly between the bases of the antorbital processes and extending posteriorly to just below the anterior margin of the optic foramen (Figs. 9, 13, 15, 21, 22: mvpr). This process is located immediately anterior to the anterior margin of the palatoquadrate, as illustrated by UERJ-PMB-114 (Fig. 13B). This median ventral process was referred to as the basicranial process by Maisey and Carvalho (1997). It is possible that the basicranial process is homologous to the caudal internasal keel of other hybodonts, due to its ventromedial position and location in the anterior region of the braincase (also originating as an outgrowth of the embryonic trabeculae), and its probable similar involvement in jaw suspension (perhaps as an attachment point for soft tissues involved in jaw support in the case of *Tribodus*, rather than directly abutting the palatoquadrates as in *Egertonodus*). In *Egertonodus* the caudal internasal keel extends from the tip of the rostrum to the anterior margin of the suborbital shelf. This includes the area where the ventral process is located in *Tribodus*, further suggesting that the two structures could be homologous. However, the basicranial process of *Tribodus* differs from the caudal internasal keel of *Egertonodus* in its much

shorter anteroposterior extent. It is also possible that the median ventral process of *Tribodus* is homologous to a ventral interorbital septum, as in *Squaliolus* (Maisey, 2007), which like the process in *Tribodus* forms a solid wall of cartilage in the basicranium, and is located between the antorbital process and optic foramen.

The median basicranial process in *Tribodus* could alternatively be homologous to the keel process of some modern squalean sharks (e.g., *Centroscyllium*, *Etmopterus*; Maisey, 2007), which also typically terminates immediately anterior to the palatoquadrates and is located between the optic foramen and antorbital process. In extant elasmobranchs, the preorbitalis muscle (= suborbitalis of Shirai, 1992: Maisey, 2007) originates at the dorsal end of this process in *Etmopterus* and *Centroscyllium*. According to Maisey (2007), the interorbital septum of *Squaliolus* is probably not homologous to the keel process of the aforementioned sharks, because the latter forms later in ontogeny and differs in its ontogenetic point of origin. Because *Tribodus* is extinct and its ontogeny is unknown, the exact homology of its median ventral process to similar structures of modern forms remains uncertain. However, due to its location and probable function (confined to the anterior of the orbit between the antorbital processes and optic foramen; immediately anterior to palatoquadrate symphysis; not directly articulating with a forwardly extended palatoquadrate), it seems more likely that this process was homologous to the ventral orbital processes of modern elasmobranchs than to the caudal internasal keel of *Egertonodus*. A similar basicranial process occurs in embryos of the extant batoid *Torpedo*, but disappears later in ontogeny (Holmgren, 1940: fig. 162: m.a.). This process was described by Holmgren (1940: p. 169) as a "distinct rudiment...corresponding to the posterior part of the medial area in *Etmopterus* and *Squalus*," and is positioned in front of

the palatoquadrate symphysis. In *Torpedo*, this process is continuous with an anteroposteriorly elongated ridge or medial lamella (the "medial area" of Holmgren), which extends from nearly the anterior tip of the braincase to just in front of the palatoquadrate, but later disappears. Interestingly, this elongated ridge covers the same area as the caudal internasal keel of *Egertonodus*. The last part of the ridge to remain during ontogeny is the small, anteroposteriorly compressed median process (the 'rudiment' described above), which superficially resembles the median ventral process of *Tribodus*. Whether the "medial area" of *Torpedo* is homologous to the median ventral process of *Tribodus*, and/or the caudal internasal keel of other hybodonts, is uncertain. However, it suggests that the two structures found in hybodonts could be homologues of each other, resulting from similar ontogenetic processes.

As in *Egertonodus* and *Chlamydoselachus*, the anteroventral margin of the precerebral fontanelle in *Tribodus* is defined by the slightly upturned forward part of the internasal septum (Maisey, 1983). The precerebral fontanelle is infilled with matrix, making structures on the interior walls and floor of the fontanelle difficult to examine; however, these structures can be observed with the aid of CT scanning (Fig. 15A–D). In a three-dimensional image of the braincase made from CT scans of AMNH 13958, the olfactory nerve foramen is visible as a large opening in the internasal septum connecting the precerebral fontanelle with the olfactory chamber (Fig. 26, I). The olfactory nerve canal is visible on the interior of the braincase as an elongated furrow on the ventrolateral wall of the ethmoid region (Fig. 26, olf can).

VASCULARIZATION AND INNERVATION OF THE ETHMOID REGION: Allis (1923) and Jarvik (1942) noted three major groups of nerves and blood vessels in the anterior of the orbit in

*Chlamydoselachus*: a set of dorsal and ventral foramina within the orbit, and an additional group of structures that pass superficially, lateral to the ectethmoid process (Maisey, 1983). These include the maxillary artery, the facial vein, and two nerve rami: the maxillary ramus of the trigeminal nerve, and the buccal ramus of the facial nerve (now revised as the buccal ramus of the anterodorsal lateral line nerve; Northcutt and Bemis, 1993). Based on comparison with modern elasmobranchs such as *Chlamydoselachus*, Maisey (1983) provided an interpretation of the innervation and vascularization of the ethmoid region of *Egertonodus basanus*. Based on this interpretation and on CT scan images of *Tribodus limae* (AMNH 13958), small paired foramina on the ventral surface of the internasal lamina (located directly posterior to the nasal capsules and opening into them) are interpreted as anterior openings for the orbitonasal vein canals (Fig. 3A, 6B, 11: onc). These connect internally with corresponding small ventrally located openings in the anterior of each orbit, where the orbitonasal veins presumably exited the orbit (Figs. 2C, 6B–F, 11, 13: onc). The positions of these foramina for the orbitonasal vein are consistent with those described in *Egertonodus* and other elasmobranchs (e.g., *Chlamydoselachus* and *Notorynchus*; Allis, 1923; Maisey, 1983; Shirai, 1992; Maisey, 2004b). Allis (1923) described the orbitonasal vein in *Chlamydoselachus* as originating in the nasal capsule and traversing the ectethmoid chamber before entering the orbit via the orbitonasal foramen. The positions of the orbitonasal foramina in *Tribodus* are consistent with this description. Based on the inferred position of the orbitonasal canal, the part of the postnasal wall lateral to the orbitonasal foramen in *Tribodus limae* is then the *planum antorbitale* or antorbital

process, (Figs. 3A, C; 10–13; ant) originating from the *lamina orbitonasalis* of the embryonic trabecula, according to the interpretation given by De Beer (1931).

On the ventromedial surfaces of the antorbital processes of AMNH 13958 are small, paired, rounded structures, immediately lateral to a large notch separating the distal end of the antorbital process from the interorbital wall (Figs. 3A, 11, 12: pr.art). The rounded shape of these paired structures, together with their lack of prismatic cartilage distally, indicate that they may have served as an attachment point for muscles or ligaments involved in jaw suspension. There are several examples of extant elasmobranchs in which the antorbital processes serve as muscle attachment sites: the suborbitalis (= preorbitalis, Maisey, 2007) muscle in *Chlamydoselachus*, hexanchoids, and the squalean *Echinorhinus* originates at the tip of the antorbital process, and the *adductor mandibularis superficialis* muscle in hexanchoids inserts on the antorbital process as well as behind the eye (Shirai, 1992). In extant carcharhinoids, the ventral head of the preorbital (= suborbitalis, Maisey, 2007) muscle originates in the anterior of the orbit or on the posterior of the nasal capsule (Compagno, 1988, figure 8.1). Interestingly, small rounded processes similar in appearance to those mentioned in *Tribodus* occur on the medial part of the antorbital processes in embryonic *Torpedo* (the "short, caudally directed process" described by Holmgren, 1940: p. 166, figs. 157, 158). According to Holmgren, these small rounded processes act as insertion points for the *musculus depressor rostri*, as well as another muscle that Holmgren did not identify (possibly the preorbitalis; cf. Holmgren, 1940, fig. 157).

Immediately lateral to the paired rounded processes is a smaller notch, interpreted here as possibly housing the lateral ramule of the buccal and maxillary ramus (lr) as in

*Notorynchus* (Maisey, 2004b). However, in *Notorynchus*, this ramus is more fully enclosed within the ectethmoid process (Maisey, 2004b). The maxillary artery and facial vein may also have passed through this notch, as these structures have also been described as superficially located along with the buccal and maxillary rami in extant elasmobranchs (Maisey, 1983). As these nerves and vessels generally pass lateral to the ectethmoid process, at least in extant elasmobranchs (Maisey, 1983), the small rounded paired processes in *Tribodus* described above (located medial to these structures) could be homologous to the ectethmoid processes of other elasmobranchs. Anterior to passing lateral to the ectethmoid process, it is likely that the maxillary artery and facial vein would have passed mesially into the nasal capsule via a small aperture in its lateral margin, as in *Chlamydoselachus* (Jarvik, 1942; Maisey, 1983). *Egertonodus basanus* was described by Maisey (1983) as having an ectethmoid process like that of *Chlamydoselachus*, in the form of a laterally directed, pointed flange extending outward from the anterior edge of the postnasal wall. *Hybodus reticulatus* was also reconstructed as having an ectethmoid process like that of *Egertonodus*, although this part of the specimen was not preserved (Maisey, 1987).

ORBITONASAL VEIN, ANTERIOR CEREBRAL VEIN, AND PROFUNDUS NERVE: In the anterior of the orbit are several foramina, the ventral-most of which is considered to have contained the orbitonasal vein (see above). Dorsal to this is an additional foramen, interpreted here as possibly housing the anterior cerebral vein (Figs. 15G, 25, 26; acv) as in *Egertonodus basanus* and *Orthacanthus* (Maisey, 1983). The anterior cerebral vein may have exited the orbit through this foramen, which opens into the precerebral fontanelle, and then passed along the interior edge of the fontanelle wall and into the

nasal capsule via the olfactory foramen. Alternatively, the anterior cerebral vein may have passed through the profundus foramen alongside the nerve, as in some modern elasmobranchs such as *Chlamydoselachus* (Maisey, 1983; Jarvik, 1942), although this would leave this medial foramen (above the orbitonasal foramen and below the profundus foramen) without explanation. According to Maisey (1983), most extant sharks (except *Chlamydoselachus* and *Squatina*) have separate foramina for the anterior cerebral vein, orbitonasal vein, and profundus nerve. Unlike *Egertonodus* (Maisey, 1983), *Tribodus* lacks paired foramina in the floor of the precerebral fontanelle for the anterior cerebral vein.

Dorsal to the foramen for the anterior cerebral vein is an additional foramen, which appears to emerge on the dorsal surface of the braincase posterior to the nasal capsules (Figs. 15B–F; 19; 25: prof). This foramen is here interpreted as housing the profundus nerve. As Maisey (1983) concluded to be the case in *Egertonodus basanus*, it seems unlikely that the profundus nerve passed through the orbitonasal canal, because this canal emerges on the ventral side of the braincase where it appears to enter the olfactory capsule (although according to Maisey, 1983, the possibility of a common foramen for the orbitonasal vein and profundus nerve in *Egertonodus* could not be ruled out). According to Allis (1923), in *Chlamydoselachus* the profundus nerve emerges on the dorsal surface of the nasal capsule. The profundus nerve in *Tribodus* may have exited the orbit from a separate foramen dorsal to the orbitonasal foramen, and emerged from a small opening visible on the dorsal surface of the nasal capsule in AMNH 13958. A large foramen located dorsal to the profundus foramen in the anterior part of the orbit of AMNH 13958 is here interpreted as the opening of the preorbital canal (Figs. 19, 25:

pre). Through this canal would have passed the orbital artery and vein and the superficial ophthalmic ramus of the anterodorsal lateral line nerve (originally referred to as the superficial or lateral ophthalmic ramus of the facial nerve; Jarvik, 1942: fig. 3: r.o.lat; Maisey, 1983: fig. 12: loph VII; Allis, 1923: p. 23: ramus ophthalmicus superficialis trigemini), as in *Egertonodus* and extant elasmobranchs (Maisey, 1983; Northcutt and Bemis, 1993).

As in *Egertonodus basanus* (Maisey, 1983), and *Tristychius arcuatus* (Dick, 1978), a basal communicating canal (rostral fenestra of Schaeffer, 1981) is absent in *Tribodus limae*. According to Maisey (1983), this opening is found in squaloids, *Heptranchias*, and *Pristiophorus* (Holmgren, 1941), but not in other extant elasmobranchs, and it is also absent in *Xenacanthus*, *Tamiobatis*, "*Cladodus*" (Schaeffer, 1981; Maisey, 1983), and "*Cobelodus*" (Maisey, 1983). It has been proposed that a basal communicating canal may be a synapomorphy of some modern sharks (Maisey, 1980; 1983), and its absence in *Tribodus* and other hybodonts appears to be a conserved feature.

An epiphyseal foramen, if one was present, is not preserved in AMNH 13958, as the dorsal midline of the braincase has been worn away from the posterior edge of the precerebral fontanelle to approximately the middle of the orbit. However, no evidence of an epiphyseal foramen was observed in any of the other specimen of *Tribodus* observed for the present paper, or in those described by Brito (1992). The epiphyseal foramen in *Egertonodus basanus* has been described as located in the dorsal midline just posterior to the margin of the precerebral fontanelle (Maisey, 1983). In the absence of better specimens of *Tribodus*, it remains possible that an epiphyseal foramen may have been present and positioned similarly to that of *Egertonodus*. Alternatively, the epiphysis may

have been located within the precerebral fontanelle, as in some extant elasmobranchs, in which case no foramen would be visible. According to Maisey (1983), a separate epiphyseal foramen is present in extant squaloids, hexanchoids, and scylliorhinids, while it is absent in *Heterodontus*, triakids, most carcharhinids, lamnoids, and orectoloboids. In these latter forms, the epiphysis is located near the posterior margin of the precerebral fontanelle. Maisey (1983) states that an epiphyseal foramen is also absent in *Cladodoides* ("*Cladodus*"), *Tamiobatis*, *Orthacanthus* ("*Xenacanthus*"), the hybodontiform shark *Tristychius*, and "*Cobelodus*," and suggests that the epiphysis in these taxa was probably also located towards the back of the precerebral fontanelle. In the absence of any evidence of an epiphysis in *Tribodus*, even with well-preserved cranial material available, it seems very possible that the epiphysis in *Tribodus* did not have a separate foramen, and was located within the precerebral fontanelle as in the aforementioned taxa.

### ORBITOTEMPORAL REGION

Unlike other hybodonts in which cranial material is known (e.g., *Hamiltonichthys mapesi*, Maisey, 1989; *Egertonodus basanus*, Maisey, 1983, 1987; *Egertonodus fraasi*, Maisey, 1986, 1987; *Hybodus reticulatus*, Maisey, 1987), *Tribodus* (Figs. 21, 22, 25) lacks suborbital shelves. Instead, the ventral part of the basicranium in the orbital region is smoothly rounded and convex, and narrower than the orbital walls farther dorsally, so that a transverse section through the braincase in this area resembles an inverted triangle with a rounded point (Fig. 16B–H). Overall, the orbit in *Tribodus* is more completely enclosed by cartilage than in other known hybodonts, with large antorbital and postorbital

processes (Figs. 21, 22, 25) that extend ventrally below the level of the interorbital wall, as noted by Maisey and Carvalho (1997).

ROOF OF THE ORBITOTEMPORAL REGION: The cranial roof in the orbitotemporal region (Figs. 9B, 19, 23, 24) is convexly domed dorsomedially, as in *Egertonodus* (Maisey, 1983). Lateral to this on either side of the cranial roof are pronounced supraorbital crests overhanging the orbits, which slope upwards dorsolaterally in cross-sectional view (Figs. 9B, 15C–H, 16A–H, 19: supc). Between the supraorbital crests and the dorsomedial dome of the braincase are narrow, anteroposteriorly elongated concave regions, which contain the foramina (Figs. 9B, 16A, 19, 25: soph) for the branches of the superficial ophthalmic nerve complex (trigeminal and anterodorsal lateral line nerves) supplying the supraorbital sensory canals. These foramina form a single row extending anteroposteriorly, and this row forms a laterally concave curve, following the shape of the supraorbital crest. In most of the specimens examined the median dorsal roof of the braincase is not preserved anteriorly.

OPTIC, TROCHLEAR, AND OCULOMOTOR NERVES: The optic foramen is a large, round opening ventral to the center of the orbit, and immediately posterior and dorsal to the median ventral basicranial process (Figs. 9C, 16A, 21, 22, 25, 26; II). The optic nerve and artery likely passed through this foramen together, as in many other elasmobranchs (e.g., *Chlamydoselachus*, Allis, 1923; *Cladodoides*, Maisey, 2005). The optic foramen marks the boundary between the embryonic orbital and trabecular cartilages in extant elasmobranchs (El-Toubi, 1949). The foramen for the trochlear nerve (IV), which innervates the dorsal oblique eye muscle in gnathostomes, is visible on the interorbital wall near the base of the supraorbital crest, dorsal and anterior to the optic foramen (Figs.

15H, 25, 26; IV). This position for the trochlear foramen (anterodorsal to the optic foramen) also occurs in *Egertonodus basanus* and other hybodonts, and may be of phylogenetic importance as a shared hybodont feature (Maisey, 2004a). Ontogenetically, the trochlear foramen forms within the embryonic orbital cartilage and is surrounded by it on all sides (El-Toubi, 1949).

Posterior and slightly dorsal to the optic nerve foramen is a much smaller foramen, here interpreted as housing the oculomotor (III) nerve (Figs. 16B–C, 25, 26). This interpretation is further supported by CT scan images and digital reconstructions of the cranial endocast, which show a small outgrowth from the endocast at the approximate position of this foramen (Figs. 28, 30), located behind the optic nerve and immediately dorsal to the anterior of the hypophyseal chamber (the location of the oculomotor nerve in *Notorynchus* and many other neoselachians; Maisey, 2004b). The oculomotor foramen is well preserved in UERJ-PMB-40, in which it is visible as a small foramen with an anteriorly directed opening, located posterodorsal to the optic foramen and immediately anteroventral to the prootic foramen (see section on trigeminal and facial nerves, below). The oculomotor foramen in *Tribodus* is located slightly anterior to its inferred position in *Egertonodus basanus* (Maisey, 1983, fig. 26A), in which it is identified as dorsal and slightly posterior to the efferent pseudobranchial foramen (confirmed by CT scans of *Egertonodus*; see section on endocranial morphology of *Egertonodus basanus,* below).

There is no conclusive evidence of an optic pedicel (= eyestalk; optic stalk) in *Tribodus*, although it remains possible that one could have been present in the region of the oculomotor nerve, as in many other elasmobranchs. However, there is also no evidence of an optic pedicel in any other known hybodont. Optic pedicels are known in

extant neoselachians (e.g., *Chlamydoselachus*, *Squalus*, Allis, 1923; Shirai, 1992; Maisey, 2007; batoids, many squaloids and galeomorphs, Shirai, 1992), as well as extinct chondrichthyans (e.g., "*Cobelodus*," *Cladodoides*, Maisey, 2005; 2007; *Tamiobatis*, Schaeffer, 1981; *Synechodus*, Maisey, 1985), extinct osteichthyans (e.g., *Ligulalepis*, *Psarolepis*, Basden et al., 2000; Zhu et al., 2001; Maisey, 2007) and placoderms (Young, 1986). Presence of an optic stalk may be primitive for gnathostomes, although this feature is absent in extant osteichthyans and chimaeroids (Maisey, 2005) as well as in some extant neoselachians (e.g., many carcharhinoids and the squalean *Isistius*, Shirai, 1992). In elasmobranchs and placoderms, the optic pedicel is typically located posterior to the optic foramen and ventral to the oculomotor foramen (Maisey, 2005). Ontogenetic studies of extant elasmobranchs such as *Squalus acanthias* show that the optic pedicel forms as a separate cartilage independent of the developing braincase, with which it later joins (El-Toubi, 1949). In AMNH 13958, a laterally convex, uncalcified region is present posterior to the optic foramen and posteroventral to the oculomotor foramen on both sides of the braincase, and could possibly represent the attachment site for an optic pedicel. A similar raised, rounded, uncalcified area posteroventral to the oculomotor foramen and ventral to the foramen for the superficial ophthalmic complex is also present in UERJ-PMB-40. However, in *Egertonodus* no evidence of an eyestalk has been reported (Maisey, 1983; 1986, 1987), and in other hybodonts (e.g., *Hybodus reticulatus* and *Hamiltonichthys mapesi*) as a result of poor preservation not enough evidence exists to determine if an optic pedicel was present.

TRIGEMINAL, FACIAL, AND ANTERODORSAL LATERAL LINE NERVES: According to Goodrich (1930), the foramen for the main branch of the facial nerve is closed off in

adult gnathostomes by a prefacial commissure, a narrow strip of cartilage that extends from the basal plate to the auditory capsule. This structure separates the foramina for nerves V and VII, creating an anterior (prootic) foramen and a posterior (facial) foramen. The prefacial commissure is absent in some extant chondrichthyans (Scylliodei and several others, Shirai, 1992), and also in some osteichthyans (Goodrich, 1930).

Developmentally, in extant elasmobranchs, the embryonic fenestra prootica (an opening between the orbital cartilage and otic capsules) contains the profundus, trigeminal, and abducens nerves, part of the facial nerve, and the anterior lateral line nerves (Goodrich, 1930; Holmgren, 1940; El-Toubi, 1949; Northcutt and Bemis, 1993). Generally, the prootic foramen in adult gnathostomes contains the ophthalmic rami of the trigeminal and anterodorsal lateral line nerves, the entry of the profundus nerve into the orbit, the buccal ramus of the anterodorsal lateral line nerve, and the maxillary and mandibular branches of the trigeminal nerve (V); whereas the palatine and hyomandibular branches of the facial nerve (VII), and the anteroventral lateral line nerve, emerge from the facial foramen (Goodrich, 1930; Northcutt and Bemis, 1993). This arrangement, with two foramina for the above-mentioned nerves, occurs in squaleans, *Heterodontus*, and some fossil outgroups (Shirai, 1992). However, according to Shirai (1992) at least three other patterns are observed in extant neoselachians. Among squaleans, a single trigemino-facial foramen is found in *Echinorhinus*, whereas *Zameus* has three separate foramina: an anterior, containing the profundus nerve and the maxillary and mandibular rami of the trigeminal nerve; a central, containing the superficial ophthalmic complex and the buccal ramus of the anterodorsal lateral line nerve; and a posterior foramen, containing the hyomandibular ramus of the facial nerve.

In many galeomorphs, two foramina are present but the more dorsal foramen contains only the superficial ophthalmic complex (Shirai, 1992).

In *Tribodus limae*, three foramina for the trigeminal, facial, profundus and anterior lateral line nerves appear to have been present: a moderately sized anterodorsal foramen (Figs. 9C, 16D–H, 25, 26; V oph, alln, prof), a larger foramen ventrolaterally (Figs. 9A, 17A, 21, 22, 26: V, VII), and a small foramen immediately posterior to the large foramen (Figs. 21, 22, 26: VII hm). The anteriorly directed foramen posterior and dorsal to the oculomotor foramen is here interpreted as having probably contained the superficial ophthalmic complex and profundus nerve. The larger foramen immediately posteroventral to this corresponds to the "trigemino-facial" (V-VII) foramen of previous authors (e.g., Maisey, 1983; Brito, 1992), and likely contained the main trigeminal-anterodorsal lateral line complex (formerly considered the trigemino-facial complex; revised by Northcutt and Bemis, 1993), including the maxillary and mandibular rami of nerve V, and the buccal ramus of the anterodorsal lateral line nerve. In the present thesis the abbreviation "V, VII" is retained for this foramen in the figures for clearer comparison with previous works. Finally, the small posteriormost foramen likely contained the main trunk of the anteroventral lateral line and facial nerves, including the hyomandibular ramus of the facial nerve (and possibly also its palatine ramus, as in *Heterodontus*; Goodrich, 1930: fig. 284), and the mandibular ramus of the anteroventral lateral line nerve. This interpretation of the trigemino-facial foramina in *Tribodus*, if correct, indicates a noticeably different pattern from that previously described in other fossil elasmobranchs, including previous descriptions of *Tribodus* (e.g., Brito, 1992), and may indicate a shared feature of hybodonts. Comparison with *Egertonodus* (see section

on endocranial morphology of *Egertonodus basanus*, below) lends some support to this hypothesis. The presence of a separate superficial ophthalmic foramen in hybodonts is at least superficially similar to the condition in some galeomorphs, although these forms lack an additional foramen for the hyomandibular ramus. However, variations in closure of the embryonic incisura prootica can produce at least four separate patterns of foramina in modern elasmobranchs, differing even among closely related taxa (e.g., *Zameus*, *Echinorhinus*; Shirai, 1992). Therefore, an additional pattern such as that found in *Tribodus* could probably be arrived at fairly easily, at least from an embryological perspective.

This interpretation of the foramina for the trigeminal, facial, profundus, and anterior lateral line nerves in *Tribodus* differs from that of Brito (1992), who identified the more anterodorsal foramen as the prootic foramen, as did Maisey in his description of *Egertonodus* (Maisey, 1983). In *Tribodus*, the prootic foramen (if one can be identified) would more properly be the largest of the three foramina, containing the main trigeminal-anterodorsal lateral line complex, identified as the hyomandibular foramen by Brito (1992). The prefacial commisure would then be the narrow strip of cartilage separating it from the smaller hyomandibular (facial) foramen immediately posterior to it.

However, the position of the prootic foramen in *Tribodus* and *Egertonodus* differs from that of *Cladodoides* (Maisey, 2005) in being located anteromedial, rather than posteromedial, to the postorbital process. Directly posterior to the dorsal edge of the superficial ophthalmic foramen in UERJ-PMB-40 is a tiny foramen whose opening is directed posterodorsally. From its opening, a narrow indented furrow is distinctly visible extending dorsally, terminating just anteroventral to one of the superficial ophthalmic

foramina on the ventral side of the supraorbital crest. A similar narrow furrow is visible extending dorsally from the middle of the dorsal surface of the main prootic foramen. These furrows probably represent the paths of individual rami of the superficial ophthalmic complex.

### TRIGEMINO-FACIALIS RECESS

A large recess is present on the external posterolateral surface of the orbit in *Tribodus limae* (AMNH 13958 and UERJ-PMB-40: Figs. 9C, 16E, 25: rec). As in *Egertonodus* (Maisey, 1983), this recess is considered here to be homologous to the trigemino-facialis recess of Allis (1923), although (also as in *Egertonodus*, as well as *Cladodoides* and "*Cobelodus*," Maisey, 2007) it does not contain foramina for the trigeminal or facial nerves. CT scans show that it also did not contain the pituitary vein in *Tribodus*. This recess is located posterior to the oculomotor foramen, ventral to the superficial ophthalmic foramen, and anterior to the prootic foramen. A clearly defined opening at the anterodorsal end of the trigemino-facialis recess is interpreted as the oculomotor (III) foramen, as described above. Within the recess itself are two additional foramina, probably for the abducens nerve and efferent pseudobranchial artery (supported by CT scan data), and a small posterior depression which may have contained the origin of the external (= lateral or posterior) rectus eye muscle, which was innervated by the abducens nerve.

ABDUCENS NERVE: A small opening at the posterodorsal end of the trigeminofacialis recess is here interpreted as having contained the abducens (VI) nerve (Figs. 16F–H, 25: VI). This position for the abducens foramen in *Tribodus limae* is supported by evidence

from extant elasmobranchs, in which it is usually located in the vicinity of the prootic foramen (in the latter, the nerve typically exits either through the foramen (e.g., *Heterodontus*) or anterior to it (e.g., *Squalus*) (Goodrich, 1930, figure 284). This interpretation is also supported by CT scan evidence, which shows that this foramen leads internally to a small canal that joins posteriorly with the larger canal leading to the superficial ophthalmic foramen. This canal originates at the base of the trigeminal-facial-anterodorsal lateral line nerve trunk farther posteriorly, a location consistent with the abducens nerve leaving the cranial cavity. The abducens nerve typically originates on the ventral side of the brain slightly mesial to the octaval and hyomandibular trunks, and then proceeds anterolaterally, following the pathway of the superficial ophthalmic complex and nerves V and VII (which typically exit through the prootic foramen) (Wischnitzer, 1993, figure 8-2). Additional evidence in support of this conclusion is the position of this foramen just below the level of the oculomotor foramen, on a level with the presumed location where the optic pedicel would be if one were present. This position is consistent with the location of the abducens foramen in neoselachians and *Cladodoides* (Maisey, 2005). It is also within the trigemino-facialis recess, close to the presumed origin of the external rectus eye muscle, which it innervated. However, although the abducens foramen was identified in a similar location (anterior to the facial foramen, in the posterodorsal rim of the trigemino-facialis recess) in *Egertonodus* (Maisey, 1983), CT scans indicate that this foramen in *Egertonodus* probably housed the pituitary vein instead. It is possible that the abducens nerve in *Egertonodus* was contained within the prootic foramen, as in extant *Heterodontus*.

Alternatively, the fact that the above-mentioned foramen is internally connected with the superficial ophthalmic foramen could suggest a different interpretation in which this foramen is instead a branch of nerves V, VII, or the anterodorsal lateral line nerve (such as the mandibular ramus of nerve V), or perhaps a separate exit for the profundus nerve. An interpretation of this foramen as the profundus foramen may be supported by CT scan images, which could instead show the ophthalmic rami of the trigeminal and anterodorsal lateral line nerves diverging into two separate canals as they leave the cranial cavity (as in extant neoselachians such as *Squalus*, Wischnitzer, 1993, fig. 8-2) and exiting separately from the braincase. The larger canal (interpreted as housing the superficial ophthalmic complex and its associated nerves) exits through the dorsal foramen, and the smaller canal (possibly the profundus nerve) exits through the more posteroventral foramen, located in the rear of the trigemino-facialis recess. This alternative interpretation is further supported by the fact that the nerve trunk that diverges into these two canals is positioned anteriorly on the cranial endocast with respect to the large trigeminal-facial-anterodorsal lateral line nerve trunk that branches from the endocast laterally, and appears to correspond to the location of the superficial ophthalmic, infraorbital, mandibular, and profundus nerves in extant neoselachians such as *Squalus* (Wischnitzer, 1993, fig. 8-2). A separate profundus foramen is also present in *Cladodoides*, located anteroventral to the prootic foramen (Maisey, 2005), and one may also have existed in *Orthacanthus* (Schaeffer, 1981). This arrangement also occurs in chimaeroids (e.g., *Callorhinchus*: De Beer, 1937, pl. 22). However, a separate profundus foramen was not reported in *Egertonodus* (Maisey, 1983), and is absent in most

neoselachians (Maisey, 2005). Also, this foramen in *Tribodus* is located posteroventral to the prootic foramen, rather than anteroventral to it as in *Cladodoides* (see Maisey, 2005).

The latter interpretation would also necessitate a different location for the abducens foramen. One alternative is that the abducens nerve exited the braincase through the prootic foramen as in *Heterodontus* (and possibly *Egertonodus*). It is additionally possible that a small foramen located directly posterior and ventral to the prootic foramen (discussed above, and identified as the hyomandibular foramen) is instead the abducens foramen. CT scans of the interior of the braincase show that this foramen originates on its ventrolateral wall (dorsal to the dorsum sellae and about halfway along its length), and is located between and ventral to two larger foramina, here interpreted as the anterior and posterior rami of the octaval (VIII) nerve (see section on octaval, glossopharyngeal, vagus, and spino-occipital nerves, below). This interpretation would be supported by the fact that the abducens nerve exits the braincase in this position in *Cladodoides* (Maisey, 2005, figures 7, 17). Also, according to Maisey (2005), having the abducens foramen located below and behind the dorsum sellae may be a primitive gnathostome feature. This feature is also found in chimaeroids and some neoselachians, and may be primitive for chondrichthyans (Maisey, 2005). However, in *Cladodoides* this foramen is level with the eyestalk (as is the abducens nerve in neoselachians), whereas in *Tribodus* this more ventral foramen is not on a level with the region where an eyestalk typically would be found. Also, in *Cladodoides* this position is within the orbit, ventral to the prootic foramen and anterior to the hyomandibular foramen, whereas in *Tribodus* the aforementioned foramen is posterior to the presumed hyomandibular foramen and far posterior to the "prootic" foramen (interpreted here as the superficial ophthalmic

foramen, as discussed above). Because the abducens nerve in gnathostomes innervates the external rectus eye muscle, it seems unlikely that it would emerge this far back from the trigemino-facialis recess, where that muscle would have originated. The foramen in the posterodorsal rim of the trigemino-facialis recess is thus here considered more likely to be the abducens foramen, and the more posterior foramen is interpreted as the hyomandibular (facial) foramen.

EFFERENT PSEUDOBRANCHIAL ARTERY: A foramen located centrally within the trigemino-facialis recess in *Tribodus* and near its ventral margin is interpreted here as the foramen for the efferent pseudobranchial artery (Figs. 16D, 25, 26, 37: epsa). Maisey (1983) identified the efferent pseudobranchial artery as occupying a similar location in *Egertonodus basanus*, also in the mid-ventral part of the trigemino-facialis recess. However, CT scans show that the efferent pseudobranchial foramen in *Egertonodus* was located somewhat farther anteriorly (see section on *Egertonodus* endocranial morphology, below). As in *Tribodus*, smaller foramina occur anterodorsally and posterodorsally within this recess in *Egertonodus*. The more anterior of these foramina in *Egertonodus* has been interpreted as the oculomotor foramen, as in *Tribodus* (Maisey, 1983). The more posterior foramen in *Egertonodus* was interpreted by Maisey (1983) as the abducens foramen. It is here interpreted that the efferent pseudobranchial and ophthalmic arteries in *Tribodus* diverged external to the braincase, after exiting together through a common foramen (as in many extant neoselachians).

This location for the efferent pseudobranchial foramen is supported by several factors. First, because the efferent pseudobranchial foramen marks the anterolateral margin of the embryonic polar cartilage in elasmobranchs, whereas the pituitary vein foramen marks its

posterolateral end, it is generally considered that the efferent pseudobranchial artery must be located anterior to the pituitary vein (although during a brief developmental stage in embryonic *Torpedo*, the two vessels share a common foramen, Holmgren, 1940). This is certainly the case in *Tribodus*, in which the efferent pseudobranchial artery is located well in front of the dorsum sellae and pituitary vein. Second, CT scan images reveal paired foramina (Fig. 26: ica) in the floor of the cranial cavity, several millimeters anterior to the anterior tip of the dorsum sellae and slightly anterior to the foramen just described. CT scans indicate that the internal carotid arteries entered the cranial cavity through these foramina, after entering the braincase farther posteriorly and tunneling through the basicranial cartilage (see section on lateral dorsal aortae, internal carotid arteries, hypophyseal foramen, and pituitary vein, below).

FACIAL NERVE AND ACOUSTICO-TRIGEMINO-FACIALIS RECESS: Brito (1992) identified a large foramen posteroventral to his "prootic" foramen on the exterior of the braincase as representing the foramen for the hyomandibular ramus of the facial nerve (Fig. 14C: VII hym). Brito's "prootic" foramen is here interpreted as housing the superficial ophthalmic complex, and the larger, more posterior foramen is interpreted as the main trigemino-facial (V, VII) foramen (which probably contained the maxillary and mandibular rami of the trigeminal nerve, and the buccal ramus of the anterodorsal lateral line nerve, in *Tribodus*, following cranial nerve terminology of Northcutt and Bemis, 1993). Additional support for this hypothesis is provided by CT scans and digital images of the interior of the braincase. These scans show that this foramen (Fig. 26: V, VII) opens internally in the anterior part of a large recess (interpreted as the acoustico-trigemino-facialis recess), immediately posteroventral to another foramen that leads anteriorly to the superficial

ophthalmic foramen (Fig. 26: V oph, alln, prof) and anterior to a larger foramen interpreted as the anterior ramus of the octaval nerve (Fig. 26: VIIIa). This position is consistent with the location of the trigemino-facial foramen in many neoselachians. In addition to the superficial ophthalmic and trigemino-facial foramina, the acoustico-trigemino-facialis recess contains two additional large foramina posteriorly, both of which exit the cranial cavity and enter the otic capsule. These foramina likely contained the anterior and posterior branches of the octaval (VIII) nerve (see section on endocranial space, cranial endocast, and skeletal labyrinth of *Tribodus*, below).

An additional, smaller foramen in the region of the acoustico-trigemino-facialis recess, located between and immediately ventral to the trigeminal-facial-anterodorsal lateral line and octaval foramina; is here interpreted as the hyomandibular (facial) foramen (Fig. 26: VII hm). However, it is alternatively possible that this foramen housed the abducens nerve, as discussed above, or perhaps the palatine ramus of the facial nerve (unlikely, because this is usually directed anteriorly, not posteriorly, and generally diverges from the hyomandibular ramus external to the cranial cavity). The foramen arises in the correct location on the floor of the cerebellar region to be consistent with the abducens nerve (above and behind the anterior of the dorsum sellae; slightly medial to the acoustico-trigemino-facialis recess). The abducens foramen is located at this position in *Squalus* (Marinelli and Strenger, 1959), *Cladodoides* (Maisey, 2005), and "*Cobelodus*" (Maisey, 2007). However, the abducens nerve usually exits the braincase farther anteriorly, in the region of the external rectus eye muscle, which it innervates (Shirai, 1992).

In *Cladodoides*, the palatine ramus of the facial nerve diverges to form separate anterior and posterior ramuli, which exit through the floor of the braincase immediately below the base of the postorbital processes (Maisey, 2005). Although in *Cladodoides* the rami of the facial nerve diverge after exiting the braincase, it is possible that during ontogeny in *Tribodus* they could have been individually enclosed in cartilage to form separate foramina. In *Squalus*, there are separate foramina for the palatine and hyoid rami of nerve VII in the wall of the braincase (Goodrich, 1930, fig. 284). In any case, due to its position and relationship to the intracranial space (opening into the acoustico-trigemino-facialis recess), it seems fairly certain that this foramen was for a nerve ramus (probably of nerves V, VII, or the anterior lateral line nerves), rather than for an artery or vein.

## BASICRANIUM

The basicranium in the ethmoid region, including the internasal lamina and median ventral process, were discussed in a previous section (see above). The basicranium in the suborbital and otico-occipital regions of *Tribodus limae* is not uniformly level as in *Egertonodus basanus* (Maisey, 1983), but instead shows a concave curve ventrally, extending posteriorly from the ventral basicranial process to the occiput (Figs. 9C, 25). A curved basicranium has not been described in any other hybodont, although in the fossil neoselachian *Synechodus dubrisiensis* (Maisey, 1985, figs. 2, 4E) and some batoids (e.g., *Rhinobatis*: Daniel, 1934, fig. 68) the neurocranium shows a similar ventral arch between the occiput and the anterior of the orbit. Unlike *Synechodus*, however, the neurocranium of *Tribodus* is not arched dorsally, and does not show the pronounced downward curvature of the ethmoid region seen in *Synechodus* as well as in extant *Heterodontus*,

galeomorphs, and batoids (Maisey, 1985). As discussed previously, no suborbital shelves are present in *Tribodus* (unlike other previously described hybodonts such as *Egertonodus*, Maisey, 1983), and the suborbital region of the basicranium is convexly rounded ventrally and continuous with the orbits, as in some extant squaleans (Shirai, 1992). Other elasmobranchs lacking suborbital shelves include *Synechodus*, extant carcharhinid galeomorphs, *Chlamydoselachus*, hexanchoids, squaloids, and batoids (Maisey, 1985; Shirai, 1992).

In *Tribodus limae*, there is a large median opening located directly posterior to the bases of the postorbital processes (best seen in AMNH 13958 and UERJ-PMB-40) (Figs. 9A, 12B, 21, 22, 35–37: hf). This could either be an internal carotid foramen or a hypophyseal foramen (see Discussion). Although in AMNH 13958 it appears to be flanked by two shallow grooves in the cartilage (superficially resembling pathways for the internal carotid arteries seen in *Egertonodus* and other elasmobranchs), closer inspection and comparison with additional specimens reveals that these grooves are more likely small scratches in the surface of the fossil.

Several millimeters posterior to this median foramen and lateral to it are paired ventral processes, whose distal ends point posterolaterally (Figs. 9A, C; 12B; 18B; 21–25; 36; 37: pvpr). Although only the left process is preserved in AMNH 13958, both processes are well preserved in UERJ-PMB-40 (Figs. 12B, 36, 37). These structures are located directly posterior to a notch in the ventrolateral surface of the basicranium that originates immediately below the postorbital process, and when the palatoquadrates are placed against the neurocranium they appear to fit loosely into the anterior part of this notch between the ventral process and postorbital process. This indicates that these paired

ventral processes may have helped to align the upper jaw where it contacted the neurocranium.

LATERAL DORSAL AORTAE, INTERNAL CAROTID ARTERIES, HYPOPHYSEAL FORAMEN, AND PITUITARY VEIN: In *Tribodus limae* (UERJ-PMB-40 and AMNH 13961), paired foramina are visible immediately dorsal to the paired ventral processes in posterior view (located on the ventromedial side of the base of each process, Figs. 21, 22, 36: lda). They are especially well preserved in UERJ-PMB-40 (Fig. 36). These probably represent the points of entry of the lateral dorsal aortae into the braincase.

If the lateral dorsal aortae entered the braincase here and continued anteromedially within the basicranial cartilage, then the median basicranial foramen is not an entry point for the internal carotids, and requires further explanation. The most obvious explanation is that this latter opening is a hypophyseal foramen. This explanation is supported by CT scans and digital reconstructions of the braincase, which show that this foramen opens internally into a large cavity posteroventral to the main endocranial space (in the rear of the hypophyseal chamber) (Figs. 17E, F; 26). This cavity is connected anteriorly with the endocranial space by a narrow medial canal (Figs. 17C, 23, 24, 28, 30: hd), indicating that it may represent the posterior lobe of a bipartite hypophysis as in some extant elasmobranchs (Daniel, 1934, p. 233). According to Maisey (1983), an open hypophyseal duct occurs in *Egertonodus basanus*, and also in *Xenacanthus*, *Tamiobatis*, "*Cladodus*," and *Cladoselache*, but is lacking in adult neoselachians.

A small foramen located beneath the anterior part of the dorsum sellae and visible in digitally reconstructed sagittal sections of the braincase likely represents the interorbital canal, through which the pituitary vein passed to exit the braincase laterally through a

small foramen ventromedial and posterior to the opening for the facial and anteroventral lateral line nerves (Figs.17B, 26, 28, 37: pit v). This location for the pituitary vein is in keeping with the typical elasmobranch arrangement, in which the pituitary vein foramen is located posterior to the efferent pseudobranchial foramen and marks the boundary between the embryonic polar cartilage and the parachordal cartilage posteriorly.

EFFERENT HYOIDEAN AND ORBITAL ARTERIES: In *Tribodus limae*, anterior to the paired ventral processes and posterolateral to the hypophyseal foramen are two additional, larger pairs of foramina, best preserved in UERJ-PMB-40 (Fig. 37). The more posterior pair of foramina exit the floor of the braincase posterolateral to the hypophyseal foramen, and open into the anterior part of an elongated, posterolaterally-extending groove (Fig. 37: eha). These foramina are here interpreted as housing the efferent hyoidean arteries, which passed posterolaterally from the lateral dorsal aortae to supply the hyoid arch. The more anterior pair of foramina is directed anterolaterally, and CT scan images of AMNH 13958 show that both these and the aforementioned pair of foramina are connected internally to the posterior foramina dorsal to the paired ventral processes. Based on these considerations, the anterolateral pair of foramina are here interpreted as representing the exits of the orbital (= stapedial) arteries from the braincase (Fig. 37: ora). Narrow grooves in the cartilage extending anteriorly from these foramina towards the orbit further support the interpretation that the passage for the orbital arteries was located here. However, this interpretation is unusual in comparison to the typical pattern of cranial circulation in other elasmobranchs, and requires further explanation (see Discussion). It is unlikely that these foramina contained any cranial nerve rami, because CT scans do not show them connecting internally with any nerve passages, and they are located beneath the dorsum

sellae where no cranial nerves originate. The only possible alternative is that these paired lateral foramina could represent the interorbital canal containing the pituitary vein. However, CT scans indicate that the pituitary vein was probably located slightly farther anteriorly, in front of the narrow canal leading to the posterior chamber of the hypophysis (as described above), and the presence of external foramina in that location interpreted as the pituitary vein foramina in UERJ-PMB-40 further support that hypothesis. Additionally, because the pituitary vein typically joins the lateral head vein anterior to the postorbital processes (through which the latter vein passes on its way to the orbit), the large lateral foramina mentioned previously may well be located too far posteriorly to represent the pituitary vein.

In UERJ-PMB-40 (Fig. 12), the posteroventral part of the braincase is well preserved, including both of the paired ventral processes. In this specimen, small, paired foramina are present just posterior to the occiput in ventral view, at the same level as the base of the small pointed posterior processes located immediately lateral to the occiput. Similar paired foramina are also visible in UERJ-PMB-114 and AMNH 13961. Although it may appear at first glance that the paired lateral dorsal aortae entered the braincase here, as previously reconstructed in *Egertonodus* (Maisey, 1983), CT scan slices of *Tribodus* show no evidence of paired canals for the lateral dorsal aortae passing within the basicranial cartilage in the occipital region. However, CT scans do reveal the presence of paired narrow canals extending dorsomedially within the occipital region from these paired foramina, and opening dorsally into the posteromedial floor of the glossopharyngeal-vagus foramen on both sides of the braincase (Figs. 18E, F; 21, 22, 27–30: oc art). These canals may represent occipital arteries branching from the main trunk

of the lateral dorsal aorta ventrally and entering the cartilage of the braincase to supply structures located farther dorsally. The paired ventral foramina just anterior to the occiput in *Tribodus* are thus interpreted here as entry points for the occipital arteries into the braincase. CT scans of *Egertonodus* show that its corresponding set of paired foramina also open into a similar pair of dorsally extending canals that also enter the glossopharyngeal-vagus foramen, changing the previous interpretation and indicating that at least two hybodonts (*Tribodus* and *Egertonodus*) have this arrangement of the occipital arteries and their foramina. Similarly positioned foramina for the occipital arteries have also been reported in the Carboniferous (Viséan–Namurian) hybodontiform *Tristychius arcuatus* (Dick, 1978). In *Tristychius arcuatus*, according to Dick (1978: p. 80; fig.2), the ventral foramina of the occipital arteries are located within anteroposteriorly elongated, narrow indents for the "common carotid arteries" or lateral dorsal aortae. This is very similar to the arrangement found in *Egertonodus* (see Discussion), in which similar indents for externally located lateral dorsal aortae also contain the occipital artery foramina. In *Tribodus*, no external indents for the lateral dorsal aortae are visible, but it is likely that they traveled exterior to the braincase in the occipital region, connecting with the occipital arteries in an arrangement similar to that of *Egertonodus* and *Tristychius*. In *Tristychius*, the occipital arteries emerge dorsolaterally posterodorsal to the vagus nerve foramina (Dick, 1978).

### OTICO-OCCIPITAL REGION

POSTORBITAL PROCESSES: The postorbital processes in *Tribodus limae* (Figs. 9A, C; 21–25: popr) are long, narrow, and tapered toward their distal ends; and are generally

much more slender and gracile than those of *Egertonodus* (Maisey, 1983). Most of the left postorbital process is preserved in *Tribodus limae*, AMNH 13958 (although its distal part is missing), whereas the right postorbital process is not preserved except for its base. This is typical of most fossil hybodont specimens, in which the postorbital processes are often broken off or missing, and may reflect that these processes were only weakly attached to the braincase (Maisey, 1982, 1983). The postorbital processes originate on the lateral wall of the otic capsule, and extend anteroventrally at an angle of approximately 45 degrees to the horizontal aspect of the braincase, defining the posterior margin of the orbit. These processes also extend farther laterally than the antorbital processes. Unlike *Egertonodus*, the widest part of the braincase in *Tribodus* is not the postorbital processes but the otic region farther posteriorly, at the point where the cephalic spines articulated. A large fenestra in the proximal part of the postorbital process is interpreted here as the jugular canal (Figs. 9A, 17B, 21, 23: jc), through which passed the jugular or lateral head vein, and possibly also the hyomandibular ramus of the facial nerve (after exiting the braincase through the facial foramen). The supraorbital crest ends dorsal to the anterior margin of the base of the postorbital process, and is separated from it by a rounded notch.

According to Maisey (2008) and Holmgren (1940), the postorbital process in chondrichthyans forms ontogenetically from two structures: a primary process (which is a posterolateral outgrowth of the supraorbital shelf), and the lateral commissure (fused in part with the side wall of the otic capsule, and fused dorsally either with the otic capsule to enclose the hyomandibular trunk of the facial nerve, or with the ventrolateral margin of the primary process to enclose the lateral head vein). Based on the structure and position of the postorbital process in *Tribodus*, it is concluded here that it was formed at least in

part by the embryonic lateral commissure, which was chondrified in the adult. This interpretation is based on the fact that the postorbital process in *Tribodus* is fused dorsally and medially with the otic capsule and encloses the jugular canal, which presumably housed the lateral head vein. In the same way, a chondrified lateral commissure was probably also present in *Egertonodus*, as was suggested previously by Maisey (1983).

A postorbital articulation was absent in most hybodontiforms (including *Tribodus*), whose jaw suspension is hyostylic (except for *Tristychius*, which had a postorbital articulation; Dick, 1978; Maisey, 2008). Thus, unlike other fossil chondrichthyans with a lateral commissure (e.g., *Cladodoides*, Maisey, 2005; "*Cobelodus*," Maisey, 2007), the postorbital process in most hybodonts lacks an articular facet for the palatoquadrate.

OCTAVAL, GLOSSOPHARYNGEAL, VAGUS, AND SPINO-OCCIPITAL NERVES: CT scan images of the interior of the braincase show two large foramina located posterior to the foramen for the hyomandibular ramus of the facial nerve, both of which exit into the otic capsule. These are here interpreted as having housed the anterior and posterior rami of the octaval nerve, respectively (Figs. 17B, D–G, 26: VIII a, p). Posterior to the octaval nerve foramina and located ventrolaterally on the endocranial wall is a much smaller foramen (Fig. 26: IX). This foramen is here interpreted as having housed the glossopharyngeal nerve, and joins the glossopharyngeal-vagus canal at a location ventral to the preampullary canal. It is positioned similarly to the glossopharyngeal nerve of neoselachians (e.g., *Squalus*, Marinelli and Strenger, 1959; Gegenbaur, 1872). After exiting the cranial cavity, the glossopharyngeal nerve traveled through a narrow canal beneath the otic capsule, which widens posteriorly (Figs. 27, 28, 29B, 30: IX). This canal exits on the posterior of the braincase together with the vagus nerve through a single,

of the anterior and posterior semicircular canals, respectively. The ridge overlying the anterior semicircular canal extends anterolaterally at an angle of approximately 35 degrees from the midline of the specimen, while the posterior ridge extends laterally at about 45 degrees to the midline.

As discussed previously, paired rectangular laterally concave areas located on the lateral part of the otic region represent the points of articulation for the cephalic spines (Maisey & Carvalho, 1997), indicating that AMNH 13958 was a male (female specimens of *Tribodus* lack cephalic spines, as well as the paired platforms for their articulation; the posterolateral part of the braincase is instead smoothly rounded). The convex platforms for the cephalic spines in AMNH 13958 lack a covering of prismatic cartilage, and appear fibrous. A photograph of the original specimen immediately after acid preparation shows that the cephalic spines sat in these convex platforms with their cusps directed posteroventrally (Fig. 109: csp). Posteromedial to the cephalic spine platforms are two lateral processes, here interpreted as lateral otic processes as in *Egertonodus* (Maisey, 1983) (Figs. 9B, C; 19: lotpr). It has been suggested that the hyomandibula articulated on these processes (Maisey & Carvalho, 1997). This interpretation is supported by the new material of *Tribodus*, which shows a rounded concave notch for the dorsal head of the hyomandibula on the medial surface of the lateral otic process on each side of the specimen, between the lateral otic process and a small, triangular, posteriorly directed process posteromedial to it (Figs. 9A, 21, 22, 23: hm art). The hyomandibular articulation is posterior and lateral to the glossopharyngeal-vagus foramen, and the lateral otic process is located entirely lateral to this foramen. Paired posterior triangular processes are

located immediately posterior to the glossopharyngeal-vagus foramina, flanking the occiput laterally.

FORAMEN MAGNUM AND OCCIPUT: Situated directly between the paired glossopharyngeal–vagus foramina on the posterior of the braincase is the foramen magnum, through which the spinal cord exited the braincase (Figs. 9B, 19, 23B, 25: fm). The foramen magnum is a rounded opening, slightly elongated dorsoventrally. Above the foramen magnum is a dorsally-extending occipital crest, which terminates at the posterior margin of the parietal fossa, representing the point of closure of the occipital arch during ontogeny. A similar crest is seen in *Notorynchus* (Maisey, 2004b). The occipital cotylus, located directly ventral to the foramen magnum (Figs. 9A, 18C–F, 21, 23B, 25: oc cot), is fibrous and has a concave posterior surface, as in *Egertonodus* (Maisey, 1983). The lateral sides of the occiput are fully formed, but the dorsal and ventral sides are not well developed and the occipital cotylus opens dorsally into the foramen magnum. Like other hybodonts (such as *Egertonodus*, Maisey, 1983), and unlike the condition in extant neoselachians, there is no occipital hemicentrum in *Tribodus* (and this form also lacks calcified vertebral centra, as do other non-neoselachian elasmobranchs). The occipital region in *Tribodus* is broader than in *Egertonodus*, and the occiput does not extend as far posteriorly behind the otic capsules as it does in *Egertonodus*. This feature of *Tribodus* is similar to many modern sharks, in which the occiput is also situated between the otic capsules (Maisey, 1983).

shared foramen lateral to the foramen magnum on either side (Figs. 9B, 18D–F, 19, 23B: IX, X). Each of these shared foramina is located immediately anterior to the hyomandibular articulation, and is oval in outline.

In sagittal view, foramina for rami of the vagus nerve are visible as two small openings in the mesial wall of the braincase, posterior to the glossopharyngeal foramen (Fig. 26: X). They are located beneath the domed roof of the medullary chamber, similar to the position of the internal vagus foramen in neoselachians (e.g., *Notorynchus*, Maisey, 2004b), and are arranged one above the other. These foramina open into canals that exit the braincase through the glossopharyngeal-vagus foramen.

ROOF OF THE OTIC REGION: The otic region of *Tribodus limae* (AMNH 13958) is relatively complete, although the right postorbital process is missing. As in *Egertonodus basanus*, the paired otic capsules in *Tribodus* constitute approximately one-third of the total length of the braincase. The parietal (endolymphatic) fossa is large, elongated, and ovate, and is located centrally between the otic capsules (Figs. 9B, 19: p fos). An anterior pair of small, rounded foramina located laterally within the parietal fossa represents the endolymphatic foramina (Figs. 19, 26: end f), and a more posterior pair represent the perilymphatic fenestrae (Figs. 18A, 26, pf). Other than these two pairs of foramina, the parietal fossa has a continuous cartilaginous floor, probably formed by an embryonic taenia medialis as in extant elasmobranchs (Holmgren, 1940) (Fig. 17B: t med). In extant elasmobranchs, this structure can be produced either as a posterior outgrowth from the synotic tectum (e.g., *Squalus*), or as an anterior outgrowth from the posterior tectum (where one is present, e.g., *Scyllium*) (Holmgren, 1940). Paired elevated ridges in the cartilage located laterally, anterior and posterior to the parietal fossa, indicate the location

## ENDOCRANIAL SPACE, CRANIAL ENDOCAST, AND SKELETAL LABYRINTH

CRANIAL ENDOCAST AND ENDOCRANIAL SPACE: A generalized description of endocranial morphology in *Tribodus* was provided by Maisey (2004a) as part of a comparative study of elasmobranch neurocrania. However, a detailed description of endocranial morphology in *Tribodus* has not yet been provided, and a reconstruction of the cranial endocast in *Tribodus* (or any other hybodont) has not been presented until now. The cranial endocast of *Tribodus* is similar in many respects to that of some extant neoselachians such as *Notorynchus*, particularly in dorsal and lateral views. As in *Notorynchus* and *Squalus*, the telencephalic chamber broadens anteriorly, with proportionally thick olfactory canals and widely spaced olfactory chambers (Figs. 27, 28: tel). This condition is unlike that of *Cladodoides* (Maisey, 2005), in which the telencephalic region is more narrow and uniform in width from side to side, and actually narrows anterior to the cerebellar chamber. It is also considerably different from "*Cobelodus*" (a tropibasic form), in which the endocast is extensively foreshortened and the telencephalic region also tapers anteriorly in dorsal view. As Maisey (2004a) also pointed out, in both *Tribodus* and *Egertonodus* the floor of the telencephalic chamber above the median ventral process is flat to slightly convex and does not follow the shape of the underlying external morphology (Fig. 26), a feature shared with neoselachians. As noted by Maisey (2004a), no constriction between the telencephalic and mesencephalic regions (such as that found in *Squalus*) is present in *Tribodus*. Also, the myelencephalic (medullary) chamber of *Tribodus* is domed as in *Notorynchus* and *Squalus*, as pointed out by Maisey (2004a). The vagus (X) nerve exits the cranial cavity in a similar location to

that of *Notorynchus* and *Squalus*, near the center of the medullary chamber (Figs. 26, 27, 29, 30: X).

Maisey (2004a) noted that in both *Tribodus* and *Egertonodus*, the optic foramen is positioned centrally within the orbit and the trochlear foramen is located anterior and dorsal to the optic foramen, which he describes as an unusual configuration for elasmobranchs (in which the trochlear foramen is typically dorsal, but posterior to the optic foramen). This is confirmed by CT scans and digitally reconstructed endocasts of both *Tribodus* and *Egertonodus* that show a lateral outgrowth in the correct position on the endocast to correspond to the trochlear nerve (Figs 27, 28, 30: IV). The optic artery also probably exited the braincase through the optic foramen, alongside the optic nerve.

Posterodorsal to the optic foramen on the *Tribodus* endocast is a smaller outgrowth, located directly above the anterior part of the infundibular region. This is in the correct position to correspond to the oculomotor nerve of many extant neoselachians (Figs. 28, 30: III). It exits the braincase through a small foramen immediately anterior to the trigemino-facialis recess. Ventral to this, the infundibular region extends posteriorly to form a hypophyseal chamber (Figs. 17A, B; 23A: hyp), visible in ventral and lateral views of the endocast (Figs. 28, 30). At the rear of the infundibular/hypophyseal region immediately anterior to the dorsum sellae are paired lateral extensions, here interpreted as the pituitary veins (Fig. 28, pit v), and comparable to those of *Cladodoides* (Maisey, 2005). Posterior to this, the hypophyseal chamber constricts to form a narrow medial tube, which joins posteriorly with a large chamber beneath the dorsum sellae (Figs. 28, 30: hd). A median ventral extension from this chamber (Fig. 28: hf) may represent either an open hypophyseal duct or a foramen for the internal carotid arteries, although the

former interpretation is considered here to be more likely (see above discussion). From the anterolateral sides of this chamber, paired elongated tubes extend forward, joining the cranial endocast posterior to the optic nerve and below the oculomotor nerve (Figs. 28, 30: ica). These paired canals were probably for the internal carotid arteries, which tunnel through the basicranial cartilage before entering the braincase and joining two additional vessels, the efferent pseudobranchial/ophthalmic arteries and the optic arteries (in order anteriorly). From the lateral sides of this chamber extend two additional sets of openings that exit the braincase laterally. Of these, the anterior pair of openings is here interpreted as the orbital arteries (Figs. 28, 30: ora), and the posterior pair is interpreted as the efferent hyoidean arteries (Fig. 28: eha). From the posterior part of this chamber, paired canals extend posterolaterally (Figs. 28, 30: lda). These are here considered to represent the lateral dorsal aortae, which entered the braincase through paired posterior foramina (at the base of the paired ventral basicranial processes) and traveled anteriorly to enter the aforementioned chamber. They then joined the orbital arteries, and continued anteromesially as shortened internal carotid arteries before joining inside the chamber and dividing again to progress anteriorly.

An acoustico-trigemino-facialis recess (De Beer, 1937, p. 56) is visible on the internal lateral wall of the sagittally sectioned half-braincase of *Tribodus* (Fig. 26), and a corresponding lateral extension appears on each side of the cerebellar region in the endocast (Figs. 27, 28, 30). This recess contained the proximal trunks of the trigeminal, facial, anterior lateral line, and octaval nerves. According to De Beer (1937) and Allis (1914), this space is intramural (mesial to the wall of the braincase) in modern *Squalus* but not intracranial, because it is located external to the dura mater, which may have also

been the case in *Tribodus*. In the anteriormost part of this recess on the endocast is a forwardly-directed canal. This canal divides immediately anterior to exiting the cranial cavity, forming a large dorsal canal and a narrower ventral canal. The larger canal is here interpreted as having housed the superficial ophthalmic complex, and possibly also the profundus nerve (Figs. 27, 28, 30: V oph, alln, prof).

The smaller canal may represent the abducens nerve (Figs. 28, 30: VI), originating on the ventral surface of the brain and extending anterodorsally to exit the braincase into the orbit in the vicinity of the trigemino-facialis recess. It may alternatively represent the profundus nerve (discussed above); however, this interpretation is considered less likely because the abducens nerve would then have to exit the braincase farther posteriorly, away from the external rectus muscle which it innervates. Posteroventral to the superficial ophthalmic and abducens canals is a second lateral extension from the acustico-trigemino-facialis recess, interpreted as the main trunk the trigeminal and anterodorsal lateral line nerves (which exit through the trigemino-facial foramen; Figs. 27, 28, 30: V, VII). Two larger lobes immediately posterior to this on the endocast are here considered to be the anterior and posterior branches of the octaval nerve, respectively (Figs. 27, 28: VIII).

Posterior to the acustico-trigemino-facialis recess and hypophyseal chamber, the dorsal surface of the endocast slopes downwards, forming a saddle-like depression into which the skeletal labyrinth fits (Figs. 27, 30, 31, 33, 34). Posterior to this, the medullary chamber again expands dorsally, forming a rounded dome (Figs. 26, 27, 30). The notochord is visible as an elongated median extension from the ventral surface of the medullary region (Figs. 28–30: nt). Dorsolateral to the notochord, at the anterior end of

the medullary dome, a small paired extension from each side of the endocast represents the glossopharyngeal nerve (Figs. 27, 28, 30: IX). Posterior to these, two additional pairs of canals extending from the dorsal and lateral sides of the medullary dome represent the vagus nerve (Figs. 27, 29B, 30: X). These canals extend posterolaterally and exit the braincase posteriorly together with larger, more laterally located canals (emerging from the ventral sides of the skeletal labyrinth, and containing the glossopharyngeal nerves) inside the large glossopharyngeal-vagus foramina. However, although the two nerves share a common foramen to exit the braincase, they do not share a single canal opening into this foramen, and instead enter the lumen of the glossopharyngeal-vagus foramen through separate smaller foramina. Posteromedial to the glossopharyngeal-vagus foramina, the medullary chamber narrows, terminating posteriorly at the foramen magnum. At least three pairs of spino-occipital nerve canals extend laterally from the sides of the medullary chamber (Figs. 26–29: soc), and several of them enter the glossopharyngeal-vagus foramen. Posteriorly, small canals extending dorsolaterally from the floor of the braincase and opening into the glossopharyngeal-vagus foramina represent paired occipital arteries (Figs. 27–30: oc art).

SKELETAL LABYRINTH: The skeletal labyrinth of *Tribodus limae* was figured and briefly described by Maisey (2005). Digital imaging of CT scans for the present work confirm Maisey's description for the most part, except that the foramen for the octaval nerve appears to have been divided by a narrow band of cartilage to form separate foramina for the anterior and posterior rami of the octaval nerve (Figs. 17B–G; 26; 27–28, 30, 32). As in neoselachians and *Egertonodus* (and unlike many Paleozoic chondrichthyans such as *Cladodoides* and *Cobelodus*, Maisey, 2005, 2007), a medial

capsular wall is present in the otic region, separating the skeletal labyrinth from the main endocranial cavity housing the brain (Figs. 17B–H, 26: mcw). This wall is fused with the parachordal-derived floor of the braincase ventrally, and with the roof of the otic region, except where it is penetrated by foramina. Anteriorly, two large foramina in the mesial wall of the braincase open into the otic capsule. These are here interpreted as separate passages for the anterior and posterior branches of the octaval nerve, which supplies the inner ear. In most gnathostomes, the anterior branch of this nerve innervates the utricular macula and the cristae of the anterior and external ampullae, whereas its posterior ramus innervates the posterior of the ear, including the preampullary canal, saccular and lagenar maculae, and macula neglecta (Cordier, 1954: p. 228; Maisey, 2001a).

As in all gnathostomes (Maisey, 2001a; Liem et al., 2001: p. 414), the skeletal labyrinth of *Tribodus limae* includes three semicircular canals (the anterior, external or horizontal, and posterior canals) (Figs. 31–34). These canals are narrow and elongate. As in other gnathostomes, the ampullae of the anterior and external canals are directly connected to the utriculus anteriorly. As in neoselachians and most gnathostomes, a utricular recess is present (Fig. 32, 33A, 34: ur). The saccular chamber is large and rounded, and a small lagena is present posteroventrally (Figs. 18B, 34: lag). Dorsally, the labyrinth opens externally via two foramina, the endolymphatic foramen anteriorly (Fig. 31, end f) and the perilymphatic foramen posteriorly (Figs. 31, 33B: pf). These are paired structures, occurring on either side of the parietal fossa. The positions of the endolymphatic and perilymphatic ducts are similar to those of neoselachians, with the endolymphatic duct originating near the base of the anterior semicircular canal dorsally, and the perilymphatic duct originating from the dorsal margin of the posterior

semicircular canal. As in neoselachians, the posterior semicircular canal of *Tribodus* forms an almost complete circuit, with a narrow preampullary canal (Fig. 32: pac) connecting the posterior ampulla with the sacculus and perilymphatic fenestra. However, the preampullary canal is tilted upward anterodorsally, rather than almost vertical as it is in *Notorynchus* (Maisey, 2005, fig. 36). As in most gnathostomes, the semicircular canals are arranged at right angles to one another, with the two vertical canals aligned at a 90 degree angle to each other and both of them perpendicular to the horizontal (external) canal. The external canal extends laterally beyond the margin of the saccular chamber, leaving a narrow space between it and the sacculus. The semicircular canals appear proportionally narrower than those of neoselachians such as *Notorynchus* (Maisey, 2005, fig. 36), whereas the saccular chamber is proportionally larger, forming nearly half the anteroposterior length of the skeletal labyrinth. Like neoselachians and unlike most other craniates, a crus commune and sinus superior are absent in *Tribodus*, as Maisey (2001a, 2005) previously pointed out.

### ENDOCRANIAL MORPHOLOGY OF *EGERTONODUS BASANUS*

In addition to the material of *Tribodus limae* already mentioned, a braincase of *Egertonodus basanus* (NHM P60110, originally described by Maisey, 1983; this paper, Fig. 38), was also CT scanned for the present study. These CT scans (Figs. 39–41) of the braincase and cranial endocast of *Egertonodus basanus*, as well as 3-D digital images made from these CT scans for the present study (Figs. 42–44; 46A–C), confirm many of Maisey's (1983) interpretations based on its external structure, providing a clearer understanding of cranial morphology in a hybodont other than *Tribodus*.

Although the braincase of *Egertonodus* examined here is not as well preserved as that of *Tribodus*, and is partly crushed, enough detail is preserved to allow useful comparisons with *Tribodus*. A digitally reconstructed sagittal section (Fig. 43) reveals that *Egertonodus*' internal cranial morphology was similar to that of *Tribodus*, but with several notable differences. The overall shape of the cranial cavity is similar to that of *Tribodus*, with a telencephalic region that broadens anteriorly in dorsal view (although less so than in *Tribodus*), a narrowing beneath the otic region, and a domed medullary chamber. As in *Tribodus*, there is a large optic foramen some distance anterior to the tip of the dorsum sellae (Fig. 43: ds), and centrally located within the orbit (Figs. 42, 43: II). A narrow groove posteroventral to the ventral edge of the optic foramen (Fig. 43) probably represents the path of the optic artery, which probably exited the braincase through the optic foramen alongside the optic nerve as in *Tribodus*. Anterodorsal to the optic foramen is a small foramen, interpreted here as the trochlear nerve (Figs. 42, 43: IV) and positioned similarly to that of *Tribodus*, but unlike that of most non-hybodont chondrichthyans.

The dorsum sellae (Fig. 43: ds) is shorter anteroposteriorly than that of *Tribodus* (Fig. 26: ds), and slants upward dorsally to form a larger angle (approximately 45 degrees) with the floor of the braincase than in *Tribodus*. As in *Tribodus*, the oculomotor foramen is located above and anterior to the tip of the dorsum sellae, but it is closer to the dorsum sellae in *Egertonodus*. At the posterior of the hypophyseal chamber beneath the dorsum sellae is a small foramen, interpreted here as housing the pituitary vein (Fig. 43, pit v). It exits the braincase externally through a small foramen in the trigemino-facialis recess at the back of the orbit (Fig. 42: pit v), in the position that Maisey (1983) interpreted as

containing the efferent pseudobranchial artery. In *Tribodus*, the pituitary vein exits the braincase farther posteriorly relative to the orbit, at the level of the postorbital processes. Beneath the pituitary foramen in *Egertonodus* is a small chamber in the basicranial cartilage, which opens ventrally through the median basicranial foramen. This chamber connects anterolaterally with paired canals, which travel a short distance anteriorly before exiting the braincase through ventrolaterally positioned foramina (Fig. 39 F, G; 42: epsa). These foramina are located posteroventral to the optic foramen, anteroventral to the pituitary foramen, and directly below the oculomotor foramen, and are interpreted here as the efferent pseudobranchial foramina. Here the morphology departs somewhat from that of *Tribodus*, in which a similarly positioned chamber below the dorsum sellae houses the orbital arteries, and the efferent pseudobranchial arteries are located more anteriorly. However, as in *Tribodus* (and most other chondrichthyans except embryonic *Torpedo*: Holmgren, 1940), the efferent pseudobranchials are located anterior to the pituitary vein foramina. Unlike *Tribodus*, the median basicranial foramen opens at the convergence point of external grooves in the basicranial cartilage (Fig. 38B), and it seems fairly certain that in *Egertonodus* these grooves contained the internal carotid arteries and other vessels of the basicranial arterial circuit, which traveled external to the basicranial cartilage. Unlike *Tribodus*, the median ventral foramen probably contained the internal carotid arteries (possibly alongside an open hypophyseal duct), and there are no ventral canals within the cartilage posterior to the median foramen in *Egertonodus*.

Directly above and behind the tip of the dorsum sellae in *Egertonodus* is a laterally located acoustico-trigemino-facialis recess. At the anterior end of this recess are two large foramina, one anterior and slightly dorsal to the other. The more dorsally located

foramen leads to an anteriorly directed canal (Fig. 43: V oph, alln, prof). This opens into the orbit via a foramen (Fig. 42) designated by Maisey (1983) as the main trigemino-facial (V, VII) foramen (Fig. 38C). Its position is identical to that of the superficial ophthalmic canal in *Tribodus*, and is also interpreted here as housing the superficial ophthalmic complex and profundus nerve. As in *Tribodus*, a smaller canal diverges ventrally from the former, but it travels through the cartilage for a much shorter distance (Fig. 40A: VI), and exits at the anterodorsal end of a larger foramen (Figs. 42, 43: V, VII) located posteroventral to the superficial ophthalmic foramen. This foramen was originally designated by Maisey (1983) as housing the hyomandibular ramus of nerve VII. It is similar in position to that of the main trigeminal-anterodorsal lateral line nerve canal of *Tribodus*, and is here interpreted as also representing the main trunk of those nerves (as in *Tribodus*).

An additional foramen located posteroventral to the main V-VII foramen in *Egertonodus* is here interpreted as housing the hyomandibular ramus of the facial nerve (Figs. 40E, 43, 44: VII hm). Its position in relation to the main V-VII foramen is similar to that of the hyomandibular foramen in *Tribodus*. In *Egertonodus*, this foramen (Fig. 40E: VII hm) is directed posteroventrally, and is located directly dorsal to a small foramen in the suborbital shelf (Fig. 40E: ora), identified by Maisey (1983) as the anterior foramen for the orbital artery (Fig. 38B, ora). It is possible that the palatine ramus of the hyomandibular trunk passed ventrally through this foramen to reach the roof of the mouth, whereas the hyoid ramus may have curved posterolaterally to enter the jugular canal on its way to the hyoid arch.

Immediately posterior to the hyomandibular foramen in medial view of the braincase is a pair of much larger foramina, which open into the otic capsule (Fig. 43: VIII). These are interpreted as representing the anterior and posterior rami of the octaval nerve, as in *Tribodus*. A smaller foramen posterior to the octaval foramina, and ventral to the anterior edge of the perilymphatic fenestra, is interpreted as the glossopharyngeal foramen (Fig. 43–44: IX). As in *Tribodus*, it opens into the posterior floor of the otic capsule, and continues posteriorly. Paired foramina for rami of the vagus nerve are located beneath the dome of the medullary region, as in *Tribodus* (Figs. 43–44: X, $X_d$) and the canals leading from the vagus and glossopharyngeal foramina also converge to exit externally through a common glossopharyngeal-vagus foramen. At least three spino-occipital nerves are present posteroventrally within the medullary region, as in *Tribodus* (Figs. 41F–H, 43–44: soc).

SKELETAL LABYRINTH OF *EGERTONODUS*: The otic region of *Egertonodus basanus* examined for the present thesis is not as well preserved as that of *Tribodus limae*. The skeletal labyrinth is best preserved on the right side of the specimen, but in the CT scans its lining of prismatic cartilage is faint and difficult to trace, particularly in the ventrolateral part of the saccular chamber and the proximal part of the preampullary canal. Nevertheless, it is well enough preserved to allow the skeletal labyrinth of *Egertonodus* to be reconstructed via digital imaging (Fig. 46A–C). As in *Tribodus*, a medial capsular wall is present in the otic region of *Egertonodus* (Fig. 40F–H, 43: mcw), separating the skeletal labyrinth from the rest of the endocranial cavity and containing foramina for the octaval, glossopharyngeal, and vagus nerves. Like *Tribodus*, there are two large foramina anteriorly that open into the otic capsule, which probably housed the

anterior and posterior branches of the octaval nerve. The presence of two octaval foramina in *Tribodus* and *Egertonodus* may indicate a hybodont synapomorphy, and is lacking in neoselachians. As in *Tribodus* and neoselachians, the glossopharyngeal nerve passes through the wall of the endocranium in the medullary region, ventral to the preampullary canal and anterior to the vagus nerve. As in *Tribodus* and neoselachians, the glossopharyngeal nerve is located ventrally in the endocranial wall. After exiting the endocranial space, it passes via a narrow canal into the glossopharyngeal-vagus foramen, as in *Tribodus*. Posterior to the glossopharyngeal foramen is a pair of additional foramina, here interpreted as housing rami of the vagus nerve. One of these is located dorsally near the dome of the medullary region, and the other is located ventrally below it. Both of these foramina join canals that connect with the glossopharyngeal-vagus foramen, and the more dorsal canal continues farther laterally, exiting the braincase dorsal to the glossopharyngeal-vagus canal.

The skeletal labyrinth of *Egertonodus* (Fig. 46A–C) is similar to that of *Tribodu*s (Fig. 41D–F) and other gnathostomes (Fig. 47) in its overall structure. The anterior, external, and posterior semicircular canals are arranged as in *Tribodus*, and a utricular recess is present anteriorly communicating directly with both the anterior and external ampullae as in many gnathostomes. A crus commune and sinus superior are absent in *Egertonodus*, as in *Tribodus* and neoselachians, and the anterior and posterior semicircular canals are widely spaced dorsally. Like *Tribodus* and neoselachians, in *Egertonodus* an endolymphatic foramen is present anterodorsally, and a perilymphatic foramen is present posterodorsally (Fig. 46B: end f, pf). The posterior semicircular canal forms a complete circuit, with a preampullary canal (Figs. 41A, B; 46C: pac) connecting the posterior

ampulla with the saccular chamber and perilymphatic fenestra. A small lagenar chamber is present in the posterior of the saccular region (Figs. 41A, B: lag), as in *Tribodus*. In both *Egertonodus* and *Tribodus*, the external semicircular canal passes mesial to the posterior canal.

## DISCUSSION

### COMPARISON OF CRANIAL CIRCULATION IN *TRIBODUS, EGERTONODUS,* AND OTHER FOSSIL AND EXTANT ELASMOBRANCHS

A reconstruction of the cranial circulation and relevant vascular foramina of *Tribodus* (Figs. 48, 49) is presented here and discussed below in comparison to that of other fossil and extant elasmobranchs (Fig. 50). Information from CT scan images and the positions of external foramina indicate that the configuration of the cranial circulation in *Tribodus* was complicated, and appears to have differed in several major respects from that of *Egertonodus basanus* (Maisey, 1983), the only other hybodont whose cranial anatomy is known in comparable detail.

EXTANT ELASMOBRANCHS: In most extant elasmobranchs, the cranial circulation follows what is probably a highly conserved pattern, in which the dorsal aorta divides into left and right branches (= lateral dorsal aortae), each of which gives off an efferent hyoidean artery posteriorly, and an orbital artery more anteriorly, before anastomosing to form a single internal carotid artery. This artery generally enters the braincase either after or just prior to anastomosing, producing either a single median internal carotid foramen (e.g., *Raja*: Allis, 1912; *Heterodontus*: Maisey, 1983; Shirai, 1992; *Squalus*: Ashley and Chiasson, 1988; *Squatina*; *Pristiophorus*; batoids: *Rhynchobatus*; hexanchoids: *Hexanchus*; many squaloids; Shirai, 1992) or a pair of foramina (e.g., *Chlamydoselachus*,

Allis, 1911, 1923; many squaloids; galeomorphs: *Proscyllium*; Shirai, 1992; Compagno, 1988). As the above-listed taxa show, this feature (presence of one vs. two internal carotid foramina) is highly variable in extant neoselachians, and does not appear at present to have much taxonomic significance. Soon after anastomosing and entering the braincase, the internal carotid artery again divides into left and right branches. Each of these gives off a lateral branch (which divides to produce the efferent pseudobranchial and ophthalmic arteries), and an anterior branch, which gives rise to the optic and cerebral arteries. In neoselachians, the posterior part of the basicranial arterial system forms what has been referred to as a "bell-shaped" circuit (Schaeffer, 1981), due to the outwardly/laterally curving position of the lateral dorsal aortae, which form the concave 'base' of the 'bell,' while the V-shaped proximal area where the lateral dorsal aortae merge posteromedially as the median dorsal aorta forms the bell's 'clapper.'

This 'bell-shaped' area is mainly external to the braincase in neoselachians, particularly in its posterior part. However, Allis (1911) describes the efferent hyoidean artery of *Chlamydoselachus* as passing briefly through a short canal in the cranial cartilage before emerging again to join the lateral dorsal aorta. More anteriorly, the orbital artery can be external to the braincase (e.g., *Chlamydoselachus*, Allis, 1923), or can pass through the cranial cartilage, as in *Heterodontus* (Maisey, 1983). Compagno (1988, fig. 6.8) illustrates several extant galeomorphs in which the efferent hyoidean and orbital (stapedial) arteries meet the lateral dorsal aortae within the basicranial cartilage, anterior to the point where the lateral dorsal aortae enter the braincase (i.e., hemigaleine hemigaleids; *Hemipristis*). Anterior to the entry of the internal carotids into the braincase, the efferent pseudobranchial and ophthalmic arteries typically exit the braincase through

a single foramen, and diverge afterward (Allis, 1911, 1912, 1923; Holmgren, 1942, fig. 18). The optic artery typically exits the braincase farther anteriorly, alongside the optic nerve.

FOSSIL CHONDRICHTHYANS: In fossil sharks, the pattern of cranial vascularization has been reconstructed based on the arrangement of basicranial foramina (and, where present, external grooves on the surface of the braincase) (e.g., *Orthacanthus*, *Cladoselache*, Schaeffer, 1981; *Cladodoides*, *Tamiobatis*, Maisey, 2005; "*Cobelodus*," Maisey, 2007). The pattern in these fossil forms is broadly similar to that of extant neoselachians in having a posterior circuit formed from the lateral dorsal aortae and internal carotids, and in the positions of the efferent hyoidean and orbital arteries relative to this circuit. In general, the basicranial circuit in fossil chondrichthyans is narrower and more elongate than it is in neoselachians, and lacks the bell-shaped curve posteriorly. In many forms (e.g., *Orthacanthus*, *Cladoselache*, *Tamiobatis*, *Cladodoides*, Schaeffer, 1981; Maisey, 2005, 2007), the lateral dorsal aortae enter the basicranial cartilage posteroventrally through paired foramina and travel anteriorly through enclosed canals. In others (e.g., "*Cobelodus*", Maisey, 2007), the dorsal aorta enters the braincase through a single posteroventral foramen and divides within the cartilage, but the lateral dorsal aortae also travel anteriorly through enclosed canals. This is notably different from the pattern in hybodonts and many neoselachians, in which the posterior part of the lateral dorsal aortae and arterial circuit are external to the cartilage. Also, the part of the arterial loop posterior to the efferent hyoidean artery is longer in xenacanths and "ctenacanths" than in other chondrichthyans, a feature that is probably related to the elongated otico-occipital regions of these taxa. Another noticeable difference between many fossil and extant

chondrichthyans is the anterior extent of the arterial system: in fossil forms including hybodonts and Paleozoic sharks, the cranial arterial system (from lateral dorsal aortae to optic arteries; based on the positions of foramina) appears to have extended nearly the entire length of the braincase, whereas in extant elasmobranchs (e.g., *Heterodontus*, *Chlamydoselachus*, Maisey, 1983) it extends anteriorly only about two-thirds the length of the braincase. This may also be related to the general shift in braincase proportions in neoselachians, with the otico-occipital regions shortening and the orbital and ethmoidal regions forming a larger proportion of overall braincase length. In many fossil sharks, the orbital and efferent hyoidean arteries have been reconstructed branching from the lateral dorsal aorta in very close proximity (*Tamiobatis*, *Orthacanthus*, *Egertonodus*, *Cladoselache*, "*Cobelodus*", Schaeffer, 1981; Maisey, 1983, 2005, 2007), whereas in *Cladodoides*, *Tribodus*, and neoselachians there is apparently some distance between their branch points (Maisey, 1983, 2005; and the present paper). However, many of these observations rely on the accuracy of previous reconstructions, which necessarily involve at least some degree of speculation.

*TRIBODUS*: Based on CT scans and digital images of the braincase of *Tribodus* (AMNH 13958), its cranial circulation can be reconstructed according to several possible scenarios, described below. In all of these, it is considered likely that the optic artery passed through the optic foramen together with the optic nerve, as in *Cladodoides* and extant neoselachians (Maisey, 2005). It is also considered probable that the efferent pseudobranchial and ophthalmic arteries divided external to the cranial wall, as in many neoselachians and as Maisey (1983) reconstructed in *Egertonodus* (and confirmed in *Egertonodus* by CT scan images in the present study). The efferent pseudobranchial

arteries are here interpreted as having passed through paired canals in the basicranial cartilage (visible in CT scan images), which emerge into the cranial cavity just anterior to the dorsum sellae. They then would have curved posterolaterally and slightly dorsally, to exit the cranial wall through a small foramen in the lateral wall of the orbit immediately anterior and ventral to the lateral hypophyseal ridge, before diverging into separate efferent pseudobranchial and ophthalmic arteries external to the braincase.

The remaining aspects of the cranial circulation are more problematic, due to the presence of several foramina not found in other fossil or extant elasmobranchs and whose significance is difficult to interpret. However, the likelihood of each morphological scenario can be weighed according to a number of ontogenetic and phylogenetic considerations, allowing the most likely configuration of cranial vascularization to be identified. On the basicranium there is a single median foramen located between the paired postorbital processes. This might normally be considered a foramen for the internal carotid arteries, as in some extant neoselachians (e.g., *Heterodontus*) in which the internal carotids meet external to the basicranial cartilage and enter the cartilage as a single vessel. This interpretation has also been suggested for *Egertonodus* (Maisey, 1983). However, unlike *Egertonodus*, *Tribodus* lacks any obvious indentations on the basicranium which could be interpreted as external arterial pathways. Also, *Tribodus* has several additional foramina in the basicranium which require explanation, casting doubt on the interpretation of the median foramen as an internal carotid opening. These include a pair of posterior foramina (located on the undersides of the paired posterior basicranial processes) and two pairs of lateral foramina (immediately lateral to the median foramen). CT scans show that all of these foramina are interconnected by internal canals. The

posterior foramina lead to paired canals which continue anteromedially, converging to open into a large chamber overlying the median basicranial foramen, and continuous with it. This chamber is also continuous with the two pairs of lateral foramina, which open ventromedial to the postorbital processes. This configuration indicates that the structures contained within these foramina may have been continuous with one another, and suggest a system of branched arteries.

In most extant elasmobranchs, the basicranial circulation forms a loop or circuit posteriorly. The dorsal aorta divides into paired lateral dorsal aortae, which diverge to form the posterior part of the loop. They meet the paired posterolaterally directed efferent hyoidean arteries slightly farther anteriorly, continue forward as the common carotid arteries, and meet with the paired anterolaterally directed orbital arteries before turning medially as the internal carotid arteries to converge and enter the basicranial cartilage (whether the internal carotids meet immediately prior to, or after, entering the braincase is variable in many extant elasmobranchs). Indentations on the basicranium in *Egertonodus* strongly suggest a similar configuration, as proposed by Maisey (1983). Moreover, most fossil chondrichthyans currently known exhibit a more or less similar pattern (e.g., *Orthacanthus*, *Tamiobatis*, Schaeffer, 1981; *Cladodoides*, Maisey, 2005; "*Cobelodus*," Maisey, 2007), with a comparable circuit and arterial arrangement (the main differences being in the shape of the circuit—bell-shaped in neoselachians vs. more narrow and elongated in other elasmobranchs—and whether the circuit is entirely external or partly contained in cartilage, which varies greatly even among extant neoselachians; e.g., Compagno, 1988). Thus, the general pattern of basicranial circulation

in elasmobranchs appears to be highly conserved, and it would seem most likely that *Tribodus* would conform to that paradigm, at least in terms of overall structure.

The internal carotid arteries extend forward within the basicranial cartilage beginning immediately anterior to the median foramen, and would have to enter the braincase somewhere posteriorly, either through the median foramen or through the foramina anterodorsal to the paired basicranial processes. The orbital arteries and efferent hyoidean arteries must also be accounted for.

In the first possible scenario of cranial circulation in *Tribodus*, the median basicranial foramen is interpreted as the internal carotid foramen (as in many extant neoselachians and *Egertonodus* as interpreted by Maisey, 1983), located where the internal carotid arteries converge to enter the braincase. Before entering the braincase, the internal carotid arteries diverge from a single median dorsal aorta posteriorly, which then divides into paired lateral dorsal aortae prior to anastomosing immediately external to the internal carotid foramen. According to this scenario, paired canals diverging posteriorly from the chamber above the internal carotid foramen are then explained as containing the efferent hyoidean arteries, the first pair of vessels to branch from the (now merged) internal carotid artery after its entry into the braincase. These canals emerge externally at the foramina above the paired basicranial processes. Immediately anterior to the junction with the efferent hyoidean arteries, the pair of canals originating in the space above the internal carotid foramen and exiting the braincase anterolaterally are then interpreted as having contained the orbital arteries. However, the posterolateral pair of foramina are then left without explanation. Anterior to the origin of the orbital arteries, the internal carotid artery would have again divided before continuing anteriorly as paired arteries

tunneling through the basicranial cartilage beneath the hypophyseal chamber, which emerge on the floor of the cranial cavity to meet the efferent pseudobranchial/ophthalmic arteries, and the optic arteries farther anteriorly.

After entering the cranial cavity and giving rise to the efferent pseudobranchial and ophthalmic arteries, the paired internal carotid arteries again continue anteriorly, diverging one more time to produce first the optic arteries, which curved laterally and exited the braincase through the optic foramen alongside the optic nerve, and finally the cerebral artery, which curved dorsally to supply the brain. The difficulty with accepting this scenario is that the efferent hyoidean and orbital arteries in chondrichthyans do not typically meet the internal carotids after they merge and enter the braincase, and such a pattern is unknown in any other fossil or extant elasmobranch. Also, the posterolateral foramina in the hypophyseal region remain unexplained. Additionally, there are no observable indentations on the external surface of the basicranium that could be consistent with the path of the internal carotids entering the median ventral foramen, although this does not necessarily mean they were not present.

In the second scenario of cranial arterial circulation, the paired posterior canals converging above the paired ventral processes are interpreted as containing the lateral dorsal aortae. After entering the braincase, the lateral dorsal aortae continue forward anteromedially and enter the median basicranial chamber above the hypophyseal foramen, giving rise first to the efferent hyoidean arteries (posteriorly) and then the orbital arteries (anteriorly) before turning mesially and anastomosing above the median ventral foramen (the “internal carotid” foramen of the previously described scenario). The efferent hyoidean arteries then curve outward posterolaterally, exiting the braincase

and passing along the posterolaterally directed grooves anterolateral to the paired ventral processes on their way to the hyoid arch. The orbital arteries exit the braincase through the paired foramina anterolateral to the median ventral foramen, as in the previous interpretation, and turn outward anterolaterally to enter the orbit. After anastomosing, the internal carotid arteries again diverge anteriorly, meeting the efferent pseudobranchial/ophthalmic, optic, and cerebral arteries as in the previous scenario. Because in this second scenario the internal carotid arteries enter the braincase through the paired posterior foramina, the medial basicranial foramen is left without explanation. Two possible interpretations are first, that this foramen represents a hypophyseal duct that remained open externally; or second, that the specimen is a juvenile in which the embryonic hypophyseal fenestra has not yet closed. However, other features of the braincase suggest that the specimen more likely represents an adult, leaving the explanation that an open hypophyseal duct was present in *Tribodus*. This interpretation is supported by the presence of a narrow internal canal (visible in CT scans) connecting the main hypophyseal chamber with the more posteroventral space beneath the dorsum sellae that opens ventrally through the median ventral foramen.

Each of the above-described scenarios is problematic. In the first scenario, although the internal carotid arteries enter the braincase through a central foramen as previously hypothesized in other hybodonts (i.e., *Egertonodus*, Maisey, 1983), the efferent hyoidean and orbital arteries join the internal carotid artery only after it anastomoses and enters the braincase, a key difference from most extant neoselachians and fossil chondrichthyans. Also, the pair of posterolateral foramina remain unexplained. In the second scenario, an open hypophyseal foramen is considered to have been present (unlike adult extant

neoselachians). However, although the efferent hyoidean and orbital arteries join the lateral dorsal aortae after the latter structures enter the braincase (unlike most neoselachians), they do so posterior to the anastomosis of the internal carotids (as in most elasmobranchs). Therefore, the second scenario of cranial circulation in *Tribodus* is accepted here as the more plausible of the two.

*EGERTONODUS*: Digital reconstructions of the braincase of *Egertonodus basanus* made from CT scan slices as part of the present thesis confirm Maisey's (1983, fig. 25) reconstruction of its basicranial circulation. These images show that the internal carotid arteries in *Egertonodus* most likely entered the braincase through the median basicranial foramen (Maisey, 1983: fig. 9b; this paper, Fig. 50A), converging into a single vessel just prior to entering the braincase. They then diverged anteriorly into left and right branches. These branches then diverged again a few millimeters anterior to the internal carotid foramen, producing a laterally directed branch (the combined ophthalmic/efferent pseudobranchial artery, which exited the braincase via a common foramen, and then presumably diverged as in extant neoselachians), and an anterior branch (giving rise to the optic artery, which exited the braincase via the optic foramen alongside the optic nerve).

## PROBABLE EXTENT OF THE EMBRYONIC CARTILAGES IN *TRIBODUS* AND *EGERTONODUS*

A reconstruction of the embryonic cartilages in *Tribodus* and *Egertonodus* is presented in Figure 51, on the basis of morphological landmarks described by Holmgren (1940) and Maisey (2005; 2007). The positions of the efferent pseudobranchial artery and pituitary vein foramina have been considered to be of developmental significance, in

marking the anterior and posterior extent of the embryonic polar cartilage, respectively (Maisey, 2007). These foramina are usually situated in the posterior of the orbit, in the region between the optic nerve foramen and the postorbital process. In neoselachians, the efferent pseudobranchial foramen is nearly always anterior to that of the pituitary vein (however, in embryos of the batoid *Torpedo ocellata* the two vessels briefly share a single foramen; Holmgren, 1940, pp. 204–227, fig. 162; and in *Torpedo* the embryonic polar cartilage is limited to a relatively narrow strip and never contacts the parachordals; Holmgren, 1940). The efferent pseudobranchial foramen is also typically located posterior to the optic and oculomotor foramina, at the same level as the optic foramen and ventral to the oculomotor foramen.

The general position of the efferent pseudobranchial foramen in *Tribodus* and *Egertonodus* is similar to that of neoselachians, with some variation between the two taxa (i.e., in *Tribodus* the efferent pseudobranchial foramen is on a level with the optic foramen, whereas in *Egertonodus* it is ventral to the optic foramen). Externally, the efferent pseudobranchial foramen in neoselachians is often located ventrally within an ovoid depression on the lateral surface of the braincase, interpreted as corresponding to the "trigemino-pituitary fossa" (Allis, 1914; De Beer, 1937). This is also the case in *Tribodus*, in which the efferent pseudobranchial artery (but not the pituitary vein) is located within the external trigemino-facialis fossa. In *Egertonodus*, the efferent pseudobranchial foramen is located slightly anterior to the main trigemino-facialis fossa. Although an opening for the pituitary vein in *Egertonodus* was not found previously (Maisey, 1983), digital reconstructions indicate that its pituitary vein was located within the trigemino-facialis recess, somewhat above and posterior to the efferent

pseudobranchial foramen and slightly anterior to the internal carotid foramen. This indicates that the polar cartilage in *Egertonodus* probably had a somewhat limited anteroposterior extent. In contrast, the pituitary vein in *Tribodus* is more posteriorly located, medial to the postorbital process on a level with the anterior part of the otic region. The hypophyseal foramen is located even farther posteriorly, indicating that the polar cartilage (which typically surrounds the hypophyseal foramen) was probably more extensive in *Tribodus* than in *Egertonodus*. In extant neoselachians, the dorsal margin of the polar cartilage is usually indicated by the position of the optic pedicel. Because this structure is absent in *Tribodus* and *Egertonodus*, the dorsal extent of the polar cartilage is estimated here based on the approximate location of the optic pedicel, if one were present.

The parachordal plate generally forms the basicranial floor, from the back of the dorsum sellae posteriorly to the occipital arch. It appears to have been less extensive in *Tribodus* than in *Egertonodus*, based on the more posterior position of the hypophyseal foramen and dorsum sellae in *Tribodus*. Anteriorly, the trabecular cartilage generally extends forward from the efferent pseudobranchial foramen, and its dorsal margin is delimited by the optic foramen. The trabeculae extend anteriorly to the rostrum, along the medioventral portion of the braincase. In *Tribodus* and *Egertonodus*, the trabeculae probably formed the median basicranial process and caudal internasal keel, respectively, as well as the rostral bar. The trabeculae probably also contributed to the ethmopalatine processes in *Egertonodus*. According to Cerny et al. (2004), the dorsal part of the first pharyngeal arch (possibly representing an ancestral premandibular arch) forms the trabeculae in the anteroventral part of the braincase, whereas the vertebrate jaw

(palatoquadrate and Meckel's cartilage) is derived from cranial neural crest cells from the ventral part of the first pharyngeal arch. The dorsal part of the orbit (between the optic foramen and superficial ophthalmic foramina) is typically formed by the orbital cartilage in extant elasmobranchs (El-Toubi, 1949). It contains the trochlear and oculomotor foramina, and its posterior margin is formed by the trigemino-facial foramina (marking the position of the embryonic incisura prooticum). Dorsal to this, the supraorbital crest (lateral to the dorsal row of superficial ophthalmic foramina) is formed by the supraorbital cartilage in *Squalus* (El-Toubi, 1949). The anterior roof of the braincase is usually formed by that cartilage and by the orbital cartilage (El-Toubi, 1949). The lamina orbitonasalis (lateral to the trabeculae) forms the anterolateral wall of the braincase lateral to the orbitonasal canal, including the antorbital or ectethmoid process (El-Toubi, 1949; De Beer, 1937). The latter is much more extensive in *Tribodus* than in *Egertonodus*, curving downward and posteriorly in the former to encircle most of the anterior portion of the orbit and forming an anteroventral attachment point for the preorbitalis muscle. The olfactory capsule forms as a separate, independent cartilage, which typically chondrifies fairly late in ontogeny (El-Toubi, 1949). Its presence in the *Tribodus* braincase adds support to the conclusion that this specimen represents a mature individual.

Much of the posterolateral part of the braincase is formed by the otic capsule, which contains the skeletal labyrinth including the semicircular canals. It extends from the level of the anterior ampulla posteriorly to the lateral otic process, and includes the dorsolateral margin of the glossopharyngeal foramen. Medial to this is the parietal fossa, whose anterior margin is formed by the synotic tectum. The taenia medialis, which forms the

floor of the parietal fossa, can be formed in extant elasmobranchs by either a posterior extension of the synotic tectum, or an anterior extension of the posterior tectum, where one is present (Holmgren, 1940). Whether a posterior tectum was present in hybodonts is difficult to determine. The posteriormost part of the braincase, including the occipital cotylus, was formed by the occipital arch (a derivative of the embryonic hyoid somite, together with the parachordals; Holmgren, 1940). Both *Tribodus* and *Egertonodus* have postorbital processes probably formed at least in part by a chondrified embryonic lateral commissure (as discussed above). This inference is based on the presence of a jugular foramen contained within the postorbital process in both of these forms, as well as on the pronounced ventral extent of their postorbital processes. The contribution of the lateral commissure was probably greater in *Egertonodus*, in which the ventral margin of the postorbital process merges with the basicranium (as in other known hybodonts, *Tristychius*, and many Paleozoic sharks). As discussed by Maisey (2008), the embryonic lateral commissure is most pronounced in Paleozoic chondrichthyans in which a postorbital articulation is present. Its contribution is significantly less in extant neoselachians (in which a postorbital articulation is generally absent except among hexanchiforms, i.e., *Notorynchus*). The lateral commisure of *Tribodus* is not shown in Fig. 51A (because the postorbital process and otic capsule are cut away to show the posterior of the orbit), but probably contributed to the ventrolateral portion of the postorbital process.

## FORMATION OF THE MEDIAL CAPSULAR WALL IN HYBODONTS AND NEOSELACHIANS

*Tribodus* is similar to *Egertonodus* and neoselachians in several aspects of its endocranial and skeletal labyrinth morphology, some of which have been addressed previously (Maisey & Carvalho, 1997; Maisey, 2004a; 2005; 2007). One of the most striking similarities is the presence of a medial capsular wall separating the skeletal labyrinth from the rest of the endocranial cavity. This structure is absent in Paleozoic chondrichthyans including *Cladodoides* and *Cobelodus* (Maisey, 2005; 2007), as well as in chimaeroids and osteichthyans (e.g., *Mimia*: Gardiner, 1984; Maisey, 2005), and may represent a synapomorphy of hybodonts and neoselachians (although a medial capsular wall is also present in placoderms). In embryonic neoselachians, the anterior part of the medial capsular wall (anterior to the glossopharyngeal nerve) is formed primarily by a dorsal outgrowth of the basicapsular lamina, the "processus dorsalis" of De Beer (1937). Holmgren (1940) describes this process in 25 mm *Etmopterus*. The basicapsular lamina is in turn connected ventrally to the lateral margin of the parachordals, and laterally to the anterior rudiment of the otic capsule (Holmgren, 1940). Posterior to the glossopharyngeal nerve is the posterior part of the basicapsular lamina, and the posterior rudiment of the auditory capsule. Later in development (30 mm *Etmopterus*), a lamella from the anterolateral wall of the otic capsule extends downward medially, contributing to the anterior part of the medial capsular wall, and caudad to join the processus dorsalis. This cartilage and the processus dorsalis fuse to form the foramen for the octaval nerve. Posterior to the glossopharyngeal nerve, the medial capsular wall is formed by the cartilage of the posterior semicircular canal ('cartilage of Källberg,' Holmgren, 1940), which grows downward to fuse with the parachordals ventrally. The occipital column

rises anterodorsally, and together with the parachordal forms a foramen for the vagus nerve. This nerve marks the boundary between the cartilage of Källberg and the occipital column (Holmgren, 1940). In *Scyliorhinus*, the part of the medial capsular wall forms much as in *Etmopterus*, but with some developmental differences (e.g., in *Scyliorhinus* the cartilage of Källberg has a much lesser extent; Holmgren, 1940). In *Torpedo* and other rays (Holmgren, 1940), the cartilage of Källberg is apparently lacking, and an anterior and posterior processus dorsalis form the medial capsular wall anterior to the vagus nerve. Comparison of these representatives of extant rays, galeomorphs, and squaleans indicates that certain aspects of medial capsular wall formation are conserved among these groups (e.g., presence of a processus dorsalis anterior to the glossopharyngeal nerve; presence of a vagus foramen at the boundary between the occipital column and cartilage of Källberg (or posterior processus dorsalis in rays). This suggests that similar embryonic structures and processes may also have been present in hybodonts, including *Tribodus* and *Egertonodus*. It also indicates an absence of these developmental (and related genetic) pathways in Paleozoic chondrichthyans, holocephalans, and other outgroups (with the possible exception of placoderms).

### General comparison of *Tribodus* with *Egertonodus* and other elasmobranchs

Maisey (2004a, 2005) noted a number of additional similarities of the otic region between *Tribodus*, *Egertonodus*, and neoselachians (isolation of the posterior semicircular canal and its pre-ampullary extension to form a nearly complete circuit; absence of a crus commune and sinus superior; presence of perilymphatic fenestrae; out-of-plane orientation of the external canal; complete parietal fossa in the cranial roof;

complete closure of the otico-occipital fissure dorsally; complete closure of the embryonic metotic fissure ventrally; presence of a lateral otic process; anterior ampulla positioned between or in front of postorbital processes; occipital block wedged between otic capsules posteriorly; saccular floor lies in the same plane as cranial cavity). All of these features are confirmed by the present study. Maisey (2004a) also noted features that could not be detected in these fossil hybodonts because they involve soft anatomical structures (e.g., elaboration and enlargement of the crista neglecta; separation of utricular and saccular regions). Hybodontiforms and neoselachians differ from many Paleozoic chondrichthyans in that the latter have paired posterior foramina for the lateral dorsal aortae located far back on the basicranium near the occiput (e.g., *Tamiobatis*, *Orthacanthus*, *Cladodoides*; Schaeffer, 1981; Maisey, 2005). Presence of these structures may represent a synapomorphy uniting these and similar taxa as a group; or may alternatively represent a primitive condition of chondrichthyans.

Cranial features shared by *Tribodu*s and *Egertonodus* (which may represent hybodont synapomorphies) include: presence of separate foramina for the anterior and posterior rami of the octaval nerve; trochlear foramen anterior to optic foramen (noted by Maisey, 2004a); presence and arrangement of three foramina for the trigemino-facial-anterodorsal lateral line complex (superficial ophthalmic complex, trigeminal-anterodorsal lateral line complex, and hyomandibular ramus of the facial nerve); presence of cephalic spines in males (e.g., Maisey, 1982, 1983, 1987, 1989; Brito and Ferreira, 1989; Antunes et al., 1990; Brito, 1992; Maisey and Carvalho, 1997); shared glossopharyngeal-vagus foramina (previously noted by Maisey, 2004a); absence of an optic pedicel. The Carboniferous 'hybodontiform' *Tristychius* shares some features with *Tribodus* and *Egertonodus*, but

lacks others: like hybodonts and neoselachians, in *Tristychius* the embryonic otico-occipital, ventral, and metotic fissures are closed in the adult, and posterior ventral foramina for the lateral dorsal aortae are lacking. As in hybodonts, there is no evidence of an optic pedicel, and according to Dick (1978) the trochlear nerve foramen may have been located anterior to the optic nerve. However, unlike hybodonts, there is no evidence of cephalic spines in *Tristychius*; its glossopharyngeal and vagus foramina are separate as in neoselachians; and there appears to have been only a single, shared foramen for the trigeminal and facial nerves (Dick, 1978). Whether or not two foramina for the octaval nerve were present in *Tristychius* remains unknown. *Tristychius* also retains several conserved chondrichthyan features, including an elongate otico-occipital region not telescoped between the postorbital processes; a postorbital articulation of the palatoquadrate (although this differs somewhat from the 'archaeostylic' articulation found in other Paleozoic sharks, Maisey, 2008); and possibly even a crus commune and sinus superior (Dick, 1978). These details, along with additional postcranial features (e.g., the presence of two non-medial denticle rows on the posterior of the dorsal fin spines, and the posteriorly concave shape of the spines in cross-section, as in 'ctenacanths'), support the view that *Tristychius* was basal to the main hybodontiform lineage (either as a basal hybodontiform, or as an outgroup to euselachians, which includes hybodonts and neoselachians).

*Tribodus* is unique in having paired ventral basicranial processes, and also differs from other known hybodonts in lacking the following structures: a suborbital shelf; ethmopalatine processes; a caudal internasal keel; an ethmoidal articulation of the palatoquadrate; postorbital processes that contact the braincase ventrally; and a

basicranial arterial circuit mainly external to the cartilage. The postorbital processes of *Tribodus* are very short anteroposteriorly compared to *Egertonodus* and other hybodontoids. *Tribodus* is also unusual in having its median basicranial foramen (hypophyseal foramen) positioned far posteriorly, indicating a similar posterior extension of the polar cartilage, and suggesting a very short parachordal region. *Tribodus* and *Egertonodus* also share numerous primitive chondrichthyan features (e.g., presence of an open hypophyseal duct; presence of an elongated basicranial arterial circuit; postorbital processes formed largely by the lateral commissure; presence of a precerebral fontanelle; presence of a parietal fossa; jugular vein passes through postorbital process; occipital hemicentrum absent). These features are also present in *Tristychius* and Paleozoic outgroups. Further study, particularly involving CT scanning to examine internal cranial anatomy of *Tristychius* and other outgroups (where possible), is necessary to reveal additional similarities and differences between these forms and crown-group elasmobranchs. Because complete neurocrania are currently known in only two hybodontiforms (Tribodus and Egertonodus), and the state of preservation of other fossil hybodonts precludes comparison of many features (including the number of trigemino-facial foramina, pattern of cranial circulation, skeletal labyrinth, and internal cranial morphology), inclusion of such features in a phylogenetic analysis would at present be premature and would succeed only in increasing the amount of missing data in the analysis. However, features that are also observable in other hybodonts as well as outgroup taxa may be included in phylogenetic analysis, and are potentially informative. Such characters are included in the character list in part III of this dissertation.

# CONCLUSIONS

The braincase of the Lower Cretaceous hybodont shark *Tribodus limae* was examined using high-resolution CT scanning, and its internal and external morphology were described based on three-dimensional digital reconstructions. This study represents the first in-depth examination of a hybodont braincase using CT scanning and digital imaging technology. The braincase of an additional Lower Cretaceous hybodont, *Egertonodus* basanus, was also digitally reconstructed and compared to *Tribodus*. A reconstruction of cranial nerves and blood vessels in *Tribodus* was presented on the basis of preserved foramina. The braincase of *Tribodus* shares many features with those of *Egertonodus* and neoselachians, providing further support for the sister-group relationship between hybodonts and extant elasmobranchs. CT scans confirm that in both *Tribodus* and *Egertonodus* the glossopharyngeal and vagus canals converge and exit from a common foramen (also found in *Chlamydoselachus*). In both of the hybodonts examined, the trochlear nerve exits the braincase anterior to the optic nerve, a possible hybodont synapomorphy. Separate foramina for the two rami of the octaval nerve are present in both *Tribodus* and *Egertonodus*, and may represent an additional hybodont synapomorphy. Also, both taxa have three separate foramina for the trigeminal, facial, and anterodorsal lateral line nerves, apparently including an individual foramen for the superficial ophthalmic complex. However, the basicranial arterial system in *Tribodus* differs considerably from that of *Egertonodus* in that the internal carotid arteries enter the braincase much farther posteriorly in the former, and through paired foramina rather than a single median foramen. The median ventral basicranial process in *Tribodus* is similar in structure and position to median ventral processes seen in some extant neoselachians

(e.g., *Etmopterus*), and in embryonic *Torpedo* (although in the latter this structure disappears during development), and thus may have had a similar ontogenetic origin.

FIGURE 14. Reproduction of original illustrations of the *Tribodus limae* braincase, modified from Brito (1992), in A, dorsal; B, ventral, and C, lateral views. Abbreviations (translated from the original French): **ald**, foramina for lateral dorsal aortae; **a.orb**, orbital artery; **cap.ot**, otic capsule; **c.j.**, jugular canal; **c.occ**, occipital cotylus; **csca**, anterior semicircular canal; ; **csce**, external semicircular canal; **cscp**, posterior semicircular canal; **f.end**, endolymphatic (parietal) fossa; **f.m.**, foramen magnum; **f.p.**, precerebral fontanelle; **q.int**, internasal keel; **p.art**, articular process for palatoquadrate; **p.ot.lat**, lateral otic process; **ppo.**, postorbital process; **V.opht**, superficial ophthalmic ramus of nerve V; **V + VII**, foramen for main branch of trigeminal and facial nerves; **VII hym**, foramen for hyomandibular branch of facial nerve; **IX + X**, glossopharyngeal-vagus foramen. Not to scale.

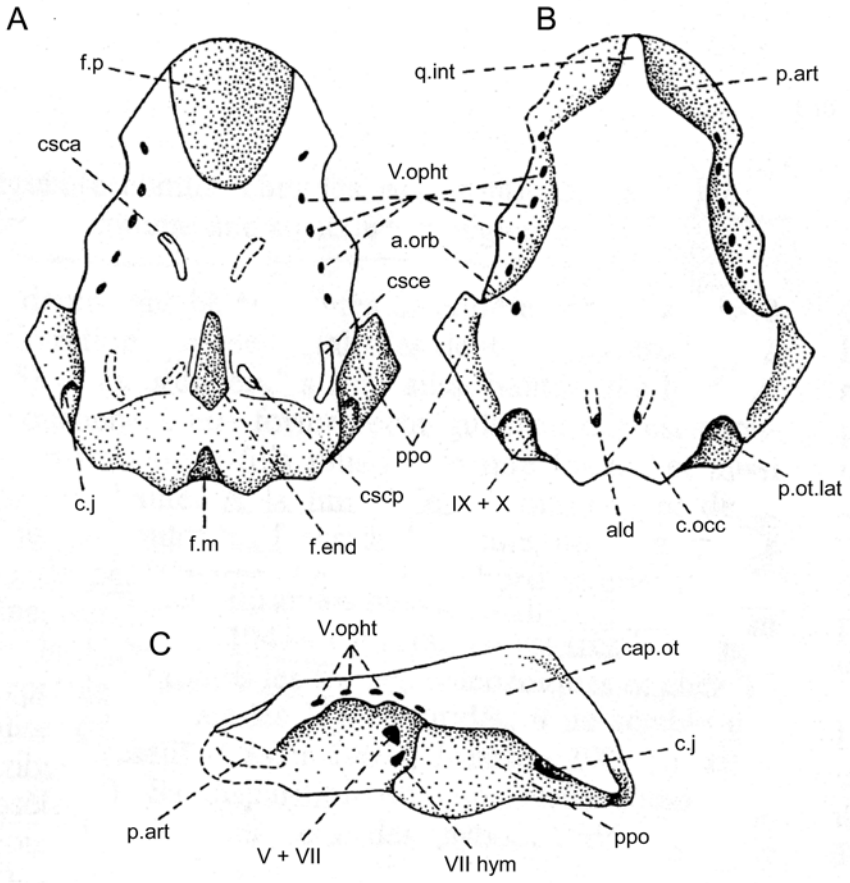

A
f.p
csca
V.opht
a.orb
csce
ppo
c.j
cscp
f.m
f.end
B
q.int
p.art
IX + X
ald
c.occ
p.ot.lat
C
V.opht
cap.ot
c.j
p.art
V + VII
VII hym
ppo

FIGURE 15. Transverse CT scan slices of the *Tribodus limae* braincase, AMNH 13958. Ethmoidal region. A, slice 57, through the olfactory chamber and precerebral fontanelle; B, slice 72, through the precerebral fontanelle showing the ventral exit of the orbitonasal canal; C, slice 83, through the precerebral fontanelle showing the orbitonasal canal traveling through the cartilage; D, E, F, slices 87, 89, and 94, respectively, through the precerebral fontanelle showing the course of the profundus nerve and orbitonasal canal; G, slice 100, at the level of the anterior cerebral canal; H, slice 159, through the anterior of the orbit at the level of the trochlear nerve and median ventral basicranial process. No scale.

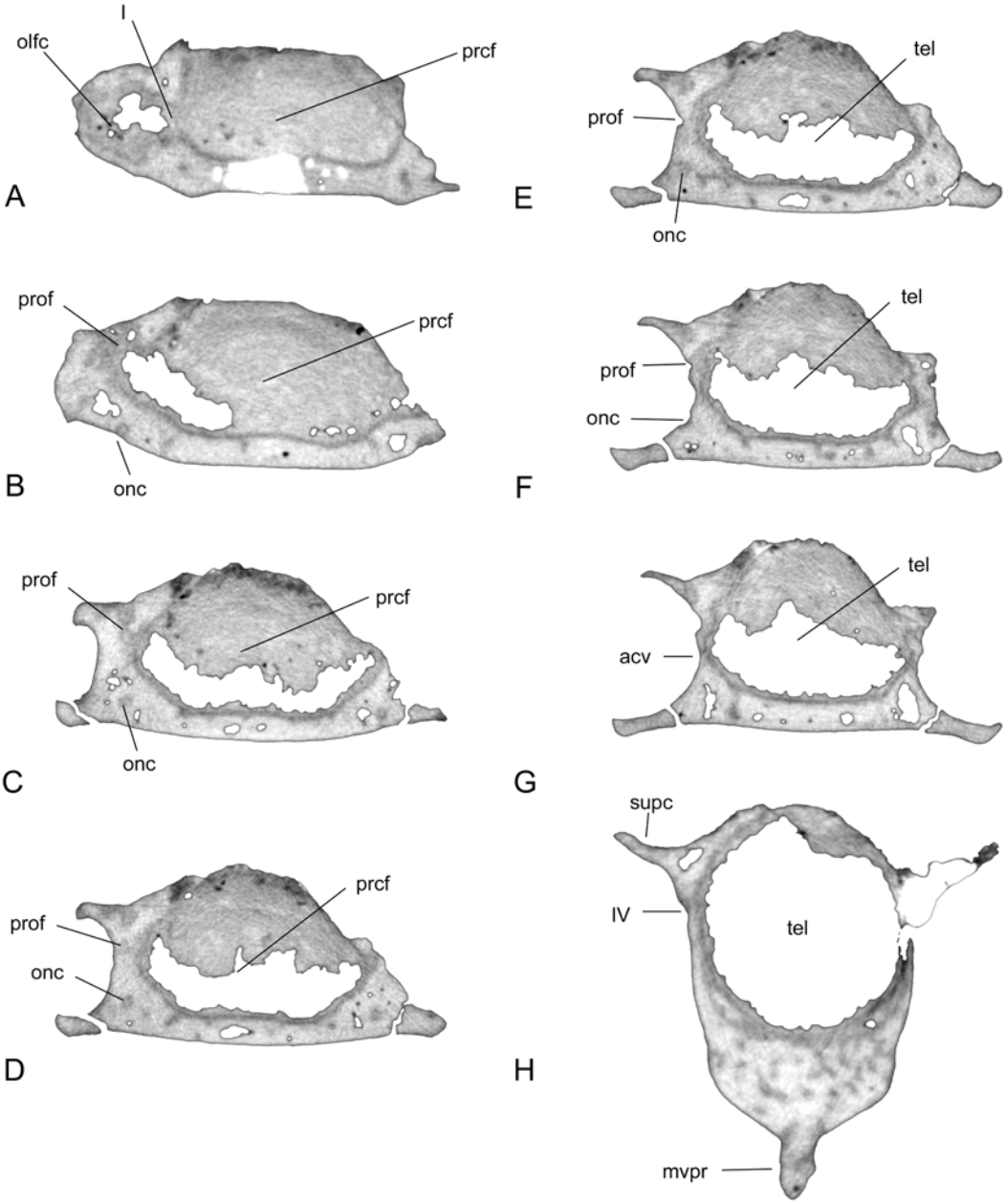

A
olfc
l
prcf
B
prof
prcf
onc
C
prof
prcf
onc
D
prof
onc
prcf
E
prof
tel
onc
F
prof
onc
tel
G
acv
tel
H
supc
IV
tel
mvpr

FIGURE 16. Transverse CT scan slices through the *Tribodus limae* braincase. Orbital region. A, slice 187, at the level of the optic nerve; B, slice 209, at the level of the oculomotor nerve; C, slice 216, at the level of the oculomotor nerve showing the anterior semicircular canal originating anterior to the postorbital process; D, E, slices 222 and 226, respectively, at the level of the efferent pseudobranchial foramen and the foramen for the superficial ophthalmic complex and profundus nerve; F, slice 239, at the level of the utricular recess and abducens foramen; G, H, slices 241 and 242, respectively, showing the course of the superficial ophthalmic complex and abducens nerve within the cartilage of the orbit. No scale.

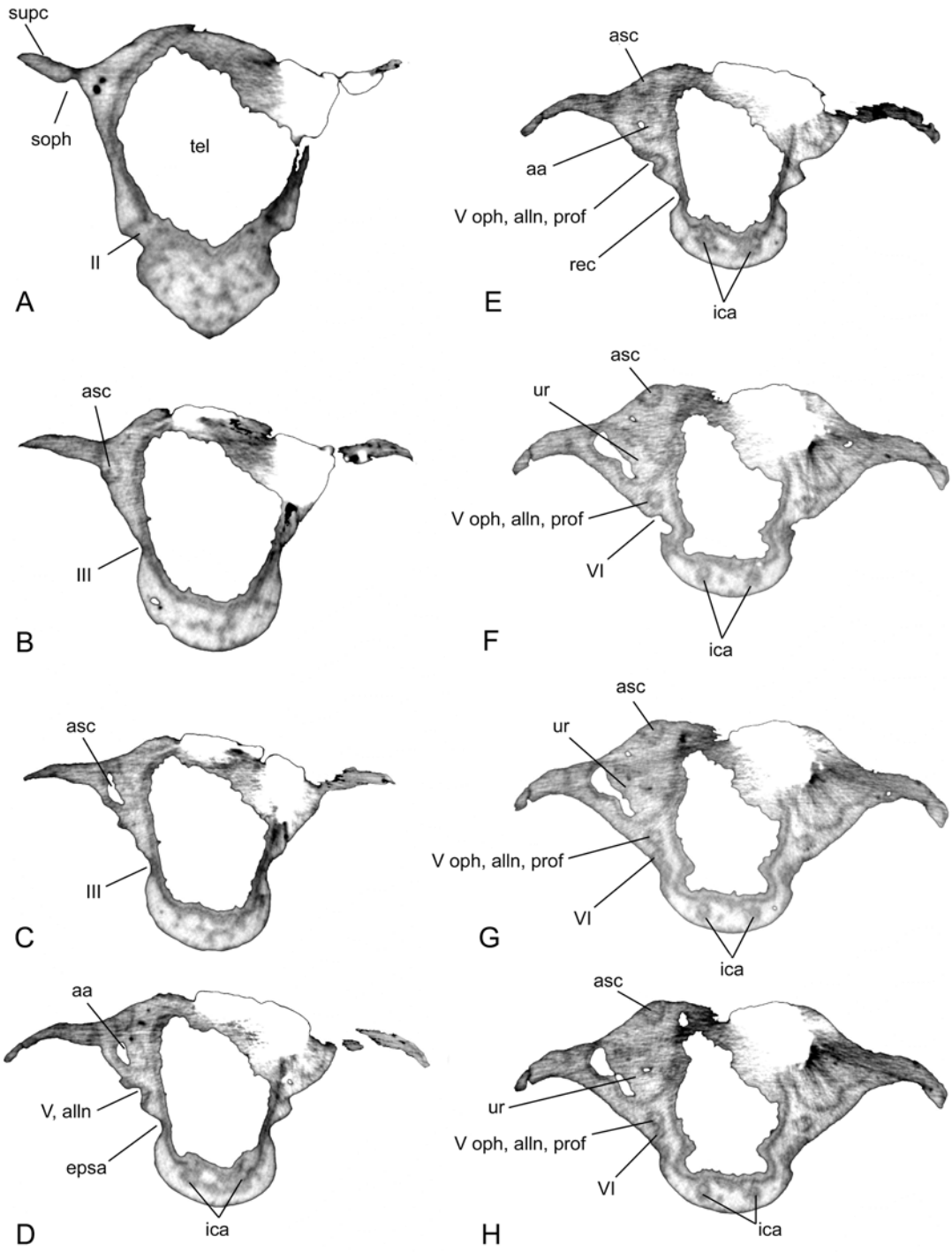

supc
soph
tel
II
A
asc
III
B
asc
III
C
aa
V, alln
epsa
ica
D
asc
aa
V oph, alln, prof
rec
ica
E
asc
ur
V oph, alln, prof
VI
ica
F
asc
ur
V oph, alln, prof
VI
ica
G
asc
ur
V oph, alln, prof
VI
ica
H

FIGURE 17. Transverse CT scan slices through the *Tribodus limae* braincase. Otic region. A, slice 257, at the level of the hypophysis and facial nerve; B, slice 270, showing the pituitary vein canal and the anterior ramus of the octaval nerve; C, slice 285, showing the hypophyseal duct and internal carotids; D, slice 290, showing the posterior ramus of the octaval nerve and the exit of the orbital arteries from the braincase; E, slice 298, at the level of the hypophyseal foramen; F, slice 303, showing the exit of the efferent hyoidean arteries from the braincase; G, slice 307, showing the canals for the lateral dorsal aortae converging to form a single chamber medial to the efferent hyoidean foramina; H, slice 313, showing the lateral dorsal aortae diverging posteriorly. No scale.

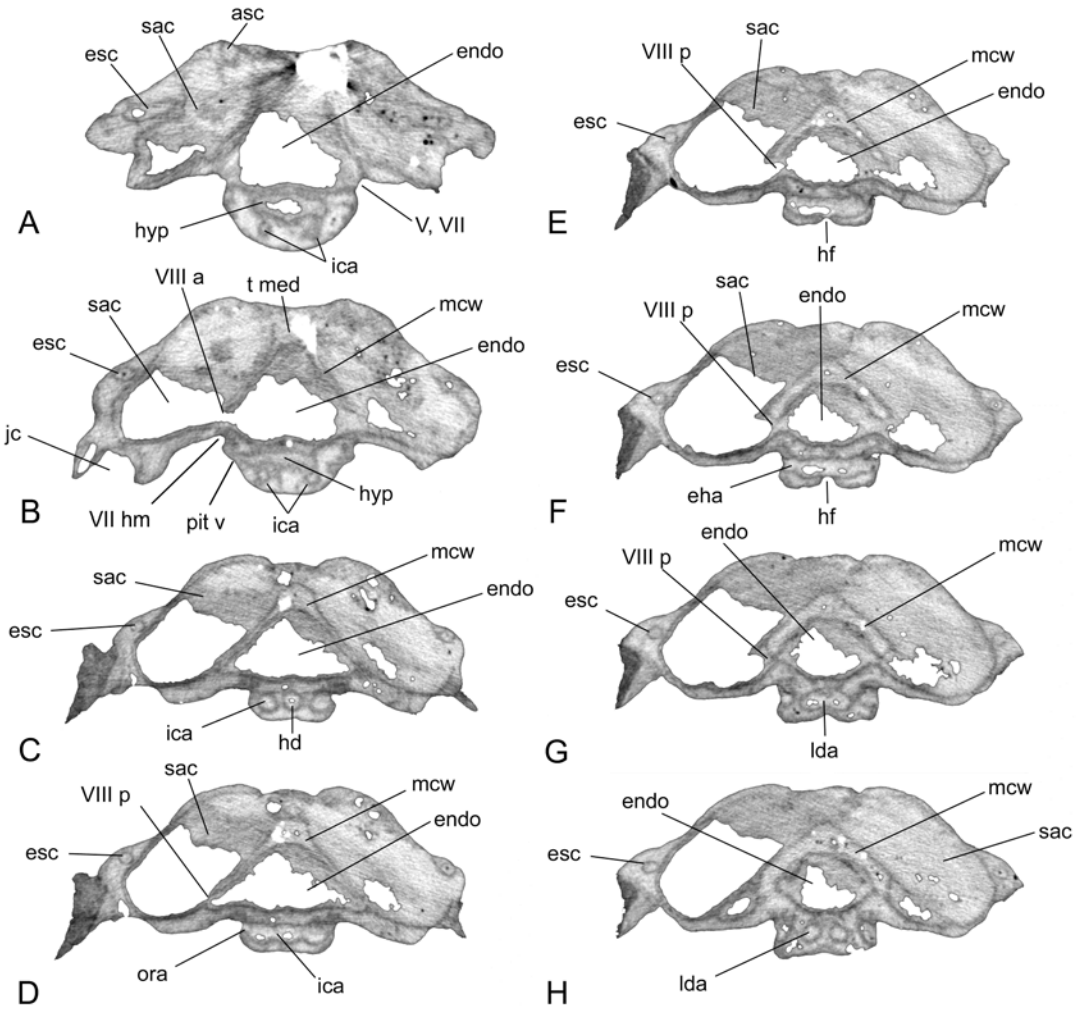

A
asc
sac
esc
endo
hyp
V, VII
ica
B
VIII a
t med
sac
mcw
esc
endo
jc
VII hm
pit v
ica
hyp
C
sac
mcw
esc
endo
ica
hd
D
sac
VIII p
mcw
esc
endo
ora
ica
E
sac
VIII p
mcw
esc
endo
hf
F
sac
endo
VIII p
mcw
esc
eha
hf
G
endo
VIII p
mcw
esc
lda
H
endo
mcw
esc
sac
lda

FIGURE 18. Transverse CT scan slices through the *Tribodus limae* braincase. Occipital region. A, slice 334, at the level of the preampullary canals and perilymphatic foramina; B, slice 369, at the level of the posterior ampullae and glossopharyngeal canal; C, slice 395, at the level of the vagus nerve; D, slice 400, at the level where the vagus canal exits into the glossopharyngeal foramen; E, slice 418, showing canals for the occipital arteries and spino-occipital nerves; F, slice 423, at the level of the occipital cotylus. No scale.

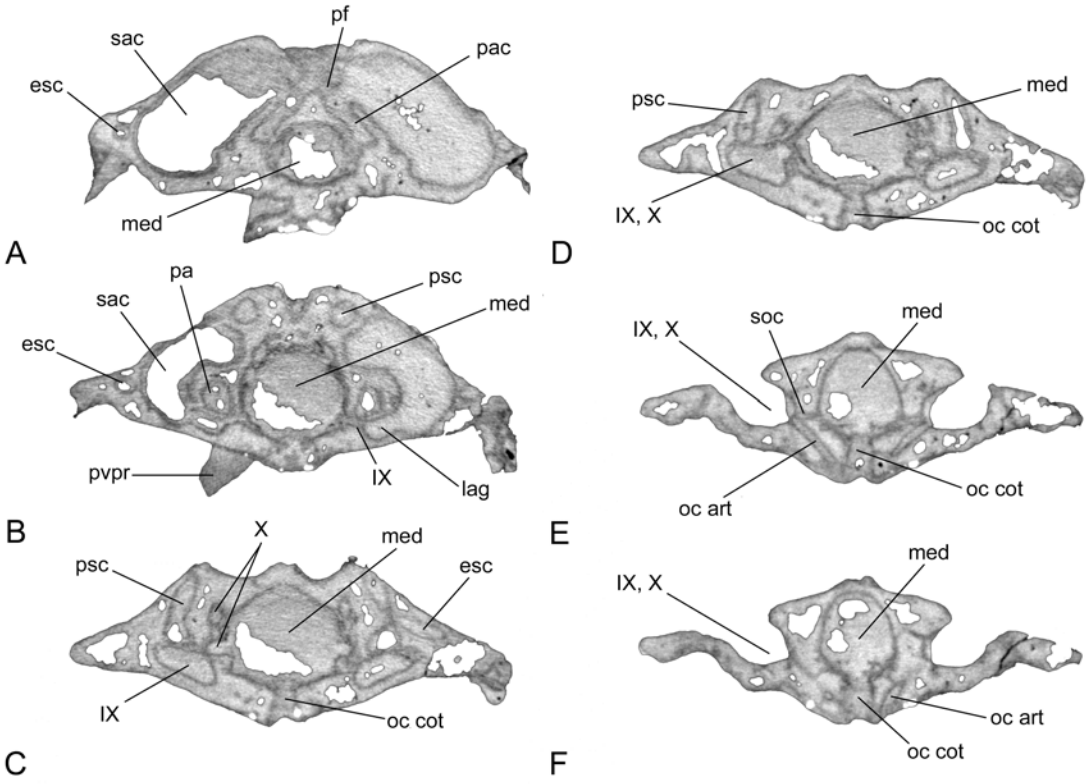

A
pf
sac
pac
esc
med
B
pa
psc
sac
med
esc
pvpr
IX
lag
C
X
med
psc
esc
IX
oc cot
D
psc
med
IX, X
oc cot
E
IX, X
soc
med
oc art
oc cot
F
med
IX, X
oc art
oc cot

FIGURE 19. Dorsal view of the *Tribodus limae* braincase, AMNH FF 13958, anterior at top (surface rendering). No scale.



FIGURE 20. Dorsal view of the *Tribodus limae* braincase, line drawing.

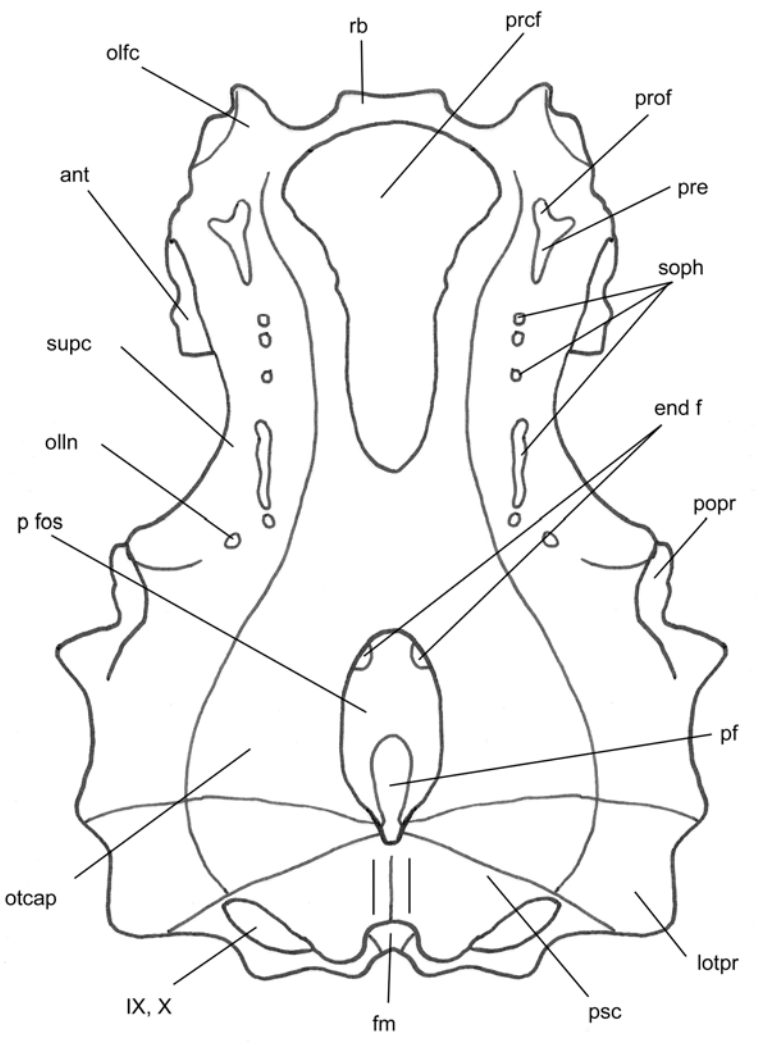

rb
prcf
olfc
prof
ant
pre
soph
supc
end f
olln
popr
p fos
pf
otcap
lotpr
IX, X
fm
psc

FIGURE 21. Ventral view of the *Tribodus* braincase, anterior at top (surface rendering). No scale.

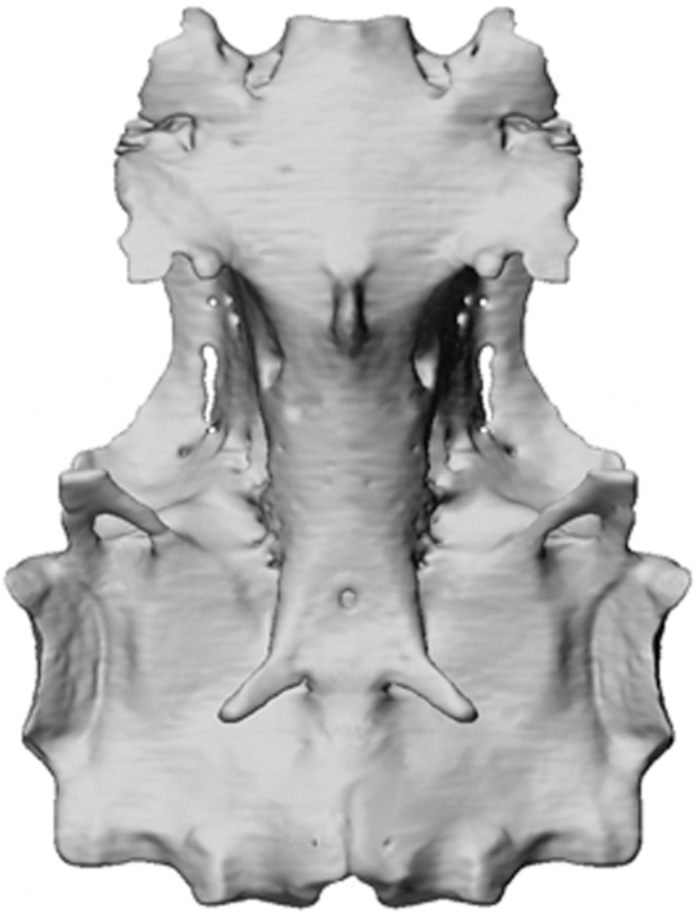


FIGURE 22. Ventral view of the *Tribodus* braincase, line drawing.

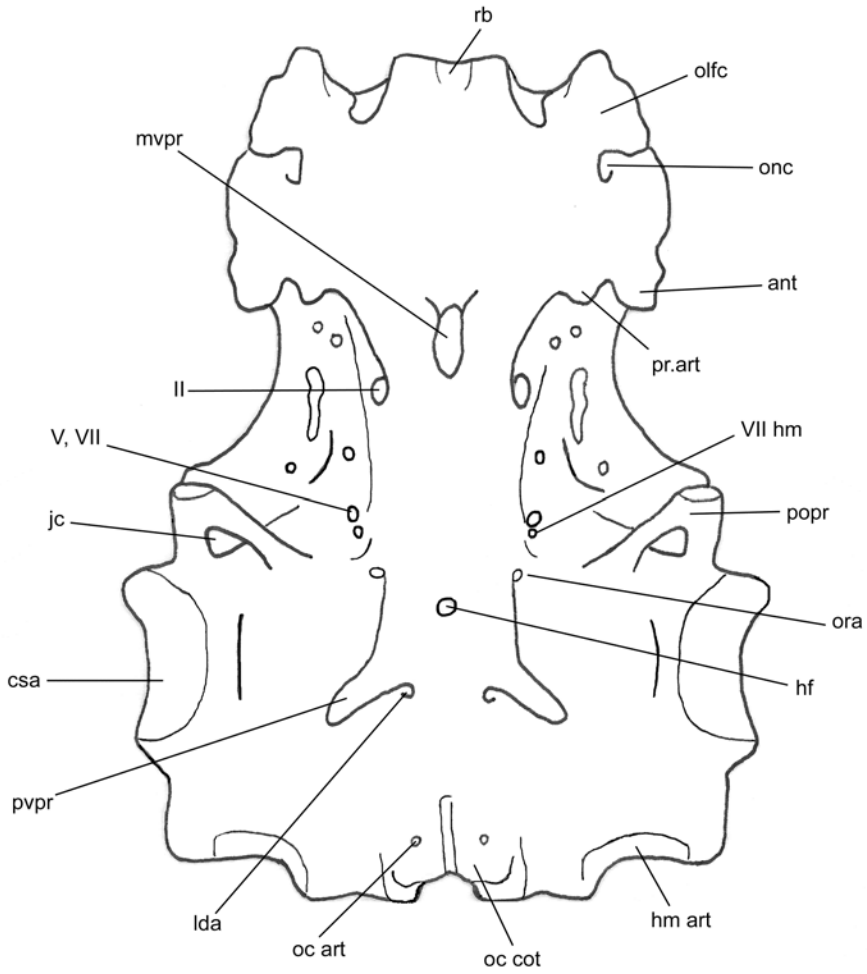
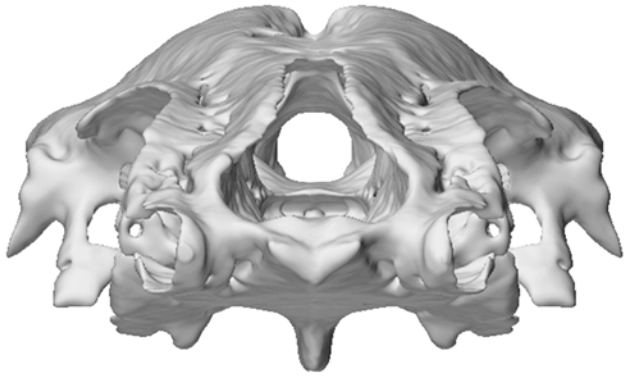
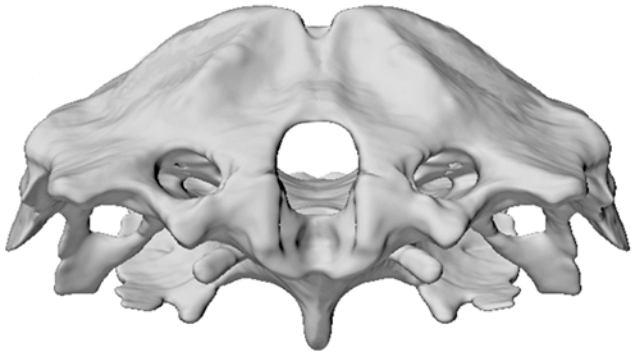

rb
olfc
mvpr
onc
ant
pr.art
II
V, VII
VII hm
jc
popr
ora
hf
csa
pvpr
lda
oc art
oc cot
hm art

FIGURE 23. Anterior (A) and posterior (B) views of the *Tribodus* braincase (surface renderings). No scale.



A



B

FIGURE 24. Anterior (A) and posterior (B) views of the *Tribodus* braincase, line drawing.

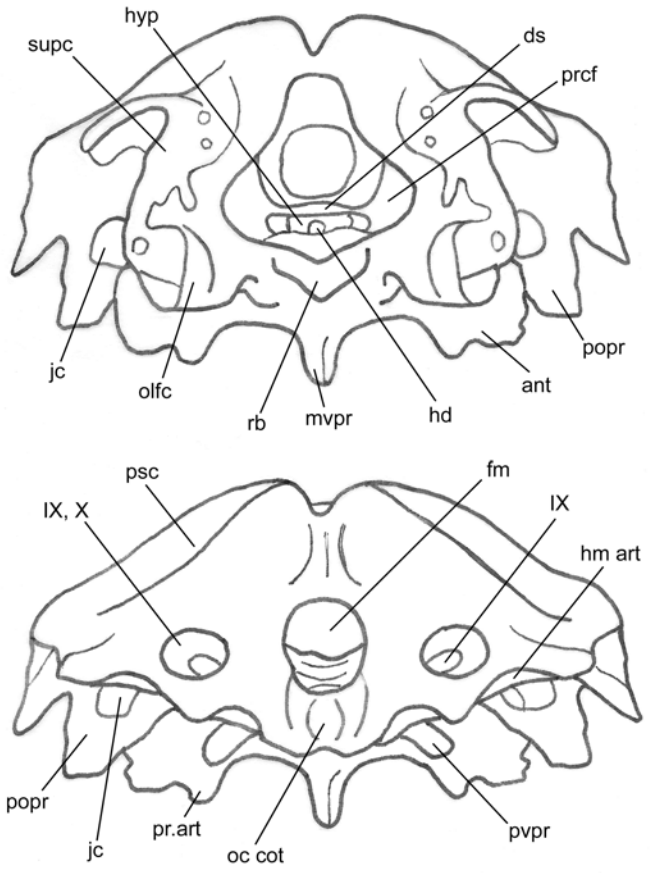

hyp
supc
ds
prcf
jc
olfc
rb
mvpr
hd
ant
popr
psc
IX, X
fm
IX
hm art
popr
jc
pr.art
oc cot
pvpr

FIGURE 25. Lateral view of the *Tribodus* braincase, anterior to the right (surface rendering). No scale.

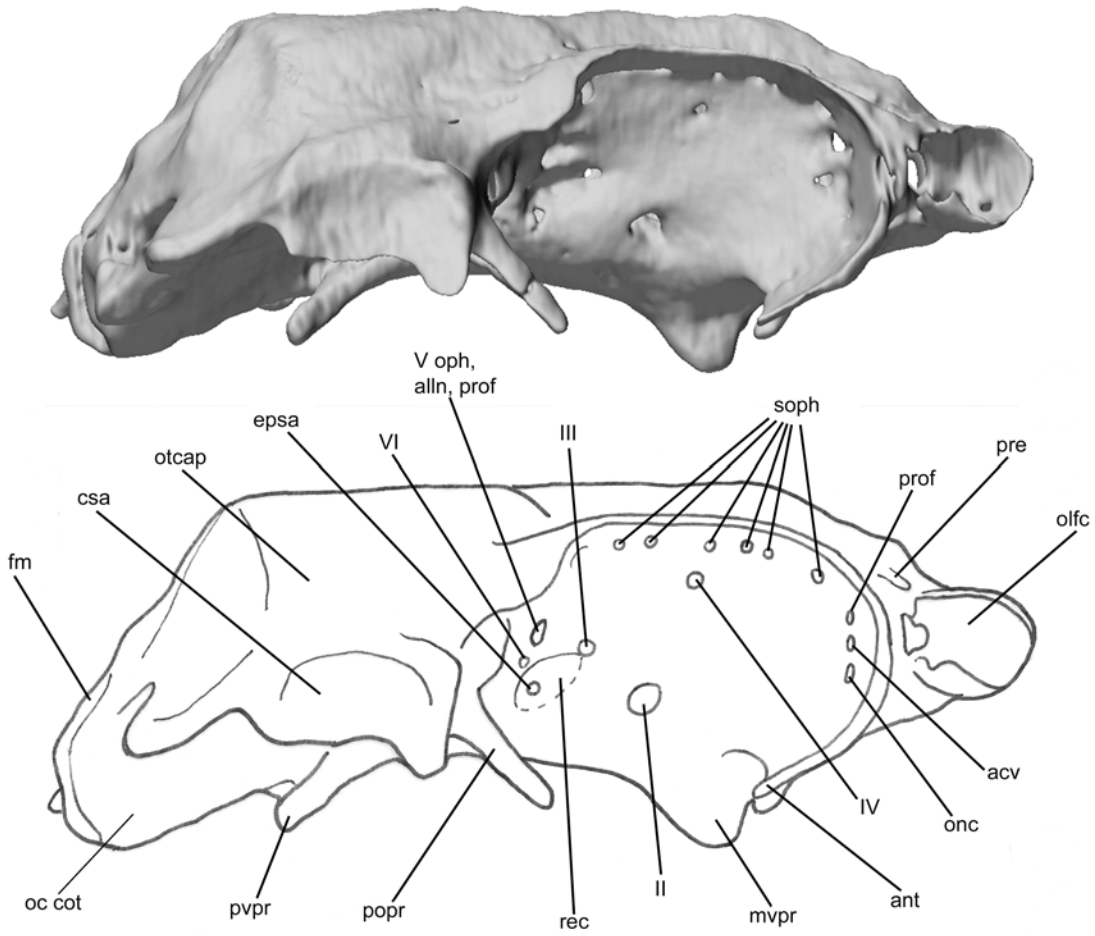

V oph,
alln, prof
soph
epsa
VI
III
otcap
pre
prof
csa
olfc
fm
acv
IV
onc
oc cot
pvpr
popr
rec
II
mvpr
ant

FIGURE 26. Medial view of the *Tribodus* braincase sliced through the sagittal plane, anterior to the left (surface rendering). No scale.

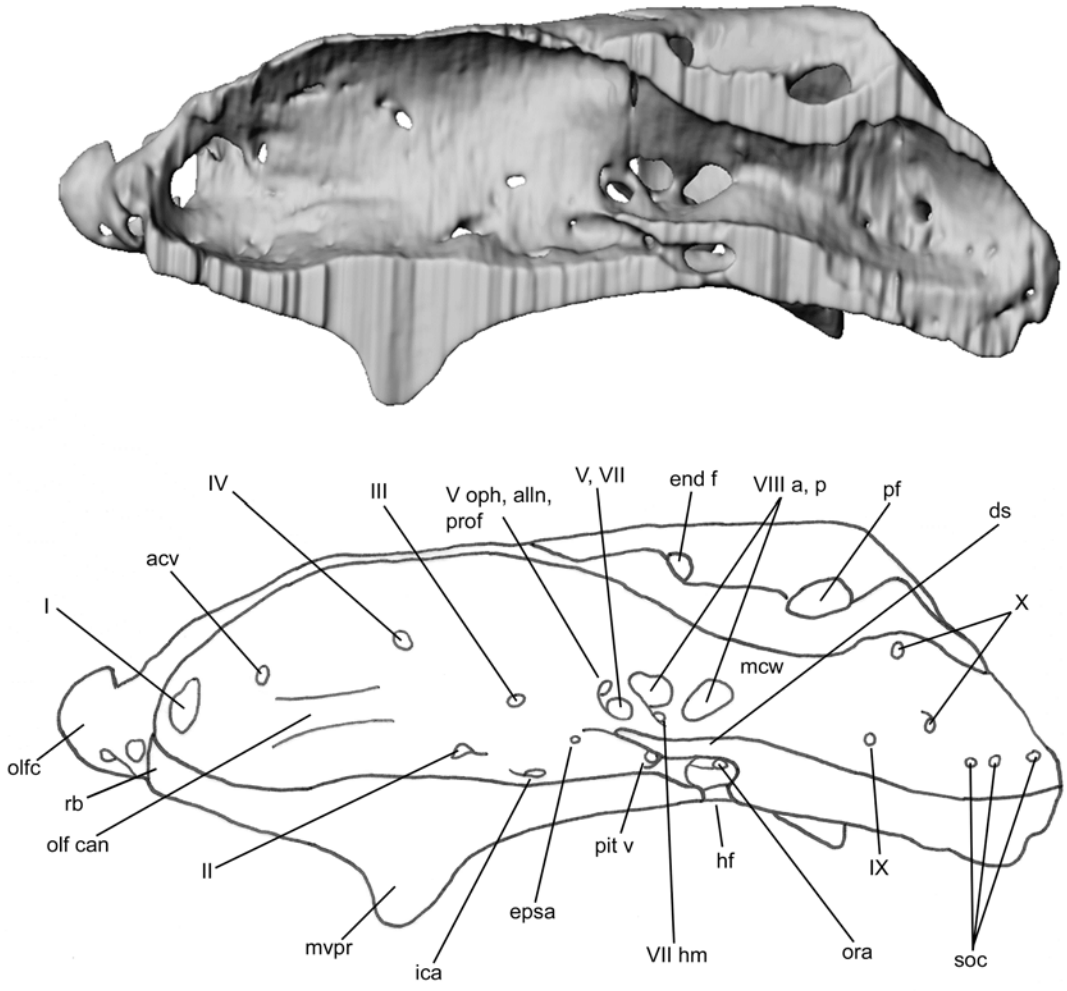

IV
III
V oph, alln, prof
V, VII
end f
VIII a, p
pf
ds
acv
I
X
mcw
olfc
rb
olf can
II
pit v
hf
IX
epsa
mvpr
ica
VII hm
ora
soc

FIGURE 27. Dorsal view of the *Tribodus limae* endocast with otic labyrinth removed, anterior at top (surface rendering). No scale.

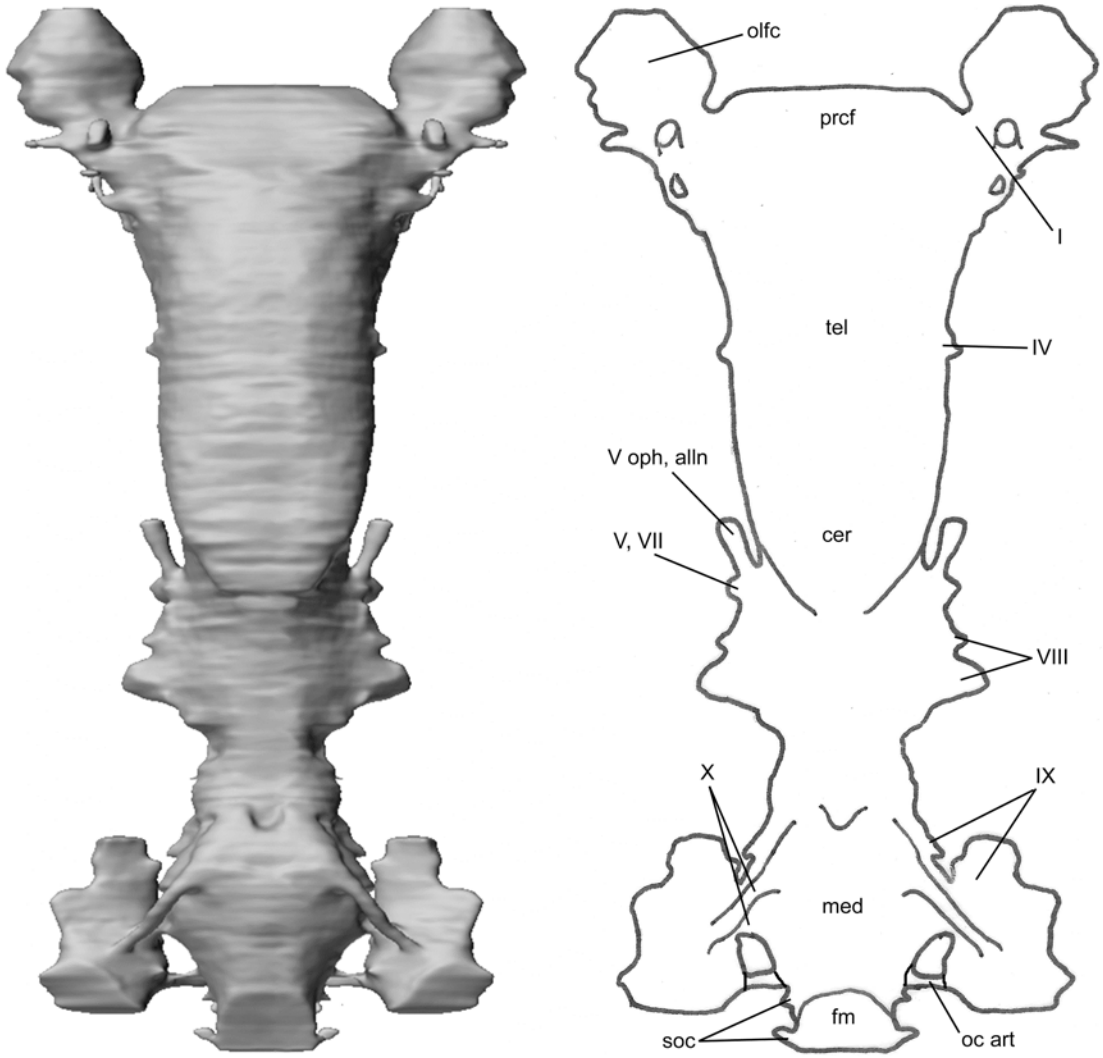

olfc
prcf
I
tel
IV
V oph, alln
V, VII
cer
VIII
X
IX
med
fm
soc
oc art

FIGURE 28. Ventral view of the *Tribodus limae* endocast with otic labyrinth removed, anterior at top (surface rendering). No scale.

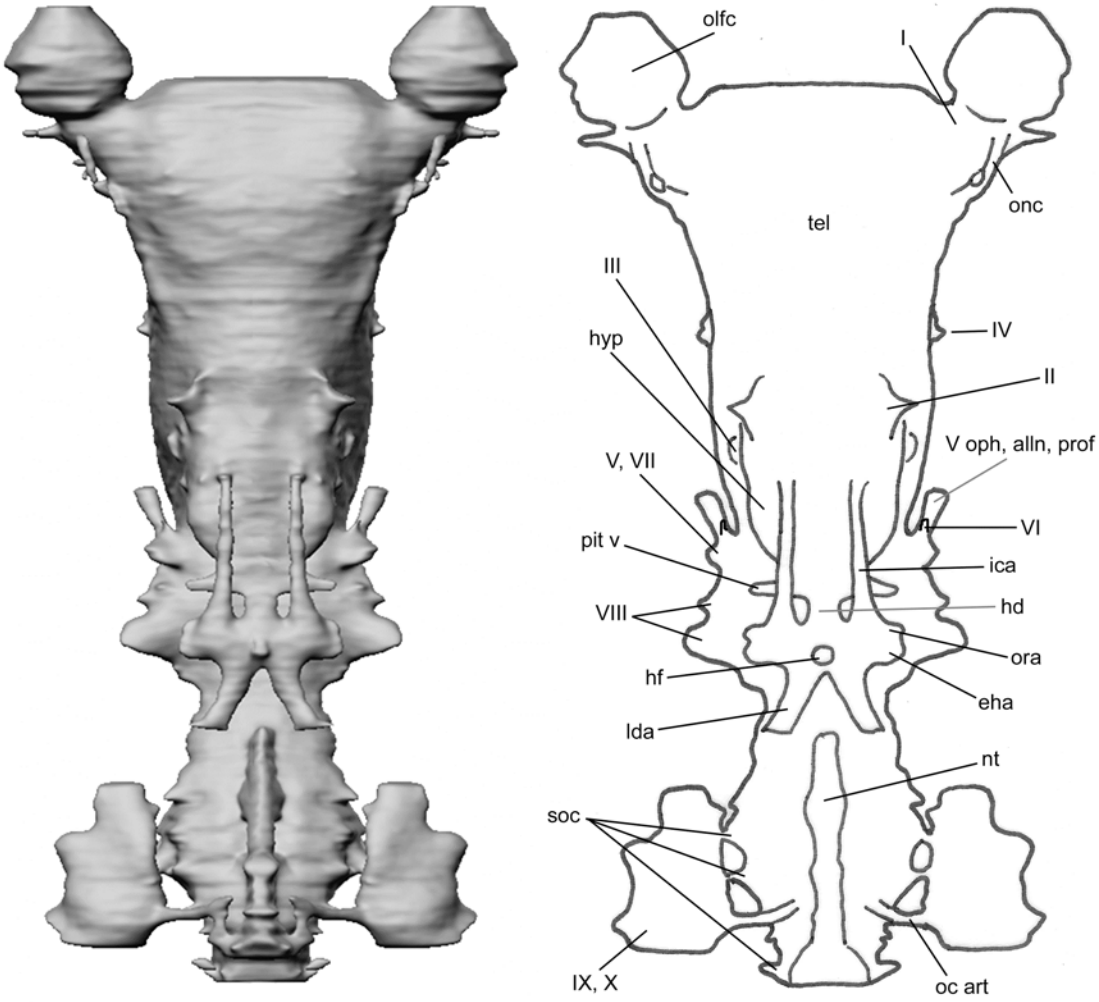
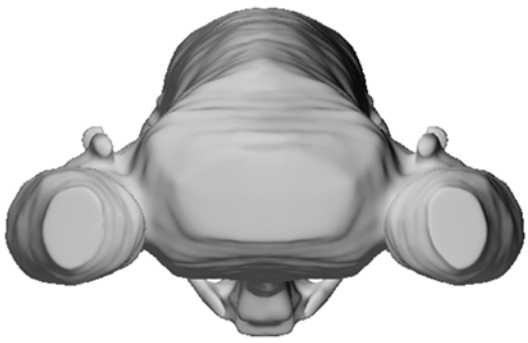
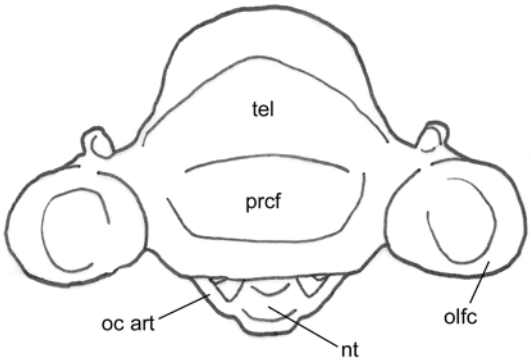
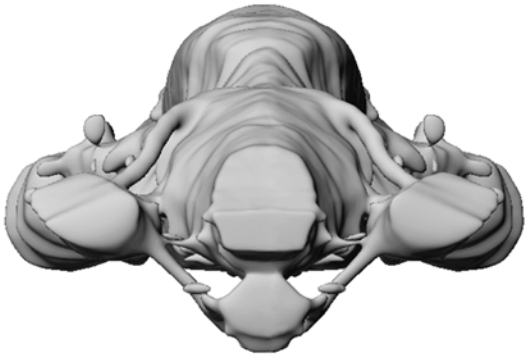

olfc
I
onc
tel
III
hyp
IV
II
V oph, alln, prof
V, VII
VI
pit v
ica
VIII
hd
ora
hf
eha
lda
nt
soc
IX, X
oc art

FIGURE 29. Anterior (A) and posterior (B) views of the *Tribodus* endocast with otic labyrinth removed, (surface renderings). No scale.



A



B

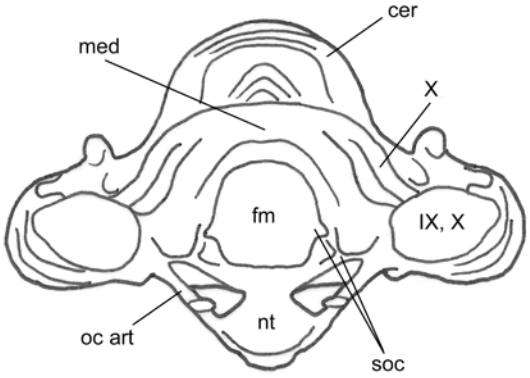


FIGURE 30. Lateral view of the *Tribodus limae* endocast with otic labyrinth removed, anterior to the right (surface rendering). No scale.

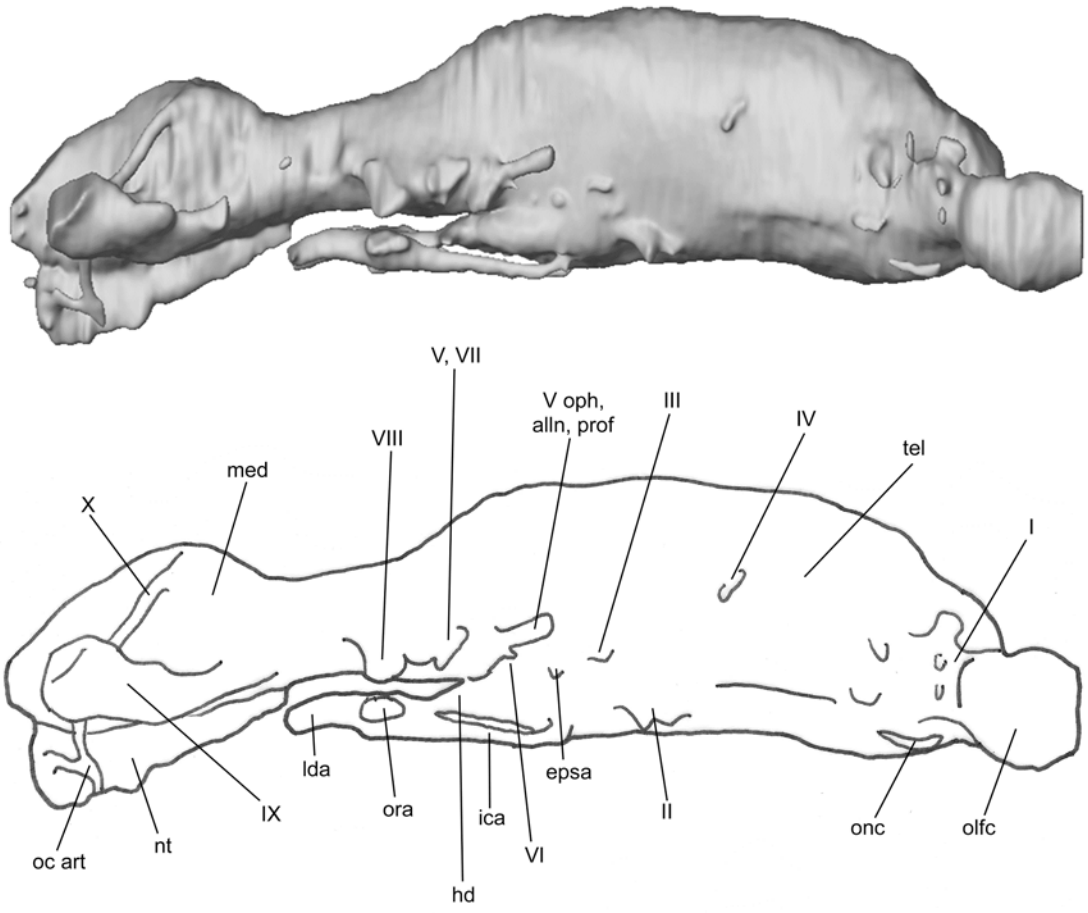

V, VII
V oph,
alln, prof
III
IV
VIII
tel
med
X
I
lda
epsa
IX
ora
ica
II
onc
olfc
nt
VI
oc art
hd

FIGURE 31. Dorsal view of the *Tribodus* endocast and skeletal labyrinth, anterior at top (surface rendering). No scale.

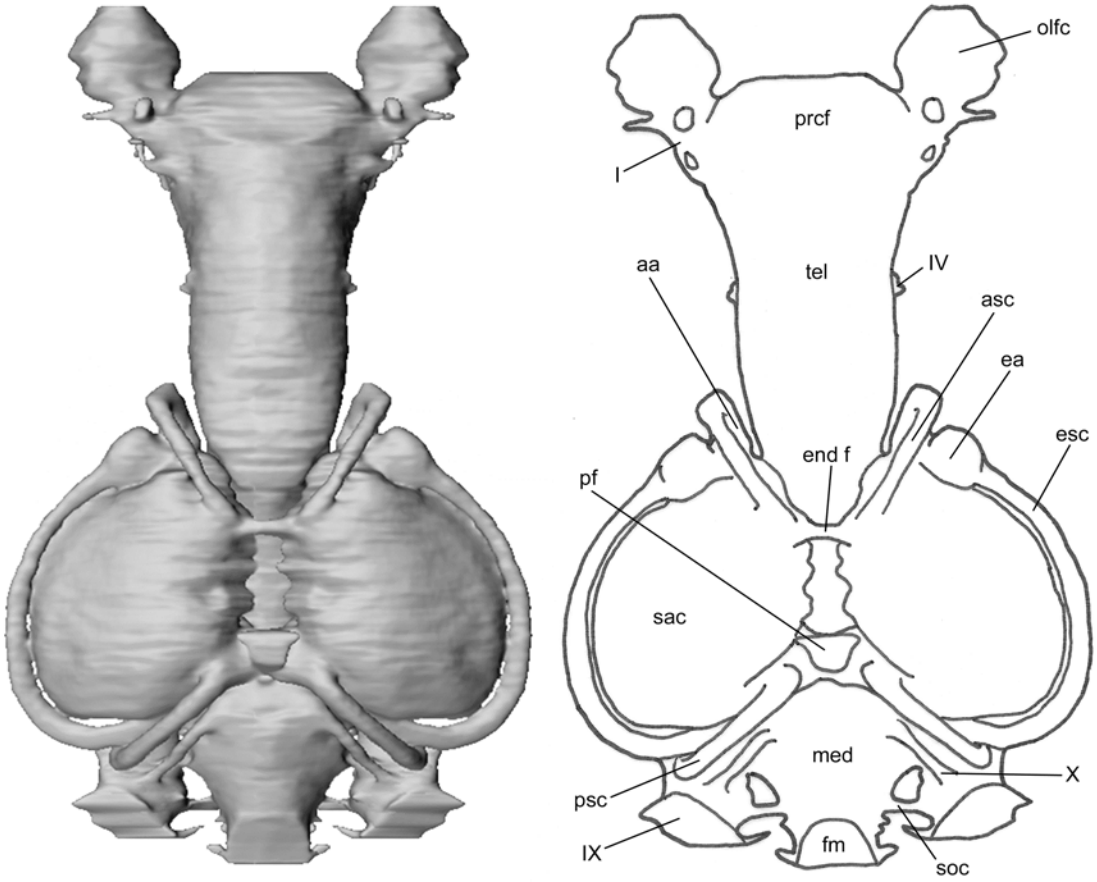

olfc
prcf
I
aa
tel
IV
asc
ea
esc
end f
pf
sac
med
X
psc
IX
fm
soc

FIGURE 32. Ventral view of the *Tribodus* endocast and skeletal labyrinth, anterior at top (surface rendering). No scale.

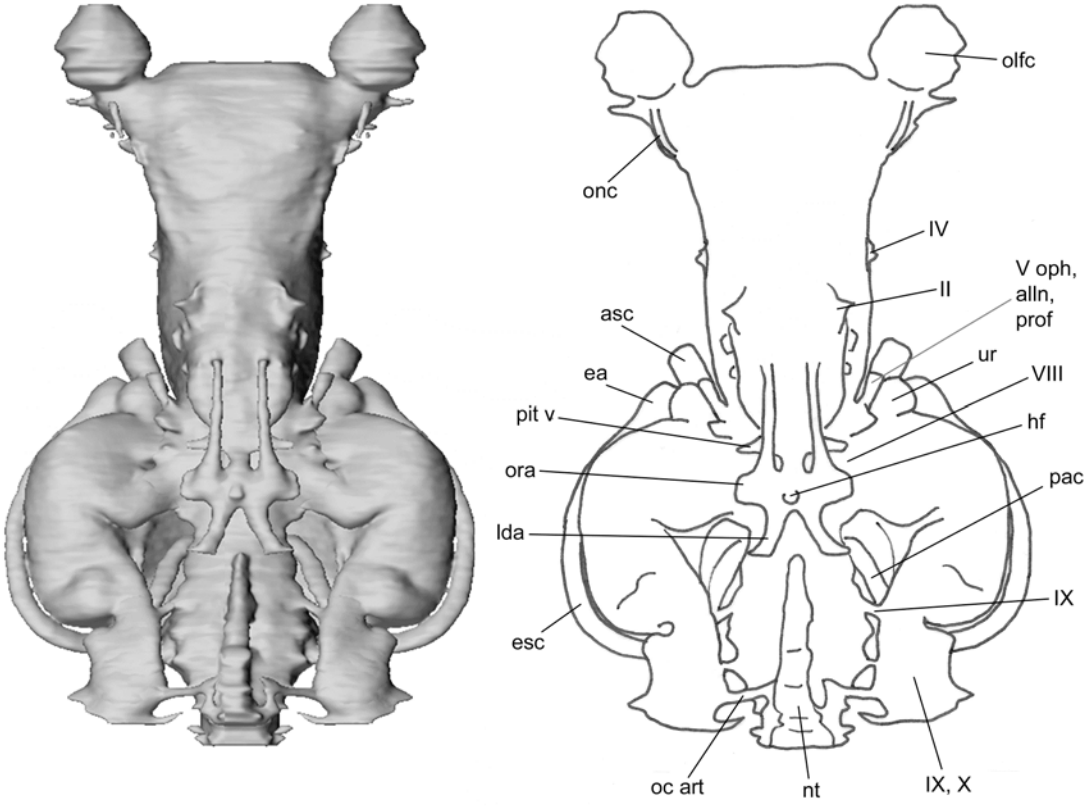

olfc
onc
IV
V oph,
alln,
prof
II
asc
ur
ea
VIII
pit v
hf
ora
pac
lda
IX
esc
oc art
nt
IX, X

FIGURE 33. Anterior (A) and posterior (B) views of the *Tribodus* endocast and skeletal labyrinth (surface renderings). No scale.

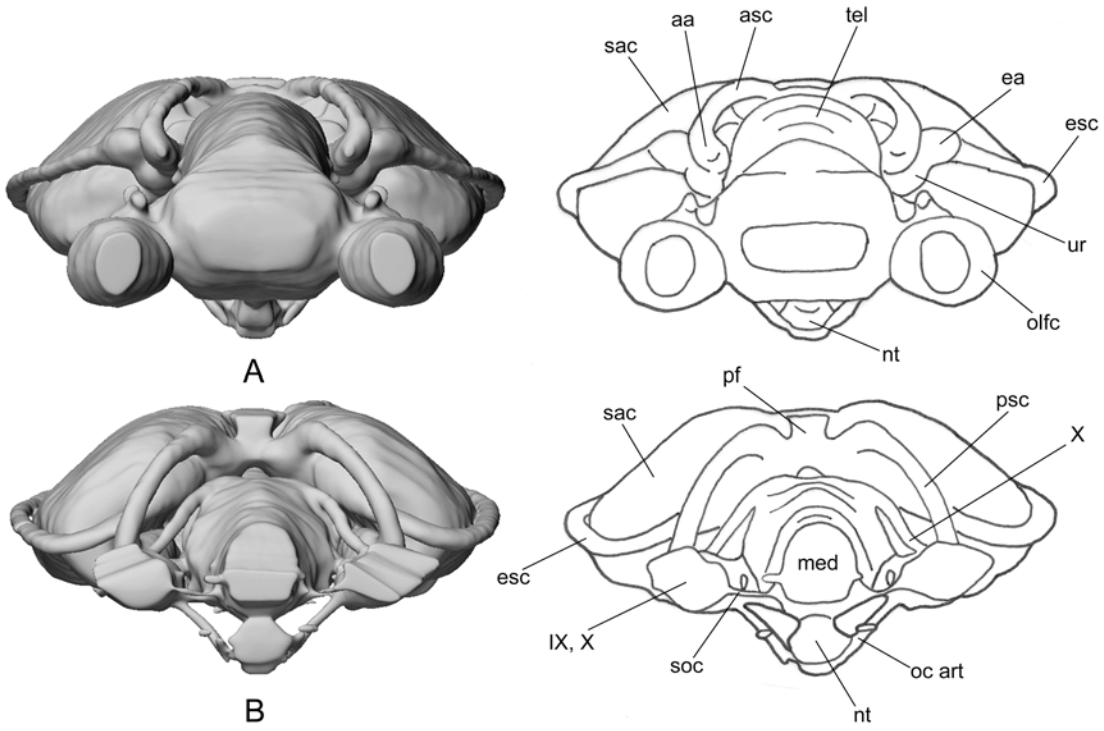

A
B
sac
aa
asc
tel
ea
esc
ur
olfc
nt
pf
sac
psc
X
esc
med
IX, X
soc
oc art
nt

FIGURE 34. Lateral view of the *Tribodus* endocast and skeletal labyrinth, anterior to the right (surface rendering). No scale.

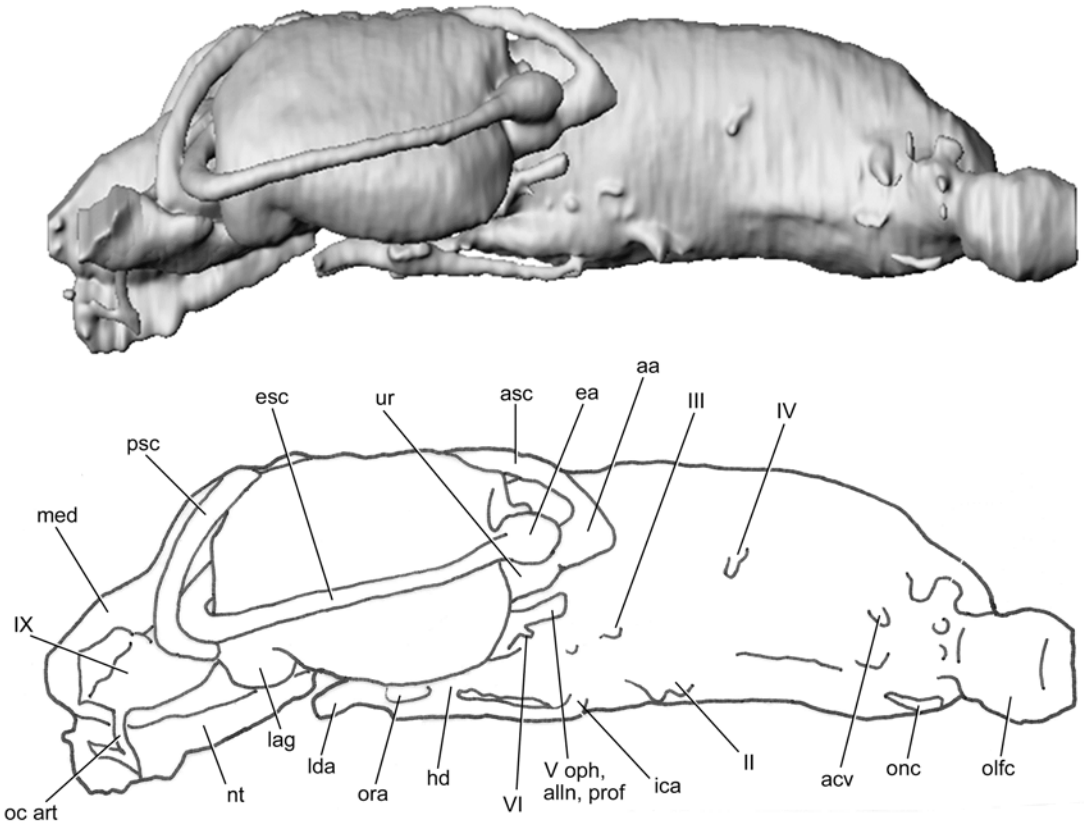

esc
ur
asc
ea
aa
III
IV
psc
med
IX
oc art
nt
lag
lda
ora
hd
VI
V oph,
alln, prof
ica
II
acv
onc
olfc

FIGURE 35. *Tribodus limae*, UERJ-PMB-40, closeup showing braincase in ventral view.



FIGURE 36. Close-up of posterior basicranial foramina in *Tribodus limae* (UERJ-PMB-40). Scale bar is 1 cm.

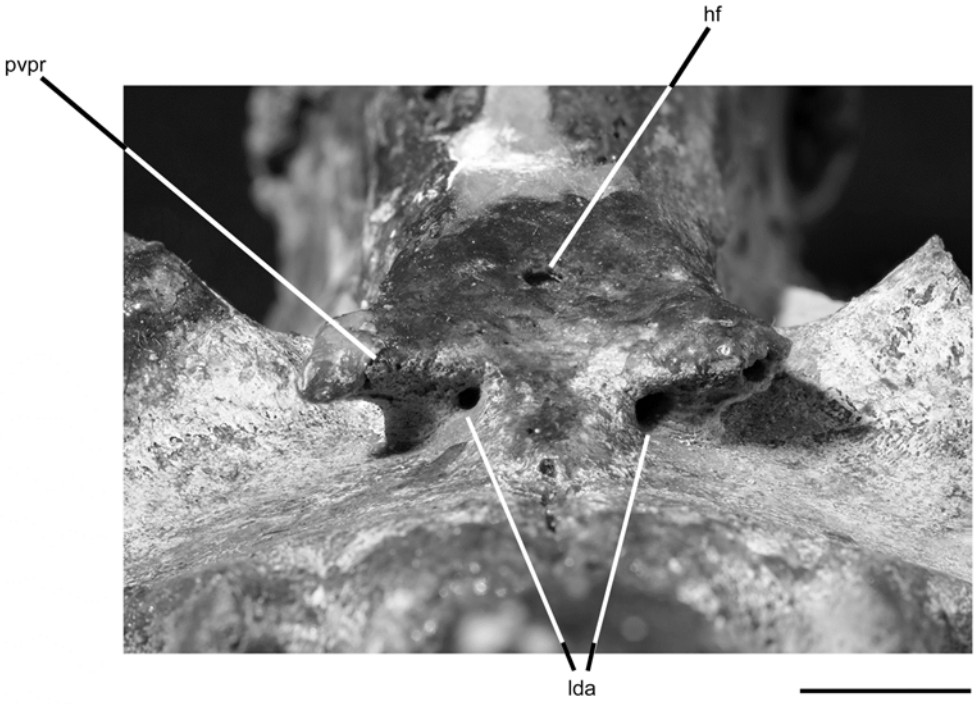

hf
pvpr
lda

FIGURE 37. Close-up of lateral basicranial foramina in *Tribodus limae* (UERJ-PMB-40). Scale bar is 1 cm.

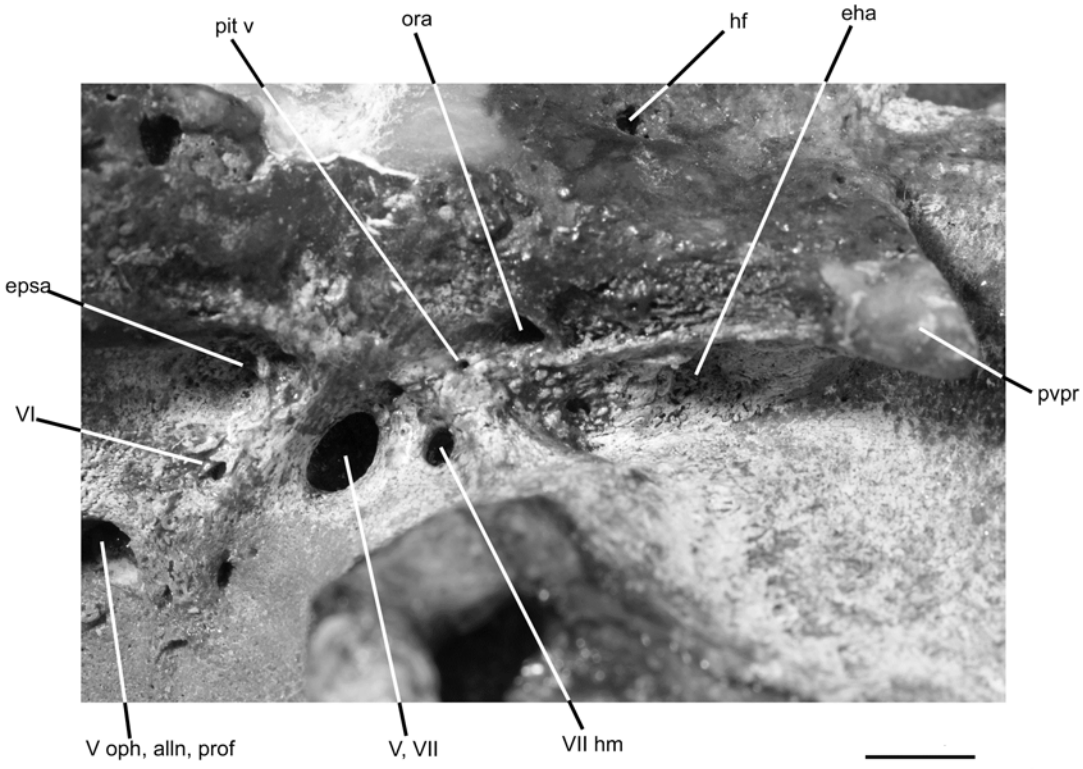

pit v
ora
hf
eha
epsa
pvpr
VI
V oph, alln, prof
V, VII
VII hm

FIGURE 38. Braincase of *Egertonodus basanus* NHM P60110, which was CT scanned for the present study. A, dorsal; B, ventral, and C, left lateral views. After Maisey, 1983. Features labeled according to Maisey's (1983) original description; an alternative interpretation is presented in Figs. 28–32 and in the text of the present thesis. Scale bar is 2 cm.

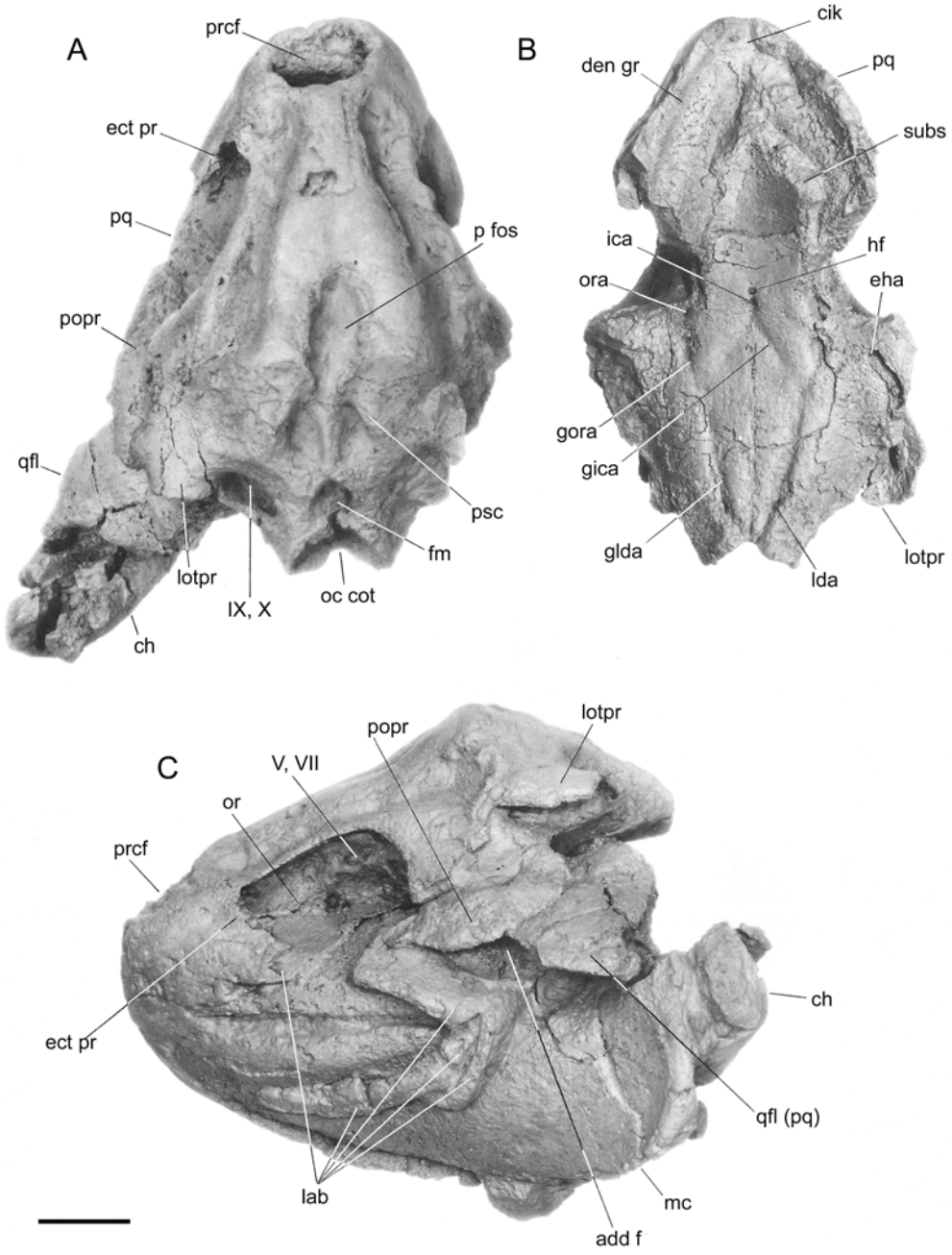

A
prcf
ect pr
pq
p fos
popr
qfl
psc
fm
lotpr
IX, X
oc cot
ch
B
cik
pq
den gr
subs
ica
hf
ora
eha
gora
gica
glda
lda
lotpr
C
lotpr
popr
V, VII
or
prcf
ch
ect pr
qfl (pq)
lab
mc
add f

FIGURE 39. Transverse CT scan slices of the *Egertonodus* braincase, NHM P60110. Ethmoidal and orbital regions. No scale.

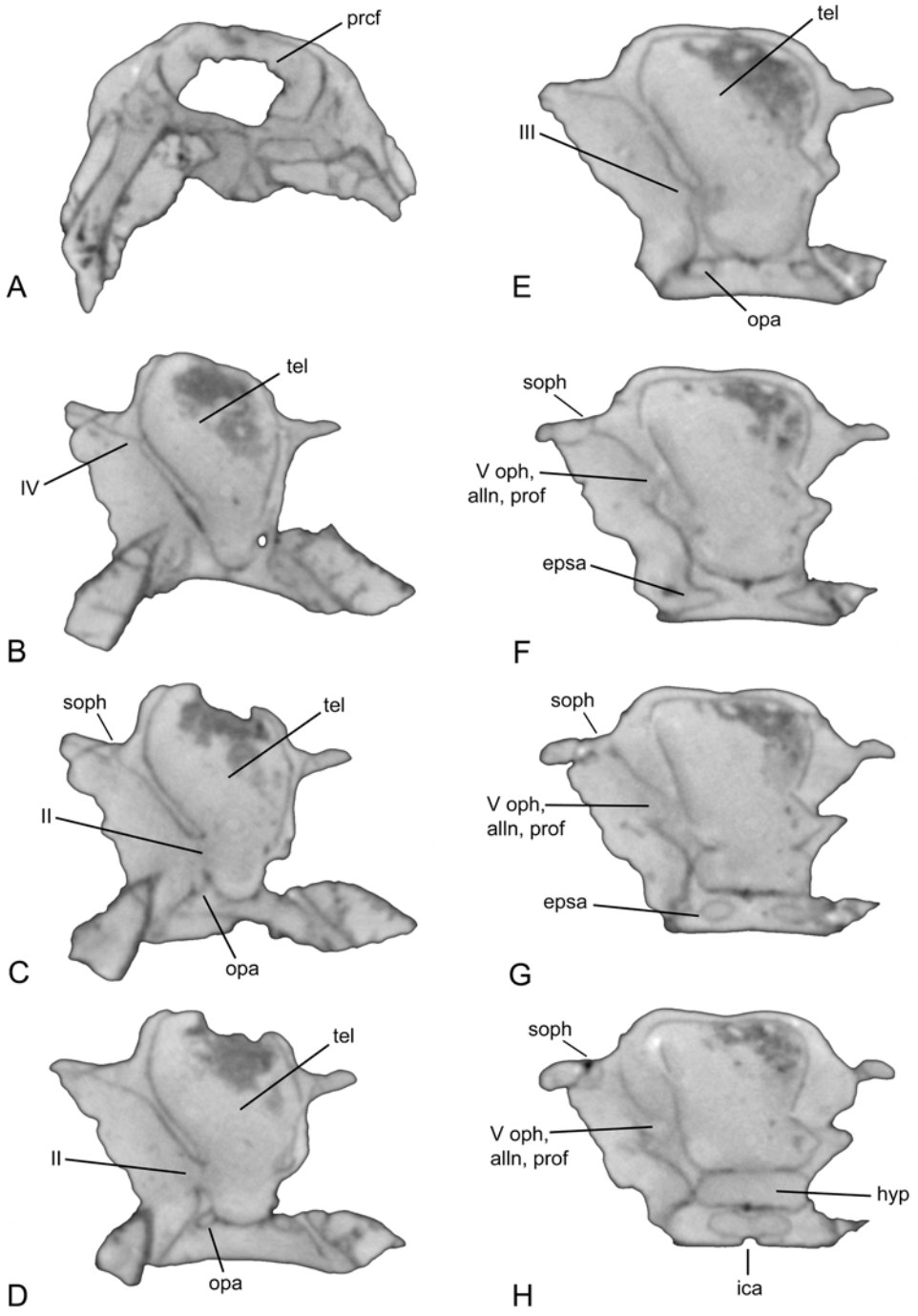

prcf
A
tel
III
E
opa
tel
IV
B
soph
V oph,
alln, prof
epsa
F
soph
tel
II
C
opa
soph
V oph,
alln, prof
epsa
G
tel
II
D
opa
soph
V oph,
alln, prof
hyp
ica
H

FIGURE 40. Transverse CT scan slices of the *Egertonodus* braincase, NHM P60110. Orbital and otic regions. No scale.

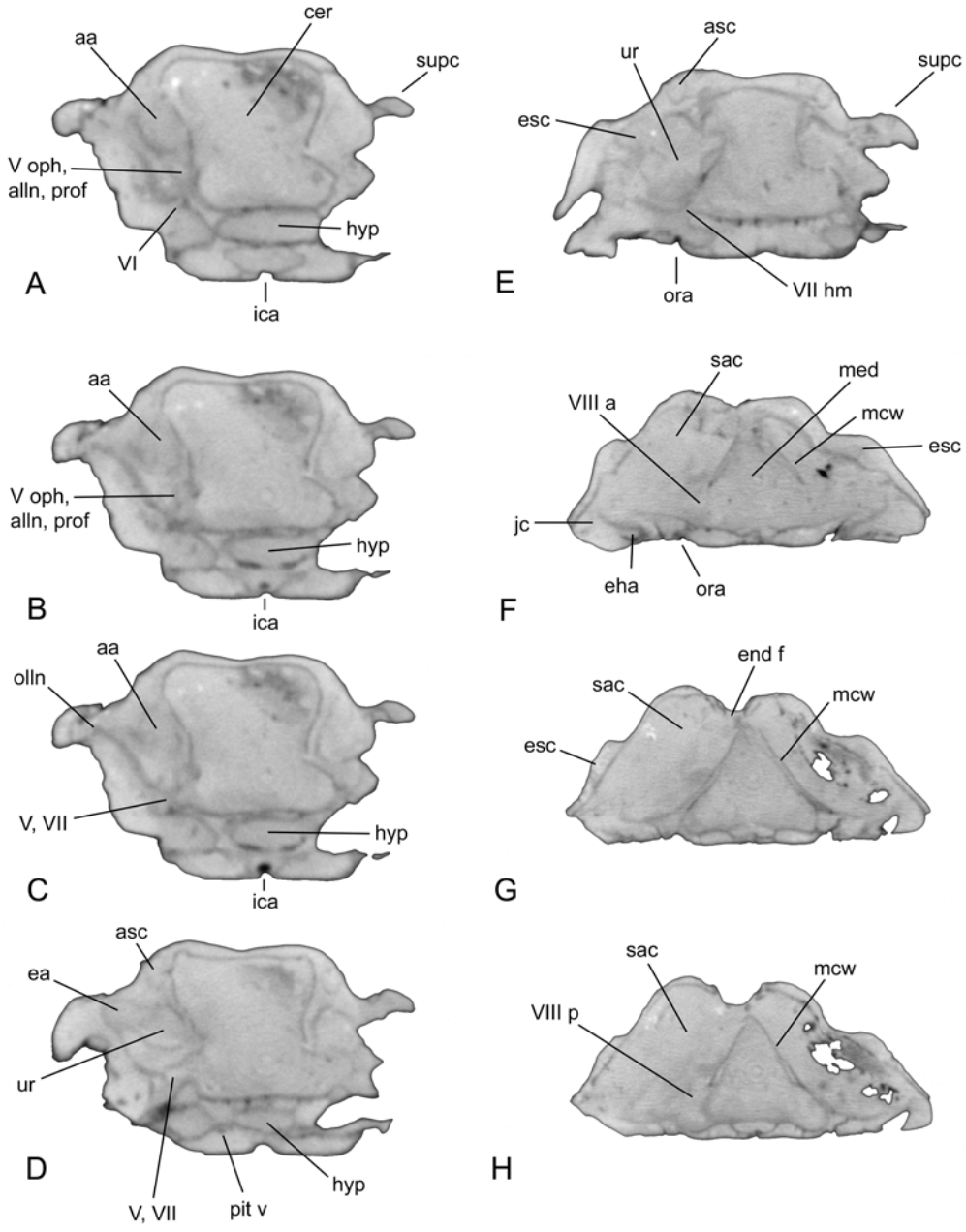

A
aa
cer
supc
V oph,
alln, prof
VI
hyp
ica
B
aa
V oph,
alln, prof
hyp
ica
C
aa
olln
V, VII
hyp
ica
D
asc
ea
ur
V, VII
pit v
hyp
E
asc
ur
supc
esc
ora
VII hm
F
sac
med
VIII a
mcw
esc
jc
eha
ora
G
end f
sac
mcw
esc
H
sac
mcw
VIII p

FIGURE 41. Transverse CT scan slices of the *Egertonodus* braincase, NHM P60110. Otic and occipital regions. No scale.

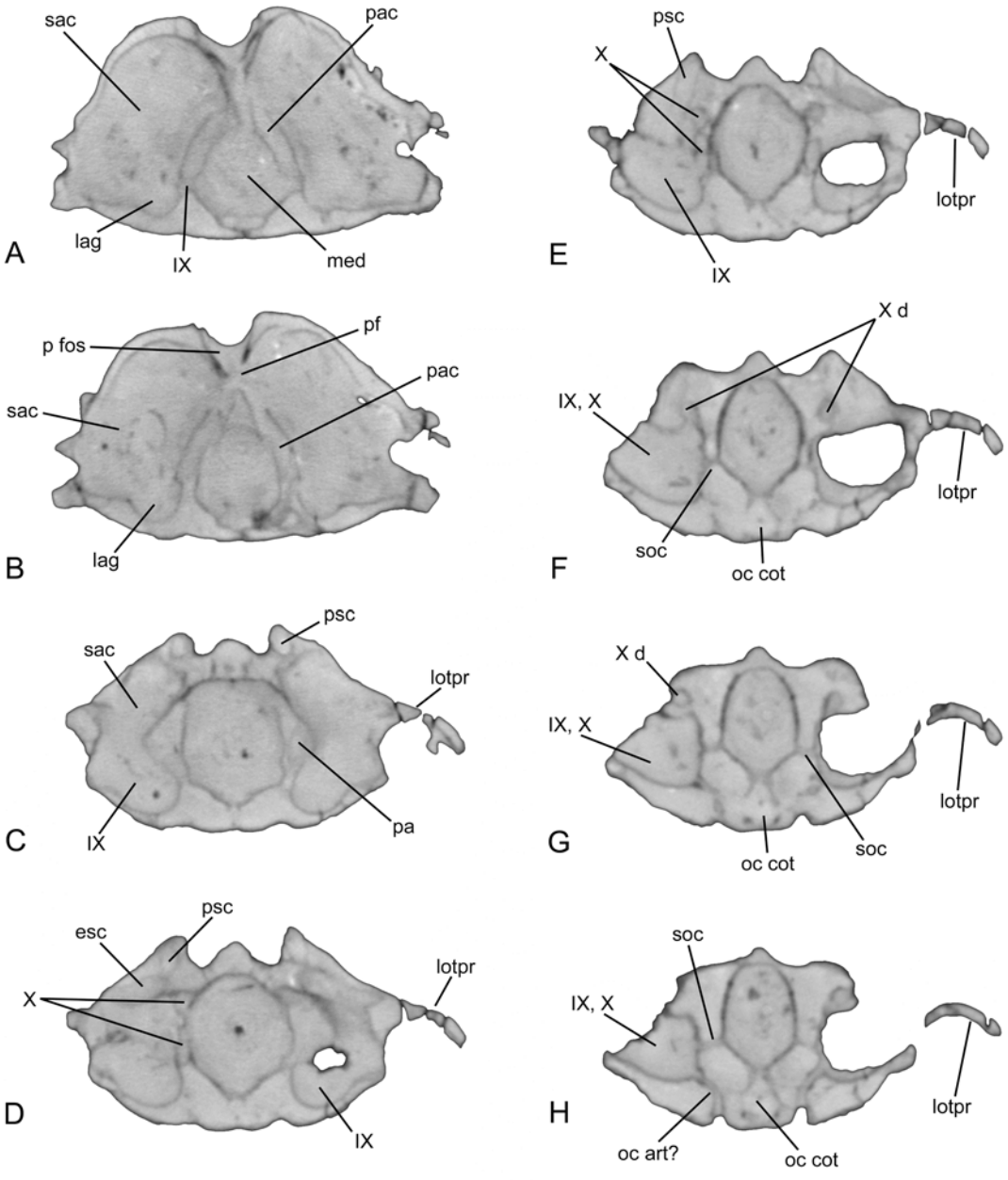

A
sac
pac
lag
IX
med
B
p fos
pf
pac
sac
lag
C
psc
sac
lotpr
IX
pa
D
psc
esc
X
lotpr
IX
E
psc
X
lotpr
IX
F
X d
IX, X
lotpr
soc
oc cot
G
X d
IX, X
lotpr
oc cot
soc
H
soc
IX, X
lotpr
oc art?
oc cot

FIGURE 42. Lateral view of the *Egertonodus* braincase (NHM P60110), anterior to the left (surface rendering). No scale.

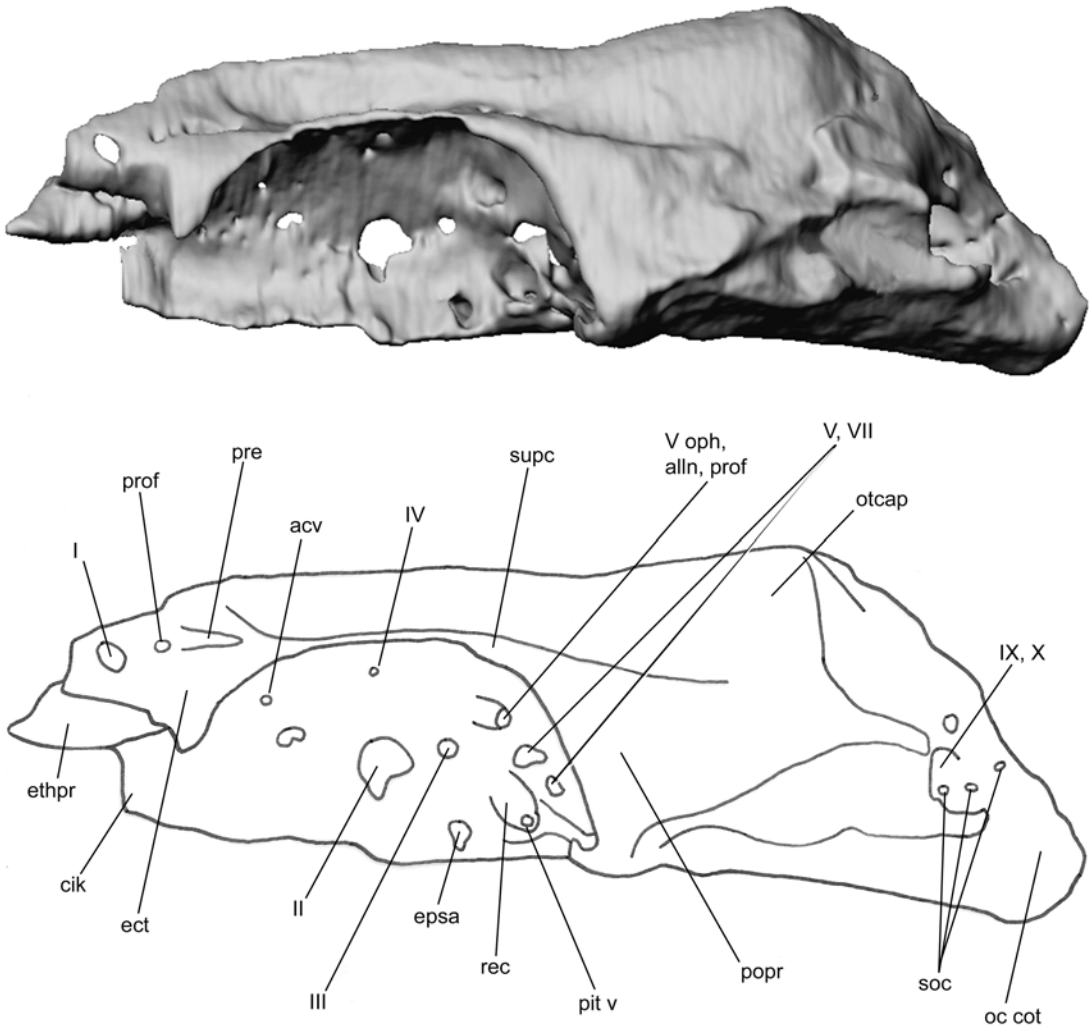

I
prof
pre
acv
IV
supc
V oph,
alln, prof
V, VII
otcap
IX, X
ethpr
cik
ect
II
III
epsa
rec
pit v
popr
soc
oc cot

FIGURE 43. Medial view of the *Egertonodus* braincase (NHM P60110), sliced through the sagittal plane, anterior to the left (surface rendering). No scale.

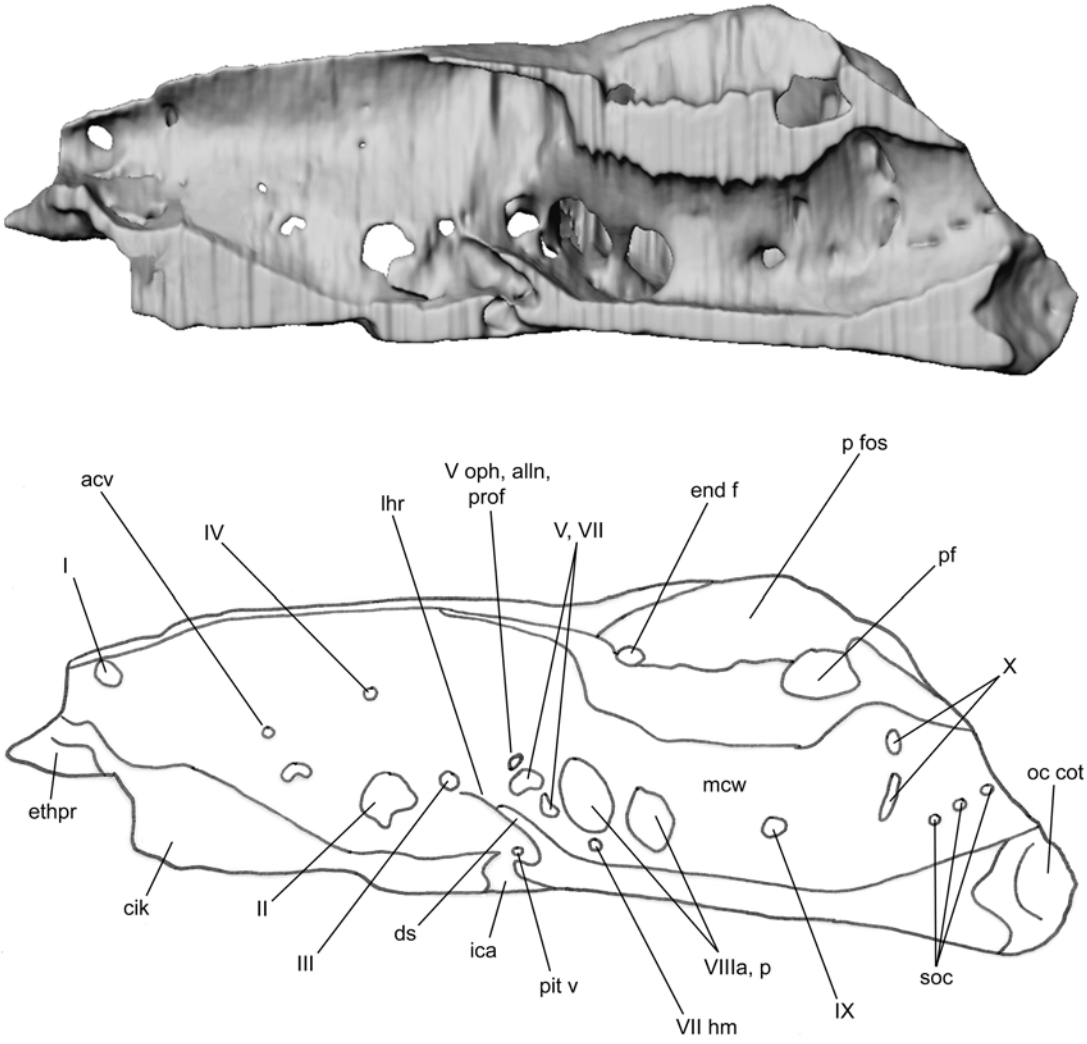

p fos
acv
V oph, alln,
prof
lhr
end f
IV
V, VII
pf
I
X
oc cot
mcw
ethpr
cik
II
III
ds
ica
pit v
VIIIa, p
VII hm
IX
soc

FIGURE 44. A, dorsal; B, ventral; and C, lateral views of the *Egertonodus* (NHM P60110) endocast (surface renderings). No scale.

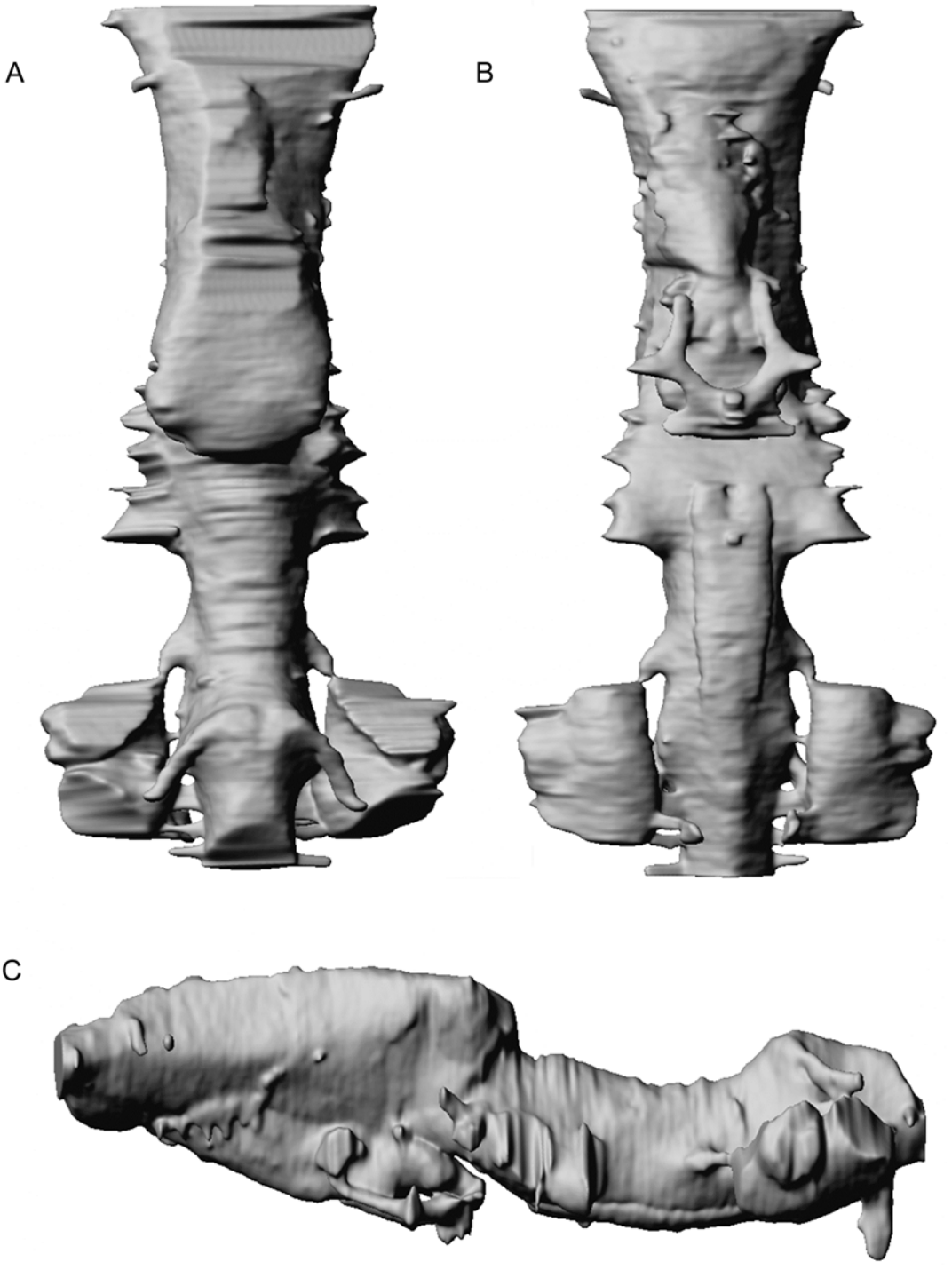

A
B
C

FIGURE 45. Line drawings of the *Egertonodus* endocast (NHM P60110). A, dorsal; B, ventral; and C, lateral views.

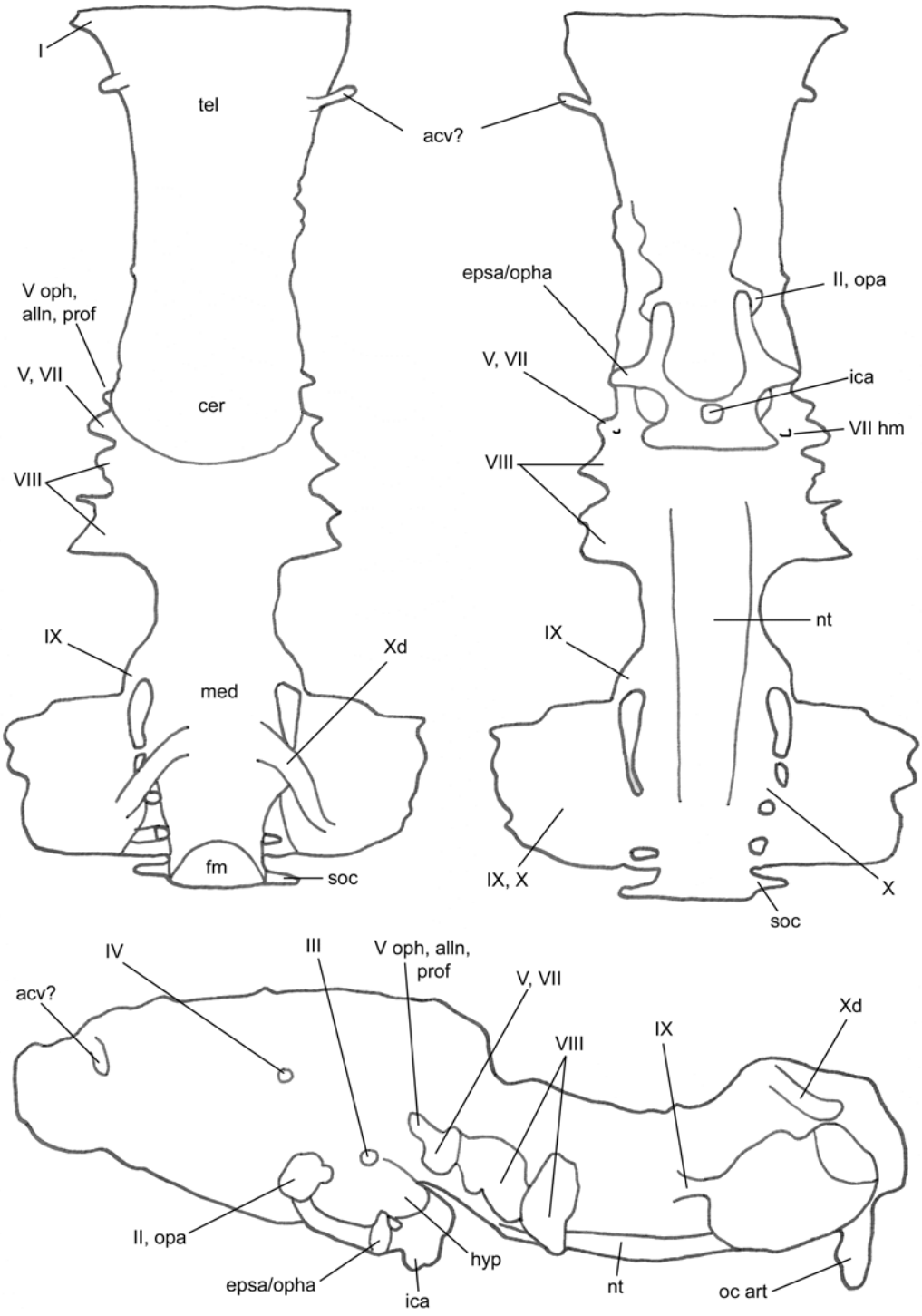

I
tel
acv?
V oph,
alln, prof
V, VII
cer
VIII
IX
Xd
med
fm
soc
epsa/opha
II, opa
V, VII
ica
VII hm
VIII
nt
IX
IX, X
X
soc
IV
III
V oph, alln,
prof
V, VII
acv?
VIII
IX
Xd
II, opa
hyp
epsa/opha
ica
nt
oc art

FIGURE 46. A–C, Skeletal labyrinth of *Egertonodus basanus*, NHM P60110 (surface renderings), A, lateral; B, dorsal; C, medial views. D–F, Skeletal labyrinth of *Tribodus limae*, reconstructed by Maisey (2005), D, lateral; E, dorsal; F, medial views. No scale.

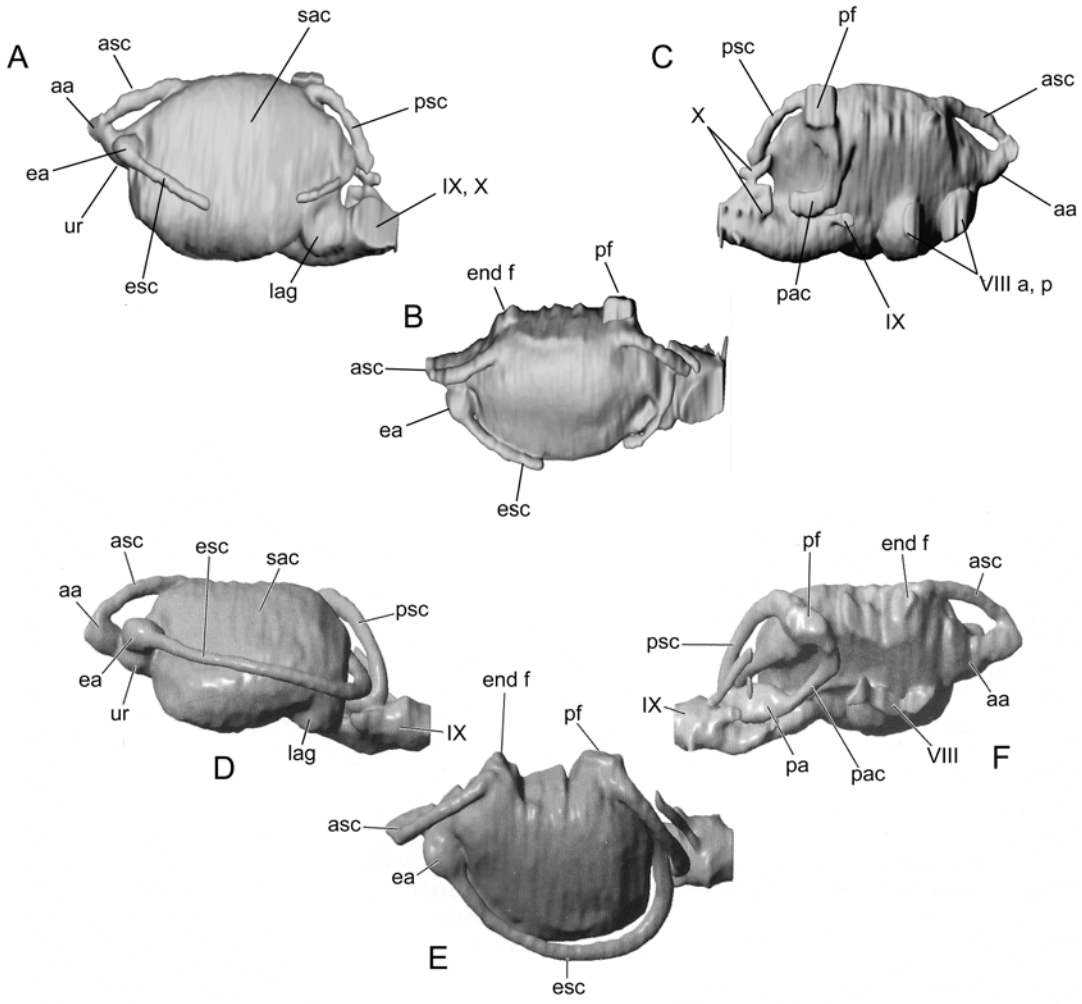

A
asc
sac
aa
psc
ea
IX, X
ur
esc
lag
B
end f
pf
asc
ea
esc
C
pf
psc
asc
X
aa
pac
IX
VIII a, p
D
asc
esc
sac
aa
psc
ea
ur
IX
lag
E
end f
pf
asc
ea
esc
F
pf
end f
asc
psc
IX
aa
pa
pac
VIII

FIGURE 47. Skeletal labyrinth structure in other elasmobranchs. A–C, extant *Notorynchus*, A, lateral; B, dorsal; C, medial views; D, *Cladodoides*, lateral view. After Maisey, 2005. No scale.

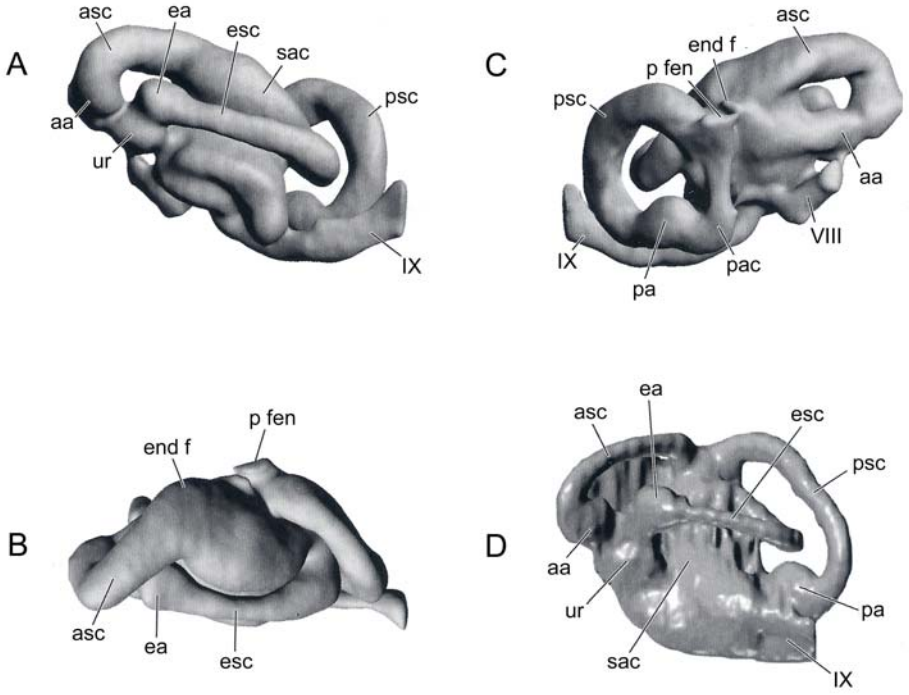

A
asc
ea
esc
sac
psc
aa
ur
IX
B
p fen
end f
asc
ea
esc
C
asc
end f
p fen
psc
aa
VIII
IX
pac
pa
D
ea
asc
esc
psc
aa
ur
pa
sac
IX

FIGURE 48. Reconstructions of the basicranial circulation in *Tribodus limae*. A, ventral (external) view of the braincase showing the basicranial arterial circuit; solid lines represent vessels visible on the surface or external to the cartilage, and dashed lines represent those internal to the cartilage or endocranial space; B, dorsal cutaway (interior) view of the floor of the cranial cavity, showing the same vessels as seen from above; note the internal carotid arteries emerging from the basicranial cartilage through paired foramina in the floor of the braincase anterior to the dorsum sellae, and then diverging to form the optic artery anteriorly and the efferent pseudobranchial/ophthalmic artery posteriorly (the latter divides after exiting the braincase). Solid lines represent vessels visible on the surface of the cutaway (on the floor of the cranial cavity), and dashed lines represent vessels internal to the cartilage or ventral to the basicranium (compare with A). No scale.

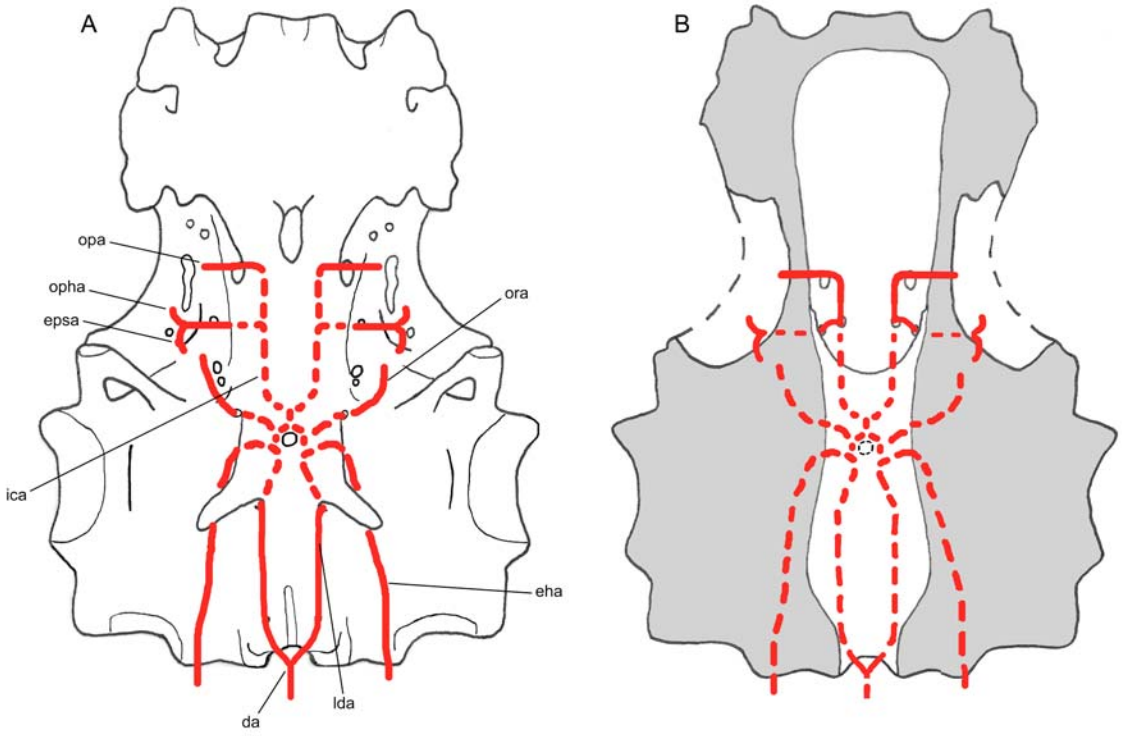

A
B
opa
opha
epsa
ica
ora
eha
da
lda

FIGURE 49. Oblique medial view of the *Tribodus* braincase showing the foramina for the efferent pseudobranchial and ophthalmic arteries. The internal carotid arteries emerge on the internal floor of the braincase after tunneling through the basicranial cartilage, and diverge to form a posterolaterally curving branch, which further diverges into the efferent pseudobranchial and ophthalmic arteries external to the cartilage, and an anterolaterally curving branch, the optic artery, which exits through the optic foramen. No scale.

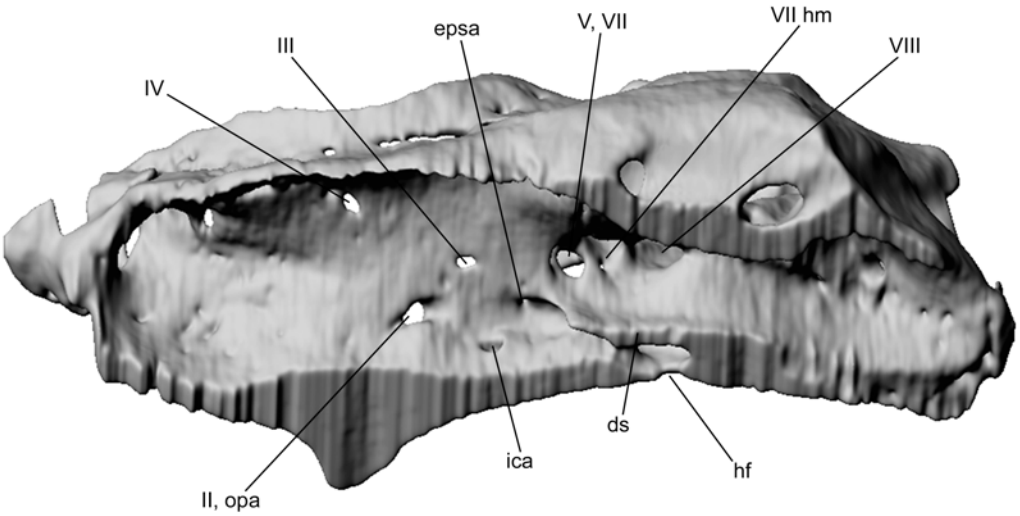

III
epsa
V, VII
VII hm
VIII
IV
ds
ica
hf
II, opa

FIGURE 50. Basicranial circulation in other elasmobranchs. A, *Egertonodus* (*Hybodus*) *basanus*, after Maisey, 1983; B, extant *Heterodontus*, after Maisey, 1983; C, extant *Chlamydoselachus*, after Allis, 1923 (reproduction from Maisey, 1983: fig. 25; positions of "ora" and "opha" reversed to reflect their correct positions); D, *Cladodoides*, after Maisey, 2005; E, *Tamiobatis*, after Maisey, 2005 (left side: interpretation of Williams, 1998; right side: interpretation of Maisey, 2005); F, *Orthacanthus*, after Schaeffer, 1981. No scale.

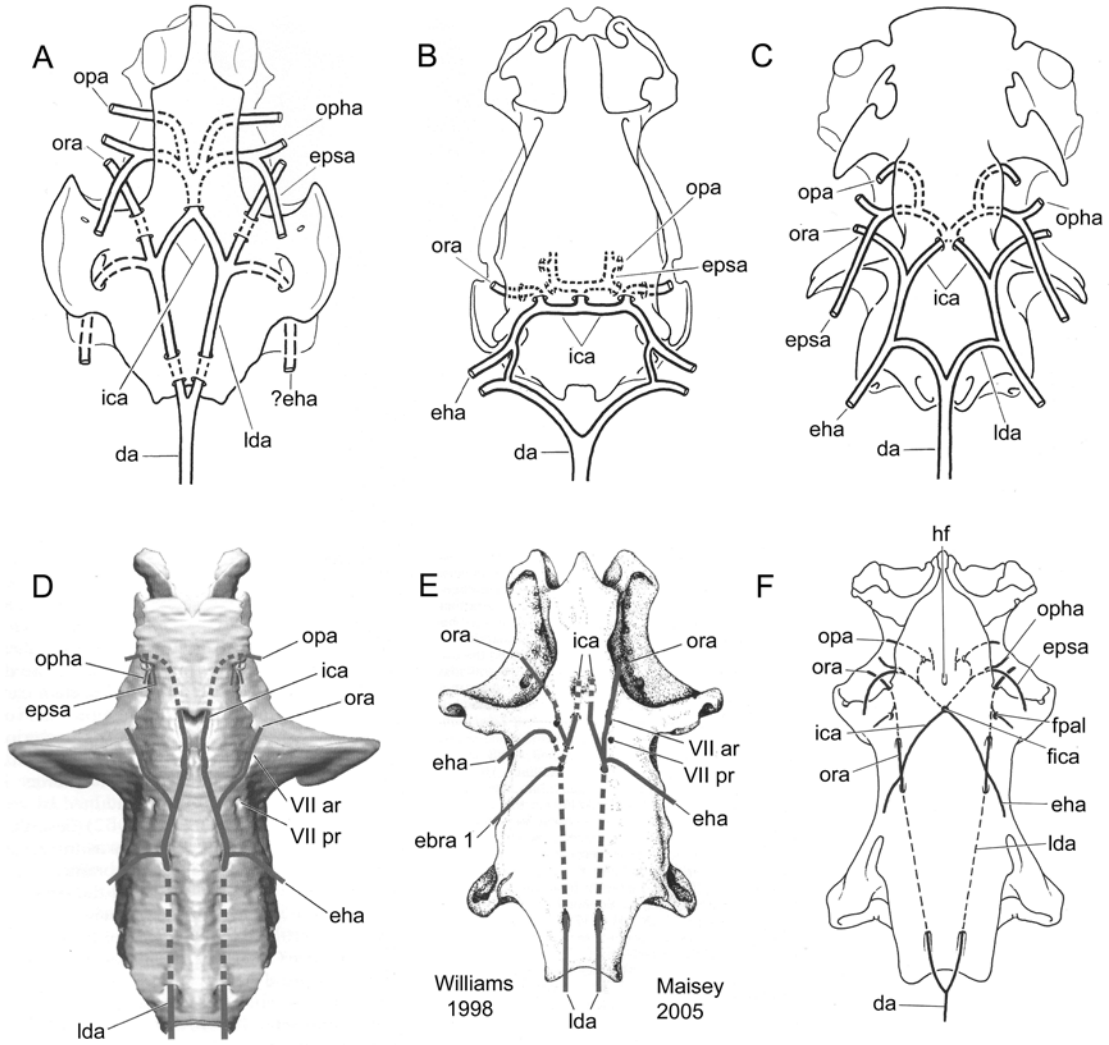
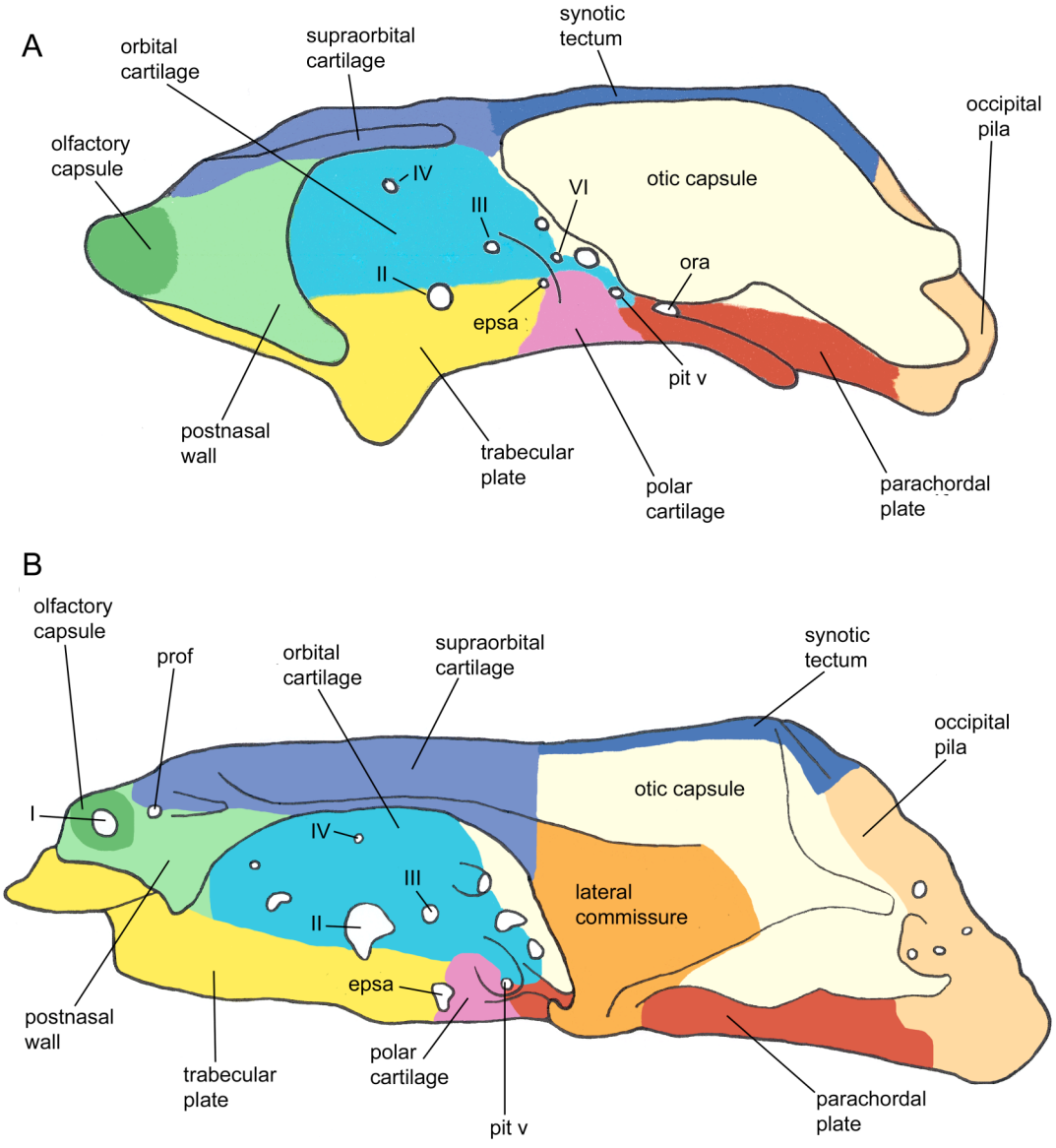

A
opa
opha
ora
epsa
ica
?eha
lda
da
B
opa
ora
epsa
ica
eha
da
C
opa
opha
ora
ica
epsa
eha
da
lda
D
opha
opa
ica
epsa
ora
VII ar
VII pr
eha
lda
E
ora
ica
ora
VII ar
VII pr
eha
eha
ebra 1
Williams
1998
Maisey
2005
lda
F
hf
opha
opa
epsa
ora
fpal
ica
fica
ora
eha
lda
da

FIGURE 51. A, Composite reconstruction showing probable extent of embryonic cartilages in *Tribodus limae*; the postorbital process, otic capsule, and antorbital process have been cut away to show the foramina. B, Reconstruction showing probable extent of embryonic cartilages in *Egertonodus basanus*. Color scheme based on Maisey (2005), for easier comparison with his reconstructions of the embryonic cranial cartilages in other elasmobranchs. No scale.


A
orbital cartilage
supraorbital cartilage
synotic tectum
occipital pila
olfactory capsule
IV
VI
III
otic capsule
II
ora
epsa
pit v
postnasal wall
trabecular plate
polar cartilage
parachordal plate
B
olfactory capsule
prof
orbital cartilage
supraorbital cartilage
synotic tectum
occipital pila
otic capsule
I
IV
III
lateral commissure
II
epsa
postnasal wall
trabecular plate
polar cartilage
pit v
parachordal plate

# CHAPTER 6: VISCERAL SKELETON OF *TRIBODUS* AND RECONSTRUCTION OF ITS JAW SUSPENSION

[Adapted from: Lane, J.A. In preparation. Visceral Skeleton and Jaw Suspension in the Durophagous Hybodontid Shark *Tribodus limae*, from the Lower Cretaceous of Brazil. Planned for submission to Journal of Morphology.]

## INTRODUCTION

Well-preserved skeletal material of fossil chondrichthyans is extremely rare compared to isolated hard parts (e.g., teeth and fin spines, on the basis of which numerous taxa have been named). For this reason, jaws of hybodontids are currently known from only a handful of taxa, i.e., *Hamiltonichthys* (Maisey, 1989A); *Lissodus* (Broom, 1909; Brough, 1935); *Lonchidion* (Gomez-Pallerola, 1985, 1992; Maisey et al., 2004); *Hybodus* (Agassiz, 1833–1844; Koken, 1907; Maisey, 1982, 1987); *Egertonodus* (Brown, 1900; Woodward, 1916; Maisey, 1983; 1986); *Asteracanthus* (Peyer, 1946; Rieppel, 1981; Maisey, 1982); and *Acrodus* (Agassiz, 1833–1844; Woodward, 1916, 1919; Kuhn, 1945; Maisey, 1982). The majority of hybodontids had anteriorly long jaws that reached the ethmoid region and a jaw suspension that has been described as "hyostylic" sensu stricto (i.e., having a suspensory hyomandibula and ethmopalatine process, but no postorbital articulation; Huxley; 1876; Gregory, 1904). However, all chondrichthyans with a suspensory hyoid arch can be considered "hyostylic" sensu lato, differing mainly in the number and identity of their additional jaw articulations (Gregory, 1904; Maisey, 2008). In the present paper, the term "hyostylic" is used in the strict sense (referring to the

condition found in many hybodonts, and some galean sharks including heterodontiforms, carcharhiniforms, and lamniforms; Wilga, 2005). Several hybodont taxa differed from this pattern in having shortened jaws that do not extend to the ethmoid region (e.g., *Asteracanthus*, *Lissodus*, and *Lonchidion*), and a few (e.g., *Asteracanthus* and *Acrodus*) had a durophagous dentition, with low-crowned, rounded cuspidate or occlusally flattened teeth. This morphological diversity among hybodonts appears to parallel that observed among extant neoselachians, in which a small percentage of taxa have also independently evolved a durophagous lifestyle (e.g., *Heterodontus*; *Sphyrna tiburo*; many myliobatid stingrays; Summers, 2000; Wilga, 2000).

The discovery of exceptionally well-preserved material of the Lower Cretaceous (Aptian/Albian) hybodont *Tribodus limae* Brito and Ferreira, 1989, including a nearly complete braincase with complete, three-dimensional mandibular and hyoid arches and a well-preserved pectoral girdle (AMNH 13958; Maisey and Carvalho, 1997; Lane and Maisey, 2009; Lane, in prep.), provides valuable new information regarding hybodont morphology and taxonomic diversity. The well-preserved mandibular arch elements of this and other specimens allow for a full description of jaw morphology in *Tribodus*, including the opportunity to reconstruct its jaw musculature for the first time (no reconstructions of hybodont jaw musculature have yet been published). Additional well-preserved specimens of *Tribodus* reposited in Brazilian museum collections provide further evidence including gill arch structure, which is not preserved in any of the AMNH material.

Jaw musculature has been reconstructed previously in only a few fossil chondrichthyans, including a cladoselachian shark from the Late Devonian of Tennessee

(Maisey, 1989B) and the symmoriiform "*Cobelodus"* (Maisey, 2007). Both of these sharks differ from hybodontoids in having an archaeostylic jaw suspension (sensu Maisey, 2008). Archaeostyly is defined as a suspensory arrangement in which a postorbital articulation is present and located on the ventrolateral part of the lateral commissure, and differs from amphistyly (found in extant hexanchiform sharks), in which the articular facet is located on the primary postorbital process (Maisey, 2008). Unlike hybodontoids, "*Cobelodus*" and cladoselachians have 'cleaver-shaped' jaws with an enlarged palatoquadrate otic region like those of xenacanths and ctenacanths.

The extant phylogenetic bracket method (Witmer, 1995) has been proposed and used previously as a means of predicting the arrangement of soft anatomical features in fossils on the basis of their structure in the two extant groups 'bracketing' the fossil taxon (i.e., the closest living member of the fossil taxon's sister group, and the closest living member of the outgroup to the fossil plus its sister taxon). Unfortunately, when applied to fossil hybodonts such as *Tribodus*, this method is less than perfect for determining the arrangement of soft anatomic features of the jaw suspension. The reason for this difficulty is that the two extant 'bracket' groups for hybodonts are 1) living neoselachians (the sister group of hybodonts) and 2) holocephalans (the closest living outgroup to hybodonts + neoselachians). Whereas extant neoselachians appear to provide a good model for reconstructing jaw morphology in hybodonts, the comparison to the outgroup 'bracket' (holocephalans) fails because the holostylic jaw suspension of the latter group is so derived as to provide very little useful information for comparison. The next closest living 'bracket' group is extant osteichthyans, which are still more distant. As Wilga (2005) pointed out, because the upper jaw is fused to the braincase in holocephalans,

cranial-palatoquadrate ligaments and joints are lacking, and the arrangement of muscles differ. Previous phylogenetic analyses have placed holocephalans as a derived group within symmoriiforms (e.g., Coates and Sequeira, 2001A, B), and their overall morphology is highly derived. As such, they may not represent the ancestral state to hybodonts + neoselachians, or even the ancestral state within their own group (if they are indeed derived symmoriiforms). For this reason, it is unlikely that comparisons between the jaw apparatus of extant holocephalans and neoselachians can provide a useful 'bracket' for accurately determining the condition of soft anatomical features in hybodonts, except in a very broad sense. However, comparisons with extant neoselachians, and observation of the common features shared by all extant neoselachian groups, is potentially useful in determining the ancestral condition which may have been present in hybodonts (although the lack of an adequate lower bracket makes such a determination largely speculative).

The goal of the present chapter is to describe the visceral skeleton of *Tribodus limae* on the basis of available well-preserved specimens (including using CT scanning technology to provide a description of internal jaw structure), to present a reconstruction of jaw musculature in *Tribodus* on the basis of skeletal morphology and comparison with other fossil and extant chondrichthyans, and to discuss these results as they relate to evolutionary relationships and possible function and behavior of *Tribodus limae*.

## DESCRIPTION

### MANDIBULAR ARCH

**Palatoquadrates—**Anteriorly, the palatoquadrates of *Tribodus* (Figs. 52–54) have a flat, vertical symphysial surface medially, where they appear to have contacted each other (Figs. 52B, 53). However, palatoquadrates of *Tribodus* were not fused (unlike some extant myliobatid rays; Summers, 2000). The palatoquadrates of *Tribodus* do not rise into the orbit dorsally (unlike in *Egertonodus*; Maisey, 1983), and the dorsal surface of the palatoquadrate is smooth and continuously convex in lateral view, consistent with Brito's (1992) interpretation that *Tribodus* lacked an orbital process. However, located approximately halfway along the length of the palatoquadrate is a small dorsomedial flange (Figs. 53B, D; 54A, B) (possibly corresponding to the dorsal postorbital or otic flange of other elasmobranchs), which appears to have rested beneath the otic region at the same level as the proximal end of the paired basicranial processes and may represent an orbital or palatobasal process (Fig. 54: palpr?). A similar dorsomedial process or flange on the palatoquadrate is known in several other hybodonts (e.g., *Hybodus reticulatus*; *Acrodus* sp.; Maisey, 1987; Thomson, 1982), although in these taxa it is positioned farther anteriorly beneath the orbit. The location of this process varies somewhat among taxa, but its general position (dorsomedially, in the basicranial region) suggests that it may represent a palatobasal articulation. When reconstructed in ventral view, the upper jaw fits neatly in the space between the medial basicranial process anteriorly and the ventral basicranial processes posteriorly, with the latter abutting the medial posterodorsal surface of the palatoquadrates. Posteriorly, the upper jaw fits into the space between the postorbital processes and the paired ventral basicranial processes,

which may have acted as limits to anteroposterior jaw movement and may have provided ligamentous attachment surfaces.

The anterior portion of the palatoquadrates in *Tribodus* is rounded in dorsal and ventral view, and their anterior edge is nearly vertical in lateral view, and dorsoventrally quite deep. The anterodorsal surface of each palatoquadrate shows a medial depression, and seems to fit against a corresponding rounded suborbital portion of the basicranium, which extends between the median basicranial process and the paired verntral processes in the resting position. The jaws may have rested against this rounded suborbital surface, from which they may have been extended anteroventrally during feeding as in many extant neoselachians. An anterior dorsoventral constriction is also seen in the palatoquadrates of many other hybodonts (e.g., *Hybodus*, *Egertonodus*, *Acrodus*), located between the palatine and quadrate regions of the cartilage.

The mesial surface of the palatoquadrates is smooth, and is concave posteriorly and weakly convex anteriorly. Anterodorsally there is a faint groove (dp), extending posterodorsally to approximately the level of the palatoquadrate dorsomedial flange and curving ventrally just anterior to the quadrate flange, which may mark the posterior boundary of the pavement dentition that probably extended laterally as far as the ventral jaw margin. Posteriorly, each palatoquadrate has a broad, laterally positioned quadrate flange (Fig. 53, qfl) that widens ventrally, overhanging a dorsoventrally deep fossa for the adductor muscle. The quadrate flange was positioned ventral to the postorbital process of the neurocranium. The ventral end of this flange widens to form an elongated, narrow process posteriorly, terminating in a condyle which forms the primary mandibular articulation with Meckel's cartilage (the “rounded process” of Brito, 1992), and a broader

anterior process. The medial and posterior face of the palatoquadrate is smooth and gently convex dorsal to the mandibular joint. There is no trace of a groove or shelf for the hyomandibula.

**Meckel's cartilages—**Like the upper jaws, the paired Meckel's cartilages were joined but not fused at a median symphysis. Their anterior edge is steeply inclined posteroventrally in lateral view (Figs. 52A, 54D, 55). The anterodorsal margin of Meckel's cartilage protrudes to form a narrow ridge. Posteroventrally, the surface of the cartilage is broadly concave, forming a large fossa for the adductor muscle (Figs. 52A, 53B, C, 54D–F, 55). On the mesial surface of Meckel's cartilage (Fig. 54E), there is a clearly demarcated groove above which the surface of the cartilage curves to form a convex slope anteriorly, forming a platform for the teeth, but there is no obvious dental groove to accommodate the tooth families as in *Egertonodus* and *Hybodus*.

As in many other chondrichthyans, the mandibular joint in *Tribodus* forms a double articulation (Figs. 53C, 54C–F). The primary mandibular articulation is located posterolaterally and comprises an elongate, anteroposteriorly broad mandibular glenoid fossa that corresponds to a knob-like articular condyle on the palatoquadrate (Fig. 53, art k). The auxiliary mandibular knob (Fig. 53, mk) is located anteromedially on Meckel's cartilage, and articulates with a concave surface on the palatoquadrate. A double mandibular articulation is present in most chondrichthyans, (including extant neoselachians), as well as in placoderms, acanthodians, and osteichthyans, although in extant chimaeroids the glenoid fossa and corresponding palatoquadrate condyle are only weakly developed (Maisey, 1989B). Reconstruction of the jaws shows that the mandibular joint of *Tribodus* was arranged nearly horizontally, with the primary and

auxiliary articular surfaces on a level with each other mesiolaterally. As in xenacanths, *Hybodus*, and *Egertonodus*, the mandibular joint of *Tribodus* (measured mesiolaterally from auxiliary to primary articulations) comprises over 25% of total mandibular length (Maisey, 1989B).

On the mesial surface of Meckel's cartilage just ventral to the articular surface is a small circular indentation, here interpreted as housing the proximal end of the ceratohyal. It is overlain anterodorsally by a small ridge, as in extant elasmobranchs, xenacanths, and *Hybodus,* but lacking in some Paleozoic sharks (e.g., cladoselachians) (Maisey, 1989B).

Maisey (1989B) showed (using measurements from a Late Devonian cladoselachian) that the mandibulo-hyoidean ratios of Zangerl and Williams (1975), which supposedly indicate whether the hyoid arch was nonsuspensory, are probably uninformative. Measurement data from *Tribodus* obtained for the present paper further support Maisey's conclusion. Maisey (1989B) used the following two ratios of Zangerl and Williams (1975):

$$\text{Index A} = \frac{\text{length of epihyal} \times 100}{\text{distance from mandibular joint to tip of palatoquadrate otic process}}$$

$$\text{Index B} = \frac{\text{length of ceratohyal} \times 100}{\text{length of Meckel's cartilage}}$$

According to Maisey, values of A between 87 and 100, and values of B over 75, were considered as indicating that the hyoid arch was nonsuspensory because the hyoid extended past the mandibular joint. Measurements of the jaws and hyoid arch elements of *Tribodus limae* (AMNH 13958) were taken, and the appropriate measurements were inserted into the above equation to determine the outcome. The length of the left epihyal (=hyomandibula) was measured as 29.7 mm, and the distance from the left mandibular joint to the tip of the palatoquadrate otic process was measured as 29.6 mm, producing an A value of 100.4. The length of the left ceratohyal was measured as 49.4 mm, and the length of the left Meckel's cartilage was measured as 66.2, producing a B value of 74.7, close to 75. Thus, both A and B values are at the upper limit of their respective ranges, suggesting that the hyoid arch should be nonsuspensory or nearly so. However, in *Tribodus* there are no cranio-palatine joints, indicating that the hyoid arch clearly had to be suspensory and in fact provided the only skeletal support for the jaws. Thus, the measurement data from *Tribodus* further supports Maisey's (1989B) conclusion that these ratios are not informative.

## HYOID ARCH

Elements of the hyoid arch are preserved in AMNH 13958; AMNH 13959; MN 5807-V; MN 5808-V; UERJ-PMB-40; UERJ-PMB-114; and UERJ-PMB-119. Hyoid arch elements of AMNH 13958 are shown in Figure 56. Three hyoid arch elements were present: an anteroposteriorly narrow and transversely elongated, bar-shaped basihyal (Fig. 56A, B); a narrow, proximally bifurcated ceratohyal twice as long as the hyomandibula (Fig. 56G–J); and a short, robust hyomandibula that is broad

ventrally and more tapered dorsally (Fig. 56C–F. The hyomandibula was located dorsally between the 'lateral otic process' of the braincase and the palatoquadrate, whereas the ceratohyal was arranged with its bifurcated end contacting the hyomandibula and Meckel's cartilage and its elongate distal portion tucked behind Meckel's cartilage mesially. The hyomandibula appears to have been directed downward, outward, and slightly anteriorly, as in *Tristychius* and many extant sharks (Dick, 1978; Maisey, 1983).

The relatively short hyomandibula articulates ventrally with the mandibular arch and with the ceratohyal. The larger, more dorsal and medial of the two processes of the bifurcated ceratohyal articulates with the distal end of the hyomandibula, while the smaller, more laterally located ventral process and the anteromedial extension of the ceratohyal probably provided support to the lower jaw via ligaments. A deep pit located on the dorsolateral surface of the ceratohyal several millimeters anterior to its bifurcated proximal end may have articulated with the posteromesial surface of the lower jaw adjacent to the primary articulation of the jaw joint. Although the hyoid arch is disarticulated in AMNH 13958, it is inferred that the basihyal was probably located between the distal ends of the ceratohyals at the anteroventral extremity of the hyoid arch, as in extant elasmobranchs. The basihyal is slender anteroposteriorly, with widened lateral ends (where it articulated with the ceratohyals) and a slight medial posteroventral bulge. The basihyal of *Tribodus* forms a wide transverse bar (as in many extant neoselachians, in which it probably arose independently and has been considered an advanced feature). The basihyal of *Tribodus* has a smooth horizontal anterodorsal margin, and a concavely arched ventral margin flanked laterally by paired triangular ventral extensions, superficially resembling the basihyal in *Squalus acanthias*

(Wischnitzer, 1993). According to Goodrich (1958, p. 399), the basihyal in *Raja* is also arched and "bow-like" in shape, and concave posteriorly. Based on examination of specimens, the hyoid arch in *Tribodus* is here inferred to have been suspensorial and intact (i.e., with all of its elements articulated).

**BRANCHIAL ARCHES**

The branchial arches are not well preserved in any of the AMNH specimens of *Tribodus*. However, branchial arches are preserved in MN 5807-V (Fig. 57); MN 5808-V (Fig. 58); UERJ-PMB-40; UERJ-PMB-114; and UERJ-PMB-119. Pharyngobranchials are preserved in MN 5807V and MN 5808V (Figs. 57–59; 61–63), as well as in UERJ-PMB-114. Five branchial arches were observed (consistent with previous descriptions of *Tribodus*; Brito, 1992), as in other hybodonts (Maisey, 1982) and most elasmobranchs (Fig. 64), and this feature may be primitive for elasmobranchs. Pharyngobranchials, epibranchials, and ceratobranchials can be identified, in order dorsoventrally. However, there is no trace of hypobranchials or basibranchials, although these elements were presumably present. Brito (1992) interpreted the dorsalmost branchial elements in MN 5808-V (formerly CD-P-106) as ceratobranchials, but these are here interpreted as pharyngobranchials (Figs. 61–63). The pharyngobranchials are angled backward posterodorsally, and have a triangular dorsal tip with a posterior barb interpreted here as a pharyngobranchial blade (also found in extant galean sharks, e.g., *Heterodontus* (Fig. 64E); and possibly some hybodonts; Maisey, 1982, fig. 9E; Shirai, 1992; de Carvalho, 1996). Presence of a pharyngobranchial blade in *Tribodus* appears to support the view that this feature may be plesiomorphic in neoselachians (Shirai, 1992; de Carvalho; 1996).

There is no evidence that pharyngobranchials of *Tribodus* (or any other hybodont) were fused posteriorly. In neoselachians, this fusion has been termed the "gill pickaxe," and occurs between the posteriormost pharyngobranchials (sometimes also including the corresponding epibranchials), usually of the fourth and fifth gill arches (Shirai, 1992; Fig. 64E, F). However, in hexanchiforms, in which additionall gill arches are present, the fusion involves the fifth and sixth pharyngobranchials (*Hexanchus*), or the six and seventh (*Heptranchias*). Fusion of the posteriormost pharyngobranchials also occurs in chimaeroids (e.g., *Hydrolagus*), but has not been reported in any other chondrichthyan taxa.

**LABIAL CARTILAGES**

Brito (1992) reported three (superior, anterior, and posterior) labial cartilages in *Tribodus*, although according to Brito (1992) these were quite damaged and seemed to be smaller than those of hybodonts such as *Egertonodus*. However, no evidence of labial cartilages was observed in any of the Brazilian specimens of *Tribodus* in the present study, although two small, narrow columnar fragments of cartilage in AMNH 13959 (one on the right upper jaw and one on the left lower jaw) may represent labials. Massive labial cartilages have been reported in other hybodonts (e.g., *Egertonodus* and *Hybodus*; Maisey, 1982, 1983). Due to the otherwise excellent state of preservation of the *Tribodus* material, the lack of any evidence of massive labial cartilages suggests that these were absent or reduced in *Tribodus*. It is possible that massive labial cartilages represent a synapomorphy of some Mesozoic hybodonts (extant sharks typically have three or fewer

small labial cartilages on each side; Maisey, 1982; Shirai, 1992; and some extant rajiforms such as *Rhinobatos* and *Torpedo* lack labial cartilages altogether; Shirai, 1992).

**CT SCANNING OF INTERNAL JAW STRUCTURE**

CT scan sections of both the palatoquadrate and Meckel's cartilage of AMNH 13958 reveal the presence of endochondral "struts" or buttresses, visible as dark linear streaks extending diagonally through the cartilage (Fig. 65). These structures appear to correspond to the endochondral “trabecular cartilage” found in some extant batoids (Summers, 2000; Dean and Motta, 2004; Figs. 77, 78), possibly representing the first time such endochondral struts have been found in a non-batoid elasmobranch, as well as in a fossil chondrichthyan. Like the endochondral struts of batoids, these struts also appear to be lined with prismatic calcified cartilage, and some clearly show a hollow internal lumen, which is lighter in color than the surrounding cartilage (best visible in Fig. 65A–E).

The struts are most heavily concentrated in the anterior parts of the jaws in the region of the biting surfaces, and posteriorly near the quadratomandibular joint. Anteriorly, they are arranged directly perpendicular to the biting surface as in batoids (Fig. 65, arrows indicate biting surface; Fig. 77), and perhaps served a similar role in providing structural support to counter the forces generated by biting down on hard prey items (Summers et al., 1998; Summers, 2000; Dean and Motta, 2004). In the region of the mandibular joint, the cartilage struts are oriented perpendicular to the inner surface of the articular cotylus where the forces generated by movement of the jaw joint were presumably concentrated,

suggesting that the struts added support at the jaw joint as in extant batoids (Summers, 2000). Moreover, the palatoquadrate lacks trabecular struts in the region of the jaw joint. However, similar strut-like calcification is also extensive in the basicranium of *Tribodus*, including regions that are remote from the jaws and probably not subjected to high stress.

Multiple layers of prismatic cartilage may have been present in the lower jaw (Fig. 65), where a second (internal) layer of prismatic cartilage is inferred in CT-scan slices by a dark line around the perimeter of the cartilage and separated from the surface layer by a more lightly colored (uncalcified?) region. This inner layer appears to be continuous with the endochondral struts.

## RECONSTRUCTION OF THE JAW SUSPENSION IN *TRIBODUS*

A complete analysis of functional morphology and jaw mechanics in *Tribodus* is beyond the scope of the present study. However, the excellent state of preservation in several specimens of *Tribodus* provides an opportunity to reconstruct its jaw musculature (Fig. 66). Comparison with extant neoselachians and holocephalans yields the following interpretations concerning the probable conditions of jaw muscles and ligaments in *Tribodus*.

**Anterior ligaments—** In *Tribodus*, the jaws do not extend into the ethmoid region, raising the possibility that an ethmopalatine ligament may have been lacking. Cranial-palatine ligaments are absent in batoids (Wilga, 2005), in which the jaws also do not reach the ethmoid reagion. However, it seems more likely that the median ventral keel process of *Tribodus*, which is located immediately anterior to the jaws, may have provided an attachment surface for an ethmopalatine ligament. Small indentations on

either side of the median ventral process may have formed attachment sites for such a ligament. A sleeve-like ethmopalatine ligament is present in numerous neoselachian groups, and has been considered primitive for elasmobranchs (Wilga, 2005; Fig. 67). Ethmopalatine ligaments may also have been present in hybodonts other than *Tribodus* (e.g., *Egertonodus*), in which the jaws do extend into the ethmoid region and bear ethmoidal articular facets (a similar arrangement to that of extant carcharhiniforms; Wilga, 2005). Cranial-palatine ligaments are lacking in holocephalans, due to fusion of the upper jaw with the cranium (Wilga, 2005). There is no evidence that *Tribodus* had a palatonasal ligament like that of modern lamniforms (Wilga, 2005).

**Preorbitalis—** The presence of small, paired, rounded processes in *Tribodus* on the mesial margins of the antorbital processes and lacking prismatic cartilage distally strongly suggests an attachment area for muscles, similar in position to the origin of the preorbitalis muscles (= suborbitalis, abbreviation: so) in extant elasmobranchs (e.g., *Chlamydoselachus*, hexanchoids, some squaleans; Shirai, 1992; most galeomorphs, batoids; Wilga, 2005; Figs. 68–71). This suggests that a preorbitalis muscle may have been present in *Tribodus* (although it is alternatively possible that these processes could have provided attachment for an ethmopalatine ligament). Small rounded processes on the medial parts of the antorbital processes similar in appearance to those of *Tribodus* also occur in embryonic *Torpedo* (Holmgren, 1940, fig. 158), and form insertion points for the depressor rostri muscle. However, that muscle occurs only in extant rajiforms, and was probably absent in *Tribodus.*

According to Anderson (2008), a preorbital muscle innervated by the trigeminal nerve is primitive for crown-group gnathostomes, occurring in elasmobranchs, chimaeroids,

and osteichthyans. It originates on the preorbital part of the skull, and inserts on the mandible and in some cases also on the adductor muscles and labial cartilages (Anderson, 2008). In extant *Heterodontus* and orectolobiforms the preorbitalis is sudivided (Wilga, 2005), and this may also have been the case in *Tribodus*. It is possible that in *Tribodus* an additional slip of the preorbitalis originated on the ventral part of the interorbital wall, either at the base of the median ventral "keel process" (as in extant etmopterids; Shirai, 1992), or more broadly covering the ventrolateral surface of the orbital region behind the median ventral process (e.g., *Squaliolus*, Shirai, 1992). The presence of small uncalcified areas on the basicranium of *Tribodus* dorsolateral to the median ventral process on either side may represent attachment sites for these muscle slips. In some batoids, the preorbital muscle forms multiple (as many as five) separate slips (Daniel, 1934, p. 101), but this condition is likely derived.

**Adductor mandibulae—**An adductor mandibulae muscle (am) was presumably present in *Tribodus*. Anderson (2008) concluded that the presence of a subdivided adductor mandibulae (innervated by the trigeminal nerve, and used to raise the mandible) is primitive for crown-group gnathostomes, and may also have been present in placoderms (Miles, 1969). In extant elasmobranchs, the adductor mandibulae typically originates on the palatoquadrate and inserts on the lower jaw; whereas in osteichthyans and chimaeroids it originates directly on the neurocranium (Anderson, 2008). Maisey (1989B, 2007) hypothesized the presence of an adductor mandibulae similar to that of extant elasmobranchs in cladoselachian sharks (1989B) and "*Cobelodus*" (2007) (Fig. 72).

The adductor mandibulae of *Tribodus* was probably compact anteroposteriorly, corresponding to the reduced length of the jaws relative to the braincase in *Tribodus*. As in extant elasmobranchs, the adductor mandibulae probably formed two main divisions (a dorsal division on the palatoquadrate and a ventral division on Meckel's cartilage), separated by a mid-lateral raphe along their contact point. The dorsal division probably originated in the deep adductor fossa underlying the quadrate flange anteriorly, and the underside of the flange may have provided increased surface area for the muscle to attach. The ventral division of the adductor mandibulae probably covered most of the lower jaw, terminating beneath a ridge at the anterodorsal margin of the jaw. The presence of a durophagous dentition in *Tribodus* suggests a powerful adductor mandibulae, as in many extant elasmobranchs with a crushing dentition (e.g., *Heterodontus* and batoids; Daniel, 1934).

**Adductor mandibulae superficialis—**It is possible that an adductor mandibulae superficialis (ams) was present in *Tribodus*, and one is included in the reconstruction presented here (Fig.66), although this is speculative. This muscle occurs in basal members of each of the major neoselachian groups (orbitostylic sharks, *Heterodontus*, and batoids; Shirai, 1992) raising the possibility that it could be primitive for neoselachians. The adductor mandibulae superficialis typically originates on the mandibular arch and inserts on subcutaneous tissue behind the eye, but in a few taxa it inserts elsewhere (e.g., on the antorbital process in hexanchoids; Shirai, 1992). If present in *Tribodus*, this muscle may have originated on the posterior or posteroventral part of the adductor mandibulae or palatoquadrate, and inserted on subcutaneous tissue of the

eye region (as suggested in Fig. 66); or alternatively, on the small knob-like projections on the antorbital processes, as in extant hexanchoids.

**Levator palatoquadrati—** A levator palatoquadrati muscle (lp; innervated by the trigeminal nerve, and used for upper jaw retraction) was probably present in *Tribodus*, originating on the otic region of the braincase and inserting on the palatoquadrate as in gnathostomes generally (Wilga, 2005; Anderson, 2008). Part of the muscle may have additionally originated on the posteroventral part of the postorbital process, although this is speculative. In Recent elasmobranchs, the levator palatoquadrati is located between the spiracle and the orbit, typically originating on the otic region of the braincase (often from a sphenopterotic ridge) or from the adjacent epaxial muscle, and inserting on the dorsal part of the palatoquadrate (Shirai, 1992). According to Anderson (2008), the levator palatoquadrati is most parsimoniously considered primitive for crown-group gnathostomes, and subsequently lost in chimaeroids (associated with development of a holostylic jaw suspension).

**Intermandibularis—**An intermandibularis muscle (im) innervated by the trigeminal nerve (originating on the midventral raphe and inserting on the mesial sides of the lower jaws, as in most neoselachians, Wilga, 2005) was presumably present in *Tribodus*. It has been proposed that an intermandibularis is primitive for crown-group gnathostomes (Anderson, 2008), and one has been reconstructed in a fossil cladoselachian shark from Tennessee (in which muscle impressions are well preserved; Maisey, 1989B). A homologue of this muscle is present in chimaeroids, but differs in its topology from that of other chondrichthyans (Anderson, 2008). Among living neoselachians, a degree of morphological variation in the interhyoideus (ih) exists between taxa (for example, some

lamniforms lack a mid-ventral raphe between the paired interhyoideus muscles; whereas in *Isurus* the muscle also extends between the edges of the palatoquadrate; Wilga, 2005).

**Levator hyomandibularis—** A levator hyomandibularis (lh; used for lower jaw retraction) was probably present in *Tribodus*, and probably originated on the posterior of the otic capsule and inserted directly on the dorsal surface of the hyomandibula. This muscle has been considered primitive for crown-group gnathostomes, in which it generally originates on the neurocranium and inserts on the hyomandibula, and is innervated by the facial nerve (Anderson, 2008). It is possible that an anterior slip of the levator hyomandibularis in *Tribodus* may have additionally inserted on the palatoquadrate, as in some extant squaloids. The levator hyomandibularis in extant elasmobranchs is generally continuous with the series of superficial constrictors immediately following it, except in rajiforms, *Heterodontus*, and orectoloboids (although the rajiform and *Heterodontus*/orectoloboid conditions may not be homologous; Shirai, 1992).

**Interhyoideus—**An interhyoideus muscle (ih) was probably present in *Tribodus*, stretching between the left and right halves of the hyoid arch ventrally and innervated by the facial nerve as in other gnathostomes (Anderson, 2008). Anderson (2008) proposed that this muscle is most parsimoniously considered present in the ancestor of crown-group gnathostomes, and lost secondarily in chimaeroids (possibly linked to their nonsuspensory hyoid arch). A homologue of the interhyoideus muscle is termed the depressor hyomandibularis in rays (Shirai, 1992). In extant elasmobranchs, the intermandibularis originates from a median raphe of connective tissue (as does the intermandibularis), and inserts on the distal edge of the hyomandibula in rays and on the

ventroposterior edge of the ceratohyal in sharks (Shirai, 1992; Wilga, 2005). It is located deep to the intermandibularis. The shark-like condition (in which the interhyoideus inserts on the ceratohyal) was probably present in *Tribodus*.

**Dorsal hyoid constrictor—**A hyoid constrictor muscle innervated by the facial nerve was interpreted as primitive for crown-group gnathostomes by Anderson (2008), and this muscle was presumably also present in *Tribodus*. In extant elasmobranchs, the dorsal hyoid constrictor originates on the side of the braincase and from the fascia extending behind it, and typically inserts on the dorsal margin of the hyomandibula (although in most squaloids and pristiophoroids, the muscle inserts on the palatoquadrate and hyomandibula; Shirai, 1992). The hyoid constrictors are typically continuous with the superficial branchial constrictors posteriorly, except in rajiforms and some galeomorphs (Shirai, 1992). In chimaeroids, a homologous muscle series is termed the opercular constrictor series (Anderson, 2008). The arrangement of the hyoid constrictor muscles in *Tribodus* was probably similar to that of neoselachians, although it is unknown if they were continuous with the posterior constrictor series.

**Coracomandibularis—**Due to the inferred presence of a coracomandibularis (com) in the ancestor of crown-group gnathostomes (Anderson, 2008), and its presence in both neoselachians and chimaeroids, it is considered here that this muscle was also present in *Tribodus*. The coracomandibularis in *Tribodus* was probably similar to that of other hyostylic elasmobranchs with an intact and suspensory hyoid arch (i.e., extant galean and squalean sharks), originating on the pectoral girdle and inserting on both sides of the mandibular symphysis. As in other chondrichthyans, and gnathostomes in general (except teleosts; Wilga et al., 2000; Fig. 73), it is here inferred that the coracomandibularis in

*Tribodus* functioned to depress the lower jaw. The coracomandibularis is generally innervated by branches of the spinal accessory nerve (Anderson, 2008).

**Coracohyoideus—** It is inferred here that a coracohyoideus muscle (coh) was present in *Tribodus*, and was probably morphologically similar to that of most extant elasmobranchs (i.e., inserting on the basihyal cartilage and originating on the coracoid bar of the pectoral girdle and/or the coracoarcual muscles). The basihyal cartilage of *Tribodus* has a rounded protuberance on its posteroventral surface, which may have formed an anchor point for the insertion of the coracohyoideus. The coracohyoideus is considered primitive for crown-group gnathostomes (Anderson, 2008), and typically functions to depress the hyoid arch (Wilga et al., 2000; Fig. 73). In chimaeroids, this muscle connects with the coracomandibularis muscle (Anderson, 2008). Like the coracomandibularis, the gnathostome coracohyoideus is generally innervated by the spinal accessory nerve (Anderson, 2008).

**Coracobranchialis—** It is interpreted here that a coracobranchial series of muscles was probably present in *Tribodus*, with points of origin and insertion comparable to those of extant sharks (originating on the pectoral girdle and inserting on the visceral skeleton). According to Anderson (2008), the coracobranchial muscles are most parsimoniously interpreted as primitive for crown-group gnathostomes, and lost in *Latimeria*. There are typically five coracobranchial muscles located ventral to the floor of the pharynx in extant elasmobranchs (Shirai, 1992). The first coracobranchial (Fig. 69D: cob1) originates on the anterior of the coracoarcual and inserts on the posterolateral ends of the basihyal and/or the distal part of the ceratohyal in Recent shark-like elasmobranchs (including squaleans and galeomorphs); in many batoids it is called the

coracohyomandibularis (Fig. 69E: cohm), and inserts on the distal part of the hyomandibula via a tendon (Shirai, 1992).

**Cucullaris—**Anderson (2008) considered a cucullaris muscle group to be primitive for crown-group gnathostomes, and one was presumably present in *Tribodus*. In neoselachians, the cucullaris muscles originate as part of the epibranchial musculature and insert on the pectoral girdle, and are innervated by the vagus nerve (Anderson, 2008). However, in chimaeroids and *Amia*, this muscle series extends from the braincase to the pectoral girdle and branchial arches, and is innervated by the vagus and glossopharyngeal nerves (Anderson, 2008). It is likely that the cucullaris muscle in *Tribodus* was more closely similar to that of neoselachians.

## DISCUSSION

### Comparison of the Jaws in *Tribodus* and Other Hybodonts

The jaws of *Tribodus limae* are much shorter anteriorly than jaws of *Egertonodus basanus* (Fig. 60) and most other hybodonts (Fig. 74A–D) (although all hybodonts and most neoselachians have short jaws compared to many Paleozoic sharks, in which the jaw joint is often extended behind the otic region). Anteriorly short jaws like those of *Tribodus* are also found in a few other hybodont taxa, including *Asteracanthus* (Fig. 74E–H), *Lissodus*, and *Lonchidion*. Jaws of *Tribodus* were oriented nearly transversely (unlike in *Egertonodus* and other long-jawed hybodontoids). The hyoid arch of *Tribodus* was suspensory, as in most elasmobranchs, but no obvious articular facets connecting the palatoquadrates and braincase are present.

Brito (1992) originally reconstructed the braincase of *Tribodus limae* as similar to that of some other hybodonts such as *Egertonodus basanus*, with paired ethmopalatine processes (Brito, 1992, fig. 1: p. art.) and an internasal keel (Brito, 1992, fig. 1: q. int). Brito (1992) described the palatoquadrates of *Tribodus* as having a single point of articulation with the neurocranium, occurring at the anterior of the snout by "une solide junction avec le processus ethmopalatin, separe de son symetrique par la quille internasale….En consequence, les deux palatocarres ne sont pas unis sur la ligne mediane du crane par une symphyse, mais sont libres." [a solid junction with the ethmopalatine process, separated symmetrically by the internasal keel….in consequence, the two palatoquadrates are not united along the median line of the cranium by a symphysis, but are free] (Brito, 1992:146). However, Brito's (1992) description was based on a specimen in which the braincase was damaged, and examination of additional specimens of *Tribodus* (particularly AMNH 13958, UERJ-PMB-40, and UERJ-PMB-114) shows that the former interpretation is incorrect.

Inflated ethmopalatine processes and an internasal keel in the ethmoid region (forming an ethmoidal articulation with the palatoquadrates) are absent in *Tribodus*. However, an anteroposteriorly short median basicranial process (resembling the "keel process" of some extant squalean sharks; Shirai, 1992) is present beneath the anterior part of the orbit, between the antorbital process and optic foramen. In *Egertonodus*, the palatoquadrates abut the internasal keel laterally, and are separated by it (Maisey, 1982, 1983). However, it is unlikely that the median keel process in *Tribodus* separated the palatoquadrates, because the jaws terminate posterior to it and do not extend beyond the midpoint of the orbit. It is possible that an ethmopalatine ligament was present anteriorly

connecting the palatoquadrate to the braincase (possibly to the median basicranial process, or to paired rounded processes on the distal ends of the antorbital processes), as in some extant galeomorph sharks (Wilga, 2005). If this were the case, *Tribodus* could be considered "hyostylic" in the same sense as some extant basal lamniform taxa, in which the ethmoidal connection with the braincase is mainly ligamentous and lacks the ethmoidal articular facets found in carcharhiniforms (Wilga, 2005). Similarly, presence of a small flange on the dorsal surface of the palatoquadrate posteriorly suggests that there may have been a ligamentous posterior connection between the palatoquadrates and braincase, possibly homologous to a palatobasal articulation.

**Jaw Suspension in *Tribodus***

The jaw suspension of *Tribodus* can best be described as intermediate between hyostyly and euhyostyly (sensu Gregory, 1904; and Wilga, 2005; Fig. 75), in that direct skeletal support was provided only by the hyoid arch (as in batoids); articular facets on the palatoquadrate are absent; and the jaws do not reach the ethmoid region. However, unlike batoids, the hyoid arch in *Tribodus* is intact, as in neoselachian sharks and most other chondrichthyans (i.e., composed of articulated hyomandibular, ceratohyal, and basihyal cartilages).

Although ethmoidal articular facets on the palatoquadrate are absent in *Tribodus*, there is evidence that a ligamentous ethmoidal articulation may have been present, as in some extant lamniform sharks that have been described as hyostylic (Wilga, 2005). An ethmoidal articulation has been described as plesiomorphic for chondrichthyans (Maisey, 2008; Fig. 76), and some kind of sliding connection is present in the ethmoid region of

hybodonts in which the upper and lower jaws extend to the tip of the snout (e.g., *Egertonodus*: Maisey, 1983). However, an ethmoidal articulation and ethmopalatine ligaments are absent in batoids, in which the jaws do not reach the ethmoid region and an anterior basicranial process for jaw support is lacking.

A postorbital articulation is absent in *Tribodus* and many other hybodonts. However, a palatoquadrate articulation with the ventral part of the postorbital process was present in *Tristychius* (Maisey, 2008; Fig. 76), and there is some evidence that a similar articulation was present in a Triassic hybodont (Thomson, 1982). A postorbital articulation is found in many Paleozoic chondrichthyans (e.g., xenacanths, symmoriiforms, *Pucapampella*) as well as in modern hexanchiforms, although in the latter this structure is considered to be secondarily derived (Maisey, 2008). A specialized orbital articulation (extending dorsally between the optic pedicel and optic foramen) like that found in extant squalean sharks (e.g., *Squalus*), has never been observed in hybodonts (Maisey, 1980). An orbital articulation is primitively present in many chondrichthyans, but this too appears to be lacking in *Tribodus* although a "basal" articulation has been reported in other hybodonts (e.g., *Acrodus* sp.; Thomson, 1982). However, *Tribodus* may have had a ligamentous palatobasal articulation posteriorly, in the region of the paired basicranial processes.

**Notes on jaw function in *Tribodus* and other elasmobranchs**

Although the jaws of *Tribodus* were relatively free (i.e., a "direct" cranio-palatine articulation was absent, and the jaws were supported primarily by the hyoid arch), its jaw mobility was dependent on a number of factors, and cannot be inferred based on jaw suspension alone. According to Wilga (2002), the degree of jaw protrusibility is related

more with the length of the ethmopalatine ligament than with the type of jaw suspension, in that a long ethmopalatine ligament (or total lack of that ligament) increases jaw protrusibility.

If present, the ethmopalatine ligament of *Tribodus* would have had to be relatively long (due to the lack of any direct articulation of the palatoquadrate with the braincase), which would presumably allow for considerable jaw mobility (Wilga, 2002). Alternatively, an ethmopalatine ligament may have been lacking in *Tribodus* (although this seems less likely, based on the presence of the median basicranial process in close proximity to the jaws). An ethmopalatine ligament is absent in batoids, many of which have highly protrusible jaws (Dean and Motta, 2004). Thus, whether *Tribodus* had no ethmopalatine ligament (as in batoids) or a long ligament (as in *Squalus*), it is here inferred that the jaws of *Tribodus* were protrusible and highly mobile. Jaw protrusibility of *Tribodus* was probably intermediate between *Heterodontus* (in which an ethmopalatine buttress limits jaw mobility; Wilga, 2002), and batoids (in which decoupling of the mandibular and hyoid arches generally allows for increased jaw flexibility; e.g., *Narcine*; Dean and Motta, 2004), and may have been comparable to extant *Squalus* and lamniform sharks (Wilga, 2002). Neoselachians with shorter, anteriorly directed hyomandibulae and shorter jaws have been found to have the largest upper jaw protrusion distance (Wilga, 2002), further suggesting that *Tribodus* may have had a high degree of upper jaw protrusion compared with other hybodonts.

Although *Tribodus* had a durophagous dentition similar to that of extant batoids, its jaws were not fused symphysially (although they were connected ligamentously), suggesting that a 'nutcracker-type' feeding mechanism such as that used by extant

myliobatid rays for force amplification in crushing hard prey; Summers, 2000) was probably absent in *Tribodus*. Another adaptation for durophagy found in some neoselachians (e.g., orectolobiforms; *Squalus*) is a jaw joint that is ventrally offset from the occlusal planes of the jaws. However, this is primarily a functional adaptation that allows teeth with a clutching-type morphology to be used for crushing hard prey (Ramsay and Wilga, 2007), and appears to be absent in *Tribodus*, in which it is functionally unnecessary because the teeth are already adapted for durophagy.

Summers (2000) listed multiple layers of prismatic cartilage and presence of supporting endochondral struts, both reported here for the first time in *Tribodus*, as further morphological adaptations for durophagy in myliobatid stingrays and numerous other extant chondrichthyans (e.g., *Pristis*; *Isurus*; chimaeroids) (Fig. 77, 78). Summers (2000) termed these endochondral struts "trabecular cartilage"; however, that term is considered somewhat misleading in that it is easily confused with the trabeculae of the embryonic basicranium. According to Summers et al. (1998) and Summers (2000), endochondral struts in batoids are an adaptation providing added structural support to an otherwise relatively soft material (i.e., cartilage), and producing a strong but lightweight structure (comparable to the steel framework upholding some modern buildings). They represent an interesting evolutionary novelty, allowing the adaptation of strong crushing jaws within the evolutionary constraints of a soft cartilaginous skeleton. The presence of endochondral struts was originally considered as a potential synapomorphy of extant myliobatoid rays (Summers et al., 1998; Summers, 2000; Fig. 78). However, it has since been discovered to be more widespread among batoids, occurring also in the torpediniform *Narcine brasiliensis* (which is not durophagous, but requires added support

when protruding its jaws into the substrate to feed on soft polychaetes). Further research is needed to determine if endochondral struts might also occur in extant non-batoid neoselachians. According to Summers (2000), the struts typically are arranged in such a way as to transfer the force from prey crushing to the multiple layers of prismatic cartilage lining the jaw surface. The cartilage struts have been observed even in embryos of planktivorous myliobatoids, suggesting that they may have a phylogenetic rather than a functional origin (Summers, 2000). This view may be further supported by the presence of endochondral struts elsewhere in the skeleton of *Tribodus* (e.g., in the basicranial wall). The occurrence of these struts in jaws of *Tribodus* suggests that their presence in neoselachians may be plesiomorphic, rather than representing a derived feature of extant batoids. Alternatively, they may have arisen independently in *Tribodus* and batoids.

Multiple layers of prismatic cartilage have previously been considered to be present only in a few fossil chondrichthyans (e.g., xenacanths and 'ctenacanths,' but generally absent in symmoriiforms; Summers, 2000; Schaeffer, 1981). However, multiple layered prismatic cartilage throughout the skeleton may still be characteristic of a subgroup of extinct elasmobranchs, because in neoselachians and *Tribodus* this feature seems to be restricted to the jaw region (Summers, 2000). It is unknown whether multiple-layered cartilage has any phylogenetic significance, or whether it represents a widespread structural adaptation in skeletal elements that are subjected to increased force (e.g., jaws), but according to Summers (2000) it may be plesiomorphic for Chondrichthyes.

**Feeding behavior and ecology of *Tribodus***

Durophagy has apparently evolved independently several times within neoselachians (e.g., some galean sharks and batoids; Huber et al., 2008), and in holocephalans (Fig. 78), and is generally characterized by a suite of morphological features including a molariform or pavement dentition of stout flattened teeth (Fig. 80) (primitively present in stem holocephalimorphs, but lost or modified in chimaeras); hypertrophied jaw adductor muscles capable of high force production; robust, well-calcified jaws; and high jaw leverage (Huber et al., 2008). The presence of a molariform or pavement dentition (Fig. 80) has been strongly correlated with durophagy in modern elasmobranchs (Huber et al., 2008). Durophagy is inferred in several hybodont taxa besides *Tribodus* (e.g., *Acrodus* and *Asteracanthus* (Fig. 81). However, *Acrodus* possesses occlusally rounded, ornamented, molariform teeth (comparable to those of *Heterodontus*), whereas teeth of *Asteracanthus* are flattened occlusally and elongate, suggesting possible differences in their feeding mechanisms and prey types. This difference may be further supported by the presence of acuminate (sharply pointed) anterior teeth in *Acrodus* (presumably used for grasping prey), whereas anterior teeth of *Asteracanthus* are rounded and blunt occlusally. *Tribodus*, *Acrodus* and *Asteracanthus* all possess teeth with columnar osteodentine, and have been classified together in the family Acrodontidae on the basis of this character (Brito, 1992; Maisey et al., 2004). Most other hybodontiforms (e.g., *Hybodus*, *Egertonodus*) lack a durophagous dentition.

*Asteracanthus* palatoquadrates are morphologically similar to those of *Tribodus* in several respects (e.g., presence of a broad dental pad with a strongly projecting anterolateral rim; strongly overhanging quadrate flange and deep adductor fossa;

presence of a palatoquadrate symphysis; and the overall shape of the dorsal margin of the palatoquadrate) and probably did not extend to the ethmoid region (inferred from the absence of an ethmoidal articulation, and (like *Tribodus*) appear to have been orientated more transversely than those of other hybodonts. *Asteracanthus* palatoquadrates differ from those of *Tribodus* in having a more rounded and dorsoventrally convex mesial surface (it is concave in *Tribodus*), and the anterior of the palatoquadrate is more pointed and slopes downward at a much steeper angle than in *Tribodus*.

Dentition types associated with durophagous prey in neoselachians include the crushing type (e.g., *Raja*); grinding type (e.g., *Myliobatis*); and clutching-grinding type (e.g., *Heterodontus*) (Wilga and Motta, 1998). Wilga and Motta (1998) defined crushing as "the forceful occlusion of the opposing dental surfaces" and grinding as "dental surfaces not only oppose one another...but also slide past one another." Teeth used for crushing can be low-cusped or molariform, are small and numerous, and typically form a bumpy surface. In *Heterodontus*, the anterior teeth have cusps for grasping prey, whereas the posterior teeth are molariform and specialized for crushing. In neoselachians with a grinding dentition, the teeth are typically flat, forming an imbricated pavement of tooth plates; the jaws are strengthened by calcified struts, and a lever system amplifies the force of the adductor muscles (Wilga and Motta, 1998). A pavement of flat hexagonal teeth similar to that of *Tribodus* is found in some myliobatid rays, which use them to grind molluscs and crustaceans (Wilga and Motta, 1998). Some rays have evolved further features adapted for grinding, such as fusion of the upper and lower jaw symphyses, a restricted gape, and asynchronous activation of the jaw adductors (Wilga and Motta, 1998).

The presence of flattened, hexagonal teeth forming an imbricated pavement dentition in *Tribodus* suggests that it was likely a benthic feeder with a partly or completely durophagous diet (Brito and Ferreira, 1989; Brito, 1992; Maisey and Carvalho, 1997). Its feeding pattern probably consisted of crushing and grinding prey (although its jaws were not as highly specialized for grinding as those of myliobatid stingrays and lack a fused symphysis; Summers, 2000). The absence of cuspidate teeth suggests that teeth were probably not used for grasping prey (unlike *Heterodontus*). This interpretation is further supported by the anteroposteriorly shortened jaws with a batoid-like, semi-euhyostylic jaw suspension; anteroventrally downward-sloping braincase; large orbit (possibly indicating large eye size adapted for vision in a reduced-light habitat).

Whether *Tribodus limae* was a specialist on one type of prey or a generalist with a variety of prey types is unknown. However, the discovery of fossilized shrimp and coarse sand grains inside the body cavity of *Tribodus* (Maisey and Carvalho, 1997) raises the possibility that it was a benthic feeder that specialized on crustaceans. Alternatively, it may have been a generalist feeder, similar to extant rhinobatoids and rajoids (Wilga et al., 2007). However, *Tribodus* was apparently a mechanistic specialist (adapted to crushing prey) and an ecological specialist (adapted to a benthic lifestyle).

**Conclusions—**The following conclusions can be drawn from the present study:

1) Both upper and lower jaws of *Tribodus limae* contain endochondral struts similar to those found in extant myliobatid batoids (Summers, 1998, 2000), which may have provided added structural support to the jaws. Like the endochondral struts of batoids, those of *Tribodus* seem to have a hollow lumen lined with prismatic cartilage, they are concentrated primarily in parts of the jaws subjected to the

highest forces during biting and jaw opening/closing (i.e., at the mandibular articulation and in the region of the dental pads), and they are arranged perpendicular to the jaw surface, but normal to the inferred direction of force. This represents the first report of endochondral struts in a fossil chondrichthyan, and the first description of this feature in any non-batoid elasmobranch. At least two layers of prismatic cartilage also appear to have been present in jaws of *Tribodus*, as in numerous extant neoselachian taxa.

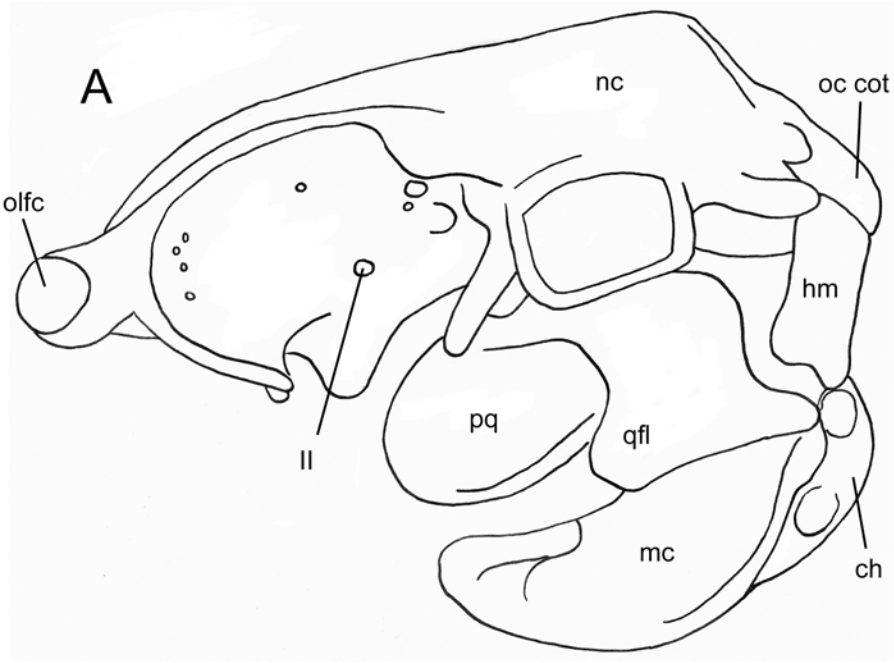
2) The jaw suspension of *Tribodus* appears to have been functionally intermediate between the hyostylic suspension of many hybodonts and the euhyostylic suspension of batoids, and may have been similar to that of some extant lamniforms (in which the cranio-palatoquadrate articulations are primarily ligamentous; articular facets are lacking; and skeletal support for the jaws is primarily by the hyoid arch). The hyoid arch of *Tribodus* is intact and articulated, unlike the batoid condition.
3) *Tribodus* had palatoquadrates not extending anteriorly as far as the ethmoid region, unlike many hybodonts (e.g., *Egertonodus*; *Hybodus*; *Acrodus*), but similar to some hybodont taxa including *Asteracanthus*. Similarities in palatoquadrate morphology in *Tribodus* and *Asteracanthus* suggest a potentially close phylogenetic relationship between them. Palatoquadrates not extending to the ethmoid region are also found in some extant neoselachians, including batoids and many orbitostylic sharks, but not in hexanchoids or most galeomorphs. Jaws of *Tribodus* also were orientated more transversely than those of most other

hybodonts (Maisey and Carvalho, 1997), superficially resembling jaws of some extant squalean sharks and batoids.

4) Five branchial arches were probably present in *Tribodus*, and those features which can be observed are morphologically similar to those of other hybodonts. Pharyngobranchials, epibranchials, and ceratobranchials are identified; hypobranchial and basibranchial elements were presumably present, but may have been uncalcified. A pharyngobranchial blade is present in *Tribodus*, as in several other hybodontiforms (e.g., *Tristychius*; *Lissodus*) and extant galeomorphs, supporting the view that a pharyngobranchial blade may be primitive for neoselachians (Shirai, 1992; cf. de Carvalho, 1996).
5) Features of the visceral skeleton in *Tribodus* and comparison with neoselachians suggests that *Tribodus* had a muscle similar or homologous to the suborbitalis/preorbitalis of extant elasmobranchs, which inserted on the antorbital processes. On the basis of its lack of direct cranio-palatine articulations and probable presence of a long ethmopalatine ligament, it is likely that jaws of *Tribodus* had a high degree of protrusibility. However, it is unlikely that *Tribodus*' jaws were as protrusible as those of some extant batoids (e.g., *Narcine*).
6) A number of morphological features (an imbricated pavement dentition of relatively large, hexagonal, flat teeth; presence of endochondral struts in in the region of the biting surface and the jaw joint; jaws with multiple-layered prismatic cartilage; previous discovery of shrimp and coarse sand grains in fossilized stomach contents) support the view that *Tribodus* was a benthic feeder with a durophagous diet. However, the lack of a fused jaw symphysis suggests that

*Tribodus* may have been less capable of handling harder prey (e.g., hard-shelled mollusks) than are extant durophagous myliobatids (Summers, 1998; 2000).

FIGURE 52. A, reconstruction of *Tribodus* head region in lateral view, showing position of mandibular and hyoid arch elements in relation to the basicranium. B, Reconstruction of *Tribodus* head region in ventral view, showing position of mandibular and hyoid arch elements in relation to the basicranium.


A
nc
oc cot
olfc
hm
pq
qfl
II
mc
ch

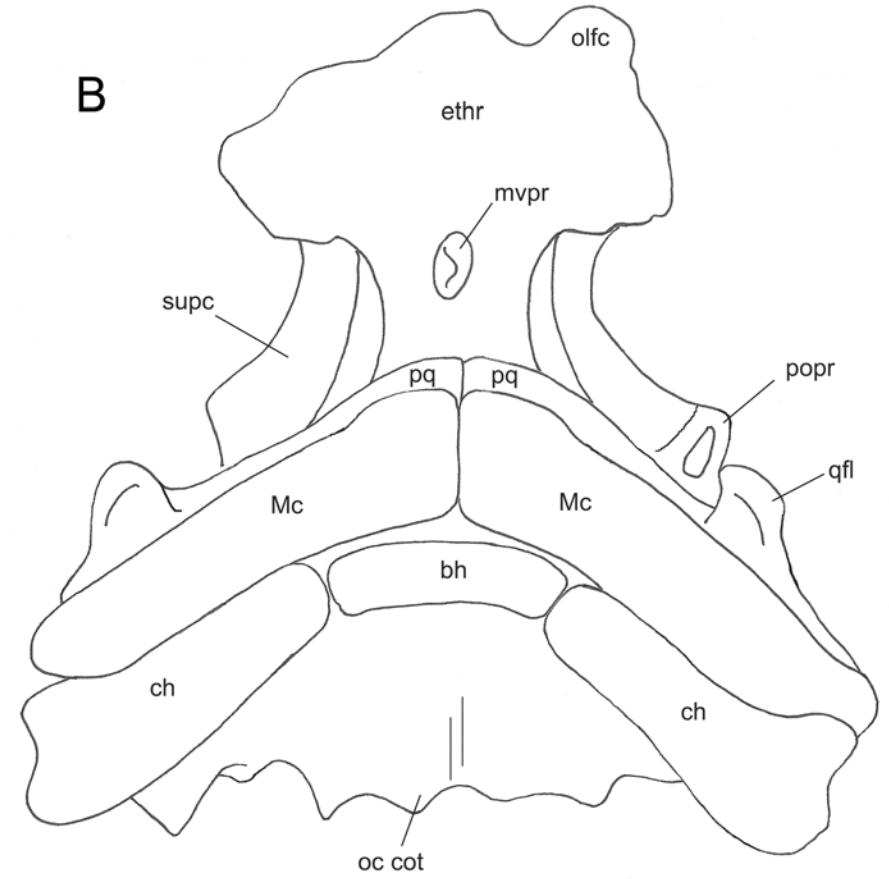

B
olfc
ethr
mvpr
supc
pq
pq
popr
qfl
Mc
Mc
bh
ch
ch
oc cot

FIGURE 53. Jaws of *Tribodus limae*, AMNH 13958. A, articulated upper and lower jaws, anterior view, jaws open; B, articulated upper and lower jaws, anterior view, jaws closed; C, upper (top) and lower (bottom) jaws in occlusal view; D, upper jaws in dorsal view. Scale bars equal two centimeters.

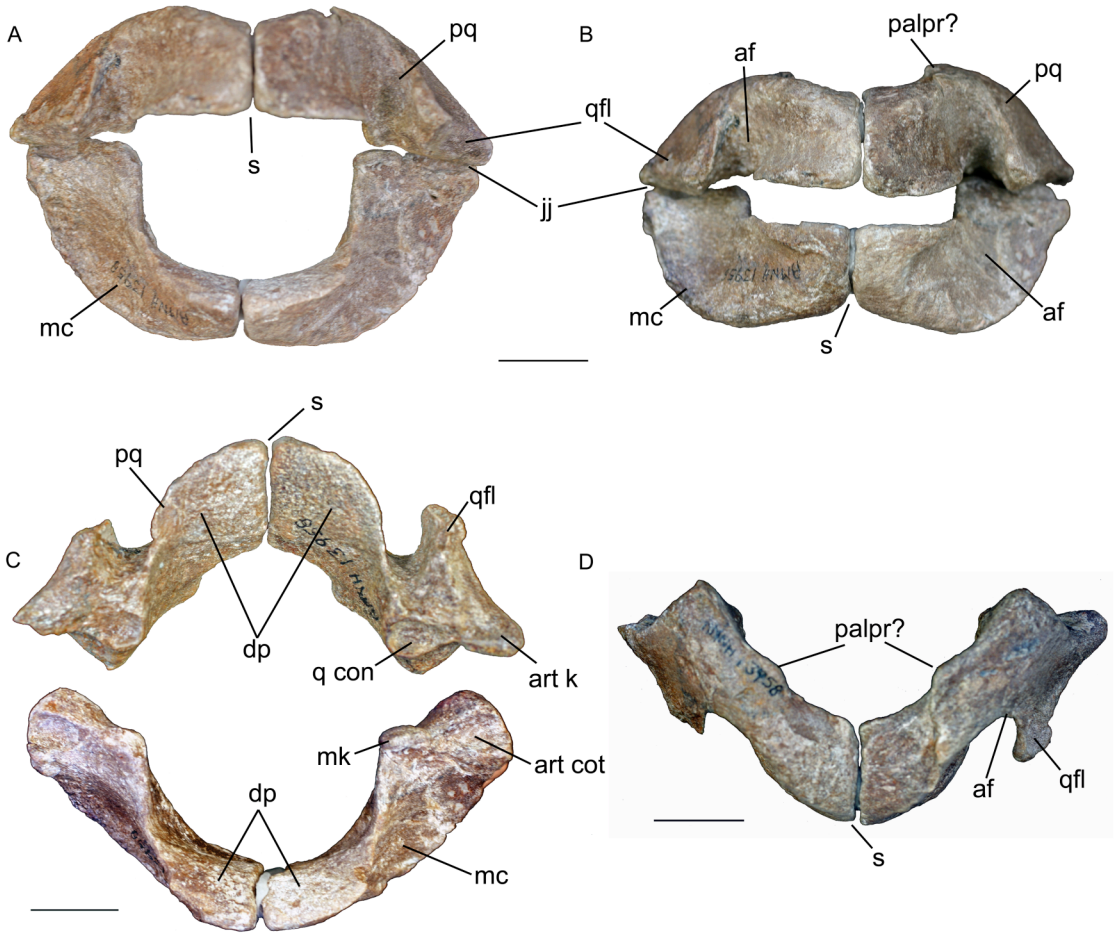

A
pq
s
mc
B
palpr?
af
pq
qfl
jj
mc
af
s
C
s
pq
qfl
dp
q con
art k
mk
art cot
dp
mc
D
palpr?
af
qfl
s

FIGURE 54. Jaws of *Tribodus limae*, AMNH 13958. A–C, left palatoquadrate, in A, lateral; B, mesial; and C, occlusal views. D–F, left Meckel's cartilage of the same specimen, in D, lateral; E, mesial; and F, occlusal views.

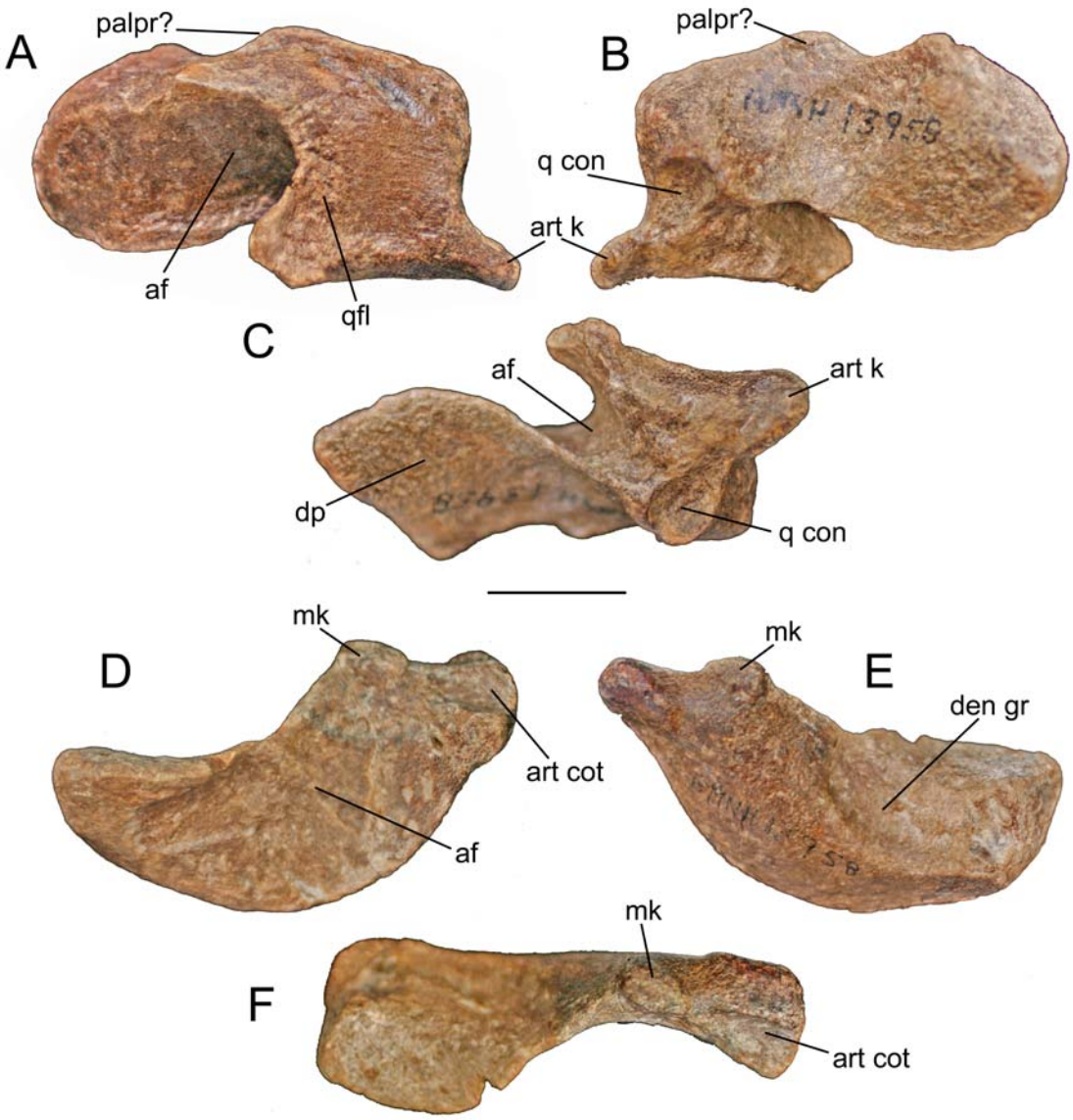

A
palpr?
af
qfl
B
palpr?
q con
art k
C
af
art k
dp
q con
D
mk
art cot
af
E
mk
den gr
F
mk
art cot

FIGURE 55. Left Meckel's cartilage of *Tribodus limae*, AMNH 13961, with partial dentition preserved. Scale bar equals two centimeters.

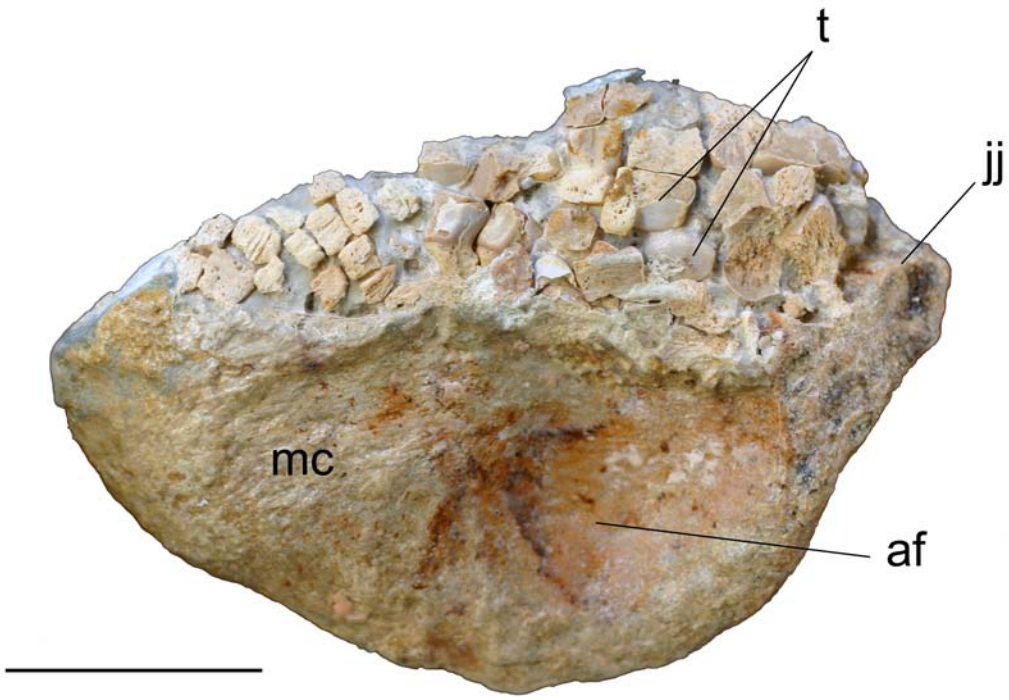

t
jj
mc
af

FIGURE 56. Hyoid arch elements of *Tribodus limae*, AMNH 13958. A–B, basihyal in posterior (A) and anterior (B) views; C–D, left hyomandibula in lateral (C) and mesial (D) views; E–F, right hyomandibula in lateral (E) and mesial (F) views; G–H, left ceratohyal in mesial (G) and lateral (H) views; I–J, right ceratohyal in mesial (I) and lateral (J) views.


A
C
E
post
ant
B
D
F
G
H
distal
I
J
proximal

FIGURE 57. Anterior of *Tribodus limae*, MN 5807V, showing jaws in relation to neurocranium. Scale bar equals 5 cm.


adfs
nc
bp
pbr
pq
qfl
sc
t
mc
r
mc

FIGURE 58. Anterior of *Tribodus limae*, MN 5808V, showing branchial skeleton in relation to other anterior structures. Scale bar equals 5 cm.


adfs
vert
nc
pbr
ebr
pq
t
cbr
sc
r
mc

FIGURE 59. *Tribodus limae*, MN 5807V. Closeup of Fig. 57 showing jaws, hyoid arch cartilages, and branchial elements. Note position of the hyomandibula and ceratohyal in relation to the jaws and neurocranium. Scale bar in millimeter increments.

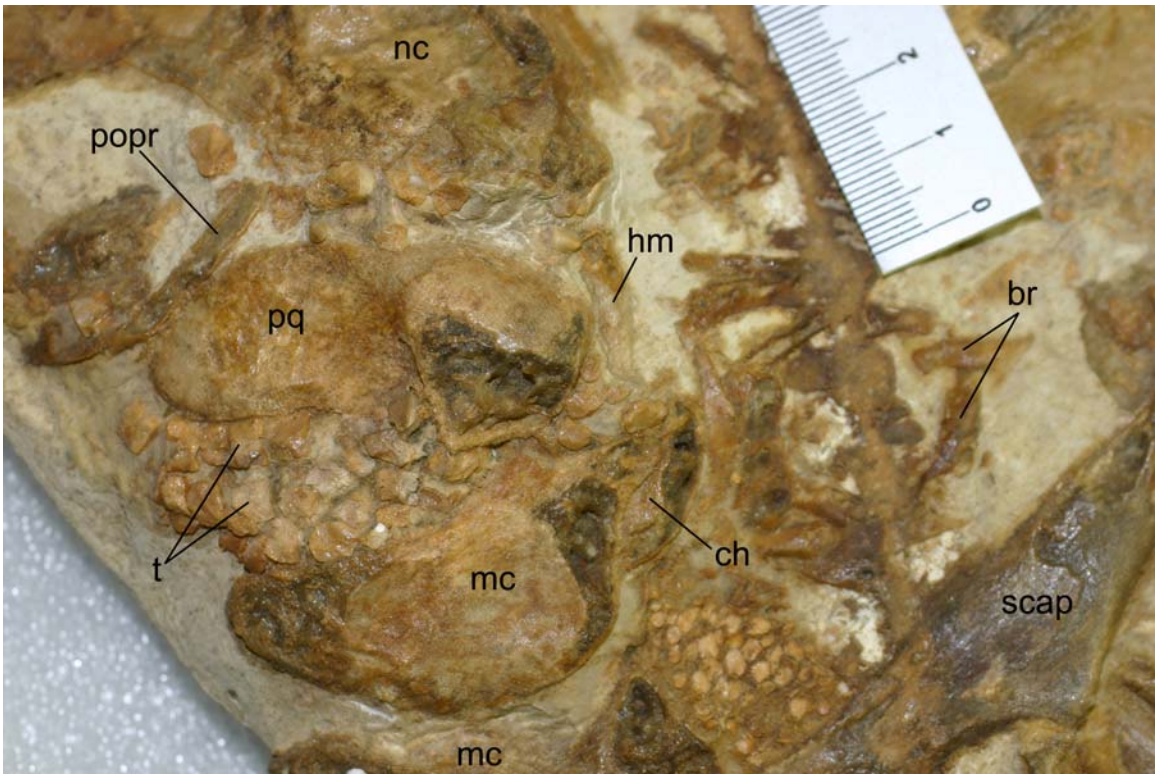

nc
popr
hm
pq
br
t
ch
mc
scap
mc

FIGURE 60. Jaw suspensions of *Egertonodus basanus* (A) and *Tribodus limae* (B) in left lateral view. Note extensive series of labial cartilages and anteroposterior extent of the jaws in *Egertonodus*. Scale bars equal 50 mm. After Maisey, 2008.

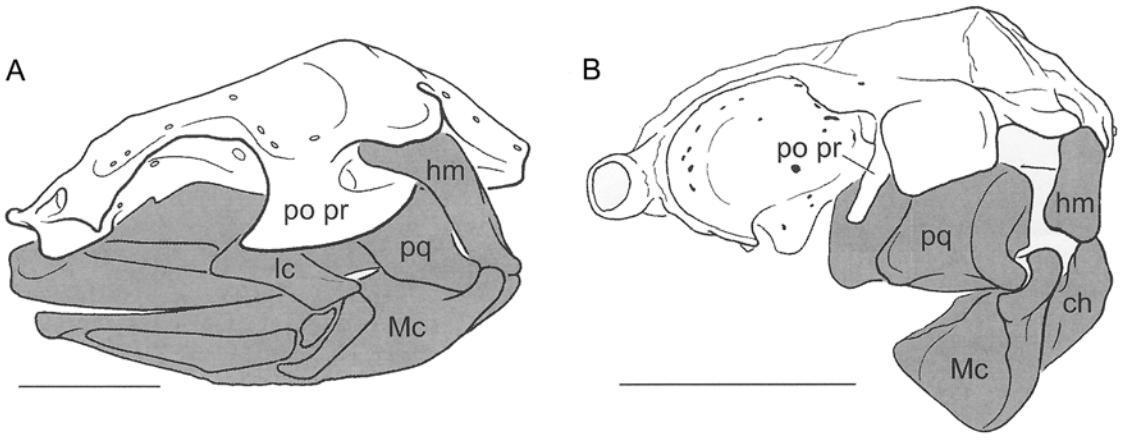

A
hm
po pr
pq
lc
Mc
B
po pr
hm
pq
ch
Mc

FIGURE 61. *Tribodus limae*, MN 5808V, closeup showing branchial skeleton. Scale bar in centimeters, with millimeter increments.

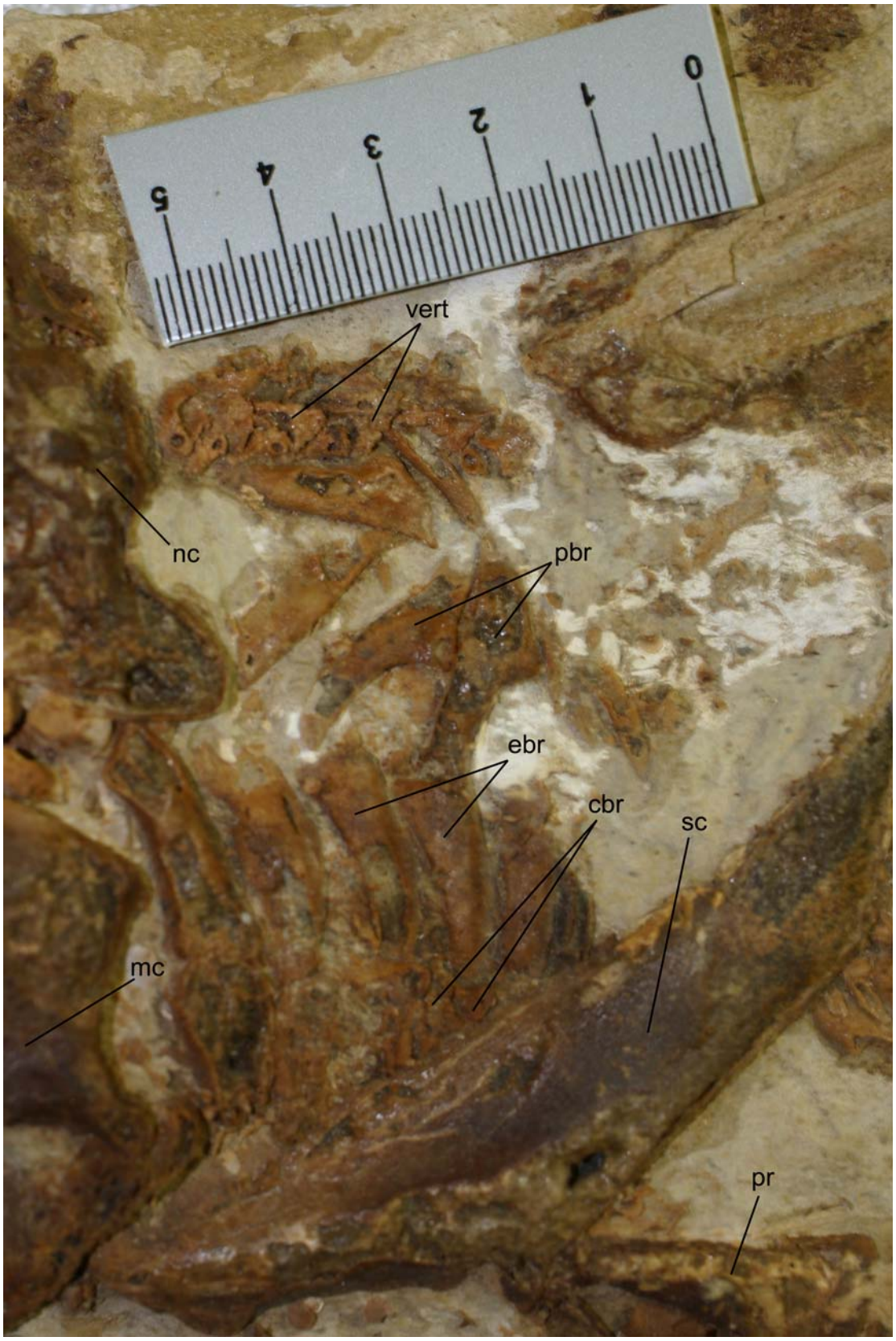
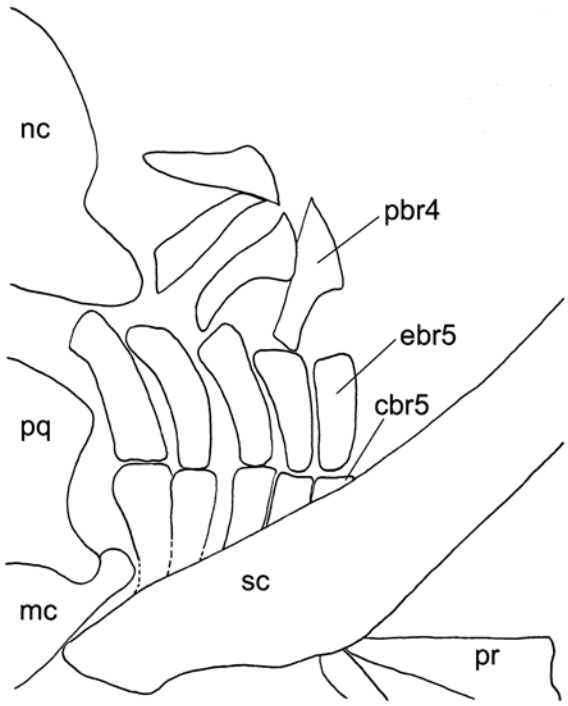

vert
nc
pbr
ebr
cbr
sc
mc
pr

FIGURE 62. *Tribodus limae*, MN 5808V, closeup of pharyngobranchials. Scale bar in centimeters, with millimeter increments.


pbr
ebr
5
4
3
2

FIGURE 63. Gill arches of *Tribodus limae*. A, line drawing of MN 5808V (Fig. 61), showing branchial elements as preserved. B, Gill arches of *Tribodus limae*, restored. Not to scale.

A




B

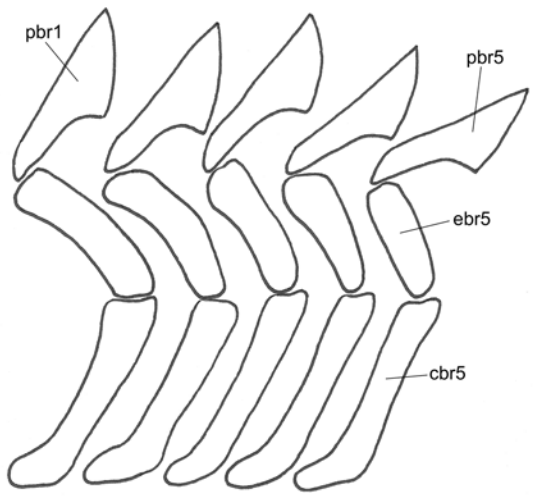


FIGURE 64. Gill arches of other hybodontids and extant sharks; after Maisey, 1982. A, *Lissodus cassangensis*; B, *Egertonodus fraasi*; C, *Hybodus hauffianus*; D, *Lissodus cassangensis*, restored; E, the extant shark *Heterodontus francisci*; F, the extant shark *Galeocerdo cuvier*. Not to scale.

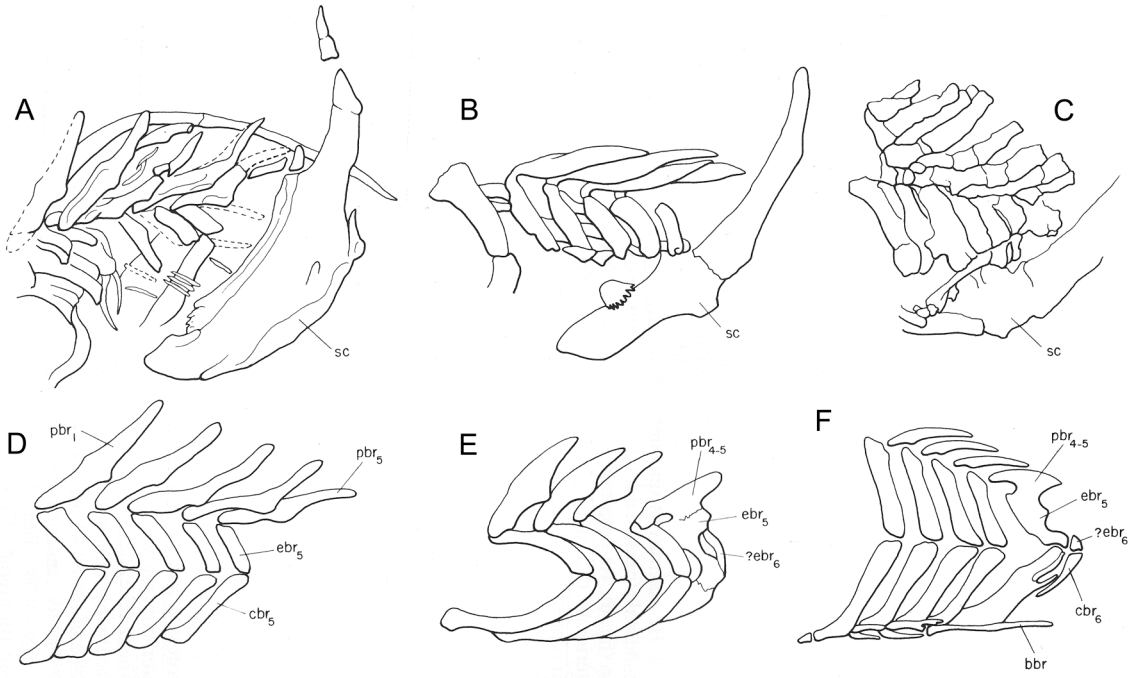

A
sc
B
sc
C
sc
D
pbr1
pbr5
ebr5
cbr5
E
pbr4-5
ebr5
?ebr6
F
pbr4-5
ebr5
?ebr6
cbr6
bbr

FIGURE 65. CT scan slices of *Tribodus limae* (AMNH 13958) upper and lower jaws, showing endochondral "struts." Struts appear as darkened, diagonal lines through the interior of the cartilage. Interior layer of prismatic cartilage particularly visible in slices B–E of lower jaw. A–E, Meckel's cartilage (lower jaw). Overview at left shows slice position on lower jaw, in mesial view. Mesial surface to lower right in A–E. A, articular region of lower jaw, slice 345; B–E, at the level of the dental pad. B, slice 693; C, slice 716; D, slice 745; E, slice 750. F–J, palatoquadrate (upper jaw). Mesial to lower left in F–J. All slices at the level of the dental pad. Overview at left shows slice position on upper jaw, in lateral view. F, slice 651; G, slice 704; H, slice 726; I, slice 742; J, slice 750. Asterisk indicates articular fossa of lower jaw. Small arrows indicate biting surface. Not to scale.

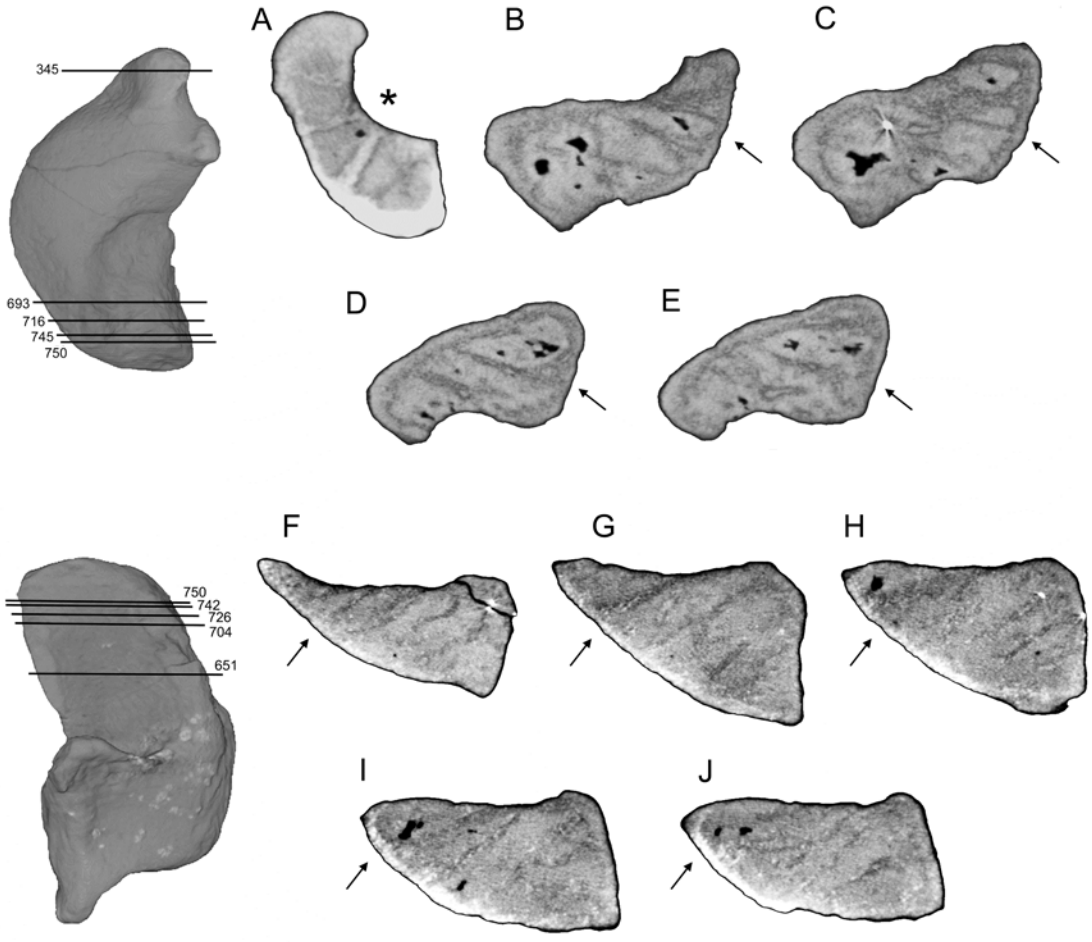
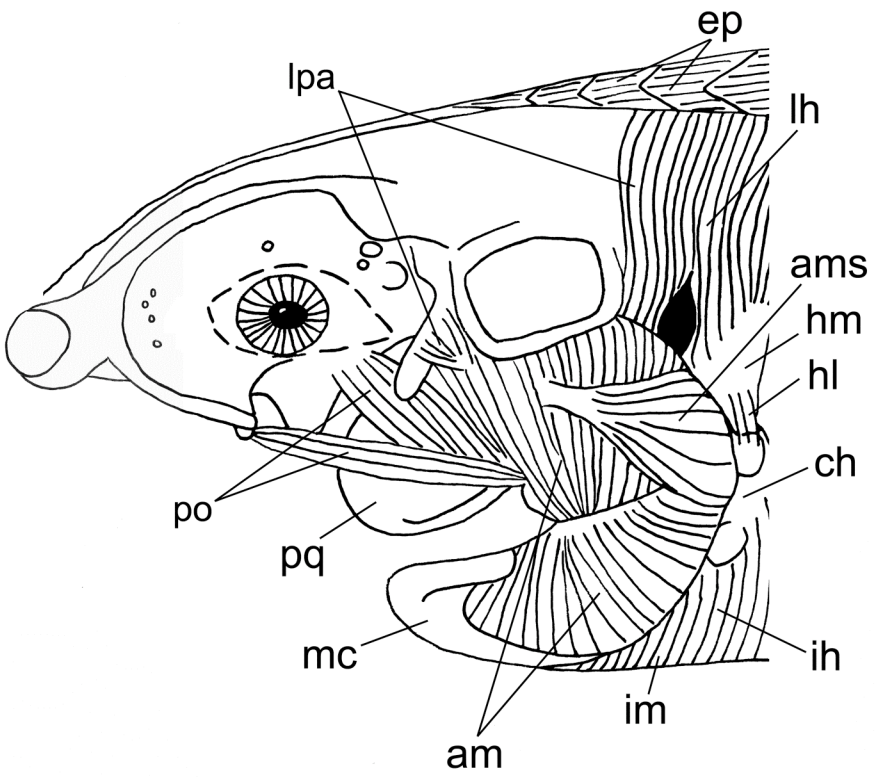

345
693
716
745
750
A
*
B
C
D
E
750
742
726
704
651
F
G
H
I
J

FIGURE 66. A, reconstructions of the jaw musculature in *Tribodus limae* in lateral (A) and ventral (B) views. In B, external muscles shown on the left, internal muscles shown on the right. Coracomandibularis shown in cutaway view to reveal the underlying musculature. Not to scale.


ep
lpa
lh
ams
hm
hl
ch
po
pq
mc
ih
im
am

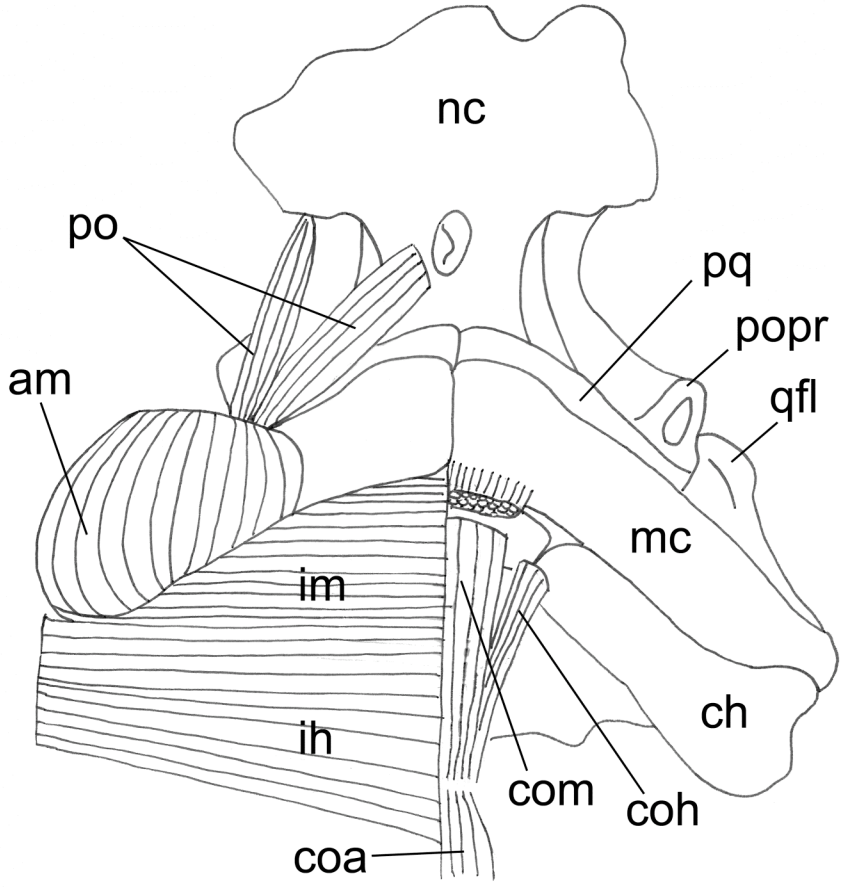
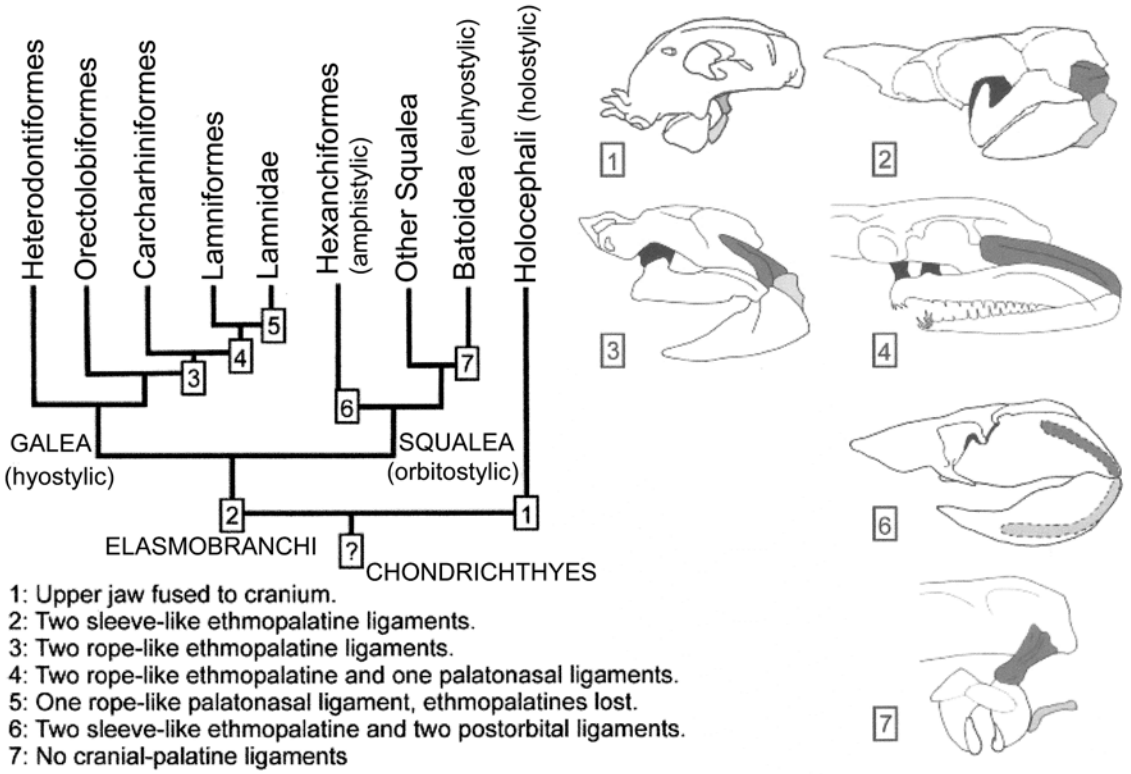

nc
po
pq
popr
am
qfl
mc
im
ch
ih
com
coh
coa

FIGURE 67. Evolution of cranial-palatoquadrate ligamentous connections in elasmobranchs, with holocephalans as the outgroup (after Wilga, 2005). 1, holostylic condition of holocephalans (e.g., *Callorhinchus milli*); 2, Basal elasmobranch condition (e.g., *Squalus acanthias*); 3, Carcharhiniform and lamniform condition (e.g., *Negaprion brevirostris*); 4, Basal lamniform condition (e.g., *Mitsukurina owstoni*); 5, Lamnid condition (e.g., *Isistius oxyrhinchus*); 6, Hexanchiform condition (e.g., *Heptranchias perlo*); 7, batoid condition (e.g., *Rhinobatos lentiginosus*). Note: this diagram adapts the position of Shirai (1992) that batoids are a derived group of squalean sharks, based mainly on morphological characters. Molecular trees support the opposing view, that batoids are basal neoselachians (Maisey et al., 2004). Although batoids lack any cranial-palatine ligaments, this may represent a derived condition. This is further supported by the presence of cranio-palatine articulations in many fossil elasmobranchs, suggesting that the basal neoselachian condition proposed by Wilga, 2005 (condition 2, two sleeve-like ethmopalatine ligaments) cannot be ruled out for fossil elasmobranchs with cranio-palatine articulations.




1: Upper jaw fused to cranium.
2: Two sleeve-like ethmopalatine ligaments.
3: Two rope-like ethmopalatine ligaments.
4: Two rope-like ethmopalatine and one palatonasal ligaments.
5: One rope-like palatonasal ligament, ethmopalatines lost.
6: Two sleeve-like ethmopalatine and two postorbital ligaments.
7: No cranial-palatine ligaments

FIGURE 68. Superficial jaw muscles in Recent elasmobranchs, after Shirai (1992). A, *Etmopterus spinax* in left lateral view; B, C, *Centroscyllium excelsum*, in left lateral (B) and ventral (C) views; D, *Heterodontus zebra*; E, *Orectolobus japonicus*; F, *Scyliorhinus torazame*; G, *Heptranchias perlo*; H, *Zameus squamulosus*, and I., *Echinorhinus brucus*; in left lateral views. Scale bars equal 10 mm.

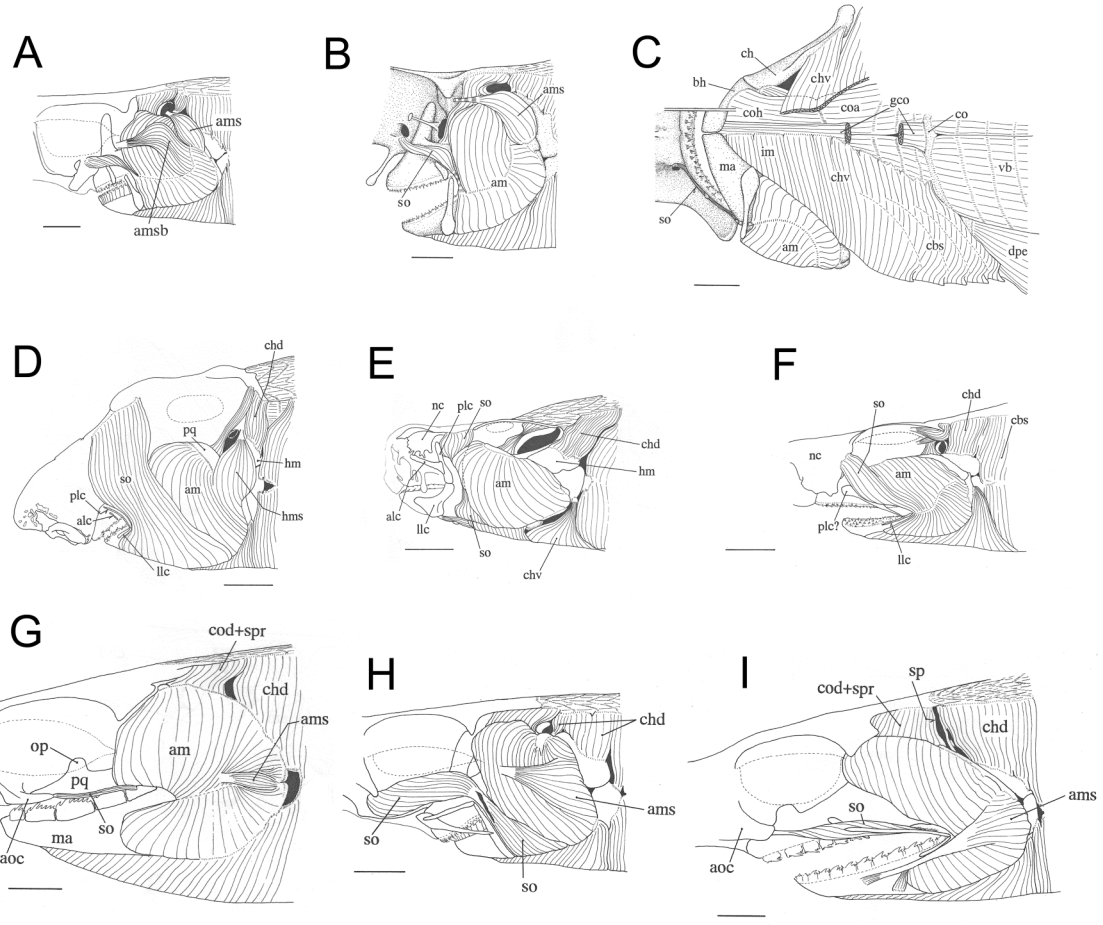

A
ams
amsb
B
ams
am
so
C
ch
bh
chv
coh
coa
gco
co
im
ma
vb
chv
so
am
cbs
dpe
D
chd
pq
hm
so
am
plc
alc
hms
llc
E
nc
plc
so
chd
hm
am
alc
llc
so
chv
F
so
chd
cbs
nc
am
plc?
llc
G
cod+spr
chd
ams
op
am
pq
so
ma
aoc
H
chd
ams
so
so
I
sp
cod+spr
chd
ams
so
aoc

FIGURE 69. Ventral jaw muscles in Recent elasmobranchs, after Shirai (1992). A–C, outer (ventral) muscle layer; A, *Squalus asper*; B, *Centrophorus squamosus*; C, *Pristiophorus nudipinnis*. D–G, inner (dorsal) muscle layer; D, *Etmopterus lucifer*; E, *Rhinobatos hynnicephalus*; F, *Isistius brasiliensis*; G, *Dalatias licha*. Scale bars equal 10 mm.

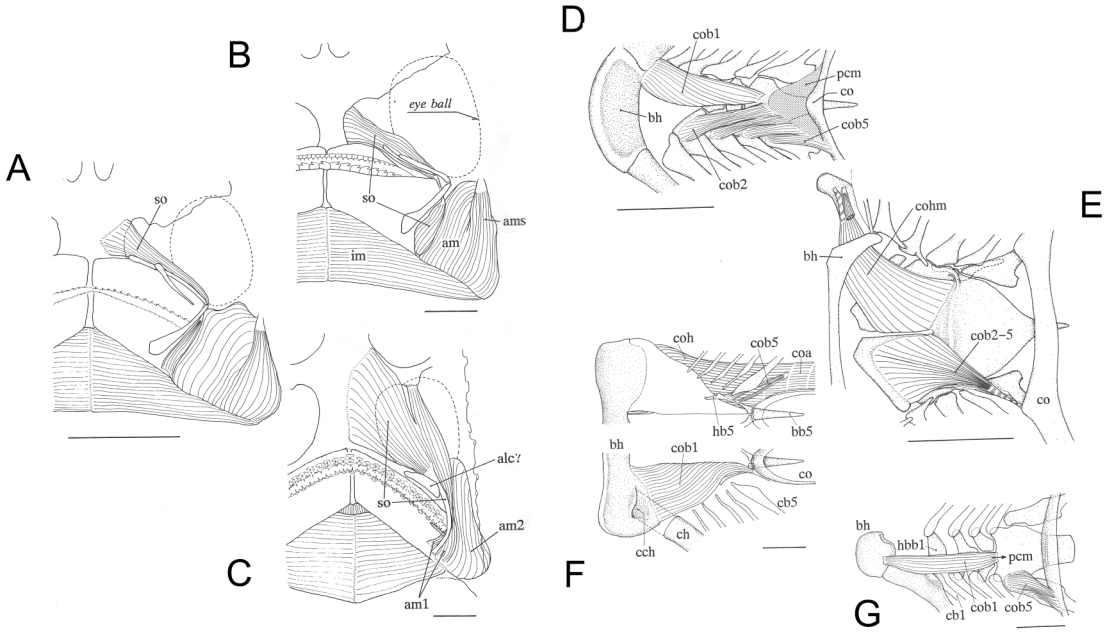

A
so
B
eye ball
so
ams
am
im
C
alc?
so
am2
am1
D
cob1
pcm
co
bh
cob5
cob2
E
cohm
bh
cob2–5
co
F
coh
cob5
coa
hb5
bb5
bh
cob1
co
cb5
ch
cch
G
bh
hbb1
pcm
cb1
cob1
cob5

FIGURE 70. Head and jaw muscles of carcharhinoid sharks (Galea). A, *Scyliorhinus rotifer*; B, *Eridacnis barbouri*; C, *Leptocharias smithii*; D, *Triakis semifasciata*; E, *Galeorhinus galeus*; F, *Paragaleus* sp.; G, *Scoliodon laticaudus*; H, *Loxodon macrorhinus*; I, *Triaenodon obesus*; J, *Sphyrna tiburo*; K, *Sphyrna zygaena*; L, *Eusphyra blochii*. Abbreviations: MAM, adductor mandibulae; MC, Meckel's cartilage; MLH, Levator hyomandibularis; MLN, levator palpebrae nictitantis or NLE muscle; MLP, levator palatoquadrati; MPD, dorsal head of preorbitalis; MPR, preorbitalis or levator labii superioris; MPV, ventral or main head of preorbitalis; NC, nasal capsule; PQ, palatoquadrate; PT, postorbital process; SC, supraorbital crest. Modified from Compagno, 1988: fig. 8.1.

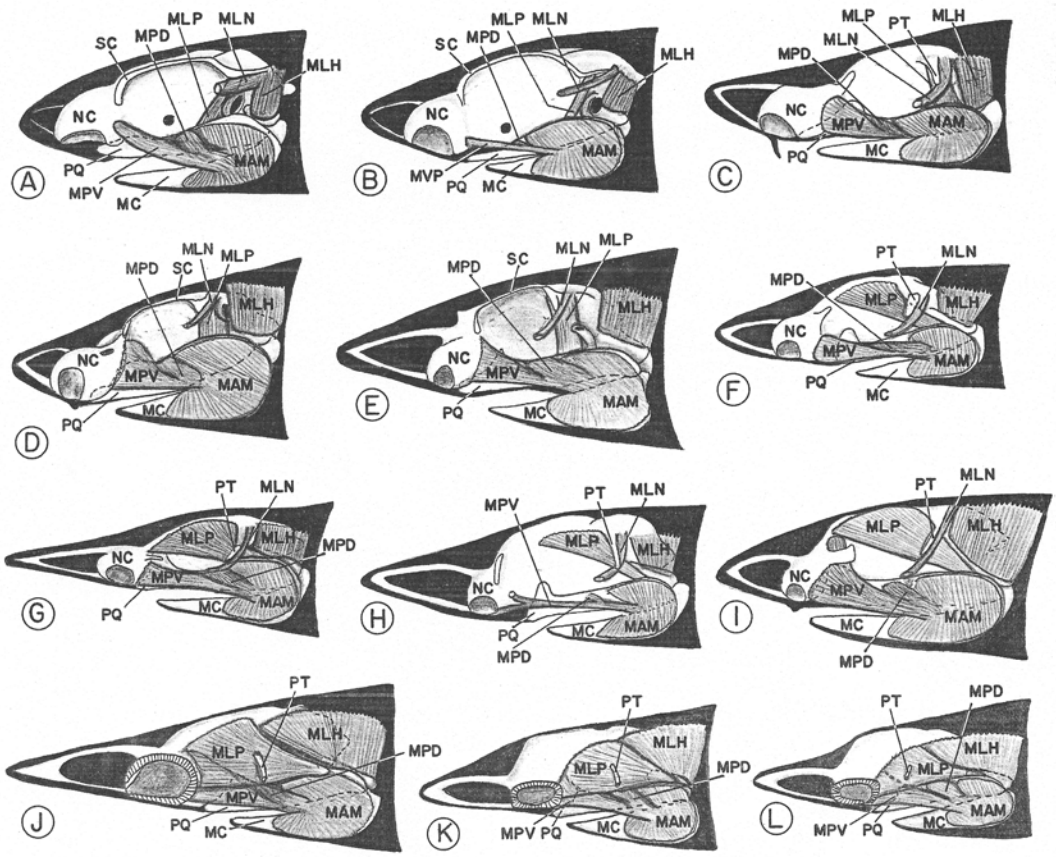
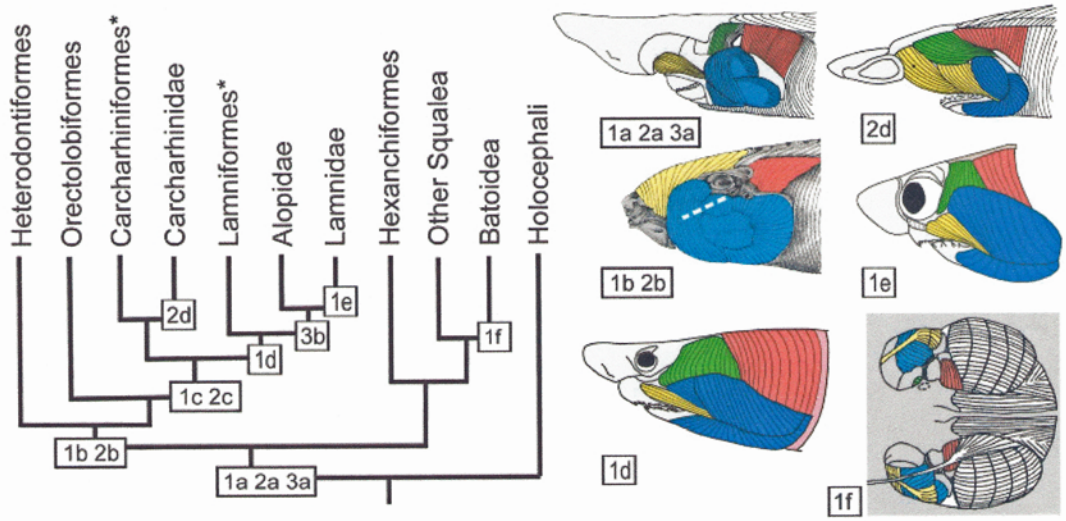

A
SC
MPD
MLP
MLN
MLH
NC
PQ
MPV
MC
MAM
B
SC
MPD
MLP
MLN
MLH
NC
MVP
PQ
MC
MAM
C
MLP
PT
MLH
MLN
MPD
NC
MPV
MAM
PQ
MC
D
MPD
SC
MLN
MLP
MLH
NC
MPV
MAM
PQ
MC
E
MPD
SC
MLN
MLP
MLH
NC
MPV
PQ
MC
MAM
F
PT
MLN
MPD
MLP
MLH
NC
MPV
MAM
PQ
MC
G
PT
MLN
MLP
MLH
MPD
NC
MPV
PQ
MC
MAM
H
MPV
PT
MLN
MLP
MLH
NC
PQ
MC
MAM
MPD
I
PT
MLN
MLP
MLH
NC
MPV
MC
MAM
MPD
J
PT
MLH
MLP
MPD
MPV
PQ
MC
MAM
K
PT
MLH
MLP
MPD
MPV
PQ
MC
MAM
L
PT
MPD
MLH
MLP
MAM
MPV
PQ
MC

FIGURE 71. Upper jaw musculature mapped onto a phylogeny of extant elasmobranchs (after Wilga, 2005). 1a2a3a, basal elasmobranch condition (illustrated by *Squalus acanthias*); 1b2b, basal galeomorph condition (illustrated by *Ginglymostoma cirratum*); 1d, basal lamniform condition (illustrated by *Carcharius Taurus*); 2d, derived Carcharhiniform condition (illustrated by *Sphyrna tiburo*); 1e, derived Lamniform condition (illustrated by *Isurus oxyrinchus*); 1f, batoid condition (*Rhinobatos lentiginosus*). Dotted line: location of levator palatoquadrati muscles overlain by adductor mandibulae and preorbitalis muscles. Blue: quadratomandibularis (adductor mandibulae); green: levator palatoquadrati; red: levator hyomandibularis; yellow: preorbitalis. Note: this phylogeny adapts the view of Shirai (1992) that batoids are derived squaleans; however, molecular data places batoids as the sister group to other living neoselachians. Duplication of the preorbitalis muscle in batoids may reflect a derived condition of that group.




1a: One horizontal preorbitalis muscle for upper jaw protrusion.
1b: Duplication of preorbitalis, both vertical, modification of insertion to lower jaw for adduction.
1c: Reversal of preorbitialis from vertical to horizontal orientation, back to protrusion.
1d: Loss of new preorbitalis division.
1e: Duplication of preorbitalis, still for upper jaw protrusion.
1f: Duplication of preorbitalis, modification of new division to vertical for upper jaw elevation.
2a: Vertical levator palatoquadrati for upper jaw retraction.
2b: Modification of levator palatoquadrati to horizontal, still for retraction.
2c: Reversal of levator palatoquadrati from vertical to horizontal, back to retraction.
2d: Modification of levator palatoquadrati to horizontal and for upper jaw protrusion.
3a: Levator hyomandibularis insertiononto hyomandibula for jaw retraction.
3b: Modification of levator hyomandibularis to insert also onto mandible, still for retraction.

FIGURE 72. Previous reconstructions of jaw musculature in fossil chondrichthyans, both left lateral views. A, "*Cobelodus*" (FMNH PF 13242); after Maisey, 2007. Not to scale. B, the "Tennessee cladoselachian" (NMNH 20675); above, visceral skeleton, hyoid arch in dark gray; below, visceral musculature. Scale bar equals 5 mm. After Maisey, 1989B.

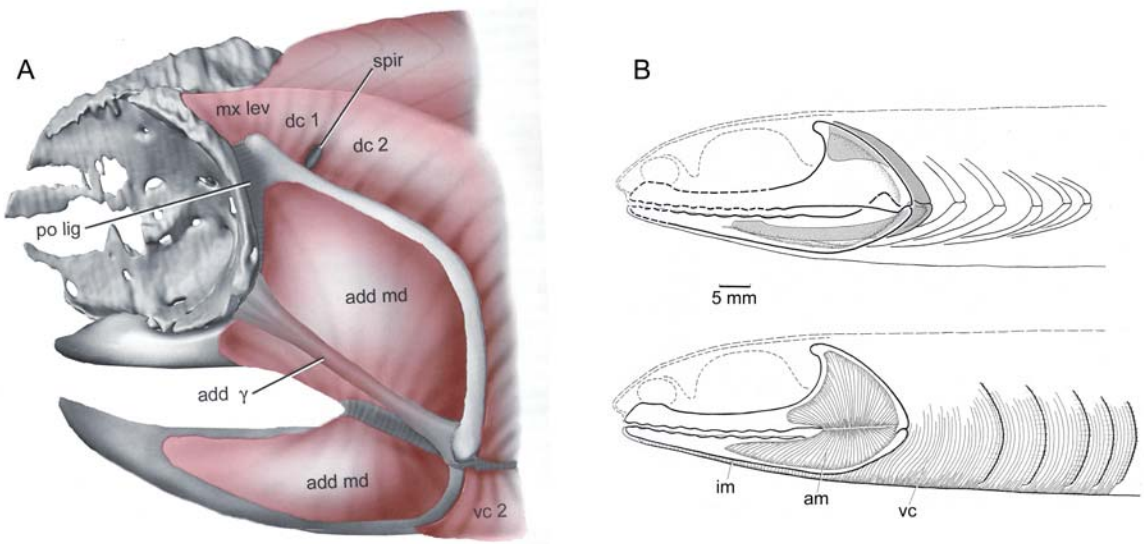
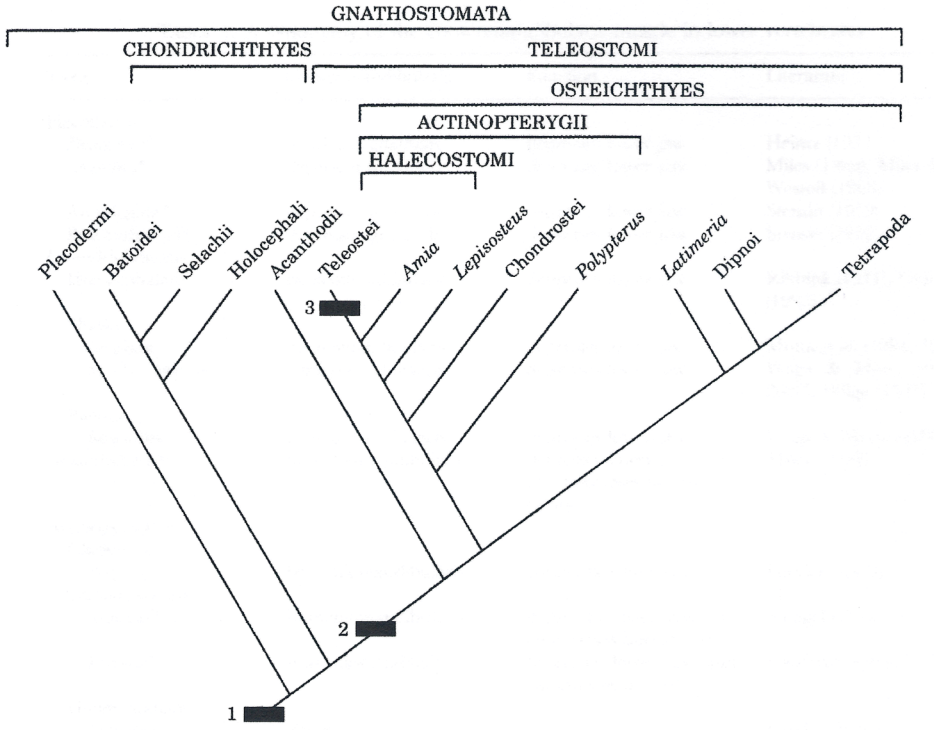

A
spir
mx lev
dc 1
dc 2
po lig
add md
add γ
add md
vc 2
B
5 mm
im
am
vc

FIGURE 73. Gnathostome phylogeny showing evolution of lower jaw depression mechanisms and function of the coracomandibularis and coracohyoideus muscles (After Wilga et al., 2000).




1. Coracomandibularis coupling (depressor gnathalis in Placodermi) attaches mandible to the pectoral girdle and functions to depress the mandible. Coracohyoideus coupling attaches pectoral girdle to hyoid and functions to depress hyoid. Mandibulohyoid ligament present but does not function in mandibular depression.
2. Coracomandibularis coupling (branchiomandibularis in Osteichthyes; geniothoracis in Dipnoi; geniohyoideus in Amphibia) attaches mandible to hyoid and other branchial arches and functions in buccal compression, hyoid protraction and limited depression of the mandible. Coracohyoideus coupling (sternohyoideus in Actinopterygii and Sarcopterygii; rectus cervicis in Dipnoi and Amphibia) depresses hyoid and mandible via the mandibulohyoid ligament.
3. True coracomandibularis coupling lost, analogous coupling (protractor hyoideus, formed from fusion of intermandibularis posterior and interhyoideus muscles) attaches mandible to hyoid and functions primarily to protract hyoid or compress buccal cavity, although it may contribute to mandible depression.

FIGURE 74. Jaws of other hybodontoids, in right lateral view. A, *Egertonodus basanus*; B, *Hybodus hauffianus*; C, *Acrodus* sp.; D, *Acrodus* ?*nobilis* (NHM [formerly BM(NH)] P50869, listed as BM(NH) P50809 by Maisey, 1982). E–F, *Asteracanthus* sp., palatoquadrates; E, anterior view proposed by Peyer (1946); F–H, NHM P12614; F, anterior; G, left lateral; and H, dorsal views. After Maisey, 1982.

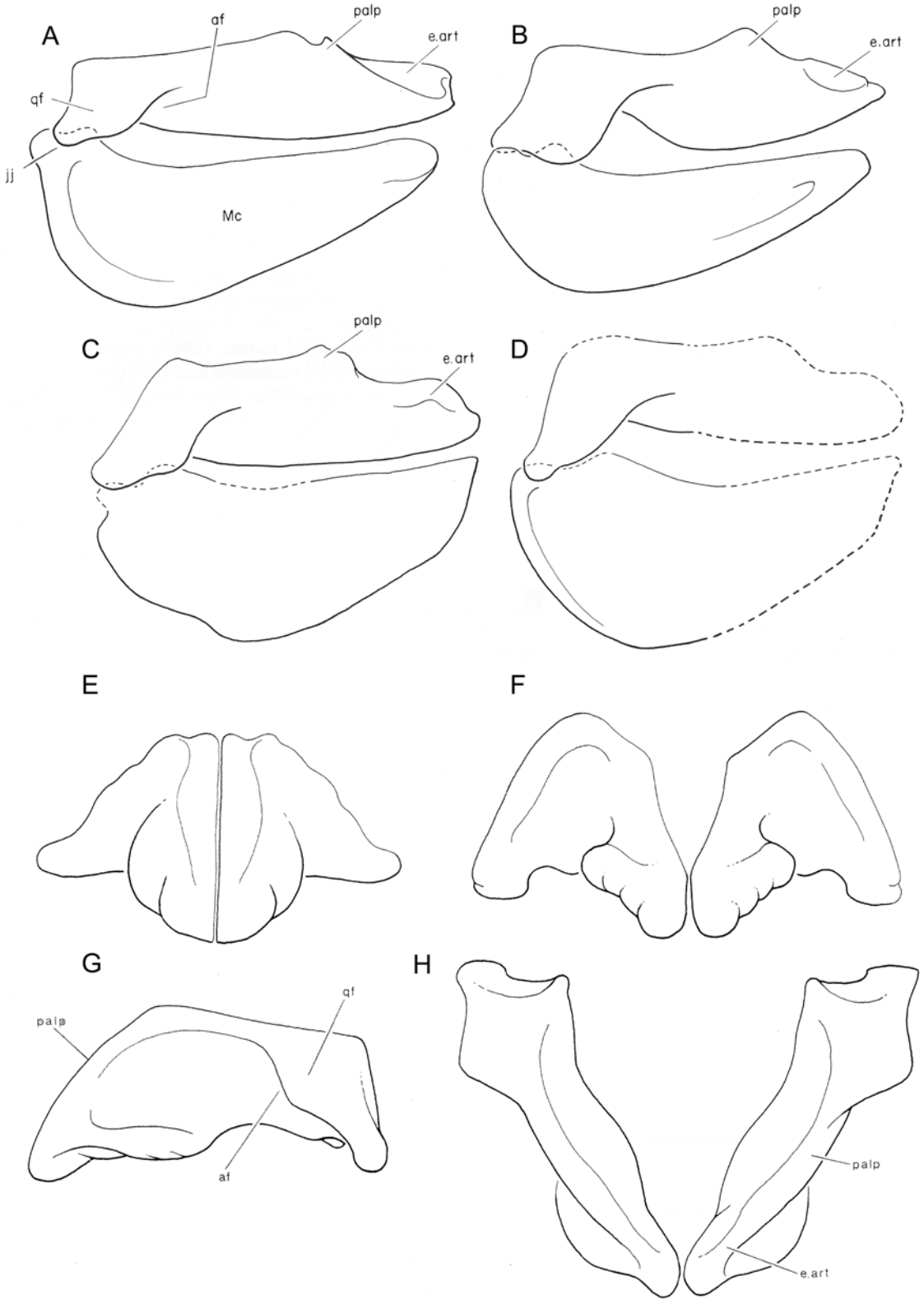
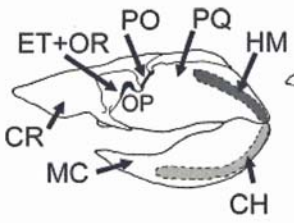
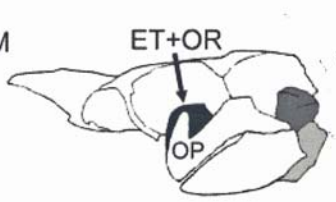

A
af
palp
e.art
qf
jj
Mc
B
palp
e.art
C
palp
e.art
D
E
F
G
palp
qf
af
H
palp
e.art

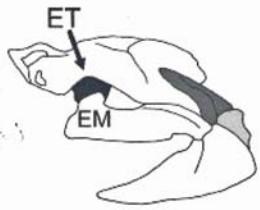
FIGURE 75. Jaw suspension types found in extant elasmobranchs. Representative taxa: the hexanchiform *Notorynchus cepedianus* (amphistyly); the squalean *Squalus acanthias* (orbitostyly); the carcharhiniform *Negaprion brevirostris* (hyostyly); and the batoid *Rhinobatos lentiginosus* (euhyostyly). CR, cranium; CH, ceratohyal; ET, ethmopalatine articulation; EM, ethmoid process of palatoquadrate; HM, hyomandibula; HY, hyoid arch (hyomandibula + ceratohyal); MC, Meckel's cartilage; OP, orbital process of palatoquadrate; OR, orbital articulation; PO, postorbital articulation; PQ, palatoquadrate; UJ, upper jaw (palatoquadrate). Black: ethmopalatine and postorbital ligaments; light gray: ceratohyal; dark gray: hyomandibula. (After Wilga, 2005).




**AMPHISTYLY**
UJ tight
2 CR-PQ joints
Short OP process
HY intact




**ORBITOSTYLY**
UJ loose
1 CR-PQ joint
Long OP process
HY intact




**HYOSTYLY**
UJ loose
1 CR-PQ joint
Short EM process
HY intact



**EUHYOSTYLY**
UJ free
0 CR-PQ joints
No UJ process
HY broken-up

FIGURE 76. Current hypothesis of jaw evolution in chondrichthyans, after Maisey, 2008. Yellow, neurocranium; red, palatoquadrate; purple, Meckel's cartilage; gray, hyoid arch elements. Dashed lines indicate taxa whose taxonomic positions are considered controversial. A, archaeostylic primitive condition. B, loss of postorbital articulation; B1 represents hypothetical primitive autodiastylic holocephalans, B2 represents more derived holostylic holocephalans. C, ethmoidal articulation lost. D, archaeostylic postorbital articulation lost. E, palatobasal articulation lost (hybodonts). F, neoselachians. G, palatobasal articulation lost (galeomorphs). H, palatoquadrate braced secondarily against ethmoid region. I, derived anterior ligamentous jaw attachments. J, palatobasal articulation invades orbit (orbitostylic sharks). Bat 1, Bat 2: alternative possible positions for batoids, which have a euhyostylic jaw suspension.

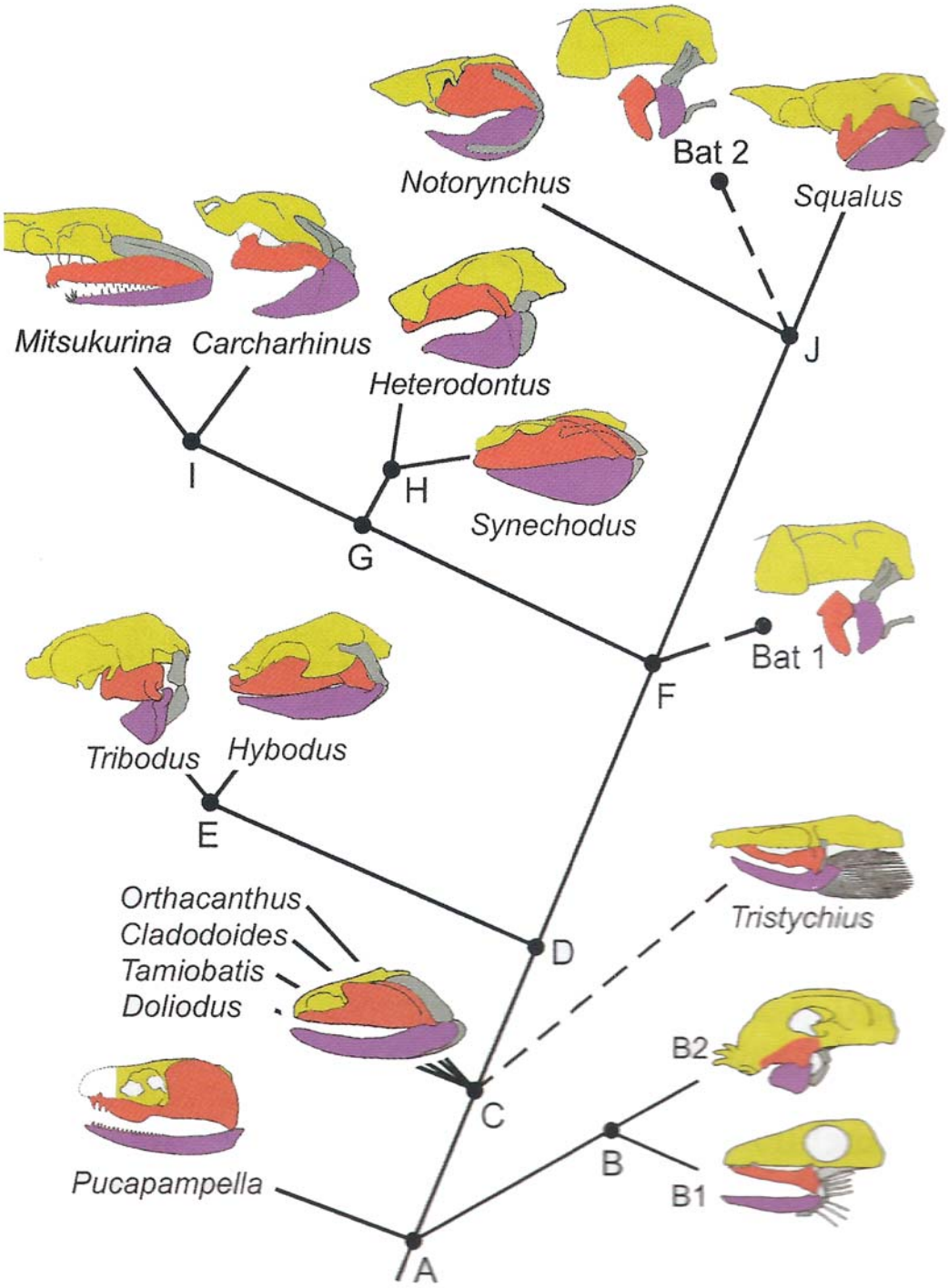

Notorynchus
Bat 2
Squalus
Mitsukurina
Carcharhinus
Heterodontus
J
I
H
Synechodus
G
Bat 1
F
Tribodus
Hybodus
E
Orthacanthus
Cladodoides
Tamiobatis
Doliodus
Tristychius
D
B2
C
Pucapampella
B
B1
A

FIGURE 77. Endochondral “struts” in the extant batoid *Rhinoptera bonasus* (Myliobatidae), after Summers et al. (1998). A, Outline showing the plane of sectioning shown in the other three illustrations. Scale bar equals 10 cm. B, sagittal section through the head showing the relative position of the jaws to hard prey items being crushed (black circles). C, Radiograph of a sagittal section through the jaws showing trabecular cartilage “struts.” Scale bar equals 1 cm. D, Section through palatoquadrate, showing that trabecular struts and multiple outer layers of prismatic cartilage (red arrows). Scale bar equals 1 mm.

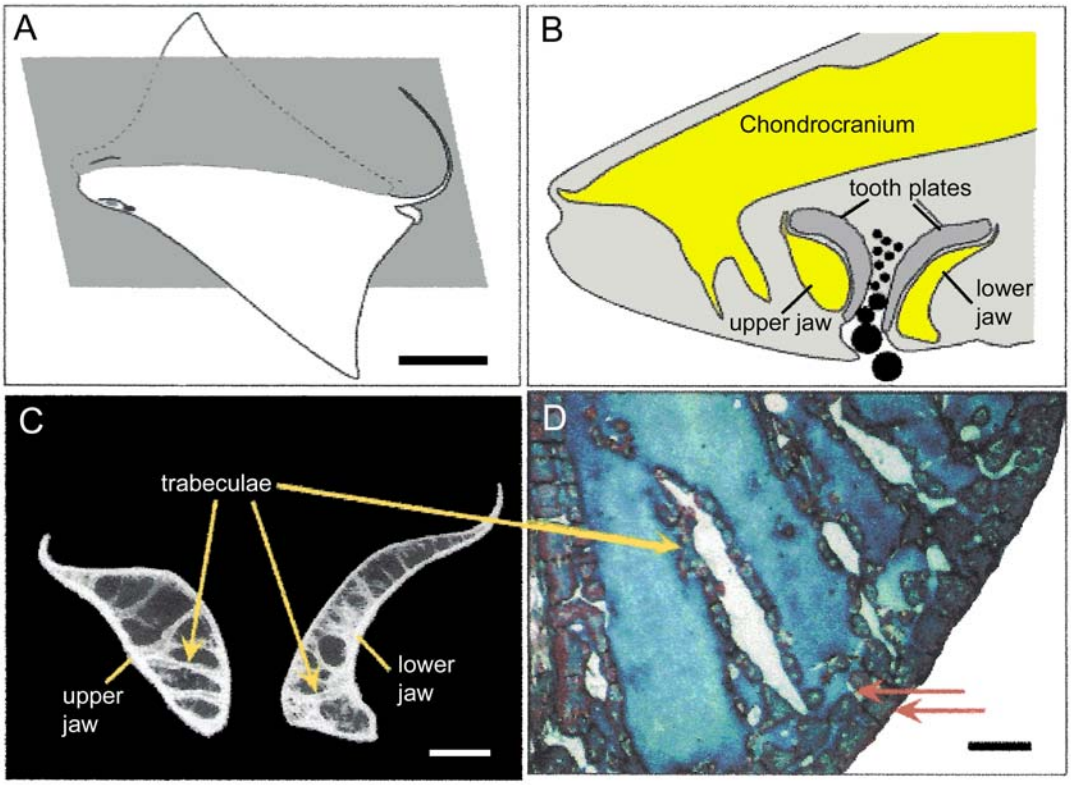

A
B
Chondrocranium
tooth plates
upper jaw
lower jaw
C
trabeculae
upper jaw
lower jaw
D

FIGURE 78. Occurrence of endochondral “struts” in extant myliobatid stingrays, mapped onto phylogeny. Phylogeny includes Myliobatiformes (stingrays) plus two outgroups, the Rajidae (skates) and *Rhinobatos* (the guitarfish). Dark gray highlighting indicates durophagous taxa. Hatched circles indicate presence of endochondral “struts”; open circles indicate absence of endochondral “struts”; no circles indicate unsampled taxa. Modified from Summers, 2000.

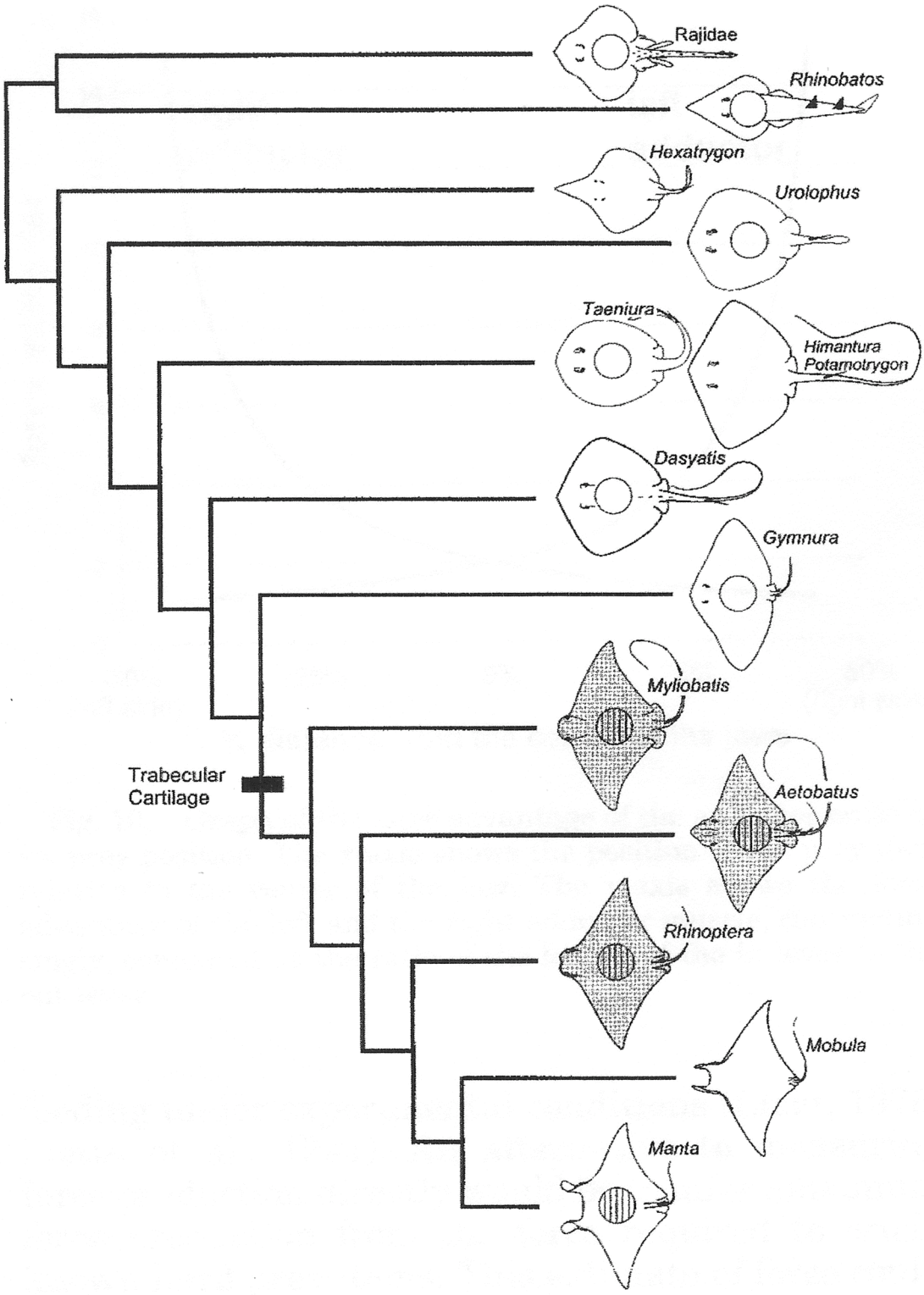

Rajidae
Rhinobatos
Hexatrygon
Urolophus
Taeniura
Himantura
Potamotrygon
Dasyatis
Gymnura
Myliobatis
Trabecular
Cartilage
Aetobatus
Rhinoptera
Mobula
Manta

FIGURE 79. Durophagy in extant chondrichthyans. Circle size indicates total number of genera in the taxonomic group indicated. Black: proportion of durophagous taxa; gray, proportion of non-durophagous taxa. (Modified from Huber et al., 2008).

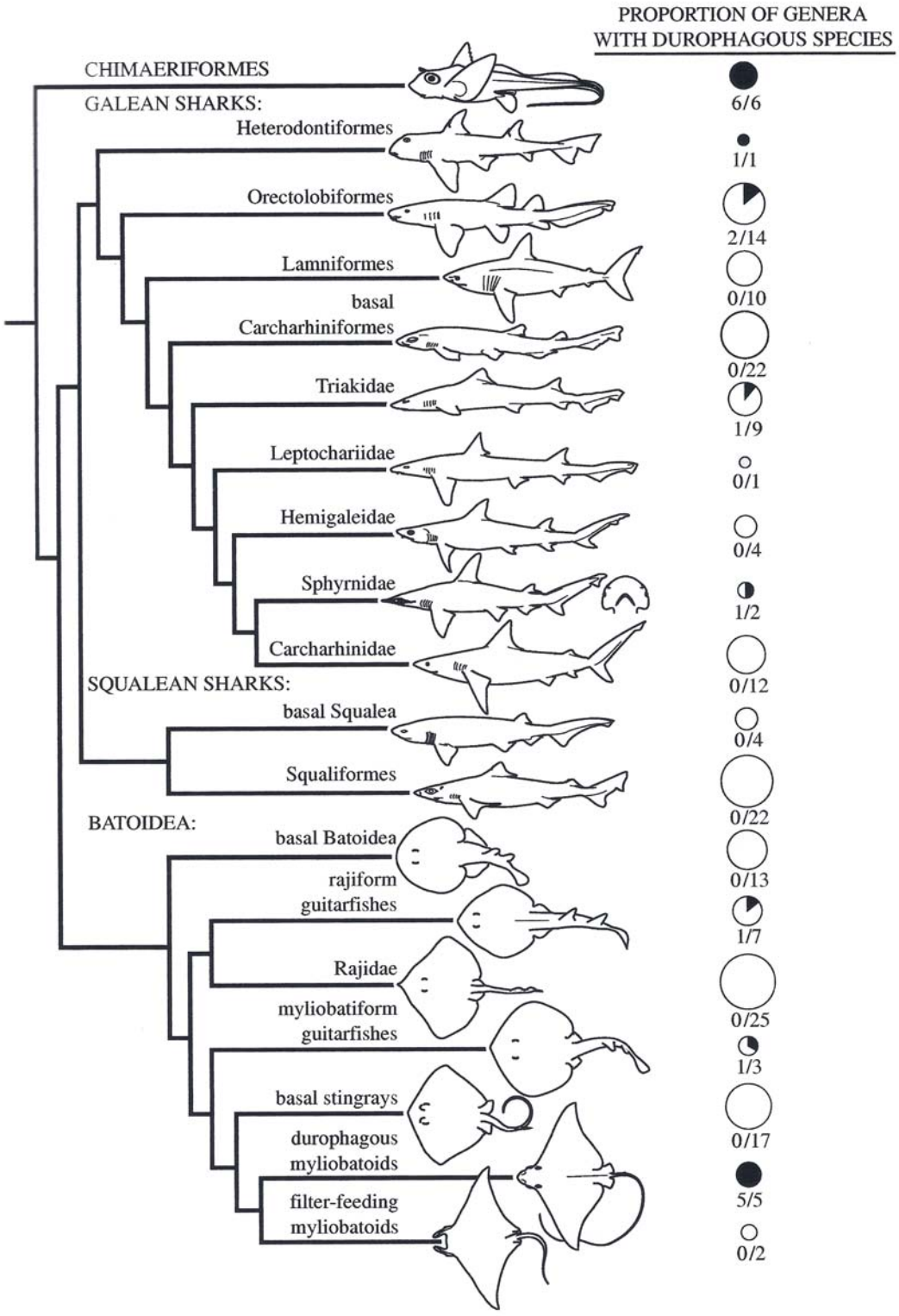
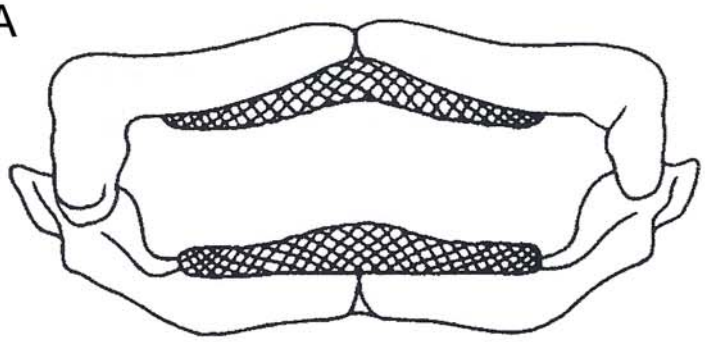
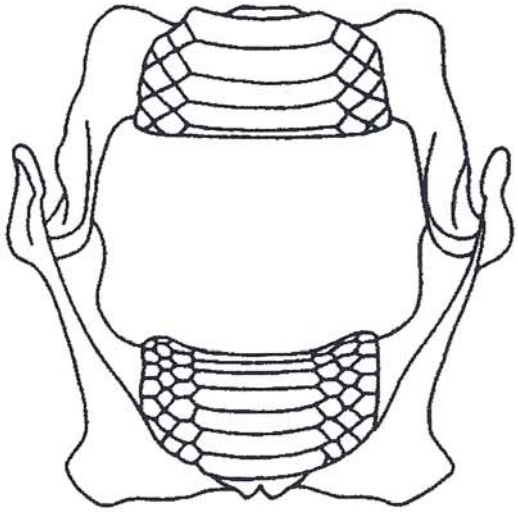

PROPORTION OF GENERA
WITH DUROPHAGOUS SPECIES
CHIMAERIFORMES
6/6
GALEAN SHARKS:
Heterodontiformes
1/1
Orectolobiformes
2/14
Lamniformes
0/10
basal
Carcharhiniformes
0/22
Triakidae
1/9
Leptochariidae
0/1
Hemigaleidae
0/4
Sphyrnidae
1/2
Carcharhinidae
0/12
SQUALEAN SHARKS:
basal Squalea
0/4
Squaliformes
0/22
BATOIDEA:
basal Batoidea
0/13
rajiform
guitarfishes
1/7
Rajidae
0/25
myliobatiform
guitarfishes
1/3
basal stingrays
0/17
durophagous
myliobatoids
5/5
filter-feeding
myliobatoids
0/2

FIGURE 80. Jaws and dentitions of representative types of durophagous extant elasmobranchs. A, crushing dentition (e.g., *Raja*); B, grinding dentition (e.g., *Myliobatis*); C, clutching-grinding (e.g., *Heterodontus*). (After Wilga and Motta, 2000).

A



B



C

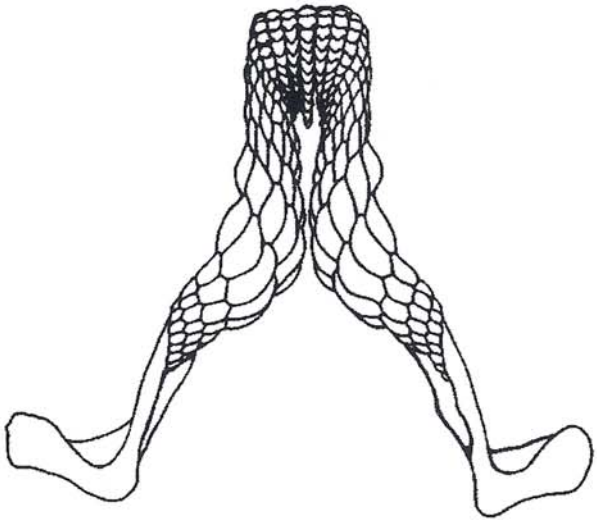
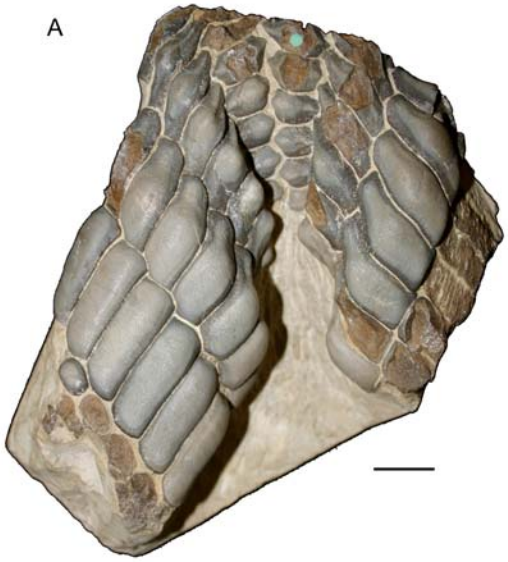


FIGURE 81. Teeth of other durophagous hybodontoids. Above: *Asteracanthus ornatissimus*. A, overview showing partial dentition; B, closeup showing individual elongate lateral teeth. Below: *Acrodus* sp. C, overview showing nearly complete dentition; D, closeup showing individual teeth. Scale bars equal 2 cm.


A


B


C


D

# CHAPTER 7: PECTORAL GIRDLE AND FIN

[Adapted from Lane, J.A., and Maisey, J.G. 2009. Pectoral anatomy of *Tribodus limae* (Elasmobranchii: Hybodontiformes) from the Lower Cretaceous of Northeastern Brazil. Journal of Vertebrate Paleontology 29(1):25–38.]

## INTRODUCTION

*Tribodus limae* Brito and Ferreira, 1989, was placed by Brito (1992) in the subfamily Acrodontinae (within the suborder Hybodontoidei, which includes Mesozoic hybodonts and the Paleozoic form *Hamiltonichthys* Maisey, 1989), on the basis of dental characteristics. Previously described material of *Tribodus* includes the holotype and four additional specimens reposited in Brazil (Brito and Ferreira, 1989; Brito, 1992), and the braincase, jaws, and hyoid arch described by Maisey and Carvalho (1997). The pectoral girdle of that specimen is described here.

The original diagnosis and description of *Tribodus limae* by Brito and Ferreira (1989) does not include any pectoral skeletal features, and pectoral anatomy of this taxon was first described by Brito (1992). Brito's (1992; Fig. 89A) reconstruction of the pectoral endoskeleton of *Tribodus limae* was based on the only pectoral material then available, a nearly complete fish preserved in lateral view. Known specimens of pectoral girdles in other hybodontoids also typically show only the lateral or medial view, a fact that has been reflected in most previous reconstructions and descriptions (e.g., Brown, 1900; Jaekel, 1906; Koken, 1907; Woodward, 1916, 1924; Moy-Thomas, 1936; Maisey, 1982, 1986, 1989). The new material of *Tribodus limae* described here presents the first

opportunity to view the posterior surface of the scapulocoracoid in this taxon, allowing for a significant revision of its pectoral morphology. This revision, along with description of other pectoral features of *Tribodus* and their potential phylogenetic significance, constitutes the focus of this article.

Coates and Gess (2007) provided a list of hybodont pectoral characters, which (together with additional characters from their list) support the phylogeny previously suggested by Maisey (1989) and Maisey et al. (2004). These pectoral characters are examined here with specific reference to *Tribodus*, and are considered in a later chapter (Part III) for inclusion in the present phylogenetic analysis.

*Tribodus* and other hybodonts have been united broadly with ctenacanths, xenacanths, and neoselachians on the basis of several characters, including a tribasal pectoral fin with three basal cartilages (propterygium, metapterygium, and mesopterygium) that articulate with the pectoral girdle (Maisey, 1984; Coates and Sequeira, 2001). Because of the potential importance of pectoral anatomy in determining chondrichthyan interrelationships (e.g., Maisey, 1984; Carvalho, 1996: characters 37–42; Coates and Sequeira, 2001: characters 23–38), a closer examination of the morphology of the pectoral fin and girdle in hybodonts in relation to other forms is of value, especially for future phylogenetic analyses including the one presented in a later part of this dissertation. The purpose of the present paper is to provide new data on the morphology of the pectoral fin and shoulder girdle in *Tribodus* on the basis of the new material, to provide a revised reconstruction of the pectoral endoskeleton in *Tribodus*, and to examine the phylogenetic relationships of *Tribodus* to other elasmobranch taxa based on

potentially new and previously described pectoral skeletal characters and a recently proposed phylogeny.

## DESCRIPTION

### Pectoral Girdle

Basic morphology of the pectoral girdle and fins of *Tribodus limae* resembles that of other previously described hybodontoids, except in the structure and position of the fin articulation. The pectoral girdle of *T. limae* consists of paired scapulocoracoids which appear to have contacted each other at the ventral midline, as in some less derived living sharks such as hexanchoids (Compagno, 1999) and the Paleozoic hybodontiform *Onychoselache traquairi* Dick, 1978 (Coates and Gess, 2007), but were not fused as they are in most modern elasmobranchs. The scapulocoracoid has a short, broad, blunt-ended coracoid process ventrally, and a more slender and tapered scapular process dorsally (Fig. 89A), as in most other hybodontiforms and neoselachians (Maisey, 1982).

The scapulocoracoids of *Tribodus limae* especially in the coracoid region are similar to those of other Mesozoic hybodonts in being fairly robust, and unlike those of *Hamiltonichthys* which are more slender (Maisey, 1989). AMNH FF 13957, a nearly complete fish with shoulder girdle in situ (Fig. 8A), shows the orientation of the scapulocoracoid to be inclined posterodorsally at an angle of approximately 60–70° to the long axis of the body, with the coracoid process anteroventral to the scapular process. A similar orientation of the scapulocoracoid is seen in the hybodontiform *Onychoselache* (Dick and Maisey, 1980), and in some recent sharks such as *Notorynchus* (Daniel, 1934; Dick, 1978). The dorsal part of the scapular process in AMNH FF 13957 curves

anteriorly and mesially, terminating just lateral to the basal plate of the anterior dorsal fin spine (Fig. 8A, C), as in *Onychoselache* and hybodontoids (Coates and Gess, 2007). Among the new AMNH specimens, AMNH FF 13957 is the only one in which the dorsal-most end of the scapulocoracoid is preserved in its entirety. As in most other hybodontoids except *Lissodus* Brough, 1935 (Maisey, 1982), there is no evidence of a separate suprascapular element in *T. limae*. The dorsal anterior margin of the scapulocoracoid is slightly rounded (Fig. 84C), and probably served as the insertion for the cucullaris muscle as in modern elasmobranchs (Ashley and Chiasson, 1988; Coates and Gess, 2007).

The anteromedial margin of the scapulocoracoid is continuously convex (Figs. 8, 83–85), and there is no evidence of a coracoid anterodorsal shoulder or posterolateral angle such as that found in some earlier chondrichthyans (Coates and Gess, 2007; Fig. 87). An elongate groove on the anterior margin of the scapulocoracoid (the coracobranchial fossa), which presumably housed the coracoarcual and last coracobranchial muscles (Maisey, 1982), is found in *Onychoselache*, *Hybodus* Agassiz, 1837, and *Lissodus* (Maisey, 1982; Duffin, 2001; Coates and Gess, 2007). Unlike those other hybodontiforms, *Tribodus* lacks an extensive coracobranchial fossa, and the only indication of this structure is a faint indent in the anterodorsal margin of the scapulocoracoid in AMNH FF 13958 and 13961. The anteroventral edge of the scapular process is smooth and rounded (Fig. 84). The anterior margin of the scapular process is slightly concave, ending ventrally at a slight anterior projection at about the level of the uppermost (lateral) facet of the articular ridge (Figs. 9C, 83A, 84A, B, 85). This projection does not resemble the anterior shoulder of early chondrichthyans (Coates and

Gess, 2007; Fig. 87). The anterior margin of the coracoid descends anteroventrally from this projection, and is also slightly concave (Figs. 83A, 84A, B, 85). A posterior flange on the lowermost one-third of the scapular process, such as that described in *Onychoselache* and *Lissodus* by Coates and Gess (2007), is lacking in *Tribodus limae*.

The medial surface of the scapulocoracoid is concave, whereas its lateral surface is convex (Fig. 84A–D). The posterior dorsolateral and posterior ventrolateral surfaces are weakly concave and triangular (widening toward the articular region) and are separated by the obliquely angled articular process for the pectoral fin (Figs. 84D, 85A, B). Comparison with modern sharks (e.g., Shirai, 1992:pls. 43–45) suggests that these areas were attachment surfaces for the pectoral fin musculature, with the levator pectoralis originating on the posterior dorsolateral surface and the depressor pectoralis on the posterior ventrolateral surface. In AMNH 13958, the anterior ventrolateral surface of the coracoid appears wrinkled (Fig. 84A) and may represent the region of origin for the ventral hypobranchial musculature (i.e., the coracoarcualis, Maisey, 1982; Ashley and Chiasson, 1988).

Foramina for the diazonal nerves and circulatory vessels of the fin are evident on three surfaces of the coracoid region: one foramen on the medial surface and two on the lateral surface (Figs. 8C, D, 82, 84A–D, 85, 86). Three main openings of the diazonal canal are also present in the Permian xenacanth *Orthacanthus texensis* (Fig. 87), in an arrangement relatively similar to that of *T. limae* (Figs. 84–86). Many neoselachians also have paired diazonal foramina located dorsal and ventral to the articular process (Coates and Gess, 2007), and a third diazonal foramen located on the medial surface of the girdle (e.g., *Carcharhinus*). An additional small opening is visible on the lateral surface of AMNH FF

13958, just ventral to the articular process and medial to the ventral diazonal foramen, and is here referred to as the posteroventral diazonal foramen (Figs. 84A, D, 85).

A surface rendering made from CT scans of the scapulocoracoid in AMNH FF 13958 (Fig. 86) shows that the main diazonal canal originates on the medial surface of the scapulocoracoid, and then bifurcates, terminating in the paired dorsal and ventral foramina on the lateral surface of that cartilage. The posteroventral foramen is the opening of an additional, smaller canal that originates on the medial surface of the scapulocoracoid (Fig. 86B) posteroventral to the main diazonal foramen. This small canal passes completely through the scapulocoracoid and does not connect with the main diazonal canal. Although a corresponding posteroventral diazonal foramen is not clearly visible in any of the other new specimens of *Tribodus limae*, AMNH FF 13961 shows a slight indentation in the same location (visible when the specimen is turned in indirect light) which may be a foramen infilled with matrix.

The articular process for the pectoral fin is best seen in AMNH FF 13958 (Figs. 83A, 84–86), AMNH FF 13959 (Figs. 8B, 82), and the reverse (right scapulocoracoid) of AMNH FF 13961 (Fig. 8D). It is a relatively narrow ridge located posterolaterally and about midway along the length of the scapulocoracoid, slanting obliquely ventromedially at an angle of approximately 45° from horizontal between the dorsal and ventral diazonal foramina on the posterolateral surface of the scapulocoracoid. A similar ridge is found in many neoselachians (e.g., *Squalus*, *Heptranchias*, *Negaprion*, *Sphyrna*, *Carcharhinus*; also *Centroscyllium*, Shirai, 1992:pl. 47; Fig. 88A) and in *Orthacanthus* (Fig. 87). However, the articular ridge in *Tribodus limae* slants downward ventromedially (Figs. 84D, 85B, 86A), whereas that in *Orthacanthus* slants ventrolaterally (Fig. 87B), although

the ridge slants at a similar angle in both taxa. The articular ridge of *T. limae* is also not as rounded posteriorly (Fig. 87B, C) as that of *Orthacanthus*.

Two indentations located on the posterior surface of the articular ridge of *Tribodus limae* are interpreted as articulation facets for the propterygium and metapterygium (Figs. 84D, 85B, 86A). AMNH 13959 (Figs. 8B, 82) shows that the articular surfaces of these facets have a rough texture. Comparison with other chondrichthyans (e.g., Maisey, 1982; Ashley and Chiasson, 1988; Shirai, 1992) suggests that the propterygium attached to the lateral articular facet and the metapterygium to the medial one, whereas the mesopterygium was probably attached to the ridge between them (Fig. 88). Alternatively, the mesopterygium may have shared an articulation facet with either the propterygium or metapterygium. However, the mesopterygium does not extend as far proximally as the other two basals (Fig. 83A), and may not have articulated directly with the scapulocoracoid.

.

**Pectoral Fin**

A partial right pectoral fin is preserved in AMNH FF 13958 adjacent to the right scapulocoracoid (Fig. 83A). It preserves the three basal cartilages, but none of the radials are preserved. AMNH FF 13958 also includes one incomplete basal cartilage from the left pectoral fin (Fig. 83B), probably representing the metapterygium because its shape is similar to that of this element in the right fin (Fig. 83A).

As in most other hybodont fossils, the right pectoral fin and scapulocoracoid in AMNH FF 13958 were positioned with the fin lying flat in the matrix adjacent to the posterior margin of the scapulocoracoid and with the basals arranged dorsoventrally,

parallel to the vertical axis of the specimen (Fig. 83A). However, once the girdle was removed from the matrix so that its posterior surface was visible and its original articular arrangement could be examined in three dimensions (Figs. 84, 85), it became clear that the fin was inverted and rotated out of its original position by approximately 135°, and that the proximal part of the fin would have articulated with the posterolateral surface of the scapulocoracoid along its oblique posterior ridge (Fig. 89B), as in some neoselachians (Shirai, 1992) and *Orthacanthus* (Fig. 87). The medial part of the right pectoral fin presumably became detached from the scapulocoracoid during burial, so that the fin rotated outward laterally and settled in the matrix adjacent to the scapulocoracoid with its dorsal surface exposed. In our revised reconstruction based on this new interpretation (Fig. 89B), the fin attaches to an articular ridge located on the posterior of the scapulocoracoid between the dorsal and ventral diazonal foramina at a height approximately one third the total height of the scapulocoracoid. The articular ridge is tilted ventromedially at an angle of approximately 135° to the dorsoventral axis of the scapulocoracoid, and the proximal part of the fin would have been similarly oriented.

The basal cartilage located on the far right in AMNH FF 13958 (Fig. 83A) is here interpreted as the propterygium (which originally attached to the lateral articulation facet on the scapulocoracoid) by following the previous reconstruction of pectoral anatomy in *Tribodus limae* by Brito (1992). This element is similar in size and shape to the ventral most basal of the specimen described by Brito (1992: fig. 1), which that author interpreted as the propterygium. This interpretation is also supported by the close proximity of this element in AMNH FF 13958 to the lateralmost articulation facet on the scapulocoracoid articular process (Figs. 85, 86), where the propterygium typically

attaches to an oblique posterior articular ridge in neoselachians (Fig. 88). The propterygium has also generally been interpreted as the most lateral element in pectoral fins of other hybodonts (Maisey, 1982, 1986, 1989). The propterygium of AMNH FF 13958 is broad distally and tapered proximally, and its sides are slightly concave. The proximal end of the propterygium is similar in proportion to the lateral articular facet of the scapulocoracoid with which it presumably articulated. The size of the propterygial facet indicates that the fin articulation of *Tribodus limae* probably had strong propterygial support, as in other hybodontoids (Maisey, 1989).

The central basal is the mesopterygium, which may have attached to the central part of the articular process (see Fig. 88). The mesopterygium is broad compared to the other two basals, and is only slightly tapered at its proximal end. As discussed above, the mesopterygium does not extend as far proximally as the propterygium and metapterygium, suggesting that it may not have participated in the fin articulation. However, a short mesopterygium is also seen in dorsal views of the pectoral fins in some modern sharks (e.g., the carcharhinoid galeomorph *Sphyrna*, AMNH 218154SD) in which all three basals articulate directly with the scapulocoracoid, so it is possible that the mesopterygium in *Tribodus* also articulated directly with the girdle.

The basal on the left in Figure 83A is interpreted here as the metapterygium. Presence of a medial articular facet on the scapulocoracoid (Figs. 84D, 85, 86A) suggests that, like the propterygium, the metapterygium also probably had a direct articulation with the scapulocoracoid (Figs. 88B, 89B). The shape of this element, most visible in its counterpart from the left fin (Fig. 83B), is consistent with that of other hybodont metapterygia in having a shortened distal end medially (e.g., Maisey, 1982). Presumably,

the metapterygial radials would have attached along the mediodistal margin of this cartilage as in other hybodonts. In other hybodonts, the metapterygium is associated with several radial series, but these are missing in AMNH FF 13958. As preserved, the length of the pectoral fin base corresponds to approximately two thirds the length of the scapulocoracoid articular process. The remaining space was presumably occupied by soft tissues supporting the fin articulation.

No pectoral radials are preserved in any of the *Tribodus limae* specimens examined here, although Brito (1992; Fig. 89A) described them in other specimens of *T. limae*. Because radials and ceratotrichia are lacking and dermal denticles covering the fins are somewhat scattered, the new material does not provide enough information to determine the overall shape and dimensions of the pectoral fin in *T. limae*. Pectoral girdles and fins are also well preserved in MN 5807V and MN 5808V (Figs. 90–93), one of which (MN 5807V, Figs. 90, 91) was the basis for Brito's (1992) reconstruction of pectoral fin anatomy in *Tribodus*.

## DISCUSSION

### Comparison with previous reconstructions of the pectoral fin in hybodonts

The new reconstruction of the pectoral skeleton in *Tribodus limae* (Fig. 89B) differs considerably from previous reconstructions of *Tribodus* (Fig. 89A) and other hybodontoids (e.g., Woodward, 1916; Maisey, 1982, 1986, 1989) in the arrangement of the pectoral fin articulation. The differences between this and previous reconstructions highlight some of the difficulties in interpreting hybodont pectoral anatomy, mainly due

to the state of preservation of most specimens. All previous reconstructions of hybodontoid pectoral fins were based on two-dimensionally preserved specimens (the only material known), most of which show only the lateral surface with the pectoral girdle embedded in matrix and often crushed or distorted. Brito's (1992; Fig. 89A) previous reconstruction of *Tribodus limae* shows its pectoral skeleton largely as it appears in the fossil, but with the fin repositioned to fit inside a hypothesized glenoid fossa. Brito's reconstruction is similar to reconstructions of other hybodontoids (e.g., Maisey, 1982, 1986, 1989), differing mainly in the location of the pectoral articulation (Fig. 89B). None of the previous reconstructions indicate the presence of an oblique posterior articular ridge in hybodonts. However, this feature occurs not only in many neoselachians (e.g., *Squalus*, *Heptranchias*, *Negaprion*, *Sphyrna*, *Carcharhinus*; Shirai, 1992: pl. 47; Fig. 88A), but also in some fossil sharks such as xenacanths (e.g., *Orthacanthus*, Fig. 87) and ctenacanths (e.g., an undescribed Permian 'ctenacanth' scapulocoracoid, FHSM VP-15012) considered the outgroups to hybodonts plus neoselachians (Coates and Sequeira, 2001A, B). Presence of a posteriorly directed articular ridge in *Tribodus limae* implies that its pectoral articulation (and possibly that of other hybodontoids) was very similar to that of neoselachians.

**Comparative pectoral skeletal morphology in *Tribodus* vs. other chondrichthyans**

**Pectoral girdle—**The scapulocoracoid in *Tribodus* is similar to that of other hybodontiforms and neoselachians in its general shape and proportions, suggesting a highly conserved pattern. In these taxa, the pectoral articulation is typically located at a height of approximately one-third to half of its total length (as opposed to much farther

ventrally, as in chimaeroids: Stahl, 1999; or dorsally, as in iniopterygians: Zangerl and Case, 1973; Janvier 1998; both of which probably represent independent autapomorphies).

In hybodontiforms and neoselachians, as well as xenacanths (e.g., *Orthacanthus*, Fig. 87), and ctenacanths (FHSM VP-15012), the scapular region is typically more slender than and as long as or somewhat longer than the coracoid region (whereas in the Paleozoic shark *Cladoselache* Dean, 1894, the scapular region is more robust than the coracoid: Bendix-Almgreen, 1975:fig. 1). Scapulocoracoids of Mesozoic hybodonts such as *Tribodus* are typically more robust than those of neoselachian sharks, but less robust than those of xenacanths and ctenacanths (especially in the scapular region).

In many early chondrichthyans (e.g., cladoselachians, symmoriiforms, and stethacanthids) the scapular region exhibits a broad posterolateral angle, considered a primitive chondrichthyan feature (Coates and Gess, 2007). Xenacanths (e.g., *Orthacanthus*, Fig. 87) and ctenacanths (FHSM VP-15012) also retain this feature, and its absence in neoselachians and hybodontiforms is probably apomorphic. Presence of a posterolateral angle in *Tristychius* could be a reversal (Coates and Gess, 2007). According to Coates and Gess (2007), a scapulocoracoid anterodorsal shoulder (i.e., a dorsal projection on the anterior margin of the scapulocoracoid, approximately level with or slightly ventral to the fin articulation) is present in Paleozoic chondrichthyans (e.g., *Akmonistion*, *Plesioselachus*) and in some basal elasmobranchs such as *Orthacanthus* (Fig. 87). However, this feature is absent in neoselachians, and in *Tristychius* and other hybodontiformes (Coates and Gess, 2007).

A diazonal canal with three openings (one medial and two lateral) as in *Tribodus* and *Orthacanthus* is found in many neoselachians (e.g., *Carcharhinus*), and Goodrich (1930) states that the presence of three main foramina is typical in neoselachians. The posteroventral canal in AMNH FF 13958 (Fig. 86) is unknown in other hybodonts, and may be autapomorphic for *Tribodus*. It may have contained a subdivision of one of the nerves and/or blood vessels supplying the pectoral fin. According to Coates and Gess (2007) diazonal foramina may be absent in *Tristychius*, and only a ventral diazonal foramen is known in *Onychoselache*. In most Paleozoic chondrichthyans (such as *Akmonistion*) and extant holocephalans, there is a diazonal foramen dorsal to the posterior part of the pectoral articulation (Coates and Gess, 2007). Presence of one diazonal foramen anterior and dorsal to the fin articulation may be a general condition of early chondrichthyans (Coates and Gess, 2007).

In *Orthacanthus* (Fig. 87C), the lateral surface of the scapulocoracoid is crushed as in the specimen of *Tristychius* described by Coates and Gess (2007), so that the probable area of insertion for the hypaxial flank muscles forms a tall, shallow recess, whereas the anterior margin of the scapulocoracoid is buttressed as it is in *Tristychius*. In *Tribodus*, the specimen is not crushed, and the likely area of insertion for the hypaxial muscles is broad with a slight dorsoventrally convex curve. The anterior margin of the scapular process in *Tribodus* is not as strongly buttressed as in *Orthacanthus*. As in *Tristychius* and *Plesioselachus macracanthus* Anderson, Long, Gess, and Hiller, 1999 (Coates and Gess, 2007), *Orthacanthus* (Fig. 87) has a pronounced ventrolateral ridge marking the anterolateral extent of the pectoral depressor muscles. In *Tribodus*, this ridge is far less pronounced, but forms the highest part of the convexly curved lateral surface of the

coracoid. The anterolateral surface of the coracoid in *Tribodus* is concave (again as in *Orthacanthus*, Fig. 87; and *Tristychius*, Coates and Gess, 2007), but this part of the coracoid is much narrower in *Tribodus* than in *Orthacanthus*, and consequently the area of attachment for the coracoarcual and coracobranchial musculature was narrower. A similar arrangement occurs in other hybodontoids (e.g., Maisey, 1982: fig.12, 1986, 1989).

Figure 94 presents a reconstruction of the anterior part of the body of *Tribodus limae*, illustrating the position of the pectoral skeleton. Based on AMNH FF 13957, the dorsal part of the scapular process in *T. limae* was apparently level with the basal cartilage of the anterior dorsal fin. Such an arrangement has not been noted previously in other hybodonts, possibly due to displacement of the skeletal elements during burial; however, in many hybodont taxa the scapulocoracoids do appear to extend dorsally almost to the basal plate of the first dorsal fin (e.g., Maisey, 1982: fig. 10). In extant sharks such as *Squalus*, the scapulocoracoid extends dorsally as far as the top of the vertebral column, similar to the condition seen in most hybodonts. The pectoral girdle is located beneath the first dorsal fin in many Paleozoic sharks, (e.g., *Ctenacanthus* Agassiz, 1835; *Goodrichthys* Moy-Thomas, 1951; *Tristychius*, *Onychoselache*), and this may be a highly conserved arrangement in *Tribodus*. By contrast, in many neoselachians the first dorsal fin is located farther posteriorly (e.g., *Squalus*), which may be apomorphic. The hydrodynamic consequences of having the first dorsal fin in line with the pectorals are difficult to assess because no extant shark has such an arrangement, but the modern configuration may confer advantages absent in *Tribodus*: a dorsal fin located directly above the girdle limits the anterior extent of epaxial and hypaxial musculature, which are

utilized in elevating and depressing the head and anterior body during rising and sinking (Wilga and Lauder, 2004). Extinct sharks such as *Tribodus* may therefore have been less efficient than modern sharks in elevating and depressing the head in this manner.

**Pectoral articulation**— The new material of *Tribodus limae* indicates that its pectoral articulation was mediolateral, with the fin directed at an angle of approximately 135° to the scapulocoracoid and attached along a posteriorly positioned articular ridge (Fig. 89B). In modern sharks, the pectoral basals also articulate on a narrow ridge located on the posterolateral portion of the scapulocoracoid (Shirai, 1992; Fig. 88A). In some fossils, there may be a steep slope between the points of articulation for the fin basals (e.g., *Tristychius*, Dick, 1978). The fin articulation is commonly oblique to the articular ridge (e.g., *Tribodus*, *Orthacanthus*, many galeomorphs and orbitostylic sharks), but lies in the horizontal plane in batoids, and is more vertical in some squaloids (Shirai, 1992). The articular surface of *Onychoselache* differs from that of *Tribodus* in having a lateral fin articulation comprising an anterior glenoid fossa and a posterior condyle (Coates and Gess, 2007).

Unlike *Tribodus* and most neoselachians sharks, in batoids, *Heterodontus*, and several other derived neoselachians the articular process is rounded and knob-like rather than ridge-like, and may be arranged laterally rather than posteriorly (Shirai, 1992). In chimaeroids, the pectoral fin is dibasal and the articular surface is located farther ventrally than in elasmobranchs, with an elongated, posteriorly facing crest and a knob on one side that fits into a shallow socket on the fin, plus a flat abutment on the opposite side for the propterygium (Stahl, 1999).

In contrast to *Tribodus* and most elasmobranchs, in some Paleozoic chondrichthyans (e.g., *Cladoselache* and symmoriiforms: Bendix-Almgreen, 1975; Sequeira and Coates, 2000), the pectoral fin is long-based (eurybasal) and comprises a posterior metapterygium plus several pre-metapterygial radials articulating directly with the shoulder girdle. The articular process is nearly horizontal, and projects ventrolaterally from the lateral side of an elongated posterior process on the girdle (*Cladoselache*, Bendix-Almgreen, 1975: fig. 1; *Akmonistion* Coates and Sequeira, 2001B [fig. 10]). Although a long-based articulation is also found in advanced euarthrodire placoderms (Stensio, 1959, 1969; Bendix-Almgreen, 1975), recent evidence strongly suggests that presence of only a single fin radial is the primitive condition in placoderms, and probably in gnathostomes generally (Janvier, 1998; Goujet, 2001; Coates, 2003; Goujet and Young, 2004; Janvier et al., 2004).

Pectoral fin morphology in eurybasal Paleozoic chondrichthyans is similar to that of stenobasal sharks in having a metapterygium that attaches to a posterior process on the scapulocoracoid. However, the articular ridge in *Cladoselache* faces laterally rather than posteriorly, and the remainder of the fin base comprises numerous radials rather than one or two basals. The more lateral articulation of the pre-metapterygial basals in *Cladoselache* and other eurybasal sharks may therefore be derived. In contrast, a posteriorly located metapterygium occurs in osteichthyans as well as chondrichthyans, and in both groups this element appears to develop according to a highly conserved ontogenetic pattern, suggesting that this condition may be primitive for crown-group gnathostomes (Balfour, 1881; Davis et al., 2004; Mabee and Noordsy, 2004).

Homology between the pre-metapterygial fin elements of *Cladoselache* and the

pre-metapterygial basals of hybodonts and neoselachians is unclear. While it is conceivable that the short-based fins of elasmobranchs and chimaeroids resulted evolutionarily through fusion of formerly separate radials to form basals as well as concentration of the fin base around the posterior part of the articular process, there is no evidence of fusion during ontogeny and it therefore seems likely that the series of pre-metapterygial radials seen in Paleozoic sharks such as *Cladoselache* represents a derived rather than primitive condition. Instead, it is possible that the multiple radials of *Cladoselache* arose secondarily by splitting of cartilage within the fin as in modern teleosts and neoselachians, where the pre-metapterygial basals and associated radials originate ontogenetically as a single cartilaginous disc that later divides via localized cell apoptosis (e.g., Balfour, 1881; Davis et al., 2004; Mabee and Noordsy, 2004). This ontogenetic pattern in teleosts and neoselachians is reminiscent of the phylogenetic pattern suggested by fossils, beginning with a single basal in primitive stem gnathostomes (e.g., *Escuminaspis*; Janvier et al., 2004) and progressing to three or more basals in crown group gnathostomes plus acanthodians (Goujet, 2001; Coates, 2003; Davis et al., 2004; Goujet and Young, 2004; Janvier et al., 2004; Mabee and Noordsy, 2004). The presence of multiradiate fins in some advanced placoderms, as mentioned above, may represent an independent autapomorphy.

Coates and Sequeira (2001B) found a eurybasal fin articulation to be congruent with other characters forming a clade comprising *Cladoselache*, symmoriiforms, and several additional taxa (e.g., chimaeroids, in which the long-based pectoral fin may have been lost secondarily). This character may thus be a derived feature uniting *Cladoselache* and

symmoriiforms, rather than the 'primitive' condition for chondrichthyans as suggested in the past (e.g., Goodrich, 1930; Zangerl, 1981; Carroll, 1988).

Presence of a stenobasal, tribasal fin is congruent with other characters uniting xenacanths, ctenacanths, hybodonts, and neoselachians. A dibasal fin is a derived feature among holocephalans (Coates and Sequeira, 2001B), and probably independently apomorphic in *Tristychius* (according to Coates and Gess, 2007) and in a few modern squaleans such as *Somniosus* (Helbing, 1904). The posterior-versus-lateral position of the fin articulation, and absence of an elongated posterolateral articular process, may represent further features distinguishing elasmobranchs from *Cladoselache* and related forms.

Among extant tribasal neoselachians, there is some variation in the way the basals are arranged on the articular process (for example, in some orbitostylic taxa like *Chlamydoselachus* and *Heptranchias*, there is a single, linear, ventromedially slanted articular ridge, with the basals aligned in a row in close contact with each other (Smith, 1937:figs. 37, 38; Gans and Parsons, 1981: pl. 7), whereas in many carcharhiniforms, the articular region is triangular, with the basals splayed around it in a corresponding arrangement (in dorsal view, the basals are aligned in a row as in other taxa; however, in lateral and ventral views, they overlap). Only the mesopterygium actually attaches along the articular ridge, whereas the metapterygium attaches to the underside of the ridge in a ventromedial position, and the propterygium attaches above and lateral to the ridge at the base of the scapular process. Among extinct tribasal sharks, *Orthacanthus*, *Ctenacanthus*, and *Tribodus* appear to display a similar pattern to the former, although the precise arrangement of basals on the articular ridge is unknown. In *Tribodus*, the articular facets

were clearly located entirely on the posterolateral surface of the scapulocoracoid along the elevated articular ridge, with at least two articular facets (for the propterygium and metapterygium), and possibly a third narrow attachment area between them for the mesopterygium (AMNH FF 13958).

Based on these features, it is here inferred that the pectoral fin of *Tribodus* probably projected outward and posteriorly from the scapulocoracoid at approximately 45° to the horizontal axis, as in many modern sharks. Because the structure and position of the pectoral fin articulation in *Tribodus* are so similar to those of many modern sharks, its fin mobility and mode of swimming may also have been similar (see e.g., Liem and Summers, 1999), but further discussion of this is beyond the scope of the present thesis. The ridge-like articular process in *Tribodus* may have provided considerably greater fin mobility than would be possible according to previous reconstructions of hybodont pectoral fins (Maisey, 1982, 1986, 1989; Brito, 1992). The structure of the pectoral endoskeleton in *T. limae* closely resembles that of neoselachian sharks, xenacanths and ctenacanths, and clearly represents a successful and highly conserved arrangement, although its phylogenetic significance is not yet well resolved.

**Pectoral fin skeleton**—The endoskeleton of the pectoral fin in *Tribodus* is typical of hybodonts and other tribasal chondrichthyans in consisting of three proximal basals (propterygium, mesopterygium, and metapterygium) plus numerous radial series distally. No radials were observed in any of the specimens of *T. limae* examined here, although Brito (1992) described their arrangement based on one of his specimens as being similar to that of other hybodonts, in which the propterygium supports a single, short, pointed radial, and the mesopterygium and metapterygium each support several radials. Coates

and Sequeira (2001B) identified two characters of the pectoral radials uniting hybodonts in their study: the presence of a broad propterygium, and the presence of three or more distal radials on the mesopterygium. *Tribodus* agrees in both of these characters, having at least three distal mesopterygial radials (Brito, 1992) and a broad propterygium. The radials (apart from the propterygial radials, except in *Hybodus hauffianus* Fraas, 1889: Maisey, 1986) are typically jointed regularly in both hybodontiforms and neoselachians, a feature that may be apomorphic (Maisey, 1982). However, since according to Brito (1992) only the proximal set of radials are known in *Tribodus*, it is unknown whether its radials were similarly jointed. The short, tapered shape of the single propterygial radial in *T. limae* (Brito, 1992: fig. 2) suggests that, as in other hybodontiforms, this element probably was not jointed.

**Morphological characters of the pectoral skeleton in *Tribodus* vs. other hybodonts**

Coates and Gess (2007) listed 12 characters of the pectoral endoskeleton (in their total list of 50 skeletal characters) as potentially important in determining hybodont relationships. Positions of pectoral characters are indicated on the phylogeny shown in Figure 95. Each of these characters is reviewed here in the order presented by Coates and Gess (2007), and its state in *Tribodus* is identified as follows. Some of these characters are included in the present phylogenetic analysis (Part III of this thesis).

(1) Scapular process narrow dorsally and lacking posterolateral angle (Fig. 95A): present in *Tribodus*. This character is shared by most hybodonts and neoselachians, but absent in *Tristychius* and in Paleozoic chondrichthyans such as *Akmonistion*,

*Plesioselachus* (Coates and Gess, 2007) and *Orthacanthus* (Fig. 87), which have a posterolateral angle.

(2) Scapulocoracoid with a continuously concave anteromedial edge (coracoid anterodorsal shoulder reduced or absent; Fig. 95A): present in *Tribodus*. Absent in some Paleozoic chondrichthyans (Coates and Gess, 2007) and in *Orthacanthus* (Fig. 87).

(18) Imperforate scapulocoracoid (i.e., diazonal foramen missing; Fig. 95B): absent in *Tribodus*. According to Coates and Gess (2007), absence of a diazonal foramen in *Tristychius* may represent an autapomorphy. However, these authors point out that a damaged area on the specimen may in fact be a remnant of this foramen, and it may also be possible that the foramen is on a part of the fossil not visible in the preserved view, such as its posterior surface. The alternative would be that the fundamental innervation and vascularization patterns of the pectoral fin had become highly modified in *Tristychius*, so that nerves and blood vessels skirted around the scapulocoracoid instead of passing through it. Diazonal foramina are certainly present in *Onychoselache* and hybodontoids (Maisey, 1982, 1989; Coates and Gess, 2007). However, the extant hexanchiform *Heptranchias* has only two (lateral and medial) diazonal foramina. It is hypothesized here that presence of three diazonal foramina is primitive for elasmobranchs.

(23) Coracobranchial fossa (grooved leading edge; Fig. 95C): possibly present in *Tribodus*. Although the anterodorsal margin of the scapular process is damaged in AMNH FF 13958, it does show a slight indentation which may be evidence of a coracobranchial fossa, and a similar indentation is also present in AMNH FF 13961. However, the anteroventral edge of the scapular process is smoothly rounded, indicating

that even if a coracobranchial fossa was present in *Tribodus*, it did not extend as far ventrally as in other hybodontoids. A coracobranchial fossa has been reported in *Onychoselache* by Coates and Gess (2007), as well as in *Lissodus* and *Hybodus* (Maisey, 1982), and its occurrence in *Tribodus* would be consistent with earlier views of hybodont phylogeny (Maisey et al., 2004; Coates and Gess, 2007). This feature is absent in *Tristychius* and neoselachians (Coates and Gess, 2007).

(32) Pectoral fin articulation on lateral face of coracoid (Fig. 95C): absent in *Tribodus*. This occurs in *Onychoselache* (a possible reversal) and in some Paleozoic chondrichthyans such as *Cladoselache* and symmoriiformes (Coates and Gess, 2007).

(33) Pectoral fin articulation oriented anterodorsally (propterygium uppermost; Fig. 95C): According to Coates and Gess (2007), this character is autapomorphic for *Onychoselache*. Although the propterygium is uppermost in *Tribodus* (due to the ventromedial slant of the articular ridge), the location of the ridge is posterior, not lateral as in *Onychoselache*, and furthermore an anterodorsal orientation is not present as in that genus. The condition in *Onychoselache* appears to be linked to the lateral location of the fin articulation. It should also be pointed out that in AMNH FF 13958 as originally preserved (Fig. 83A), the propterygium appears to be ventral or lowermost because of the way the specimen was fossilized. Unfortunately, the posterior surface of the scapulocoracoid is unknown in other hybodonts, and consequently it is not known whether a posterior ridge was present in those taxa; the orientation of their basal cartilages is therefore uncertain. However, if the pectoral articulation in those taxa was similar to that of *Tribodus*, the character ‘propterygium uppermost’ would include most

hybodontiforms. It is concluded that only the anterodorsal orientation of the fin is autapomorphic for *Onychoselache*, not having the propterygium uppermost.

(40) Coracoid and scapular regions of subequal length (Fig. 95E): Coates and Gess (2007) retained this character from Maisey (1989) and Maisey et al. (2004), which supposedly unites most hybodontoids but excludes *Hamiltonichthys*. However, the character itself is ambiguous, and requires a more precise definition. Maisey (1989) differentiated *Hamiltonichthys* from Mesozoic hybodontoids in that in *Hamiltonichthys*, the coracoid region is only one-third the length of the scapular region, whereas in Mesozoic hybodontoids, the two regions are of near-equal length. However, no specific point of reference for this measurement was identified, and if the metapterygium is used as the point of reference, it could be argued that the scapular and coracoid regions of *Hamiltonichthys* are of near-equal length. (Fig. 95D). Although the scapular and coracoid regions seem superficially to be nearly equal in Mesozoic hybodontoids, as the new material of *Tribodus* demonstrates (especially AMNH FF 13958; Figs. 83–85), only three-dimensionally preserved material accurately displays the position of the pectoral articulation. The articular process is the default landmark generally used to distinguish the scapular and coracoid regions; thus, its position must be accurately determined before these regions can be defined. Additionally, wherever the articular process is angled ventromedially, it is necessary to identify a more specific landmark on this process from which accurate measurements of the scapular and coracoid regions can be made. If the propterygial facet (the only part of the articular process typically visible in laterally preserved specimens) is used, then all hybodontoids have a coracoid process that is approximately 70-80% of the scapular process, indicating that this character is

inconclusive for differentiating members of this group. Although the metapterygial facet would probably be a more accurate landmark (because the metapterygium forms developmentally as an outgrowth of the scapulocoracoid), for preservational reasons its true position is unknown in hybodontoids other than *Tribodus*.

(19) Dibasal fin, separate mesopterygium missing (Fig. 95B): absent in *Tribodus*. According to Coates and Gess (2007), this character appears to be an autapomorphy of *Tristychius*.

(22) Pattern of pectoral basals and radials (i.e., no specialized cartilages forming axis distal to metapterygial plate; Fig. 95C): probably present in *Tribodus* (cf. Brito, 1992: fig. 2; Fig. 89A), although no radials are preserved in the new material described here. This feature is also present in *Onychoselache* and hybodontoids, and may be a synapomorphy of this unnamed group (Coates and Gess, 2007).

(25) Propterygium with convex leading edge (Fig. 95C): present in *Tribodus*. This character is also found in *Onychoselache* (according to Coates and Gess, 2007) and hybodontoids (e.g., *Hamiltonichthys*, *Lissodus*, *Hybodus*, *Egertonodus*, Maisey, 1982, 1989), and may be a synapomorphy of this unnamed group.

(34) Mesopterygium sickle-shaped (Fig. 95C): absent in *Tribodus*. Coates and Gess (2007) suggest that this may be an autapomorphy of *Onychoselache*.

(35) Five or more simple radials distal to the metapterygium (Fig. 95D): probably present in *Tribodus*, based on previous descriptions (Brito, 1992: fig.2; see Fig. 89A here). This character has been used to unite hybodontoids (Coates and Gess, 2007).

**Phylogenetic implications**

A complete phylogenetic analysis including several characters from the pectoral fin skeleton is included in Part III of this thesis. Figure 95 depicts hypothesized relationships among hybodontiform elasmobranchs (after Maisey, 1989; Maisey et al., 2004; Coates and Gess, 2007), and is currently supported by a total of 50 morphological characters listed by Coates and Gess (2007). *Tribodus* is tentatively placed within the hybodontoid subfamily Acrodontinae, which also includes *Acrodus* Agassiz, 1837 and *Asteracanthus* Agassiz, 1937 (Maisey, 1989), on the basis of a single histological character in the teeth (presence of irregular dentine; Brito, 1992). Coates and Gess (2007) link *Tribodus* with *Acrodus* and *Asteracanthus* on the basis of the character 'teeth with columnar osteodentine' (their character 49), and further link *Tribodus* with *Asteracanthus* based on the character 'palatoquadrates lacking ethmoid buttresses and orientated transversely' (their character 50). It now seems likely that 'short', transversely oriented jaws characterize an even wider subset of hybodont genera including *Lissodus* and *Lonchidion* Estes, 1964, although it is unknown at present whether their palatoquadrates also lack an ethmoid buttress.

Unfortunately, *Acrodus* and *Asteracanthus* are known largely from isolated teeth or partial dentitions, isolated jaws, and fin spines, but well-preserved skeletal fossils are unknown. The pectoral skeleton is also unknown in *Palaeobates* Meyer, 1849. Without knowing the pectoral morphology in *Acrodus* and *Asteracanthus*, it is impossible to identify any pectoral characters specific to Acrodontinae. The posteroventral diazonal foramen of *Tribodus* may be autapomorphic, or could alternatively unite a larger group if it is found to be present in other hybodontoids. Due to the two-dimensional preservation

of most hybodont specimens, identifying potential hybodont pectoral synapomorphies is difficult at present.

Hybodontiforms except *Tristychius* are united by characters 22 (‘no specialized cartilages forming axis distal to metapterygial plate’), 23 (‘presence of coracobranchial fossa’), and 25 (‘propterygium with convex leading edge’), although character 23 may be lost in *Tribodus*. Characters 1 (‘scapular process narrow dorsally and lacking posterolateral angle’) and 2 (‘coracoid anterodorsal shoulder reduced or absent’) unite neoselachians and hybodontiforms including *Tribodus*, although character 1 is reversed in *Tristychius*. Character 33 (‘pectoral fin articulation orientated anterodorsally; propterygium uppermost’) of *Onychoselache* is ambiguous: the propterygium is also uppermost in *Tribodus*, and possibly all Hybodontoidei (although this is unknown pending discovery of additional hybodont specimens), but the articular ridge in *Tribodus* is positioned more posteriorly, and differs morphologically from that of *Onychoselache*, so it is difficult to determine whether the anterodorsal articulation of *Onychoselache* is homologous to the more dorsolateral articulation of *Tribodus*. It would seem clearer to separate these into two distinct characters (i.e., ‘anterodorsally orientated pectoral articulation’ and ‘propterygium uppermost’). It is also worth noting that the narrow dorsal part of the scapular process is curved anteriorly in all hybodontiforms except *Tristychius*, possibly representing an additional synapomorphy of this group.

The presence of an oblique posterior articular ridge in *Tribodus* unites it with neoselachians, xenacanths (e.g., *Orthacanthus*), and ctenacanths; its absence in symmoriiforms and *Cladoselache* could be interpreted either as a primitive or derived condition, but seems to be correlated with the multibasal condition of the pectoral fin.

FIGURE 82. *Tribodus limae* Brito and Ferreira, 1989. Close-up of Fig. 8B (AMNH FF 13959) showing articular process of left scapulocoracoid. Scale bar equals 2 cm.

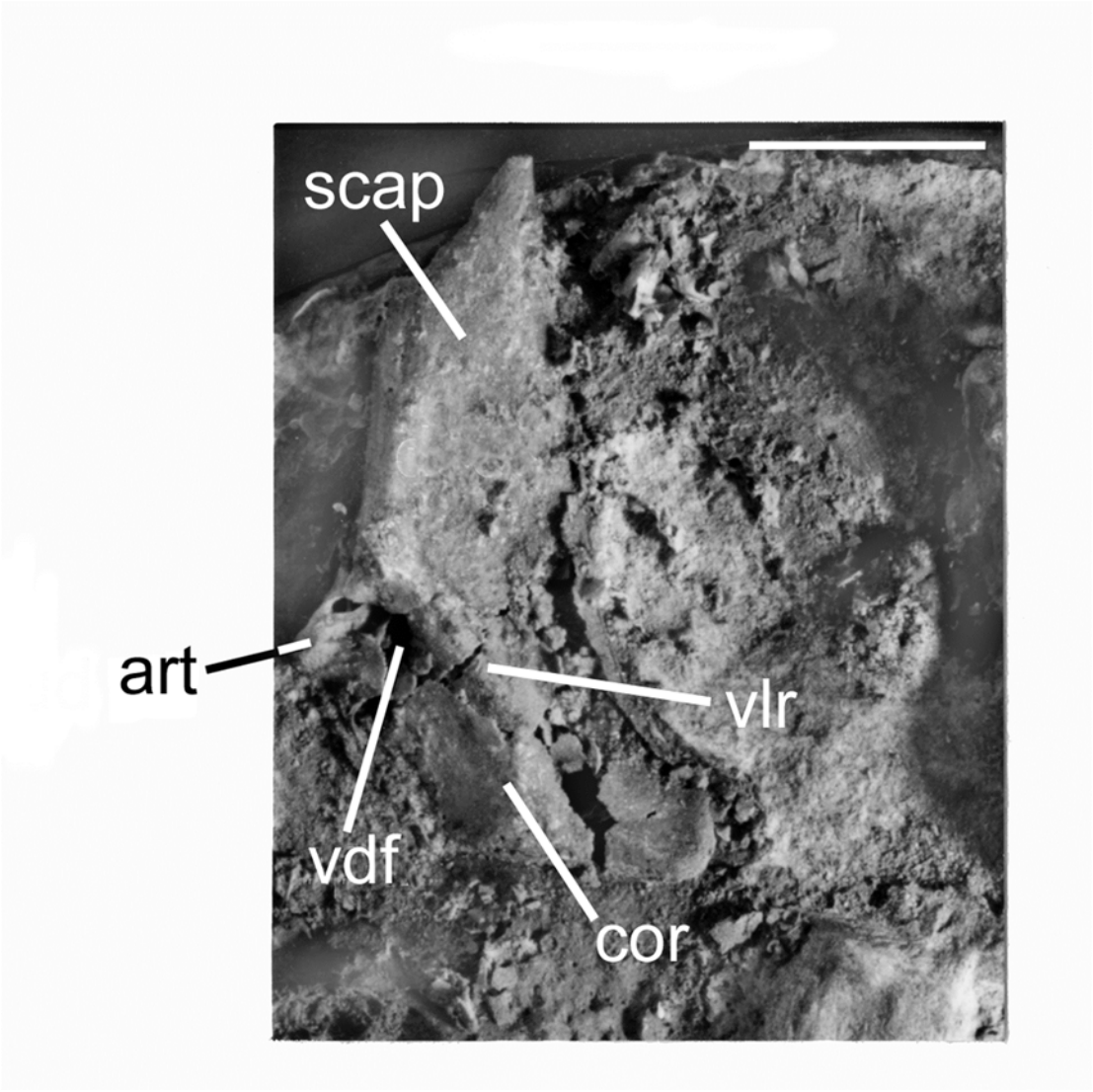
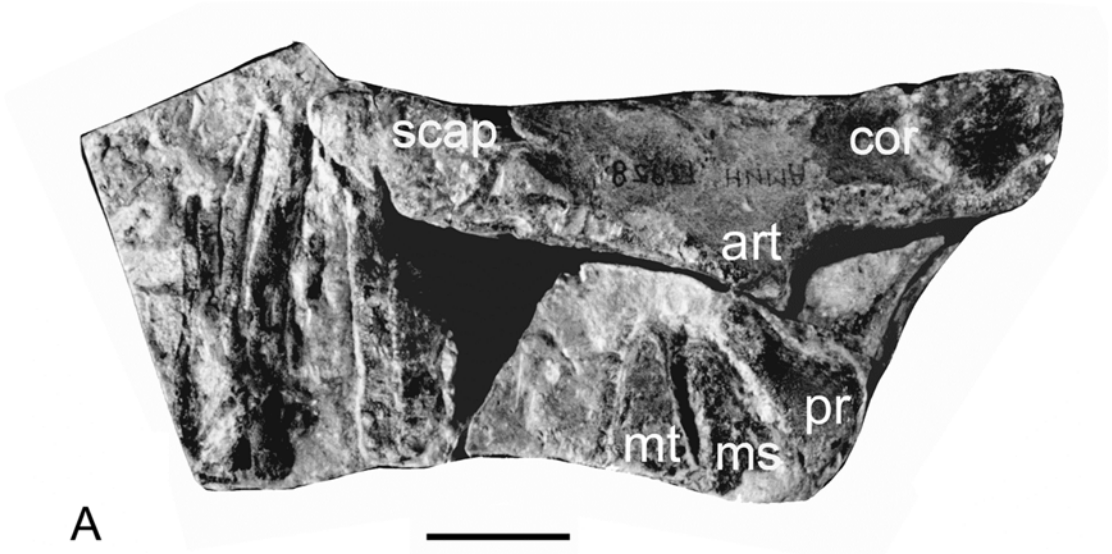

scap
art
vlr
vdf
cor

FIGURE 83. *Tribodus limae* Brito and Ferreira, 1989. A, AMNH 13958, right scapulocoracoid (lateral view) with basal cartilages of right pectoral fin in ventral view; B, dorsal (left) and ventral (right) views of one of the basal cartilages of left pectoral fin (possibly propterygium). Scale bars equal 2 cm.


scap
cor
art
pr
mt
ms
A

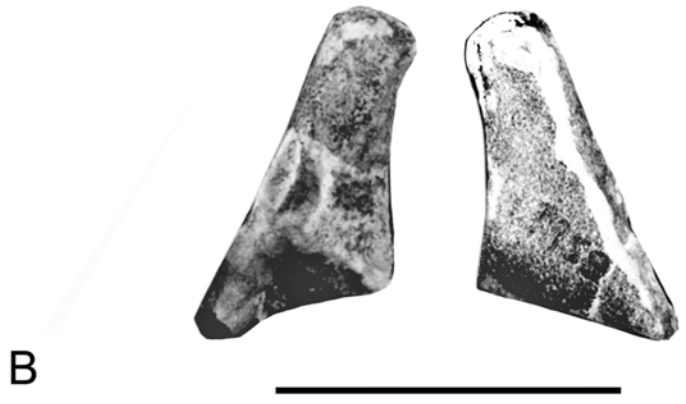

B

FIGURE 84. *Tribodus limae* Brito and Ferreira, 1989. Right scapulocoracoid, AMNH 13958, in stereophotographic views. A, lateral; B, medial; C, anterior; D, posterior. Scale bar equals 2 cm.


A
B
C
D

FIGURE 85. *Tribodus limae* Brito and Ferreira, 1989. Line drawing of right scapulocoracoid (AMNH FF 13958) seen in Figure 84. A, lateral, B, posterior, and C, medial view. Not to scale.

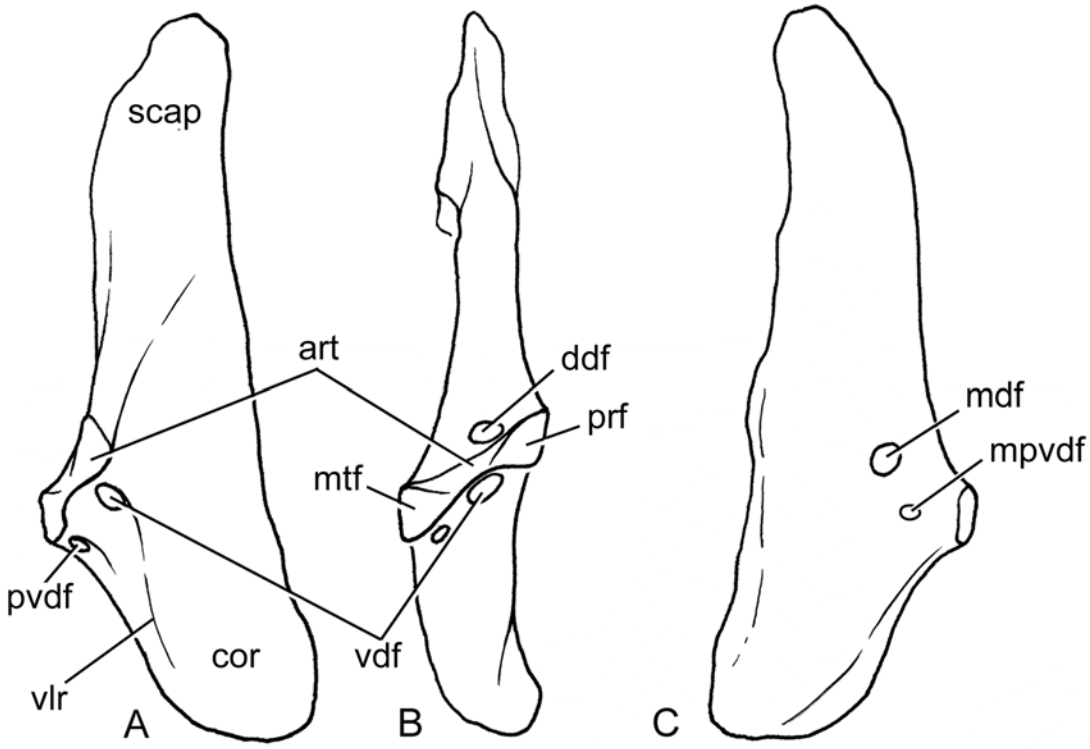

scap
art
ddf
prf
mtf
pvdf
cor
vdf
vlr
A
B
C
mdf
mpvdf

FIGURE 86. *Tribodus limae* Brito and Ferreira, 1989. CT scan images of articular region of right scapulocoracoid (AMNH FF 13958). A, posterior view; B, medial view. Not to scale.

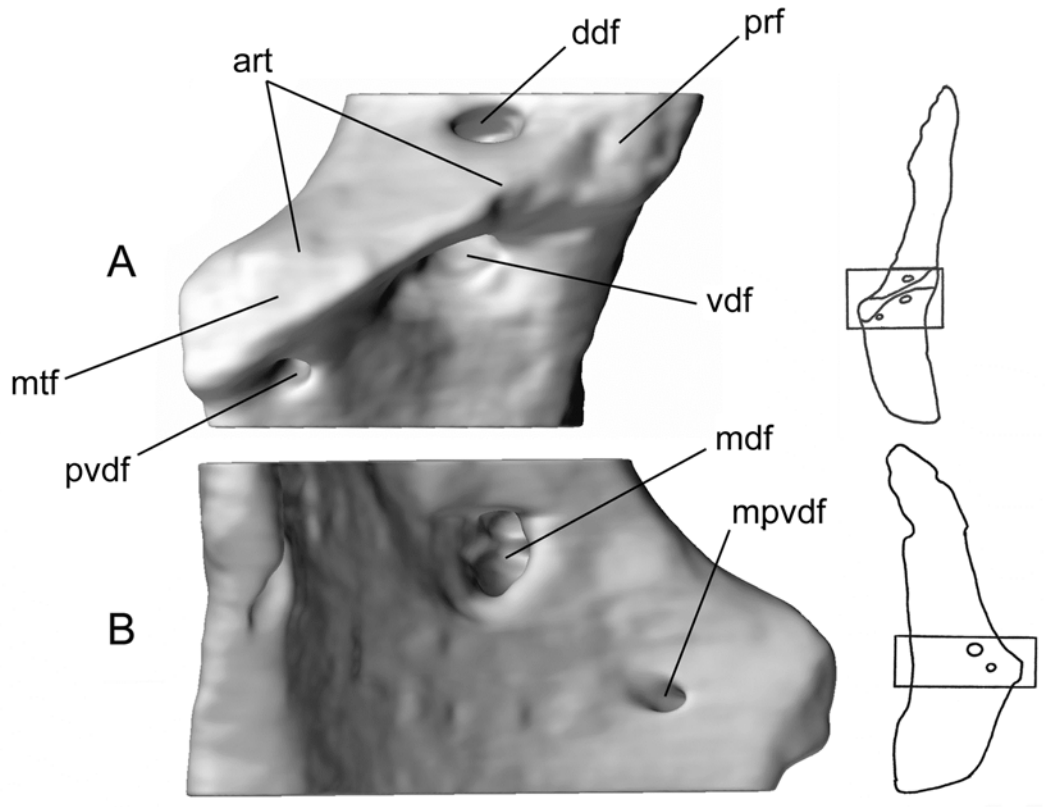

art
ddf
prf
A
vdf
mtf
pvdf
mdf
mpvdf
B

FIGURE 87. *Orthacanthus texensis* (Cope, 1888). Right scapulocoracoid (AMNH FF 20273). A, medial; B, posterior; and C, lateral views. Scale bar equals 2 cm.

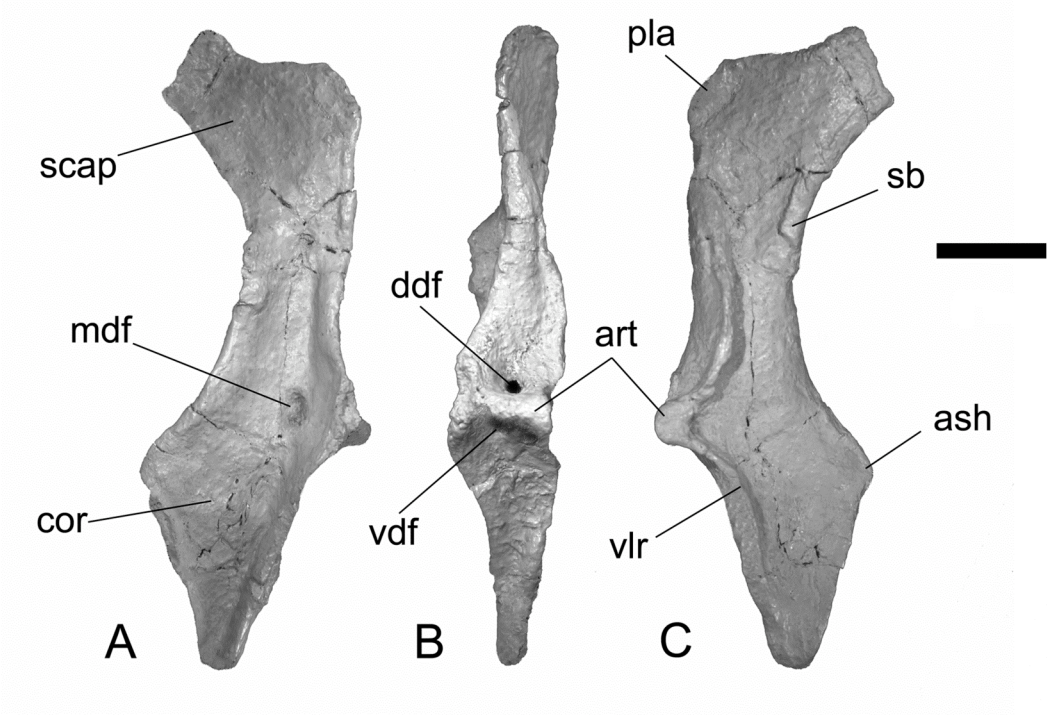

scap
mdf
cor
A
ddf
vdf
B
pla
sb
art
ash
vlr
C

FIGURE 88. Comparison of pectoral fin articulation in *Tribodus* and neoselachians. A, pectoral fin articulation in the extant squaliform neoselachian *Centroscyllium* (after Shirai, 1992); B, reconstruction of pectoral fin articulation in *Tribodus limae* based on AMNH FF 13958. Not to scale.

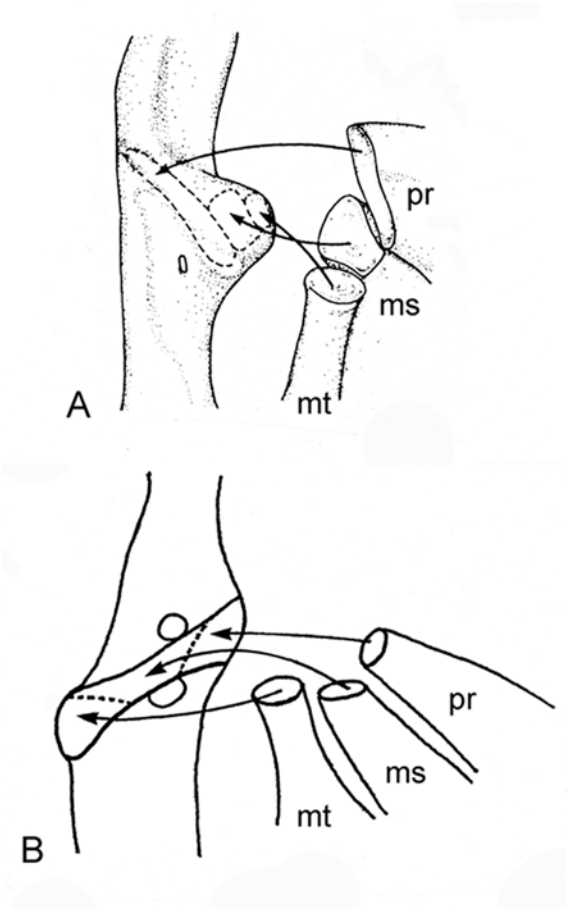

pr
ms
mt
A
pr
ms
mt
B

FIGURE 89. Comparison of previous and revised reconstructions of the pectoral endoskeleton in *Tribodus limae*. A, Previous reconstruction (after Brito, 1992); B, revised reconstruction based on the new material (AMNH FF 13957–13959, 13961). Additional abbreviations: **ars**, articular surface of pectoral fin; **gf**, glenoid fossa; **r**, radials. Not to scale.

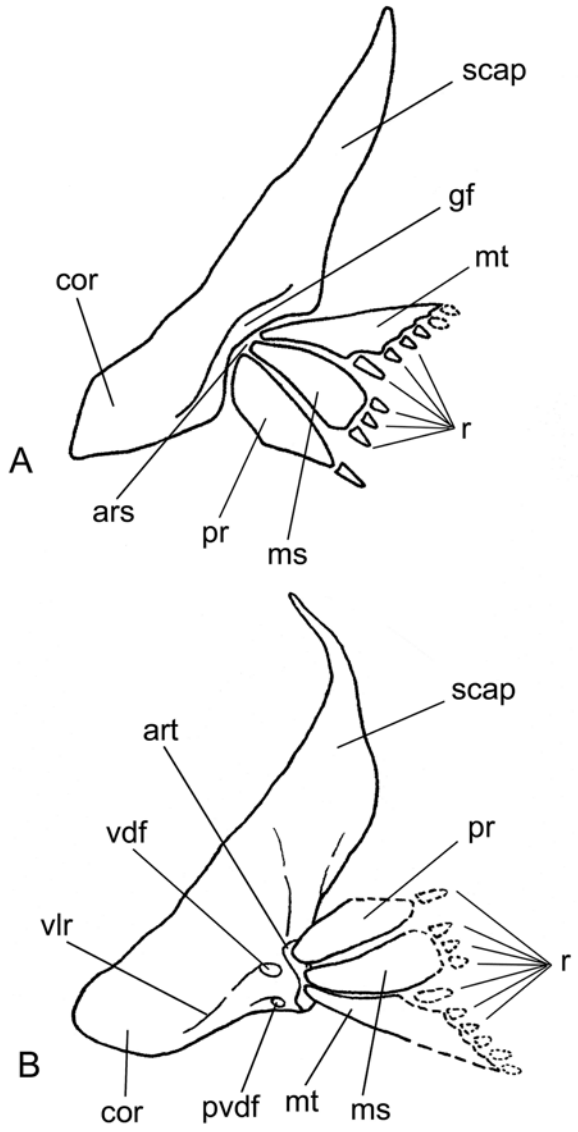

scap
gf
mt
cor
r
A
ars
pr
ms
scap
art
vdf
pr
vlr
r
B
cor
pvdf
mt
ms

FIGURE 90. *Tribodus limae*, MN 5807V, left scapulocoracoid and pectoral fin. Scale bar equals 5 cm.


scap
r
mt
art
ms
pr
cor

FIGURE 91. *Tribodus limae*, MN 5807V, closeup of articular region of left pectoral fin. Scale bar in centimeters, with millimeter increments.

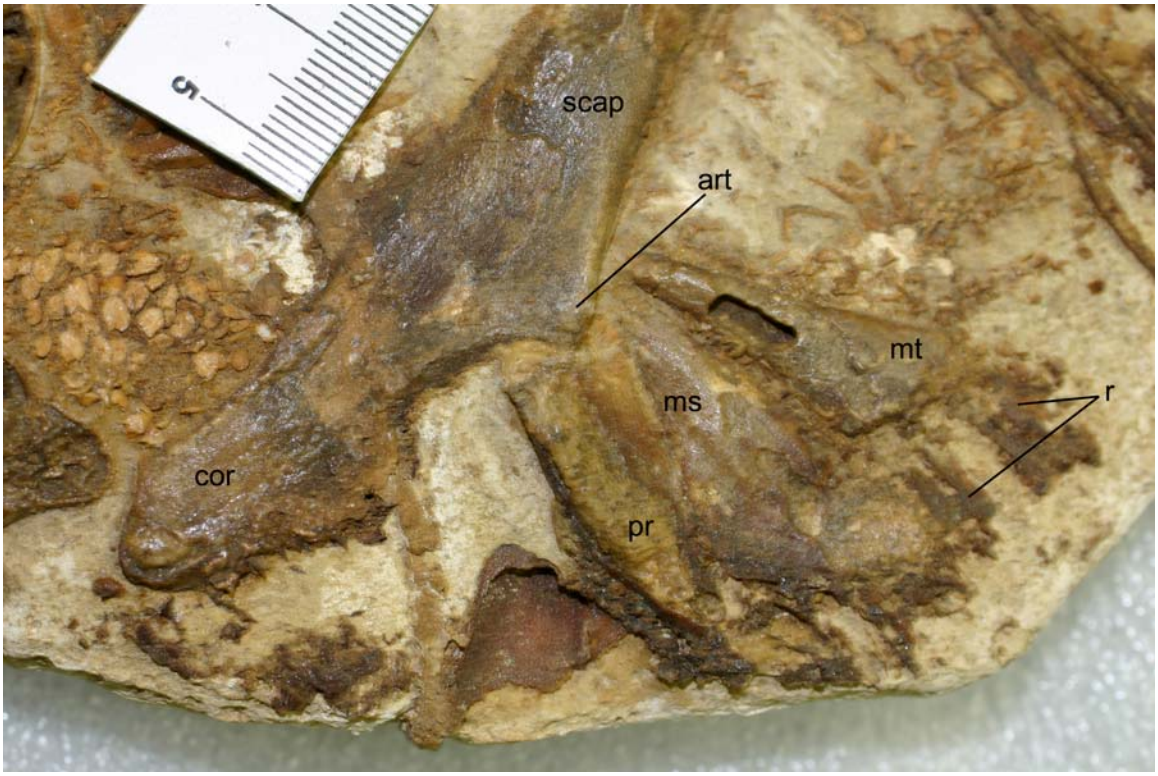

scap
art
mt
ms
r
cor
pr

FIGURE 92. Left scapulocoracoid of *Tribodus limae*, MN 5808V. Scale bar in millimeter increments.

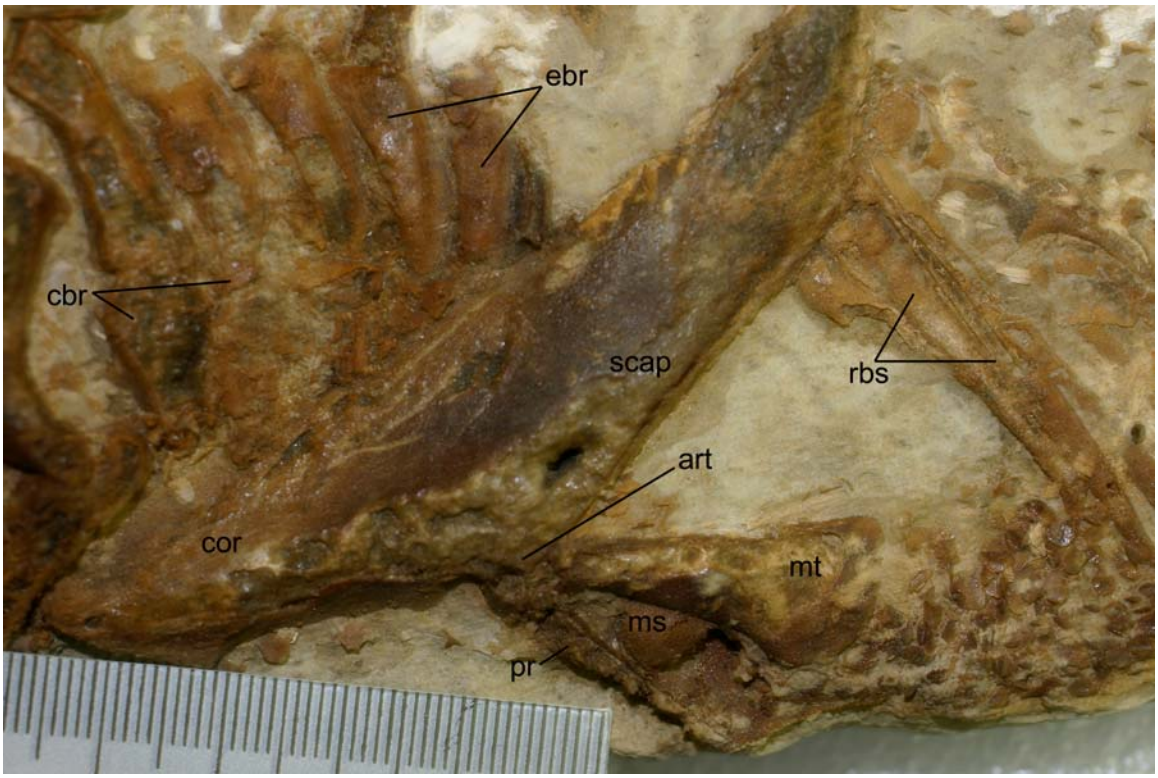

ebr
cbr
scap
rbs
art
cor
mt
ms
pr

FIGURE 93. *Tribodus limae*, MN 5808V, closeup of left pectoral fin. Scale bar in centimeters, with millimeter increments.

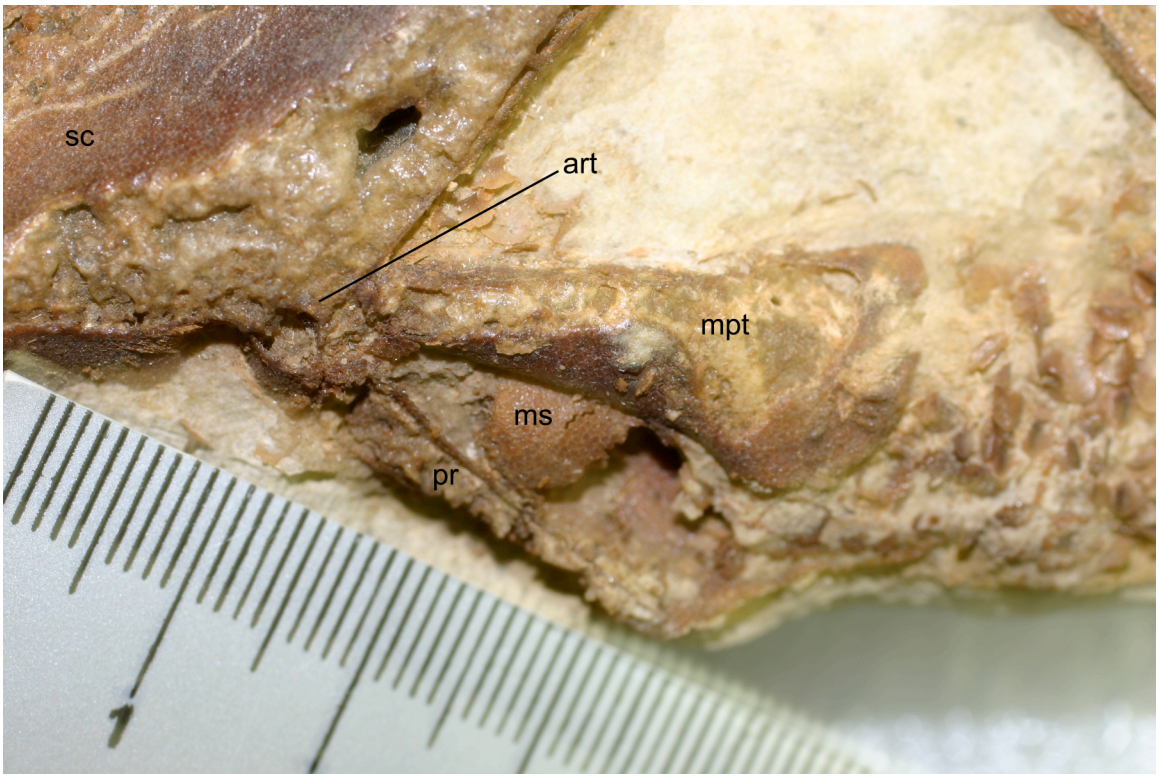

sc
art
mpt
ms
pr

FIGURE 94. *Tribodus limae* Brito and Ferreira, 1989. Composite reconstruction based on the new material and previous knowledge of hybodont skeletal anatomy. Braincase, dorsal fin and pectoral skeleton based on AMNH FF 13957–13959, 13961; branchial and vertebral elements from a previous reconstruction of *Hybodus* sp. (Maisey, 1982).

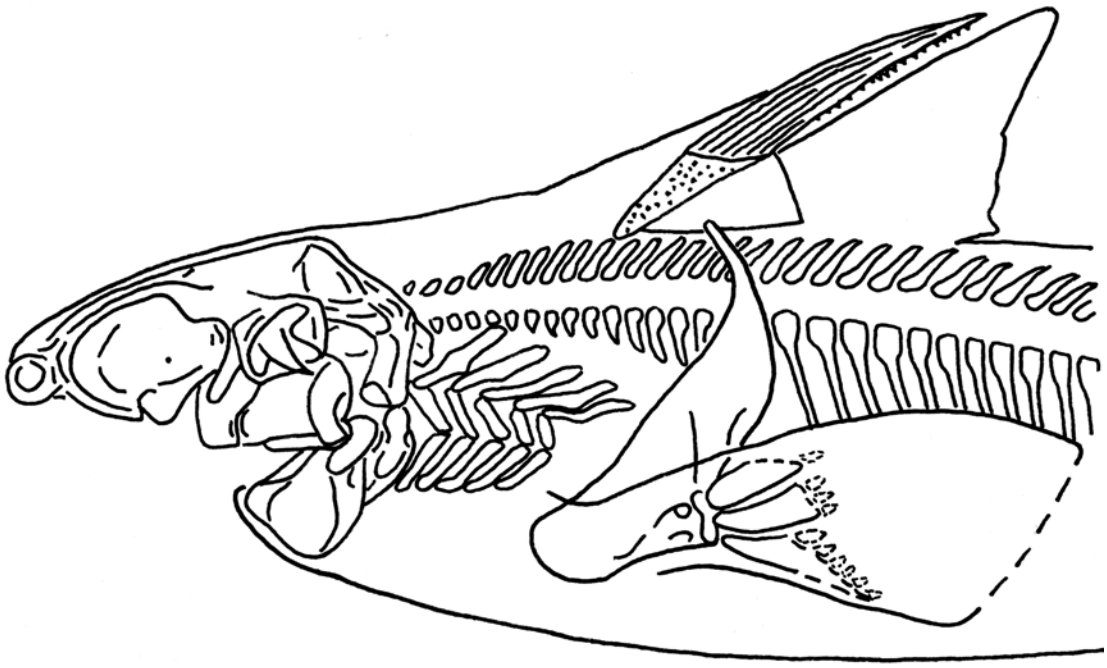
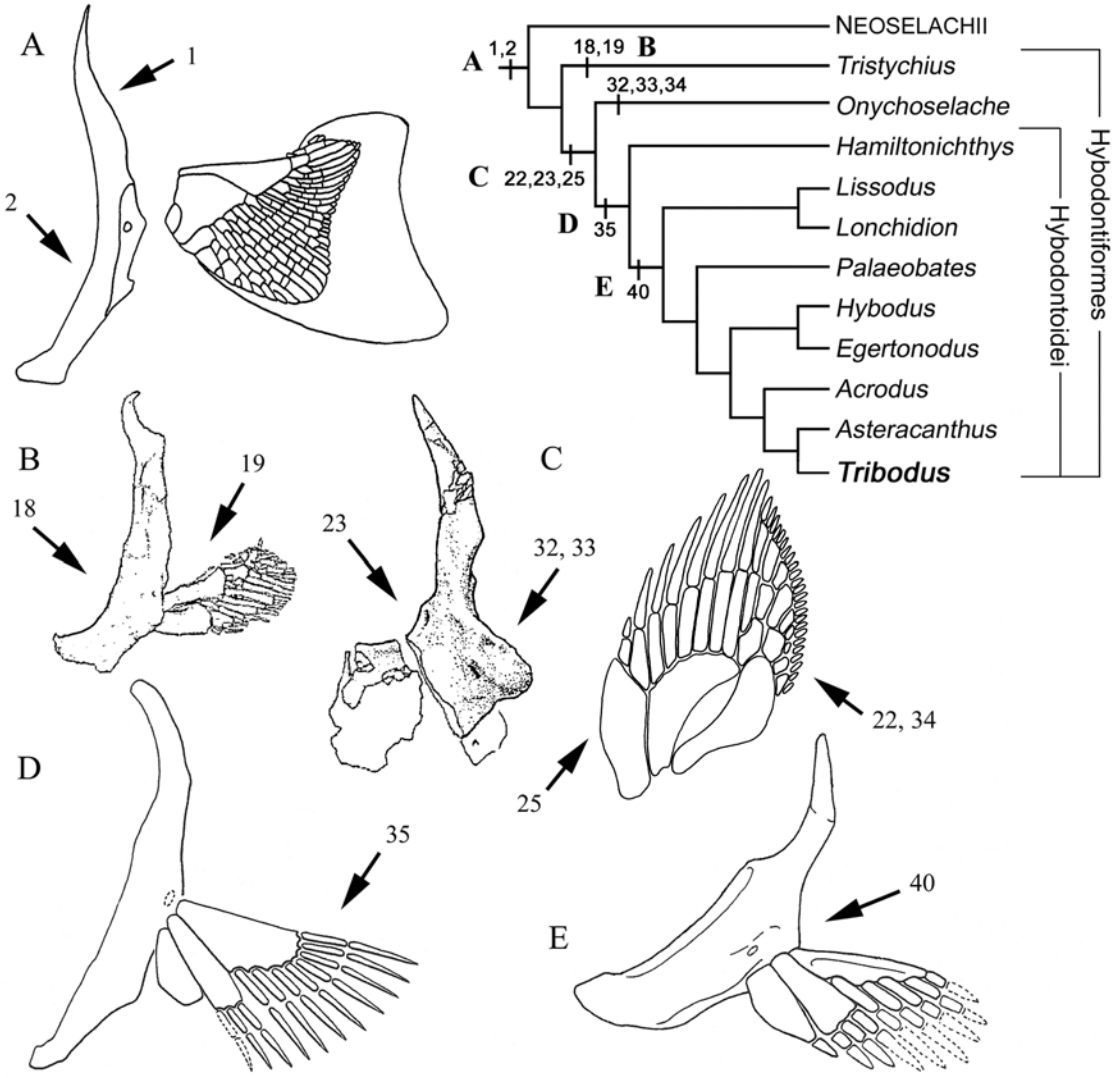


FIGURE 95. Previously proposed phylogenetic relationships among hybodontiform elasmobranchs, showing positions of pectoral skeletal characters on the tree (after Coates and Gess, 2007). *Tribodus* is indicated in boldface. Numbered characters are from Coates and Gess (2007), as listed in the text. Letters correspond to nodes on the tree, as exemplified by A, *Notorynchus*, a neoselachian (after Daniel, 1934: fig. 54); B, *Tristychius* (after Coates and Gess, 2007); C, *Onychoselache* (after Coates and Gess, 2007); D, *Hamiltonichthys* (after Maisey, 1989); and E, *Lissodus* (after Maisey, 1982).


A
1
2
B
18
19
23
C
32, 33
22, 34
25
D
35
E
40
NEOSELACHII
A 1,2
18,19 B
Tristychius
32,33,34
Onychoselache
Hamiltonichthys
C 22,23,25
Lissodus
D 35
Lonchidion
Palaeobates
E 40
Hybodus
Egertonodus
Acrodus
Asteracanthus
Tribodus
Hybodontoidei
Hybodontiformes

# CHAPTER 8: PELVIC GIRDLE AND FIN OF *TRIBODUS LIMAE*

The pelvic girdle and fin are not preserved in any of the AMNH specimens of *Tribodus limae* described here. However, Brito (1992) described the pelvic fin as well preserved in two of his specimens of *Tribodus* (USP GP/2T-IG and CD 105-P), showing a long basipterygium articulating with the pelvic girdle, and an uncertain number of elongated radials diminishing in length and size towards the posterior of the specimen. In MN 5807V (formerly CD 105-P) a partial left pelvic fin is preserved, including the pelvic girdle, basipterygium, and three proximal radials (Figs. 96, 97).

Although MN 5807V provides little information on the arrangement of the pelvic fin skeleton in *Tribodus* (due to its relative incompleteness), an additional specimen of *Tribodus* (MN uncat.) in which the pelvic fin is better preserved sheds further light on the structure of this skeletal element. In the latter specimen, five proximal radials are preserved, and traces of at least three (and possibly four) additional proximal radials are visible. The anteriormost radial appears to have been broader anteroposteriorly than the other radials, indicating that in *Tribodus limae* (as in many other hybodontoids) the first pelvic radial (or pelvic propterygium) was larger than the succeeding radials. This specimen also shows the outline of the pelvic fin, and part of its covering of dermal denticles. The fin was relatively narrow and elongate.

The pelvic radials were all directed posterolaterally, as in other hybodonts. No distal radials are preserved in either of the two MN specimens. Approximately five proximal radials were attached to the girdle, as in *Hybodus hauffianus* (but unlike *Lissodus cassangensis* and *Hamiltonichthys mapesi*, in which only three radials are attached to the

girdle; Maisey, 1982, 1989). The pelvic metapterygium appears to have supported approximately five radials. This is similar to the state in *Hybodus hauffianus* (with five metapterygial radials in males). In *Hamiltonichthys*, males also have five radials, but females have seven; in *Lissodus cassangensis* males have 6 to 7 radials (Maisey, 1989, 1982) Both MN 5807V and the uncatalogued specimen are here interpreted as females, on the basis of their lack of cephalic spines or spine platforms, and the lack of any evidence of a mixipterygium, basals, or intermediate cartilages extending posteriorly. The pelvic fin of male *Tribodus* remains unknown until further specimens are found. It is probable that the paired pelvic half-girdles were fused medially to form a continuous puboischiadic bar, as in most other hybodontoids (e.g., *Lissodus cassangensis* and *Hybodus hauffianus*) and neoselachians.

FIGURE 96. Posterior of *Tribodus limae*, MN 5807V. Scale bar equals 5 cm.


pdfs
bp
pelvg

FIGURE 97. Closeup showing pelvic fin of *Tribodus limae*, MN 5807V. Scale bar equals 2 cm.


pelvg
r
mt

# CHAPTER 9: AXIAL SKELETON

## RIBS AND VERTEBRAL ELEMENTS

A few calcified pleural (ventral) ribs and neural arches are preserved in AMNH 13957 and AMNH 13961, but their state of preservation is poor. These structures are much better preserved in some of the Brazilian specimens of *Tribodus*, notably MN 5807-V and MN 5808-V, and will be described here based on these latter specimens. In MN 5808-V (Figs. 98, 99), the vertebral column between the occiput and anterior dorsal fin is well preserved in situ, and comprises several elongate elements, each with an enclosed ventral foramen, as well as a few broader, dorsally-located elements in the shape of an inverted triangle (Fig. 99). These triangular elements are positioned between the other vertebral elements just mentioned, and appear to alternate with them. At least two of these triangular elements contain what appear to be dorsal foramina. Based on their morphology and position, it is here considered that these triangular elements may represent intercalary plates (located between the neural arches), which have not yet been identified in any hybodont shark. Intercalary plates are present in modern elasmobranchs (Fig. 100), where they typically contain the dorsal spinal nerve roots, either within their cartilage or at the boundary between the intercalary plate and basidorsal. These alternating elements (neural arches containing ventral foramina, and dorsal intercalary plates) are visible only in the anterior part of the vertebral column of *Tribodus* (between the occiput and anterior dorsal fin spine) and were not seen in the rest of the vertebral column farther posteriorly.

In modern elasmobranchs, the basidorsals contain the ventral spinal nerve roots (Goodrich, 1958; Maisey, 1982), and it is here interpreted that the more elongate elements with more ventrally located foramina represent basidorsals. Enclosed ventral foramina on the neural arch elements do not occur in other hybodonts, such as *Lissodus cassangensis*, *Egertonodus fraasi*, or *Hybodus hauffianus* (Maisey, 1982), and *Tribodus* is the only hybodont known thus far that shows any evidence of them. The triangular cartilages interpreted here as interdorsals were observed only anterior to the anterior dorsal fin, and there is no evidence of interdorsals farther posteriorly. In modern elasmobranchs, the interdorsals contain the dorsal spinal nerve root, and give rise to the vault of the neural arch. They are also generally taller than the basidorsals, and may be overlain by supraneurals.The neural spines form a double series, and as in other hybodonts the left and right sides of the neural arches do not appear to have been fused into a single arch in *Tribodus*. No evidence of diplospondyly was observed in any of the *Tribodus* specimens examined. Maisey (1982) proposed that the neural arch elements typically seen in hybodonts represent interdorsals. However, based on the morphology observed in *Tribodus*, it seems that this may not be the case. The presence of distinct foramina in the ventral parts of the 'neural arch' elements in *Tribodus* suggests that these elements may instead represent basidorsals. The more dorsally positioned “triangular” elements mentioned above could then be interdorsals, with the dorsal nerve foramina either contained within the cartilage of these latter elements or in the space between the interdorsals and basidorsals.

Farther ventrally, and ventral to the notochord, numerous elongate vertebral elements are present in MN 5808-V and MN 5807-V (Figs. 101–105). These are here interpreted

as basiventrals, although each of them contains a dorsally located foramen (Figs. 102, 103) (in neoselachians, the foramen for caudal blood vessels is located on the interventrals or in the space between ventral elements; Goodrich, 1958). In at least one specimen of *Tribodus* (MN 5807-V, formerly CD-P-105), small triangular cartilages that may represent ventral intercalary plates ("interventrals") are additionally present between the basiventral elements (Figs. 102, 103). It is possible that they simply represent broken edges of the basiventrals; however, their regular pattern more strongly suggests interventrals. There is no evidence of foramina on these putative interventrals, although in neoselachians the interventrals carry foramina for the caudal blood vessels (as mentioned above).

The basiventrals carry the calcified ribs (Figs. 104, 105), with which they appear to be fused (or it is possible that the "ribs" are actually elongated basiventrals, as suggested by Maisey, 1982). Ribs of hybodonts are elongate, whereas those of neoselachians are much shorter (Maisey, 1982). Ribs and basiventrals are separate in most modern elasmobranchs, as well as in *Orthacanthus senckenbergianus*, which has basidorsals, interdorsals, basiventrals, and interventrals (Maisey, 1982). According to Maisey (1982), some forms supposedly closely related to *Orthacanthus* (i.e., "*Pleuracanthus*" *parallelus*) have fused ribs and basiventrals and lack basidorsals and interventrals; however, there is some evidence that the latter form could actually be a hybodont (Maisey, 1982). Basiventrals are also found in acanthodians and some placoderms (Maisey, 1982).

Approximately ten ribs are preserved in MN 5807-V, and approximately nine ribs in MN 5808-V, consistent with the pattern of 10-12 ribs previously suggested for hybodonts

(Maisey, 1989). These ribs are continuous with the basidorsals, as in other hybodonts (Maisey, 1982), and are located in a ventral position, consistent with the pleural ribs (= ventral or subperitoneal ribs) described in other hybodonts by Maisey (1982). As described by Maisey (1982) and by Liem et al. (2001), ventral or pleural ribs differ from dorsal or intermuscular ribs in their position within the body. Ventral (= subperitoneal) ribs are located next to the coelom, following the course of the lateral skeletogenous septum. In contrast, dorsal ribs follow the course of the horizontal skeletogenous septum, between the epaxial and hypaxial muscle masses. During ontogeny, ribs typically form at the location of one of the skeletogenous septa, either the horizontal (dorsal or intermuscular ribs) or the lateral skeletogenous septum (ventral or pleural ribs), and typically form where myosepta intersect one of these skeletogenous septa (Liem et al., 2001).

Modern elasmobranchs have intermuscular ribs, in which the ribs and basiventrals are separate (unlike the condition in hybodonts). However, the ribs of modern elasmobranchs attach to their vertebral centra far ventrally on basapophyses (which are considered to be serially homologous with the bases of the hemal arches; Liem et al., 2001), the same attachment site as for ventral ribs in actinopterygians, suggesting that their intermuscular ribs may be secondarily derived from ventral ribs. Ventral ribs are found in hybodonts, and also in *Tristychius*, *Onychoselache*, and xenacanths. Extant chimaeroids lack ribs (possibly secondarily), and ribs are also unknown in placoderms and acanthodians, although these forms do have basiventrals. However, ventral ribs are found in some actinopterygians, and also in dipnoans. There is some evidence that ventral, or 'pleural,' ribs may be primitive for gnathostomes (Maisey, 1982; Devillers, 1954; Rosen et al.,

1981), in which case ventral ribs in hybodonts and Paleozoic sharks could be a conserved feature, representing a primitive condition of gnathostomes.

## UNPAIRED FINS

### Dorsal Fins

Like other hybodonts, *Tribodus limae* had two dorsal fins, each with a large anterior fin spine and triangular basal cartilage. Among the AMNH specimens, the dorsal fins are preserved in AMNH 13957, 13958, and 13961. Both the anterior and posterior dorsal fin spines are preserved in situ in MN 5807-V, although the fin spines are poorly preserved in this specimen. In AMNH 13961, only the lower portion of the anterior fin spine (with the entire proximal portion of the spine, and the first inch of the enameled distal portion) in left lateral view is preserved, with its associated basal cartilage. AMNH 13957 shows most of the anterior dorsal fin spine and basal plate in situ, but the anterior fin spine is embedded in matrix so that only its right lateral side is visible, and its proximal end is broken. The posterior dorsal fin is also present in this specimen, comprising the posterior fin spine and basal plate, but the fin is tilted anteriorly by approximately 45 degrees away from its original life position. Based on the relatively small size of the dorsal fin spines in AMNH 13957 compared to the other specimens, this individual may have been a juvenile. The dorsal fin spines are best preserved in AMNH 13958, which consists of an anterior fin spine in almost its entirety and twisted upwards to show the posterior denticles, and the proximal part of the posterior fin spine embedded in matrix. The posterior basal plate is preserved, although the anterior one is not. MN 5607-V clearly shows the differences in proportion between the anterior and posterior dorsal fins (Figs. 10, 106, 107): the posterior fin basal plate (Fig. 107) is much larger dorsoventrally than

its anterior counterpart (Fig. 106), and consequently carries the posterior fin spine at a much more obtuse angle than the anterior fin spine. The anterior fin spine thus appears backwardly tilted, whereas the posterior fin spine is held more vertically. This difference between the anterior and posterior dorsal fins is also found in numerous other hybodontiforms, as well as other early selachians such as *Ctenacanthus costellatus* (Moy-Thomas, 1936; Coates and Gess, 2007).

Due to the state of preservation, there is no clear evidence from any of the AMNH specimens whether or not any radial elements were present on either the anterior or posterior dorsal fin basal plates. Likewise, there is no preserved evidence of any ceratotrichia in the AMNH specimens (or in any specimens of Brito, 1992, or Brito and Ferreira, 1989). Additionally, although none of the AMNH specimens have both dorsal fins preserved in situ, the wider angle between the basal plate and fin spine in the posterior dorsal fin (as compared to the anterior dorsal fin) provides evidence that the posterior dorsal fin was held at a more vertical angle to the body than the anterior fin. This corresponds to the condition seen in Brito's (1992: figure 1) specimen, in which the two fins are preserved in situ. Many other hybodonts also share this feature, and Maisey (1984, 1989) suggests that it may be plesiomorphic for elasmobranchs in general.

In both AMNH 13961 and AMNH 13957, the basal plate of the anterior dorsal fin spine contacts the distal end of the pectoral girdle, which may reflect its position in life. In AMNH 13957, the better-preserved of the two, the elongated tip of the scapular process reaches as far dorsally as the middle of the basal plate. Brito (1992) noted that the anteroventral angle of both dorsal fin basal plates came in contact with the neural arches, although due to preservation this could not be observed in any of the AMNH specimens.

**Anal and Caudal Fins**

There is no evidence of an anal fin in any of the AMNH specimens of *Tribodus limae*, and none has been observed or described as present in any of the Brazilian specimens (Brito and Ferreira, 1989; Brito, 1992). However, presence of an anal fin may be expected in *Tribodus*, as this structure is known in other hybodonts including *Egertonodus fraasi* (Maisey, 1986), *Hybodus hauffianus* (Koken, 1907; Maisey, 1982), *Lissodus africanus*, *Hamiltonichthys* (Maisey, 1989), *Onychoselache* (Dick and Maisey, 1980), and *Tristychius* (Dick, 1978). Likewise, the caudal fin is missing from all of the AMNH specimens, and apparently all of the Brazilian specimens as well (Brito and Ferreira, 1989; Brito, 1992).

FIGURE 98. Closeup of anterior part of MN 5808V showing anterior vertebrae in relation to other skeletal elements. Scale bar equals 5 cm.


0
1
2
3
4
5

FIGURE 99. Anterior vertebrae of *Tribodus limae*, MN 5808V. Scale bar in millimeters.

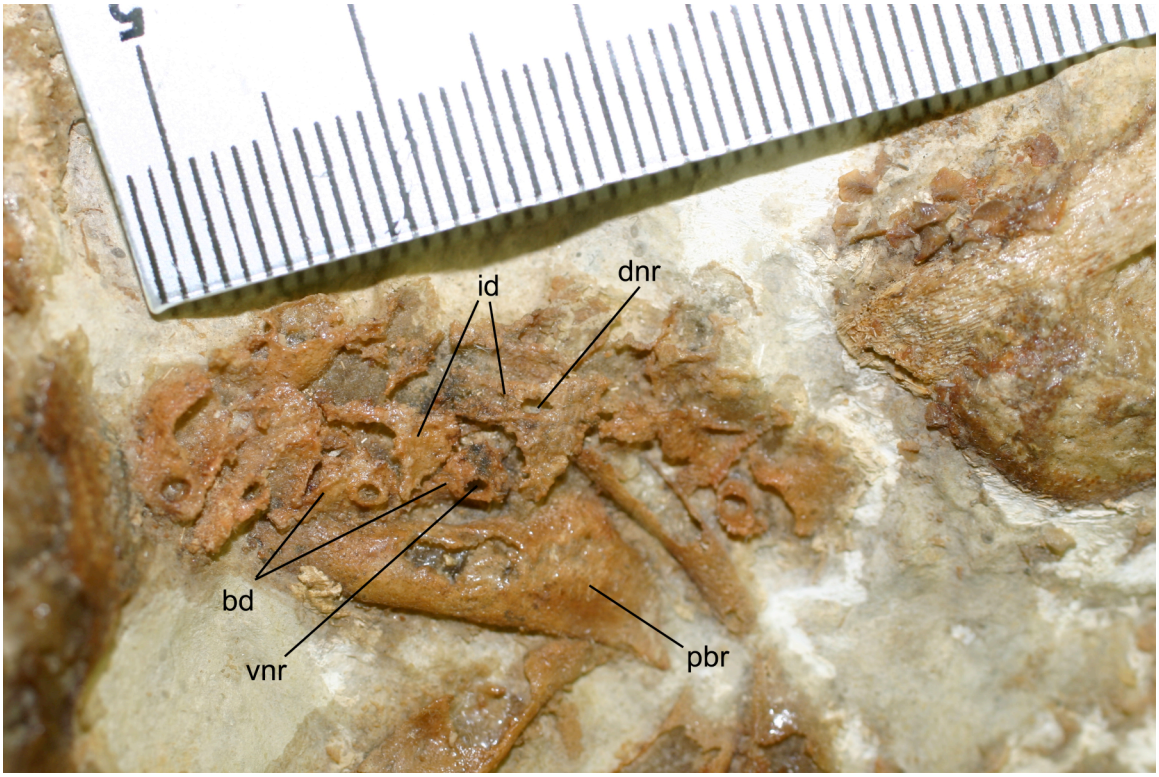

id
dnr
bd
vnr
pbr

FIGURE 100. Morphology of the anterior part of the vertebral column of various extant elasmobranchs in right medial view, after Shirai (1992). A, *Cirrhigaleus barbifer* (an orbitostylic shark); B, *Heterodontus zebra* (a galeomorph); C, *Torpedo tokionis* (a batoid); D, *Squatina japonica* (an orbitostylic shark); E, *Pristiophorus japonicus* (an orbitostylic shark). Scale bars equal 10 mm.

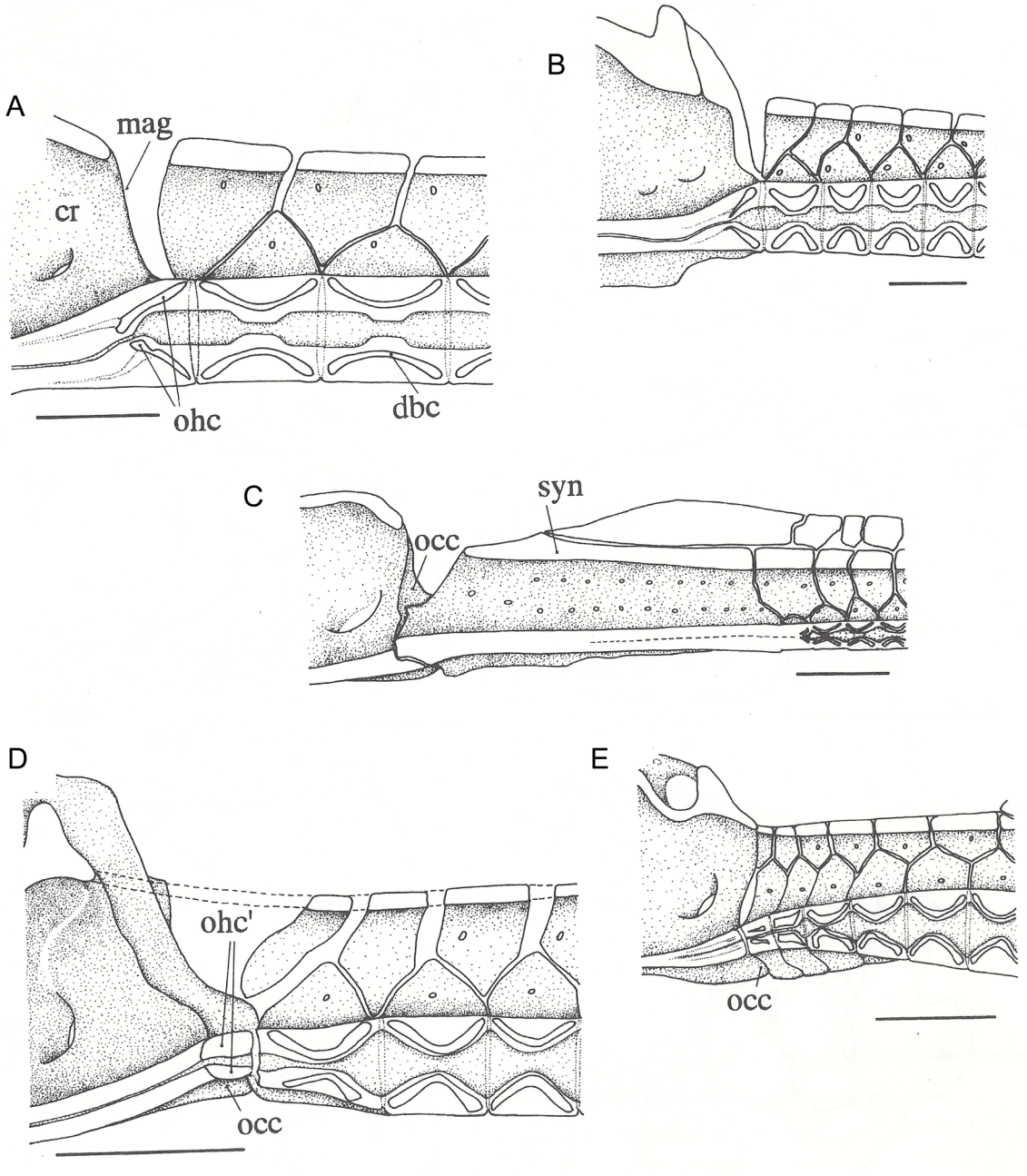

A
mag
cr
ohc
dbc
B
C
syn
occ
D
ohc'
occ
E
occ

FIGURE 101. Trunk region of *Tribodus limae*, MN 5807V. Scale bar equals 5 cm.


MN5807-V
0 1 2 3 4 5

FIGURE 102. Basiventrals of *Tribodus limae*, MN 5807V. Scale bar in millimeter increments.

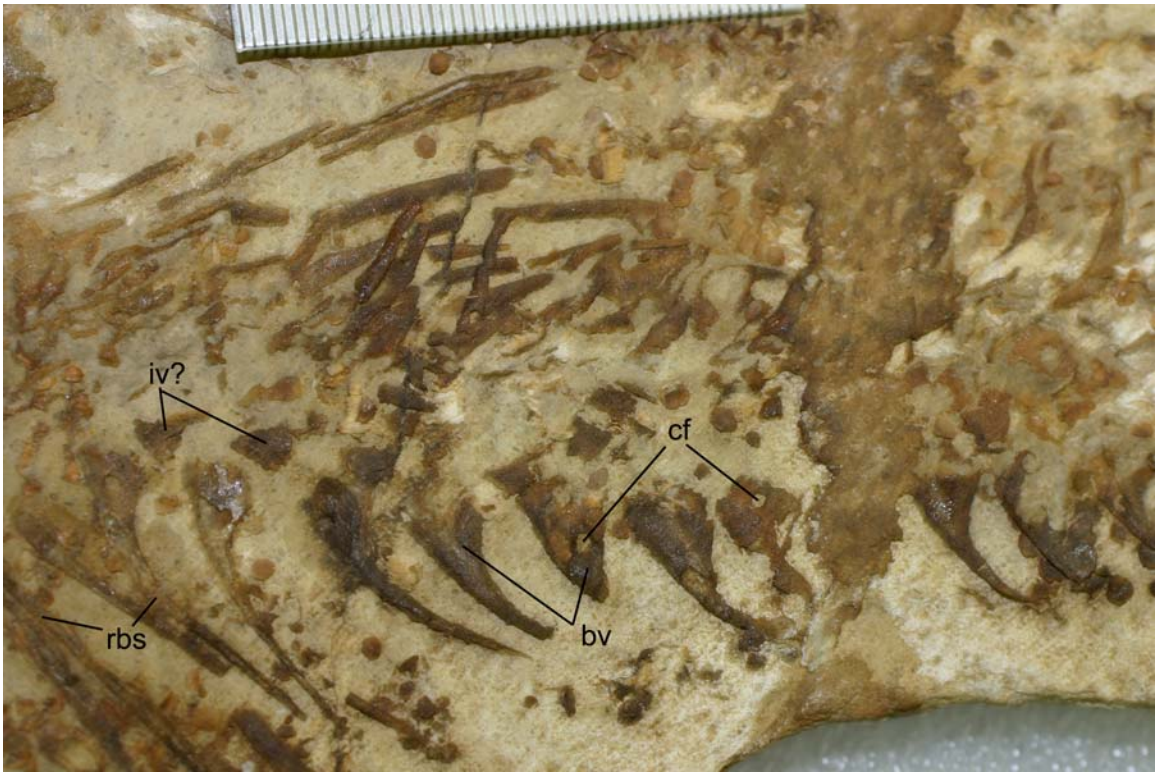

iv?
cf
rbs
bv

FIGURE 103. Closeup of basiventrals, MN 5807V, in Fig.102. Scale bar in millimeter increments.

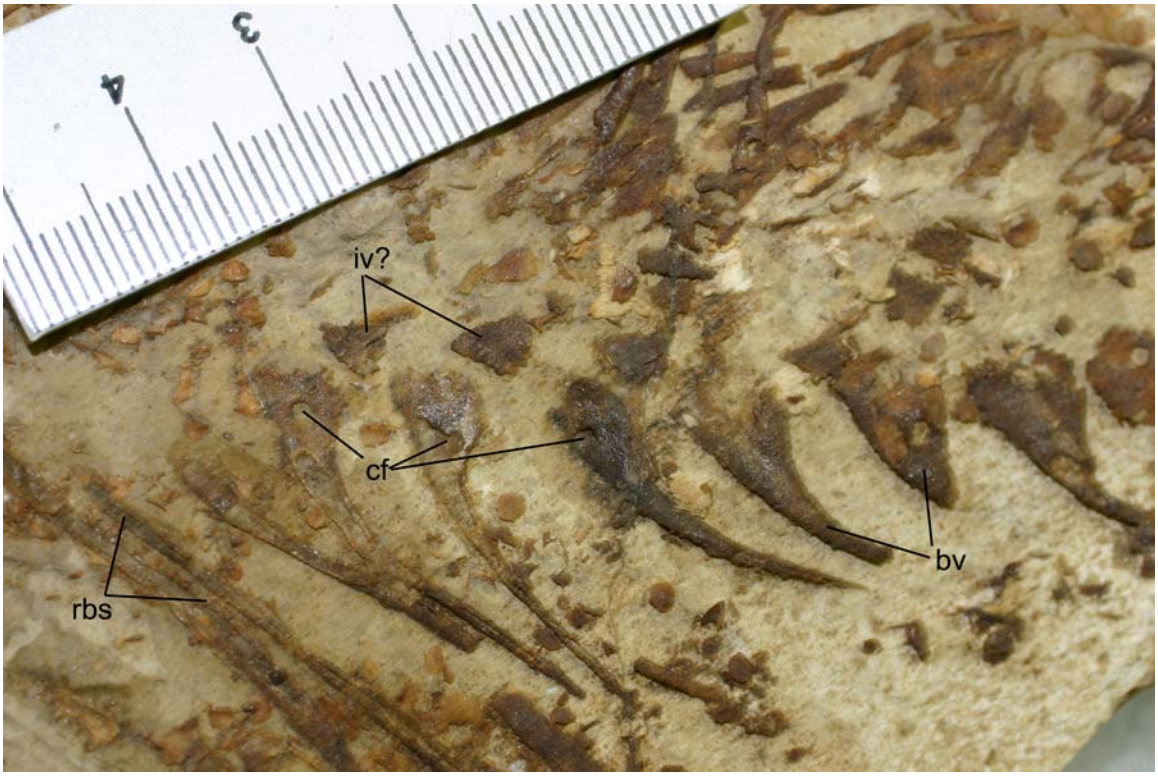

iv?
cf
bv
rbs

FIGURE 104. *Tribodus limae*, MN 5807V, closeup showing left pectoral fin and ventral vertebral elements, including calcified pleural ribs. Scale bar in centimeters with millimeter increments.


sc
rbs
bv
mt

FIGURE 105. *Tribodus limae*, MN 5808V, closeup showing left pectoral skeleton and calcified pleural ribs. Scale bar in centimeters, with millimeter increments.

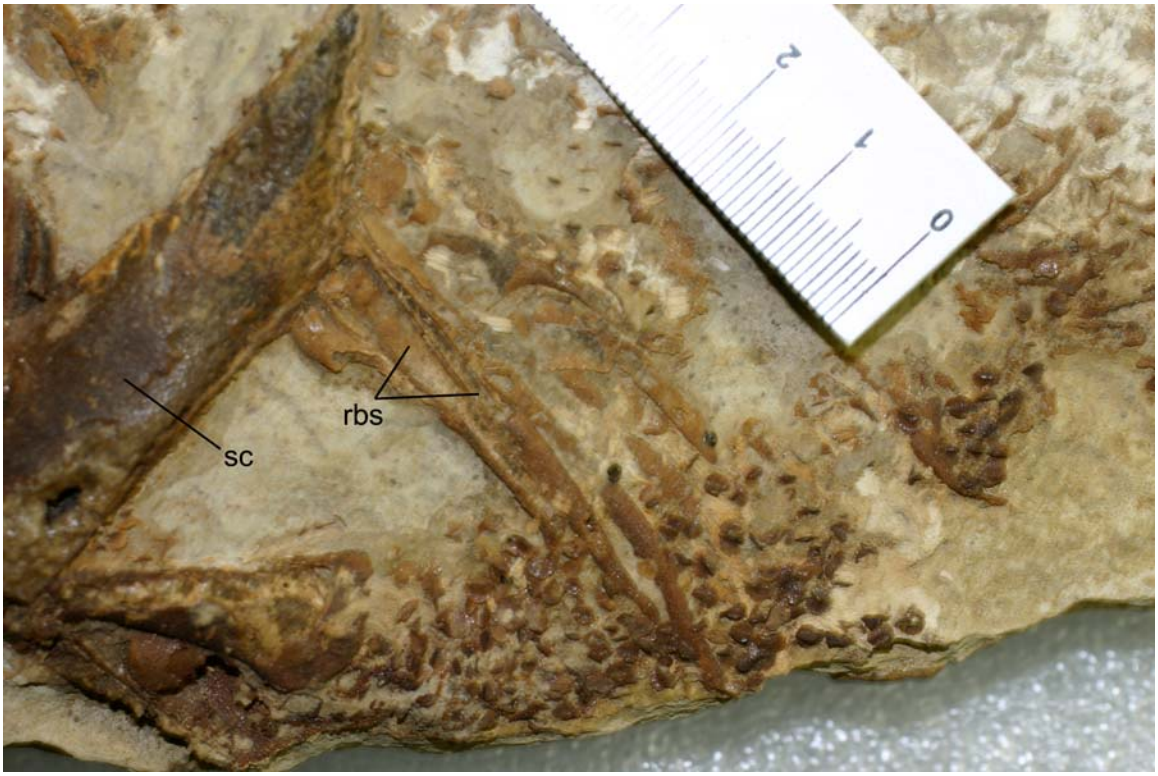

rbs
sc

FIGURE 106. Anterior dorsal fin of *Tribodus limae*, MN 5807V. Scale bar equals 5 cm.


MN 5807 -V
adfs
bp
r
0
1
2
3
4
5

FIGURE 107. Posterior dorsal fin of *Tribodus limae*, MN 5807V. Scale bar equals 5 cm.


pdfs
bp

# CHAPTER 10: DERMAL SKELETON

## DENTITION

Teeth of *Tribodus limae* are best preserved in AMNH 13961 and UERJ-PMB-40. The teeth in AMNH 13961 (Fig. 55) are somewhat jumbled and are not preserved entirely in situ, but their anteroposterior arrangement appears to have been retained. The teeth are hexagonal in shape and flattened occlusally, and all of them appear similar in size. They were apparently arranged adjacent to one another in an imbricated pattern, forming a flat pavement dentition on the anteromesial surface of the palatoquadrate. The dentition displays weak monognathic heterodonty, in which two or more different tooth morphologies occur in the same jaw (Brito and Ferreira, 1989; Brito, 1992). Evidence of dignathic heterodonty (in which tooth morphology differs between upper and lower jaws) is less clear due to the poor preservation of the dentitions.

The teeth are similar to those described in *Tribodus limae* (Brito and Ferreira, 1989; Brito, 1992). Some teeth retain their original enameloid, visible on the surface as a thin beige-white porcelain-like veneer. The sides of the teeth bear small striae, but the crown is smooth occlusally except for a single central indentation.

As described by Brito and Ferreira (1989), the posterolateral teeth are taller than they are broad, with a convex labial crest in the crown that overhangs the root, and a concave indent in lingual view. The posterolateral teeth have a crown that is rhomboid in shape in anterior view and approximately twice the height of the root. Tooth crowns are approximately hexagonal in occlusal view, at least in the more posterolateral teeth. Overall, these teeth are approximately as broad mediolaterally as they are tall. The posterolateral teeth expand in width apically. A row of small pores is present on all sides

of each tooth at the boundary between crown and root. Numerous small striae are visible in the enameloid surface of the tooth in anterior and posterior views, increasing in strength from the base of the crown toward the apex (unlike in *Tribodus aschersoni*, in which the ornamentation is stronger towards the crown base: Werner, 1989). No evidence of a pulp cavity was observed in any of the teeth examined.

The tooth base is spongy in appearance and composed of irregular osteodentine, with numerous small pores. Several larger nutritive foramina are visible near the root base, resembling the "foramens individualisés" of Casier (1947) which may be a primitive feature among hybodonts and neoselachians (Maisey, 1987). Brito (1992) also noted the presence of these foramina in teeth of *Tribodus limae*. The foramina are arranged labio-lingually and do not reach the root base (unlike the hemiaulacorhize, holaulacorhize, or polyaulacorhize patterns (sensu Cappetta, 1987) of most Recent neoselachians). Teeth of *T. limae* are consistent with Maisey's (1987) emended definition of anaulacorhize teeth (considered characteristic of hybodonts), which have a horizontal pore system but may or may not have larger "foramens individualisés." In parasagittal section the tooth interior is composed of porous osteodentine arranged in vertical columns, as in the columnar osteodentine reported in *Acrodus* and *Asteracanthus* (Maisey et al., 2004; Brito, 1992).

External to this osteodentine layer are two comparatively much thinner and more compact layers, consistent with the double layer of single crystallite enameloid (SCE) reported by Cuny et al. (2001) in *Acrodus* and *Hybodus* teeth. The average combined thickness of the two enameloid layers is approximately 60 μm on the sides of the tooth, but reaches approximately 140 μm on its occlusal surface. The outermost layer of SCE in *Tribodus* is very thin and compact (corresponding to the "outer compact layer" of Cuny

et al., 2001), whereas the underlying layer is thicker and the crystallites of apatite appear gathered together in bundles perpendicular to the tooth surface (corresponding to the "inner bundled layer" of Cuny et al., 2001, but in *Tribodus* this layer is thicker, forming approximately two-thirds of the total thickness of the enameloid surface). The border between the two enameloid layers is clearly defined, as is the border of the inner "bundled" layer with the underlying osteodentine. There is no indication in *Tribodus* of the "triple-layered enameloid" found in modern neoselachian sharks, which comprises an outer "shiny layer" of enameloid (SLE), an inner "parallel-fibred" or "parallel-bundled" layer (PFE or PBE), and an inner "tangled-fibred" or "tangled-bundled" layer (TFE or TBE) (Reif, 1973; Cuny et al., 2001; Gillis and Donoghue; 2007). The double-layered SCE of hybodonts including *Tribodus* differs from the single-layered SCE described in Paleozoic chondrichthyans (e.g., *Cladoselache*; *Ctenacanthus*; *Akmonistion*; some xenacanths; Gillis and Donoghue, 2007; Reif, 1973).

**Comparison with teeth of other species of *Tribodus***

The teeth of *Tribodus limae*, based on the new AMNH material and on previous descriptions (Brito and Ferreira, 1989; Brito, 1992), differ from those described for other species of *Tribodus* as follows: teeth of *T. limae* differ from those of *T. tunisiensis* (Cuny et al., 2004) in having ornamentation of small ridges on the lingual and labial sides that is most visible toward the crown apex (rather than at the base as in *T. tunisiensis*), a difference that has not been noted previously. Although the crown in both species can be hexagonal in apical view, the tooth root in *T. limae* is in some cases the same height as the crown, or even taller (as opposed to less than half the height of the crown in *T.*

*tunisiensis*; Brito, 1992; Cuny et al., 2004). The tooth crown in *T. limae* has a short central groove in occlusal view, whereas in *T. tunisiensis* the teeth lack ornamentation apically. Cuny et al. (2004) described teeth of *T. tunisiensis* as different from those of *T. limae* in that the former lack the baso-central enlarged foramina (="nutritive foramina") described by Brito (1992), although these authors pointed out that this may be an artifact of preservation. Cuny et al. (2004) also noted a less-developed root in *T. tunisiensis* than in *T. limae*; a lack in *T. tunisiensis* of a "labially displaced longitudinal crest" (="labial crest" of Brito, 1992) and ridges on the posterior teeth; and the lack of 'pseudo-cusps' on the apical surface of the teeth (observed in juveniles of *T. tunisiensis*).

Teeth of *Tribodus limae* and *T. tunisiensis* differ from those of *Tribodus aschersoni* (formerly *Aegyptobatus kuehnei* Werner, 1989) in that those of *T. limae* lack the lingual basally located row of specialized foramina, the highly medio-distally elongated shape, and the specialized ornamentation visible in occlusal view (Werner, 1989; Cuny et al., 2004). *Tribodus limae* has labial and lingual ornamentation of ridges that is more visible toward the apex, whereas in *T. tunisiensis* and *T. aschersoni* the ridges are more visible on the basal part of the crown. All three species have flattened teeth that are hexagonal in shape. In *T. aschersoni*, like *T. limae* but unlike *T. tunisiensis*, the root can attain a height that is greater than half the crown.

**Cephalic Spines**

Cephalic spines of *Tribodus limae* have not previously been described or illustrated in any of the published literature (e.g., Brito and Ferreira, 1989; Brito, 1992), and this represents the first description of the cephalic spines in this taxon (Figs. 109–112). Spines

are preserved in AMNH 13957 (Figs. 111, 112A–C) and 13959 (Figs. 109, 112D–E), and in UERJ-PMB-40. Cephalic spines of *Tribodus limae* are unicuspid, with a single, large, posteriorly recurved principal cusp and no accessory cusps (Fig. 109–112). In AMNH FF 13959 (an exceptionally well-preserved right cephalic spine associated with a fragmented cranium and partial scapulocoracoid), the spine base is constricted and triradiate, with paired anterior lobes and a narrow posterior lobe (Figs. 109, 112D–E: lm, ll, lp). The cephalic spine base is also well preserved in UERJ-PMB-40, although the spine cusp is missing (Fig. 110). When viewed from above, the spine base can best be described as "anchor-shaped." All three basal lobes are of approximately equal length and are slender and elongate in shape. The mesial (Fig. 110, lm) and lateral (Fig. 110, ll) lobes taper distally, whereas the distal part of the posterior lobe (Fig. 110, lp) first narrows, then expands into a broader rounded distal tip. The mesial and lateral lobes are posteriorly recurved (forming the mesial marginal indentation, mim; and the lateral marginal indentation, mil, respectively), so that the entire spine when viewed from above (e.g., lateral view, if the spine were in situ) appears nearly symmetrical on both sides. The base of the cephalic spine is composed of a porous, spongy tissue, presumably osteodentine, whereas the cusp is covered with a thin, glossy layer of enameloid, as in most other hybodonts (Maisey, 1982, 1983).

The cephalic spine cusp, or crown (Figs. 110, 111, 112: c) in *Tribodus* is slender but not acuminate, in that it shows a distal barb apically (Fig. 111: ba). The proximal part of the cusp is strongly ornamented with a series of vertical ridges anteriorly, some of which bifurcate towards the cusp base. These ridges converge approximately halfway up the spine cusp, where they join a sharp, narrow ridge, located slightly off-center, which

extends from here to the spine apex. The posterior and latero-distal sides of the spine cusp are unornamented except for a few faint parallel ridges on the posterior proximal end of the cusp, just above the spine base. In AMNH FF 13957, a left cephalic spine associated with a nearly complete fish, most of the spine base is lacking, showing the presence of a large pulp cavity in the interior of the cusp. In side view, all three lobes of the spine base slope downward posteroventrally. In *Tribodus*, the posterior lobe of the spine base extends slightly farther posteriorly than the spine apex. The distal part of the cusp is approximately horizontal in side view.

As originally preserved (prior to preparation), the cephalic spine of AMNH FF 13959 was located nearly in situ, allowing its approximate life position to be determined (Fig. 109). This specimen shows that the cephalic spine in *Tribodus limae* was located on the lateral surface of the otic region just behind the postorbital process, in a broad, rectangular, concave platform (best preserved in AMNH FF 13958). Its location most closely approximates that of the cephalic spines located above the lateral otic process in *Egertonodus basanus*, *Egertonodus fraasi*, *Hybodus hauffianus*, and *H. delabechei*, although in *Tribodus* the spine platform is located much farther ventrally, possibly representing a ventral elongation of the lateral otic process. There is no evidence of more than a single pair of cephalic spines in *Tribodus*, as is also the case in *Egertonodus basanus*.

Cephalic spines of *Tribodus limae* differ from those of *Hybodus*, *Egertonodus*, *Acrodus*, and *Asteracanthus* (e.g., genera having "*Sphenonchus*"-type cephalic spines) in that the latter taxa have a much thicker and more robust spine base, in which the lobes are much less constricted. However, *Tribodus* cephalic spines are similar to spines of these

taxa in having a barbed tip, and a dorsal, mesial, lateral, and posterior crest (see Maisey, 1982, 1987). They also differ in that the spine base in *Tribodus* is more bilaterally symmetrical than it is in these taxa. *Tribodus* cephalic spines are morphologically very different from those of *Hamiltonichthys mapesi*, which has an unconstricted spine base, multiple accessory cusps, and no ornamentation (Maisey, 1989). They differ considerably from cephalic spines of *Onychoselache*, which have more than one principal cusp and a broad, unconstricted spine base.

**Dorsal Fin Spines**

As recorded originally by Brito and Ferreira (1989), dorsal fin spines of *Tribodus limae* are elongate in shape and slightly recurved posteriorly. Brito and Ferreira (1989) described *Tribodus* fin spines as having two rows of alternating posterior denticles; however, in AMNH 13958 (Fig. 113) (the only specimen showing the posterior surface of the spine) only the more distal denticles appear to form two alternating rows, with the rest forming a single row along the midline. According to Maisey (1978), hybodontiform fin spines typically have posterior denticles in two series. The denticles extend to the distal tip of the spine. On close inspection, the distal-most denticles (extending approximately 23.0 mm from the spine tip) can be seen to alternate, although the spacing between the two rows is close enough to give the superficial appearance of a single row. There is a single row of denticles extending a further 23.1 mm proximally, after which the more proximal denticles are not preserved, although on the posteriormost part of the spine the raised area where the denticles presumably attached widens proximally before

terminating at the level of the posterior closure of the finspine. The denticles increase in size proximally from the spine apex.

Both fin spines bear a typical ‘hybodont’ pattern of ornamentation, consisting of a series of smoothly enameled, continuous parallel ribs (costae) extending proximo-distally along the length of the spine. As originally noted by Brito and Ferreira (1989), the ribs in *Tribodus* differ morphologically from those of *Asteracanthus* (in which a tuberculate ornamentation is present), but are similar to those of *Hybodus* and *Acrodus*. They differ from fin spines of *Tristychius* and *Onychoselache*, in which the denticle rows are positioned laterally (rather than along the midline), and the spine in cross-sectional view is concave posteriorly (both features that are also present in ctenacanths). Also, in *Onychoselache* only four ribs are present on each side of the dorsal fin spine, with a single rib positioned anteriorly. Fin spines with only a small number of ribs also occur in *Hamiltonichthys* (with only two or three lateral ribs and a single anterior rib). Coates and Gess (2007:1439) noted that ‘finspines with numerous bifurcating or intercalating costae or tubercle rows' are characteristic of hybodontoids exclusive of *Hamiltonichthys*, *Lissodus*, and *Lonchidion*. The presence of numerous costae (some of which are bifurcating) in *Tribodus* is a further similarity with this more derived group of hybodontoids.

Fin spines of *Tribodus* have approximately 8-14 ribs on each lateral side (8 in AMNH 13957; 11 in AMNH 13961; 14 in AMNH 13958), a range similar to the 8-10 ribs per lateral face recorded by Brito and Ferreira (1989) for *Tribodus*. There is a small anterior keel, in the form of a single rib at the midline (equal in size to, or only slightly larger in diameter than, the lateral ribs). The ornamentation begins several centimeters above the

proximal end of the fin spine, at a point that marks the boundary between the distal, smooth-textured portion of the spine and a proximal, rougher-textured, unornamented region. This boundary likely represents the point where the fin spine emerged from the body wall.

Fin spines of *Tribodus limae* were hollow (as evidenced by AMNH 13958), containing a central pulp cavity. The dorsal fin spines are wedge-shaped in cross-section, with a rounded arc anteriorly, and a broader, flatter (although still convexly curved) posterior surface. Length of the anterior dorsal fin spine is 157.5 mm in AMNH 13957, and 216.2 mm in AMNH 13958. Brito and Ferreira (1989) recorded a length of approximately 12.5 cm in their specimens.

**Dermal Denticles**

Dermal denticles are well preserved in AMNH 13957 and 13958. Dermal denticles of *Tribodus limae* have a sharp, laterally compressed, posteriorly recurved spine or "thorn" apically, increasing in height towards the posterior. The denticle base is rounded in shape with an irregular lateral margin, and has an ornamentation of ridges extending from the spine base to the apex, on which the ridges are curved posteriorly. The overall shape and morphology of the dermal denticles is in agreement with Brito and Ferreira's (1989) and Brito's (1992) descriptions of denticles of *Tribodus* as large and thorn-like in shape, with a size of approximately 2.5-3.0 mm (2.3 to 3.1 mm in the AMNH specimens).

Based on AMNH 13957, in which the shagreen of dermal denticles is preserved most extensively, these scales appear to have covered the entire surface of the body, although few are preserved from the head region in the AMNH specimens. Brito and Ferreira

(1989) described the denticles of *T. limae* as non-growing, as in *Egertonodus basanus* and *Egertonodus fraasi* (Maisey, 1982, 1983, 1987), but much larger in size than those of other Mesozoic hybodonts. Each denticle appears to have formed a distinct unit, and as in *Acrodus anningiae* and *Egertonodus basanus* (Woodward, 1889; Maisey, 1982) none of them appear to have been fused together to form compound scales. The medial (ventral) surface of the denticle base is flat. Like other hybodonts, the scales lack a pronounced neck; the absence of this feature is one of the characteristics (together with presence of a high-pointed cusp and ridged conical crown) proposed by Maisey (1982) as potential hybodont synapomorphies.

When viewed under SEM (Fig. 114), the denticle base (Fig. 114C) is observed to be composed of a porous material resembling osteodentine. There is no visible pulp cavity, and the denticle base is solid and continuous. The edges of the denticle base are rounded but irregular, with a crenulated appearance marginally. There is a clearly visible boundary between the denticle crest and the base, with the crest covered with a much smoother, thinner material. The lateral ribs extend onto the denticle base, where they are more pronounced, forming rounded ridges separated by indented valleys. On the upper part of the denticle base, near the boundary with the crest, several specimens show a row of small, regularly spaced foramina (Fig. 114D, E) (larger than the pores elsewhere on the base, which are much more minute) located between the ridges of ornamentation.

FIGURE 108. Scanning electron microscope photographs of *Tribodus limae* teeth. A, isolated tooth from AMNH 13961, overview. B, Closeup of (A) showing ornamentation of parallel vertical ridges on lateral side of tooth near occlusal surface. C-J, teeth from AMNH 13961, dentition preserved approximately in situ. C, overview of hexagonal tooth showing enameloid surface. D-F, broken teeth showing interior structure formed by columnar osteodentine. D, lateral view; E, occlusal view; F, dorsolateral view, approximately x41. G-H, closeup of (F) showing cross sections of enameloid surface layer. I-J, tooth roots showing vascular canals in lateral (I) and ventral (J) views.

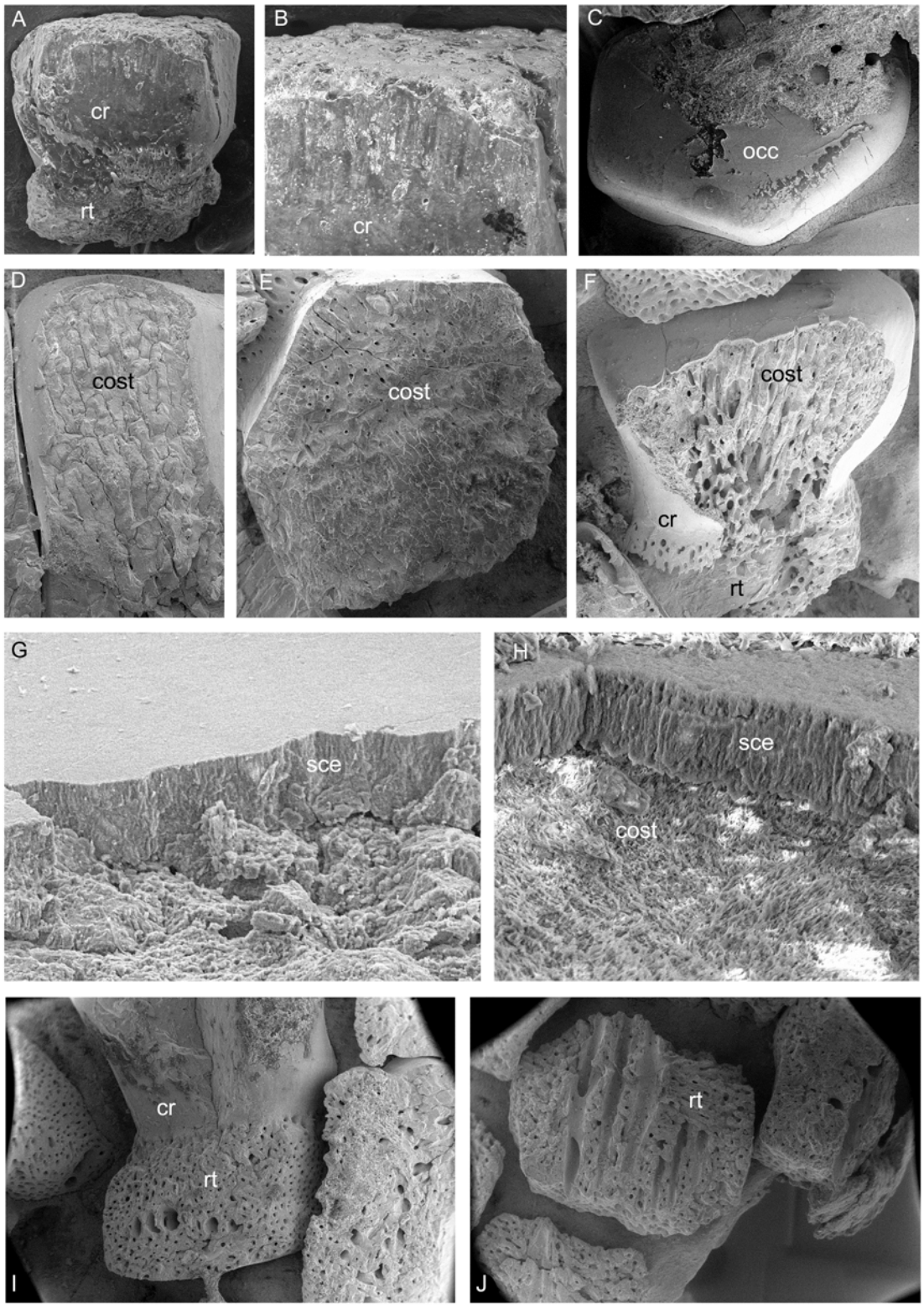

A
cr
rt
B
cr
C
occ
D
cost
E
cost
F
cost
cr
rt
G
sce
H
sce
cost
I
cr
rt
J
rt

FIGURE 109. Close-up of the head region of *Tribodus limae* AMNH 13959, showing right cephalic spine in-situ, after acid preparation. Anterior to the left. Scale bar is 1.5 cm.

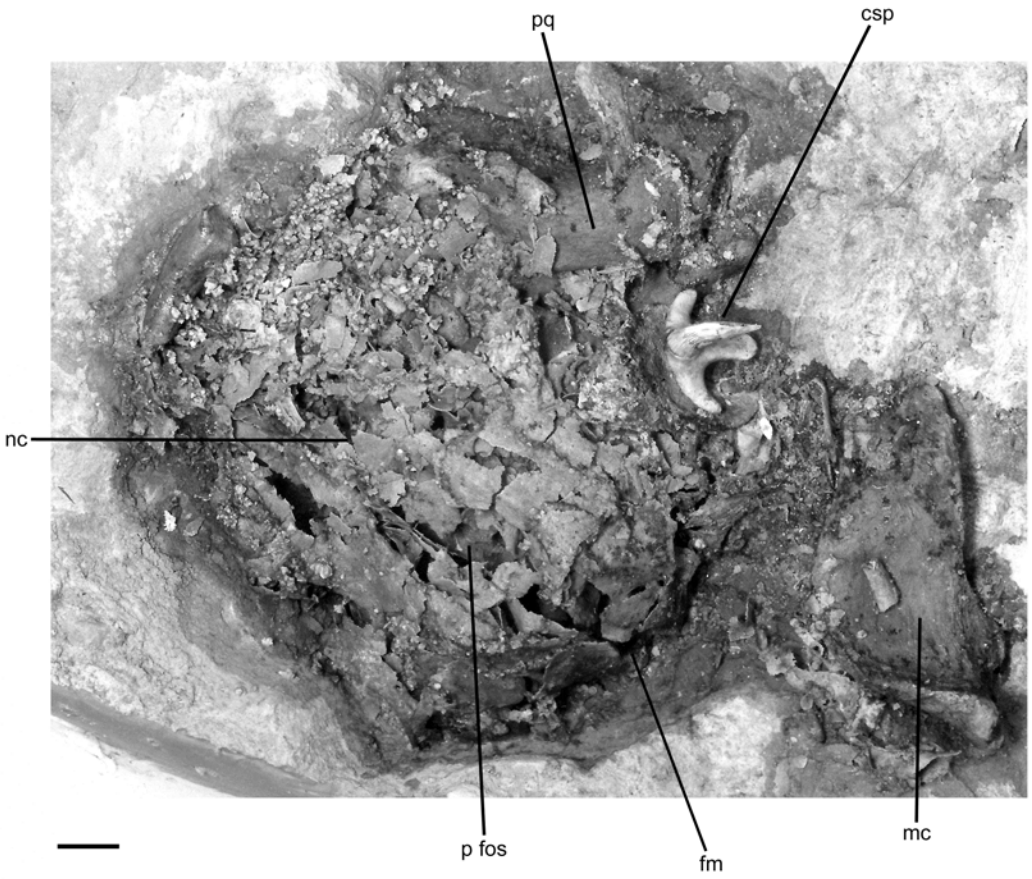

pq
csp
nc
p fos
fm
mc

FIGURE 110. (A) top, (B) bottom, and (C) lateral views of left cephalic spine of *Tribodus limae* UERJ-PMB-40. Scale bar is 1 cm.

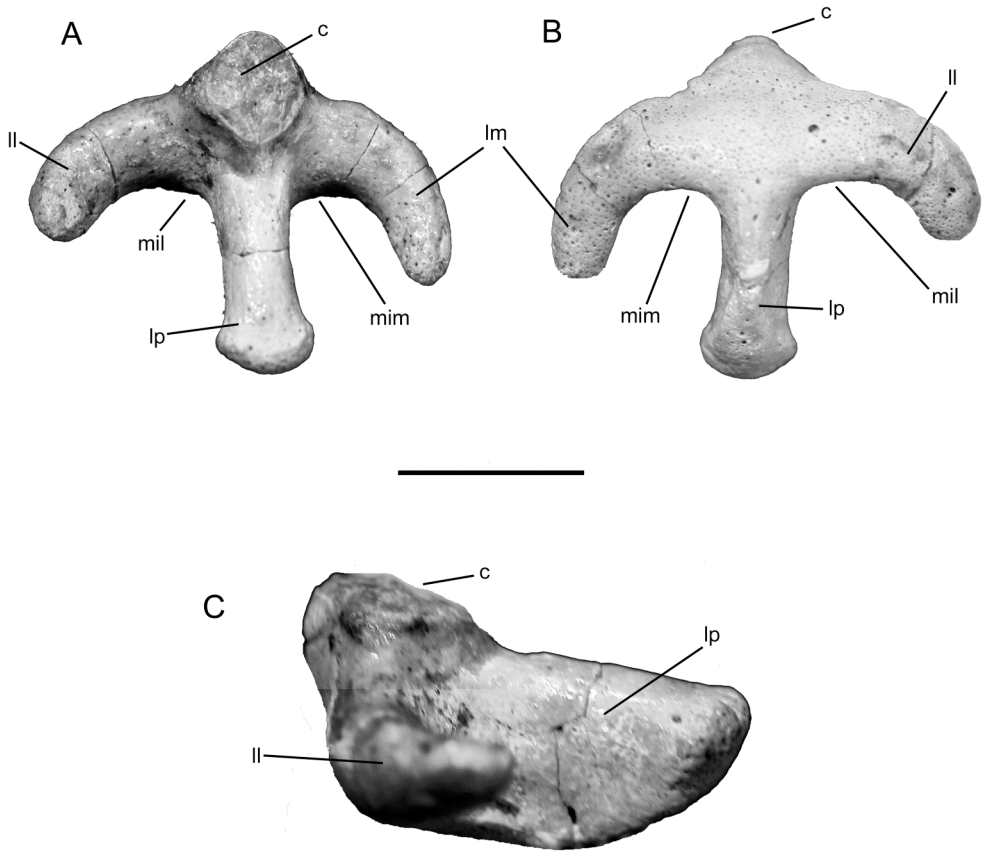

A
c
ll
mil
mim
lp
B
c
ll
lm
mim
lp
mil
C
c
lp
ll

FIGURE 111. SEM of *Tribodus limae* cephalic spine, AMNH 13959. Scale bar is 1 mm.

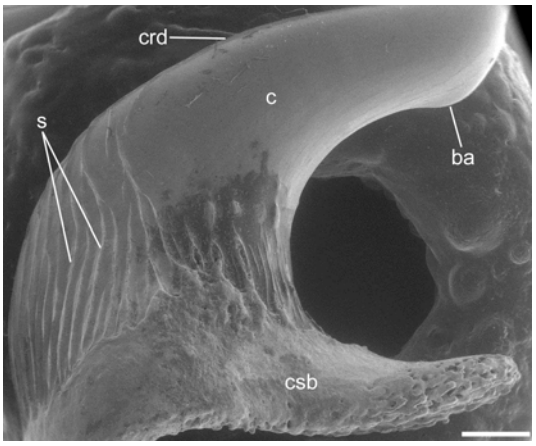

crd
c
s
ba
csb

FIGURE 112. *Tribodus limae* cephalic spines. A–C, AMNH 13957, left cephalic spine. A, lateral; B, dorsal; C, mesial views. D–E, AMNH 13959, right cephalic spine. D, mesial; E, lateral views. Scale bar is 1 cm.

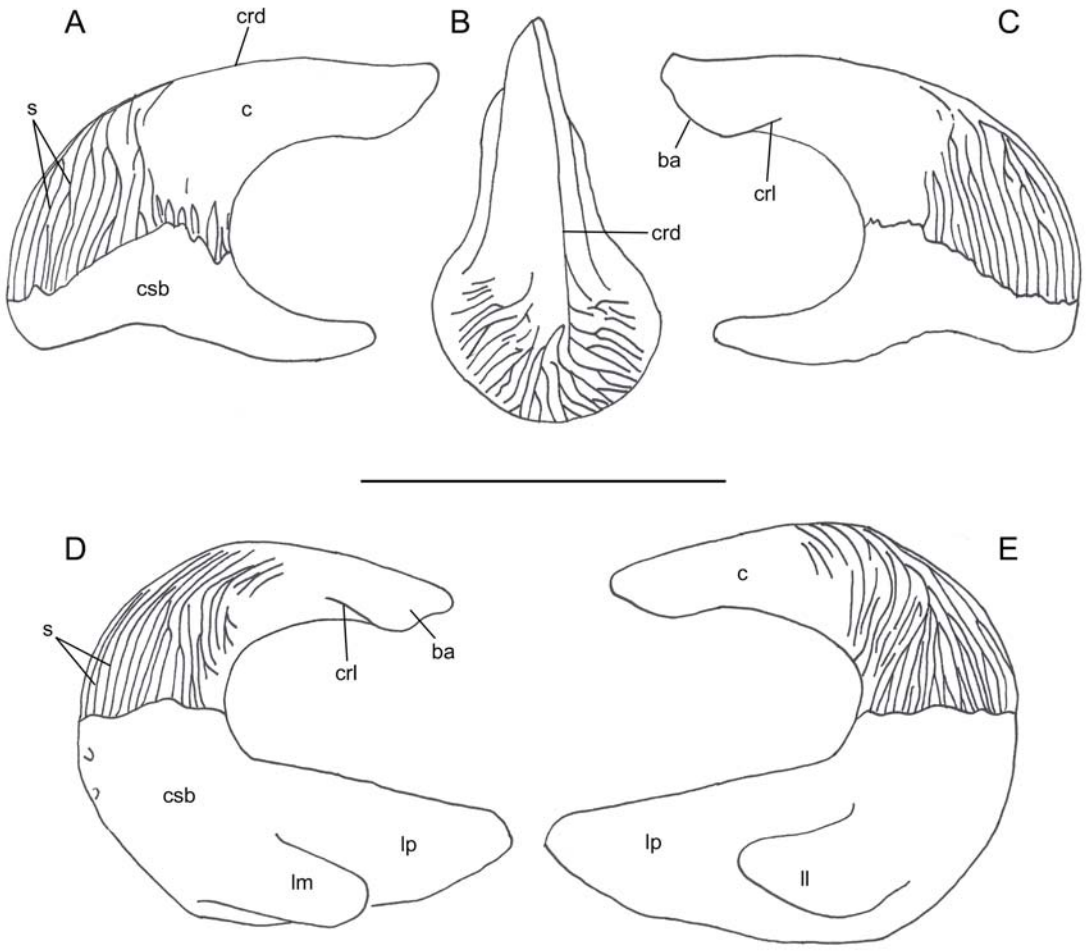

A
crd
s
c
csb
B
crd
C
ba
crl
D
s
crl
ba
csb
lp
lm
E
c
lp
ll

FIGURE 113. Dorsal fin spines of *Tribodus limae*, AMNH 13958. A, overview of specimen; B, closeup showing proximal portion of posterior dorsal fin spine and basal plate; C, proximal part of anterior dorsal fin spine; D, distal part of anterior dorsal fin spine showing single row of posterior retrorse denticles. Scale bars in B–C equal two centimeters.

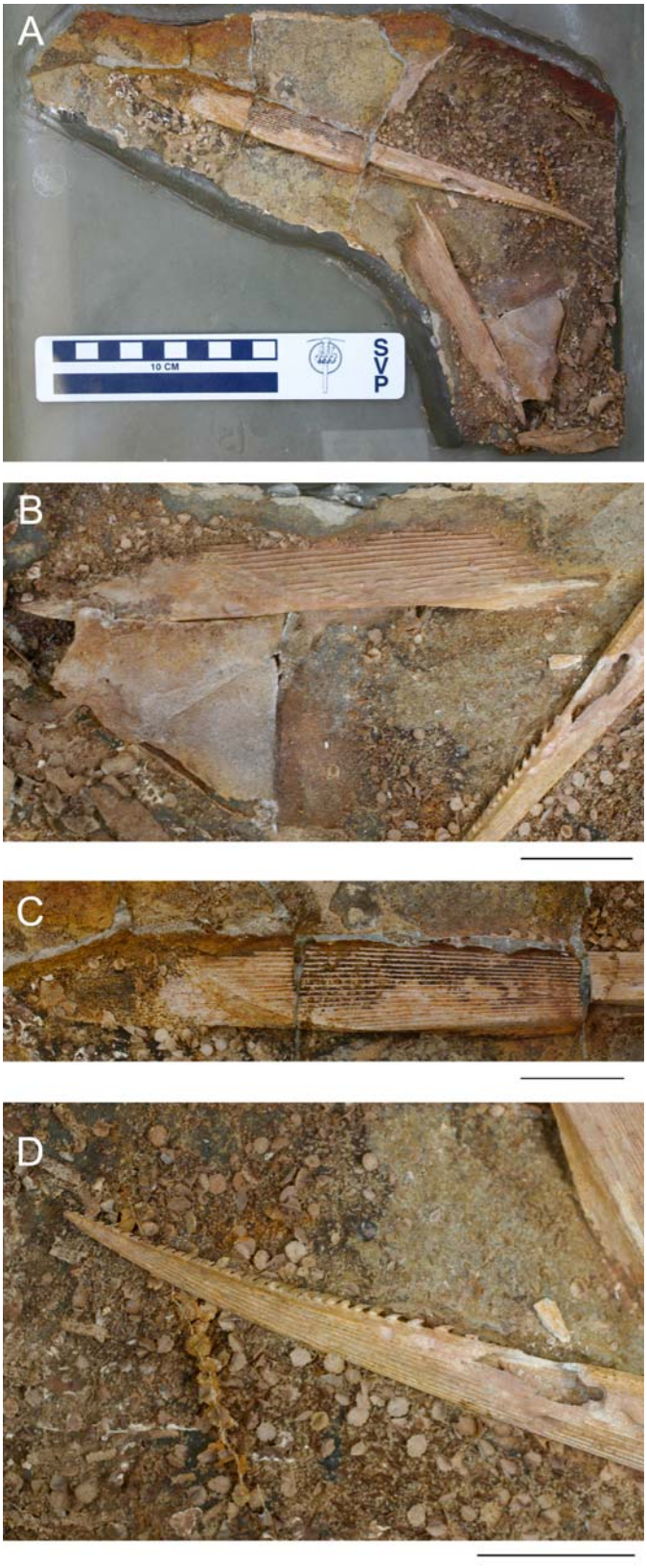
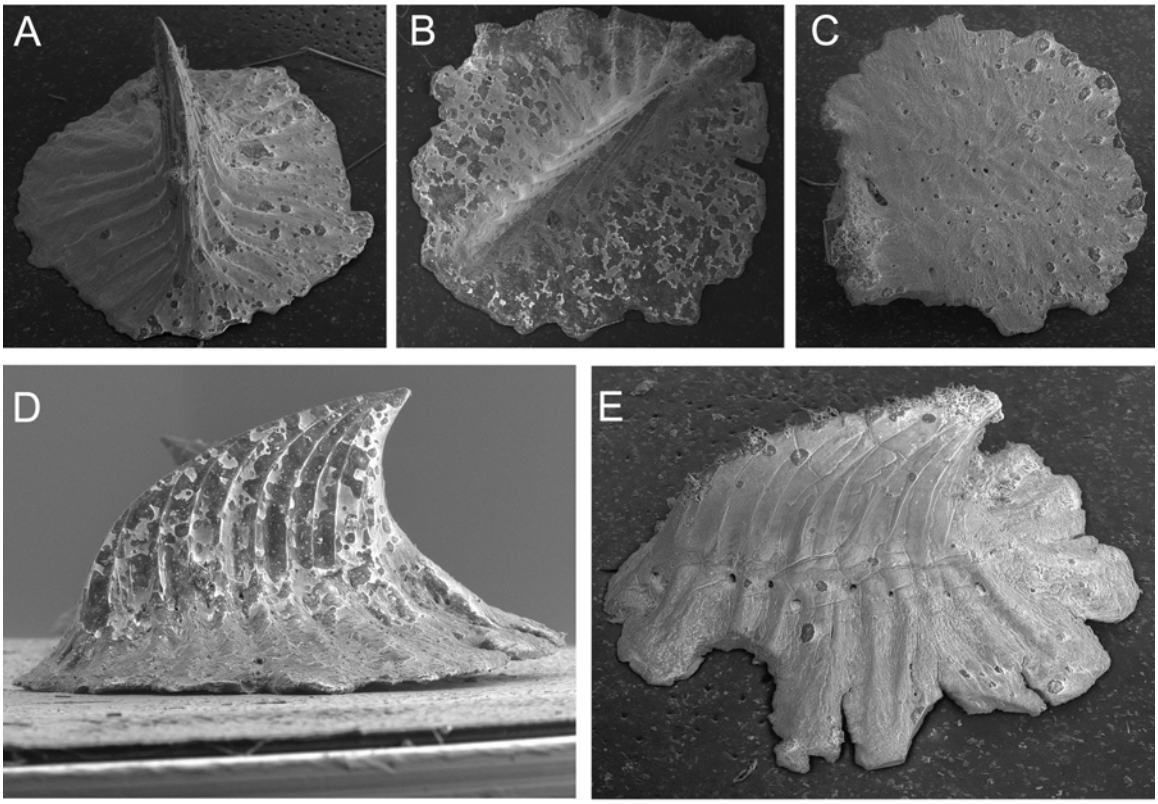

A
10 CM
SVP
B
C
D

FIGURE 114. Dermal denticles from the dorsal trunk region of *Tribodus limae*, AMNH 13958. A, anterodorsal; B, dorsal; C, ventral; D, lateral views; E, additional scale from near the same location on the same specimen, showing variation in scale morphology. Approximately x79–97.


A
B
C
D
E

# THE MORPHOLOGY AND RELATIONSHIPS OF THE HYBODONT SHARK *TRIBODUS LIMAE*, WITH A PHYLOGENETIC ANALYSIS OF HYBODONT SHARKS (CHONDRICHTHYES, HYBODONTIFORMES)

By

JENNIFER A. LANE

VOLUME II

A dissertation submitted to the Graduate Faculty in Biology in partial fulfillment of the requirements for the degree of Doctor of Philosophy, The City University of New York

2010

# PART III: PHYLOGENETIC ANALYSIS OF HYBODONTS

# CHAPTER 11: TAXON SAMPLING

A data matrix of 33 taxa and 129 characters was constructed, with the goals of testing previous hypotheses of hybodontiform monophyly and interrelationships as well as determining the phylogenetic position of *Tribodus* among Hybodontiformes based on morphological characters from complete or partial skeletal material (not limited to teeth). For this purpose, 20 ingroup taxa and 13 outgroup taxa were chosen and included in the analysis. Wherever possible, characters were coded based on direct observation of specimens, with supplemental data obtained from the relevant literature. The 20 ingroup taxa chosen all represent members of Hybodontiformes (sensu Maisey, 1989), the group traditionally referred to as "hybodonts" (although the positions of two of these taxa, *Tristychius arcuatus* and *Onychoselache traquairi*, have since been called into question: e.g., Maisey et al., 2004). Although many more hybodont taxa have been described on the basis of isolated dermal elements (mainly teeth and fin spines), only taxa in which relatively complete skeletal material is preserved were included in the present analysis (with the exception of *Lonchidion humblei* and *Lonchidion selachos*, included to provide additional information on cephalic spines of that genus, which are lacking in the more complete specimen of *Lonchidion montsechi*). The following taxa were included in the ingroup: *Tristychius arcuatus*, *Onychoselache traquairi*, *Hamiltonichthys mapesi*, *Lissodus cassangensis*, *Lissodus africanus*, *Lonchidion humblei*, *Lonchidion selachos*, *Lonchidion montsechi*, *Palaeobates angustissimus*, *Hybodus hauffianus*, *Hybodus reticulatus*, *Hybodus delabechei*, *Hybodus medius*, *Egertonodus basanus*, *Egertonodus fraasi*, *Acrodus anningiae*, *Acrodus nobilis*, *Acrodus lateralis*, *Asteracanthus*

*ornatissimus*, and the focus of this investigation*, Tribodus limae*. OTU's for hybodontiform taxa represent one or more specimens previously identified as belonging to a particular genus and species. All ingroup taxa included in the present analysis were examined firsthand on the basis of fossil material or casts reposited in various museum collections, except for *Lonchidion humblei, Lonchidion selachos*, and *Lonchidion montsechi*, for which data was taken only from the literature; and *Palaeobates angustissimus* and *Acrodus lateralis*, for which data was taken from Rieppel (1981). Specimens of *Tribodus limae* were examined at AMNH (AMNH 13957, 13958, 13959, and 13961), the Universidade do Estado do Rio de Janeiro (UERJ-PMB-40, -114, -119), and the Museu Nacional, Brazil (MN 5807V, 5808V). Specimens of *Tristychius arcuatus* were examined at the National Museums of Scotland, Edinburgh (numerous specimens, see Appendix C), the Hunterian Museum in Glasgow (HM 131310), and the Natural History Museum, London (NHM P.11383–11385, 60963a, b), and data also was obtained from Dick (1978). Two specimens of *Onychoselache traquairi*, NMS 1885.54.1 and NMS 1974.23.14, were examined at the National Museums of Scotland (Edinburgh, UK), and additional data for a third specimen (NMS 1998.35.2) was taken from Coates and Gess (2007). Data for *Onychoselache traquairi* was also obtained from Dick and Maisey (1980), and Moy-Thomas (1936). The only existing specimen of *Egertonodus fraasi*, BSPGM 1899-I-2, was studied at the Palaeontological Museum in Munich, Germany, and additional data came from Brown (1900) and Maisey (1986). Eleven specimens of *Egertonodus basanus* (NHM 40718, P.60110, 6356, P.11870, P.11817, P. 13094, P. 2082, P. 3172, and P. 40716 AND p. 40717) were studied at the Natural History Museum (London, UK), and one specimen (AMNH 4692) was examined at the American Museum

of Natural History in New York. Additional data for *Egertonodus basanus* was obtained from Woodward (1916), Patterson (1966), Maisey (1983), and Rees (2008). *Hybodus delabechei* was studied at the Natural History Museum, London (NHM 39880, P.3159, P.3160, P.3161, 40352, P.3171), and additional data came from Maisey (1982) and Reif (1978). *Hybodus medius* was studied at the Natural History Museum, London (NHM P.41103, 340), and additional data was taken from Agassiz (1843) and Woodward (1889A). *Hybodus reticulatus* was studied at the Natural History Museum, London (NHM P.2208, P.3168, P.2203D, P.3160, P.5880, P.3163, 40335, P.2198a, P.5876, P.3156, and P. 423), at the Oxford University Museum (J3088 and J3920), The Staatliches Museum fur Naturkunde, Stuttgart (*Hybodus* cf. *reticulatus*, SMNS 51949), and the Museum of Comparative Zoology, Harvard (MCZ 780, 816), and data was also obtained from Maisey (1987). *Hybodus hauffianus* was studied at the Staatliches Museum fur Naturkunde, Stuttgart, Germany (SMNS 8663, 8503, 52458, 10062, 15150, 80594, 54048, 51949, 52460, 51136, 80595, 51135, 58749, 52222, 50804, and 58748), at the Palaontologische Sammlung Institut fur Geowissenschaften Universitat Tubingen, Germany (GPIT, three uncatalogued specimens on display), and at the Natural History Museum, London (NHM P.5880), and additional data was obtained from Koken (1907), Maisey (1982), and Duffin (1997). *Acrodus anningiae* (NHM P.2146, 2731, 2732, 2734, 3152, 3153, 3155, 6332, 38125, and 32751) and *Acrodus nobilis* (NHM P.50809, 3154, 2165, 2737) were studied at the Natural History Museum, London, and data was also taken from Agassiz (1838, 1839), Woodward (1889A), and Maisey (1982). Data for *Acrodus lateralis* and *Palaeobates angustissimus* were obtained from Rieppel (1981). *Asteracanthus ornatissimus* was studied at the Natural History Museum, London (NHM

P. 12614), and additional data came from Maisey (1982) and Peyer (1946). *Lissodus africanus* specimens were examined at the Natural History Museum in London (NHM 16035–16039, 17530, 17531), the Cambridge University Museum of Zoology (UCMZ GN 949C, D; GN 333, GN 966), and the American Museum of Natural History (AMNH 8854), and additional data was ontained from Broom (1909), Brough (1935), Maisey (1990), and Duffin (2001). Firsthand examination of several additional specimens of *Lissodus africanus* (located in Oslo, Norway, and in South Africa) was not possible for the present thesis. Data for *Lissodus cassangensis* was obtained from specimen peels in the AMNH Fossil Fish collections, made from the original specimens in the Instituto de Investigação Cientifica Tropical, Lisbon, Portugal (IICT 69 and 70), and from the literature (Maisey, 1990; Duffin, 2001). Data for *Lonchidion humblei* was obtained from Murry (1981) and Duffin (2001), and data for *Lonchidion selachos* came from Estes (1964) and Duffin (2001). Data for *Lonchidion montsechi* was obtained from the literature (Gomez-Pallerola, 1979, 1985, 1992; Duffin, 2001). Although an additional complete specimen of *Lonchidion* sp. exists, located in Spain, it is currently under study by another researcher and thus cannot be included in the present thesis. *Hamiltonichthys mapesi* was studied at the American Museum of Natural History in New York (AMNH 10802, 10807), and additional data was obtained from Maisey (1989). During the course of my research for the present thesis, a new Permian hybodontiform, *Gansuselache tungshengi*, was described (Wang et al., 2009); however, I did not include it in the present phylogenetic analysis because it was not published until very recently, and such an analysis may be currently under way by the original authors. A list of specimens examined for the present analysis is included in Appendix C below.

Representative outgroup taxa were chosen from the remaining major chondrichthyan lineages, based on the previous literature. Previous studies (e.g., Coates and Sequeira, 2001A, B) strongly suggest the exclusion of these taxa from Hybodontiformes, making them viable outgroups for use here. Outgroup OTU's were chosen on the basis of being a representative sampling of the major chondrichthyan lineages currently recognized (e.g., neoselachians, holocephalans, symmoriiforms, xenacanths, 'ctenacanths', *Cladoselache*, '*Pucapampella*'). Part of the choice was also necessarily based on availability of specimens, particularly in the case of extant taxa (selected from available specimens in the AMNH Ichthyology Department collections). For the analysis, *Pucapampella* was chosen as the basalmost outgroup, because it has been proposed to represent the most primitive chondrichthyan (Maisey, 2001; Maisey and Anderson, 2001). Neoselachians are considered the monophyletic sister-group to hybodontiforms, and represent the first outgroup. For the phylogenetic analysis, the tree was rooted at *Pucapampella*, and outgroup and ingroup taxa were resolved simultaneously (as previously suggested by Maddison et al., 1984). OTU's for living outgroup taxa are individual species (as for Hybodontiformes); however, some Paleozoic chondrichthyan taxa are scored at supraspecific levels, where two or more species or genera are known with varying degrees of preservational completeness (for example, '*Orthacanthus*' here comprises *Orthacanthus texenis*, of which cranial and pectoral material is well known, and *Orthacanthus senckenbergensis*, in which postcranial material is better preserved). Similarly, 'ctenacanths' comprise *Tamiobatis* (in which the braincase is well-preserved, but postcrania are lacking), as well as *Ctenacanthus costellatus* and *Goodrichthys eksdalensis* (in which the postcranial skeleton is well preserved); and '*Pucapampella*'

includes two individual specimens tentatively assigned to that genus, one from Bolivia (Maisey, 2001) and the other from South Africa (Maisey and Anderson, 2001).

Several of the more obscure outgroup taxa were not included in the present analysis (e.g., eugeneodontids, orodontids, iniopterygians, petalodontids, and *Helodus*). These outgroup taxa were not included because the present analysis is focused on the relationships of hybodontiforms, and is not meant to be a complete analysis of chondrichthyan interrelationships. Subsequent authors may wish to include these and other outgroup taxa in future analyses, in order to determine their effect on the phylogeny.

Of the 13 outgroup taxa, five represent extant neoselachians (previously considered the sister group of hybodonts, e.g., Maisey et al., 2004). These include one batoid (*Dasyatis americana*), two orbitostylic sharks (*Notorynchus cepedianus* and *Squalus acanthias*), *Heterodontus francisci*, and one galeomorph (*Carcharhinus brevipinna*). Of the remaining eight outgroup taxa, one is an extant holocephalan (*Hydrolagus collei*), and the rest are Paleozoic chondrichthyans known from relatively complete skeletal material, including the putative stem chondrichthyan *Pucapampella*, *Cladoselache*, two xenacanths (*Orthacanthus* and *Diplodoselache*), a symmoriiform (*Akmonistion*), 'ctenacanths' (comprising *Tamiobatis*, *Ctenacanthus costellatus*, and *Goodrichthys eksdalensis*), and *Cladodoides wildungensis* (a putative ctenacanthiform shark, Maisey, 2005). All extant taxa (neoselachians and the holocephalan *Hydrolagus collei*) were coded based on specimens from the AMNH Ichthyology Department collections (see Materials and Methods section). Additional information on these taxa came from the following sources: *Notorynchus cepedianus*: Maisey, 2004; *Heterodontus francisci*: Daniel, 1934;

*Carcharhinus brevipinna*: Compagno, 1988; *Dasyatis americana*: Carvalho et al., 2004; *Squalus acanthias*: Marinelli and Strenger, 1959; *Hydrolagus collei*: Didier, 1995. For the Paleozoic chondrichthyan taxa, data was obtained from the following sources: for '*Pucapampella*': Maisey (2001) and Maisey and Anderson (2001); for *Orthacanthus*: examination of specimens at the Museum of Comparative Zoology, Harvard, and at AMNH; and from the literature (Fritsch, 1889, 1895; Schaeffer, 1981; Heidtke, 1982; Hampe, 1988); for *Diplodoselache*: Dick, 1981; for *Cladoselache*: examination of specimens at AMNH (AMNH uncat.), and from the literature (Bendix-Almgreen, 1975; Zangerl, 1981; Maisey, 2005); for *Akmonistion*: examination of specimens at UCMZ Cambridge (UCMZ GN 1047) and the Hunterian Museum, Glasgow (HM V8246, V8250), and from the literature (Coates and Sequeira, 1998; 2001A, B); for *Cladodoides wildungensis*: Maisey, 2001C, 2005; for 'ctenacanths': *Tamiobatis*, Williams (1998) and Schaeffer (1981); *Ctenacanthus costellatus*, Moy-Thomas (1939A, B); and *Goodrichthys eksdalensis*, Moy-Thomas (1939A, B; 1951).

# CHAPTER 12: PHYLOGENETIC METHODS AND DATA ANALYSIS

CONSTRUCTION OF THE DATA MATRIX: The character/taxon matrix for phylogenetic analysis was constructed using the program NDE (Nexus Data Editor) version 0.5.0 for Windows (Page, 2001). This program uses question marks to represent missing data, and dashes to represent inapplicable data. After being written in NDE, the matrix was then imported directly into PAUP* for phylogenetic analysis.

PRINCIPLE TREE SEARCHES: The data matrix was analyzed and most parsimonious trees (MPTs) were found using the computer software package PAUP* 4.0 beta for Windows (Swofford, 2001). An alternative program, T.N.T. (tree analysis using new technology, Goloboff et al., 2003) was also used for comparison. Due to the relatively large number of taxa (33 taxa), a heuristic search was performed. All characters in the data matrix were coded as binary and non-additive, and all characters were treated as having equal weight. Character optimisation used the accelerated transformation (ACCTRAN) option. For both the PAUP* and T.N.T. analyses, Tree Bisection Reconnection (TBR) branch swapping was performed on trees found by 1,000 random-taxon-addition heuristic searches. In PAUP*, this was done using the command "hsearch addseq=random nreps=1000," with TBR automatically used by the program as its default method for branch swapping; whereas in T.N.T. the identical settings were selected.

CONSENSUS TREES AND APOMORPHY LISTS: Strict and Adams consensus trees, as well as an apomorphy list, were generated in PAUP* 4.0 based on the results of the principle tree searches. A strict consensus was also generated from the trees resulting from the

heuristic search that was run using T.N.T. (Goloboff, 2003), for the purpose of comparison. Strict consensus trees were generated in PAUP* from the set of MPTs resulting from heuristic search ("contree" option). Adams consensus trees were generated in PAUP* ("contree/adams=yes"). Lists of unequivocal apomorphies for nodes common to all MPTs (i.e., appearing in the strict consensus tree) were produced by saving the strict consensus tree to a treefile (command: "contree/treefile=[name]"), reopening it in PAUP*, and then typing the command "describe 1/apolist=yes."

VIEWING TREES: Principle trees were viewed using PAUP* 4.0 and the program TreeViewX, version 0.5.0 (Page, 2004), in order to determine the alternative placements of certain taxa.

DECAY INDICES (BREMER SUPPORT) AND OTHER SUPPORT METHODS: Support for individual nodes in the strict consensus tree generated from all MPTs was measured using Bremer Support values (Bremer, 1988, 1994) and bootstrap values (Felsenstein, 1985). Bremer Support values (also known as decay indices) were calculated using PAUP* 4.0 beta for Windows, using the "keep" command (increasing the tree length to be retained at each step by one), as outlined in the PAUP* users' manual (by typing "keep = [previous tree length + 1]" at each step). To calculate bootstrap values for a matrix of this size in PAUP*, the matrix was exported to T.N.T. (Goloboff et al., 2003). 1000 bootstrap replicates were run on the dataset using T.N.T.

# CHAPTER 13: LIST OF MORPHOLOGICAL CHARACTERS

Data sources for the phylogenetic analysis presented here are based on direct observation of specimens (see Materials and Methods), and on the following literature: *Tribodus limae* from Brito and Ferreira, 1989; Brito, 1992; Maisey and Carvalho, 1997; Maisey et al., 2004; and Maisey (2004A, 2005, 2007); *Egertonodus basanus* from Woodward (1916) and Maisey (1983, 2004A); *Egertonodus fraasi* from Brown (1900) and Maisey (1986); *Hamiltonichthys mapesi* from Maisey (1989); *Onychoselache traquairi* from Moy-Thomas (1936), Dick (1978), Dick and Maisey (1980), and Coates and Gess (2007); *Tristychius arcuatus* from Dick (1978) and from Coates and Gess (2007); *Hybodus reticulatus* from Agassiz (1837), Woodward (1889A), and Maisey (1987); *Hybodus hauffianus* from Koken (1907), Maisey (1982), and Duffin (1997); *Hybodus delabechei* from Woodward (1889A, B) and Maisey (1982); *Hybodus medius* from Woodward (1889A); *Acrodus anningiae* from Agassiz (1837), Day (1864), and Woodward (1889); *Acrodus nobilis* from Agassiz (1837) and Woodward (1889A); *Acrodus lateralis* from Woodward (1889A) and Rieppel (1981); *Asteracanthus ornatissimus* from Agassiz (1837), Woodward (1889A), Peyer (1946), and Maisey (1982); *Lissodus cassangensis* from Maisey (1990) and Duffin (1985, 2001); *Lissodus africanus* from Broom (1909), Brough (1935), and Duffin (1985, 2001); *Lonchidion* from Gomez-Pallerola (1985, 1992), Estes (1964), Murry (1981), and Duffin (1985); *Cladodoides wildungensis* from Maisey (2001C, 2005); *Cobelodus* from Maisey (2008); *Akmonistion* from Coates and Sequeira, 1998; *Pucapampella* from Maisey (2001B) and

Maisey and Anderson (2001); *Orthacanthus* from Fritsch (1889, 1895), Hotton (1952), Schaeffer (1981), and Heidtke (1982); and extant elasmobranchs from Goodrich (1930), Daniel (1934), De Beer (1937), Holmgren (1940, 1941, 1942), Compagno (1988), Shirai (1992), and Maisey (2004B). [CG] indicates character statement from Coates and Gess, 2007; [M] indicates character statement from Maisey, 1989; [MEA] indicates character statement from Maisey et al, 2004; [JGM] indicates character state from Maisey, 2001A; [JGM87] indicates character statement from Maisey, 1987; [JM] indicates character statement from Maisey, 1984; [CS98] indicates character statement from Coates and Sequeira, 1998; [CS01] indicates character statement from Coates and Sequeira, 2001A; [G] indicates character statement from Gaudin, 1991; [C] indicates character statement from de Carvalho, 1996, [S] indicates character statement from Shirai, 1992. Additional sources of characters are indicated by a bracketed author citation. New character statements are designated by [N].

Certain characters included in previous analyses of hybodontiforms (e.g., Maisey, 1989; Maisey et al., 2004; Rees, 2008) were not included in the present analysis. The decision not to include these characters was based on the following factors: 1) the original character definition was considered to be too vague or unclear; 2) the character has been described by subsequent authors as problematic; or 3) the character is inapplicable to the taxa in the present analysis (e.g., several autapomorphic features used by Rees, 2008, to define taxa known primarily from teeth, and not included here). For example, the character "pattern of pectoral basals and radials" (character 17 of Maisey, 1989:37) was not included because it is not clearly defined. Where possible, an effort was made to redefine poorly defined characters from the previous literature (for example,

"scapular and coracoid regions of subequal length," from Maisey, 1989 and Coates and Gess, 2007, was redefined as "scapular and coracoid regions of near-equal length"). Because the present analysis is focused mainly on non-dentitional characters, the majority of tooth characters used by previous authors were also not included. Additionally, characters pertaining to soft anatomy of extant neoselachians were not included, in order to reduce the amount of missing data in the analysis and because the analysis is focused on fossil taxa.

The matrix of 129 characters for the present analysis includes 86 endoskeletal characters (35 neurocranial characters, 19 characters from the visceral skeleton, 19 characters from the appendicular skeleton, and 13 characters from the axial skeleton), and 43 characters from the dermal skeleton (including cephalic spines, fin spines, dermal denticles and teeth). A total of 22 new characters were included in the analysis (some of which were based on splitting up or otherwise revising previously published characters, as well as several original characters based on examination of specimens). All characters were included in a single matrix rather than partitioning different types of data (i.e., tooth data vs. head spine data, etc.). Binary characters were used for the analysis (following Coates and Sequeira, 1998). Forty-four characters in the matrix were taken from Coates and Gess (2007), who presented a manually constructed tree of hybodontiform taxa with neoselachians as the outgroup, based on a total of 50 characters. The 129 characters and the distribution of their character states are described below.

**Neurocranium**

**Character 1:** *Precerebral fontanelle absent=0; present=1.* [CS01] A precerebral fontanelle is present (character state 1) in most chondrichthyans except holocephalans, and has been considered a synapomorphy of elasmobranchs (Maisey, 1984, 2005; Gaudin, 1991) or possibly of chondrichthyans in general (Coates and Sequeira, 1998). This feature is present in neoselachians, hybodonts, *Tristychius*, and Paleozoic chondrichthyans (including *Cladodoides*, *Tamiobatis*, *Orthacanthus*, "*Cobelodus*," and *Akmonistion*: Schaeffer, 1981; Coates and Sequeira, 1998; Maisey, 2005). It is absent (character state 0) in holocephalans. Due to preservational issues, it is unknown whether a precerebral fontanelle was present in *Pucapampella* or *Cladoselache* (Maisey, 2001, 2005, 2008; Maisey and Anderson, 2001). Its taxonomic distribution suggests that this character may have been a synapomorphy of chondrichthyans, and lost secondarily in holocephalans (as proposed by Coates and Sequeira, 1998).

**Character 2:** *Glossopharyngeal nerve passes through metotic fissure absent=0; present=1*. [CS01]. The glossopharyngeal nerve passes through the metotic fissure (character state 1) in hybodonts, *Tristychius*, neoselachians, *Orthacanthus*, ctenacanths, and *Akmonistion*. The glossopharyngeal nerve does not pass through the metotic fissure (character state 0) in *Pucapampella* and holocephalans. In hybodontiforms (including *Tribodus*), *Tristychius*, ctenacanths, and neoselachians, the metotic fissure is closed dorsally, forming an enclosed glossopharyngeal canal (formed ontogenetically between the ventral floor of the auditory capsule and the hypotic lamina). In other chondrichthyans (e.g., *Orthacanthus*; *Cobelodus*; and *Akmonistion*; Coates and Sequeira,

1998; Maisey, 2005, 2008), the otico-occipital and metotic fissures are open dorsally and the glossopharyngeal nerve exits through the metotic fissure posteroventral to the otic capsule (Coates and Sequeira, 1998). In these forms, the glossopharyngeal nerve passes through the ventral otic notch (corresponding to the metotic fissure of embryonic neoselachians); this notch is continuous dorsally with the otico-occipital fissure and is thus does not form a fully enclosed canal (Maisey, 2005).

**Character 3:** *Dorsal otic ridge has horizontal crests=0; dorsal otic ridge lacks horizontal crests=1.* [CG; CS98]: A dorsal otic ridge with horizontal crests is lacking in *Tribodus*. According to Coates and Sequeira (1998), a median dorsal ridge is present in primitive chondrichthyan neurocrania, encompassing the endolymphatic fossa in its posterior part. This ridge is absent in outgroups to chondrichthyans. In *Orthacanthus*, the posterior part of this ridge is divided to form paired horizontal crests, on either side of the endolymphatic fossa; according to Schaeffer (1981), these may have acted as attachment sites for muscles supporting the cranial (dorsal) fin spine (Coates and Sequeira, 1998; Schaeffer, 1981). However, Coates and Sequeira (1998) pointed out that these crests also occur in *Akmonistion* (which they referred to originally as the "Bearsden *Stethacanthus*," Coates and Sequeira, 1998), in which the anterior dorsal fin spine is positioned much farther posteriorly, casting doubt on the conclusion that they helped to support the cranial spine. In *Tristychius*, *Egertonodus*, and other hybodontiforms, the dorsal ridge is reduced and modified to form laterally narrow crests (Coates and Sequeira, 1998). A similar condition also occurs in *Tribodus*.

**Character 4:** *Otico-occipital fissure open behind posterior dorsal fontanelle=0; otico-occipital fissure closed behind posterior dorsal fontanelle =1.* [CG]: The otico-occipital fissure is closed in *Tribodus*. As mentioned above (character 1), a closed otico-occipital fissure (state 1) is present in adult neoselachians and hybodontiforms (including *Tristychius*). Closure of the otico-occipital fissure also occurs (probably as an independently derived feature) in chimaeroids (e.g., *Helodus*; Coates and Sequeira, 1998), which recent phylogenetic analyses suggest may be nested within symmoriforms (the group that includes *Akmonistion* and *Cobelodus*). A persistent otico-occipital fissure (state 0) occurs in primitive chondrichthyans, acanthodians, and osteichthyans (e.g., *Orthacanthus*, *Tamiobatis*, *Cladodoides*, *Cobelodus*, *Pucapampella*, *Akmonistion*; Schaeffer, 1981; Coates and Sequeira, 1998; Maisey, 2005, 2008). According to Coates and Sequeira (1998), outgroup comparison with osteostracan agnathans and placoderms indicates that chondrocranial fusion is primitive for gnathostomes, suggesting that presence of a persistent otico-occipital fissure may be a synapomorphy of chondrichthyans, acanthodians, and osteichthyans. This further suggests that among chondrichthyans fissure closure may be a synapomorphy of hybodontiforms and neoselachians, and probably independently derived in chimaeroids (which may be nested within symmoriiforms) (Coates and Sequeira, 1998).

**Character 5:** *Metotic fissure open=0; metotic fissure closed=1.* [CG; JGM]: A closed metotic fissure (character state 1) is present in *Tribodus*, as well as in other hybodontiforms (e.g., *Onychoselache*: Coates and Gess, 2007; *Egertonodus*, Maisey, 1983), *Tristychius*, *Cladodoides*, *Tamiobatis*, *Synechodus*, and adult neoselachians.

According to Maisey (2001) and Schaeffer (1981), closure of the embryonic metotic fissure in these taxa is related to formation of the hypotic lamina and glossopharyngeal canal ventral to the otic capsule. The metotic fissure is also closed (state 1) in holocephalans, but does not enclose the glossopharyngeal nerve (unlike the other taxa just mentioned; see character 2 above). The metotic fissure remains open (state 0) in many Paleozoic chondrichthyans, including *Orthacanthus*, *Akmonistion*, *Cladoselache*, and *Pucapampella*. No cranial fissure has been reported in placoderms (Maisey, 2001).

**Character 6:** *Ventral otic fissure open=0; ventral otic fissure closed=1.* [CG; CS01]: An open ventral otic fissure (character state 0), which separates the basicranium into anterior and posterior halves, is found in acanthodians, osteichthyans, and the basal chondrichthyan *Pucapampella* (Maisey and Anderson, 2001; Maisey, 2001). In higher chondrichthyans (e.g., symmoriiforms, cladoselachians, xenacanths, ctenacanths, holocephalans, and euselachians) the ventral otic fissure is closed (character state 1). The ventral fissure has been considered primitively present in chondrichthyans, acanthodians, and osteichthyans, and subsequently lost in chondrichthyans (Janvier, 1998; Maisey, 2001; Maisey and Anderson, 2001).

**Character 7:** *Occipital block not wedged between otic capsules=0; Occipital block wedged between otic capsules=1.* [CG; JGM]: the occipital block is wedged between the otic capsules in *Tribodus*. Coates and Gess (2007) list this character as "probably present" in *Onychoselache*, given its resemblance to the neurocranial proportions found in *Egertonodus*; these authors list the same character in *Tristychius* as "similarly uncertain,

although the occipital crest extends forwards to the fenestra vestibulae between the posterior semicircular canals...comparable to the condition in *Squalus*." Maisey (2001) states that this feature is present (state 1) in extant elasmobranchs, and absent (state 0) in holocephalans, most osteichthyans (except some clupeoids), acanthodians, and placoderms, all of which have the occipital block located behind the otic capsules.

**Character 8:** *Dorsal otic ridge absent=0; present=1*. [CS98]. Dorsal otic ridges (paired structures developed lateral to the posterior dorsal fontanelle) are absent (state 0) in hybodonts and neoselachians (Maisey, 2005). In other extinct sharks (e.g., *Pucapampella*, *Akmonistion*, *Cobelodus*, *Cladodoides*, *Tamiobatis*, *Orthacanthus*), dorsal otic ridges are present (state 1). In all of these latter taxa except *Pucapampella* and *Cobelodus*, the dorsal otic ridges are further developed to form horizontal crests (see character 3, above).

**Character 9:** *Crus between anterior and posterior semicircular canals. present=0; absent=1*. [CG; JGM]: absent (state 1) in *Tribodus*. Absent in *Egertonodus* and neoselachians; unknown in *Tristychius*. There is also evidence that a crus may have been absent in some placoderms (Maisey, 2001). Present (state 0) in primitive chondrichthyans, chimaeroids, and osteichthyans. A crus commune between anterior and posterior semicircular canals is present in lampreys, osteichthyans, and chimaeroids, and may have also been present in at least some extinct agnathans (Maisey, 2001). It is absent in hagfish, but whether this absence is primitive or secondarily derived is unknown (Maisey, 2001). Although Maisey (2001A) states that a crus between anterior and posterior canals was absent in the stem chondrichthyan *Pucapampella*, in Maisey

(2001B) it is stated that *Pucapampella* does indeed have a crus between the anterior and posterior canals, as in chimaeroids, osteichthyans, osteostracans, and galeaspids (possibly representing the plesiomorphic gnathostome condition).

**Character 10:** *Inner ear adapted for semi-directional low-frequency phonoreception (i.e., Pre-ampullary part of posterior semicircular canal extends dorsally to perilymphatic fenestra, so that the canal forms a complete circuit; separation of utricular and saccular regions; posterior canal duct and perilymphatic openings present; medial chondrified otic capsule wall separating labyrinth and endocranial cavity). absent=0; present=1.* [MEA; CG]: present in *Tribodus*. Also present in *Egertonodus* and neoselachians. According to Maisey (2001), in extant elasmobranchs, the preampullary part of the posterior canal extends dorsally and extends to reach the perilymphatic fenestra; whereas in holocephalans and *Acipenser*, the preampullary ramus is short and extends anteriorly toward the utricular chamber, and lacks an ascending ramus. There is little evidence of an ascending preampullary canal in placoderms, despite Stensiö's reconstructions to the contrary (mostly based on a neoselachian paradigm) (Maisey, 2001). Isolation of the posterior canal from the other semicircular canals occurs in extant elasmobranchs (e.g., *Notorynchus* and *Squalus*), as well as in hybodonts (e.g., *Tribodus* and *Egertonodus*). In contrast, in most fossil and recent agnathans, osteicthyans, and holocephalans, the anterior and posterior canals are joined to form a crus commune. A medial chondrified otic capsular wall is present in extant elasmobranchs, *Egertonodus*, and *Tribodus* (and probably in other hybodonts as well, although this remains unknown thus far pending future CT scan studies of additional taxa). It is absent in primitive

chondrichthyans (e.g., *Cladodoides*, *Orthacanthus*, *Cobelodus*, *Pucapampella*), chimaeroids, and osteichthyans (e.g., *Mimia*), but was present and well-developed in some placoderms.

**Character 11:** *Internasal keel absent=0; present=1.* [CS98]. An internasal keel is present (character state 1) in some hybodontiforms (including *Hamiltonichthys*, *Egertonodus*, and *Hybodus*), although this feature is unknown due to preservation in *Lissodus*, *Lonchidion*, *Acrodus*, and *Asteracanthus*. It is also present in *Orthacanthus* (Schaeffer, 1981). An internasal keel is absent (character state 0) in other chondrichthyans, including neoselachians, *Tristychius*, holocephalans, some hybodonts (e.g., *Tribodus*), and most Paleozoic chondrichthyans except *Orthacanthus*. An internasal keel may have been absent in hybodonts in which the jaws do not extend to the ethmoid region (possibly *Asteracanthus*, *Lissodus*, and *Lonchidion*).

**Character 12:** *Rostral bar elongated=0; short=1.* [JGM87]. Maisey (1987) listed length of the rostral bar as one of the characters distinguishing *Hybodus* from *Egertonodus*. According to Maisey (1987), the rostral bar of *Hybodus reticulatus* is comparatively longer (projecting anteriorly beyond the outer rim of the precerebral fontanelle) than that of *Egertonodus basanus* and *Egertonodus fraasi*. The rostral bar in *Hybodus hauffianus* and *Hybodus delabechei* (character state 0) is also long compared to that of species of *Egertonodus*, in which it is relatively short (character state 1). *Tribodus limae* appears to have had a short rostral bar, as in *Egertonodus*. Unfortunately, the rostral bar in other hybodont taxa (e.g., *Lissodus*, *Lonchidion*, *Palaeobates*, *Acrodus*, *Asteracanthus*) is not

sufficiently preserved for comparative purposes. The rostral bar is often not preserved in fossil chondrichthyans, although it is known in *Orthacanthus* (in which the rostral bar does not project beyond the anterior of the snout) and *Akmonistion* (in which the rostral bar projects anteriorly). Among extant neoselachians, the length of the rostrum is highly variable (Shirai, 1992), and may not be of much phylogenetic significance. A long rostrum is present in some orbitostylic sharks (e.g., *Squalus*), galeomorphs, and batoids (e.g., *Rhynchobatus*: Shirai, 1992), whereas it is absent in other batoids (e.g., *Dasyatis*) and in *Heterodontus*.

**Character 13:** *Inflated ethmopalatine processes absent=0; present=1.* [JGM87]. Inflated ethmopalatine processes are present (state 1) in some hybodonts, including *Egertonodus*, *Hybodus*, and *Acrodus*. Due to preservational issues, it is unknown whether they were present in other hybodonts (e.g., *Onychoselache*, *Hamiltonichthys*, *Lissodus*, *Lonchidion*, *Palaeobates*, and *Asteracanthus*). They are absent (state 0) in *Tribodus*, *Tristychius*, neoselachians and Paleozoic chondrichthyans.

**Character 14:** *Suborbital shelf present=0; absent=1.* [CS01]. A suborbital shelf (a lateral projection of cartilage located beneath the orbital region and formed along the margin of the trabecular-polar cartilage) is present (character state 0) in many chondrichthyans, including Paleozoic sharks (e.g., *Pucapampella*, *Cladodoides*, *Akmonistion*, *Tamiobatis*, *Cladodoides*, *Orthacanthus*), *Tristychius*, many hybodontiforms (e.g., *Egertonodus*, *Hybodus*, and *Hamiltonichthys*), and extant galean neoselachians including *Heterodontus* and galeomorphs. A suborbital shelf is absent

(character state 1) in *Tribodus*, squalean sharks, and batoids. This feature is unknown in other hybodonts due to poor preservation. It is also unknown in holocephalans, in which fusion of the palatoquadrate and braincase has obscured the basicranium anteriorly.

**Character 15:** *Suborbital shelf broad and laterally flared beneath postnasal wall: absent=0; present=1.* [JGM87]. Absent in *Tribodus*. The suborbital shelf is broad and laterally flared to form distally pointed processes in *Egertonodus basanus* and *Egertonodus fraasi* (character state 1) (Maisey, 1983, 1986, 1987). This feature is absent (character state 0) in other hybodonts in which the basicranium in the ethmoid region is known (e.g., *Hybodus hauffianus*, *Hybodus reticulatus*; *Tribodus*; *Hamiltonichthys*), as well as in *Tristychius*, neoselachians, holocephalans, and other chondrichthyans. This character was suggested by Maisey (1987) as distinguishing *Egertonodus* from *Hybodus*.

**Character 16:** *Trochlear foramen dorsal and anterior to optic foramen. absent=0; present=1.* [CG]. The trochlear nerve foramen is dorsal and above or anterior to the optic foramen (character state 1) in some hybodonts (e.g., *Tribodus*, *Hybodus*, *Egertonodus*) and probably also *Tristychius*. However, according to Dick (1978) the position of the trochlear foramen in the orbit of *Tristychius* is somewhat ambiguous, and he described it as being anterior to the optic foramen in one specimen, but more posteriorly located in another (although observation of *Tristychius* specimens suggests that the former interpretation is probably correct). It is unknown in other hybodonts. The trochlear foramen is posterior to, or directly above, the optic foramen in Paleozoic chondrichthyans, holocephalans, and neoselachians. Coates and Gess (2007) included the

character "trochlear foramen dorsal to, and above or anterior to, optic foramen" in their analysis (with the states "present/absent"), and listed it as a character linking *Tristychius*, hybodonts, and neoselachians. However, it is here considered that Coates and Gess' (2007) character requires revision, because it makes the assumption that the character states "anterior to the optic foramen" and "above the optic foramen" are homologous.

**Character 17:** *Proximal part of epihyal/hyomandibula located anteriorly in the otic region: absent=0; present=1.* [CS98]. In most chondrichthyans, the hyomandibular articulates with the posterolateral part of the braincase (Maisey, 2005). It is located on the posterior of the otic capsule (character state 0) in hybodonts, some neoselachians including batoids and orbitostylic sharks, and Paleozoic chondrichthyans including *Pucapampella*, *Orthacanthus*, *Tamiobatis*, and *Akmonistion* (Maisey and Anderson, 2001; Maisey, 2005). According to Maisey (2005), the hyomandibular articulation in *Cladodoides* was probably also located posteriorly, although its exact position is uncertain. The proximal part of the hyomandibular or epihyal is located farther anteriorly (character state 1) in extant *Heterodontus* and galeomorphs (e.g., *Carcharhinus*), *Synechodus*, *Tristychius*, and in chimaeroids (e.g., *Hydrolagus*) (Dick, 1978; Didier, 1995; Carvalho, 1996; Maisey, 2005). In *Tristychius*, the proximal part of the hyomandibular articulates with the braincase immediately posterior to the postorbital process (Dick, 1978). In outgroups to chondrichthyans (i.e., placoderms, acanthodians, and osteichthyans), the hyomandibular articulation is typically located anteriorly, in the region of the lateral commissure, suggesting that the typical chondrichthyan condition is derived (Gardiner, 1984; Maisey, 2005).

**Character 18:** *Posterior dorsal fontanelle absent=0; present=1*. [Maisey, 2005]. A posterior dorsal fontanelle (typically also referred to as a parietal or endolymphatic fossa in elasmobranchs) is present in most chondrichthyans including *Pucapampella* (character state 1) as an opening located dorsally in the otic region, between the otic capsules. This feature may be primitive for chondrichthyans, and is considered homologous to the posterior dorsal fontanelle of osteichthyans and acanthodians (Maisey, 2005). A posterior dorsal fontanelle is absent in holocephalans (character state 0), apparently lost secondarily (however, this feature may have been present in ancestors of holocephalans: Maisey, 2005). The posterior dorsal fontanelle in hybodonts and neoselachians is also referred to as the endolymphatic or parietal fossa, and contains the external openings of the endolymphatic and perilymphatic ducts. The latter features are part of a complex of structural adaptations for semi-directional low frequency phonoreception that are apparently unique to hybodonts and neoselachians (Maisey, 2001, 2005). A posterior dorsal fontanelle is absent in placoderms, and has been considered a possible synapomorphy of crown-group gnathostomes (i.e., gnathostomes above placoderms) (Maisey and Anderson, 2001; Maisey, 2005).

**Character 19:** *Occipital half-centrum absent=0; present=1*. [JM; G]. An occipital half-centrum (or "demi-centrum") has been considered a synapomorphy of non-batoid neoselachians, in which it is present (character state 1). This structure occupies the occipital cotylus, and is incorporated into the braincase (Maisey, 2004). An occipital half-centrum is absent (character state 0) in batoids, and in all other non-neoselachian

chondrichthyans currently known. In extant *Notorynchus*, a partial occipital half-centrum is present, although it is poorly calcified (Maisey, 2004), and this structure is scored as present in *Notorynchus* for the current analysis.

**Character 20:** *Efferent pseudobranchial foramen dorsal to level of suborbital shelf or base of orbit: absent=0; present=1.* [JGM87]. The position of the efferent pseudobranchial foramen was listed by Maisey (1987) as one of the features differentiating *Hybodus reticulatus* from *Egertonodus basanus*. The efferent pseudobranchial foramen is dorsal to the suborbital shelf or ventral margin of the orbit (character state 1) in the hybodonts *Egertonodus basanus* and *Tribodus*, and in extant neoselachians (e.g., *Squalus*, *Carcharhinus*, *Heterodontus*, and batoids). It is located ventrally or ventrolaterally (character state 0) in *Hybodus reticulatus*, *Cladodoides*, *Tamiobatis*, *Orthacanthus*, holocephalans, and *Pucapampella*. This feature is unknown in other hybodonts, *Akmonistion*, *Cladoselache*, and *Diplodoselache*.

**Character 21:** *Hypotic lamina absent=0; present=1*. [JGM]. According to Coates and Sequeira, there is no evidence of a hypotic lamina in outgroups to elasmobranchs (e.g., chimaeroids and osteichthyans), and presence of this feature has been considered a synapomorphy of higher chondrichthyans (neoselachians and hybodontiforms). Among chondrichthyans, a true enclosed glossopharyngeal canal (produced by contribution from the hypotic lamina) in the absence of an open otico-occipital fissure may thus represent a synapomorphy of hybodontiforms and neoselachians.

**Character 22:** *Otic capsules located between postorbital processes. absent=0; present=1.* [CG; M; MEA]: The otic capsules extend anteriorly between the postorbital processes (character state 1) in hybodontiforms (not including *Tristychius*) and neoselachians. This feature is absent (character state 0) in *Tristychius*, holocephalans, and Paleozoic chondrichthyans, in which the anterior ends of the otic capsules are located entirely behind the postorbital processes.

**Character 23:** *Large, down-turned postorbital processes. absent=0; present=1.* [CG; M; MEA]. Large postorbital processes which extend downward ventrally beyond the basicranium have been considered a hybodont synapomorphy (Maisey, 1989; Maisey et al., 2004). they are absent in *Tristychius*, holocephalans, neoselachians, and Paleozoic chondrichthyans (character state 0). They are present (character state 1) in hybodontiforms including *Tribodus*, *Hybodus*, *Lissodus*, *Egertonodus*, *Acrodus*, *Onychoselache*, and *Hamiltonichthys* (Maisey, 1982, 1983, 1986, 1987, 1989; Coates and Gess, 2007).

**Character 24:** *Postorbital process positioned over trigemino-facialis region: absent=0; present=1.* [JGM87]. This character was listed by Maisey (1987) as distinguishing *Hybodus reticulatus* from *Egertonodus basanus*. The postorbital process overlies the trigemino-facialis region in some hybodonts (*Hybodus reticulatus* and *Hybodus hauffianus*), *Tristychius*, *Cladodoides*, and *Tamiobatis* (character state 1). The postorbital process does not cover the trigemino-facialis region (character state 0) in other hybodonts (including *Tribodus limae*, *Egertonodus basanus*, and *Egertonodus fraasi*), *Akmonistion*,

*Pucapampella*, holocephalans, and neoselachians. This feature is unknown in the remaining hybodont taxa (including *Onychoselache*, *Hamiltonichthys*, *Lissodus*, *Lonchidion*, *Palaeobates*, *Hybodus delabechei*, *Acrodus*, and *Asteracanthus*). According to Maisey (1987), this feature is also present in *Orthacanthus*. However, in specimens of *Orthacanthus* figured by Schaeffer (1981) the trigemino-facialis foramen is visible in lateral view and appears to be positioned immediately anterior to the postorbital process rather than covered by it, and this feature is scored as absent in *Orthacanthus* for the present analysis.

**Character 25:** *Lateral commissure chondrified to contain jugular canal: present=0; absent=1.* [N]. The lateral commissure is chondrified and contains the jugular canal in Paleozoic chondrichthyans, *Tristychius*, and hybodontiforms (character state 0). The lateral commissure is absent or unchondrified in holocephalans and neoselachians except *Squatina* (character state 1). The postorbital process of chondrichthyans primitively comprises two components: a primary postorbital process located dorsally (which is the first to develop during ontogeny), and the lateral commissure, which is located ventral to the primary process and develops later in ontogeny (Holmgren, 1940). During embryonic growth, the primary process originates dorsally immediately anterior to the prootic foramen, and later joins with the supraorbital crest to form the "secondary postorbital process" (Holmgren, 1940; Maisey, 2005). The lateral commissure originates as a lateral outgrowth on the ventral part of the otic capsule ventral to the hyomandibular foramen and posterior to the orbital artery and palatine ramus of the facial nerve, and may extend dorsally to join the primary postorbital process and enclose the jugular vein and

hyomandibular nerve (as in extant *Squatina*, in which a chondrified lateral comissure is present: Maisey, 2005). In many extant neoselachians, the lateral commissure is present but does not chondrify, possibly representing a neoselachian synapomorphy.

**Character 26:** *Postorbital articulation with the palatoquadrate. present=0; absent=1.* [CG; M; MEA]. An articulation between the palatoquadrate and the postorbital process of the braincase is absent in *Tribodus* and most other hybodontiforms, *Tristychius*, and most neoselachians except hexanchiforms (character state 1). A postorbital articulation is present in *Tristychius*, hexanchiform neoselachians (e.g., *Notorynchus*), and Paleozoic chondrichthyans (character state 0), and has also been reported in a hybodontiform (originally referred to the genus *Acrodus*) from Madagascar (Thomson, 1982). However, the postorbital articulation of *Tristychius* and the Madagascar hybodontiform differs morphologically from that of Paleozoic chondrichthyans, in that in the former two taxa, the palatoquadrate articulates with the ventral part of the lateral commissure rather than with its posterior part (Dick, 1978; Thomson, 1982; Maisey, 2008). The postorbital articulation of extant hexanchiforms is made between the palatoquadrate and the primary postorbital process, and the lateral commissure is not chondrified (Maisey, 2005, 2008) (see character 28, below). It has been suggested that the postorbital articulation of hexanchiforms may be secondarily derived, and may not be homologous with that of earlier chondrichthyans (Maisey, 2008).

**Character 27:** *Postorbital articulation with lateral commissure present=0; absent=1.* [N]. An articulation between the palatoquadrate and the lateral commissure (the ventral

portion of the postorbital process, which encloses the jugular vein canal) is present (character state 0) in Paleozoic chondrichthyans (e.g., *Orthacanthus*, *Tamiobatis*, *Akmonistion*, *Cladodoides*, *Cladoselache*, and *Pucapampella*), as well as in *Tristychius* and a hybodontiform from Madagascar (Thomson, 1982), and may be primitive for chondrichthyans. However, the postorbital articulation of Paleozoic chondrichthyans is with the posterior part of the lateral commissure, whereas in *Tristychius* and the Madagascar hybodontiform, it is with the ventral part of the lateral commissure. In most hybodontiforms currently known, and in all neoselachians, a postorbital articulation with the lateral commisure is absent (character state 1).

**Character 28:** *Postorbital articulation with primary postorbital process absent=0; present=1.* [N]. A postorbital articulation between the palatoquadrate and the primary postorbital process (the dorsal component of the postorbital process) occurs in extant hexanchiform sharks such as *Notorynchus* (character state 1), as well as in some fossil neoselachians (e.g., *Synechodus*). It is absent in all other chondrichthyans (character state 0) (Maisey, 2008).

**Character 29:** *Lateral dorsal aortae enter basicranial cartilage prior to junction with efferent hyoidean artery=0; lateral dorsal aortae do not enter basicranial cartilage prior to junction with efferent hyoidean artery=1.* [N]. The lateral dorsal aortae enter the basicranial cartilage posterior to their junction with the efferent hyoidean artery (character state 0) in Paleozoic chondrichthyans (e.g., *Pucapampella*, *Orthacanthus*, *Tamiobatis*, *Cladodoides*, *Cladoselache*, and *Akmonistion*), as well as in the

hybodontiform *Tribodus*. The lateral dorsal aortae do not enter the basicranial cartilage prior to meeting the efferent hyoidean artery in other known hybodontiforms, *Tristychius*, holocephalans, and neoselachians (character state 1).

**Character 30:** *Lateral dorsal aortae enter braincase at level of occipital block through single posterior foramen=0; through paired foramina=1.* [N]. The lateral dorsal aortae enter the braincase through paired posterior openings (character state 1) in *Orthacanthus*, *Tamiobatis*, *Cladodoides*, and *Pucapampella* (Schaeffer, 1981; Maisey, 2001, 2005). The lateral dorsal aortae enter the braincase through a single posterior opening (character state 0) in *Akmonistion* and *Cladoselache*, although in *Cladoselache* the single posterior opening diverges to form paired foramina a short distance anteriorly (Coates and Sequeira, 1998; Maisey, 2007). In holocephalans, *Tristychius*, hybodonts and neoselachians, the lateral dorsal aortae do not enter the braincase posteriorly (scored here as "-", "inapplicable").

**Character 31:** *Lateral dorsal aortae enter basicranium at level of occipital block present=0; absent=1.* [N]. The lateral dorsal aortae enter the basicranium posteriorly (at the level of the occipital block) in Paleozoic chondrichthyans (e.g., *Orthacanthus*, *Tamiobatis*, *Cladodoides*, *Akmonistion*, *Cladoselache*, and *Pucapampella* (character state 0). In holocephalans, *Tristychius*, hybodonts (including *Tribodus*), and neoselachians, the lateral dorsal aortae do not enter the braincase at the level of the occipital block (character state 1).

**Character 32:** *Lateral dorsal aortae extend laterally to meet efferent hyoidean arteries (forming a "Bell-shaped" basicranial arterial circuit) absent=0; present=1.* [JM; G]. In neoselachians, the lateral dorsal aortae turn outward laterally to form an acute angle between the internal carotid artery and the efferent hyoidean artery (character state 1) (Schaeffer, 1981). In contrast, in other chondrichthyans (except *Pucapampella*), the basicranial arterial circuit is elongated anteroposteriorly to form a spindle-shaped loop (Schaeffer, 1981), the lateral dorsal aortae do not extend laterally, and the efferent hyoidean arteries branch off directly from the anteroposteriorly oriented lateral dorsal aortae (character state 0). In *Pucapampella*, considered a basal chondrichthyan, the basicranial arterial circuit is bell-shaped as in extant neoselachians (character state 1), and the lateral dorsal aortae curve outward laterally (indicated by mediolaterally directed grooves in the basicranial cartilage) to meet the efferent hyoidean arteries (Maisey, 2001).

**Character 33:** *Inflated and elongate jugular canal ( i.e., jugular canal extends posteriorly to midpoint of otic region) absent=0; present=1.* [CG; M]. The jugular canal is wide and elongate (passing through an anteroposteriorly broad postorbital process from the posterior of the orbit to the midpoint of the otic region) in many hybodonts, including *Onychoselache*, *Hamiltonichthys*, *Hybodus*, *Egertonodus*, and *Acrodus* (character state 1). This feature is absent (character state 0) in *Tribodus*, *Tristychius* and Paleozoic chondrichthyans, in which the jugular canal passes through the postorbital process but the process and canal are relatively narrow anteroposteriorly. It is also absent in holocephalans and most neoselachians, in which the lateral commissure is not chondrified

to contain the jugular vein. This feature has been considered a synapomorphy of hybodonts (Maisey, 1989; Maisey et al., 2004), suggesting that its absence in *Tribodus* may be secondary. The feature is unknown in remaining hybodont taxa (e.g., *Lissodus*, *Lonchidion*, *Paleobates*, and *Asteracanthus*).

**Character 34:** *Ethmoidal articulation present=0; absent=1.* [JGM]. An ethmoidal articulation (in which the anterior part of the palatoquadrate articulates with the ethmoid region of the braincase via articular facets) is present (character state 0) in some hybodonts, including *Onychoselache*, *Hamiltonichthys*, *Egertonodus*, *Hybodus*, and *Acrodus*. It is also found in extant *Heterodontus* and galeomorphs (e.g., *Carcharhinus*), as well as in *Tristychius* and all known Paleozoic chondrichthyans, and has been considered primitive for chondrichthyans. An ethmoidal articulation was apparently absent (character state 1) in *Tribodus*, and probably also *Asteracanthus*, in which ethmoidal facets on the palatoquadrate are absent, and the jaws appear short compared to those of most other hybodonts (although in the absence of preserved cranial material, this remains uncertain). This feature may also have been absent in *Lissodus* and *Lonchidion*, in which the jaws are short and may not have reached the ethmoid region (Maisey et al., 2004). An ethmoidal articulation is also absent in extant batoids and squalean sharks such as *Squalus*. Ethmoidal articular facets are lacking in advanced galeomorphs (i.e., lamnids). However, in these taxa the palatoquadrate is attached to the ethmoid region via an ethmopalatine or palatonasal ligament, and the jaws extend anteriorly beneath the ethmoid region. In *Squalus*, an ethmopalatine ligament is present, but is associated with the orbital (=palatobasal) articulation. Although an ethmopalatine ligament may have

been present in *Tribodus* (see Thesis part II, Descriptive Morphology, section on the visceral skeleton), it is questionable whether this could be classified as an ethmoidal articulation (particularly because the jaws do not extend to the ethmoid region). This character is scored as "inapplicable" ("-") in holocephalans, in which the primitive jaw articulations have become obscured by fusion of the braincase and palatoquadrate.

**Character 35:** *Palatobasal articulation absent=0; present=1.* [CS01]. A palatobasal (=basitrabecular) articulation is present (character state 1) in *Pucapampella* as well as in osteichthyans and *Acanthodes*, and has been considered as probably primitive for chondrichthyans (Maisey, 2001; Maisey and Anderson, 2001). The palatobasal articulation has also been considered homologous with the orbital articulation of orbitostylic sharks (Maisey, 2008). A palatobasal articulation is present in extant *Squalus* and *Notorynchus*, as well as in Paleozoic sharks including *Cladodoides*, ctenacanths, and *Orthacanthus*. It is also present in *Tristychius* and in hybodontiforms including *Tribodus*, *Onychoselache*, *Hamiltonichthys*, *Hybodus*, *Egertonodus*, *Acrodus*, and possibly *Asteracanthus* (although in the latter this is not known with certainty). A palatobasal articulation is absent (character state 0) in some neoselachians, including batoids, *Heterodontus*, and galeomorphs (e.g., *Carcharhinus*). For the present analysis, this character is scored as "inapplicable" ("-") in holocephalans, although it has been suggested that a palatobasal articulation may be primitively present in holocephalans but hidden by their holostylic condition (i.e., fusion of the upper jaw and braincase) (Grogan et al., 1999; Maisey, 2001).

**Visceral Skeleton**

**Character 36:** *Mandibular joint located behind occiput. present=0; absent=1.* [N]. The mandibular joint between the palatoquadrate and Meckel's cartilage is located behind the occiput (character state 0) in archaeostylic and amphistylic sharks, including Paleozoic sharks (e.g., *Cladodoides*, ctenacanths, *Akmonistion*, *Cladoselache*, and *Orthacanthus*) and extant hexanchoids (e.g., *Notorynchus*). The mandibular joint is located below or anterior to the occiput (character state 1) in hybodonts, *Tristychius*, holocephalans, and non-hexanchoid neoselachians (e.g., batoids, *Squalus*, *Heterodontus*, and galeomorphs).

**Character 37:** *Upper jaw not fused with neurocranium=0; upper jaw fused to neurocranium (holostyly)=1.* [CS01]. The upper jaw (palatoquadrate) is fused to the neurocranium in holocephalans, which have a holostylic jaw suspension (character state 1). In all other chondrichthyans, the upper jaw is free and is not fused to the neurocranium (character state 0).

**Character 38:** *Jaws extend to ethmoid region=0; jaws do not extend to ethmoid region=1.* [N]. The jaws extend anteriorly beneath the ethmoid region of the braincase (character state 0) in Paleozoic chondrichthyans (e.g., *Pucapampella*, ctenacanths, *Akmonistion*, *Cladoselache*, *Orthacanthus*, and *Diplodoselache*), as well as in *Tristychius*, many hybodonts (e.g., *Onychoselache*, *Hamiltonichthys*, *Hybodus*, *Egertonodus*, and *Acrodus*), and some neoselachians (e.g., hexanchiforms, *Heterodontus*, and galeomorphs). The jaws do not extend to the ethmoid region (character state 1) in *Tribodus* (and possibly also *Asteracanthus*), batoids, and some squalean sharks (e.g.,

*Squalus*). This character is scored as "inapplicable" ("-") in holocephalans, where the palatoquadrate and braincase are fused. The character is unknown in the hybodonts *Lissodus*, *Lonchidion*, and *Palaeobates*, although there is some evidence that at least the former two taxa may have had shortened jaws that did not reach the ethmoid region (Maisey et al., 2004).

**Character 39:** *Palatoquadrates separated symphysially by ethmoid region=0; palatoquadrates meet or are fused symphysially=1***.** [N]. Palatoquadrates separated symphysially by the ethmoid region are present (character state 0) in some Paleozoic sharks (e.g., *Pucapampella*, ctenacanths, *Akmonistion*, and *Orthacanthus*), as well as in some hybodonts (e.g., *Hamiltonichthys*, *Hybodus*, *Egertonodus*, and *Acrodus*). Palatoquadrates that meet or are fused symphysially (character state 1) are present in *Tribodus* and probably *Asteracanthus*, as well as in *Tristychius* and neoselachians (e.g., *Heterodontus*, *Squalus*, batoids, galeomorphs. The character is scored as "inapplicable" ("-") in holocephalans, in which the palatoquadrates are obscured by fusion with the braincase.

**Character 40:** *Quadrate flange extends anterolaterally to overhang adductor fossa absent=0; present=1.* [JGM87]. The quadrate flange of the palatoquadrate extends anterolaterally to overhang the fossa for the adductor mandibularis muscle (character state 1) in hybodontiforms (including *Onychoselache*, *Hamiltonichthys*, *Lissodus*, *Palaeobates*, *Tribodus*, *Hybodus*, *Egertonodus*, *Acrodus*, and *Asteracanthus*) and *Tristychius*. This feature is absent (character state 0) in other chondrichthyans (including

neoselachians, Paleozoic elasmobranchs, and holocephalans), in which the quadrate flange does not curve forward to overhang the adductor fossa.

**Character 41:** *Palatoquadrate otic process expanded dorsally behind postorbital process present=0; absent=1.* [CG]. The palatoquadrate otic process is expanded dorsally behind the postorbital process (character state 0) in archaeostylic and amphistylic sharks (which have a posterior postorbital articulation), including Paleozoic sharks and extant hexanchoid neoselachians (e.g., *Notorynchus*). The palatoquadrate otic process is not expanded dorsally behind the postorbital process (character state 1) in hybodonts, *Tristychius*, and non-hexanchoid neoselachians. This character is scored as "inapplicable" ("-") in holocephalans due to fusion of the palatoquadrate with the braincase.

**Character 42:** *Palatoquadrate "cleaver-shaped" present=0; absent=1.* [Janvier, 1998]. The palatoquadrate is "cleaver-shaped" (i.e., having a dorsoventrally narrow palatine region anteriorly, with an abruptly thicker quadrate region behind the postorbital process) in Paleozoic chondrichthyans with an archaeostylic jaw suspension (character state 0). The palatoquadrate is not "cleaver-shaped" in hybodonts, *Tristychius*, and neoselachians (including amphistylic hexanchoids).

**Character 43:** *Orbital process of palatoquadrate extends into orbit between optic pedicel and optic nerve foramen. absent=0; present=1.* [S]. The orbital (=palatobasal) process of the palatoquadrate extends into the orbit between the optic pedicel and optic

nerve foramen (character state 1) in extant orbitostylic sharks (e.g., *Squalus*; *Notorynchus*). This feature is absent (character state 0) in all other chondrichthyan taxa.

**Character 44:** *Labial cartilage complex extends from ethmoid region to postorbital process: absent=0; present=1.* [N]. An enlarged labial cartilage complex comprising up to five broad labial cartilages and extending the entire length of the jaws (from the ethmoid region to the level of the postorbital process) is present (character state 1) in some hybodontiforms (including *Egertonodus*, *Hybodus*, and *Acrodus*). It is absent (character state 0) in other hybodontiforms (including *Tribodus*, *Onychoselache*, and probably *Asteracanthus*), *Tristychius*, and neoselachians, and no evidence of an enlarged labial cartilage complex has been found in Paleozoic chondrichthyans. Large labial cartilages also occur in holocephalans, but they are limited to the anterior of the jaws and do not extend from the ethmoid region to the postorbital process.

**Character 45:** *Hyomandibula decoupled from ceratohyal: absent=0; present=1.* [S]. The hyomandibula is decoupled from the ceratohyal in most batoids except torpedinoids (character state 1) (Shirai, 1992). In taxa where this character is present, the ceratohyal and basihyal are also often reduced or absent. In all other chondrichthyans, the hyomandibular articulates with the ceratohyal (character state 0).

**Character 46:** *Basihyal forms a wide transverse bar: absent=0; present=1.* [Maisey and Carvalho, 1997]. The basihyal forms a mediolaterally wide, transversely directed bar (character state 1) in extant batoids and some orbitostylic sharks (e.g., *Squalus*), and this

feature is also present in the hybodontid *Tribodus*. It is absent (character state 0) in other known hybodonts (e.g., *Egertonodus basanus*, *Hybodus hauffianus*, *Hybodus reticulatus*, *Hybodus delabechei*), in which the basihyal is broad both mediolaterally and anteroposteriorly, forming a trapezoidal shape. This feature is also absent in extant galeomorphs (e.g., *Carcharhinus*) and *Heterodontus*, as well as in holocephalans. It is unknown in all of the Paleozoic chondrichthyans examined for the present study.

**Character 47:** *Hyoid rays elongate supporting opercular flap: absent=0; present=1.* [CS01]. The hyoid arch bears elongate rays supporting an opercular flap (character state 1) in *Akmonistion*, *Cladoselache*, *Orthacanthus*, *Tristychius*, and the extant neoselachian *Chlamydoselachus*. This feature is absent (character state 0) in hybodontiforms and most other neoselachians (including extant *Heterodontus*, galeomorphs, batoids, and many orbitostylic sharks).

**Character 48:** *Operculum supported by opercular cartilage absent=0; present=1.* [G]. An operculum supported by an opercular cartilage is a synapomorphy of holocephalans (character state 1). It is absent in other chondrichthyan taxa (character state 0).

**Character 49:** *Branchial arches beneath rear of neurocranium. absent=0; present=1.* [CG]: absent in *Tribodus*. Absent in *Onychoselache* and hybodontoids. Present in *Tristychius*. Branchial arches that extend beneath the rear of the neurocranium have been considered a characteristic feature of holocephalans, and are also present in *Tristychius* (character state 1). They are absent in other chondrichthyans (character state 0), in which

the branchial arches are posterior to the braincase, and this absence is probably primitive for chondrichthyans.

**Character 50:** *Posteriormost pharyngobranchials unfused=0; fused=1.* [C]. The posteriormost pharyngobranchials are fused together (the posteriormost pharyngobranchial is typically fused to the posteriormost epibranchial and penultimate pharyngobranchial) in most extant neoselachians to form a "gill pickaxe" (character state 1). This feature has been previously considered as a synapomorphy uniting elasmobranchs (e.g., Daniel, 1934: de Carvalho, 1996), but fossil non-neoselachian elasmobranchs lack this feature. The fusion of the posterior pharyngobranchials is incomplete in *Heterodontus*, hexanchoids, and *Chlamydoselachus*, as well as some batoids (e.g., *Narcine*) (Shirai, 1992; Carvalho, 1996), although the pharyngobranchial and epibranchial elements involved do contact each other and partial fusion may occur. Fused pharyngobranchials (the last three pharyngobranchials and last two epibranchials) also occur in living and fossil holocephalans (Didier, 1995; Carvalho, 1996). Carvalho (1996) reported that fossil hybodonts lack fused posterior pharyngobranchials (character state 0), and the present study confirms this finding. Fused posterior pharyngobranchials are also apparently absent in *Akmonistion* (Coates and Sequeira, 1998) and *Orthacanthus*.

**Character 51:** *Pharyngobranchial blade absent=0; present=1.* [C]. According to Shirai (1992), the pharyngobranchial blade (an angular, posteroventrally directed projection at the proximal end of the pharyngobranchial, on which the arcualis dorsalis and interpharyngobranchialis muscles originate: de Carvalho, 1996) is present (character state

1) in extant galeomorphs, and its absence (character state 0) is synapomorphic for squalean sharks (including hexanchiforms) and batoids. Shirai (1992) also states that a pharyngobranchial blade is present in *Tristychius* and some species of *Hybodus*. However, Carvalho (1996) and Carvalho and Maisey (1996) argued that only galeomorphs show evidence of this character. New evidence from well-preserved pharyngobranchials of *Tribodus limae* described for the first time in the present Thesis (see Part II, Descriptive Morphology) confirm the presence of a pharyngeal blade in that taxon, indicating that at least some fossil hybodonts possess a pharyngobranchial blade. This feature was also observed to be present (character state 1) in *Tristychius* (as originally suggested by Shirai, 1992), *Lissodus cassangensis*, and *Hybodus hauffianus*, as well as in the extant galean sharks *Heterodontus* and *Carcharhinus*, and there is some evidence for its presence in *Orthacanthus*. It is absent (character state 0) in extant batoids and orbitostylic sharks (including *Squalus* and *Notorynchus*), as well as in holocephalans and *Akmonistion*. It is unknown in most other fossil chondrichthyans.

**Character 52:** *Most hypobranchials directed posteriorly towards the midline absent=0; present=1.* [JM]. Maisey (1984) listed presence of this character as uniting xenacanths and living elasmobranchs. Although the branchial skeleton is rarely preserved in fossil chondrichthyans, it is well enough preserved in a few specimens to determine that hypobranchials directed posteriorly towards the midline were present (character state 1) in *Tristychius* and the hybodontids *Hamiltonichthys mapesi*, *Hybodus hauffianus*, *Hybodus reticulatus*, and *Hybodus delabechei*, as well as in extant neoselachians. This feature is absent (character state 0) in holocephalans, *Cladoselache*, and *Akmonistion*.

**Character 53:** *Basibranchials separated from basihyal by a gap: absent=0; present=1.* [JM; Nelson, 1969]. This character was used by Maisey (1984) as one of five features uniting xenacanths and extant neoselachians. The basibranchials (the ventralmost elements of the branchial arches) are separated from the basihyal by a gap (character state 1) in neoselachians and in the hybodontids *Hybodus reticulatus* and *Egertonodus basanus*. It is unknown in other hybodonts and in most fossil chondrichthyans due to poor preservation. The basibranchials are not separated from the basihyal (character state 0) in holocephalans, *Cladoselache*, and *Akmonistion*.

**Character 54:** *Posteriorly directed median basibranchial copula absent=0; present=1.* [JM]. Maisey (1984) used the presence of this character to unite symmoriiforms, chimaeroids, and extant neoselachians. The basibranchial copula (a large median cartilage located posteriorly in the branchial skeleton, visible in ventral view) is directed posteriorly (character state 1) in neoselachians, holocephalans, *Tristychius*, and hybodontids (including *Hamiltonichthys*, *Hybodus hauffianus*, and *Hybodus reticulatus*). This feature is absent (character state 0) in at least some Paleozoic chondrichthyans (e.g., *Akmonistion* and *Orthacanthus*). It is unknown in most other fossil chondrichthyans due to poor preservation.

## Paired Fins and Girdles

**Character 55:** *Scapular process narrow dorsally and lacking posterolateral angle. absent=0; present=1.* [CG]: this character is present in *Tribodus*. This character is shared

by hybodonts and neoselachians (character state 1), but absent (character state 0) in *Tristychius* and in Paleozoic chondrichthyans including *Akmonistion*, *Plesioselachus* (Coates and Gess, 2007) and *Orthacanthus*, in which a posterolateral angle is present.

**Character 56:** *Scapulocoracoid with a continuously concave anteromedial edge (coracoid anterodorsal shoulder reduced or absent). absent=0; present=1.* [CG]: present in *Tribodus*. A scapulocoracoid with a continuously concave anteromedial edge is present (character state 1) in hybodontiforms and neoselachians, and is absent (character state 0) in some Paleozoic chondrichthyans (Coates and Gess, 2007), including *Orthacanthus*.

**Character 57:** *Imperforate scapulocoracoid, foramen for diazonal nerves and blood vessels missing. absent=0; present=1.* [CG]: absent in *Tribodus*. According to Coates and Gess (2007), absence of a diazonal foramen in *Tristychius* may represent an autapomorphy. However, these authors point out that a damaged area on the specimen may in fact be a remnant of this foramen, and it may also be possible that the foramen is on a part of the fossil not visible in the preserved view, such as its posterior surface. The alternative would be that the fundamental innervation and vascularization patterns of the pectoral fin had become highly modified in *Tristychius*, so that nerves and blood vessels skirted around the scapulocoracoid instead of passing through it. Diazonal foramina are certainly present in *Onychoselache* and hybodontoids (Maisey, 1982, 1989; Coates and Gess, 2007). However, the extant hexanchiform *Heptranchias* has only two (lateral and medial) diazonal foramina.

**Character 58:** *Coracobranchial fossa (grooved leading edge) on scapulocoracoid. absent=0; present=1.* [CG]: possibly present in *Tribodus*. Although the anterodorsal margin of the scapular process is damaged in AMNH FF 13958, it does show a slight indentation which may be evidence of a coracobranchial fossa, and a similar indentation is also present in AMNH FF 13961. However, the anteroventral edge of the scapular process is smoothly rounded, indicating that even if a coracobranchial fossa was present in *Tribodus*, it did not extend as far ventrally as in other hybodontoids. A coracobranchial fossa has been reported in *Onychoselache* by Coates and Gess (2007), as well as in *Lissodus* and *Hybodus* (Maisey, 1982), and its occurrence in *Tribodus* would be consistent with earlier views of hybodont phylogeny (Maisey et al., 2004; Coates and Gess, 2007). This feature is absent in *Tristychius* and neoselachians (Coates and Gess, 2007).

**Character 59:** *Pectoral fin articulation on lateral face of coracoid absent=0; present=1.* [CG]. The pectoral fin articulation extends onto the lateral face of the coracoid (character state 1) in some Paleozoic chondrichthyans including *Cladoselache*, symmoriiforms (e.g., *Akmonistion*), and *Diplodoselache*, as well as in the hybodontiform *Onychoselache* (Coates and Gess, 2007) and in extant batoids (probably lost and secondarily regained in the latter). The pectoral fin articulation is located on the posterior face of the coracoid (character state 0) in holocephalans, ctenacanths, *Orthacanthus*, *Tristychius*, hybodontiforms, and most neoselachians.

**Character 60:** *Coracoid and scapular regions of near-equal length absent=0; present=1.* [modified from CG and M]. Coates and Gess (2007) retained the character "coracoid and scapular regions of subequal length" from Maisey (1989) and Maisey et al. (2004), which supposedly unites most hybodontoids but excludes *Hamiltonichthys*. However, the character itself is ambiguous, and requires a more precise definition. Maisey (1989) differentiated *Hamiltonichthys* from Mesozoic hybodontoids in that in *Hamiltonichthys*, the coracoid region is only one-third the length of the scapular region, whereas in Mesozoic hybodontoids, the two regions are of near-equal length. However, no specific point of reference for this measurement was identified, and if the metapterygium is used as the point of reference, it could be argued that the scapular and coracoid regions of *Hamiltonichthys* are of near-equal length. Although the scapular and coracoid regions seem superficially to be nearly equal in Mesozoic hybodontoids, as the new material of *Tribodus* demonstrates (especially AMNH FF 13958), only three-dimensionally preserved material accurately displays the position of the pectoral articulation. The articular process is the default landmark generally used to distinguish the scapular and coracoid regions; thus, its position must be accurately determined before these regions can be defined. Additionally, wherever the articular process is angled ventromedially, it is necessary to identify a more specific landmark on this process from which accurate measurements of the scapular and coracoid regions can be made. If the propterygial facet (the only part of the articular process typically visible in laterally preserved specimens) is used, then all hybodontoids have a coracoid process that is approximately 70-80% of the scapular process, indicating that this character is inconclusive for differentiating members of this group. Although the metapterygial facet

would probably be a more accurate landmark (because the metapterygium forms developmentally as an outgrowth of the scapulocoracoid), for preservational reasons its true position is unknown in hybodontoids other than *Tribodus*. Although the scapular and The coracoid region is shorter than the scapular region (equaling one third of its length or less) in Paleozoic chondrichthyans, *Tristychius*, holocephalans, basal hybodontiforms (e.g., *Onychoselache* and *Hamiltonichthys*), and batoids (character state 0). The coracoid and scapular regions are equal or near-equal in length (character state 1) in Mesozoic hybodonts (e.g., *Lissodus*, *Tribodus*, *Hybodus*, *Egertonodus*) and most extant neoselachians.

**Character 61:** *Shoulder girdle fused with vertebral column: absent=0; present=1.* [S]. The shoulder girdle is fused with the vertebral column (character state 1) in extant rajiform batoids (e.g., *Dasyatis*) (Shirai, 1992). This character is absent (character state 0) in other chondrichthyan taxa.

**Character 62:** *Tribasal pectoral fin absent=0; present=1.* [CS01]. A tribasal pectoral fin (in which the fin skeleton comprises three basal cartilages articulating proximally with the scapulocoracoid) is present (character state 1) in hybodonts, neoselachians, ctenacanths, and some xenacanths (e.g., *Orthacanthus* and *Diplodoselache*). A tribasal fin is absent in holocephalans, *Tristychius*, symmoriiforms (e.g., *Akmonistion*: Coates and Sequeira, 1998), and *Cladoselache* (Bendix-Almgreen, 1975). This feature is unknown in *Pucapampella*. In some extant squalean sharks, some or all of the pectoral basals may be

secondarily fused to produce a fin of "dibasal" (e.g., *Oxynotus*, *Somniosus*) or "unibasal" (e.g., *Echinorhinus*, *Squaliolus*) appearance (Shirai, 1992).

**Character 63:** *Dibasal fin, no separate mesopterygium. absent=0; present=1.* [CS01; CG]: absent in *Tribodus*. According to Coates and Gess (2007), this character appears to be an autapomorphy of *Tristychius*, which supposedly has a pectoral fin comprising only a propterygium and metapterygium. A dibasal fin also occurs in extant chimaeroids, but probably represents an independent autapomorphy of that group. In most most neoselachians, hybodontiforms, 'ctenacanths,' and some xenacanths, the fin is tribasal, having a propterygium, mesopterygium, and metapterygium.

**Character 64:** *Pectoral articular surface oriented horizontally=0; oriented obliquely=1.* [N]. The articular surface for the pectoral fin on the scapulocoracoid is oriented horizontally (character state 0) in *Cladoselache*, symmoriiforms (e.g., *Akmonistion*), *Diplodoselache*, and batoids (probably secondarily derived in the latter). The pectoral articular surface is oriented obliquely (character state 1) in holocephalans, *Orthacanthus*, ctenacanths, *Tristychius*, hybodontiforms, and most neoselachians.

**Character 65:** *Propterygium with convex leading edge. absent=0; present=1.* [CG]: present in *Tribodus*. This character is also found in *Onychoselache* (according to Coates and Gess, 2007) and hybodontoids (e.g., *Hamiltonichthys*, *Lissodus*, *Hybodus*, *Egertonodus*, Maisey, 1982, 1989), and may be a synapomorphy of hybodontiforms other than *Tristychius*.

**Character 66:** *Mesopterygium sickle-shaped. absent=0; present=1.* [CG]: Coates and Gess (2007) suggest that this may be an autapomorphy of *Onychoselache*. It is present (character state 1) in *Onychoselache*, and absent (character state 0) in other hybodonts, Paleozoic chondrichthyans, and neoselachians examined for the present study.

**Character 67:** *Metapterygium connecting with distinct series of distal radials articulating proximodistally to form an axis: absent=0; present=1.* [CS98]. The metapterygium connects distally with a series of distal radials to form a long axis (often referred to as a "metapterygial axis") in many Paleozoic chondrichthyans, including symmoriiforms, Cladoselache, ctenacanths, and xenacanths (character state 1). In symmoriiforms, it is often extensive, forming an elongated whip. The metapterygium does not articulate with a series of axial radials in neoselachians or hybodonts (character state 0).

**Character 68:** *Premetapterygial radials articulate with compound basal cartilages absent=0; present=1.* [JM; G]. Basal cartilages anterior to the metapterygium (i.e., a propterygium and/or mesopterygium) and articulating with premetapterygial radials are present (character state 1) in neoselachians, holocephalans, hybodonts, *Tristychius*, ctenacanths, *Orthacanthus*, and *Diplodoselache*. They are absent (character state 0) in symmoriiforms (e.g., *Akmonistion*) and *Cladoselache*. This character remains unknown in *Pucapampella*.

**Character 69:** *Puboischiadic bar in males. absent=0; present=1.* [CG; M]: A puboischiadic bar (i.e., a single, continuous bar of cartilage, fused at the midline, and forming the pelvic girdle) is present (character state 1) in male *Hamiltonichthys*, and in Mesozoic hybodontoids and neoselachians of both sexes. It is absent (character state 0) in female *Hamiltonichthys*, and in *Onychoselache*, *Tristychius*, holocephalans, and Paleozoic chondrichthyans, which instead have two unfused half-girdles, one on each side of the body.

**Character 70:** *Puboischiadic bar in females. absent=0; present=1.* [CG; M]: A puboischiadic bar is present (character state 1) in *Lissodus* and other Mesozoic hybodontoids. It is absent (character state 0) in *Hamiltonichthys*, *Onychoselache*, *Tristychius*, holocephalans, and Paleozoic chondrichthyans, which instead have a pair of unfused half-girdles.

**Character 71:** *First pelvic radial (propterygium) enlarged relative to other radials. absent=0; present=1.* [CG; M]: The anteriormost pelvic radial, or pelvic propterygium, is two or more times larger than subsequent radials (character state 1) in *Onychoselache* and other hybodontiforms, and in neoselachians. The anteriormost pelvic radial is equal in size to the other radials (character state 0) in *Tristychius*, holocephalans, and Paleozoic chondrichthyans.

**Character 72:** *Pelvic propterygium terminal, no distal cartilages. absent=0; present=1.* [CG]. The pelvic propterygium is terminal (i.e., lacking any distal radials) in *Lissodus*

and other Mesozoic hybodonts, and in ctenacanths and *Diplodoselache* (character state 1). The pelvic propterygium is not terminal, and bears distal radials (character state 0), in *Hamiltonichthys*, *Onychoselache*, most neoselachians, holocephalans, and some Paleozoic sharks (e.g., *Akmonistion* and *Orthacanthus*).

**Character 73:** *Pelvic metapterygium articulates with all but the first few radials: absent=0; present=1.* [JM; G]. The pelvic metapterygium articulates with all but the anteriormost radials (character state 1) in hybodontiforms, *Tristychius*, ctenacanths, holocephalans, and neoselachians. This feature is absent (character state 0) in *Cladoselache*, *Akmonistion*, and xenacanths, in which the pelvic girdle carries a larger proportion of radials than does the pelvic metapterygium. The state of this character is unknown in *Pucapampella*.

**Axial Skeleton**

**Character 74:** *Calcified pleural ribs. absent=0; present=1.* [CG; M]: present in *Tribodus*. Calcified pleural ribs are present (character state 1) in hybodontiforms, *Tristychius*, ctenacanths, and *Orthacanthus*. They are absent (character state 0) in *Akmonistion*, *Cladoselache*, *Diplodoselache*, holocephalans, and neoselachians. Pleural ribs differ from axial ribs in that they curve ventrally, following the course of the body cavity, rather than passing through the horizontal skeletogenous septum as in extant neoselachians.

**Character 75:** *Low number (10–12) of pleural ribs. absent=0; present=1.* [CG; M; MEA]: present in *Tribodus*. A low number of pleural ribs (between 10 and 12) is present in *Hamiltonichthys* and Mesozoic hybodontids. It is absent in *Onychoselache*, *Tristychius*, ctenacanths, and *Orthacanthus*, in which numerous ribs are present. Calcified pleural ribs are absent in other chondrichthyans (see character 76).

**Character 76:** *Vertebral column includes calcified chordal centra: absent=0; present=1.* [G; JM]. A vertebral column including calcified chordal centra has been considered a synapomorphy of neoselachians. It is present (character state 1) in all neoselachian taxa, including batoids, orbitostylic sharks, *Heterodontus*, and galeomorphs. Calcified chordal centra are absent (character state 0) in all other chondrichthyans.

**Character 77:** *Anterior vertebral arcualia unfused=0; fused to form synarcual=1.* [G]. The anterior arcualia of the vertebral column are fused to form a synarcual in extant batoids and holocephalans (character state 1), but it is likely that these two states are independently derived. This feature is absent (i.e., vertebral elements remain unfused) in other chondrichthyans (character state 0).

**Character 78:** *Anterior dorsal fin absent=0; present=1.* [N]. The anterior dorsal fin is present (character state 1) in many chondrichthyans, including hybodonts, Paleozoic chondrichthyans, holocephalans, and most neoselachians (e.g., *Heterodontus*, galeomorphs, most squaleans: Shirai, 1992). The anterior dorsal fin is absent or greatly reduced (character state 0) in some extant batoids including some torpedinoids, rajoids

and myliobatoids; however, some fossil batoids possess two dorsal fins, and the loss of one or both dorsal fins in batoids has therefore been considered derived (Shirai, 1992; Carvalho, 1996). Extant *Chlamydoselachus* and hexanchoids have a single dorsal fin. It is probable that in the former, this fin is homologous with the posterior dorsal fin of other sharks; however, in the latter the fin is farther anterior and its homology is uncertain (although Shirai, 1992, suggests it may be homologous to an anterior dorsal fin).

**Character 79:** *Anterior dorsal fin base plate uncalcified=0; calcified=1.* [CS01]. The cartilaginous basal plate of the anterior dorsal fin is calcified (character state 1) in hybodonts, some Paleozoic sharks (e.g., ctenacanths, *Akmonistion*), holocephalans, and many neoselachians (e.g., *Carcharhinus*, *Heterodontus*, *Squalus*). The anterior dorsal fin base plate is not calcified (character state 0) in some batoids (e.g., *Dasyatis*), in which an anterior dorsal fin is lacking.

**Character 80:** *Posterior dorsal fin absent=0; present=1.* [N]. A distinct posterior dorsal fin is present (character state 1) in many chondrichthyan groups, including many Paleozoic sharks (e.g., *Cladoselache*, symmoriiforms, and ctenacanths), hybodonts, and some neoselachians (e.g., *Heterodontus*, galeomorphs, orbitostylic sharks). It is absent (character state 0) in xenacanths (which have a single, elongated dorsal fin and anterior dorsal fin spine) and in some batoids (e.g., *Dasyatis*).

**Character 81:** *Posterior dorsal fin base plate uncalcified=0; calcified=1.* [CS01]. The posterior dorsal fin base plate is calcified (character state 1) in hybodonts in which the

posterior dorsal fin is known, as well as in many neoselachians (e.g., *Carcharhinus*, *Heterodontus*, *Squalus*). The posterior dorsal fin base plate is uncalcified (character state 0) in holocephalans, some Paleozoic sharks (e.g., *Akmonistion*, *Cladoselache*, and xenacanths), and some batoids (e.g., *Dasyatis*).

**Character 82:** *Complete series of perichondrally calcified radials in anterior dorsal fin absent=0; present=1.* [JM; G]. An anterior dorsal fin with a complete series of perichondrally calcified radials is present in many neoselachians, including *Heterodontus*, galeomorphs, and orbitostylic sharks. It is absent in some batoids (e.g., *Dasyatis*), which lack an anterior dorsal fin. It is also absent in hybodonts and Paleozoic sharks. In hybodonts, the anterior dorsal fin comprises only a base-plate and one or two calcified radials.

**Character 83:** *Single dorsal fin elongate, extending from near pectoral level to anal or pre-anal fin level absent=0; present=1.* [CS01]. A single, elongate dorsal fin extending from near the level of the pectoral fin to near the level of the anal fin is present (character state 1) in xenacanths and holocephalans (possibly independently derived). It is absent (character state 0) in other chondrichthyans.

**Character 84:** *Anal fin absent=0; anal fin present=1.* [CS01]. An anal fin is absent (character state 0) in some Paleozoic chondrichthyans (e.g., *Akmonistion*, *Cladoselache*), and in some extant neoselachians (e.g., some squalean sharks, *Squatina*, pristiophorids, and rajiforms: Shirai, 1992). It is present (character state 1) in ctenacanths, xenacanths,

holocephalans, hybodonts, and some neoselachians (e.g., *Heterodontus*, all galeomorphs, *Chlamydoselachus*, and hexanchoids: Shirai, 1992). In xenacanths, the anal fin is often duplicated to contain two fin endoskeletons in close succession.

**Character 85:** *Anal fin with double base-plate absent=0; present=1.* [CS01]. The anal fin has a bipartite or "double" base-plate (comprising two basal cartilages) in some hybodontiforms, including *Hamiltonichthys*, *Lissodus cassangensis*, *Lissodus africanus*, and *Hybodus hauffianus* (character state 1). The state of the anal fin is unknown in other hybodonts except *Onychoselache*, in which this character is absent (character state 0) and the anal fin comprises only a single base-plate. The anal fin is also present but lacks a double base-plate in *Tristychius*, ctenacanths, xenacanths, holocephalans, *Heterodontus*, and galeomorphs (e.g., *Carcharhinus*). The anal fin comprises a single base-plate in Heterodontus, and several smaller base-plates in hexanchoids (Shirai, 1992). The anal fin contains only segmented radials in galeomorphs such as *Carcharhinus* (Shirai, 1992). An anal fin is absent in *Akmonistion*, *Cladoselache*, and some extant neoselachians (see character 86 above).

**Character 86:** *Semilunate tail with well-developed hypaxial endoskeleton present=0; absent=1.* [Modified from CS01]. A semilunate tail containing a well-developed hypaxial endoskeleton (comprising large, well-calcified hypaxial cartilages) is present (character state 0) in Paleozoic sharks including ctenacanths, xenacanths, *Akmonistion*, and *Cladoselache*. It is absent (character state 1) in hybodontiforms, *Tristychius*,

holocephalans, and neoselachians, in which the hypaxial endoskeleton of the tail is reduced.

**Teeth, Scales, and Spines**

**Character 87:** *Single-crystallite enameloid (SCE) in teeth absent=0; present=1.* [Gillis and Donoghue, 2007]. Single-crystallite enameloid has been described as primitively present in chondrichthyan teeth. It has been reported as present (character state 1) in Paleozoic sharks (including ctenacanths, *Akmonistion*, *Cladoselache*, and *Orthacanthus*), hybodontiforms, and extant *Heterodontus*. It is absent (character state 0) in most neoselachians (e.g., *Carcharhinus*, *Squalus*, and batoids) and in holocephalans. A single layer of SCE is present in Paleozoic sharks. A double layer of SCE has been reported in at least some hybodonts (e.g., *Acrodus*), and is apparently also present in *Tribodus*; however, the latter feature has not yet been studied extensively enough in various hybodont taxa to determine its phylogenetic significance, if any.

**Character 88:** *Low-crowned teeth. absent=0; present=1.* [CG; M]. Low-crowned teeth (in which high pointed cusps are absent) occur in some hybodontiforms, including *Onychoselache*, *Hamiltonichthys*, *Lissodus*, *Lonchidion*, *Palaeobates*, *Acrodus*, *Tribodus*, and *Asteracanthus* (character state 1). They also occur in extant batoids and *Heterodontus*. Low-crowned teeth are absent (character state 0) in *Tristychius* and in Paleozoic chondrichthyans including *Cladoselache*, *Akmonistion*, xenacanths, and ctenacanths, and are also absent in many neoselachians including galeomorphs and

orbitostylic sharks. This character is scored as "inapplicable" ("-") in holocephalans, which have large flattened tooth plates instead of teeth.

**Character 89:** *Tooth crowns with a lingual swelling. absent=0; present=1.* [CG; M]: present in *Onychoselache*; absent in *Tristychius*. Tooth crowns with a lingual swelling are present (character state 1) in many hybodontiforms including *Onychoselache*, *Hamiltonichthys*, *Palaeobates*, *Acrodus*, *Tribodus*, and *Asteracanthus*. Teeth lack a lingual swelling (character state 0) in *Lissodus*, *Lonchidion*, *Hybodus*, and *Egertonodus*, as well as in *Tristychius*, neoselachians, and Paleozoic chondrichthyans. This character is scored as "inapplicable" ("-") in holocephalans, which have flattened tooth plates rather than teeth.

**Character 90:** *Elongate lateral teeth. absent=0; present=1.* [CG; M] Elongate lateral teeth are present (character state 1) in some hybodontiform taxa, including *Hamiltonichthys*, *Lissodus*, *Lonchidion*, *Palaeobates*, *Hybodus medius*, *Acrodus*, and *Asteracanthus*. They also occur in extant *Heterodontus*, and may be associated with a durphagous feeding strategy. Elongate lateral teeth are absent (character state 0) in most other hybodonts, and in most neoselachians and Paleozoic sharks.

**Character 91:** *Tooth histology: orthodont=0; osteodont=1.* [CG; M; MEA]. Glikmann (1964) used orthodont vs. osteodont teeth as the basis for his classification of chondrichthyans into two distinct subgroups. Although subsequent authors have cast doubt on that interpretation, the distinction between orthodont and osteodont teeth may

have some phylogenetic validity, and has been retained as a phylogenetic character by some recent authors (e.g., Coates and Gess, 2007). Osteodont teeth are limited in occurrence among chondrichthyans, and may represent a derived state, possibly independently evolved in hybodonts and some neoselachians. Osteodont teeth are present (character state 1) in *Hybodus*, *Egertonodus*, *Acrodus*, *Tribodus*, and *Asteracanthus*, and in extant *Heterodontus*. Other chondrichthyans have orthodont teeth (character state 0), including Paleozoic sharks (e.g., *Akmonistion*, *Cladoselache*, ctenacanths, and xenacanths), *Tristychius*, some hybodontiforms (including *Onychoselache*, *Hamiltonichthys*, *Lissodus*, *Lonchidion*, and *Palaeobates*), and some neoselachians (e.g., *Carcharhinus*, batoids, *Squalus*). *Heterodontus* has both osteodont and orthodont teeth.

**Character 92:** *"parallel-fibred" enameloid absent=0; present=1.* [JM; G]. Parallel-fibred enameloid (PFE, also called "parallel-bundled" enameloid by Cuny et al., 2001) has been considered a synapomorphy of neoselachians (character state 1). It occurs in all neoselachians except batoids, which have only "tangle-fibred" enameloid (see character 93). It is possible that batoids have lost PFE secondarily, or alternatively, that they never gained it. Parallel-fibred enameloid is absent (character state 0) in all non-neoselachian chondrichthyans known thus far.

**Character 93:** *"tangle-fibred" enameloid absent=0; present=1.* "Tangle-fibred" enameloid (or "tangle-bundled" enameloid, Cuny et al., 2001) has been considered a neoselachian synapomorphy (character state 1). It occurs in all neoselachians, including

batoids. "Tangle-fibred" enameloid is absent (character state 0) in all known non-neoselachian chondrichthyans.

**Character 94:** *High-crowned multicuspid teeth. absent=0; present=1.* [CG; M; MEA]. High-crowned multicuspid teeth are found in some hybodonts including *Hybodus* and *Egertonodus*. They also occur, probably independently, in ctenacanths, symmoriiforms (e.g., *Akmonistion*), and *Cladoselache*. High-crowned teeth with multiple cusps are absent in *Tribodus*, *Acrodus*, *Asteracanthus*, *Palaeobates*, *Hybodus medius*, *Lissodus*, *Lonchidion*, *Hamiltonichthys*, and *Onychoselache*. They are also absent in *Tristychius* (which has peg-like teeth), holocephalans, xenacanths (which have bicuspid or tricuspid "diplodont" teeth), and extant neoselachians including *Carcharhinus*, *Heterodontus*, *Squalus*, and batoids.

**Character 95:** *Teeth with columnar osteodentine. absent=0; present=1.* [CG; M; MEA]: present in *Tribodus*. Present in *Asteracanthus* and *Acrodus*. Maisey (1989), Brito and Ferreira (1989), Brito (1992), and Maisey et al. (2004) listed teeth with columnar osteodentine (osteodont teeth in which the osteodentine is arranged in columns perpendicular to the tooth surface) as a synapomorphy of Acrodontinae (comprising *Acrodus*, *Asteracanthus*, and *Tribodus*. Teeth of this type are absent (state 0) in other hybodonts.

**Character 96:** *Teeth without labial peg=0; labial peg present=1.* [Rees and Underwood, 2002]. A labial peg (i.e., a rounded protuberance from the labial surface of the tooth

crown) has been considered one of the characteristics of Lonchidiidae (*Lissodus* and *Lonchidion*), although Rees (2008) considers that the character may in fact reflect convergence between the two taxa. A labial peg is absent in other hybodonts.

**Character 97:** *Teeth with sigmoidal curvature of the cusps, slender cusplets, weak ornamentation absent=0; present=1.* [Rees, 2008]. This character was used by Rees (2008: his character 20) to differentiate *Egertonodus* from *Hybodus*. Although both taxa have high-crowned multicuspid teeth, teeth that are sigmoidal or 'S-shaped' in lateral view, and have more slender cusplets and weaker ornamentation than in *Hybodus*, occur in *Egertonodus basanus* and *Egertonodus fraasi* (Rees and Underwood, 2008).

**Character 98:** *Domed teeth with low cusp and cusplets, wide triangular labial protuberance, ornament with numerous weak folds): absent=0; present=1.* [Rees, 2008]. According to Rees (2008), teeth of this type occur only in *Lissodus*, and differentiate it from *Lonchidion*. Domed teeth occur in both *Lissodus cassangensis* and *Lissodus africanus* (Duffin, 2001), as well as in other *Lissodus* species identified from more fragmentary material.

**Character 99:** *Occlusally flattened elongate lateral teeth with reticulate ornamentation and massive root: absent=0; present=1.* [Rees, 2008]. According to Rees (2008), lateral teeth of this type (with a flattened occlusal surface, thick and elongated root, and reticulate ornamentation) are characteristic of Asteracanthus and Palaeobates (character state 1). This feature is absent in other hybodonts, including Tribodus (character state 0).

**Character 100:** *Pavement dentition absent=0; present=1.* [N]. A pavement dentition, comprising an occlusally flattened "pavement" of occlusally flattened, often hexagonal, imbricated teeth, is found in *Tribodus* and in some extant durophagous batoids (character state 1). It is absent in other chondrichthyans (character state 0).

**Character 101:** *Diplodont teeth absent=0; present=1.* [G]. Diplodont teeth, which typically have two large outer cusps and a much smaller central cusp, are present (character state 1) in xenacanths including *Orthacanthus* and *Diplodoselache*. They are absent (character state 0) in most other chondrichthyans, including neoselachians, hybodontiforms, *Tristychius*, holocephalans, and many Paleozoic sharks (e.g., *Akmonistion*, *Cladoselache*, and ctenacanths). However, they have been reported to occur in *Antarctilamna* and *Doliodus* (Maisey, pers. comm..).

**Character 102:** *Crushing teeth with rounded cusps, ornament of ridges radiating from cusp apex and bifurcating towards tooth base: absent=0; present=1.* [N]. Teeth of this type are characteristic of members of the genus *Acrodus* (state 1). They are absent in other hybodonts (state 0).

**Character 103:** *Fin spines possess large retrorse denticles and smooth ribs. absent=0; present=1.* [CG; M]: present in *Tribodus*. Dorsal fin spines having large posterior retrorse denticles and an ornamentation of smooth ribs are present (character state 1) in all hybodontiforms, including *Tristychius*, *Onychoselache*, *Hamiltonichthys*, and

Mesozoic hybodontoids. They are also present in holocephalans (e.g., *Hydrolagus*). This feature is absent (character state 0) in neoselachians (in which most taxa lack dorsal fin spines, and the few that possess them such as *Squalus* and *Heterodontus* have spines with a smoothly enameled surface lacking ribs or posterior denticles). It is also absent in Paleozoic sharks, including ctenacanths (in which the fin spines have a pectinate ornament rather than smooth ribs), xenacanths, symmoriiforms, and cladoselachians.

**Character 104:** *Fin spines have convex posterior wall, denticles adjacent to posterior midline. absent=0; present=1.* [CG; M; MEA]: present in *Tribodus*. Fin spines with a convex posterior wall and posterior denticles adjacent to the midline are present (character state 1) in *Hamiltonichthys* and Mesozoic hybodontoids. They are absent (character state 0) in *Tristychius* and *Onychoselache*, in which the posterior wall of the fin spines is concave and the posterior denticles are positioned along the lateral margins of the posterior surface. This feature is also absent in Paleozoic sharks (e.g., ctenacanths, xenacanths, *Akmonistion*, and *Cladoselache*), holocephalans, and neoselachians.

**Character 105:** *Fin spines with numerous bifurcating or intercalating costae or tubercle rows. absent=0; present=1.* [CG; MEA]: absent in *Onychoselache*. Fin spines with numerous bifurcating or intercalating costae or tubercle rows are present (character state 1) in some Mesozoic hybodonts including *Egertonodus*, *Hybodus*, *Acrodus*, *Asteracanthus*, *Palaeobates*, and *Tribodus*. This feature is absent (character state 0) in *Lissodus*, *Lonchidion*, *Hamiltonichthys*, *Onychoselache*, and *Tristychius*, in which only a small number of costae are present on the fin spines, and the costae are typically arranged

parallel to each other rather than bifurcating and intercalating. It is also absent in other chondrichthyan taxa.

**Character 106:** *Fin spines with few, widely spaced costae absent=0; present=1.* [N]. Fin spines with a small number of widely spaced costae occur (character state 1) in *Tristychius*, *Onychoselache*, *Hamiltonichthys*, *Lissodus*, and *Lonchidion*. This feature is absent (character state 0) in other hybodontiforms (e.g., *Tribodus*, *Egertonodus*, *Acrodus*, *Asteracanthus*, *Palaeobates*), in which numerous closely-spaced costae are present on the fin spines. It is also absent in other fossil and extant chondrichthyans.

**Character 107:** *Anterior dorsal fin spine absent=0; present=1.* [N]. An anterior dorsal fin spine is present (character state 1) in most chondrichthyans, including Paleozoic sharks (e.g., ctenacanths, xenacanths, *Akmonistion*, and *Cladoselache*), holocephalans, *Tristychius*, hybodontiforms, and some neoselachians (e.g., *Heterodontus*, many "squaloids" such as *Squalus*). It is absent (character state 0) in other neoselachians, including galeomorphs and batoids. It is uncertain whether the single dorsal fin in hexanchoids represents an anterior or posterior fin, although Shirai (1992) considers it an anterior fin. This fin lacks a spine in hexanchoids.

**Character 108:** *Posterior dorsal fin spine absent=0; present=1.* [N]. A posterior dorsal fin spine is present (character state 1) in ctenacanths, *Tristychius*, hybodonts, and some neoselachians (e.g., *Heterodontus*, some "squaloid" sharks including *Squalus*). It is absent (character state 0) in many Paleozoic sharks (e.g., symmoriiforms such as

*Akmonistion*, *Cladoselache*, xenacanths, holocephalans, and some neoselachians (e.g., galeomorphs and batoids).

**Character 109:** *Dorsal fin spine rounded in cross-section, ornamented only by retrorse denticles: absent=0; present=1.* [JM]. This feature has been described as characteristic of xenacanths. It is present (character state 1) in xenacanths (e.g., *Orthacanthus* and *Diplodoselache*), and absent (character state 0) in other fossil and extant chondrichthyans.

**Character 110:** *Fin spines with stellate tubercles absent=0; present=1.* [M]. Fin spines with stellate tubercles (character state 1) are apomorphic for the hybodontid genus *Asteracanthus*. They are absent (character state 0) in all other hybodonts. However, fin spines with stellate tubercles also occur in myriacanthoid holocephalans and some large Paleozoic sharks of unknown taxonomic placement, such as bythiacanthids (Maisey, pers. comm.).

**Character 111:** *Fin spines with mantle of shiny enameloid, lacking posterior denticles: absent=0; present=1.* [JM; G]. Fin spines with a mantle of shiny enameloid and lacking posterior denticles are present (character state 1) in extant neoselachians in which fin spines are present (e.g., *Heterodontus* and *Squalus*). They are absent (character state 0) in all other chondrichthyans.

**Character 112:** *Spine-brush complex absent=0; present=1.* [CS98]. The spine-brush complex (character state 1) occurs in stethacanthid symmoriiforms (e.g., *Akmonistion*), and is apparently synapomorphic for that group (Coates and Sequeira, 1998). The spine-brush complex is a modification of the anterior dorsal fin endoskeleton to form a large brush-like appendage lined dorsally with enlarged dermal denticles, apparently present only in males and possibly used in mating. This feature is absent (character state 0) in all non-symmoriiform chondrichthyans.

**Character 113:** *Male cephalic spines. absent=0; present=1.* [CG; M; MEA]: present in *Tribodus*. Paired cephalic spines are present (character state 1) on the posterior of the braincase in *Onychoselache* and hybodontoids, and have been considered a hybodont synapomorphy. They appear to occur only in male individuals, defined by the additional presence of pelvic claspers in these specimens, and may have had a role in male reproductive behavior. They are unknown in *Egertonodus fraasi*, of which the only known specimen is female. Cephalic spines are absent (character state 0) in other chondrichthyans, including Paleozoic sharks, *Tristychius*, holocephalans, and neoselachians.

**Character 114:** *Cephalic spines with constricted basal plate, lateral and posterior lobes, massive central cusp, and retrorse barb. absent=0; present=1.* [CG; M; MEA]: present in *Tribodus*. Cephalic spines with this morphology are present (character state 1) in Mesozoic hybodontoids including *Lissodus*, *Lonchidion*, *Palaeobates*, *Asteracanthus*, *Acrodus*, *Egertonodus*, and *Hybodus*. They are absent (character state 0) in

*Onychoselache* and *Hamiltonichthys* (in which the basal plate is not constricted to form lobes). Cephalic spines are absent in other chondrichthyan taxa (see character 115, above).

**Character 115:** *'Convict-arrow' shaped cephalic spines with narrow posterior lobe. absent=0; present=1.* [CG; M; MEA]. 'Convict-arrow' shaped cephalic spines have been described as occurring (character state 1) in *Lissodus* and *Lonchidion*, although it has been argued that cephalic spines of *Lissodus* can be classified as 'T-shaped' rather than 'convict-arrow' shaped (Rees, 2008; Rees and Underwood, 2002). 'Convict-arrow' shaped cephalic spines are absent (character state 0) in other hybodontiforms. Non-hybodontiform chondrichthyans lack cephalic spines.

**Character 116:** *'Sphenonchus' cephalic spines. absent=0; present=1.* [CG; M; MEA]: absent in *Onychoselache*. '*Sphenonchus*' cephalic spines (spines with a prominent barbed, ornamented central cusp and one or fewer pairs of accessory cusps) are present (character state 1) in some hybodontoids including *Hybodus*, *Palaeobates*, *Egertonodus*, *Acrodus*, *Asteracanthus*, and *Tribodus*. They are absent (character state 0) in *Onychoselache*, *Hamiltonichthys*, *Lissodus*, and *Lonchidion*, in which cephalic spines have multiple accessory cusps (or principal cusps, in the case of *Onychoselache*) and are not noticeably barbed or ornamented. Cephalic spines are absent in other chondrichthyans.

**Character 117:** *Single (posterior) pair of cephalic spimes: absent=0; present=1.* [M]. A single pair of cephalic spines is present (character state 1) in *Egertonodus* and *Tribodus*.

It may also be present in *Asteracanthus*, although this remains unknown until more complete skeletal material is discovered. This feature is absent (character state 0) in other hybodonts, in which two pairs are present. It is also absent in other chondrichthyans, which lack cephalic spines.

**Character 118:** *Two pairs of cephalic spines (anterior and posterior): absent=0; present=1.* [N]. Two pairs of cephalic spines are present (character state 1) in many hybodonts, including *Hamiltonichthys*, *Lissodus*, *Hybodus*, and *Acrodus*. This feature is absent (character state 0) in *Tribodus* and *Egertonodus* (in which there is only a single pair of cephalic spines), in *Onychoselache* (in which a compound cephalic spine is present, with multiple principal cusps and an undifferentiated basal plate), and in other chondrichthyans (in which cephalic spines are absent).

**Character 119:** *Cephalic spines with accessory cusps present=0; absent=1.* [M]. The cephalic spines have smaller accessory cusps flanking the principal cusp (character state 0) in *Hamiltonichthys*, *Lissodus*, *Lonchidion*, *Hybodus reticulatus*, *Hybodus delabechei*, and *Hybodus medius*. Accessory cusps are absent (character state 1) in *Tribodus*, *Hybodus hauffianus*, *Egertonodus basanus*, *Acrodus*, and *Asteracanthus*. This feature is unknown in *Lonchidion selachos*, *Lonchidion montsechi*, *Egertonodus fraasi*, and *Palaeobates*. It is scored as "inapplicable" ("-") in other chondrichthyans, which lack cephalic spines.

**Character 120:** *Cephalic spines with single principal cusp (with or without accessory cusps) absent=0; present=1.* [N]. Cephalic spines with a single central principal cusp, with or without accessory cusps, is present (character state 1) in *Hamiltonichthys* and Mesozoic hybodonts. It is absent (character state 0) in *Onychoselache* (in which cephalic spines have multiple principal cusps) and in other chondrichthyans (in which cephalic spines are absent).

**Character 121:** *Cephalic spines lack large accessory cusps absent=0; present=1* [Rees, 2008]. Cephalic spines with large lateral cusplets (up to approximately half the height of the principal cusp) are present (character state 1) in *Hamiltonichthys*. They are absent (character state 0) in all other hybodonts. This character is scored as "inapplicable" in other chondrichthyans, which lack cephalic spines.

**Character 122:** *Posterior lobe of cephalic spine and spine cusp of near-equal width=0; posterior lobe wider than spine cusp=1.* [N]. Cephalic spines in which the width of the posterior lobe of the basal plate is less than or equal to that of the spine cusp are present in *Tribodus*, *Lissodus*, and *Lonchidion*. They are absent in other hybodonts, in which the posterior lobe of the basal plate is wider than the spine cusp. The character is scored as "inapplicable" ("-") in other chondrichthyans, in which cephalic spines are lacking.

**Character 123:** *Cephalic spines with T-shaped basal plate absent=0; present=1.* [Rees, 2008]. Cephalic spines with a T-shaped basal plate are present (character state 1) in *Tribodus*, *Lissodus*, *Palaeobates*, *Hybodus*, *Egertonodus*, *Acrodus*, and *Asteracanthus*.

They are absent (character state 0) in *Onychoselache* and *Hamiltonichthys* (in which the cephalic spine basal plate is unconstricted), and in *Lonchidion* (in which the cephalic spine basal plate is "convict-arrow shaped"). This character is scored as "inapplicable" ("-") in other chondrichthyans, which lack cephalic spines.

**Character 124:** *Cephalic spine base plate with gracile lobes=0; with robust lobes=1.* [N]. The lobes of the cephalic spine base plate are gracile in *Tribodus*, *Lissodus*, and *Lonchidion* (character state 0). They are robust in other hybodonts, including *Hybodus*, *Egertonodus*, *Acrodus*, *Asteracanthus*, and *Palaeobates* (character state 1). This character is scored as "inapplicable" ("-") in *Onychoselache* and *Hamiltonichthys* (in which the cephalic spine base plate is not differentiated into lobes), and in other chondrichthyans (which lack cephalic spines).

**Character 125:** *Synchronomorial (non-growing) denticles. absent=0; present=1.* [CG]: present (character state 1) in *Tristychius* and *Onychoselache*. Synchronomorial (non-growing) denticles occur in many hybodonts, including *Tribodus*, *Onychoselache*, *Hamiltonichthys*, *Lissodus cassangensis*, *Hybodus*, *Egertonodus*, *Acrodus*, and *Asteracanthus*. They also occur in *Tristychius*, holocephalans, neoselachians, and *Akmonistion*. Non-growing denticles are apparently absent (character state 0) in ctenacanths and *Diplodoselache*, in which all dermal denticles are of the growing type. This feature is unknown in *Pucapampella*, *Cladoselache*, *Cladodoides*, *Orthacanthus*, and some hybodonts (e.g., *Palaeobates*, *Lissodus africanus*, and all known species of *Lonchidion*).

**Character 126:** *All dermal denticles nongrowing absent=0; present=1.* [M]. A squamation comprising only nongrowing dermal denticles (character state 1) has been described as present in some hybodonts (e.g., *Onychoselache*, *Hamiltonichthys*, *Tribodus*, *Lissodus cassangensis*, *Egertonodus*). In some other hybodonts (e.g., *Hybodus*, *Acrodus*) the squamation comprises both nongrowing and growing dermal denticles (character state 0), a feature that is also present in ctenacanths and *Diplodoselache*. All dermal denticles are also nongrowing in some Paleozoic sharks (e.g., *Akmonistion*), *Tristychius*, holocephalans, and extant neoselachians. The state of this character is unknown in *Cladodoides*, *Cladoselache*, *Orthacanthus*, *Pucapampella*, and some hybodonts (e.g., *Lonchidion*, *Palaeobates*, and *Asteracanthus*).

**Character 127:** *Dermal denticles with constricted neck absent=0; present=1.* Dermal denticles with a constricted neck occur (character state 1) in ctenacanths, some neoselachians (e.g., galeomorphs, some squalean sharks), *Tristychius*, and at least one hybodontiform (*Asteracanthus*). They are absent (character state 0) in other hybodonts, *Heterodontus*, batoids, holocephalans, and *Akmonistion*. The state of this character is unknown in *Pucapampella*, *Cladodoides*, *Cladoselache*, *Orthacanthus*, *Diplodoselache*, and several hybodont taxa (e.g., *Palaeobates*).

**Character 128:** *Ring or C-shaped scales enclosing sensory canals absent=0; present=1.* [CS01]. Ring or C-shaped scales enclosing the lateral line canal and/or other sensory canals are present (character state 1) in extant holocephalans and their immediate fossil

relatives, and in symmoriiforms (e.g., *Akmonistion*). They are absent (character state 0) in most other chondrichthyans, but have been reported to occur in a few neoselachians (e.g., *Protospinax* and Jurassic galeomorphs; Maisey, pers. comm.)..

**Character 129:** *"Cladodont" teeth absent=0; present=1.* "Cladodont" teeth (which have a large, acuminate principal cusp and several much smaller accessory cusps) are present in many Paleozoic sharks, including *Cladoselache*, symmoriiforms (e.g., *Akmonistion*), and ctenacanths. They are absent (character state 0) in xenacanths, holocephalans, *Tristychius*, hybodonts, and neoselachians. Teeth of *Pucapampella* have not yet been described.

# CHAPTER 14: RESULTS OF PHYLOGENETIC ANALYSIS

Phylogenetic analysis of the character matrix (Appendix B) performed using PAUP* 4.0b (Swofford, 2001) resulted in 70 equally parsimonious trees of length 243 steps, with a consistency index (CI) of 0.5309, a retention index (RI) of 0.7996, and a rescaled consistency index (RC) of 0.4245. Of the 129 characters included in the analysis, 15 were considered parsimony-uninformative. A strict consensus (Nelson, 1979; Schuh and Polhemus, 1980; Sokal and Rohlf, 1981; Kitching et al., 1998) of the 70 total trees was generated, and resulted in the topology shown in Fig. 115 and described below. An Adams consensus (Adams, 1972; Kitching et al., 1998; Schuh, 2000) of the 70 MPTs was also generated, but showed exactly the same topology as the strict consensus; thus contributing no additional information for the present study. An identical phylogenetic analysis was also run in T.N.T. (Goloboff et al., 2003; Goloboff et al., 2008), with very similar results (yielding only four equally parsimonious trees, all of the same length as the shortest trees generated in PAUP*, i.e., 243 steps, and with strict consensus yielding an identical topology to that generated in the PAUP* search) (Fig. 116). Both the PAUP* and T.N.T. trees were rooted with "*Pucapampella*" as the outgroup, and the other outgroup taxa included in the 'ingroup' for purposes of phylogenetic analysis, in order to accurately test the monophyly of Hybodontiformes. "*Pucapampella*" in the present analysis is a composite of two specimens attributed to that genus, one from Bolivia (Maisey, 2001) and the other from South Africa (Maisey and Anderson, 2001), coded based on the descriptions in those two papers. "*Pucapampella*" was chosen as the outgroup for the analysis because it has been proposed as possibly representing the most

basal chondrichthyan (Maisey, 2001; Maisey and Anderson, 2001), on the basis of its having a ventral otic fissure, otherwise found only in outgroups to Chondrichthyes.

In the resulting strict consensus of these 70 trees, hybodonts form a monophyletic clade, to the exclusion of *Tristychius* (making Hybodontiformes paraphyletic). Other monophyletic taxa include Hybodontoidei (*Hamiltonichthys* + Mesozoic hybodonts), Hybodontidae (Mesozoic hybodonts exclusive of *Lissodus* and *Lonchidion*), Hybodontinae (*Hybodus* + *Egertonodus*), neoselachians (appearing as the sister group of hybodonts exclusive of *Tristychius*), Squalea (orbitostylic sharks plus batoids, sensu Shirai, 1992), and a clade of xenacanths and ctenacanths, which appear as monophyletic sister taxa (which in turn are sister to a monophyletic clade including *Akmonistion* and *Cladoselache*). Neoselachians and hybodonts exclusive of *Tristychius* form a monophyletic group, to which *Tristychius* is the sister taxon. Holocephalans (represented by *Hydrolagus* in the character/taxon matrix) appear as the sister group to *Tristychius* + neoselachians + hybodonts. Within the hybodont clade, *Onychoselache* is basal, and is the sister taxon to Hybodontoidei (*Hamiltonichthys* + Mesozoic hybodonts). *Hamiltonichthys* is sister to Mesozoic hybodonts, which form a monophyletic clade. Within this Mesozoic hybodont clade, *Lissodus* and *Lonchidion* form a monophyletic clade, in which the three included species of *Lonchidion* form a polytomy at the base of a monophyletic clade comprising the two species of *Lissodus*. The *Lissodus*/*Lonchidion* clade forms a sister taxon to another clade, in which *Palaeobates* is basal to a trichotomy involving the remaining taxa of Mesozoic hybodonts. This trichotomy comprises a monophyletic *Acrodus* (with the three included species of *Acrodus* forming a polytomy), another monophyletic group including *Tribodus* and *Asteracanthus*, and a third

monophyletic clade including *Hybodus* and *Egertonodus*. Within this latter clade, *Hybodus medius* is sister to a monophyletic clade in which *Egertonodus* and the remaining three species of *Hybodus* form monophyletic sister taxa (making *Hybodus* polyphyletic).

Bremer support values (Bremer, 1988, 1994) and bootstrap percentages for nodes on the strict consensus are shown in Figs. 117 and 118. The best supported clades are *Hydrolagus* + Euselachii (with a Bremer support value of 4+ and a bootstrap of 88%), Neoselachii (with a Bremer support value of 4+ and a bootstrap of 87%), and a clade of Neoselachians + hybodonts exclusive of *Tristychius* (with a Bremer support value of 4+ and a bootstrap of 82%). A clade of hybodonts (to the exclusion of *Tristychius*) was also well supported (with a Bremer support of 2 and a bootstrap of 85%), as was the monophyletic clade formed by species of *Egertonodus* (with a Bremer support of 2 and a bootstrap percentage of 84%). Hybodontoidei (*Hamiltonichthys* + Mesozoic hybodonts) also received fairly good support, with a Bremer support value of 2 and a bootstrap of 74%. Other well-supported clades are ctenacanths (with a Bremer support value of 2 and a bootstrap of 67%), *Cladoselache* + *Akmonistion* (with a Bremer support value of 2 and a bootstrap of 70%), and Mesozoic hybodonts (with a Bremer support value of 2 and a bootstrap of 54%). Of the other taxa with bootstrap values above 50%, *Acrodus* has a Bremer support value of 1 and a bootstrap of 68%; *Lissodus* has a Bremer support of 1 and a bootstrap of 63%, and xenacanths have a Bremer support value of 2 and a bootstrap of 51%. All remaining clades occurred in less than 50% of bootstrap replicates. Of these, Hybodontidae above *Palaeobates* have a Bremer support of 2, as do Hybodontinae

exclusive of *Hybodus medius*, and the clade formed by species of *Hybodus* other than *Hybodus medius*. All remaining nodes have a Bremer support of 1 or less.

Within Neoselachii, a clade consistent with Squalea (as proposed by Shirai, 1992, 1996; and supported by Carvalho, 1996; on the basis of only morphological data) is present, containing orbitostylic sharks (*Squalus* and *Notorynchus*) and batoids (*Dasyatis*), which appear as a trichotomy in the present analysis. However, other recent studies based on molecular data (e.g., Winchell et al., 2004; Maisey et al., 2004) have shown an alternative placement of batoids, as basal to all other extant neoselachians. It is not surprising that the present analysis, which is necessarily based only on morphological data like that of Shirai, 1992 (because molecular data in fossils is not preserved), would result in a similar topology to Shirai's for squalean sharks. The absence of further resolution among squaleans may be due to the lack of any soft anatomical data in the present analysis (unlike Shirai's 1992 study, in which soft anatomical characters were included). Similarly, the placement of the two extant galean shark taxa (*Heterodontus* and *Carcharhinus*) in the present analysis differs from most recent phylogenies (e.g., Shirai, 1992, 1996; Winchell et al., 2004), in that *Carcharhinus* appears here as the sister taxon to squalean sharks, with *Heterodontus* as basal to all other neoselachians included. As in the previous example, this difference in topology is likely due to the absence of soft anatomical or molecular data in the present analysis, as many previous analyses of neoselachians have been based largely on soft anatomical features (and others have been based entirely on molecular data). If it were possible to discover and include molecular and soft anatomical data for both living and fossil taxa (i.e., a true 'total evidence' approach), this would undoubtedly have the potential to change the entire topology, to

what extent remains unknown. At present, the addition of available soft anatomical and molecular data for extant taxa to the present matrix would only serve to increase the amount of missing data among the fossil taxa, potentially contributing to error in the analysis.

Each of the 70 trees resulting from the PAUP* analysis was examined individually in order to determine the different topologies resulting in unresolved nodes in the strict consensus. These differing topologies were divided into two major categories, within which were three subcategories and additional minor changes that increased the total number of resultant trees. All of the major changes occurred within the hybodont clade (node 46, *Onychoselache* and higher).

The first category (category 1) comprised trees having a monophyletic Acrodontinae (i.e., where *Acrodus* was sister to a monophyletic clade including *Tribodus* and *Asteracanthus*). This category included a total of 42 trees. The second category (category 2), with 28 trees, comprised trees where the *Tribodus*/*Asteracanthus* clade was separated from *Acrodus*. In all of the latter trees, the *Tribodus*/*Asteracanthus* clade was sister to another clade, in which *Acrodus* formed the sister group to Hybodontinae (*Hybodus* + *Egertonodus*). Within this second category, all trees had exactly the same topology for the *Acrodus* + *Hybodus*/*Egertonodus* clade, with *Hybodus medius* as the sister group to a clade comprising the remaining species of *Hybodus* and the two species of *Egertonodus* as monophyletic sister groups. The first category of tree topologies (in which Acrodontinae was monophyletic) was further divisible into three subcategories, all involving the topology within Hybodontinae. In all three subcategories, *Palaeobates* was sister to a clade that included remaining Hybodontidae, which in turn included

Acrodontinae and Hybodontinae as sister groups. In the first subcategory (subcategory A, with 14 trees), the three species of *Hybodus* exclusive of *Hybodus* medius formed a trichotomy. In the next (subcategory B, with 14 trees), *Hybodus reticulatus* was resolved as the sister taxon to *Hybodus hauffianus*, whereas in the following subcategory (subcategory C, 14 trees), *Hybodus reticulatus* resolved as the sister taxon to *Hybodus delabechei*.

In all 70 trees, Lonchidiidae (represented by *Lonchidion* + *Lissodus*) formed a monophyletic clade. However, the topology within this clade was highly variable, increasing the total number of trees. In all trees, *Lissodus* was monophyletic. The large number of total trees was caused largely by variability in placement of the three species of *Lonchidion*. Among category 1 trees (trees with a monophyletic Acrodontinae), trees of subcategory A (with a trichotomy for *Hybodus* exclusive of *H. medius*) showed 7 different topologies: (1) a polytomy with the *Lissodus* clade; (2) a trichotomy within a monophyletic *Lonchidion* clade forming the sister group to *Lissodus*; (3) *Lonchidion montsechi* as sister to a clade of *Lissodus* + remaining *Lonchidion*; (4) *Lonchidion humblei* and *Lonchidion selachos* forming a basal trichotomy with a clade in which *Lonchidion montsechi* is basal to *Lissodus*; (5) a monophyletic *Lonchidion* clade (sister to *Lissodus*) in which *Lonchidion montsechi* is sister to remaining *Lonchidion*; (6) *Lonchidion montsechi* basal to a trichotomy between the two other *Lonchidion* species and a monophyletic *Lissodus*; and (7) *Lonchidion humblei* and *Lonchidion selachos* as sister groups, forming a clade that is sister to a *Lonchidion* + *Lissodus* clade.

The same 7 variations in topology within Lonchidiidae occur in the remaining subcategories of category 1 trees. An even greater degree of variability occurs in trees of

category 2 (in which Acrodontinae is paraphyletic), with a total of 14 possible topologies for Lonchidiidae. Among these, 6 of the 7 topologies described above are present (the first one, with *Lonchidion* forming a basal polytomy with a monophyletic *Lissodus*, did not occur). In addition, the following topologies occurred: (8) a polytomy between *Lonchidion selachos*, a clade comprising *Lonchidion humblei* and *Lonchidion montsechi*, and the *Lissodus* clade; (9) a polytomy between *Lonchidion humblei*, a clade comprising *Lonchidion selachos* and *Lonchidion montsechi*, and the *Lissodus* clade; (10) the three *Lonchidion* species as nested sister taxa, with *Lonchidion selachos* as basal and *Lonchidion montsechi* sister to *Lissodus*; (11) the same topology, but with *Lonchidion humblei* as basal and *Lonchidion montsechi* sister to *Lissodus*; (12) a monophyletic *Lonchidion* clade as sister to *Lissodus*, with *Lonchidion humblei* as sister to the other two *Lonchidion* species; (13) a monophyletic *Lonchidion* clade, sister to *Lissodus*, in which *Lonchidion selachos* is basal to the other two *Lonchidion* species; (14) *Lonchidion humblei* as basal to a trichotomy between *Lonchidion montsechi*, *Lonchidion selachos*, and *Lissodus*; (15) *Lonchidion humblei* as the sister to a clade in which remaining *Lonchidion* form a sister group to *Lissodus*.

The large amount of variation within *Lonchidion* is not surprising, because the two taxa with the largest amount of missing data (both with 71% missing data) are *Lonchidion humblei* and *Lonchidion selachos*, the only two taxa in the matrix for which skeletal material is unknown (both consist of isolated dermal elements only: fin spines, cephalic spines, and teeth). This missing data can increase the number of primary trees resulting from the analysis (Kitching et al., 1998). This is further suggested by the much smaller number of trees (only 4) produced by the T.N.T. analysis, as there is some

evidence that T.N.T. may handle missing data better than PAUP* (in which it can result in spurious tree topologies) (Kitching et al., 1998; Kearney and Clark, 2003; Goloboff et al., 2008). The only other variation in the 70 trees was in the placement of the batoid *Dasyatis*, which had two possible topologies: as sister to *Squalus*, or as sister to *Notorynchus*. This jumping taxon resulted in two possible trees for each of the previously discussed topologies, effectively doubling the total number of resultant trees in the analysis.

# CHAPTER 15: DISCUSSION

## HYBODONT SYNAPOMORPHIES

A complete list of unambiguous synapomorphies supporting each node of the strict consensus (Figure 115) is provided in Appendix E (Apomorphy List). Hybodontiformes exclusive of *Tristychius* (node 46) are supported by five unambiguous synapomorphies (character 17, hyomandibular fossa located anteriorly in the otic region: 1 => 0, CI = 0.333; character 23, large, down-turned postorbital process: 0 => 1, CI = 1.00; character 33, inflated and elongate jugular canal: 0 => 1, CI = 0.5; character 58, coracobranchial fossa on scapulocoracoid: 0 => 1, CI = 1.00; character 89, tooth crowns with a lingual swelling: 0 => 1, CI = 0.333; and character 113, male cephalic spines: 0 => 1, CI = 1.00).

Hybodontoidei (node 45) is also supported by five unambiguous synapomorphies (character 85, anal fin with double base-plate: 0 => 1; CI = 1.00; character 90, elongate lateral teeth: 0 => 1, CI = 0.250; character 104, fin spines have convex posterior wall, denticles adjacent to posterior midline: 0 => 1, CI = 1.00; character 118, two pairs of cephalic spines (new character): 0 => 1, CI = 0.333; character 120, cephalic spines with single principal cusp, with or without accessory cusps (new character): 0 => 1, CI = 1.00).

A Mesozoic hybodont clade (node 44) is supported by four unambiguous synapomorphies (character 60, coracoid and scapular regions of near-equal length: 0 => 1, CI = 0.333; character 72, pelvic propterygium terminal, no distal cartilages: 0 => 1, CI = 0.333; character 75, low number (10–12) of pleural ribs: 0 => 1, CI = 1.00; and character 114, cephalic spines with constricted basal plate, lateral and posterior lobes, massive central cusp, and retrorse barb: 0 => 1, CI = 1.00).

Hybodontidae (node 41) is supported by four synapomorphies (character 105, fin spines with numerous bifurcating or intercalating costae or tubercle rows: 0 => 1, CI = 1.00; character 106, fin spines with few, widely spaced costae (new character): 1 => 0, CI = 0.333; character 116, '*Sphenonchus*' cephalic spines: 0 => 1, CI = 1.00; and character 123, cephalic spines with T-shaped basal plate: 0 => 1, CI = 0.5). A single unambiguous synapomorphy supports node 40 (Hybodontidae above *Palaeobates*): character 91, a change in tooth histology from orthodont to osteodont (0 => 1, CI = 0.5).

Node 43, Lonchidiidae, is supported by three unambiguous synapomorphies (character 89, tooth crowns with a lingual swelling: 1 => 0, CI = 0.333; character 96, teeth without/with labial peg: 0 => 1, CI = 1.00; and character 115, 'convict-arrow' shaped cephalic spines with narrow posterior lobe: 0 => 1, CI = 1.00). *Lissodus* (node 42) is supported by character 98 (domed teeth with low cusp and cusplets, wide triangular labial protuberance, ornament with numerous weak folds: 0 => 1, CI = 1.00) and character 123 (cephalic spines with T-shaped basal plate: 0 => 1, CI = 0.5).

Node 38 (Hybodontinae) is supported by two unambiguous synapomorphies (character 88, low-crowned/high-crowned teeth: 1 => 0, CI = 0.250; and character 89, tooth crowns with a lingual swelling: 1 => 0, CI = 0.333). Two unambiguous synapomorphies support node 37 (Hybodontinae exclusive of *H. medius*), character 90 (elongate lateral teeth: 1 => 0, CI = 0.250) and character 94 (high-crowned multicuspid teeth: 0 => 1, CI = 0.333).

*Hybodus* exclusive of *H. medius* (node 35) is supported by three unambiguous synapomorphies (character 12, rostral bar elongated: 1 => 0, CI = 0.5; character 24, postorbital process positioned over trigemino-facial region: 0 => 1, CI = 0.333; and

character 126, all dermal denticles nongrowing: 1 => 0, CI = 0.333). *Egertonodus* (node 36) is supported by two unambiguous synapomorphies (character 15, suborbital shelf broad and laterally flared beneath postnasal wall: 0 => 1, CI = 1.00; and character 97, teeth with sigmoidal curvature of the cusps, slender cusplets, weak ornamentation: 0 => 1, CI = 1.00). *Acrodus* (node 39) is supported by two characters (102, 126). A clade including *Tribodus* and *Asteracanthus* (node 34) is supported by three unambiguous synapomorphies (character 34, ethmoidal articulation: 0 => 1, CI = 0.5; character 38, jaws extend to ethmoid region: 0 => 1, CI = 0.333; character 39, palatoquadrates separated symphysially by ethmoid region: 0 => 1, CI = 0.333).

Node 50 (comprising Neoselachii and hybodonts as sister groups) is supported by eight unambiguous synapomorphies: character 9 (absence of a crus between anterior and posterior semicircular canals), character 22 (otic capsules located between postorbital processes), character 26 (postorbital articulation absent), character 27 (postorbital articulation with lateral commissure absent: new character), character 47 (absence of elongate hyoid rays supporting an opercular flap), character 55 (scapular process narrow dorsally lacking posterior angle), character 62 (tribasal pectoral fin), and character 71 (first pelvic radial enlarged relative to other radials).

Support for node 51 (*Tristychius* + Neoselachii + hybodonts) is provided by five unambiguous synapomorphies. These are character 7 (occipital block wedged between otic capsules); character 42 ("cleaver-shaped" palatoquadrate absent); character 52 (most hypobranchials directed posteriorly towards the midline); character 56 (scapulocoracoid with continually concave anteromedial edge/anterodorsal shoulder reduced or absent); and character 108 (posterior dorsal fin spine present: new character).

Node 52 (comprising the previously mentioned clade plus *Hydrolagus*) is supported by seven unambiguous synapomorphies: character 4 (otico-occipital fissure closed behind posterior dorsal fontanelle); character 5 (metotic fissure closed); character 8 (dorsal otic ridge absent); character 17 (hyomandibular fossa located anteriorly in the otic region); character 29 (lateral dorsal aortae do not enter basicranial cartilage prior to junction with efferent hyoidean artery: new character); character 31 (lateral dorsal aortae do not enter basicranium at level of occipital block: new character); and character 36 (mandibular joint not located behind occiput (new character).

Neoselachii (node 49) is supported by nine unambiguous synapomorphies. These include character 19 (occipital half-centrum); character 25 (lateral commissure not chondrified to contain jugular canal: new character); character 32 (lateral dorsal aortae extend laterally to meet efferent hyoidean arteries forming "bell-shaped" circuit); character 60 (coracoid and scapular regions of near-equal length); character 76 (vertebral column includes calcified chordal centra); character 92 ("parallel-fibred" enameloid); character 93 ("tangle-fibred" enameloid); character 103 (fin spines do not possess large retrorse denticles and smooth ribs); and character 106 (fin spines with few, widely-spaced costae absent: new character).

Node 57 (comprising xenacanths, ctenacanths, *Cladoselache* and symmoriiforms) is supported by character 3 (dorsal otic ridge has horizontal crests). Support for node 55 (xenacanths + ctenacanths) is provided by four unambiguous synapomorphies: character 7 (occipital block wedged between otic capsules); character 62 (tribasal pectoral fin); character 125 (non-growing denticles absent), and character 126 (all dermal denticles nongrowing: absent). Node 53 (xenacanths) is supported by five characters: character 79

(anterior dorsal fin baseplate uncalcified); character 80 (posterior dorsal fin absent: new character); character 83 (single dorsal fin elongate, extending from near-pectoral fin level to anal or pre-anal fin level); character 101 (diplodont teeth); and character 109 (dorsal fin spine rounded in cross-section, ornamented only by retrorse denticles). Node 54 (ctenacanths) is supported by two unambiguous synapomorphies: character 5 (metotic fissure closed) and character 24 (postorbital process positioned over trigemino-facialis region). Finally, node 56 (symmoriiforms + *Cladoselache*) is supported by five unambiguous synapomorphies: character 30 (lateral dorsal aortae enter braincase at level of occipital block through single foramen: new character); character 59 (pectoral fin articulation on lateral face of coracoid); character 64 (pectoral articular surface oriented horizontally: new character); character 68 (premetapterygial radials do not articulate with compond basal cartilages); and character 84 (anal fin absent).

## PHYLOGENY OF HYBODONTIFORMES

The results of the present analysis are largely in agreement with recent hypotheses of hybodontiform phylogeny (i.e., Maisey, 1989; Maisey et al., 2004; Rees, 2008). Monophyletic clades recognized by Maisey (1989) and supported by the present analysis include Hybodontinae (*Hybodus* + *Egertonodus*); Hybodontidae (with *Palaeobates* as sister to a clade including Hybodontinae + *Asteracanthus* and *Acrodus*); a clade comprising *Lissodus* + Hybodontidae; Hybodontoidei (*Hamiltonichthys* + *Lissodus* + Hybodontidae); and a clade comprising *Onychoselache* + Hybodontoidei. In his recent study of interrelationships within Hybodontoidei, Rees (2008) presented a hand-drawn cladogram (largely based on tooth morphology) of 24 characters and 14 hybodontoid

taxa, supporting Maisey's hypotheses except in his placement of *Palaeobates* as sister to *Asteracanthus*, rather than to all other Hybodontidae (as in Maisey, 1989, and the present analysis). Rees (1998:218) based this proposed relationship to *Asteracanthus* on his characters 12 ("crushing dentition with enlarged lateral teeth, complex ornamentation") and 13 ("interlocking teeth with flat crown, asymmetrical lateral teeth, reticulate ornamentation, massive root with well-defined foramina"). Although these features do produce at least a superficial similarity between these two taxa, there is also a major difference in tooth histology (teeth of *Palaeobates* are orthodont, whereas those of *Asteracanthus* and other Hybodontids are osteodont), which formed the basis for Maisey (1989) and Maisey et al. (2004) to separate *Palaeobates* from other Hybodontidae. In the present analysis, the same feature (character 91, orthodont/osteodont teeth) is the only character supporting a clade of Hybodontidae above Palaeobates.

The cladogram presented by Maisey et al. (2004) shows the same relationships within Hybodontoidei as that of Maisey (1989) except that *Tribodus* has been added to Acrodontinae as the sister group of *Asteracanthus*, on the basis of the characters "teeth with columnar osteodentine" (proposed to unite *Acrodus*, *Asteracanthus*, and *Tribodus*) and "palatoquadrates lacking ethmoidal buttresses and oriented transversely" (uniting *Tribodus* and *Asteracanthus*). Although *Tribodus* was not included in the phylogenetic hypotheses of Maisey (1989) or Rees (2008), both of these studies also acknowledge a clade ("subfamily Acrodontinae"), comprising *Acrodus* and *Asteracanthus*. In Maisey's (1989) study, this was based on two characters, "teeth with columnar osteodentine" and "adjacent tooth rows," whereas in Rees' (2008) hypothesis it is based on a single character, "crushing dentition with enlarged lateral teeth, complex ornamentation."

However, a crushing dentition with enlarged lateral teeth is also observed in both extant *Heterodontus* and some batoids, in which it is correlated with a durophagus feeding habitus, and it could potentially have arisen independently in separate hybodont lineages with similar feeding strategies. In the present analysis, the strict consensus shows a trichotomy between *Acrodus*, Hybodontinae, and an *Asteracanthus*/*Tribodus* clade. This occurs because results of the primary analysis are equivocal for this clade, with a monophyletic Acrodontinae occurring in only 60% of MPTs. In trees where Acrodontinae was monophyletic, this clade was supported by two unambiguous characters, "teeth with columnar osteodentine" (character 95, 0 => 1; CI = 0.5) and the new character "cephalic spines with accessory cusps absent" (character 119, 0 => 1; CI = 0.333). Thus, a monophyletic Acrodontinae is not unequivocally supported by the results of the present analysis. As discussed previously, *Asteracanthus* and *Tribodus* were united by three unambiguous characters (34, 38, and 39). *Acrodus* differs notably from *Tribodus* and *Asteracanthus* in the relative length of the jaws, which extend to the ethmoid region in *Acrodus*. These factors suggest that the previously proposed relationship between *Acrodus* and *Tribodus* + *Asteracanthus* may reflect convergence in tooth morphology. "Osteodont" and "orthodont" teeth have been reported to occur among members of a single neoselachian clade (Compagno, 1988), and it remains possible that "columnar osteodentine" may have functional and structural as opposed to phylogenetic causes (e.g., the effects of pressure on teeth from durophagous feeding). Unfortunately, at present *Asteracanthus* is known only from isolated jaws and dermal elements. Future research (including fieldwork to uncover new fossil specimens) is needed to further elucidate the phylogenetic relationships between *Acrodus*, *Tribodus*, and *Asteracanthus*.

In addition to *Hamiltonichthys*, *Lonchidion*, *Lissodus*, *Asteracanthus*, *Acrodus*, *Palaeobates*, *Hybodus*, and *Egertonodus* (all known from partial or complete skeletal material, and included in the present analysis), Rees (2008) also included six taxa known only from isolated dermal elements (*Vectiselachos*, *Hylaeobatis*, and *Parvodus*, which he included in Lonchidiidae; and *Planohybodus*, *Secarodus*, and *Priohybodus*, which he referred to an unnamed subfamily). These taxa were not included in the present analysis. Although *Lonchidion* was not included in the cladogram presented by Maisey (1989), a later cladogram (Maisey et al., 2004) includes it as the sister group of *Lissodus* (based on the character "convict arrow cephalic spines"). This differs from Rees (2008), who placed *Lissodus* on a separate branch above *Lonchidion*, as the sister group to Hybodontidae (on the basis of the character "T-shaped basal plate of cephalic spines"). The status of *Lissodus* and *Lonchidion* as separate genera has been debated by previous authors, some of whom (e.g., Duffin, 1985) proposed that *Lonchidion* should be synonymized with *Lissodus* on the basis of several tooth characters, including a labial protuberance. However, Rees and Underwood (2002) proposed that a labial protuberance was a poor character, probably adapted for functional reasons, and that *Lonchidion* and *Lissodus* should be retained as valid genera on the basis of differences in tooth and cephalic spine morphology. Despite this, several more recent authors (e.g., Fischer, 2008; Duffin, 2001) have continued to uphold that the two genera should be synonymized.

In the present analysis, the two included genera of *Lissodus* resolve as sister taxa in all 70 MPTs. However, the three included species of *Lonchidion* show the highest variability in position of any of the taxa in the analysis. This may partly be due to the fact that two of them (*Lonchidion humblei* and *Lonchidion selachos*) are isolated dermal elements,

whereas the third (*Lonchidion montsechi*) is one of only two hybodonts included that lack cephalic spines. Nevertheless, in all MPTs *Lissodus* and *Lonchidion* form a monophyletic clade, apparently providing support for the family Lonchidiidae Herman, 1977.

Although the monophyly of Hybodontidae, Hybodontidae above *Palaeobates*, and Hybodontinae is weakly supported by the present analysis, one species of *Hybodus* included (*Hybodus medius*) is consistently placed outside of the rest of the genus, suggesting that in future classifications it should possibly be examined for placement in a separate genus (the name "Pyramidodus" is suggested, if available, on the basis of its triangular pyramid-shaped teeth). The rest of Hybodontinae is united by two unambiguous characters, "loss of elongate lateral teeth" (character 90) and "high-crowned multicuspid teeth" (character 94). Aside from *H. medius*, *Hybodus* forms a monophyletic genus, as does its sister group *Egertonodus* (as in previous analyses).

Maisey (1989) placed *Tristychius* as a basal hybodontiform, with Hybodontiformes forming the sister group to Neoselachii. The same phylogeny was reiterated by Coates and Gess (2007). However, Maisey et al. (2004) stated that there was considerable uncertainty about the phylogenetic positions of both *Tristychius* and *Onychoselache*, adding that a taxon including *Tristychius*, *Onychoselache*, and hybodonts might be paraphyletic if neoselachians were not also included. Several previous phylogenetic studies focused on larger-scale issues of chondrichthyan phylogeny (including several computerized cladistic analyses) have included a few hybodontiforms, usually not more than three (usually *Hybodus*, *Tristychius*, and *Onychoselache*) (e.g., Schaeffer and Williams, 1977; Young, 1982; Maisey, 1984; Gaudin, 1991; Maisey, 2001; Coates and Sequeira, 2001A, B; and Ginter, 2005). These have differed widely in their placement of

*Tristychius*, hybodonts, and neoselachians. Of the studies that included *Tristychius*, Maisey (1984) placed it as the sister group to hybodonts and neoselachians (as in the present analysis). However, Gaudin (1991) showed *Onychoselache* as basal to *Hybodus* + neoselachians, as did Coates and Sequeira (2001A, B). The results of the phylogenetic analysis presented here support the hypothesis of Maisey, 1984 with regard to *Tristychius*, suggesting that it is basal to a clade comprising remaining Hybodontiformes + Neoselachii. The latter clade is supported by eight unambiguous characters (absence of crus between anterior and posterior semicircular canals; otic capsules between postorbital processes; postorbital articulation absent; postorbital articulation with lateral commissure absent; hyoid rays elongate supporting opercular flap absent; scapular process narrow dorsally and lacking posterolateral angle; tribasal pectoral fin; first pelvic radial or propterygium enlarged relative to other radials). This neoselachian + hybodont clade is very well supported according to the present analysis, with a Bremer support value of 4+ and a bootstrap value of 82%. This suggests that in future classifications, *Tristychius* (which has been placed in its own family, Tristychiidae Moy-Thomas, 1936) should possibly be removed from Hybodontiformes and placed in a separate order, pending the results of further investigations. However, in the present analysis *Onychoselache* is resolved as a basal hybodontiform, forming a monophyletic clade well supported by the present evidence (with a Bremer support value of 2 and a bootstrap value of 85%). This suggests that *Onychoselache* should be retained within Hybodontiformes in future taxonomic classifications.

Finally, the placements of a few outgroup taxa raise several interesting questions. First, only a single holocephalan, the extant chimaeroid *Hydrolagus*, was included in the

analysis. It resolved on the strict consensus as the sister group of *Tristychius*, neoselachians, and hybodonts, forming a monophyletic clade with very good support (Bremer support 4+, Bootstrap value 88). Previous analyses differ in their placement of holocephalans, with some (e.g., Schaeffer and Williams, 1977; Young, 1982; Gaudin, 1991) placing them as basal chondrichthyans, others (e.g., Maisey), placing them as basal to all chondrichthyans except *Pucapampella*, and still others (e.g., Coates and Sequeira, 2001A, B) placing them as highly derived symmoriiforms. However, at least one analysis (Ginter, 2005) places holocephalans (in a polytomy with orodontiforms, eugeneodontiforms, and petalodontiforms) as the sister group to hybodontiforms + neoselachians, as in the results of the present analysis. It should be noted that the analysis of Coates and Sequeira (2001A, B) in particular included numerous symmoriiform and fossil holocephalan taxa not included in the current analysis, adding additional information for holocephalans that had an effect on the topology. However, in the present study, holocephalans and Palaeozoic sharks were not the focus of study, and were included only as outgroups to Hybodontiformes.

Second, in this analysis, it was somewhat surprising that xenacanths and ctenacanths formed a sister group to *Cladoselache* + *Akmonistion*, rather than being placed in their more traditional position as basal elasmobranchs (e.g., Young, 1982; Maisey, 1984; Gaudin, 1991; Coates and Sequeira, 2001A, B). However, a similar topology was found by Ginter (2005), with ctenacanths as the sister group to symmoriiforms + cladoselachiforms, and xenacanths forming an even more basal outgroup. Further phylogenetic analyses, focused on larger-scale chondrichthyan phylogeny and including more comprehensive sets of characters, will hopefully help to elucidate this issue.

# CHAPTER 16: CONCLUSIONS

1. Unusually well-preserved new fossil material of the Lower Cretaceous hybodont *Tribodus limae* reveals that hybodontiforms were a much more diverse group than was previously thought, with a range of ecologically specialized and morphologically diverse taxa paralleling that of extant neoselachians. Its batoid-like pavement dentition of occlusally flat, hexagonal teeth, as well as its jaw morphology, suggest that *Tribodus limae* was most likely a durophagous benthic feeder that specialized on hard-shelled prey such as crustaceans. *Tribodus* differs from other known hybodonts in its internal and external cranial morphology in several respects, and shows the following autapomorphic features: presence of a median ventral process; paired posterior basicranial processes; narrow postorbital process with anteroposteriorly short jugular canal; mediolaterally broad, ventrally projecting antorbital processes encircling orbit; paired foramina for lateral dorsal aortae; location of efferent pseudobranchial and pituitary vein foramina; and lateral dorsal aortae enter basicranial cartilage posterior to branchpoint for efferent hyoidean artery.

2. Examination of cranial morphology of *Tribodus limae* and *Egertonodus basanus* with the aid of CT scanning reveals the following similarities, confirming several of Maisey's morphological observations (2004A): trochlear foramen anterior to optic foramen; glossopharyngeal and vagus nerve exit posteriorly through a single foramen; otic capsules located between postorbital processes; perilymphatic foramina; median capsular wall; posterior semicircular canal forms nearly complete circuit; absence of crus between

anterior and posterior semicircular canals. It also reveals several new similarities, including: presence of three separate foramina for the trigemino-facial-anterior lateral line complex (including a separate foramen for the superficial ophthalmic complex); presence of separate foramina for the anterior and posterior rami of the octaval nerve; presence of paired basioccipital foramina for the occipital arteries (previously thought to contain a short canal for the lateral dorsal aortae in *Egertonodus*). Additionally, the following major differences were noted: 1) the pituitary vein foramen is positioned much farther posteriorly in *Tribodus*, suggesting that the extent of its embryonic polar cartilage may have been shorter than in *Egertonodus*; and 2) the pattern of cranial arterial circulation differs greatly between *Tribodus* and *Egertonodus*, in that in *Egertonodus* the entire basicranial circuit is external to the braincase and there is a single median foramen for the internal carotid artery (whereas in *Tribodus* the lateral dorsal aortae enter the basicranial cartilage posteriorly through paired foramina above the posterior basicranial processes, the efferent hyoidean and orbital arteries diverge from the lateral dorsal aortae within the cartilage, and the internal carotids do not pass through the median foramen). Because internal cranial anatomy has only been examined in a few fossil chondrichthyan taxa (e.g., *Cladodoides*, *Cobelodus*, *Orthacanthus*, *Tribodus* and *Egertonodus*) and is presently unknown in other hybodonts, many of these features were not included in the present phylogenetic analysis; however, they remain as potential characters for future such analyses as additional data becomes available.

3. *Tribodus* was similar to *Asteracanthus* in having transversely oriented jaws that did not reach the ethmoid region and lacked ethmoidal articular facets, as well as a crushing

dentition of occlusally flattened teeth containing columnar osteodentine. The hyomandibular articulation with the braincase was posteriorly positioned, as in other hybodontiforms except *Tristychius*. The posterior pharyngobranchials of *Tribodus* were not fused (unlike neoselachians). A pharyngobranchial blade was present, a feature previously considered a synapomorphy of *Heterodontus* and galeomorph sharks, but which increasing evidence suggests may be plesiomorphic for neoselachians. Presence of paired rounded prominences located on the antorbital processes and lacking prismatic calcification suggest an attachment site for the preorbitalis muscles, which may have been well developed and used for jaw protrusion during suction feeding. The presence of a pavement dentition and transversely oriented jaws with a deep adductor fossa and supported internally by endochondral "struts" similar to those of extant batoids (revealed by CT scanning) support the conclusion that *Tribodus* was a durophagous benthic feeder.

4. Well-preserved fossil material of *Tribodus limae* pectoral girdles in which the pectoral articular process is preserved in three dimensions calls for a revised reconstruction of its pectoral endoskeleton. Rather than articulating in a crescent-shaped glenoid fossa as in previous reconstructions, the pectoral fin articulated with the girdle along a posteriorly positioned, obliquely oriented ridge, similar to that of many neoselachians and unlike that of *Cladoselache* and *Akmonistion* (which is oriented horizontally). This finding suggests that morphology of the pectoral articulation in other hybodonts was probably similar, although this cannot be confirmed at present due to the lack of three-dimensionally preserved scapulocoracoids in other hybodonts.

5. The vertebral column of *Tribodus* includes both basidorsals (with foramina for the ventral spinal nerve roots) and interdorsals (with foramina for the dorsal spinal nerve roots), the first evidence of these features in any hybodontiform. Approximately 10–12 elongate calcified pleural ribs were present on each side, as in other hybodonts, and were continuous with the basiventrals. The basiventrals contain well-preserved foramina for the caudal blood vessels, and additional dorsal elements are present which may represent interventrals. Two dorsal fins, each with an anterior spine and ventral basal plate, were present as in other hybodontiforms.

5. The dermal skeleton of *Tribodus* includes dorsal fin spines similar to those of other Hybodontidae, with a convex posterior wall, two rows of posterior retrorse denticles located at the midline, and numerous costae with a bifurcating and intercalating pattern; nongrowing dermal denticles; occlusally flat hexagonal teeth with single crystallite enameloid (SCE) and lacking the parallel-fibred and tangle-fibred layers of neoselachian teeth, and possessing columnar osteodentine (similar to those of *Asteracanthus*); and a single pair of cephalic spines lacking accessory cusps and having a T-shaped, trilobate base.

6. Results of the first computer-based phylogenetic analysis of Hybodontidae, with a matrix of 129 characters and 33 total taxa, provide strong support for the monophyly of Hybodontiformes above *Tristychius* (a clade including *Onychoselache* + Hybodontoidei), and for its sister-group relationship with neoselachians. However, *Tristychius* is placed as basal to this clade, in contrast with some previous hypotheses (e.g., Maisey, 1989; Coates

and Gess, 2007) and with its current classification (but supporting a hypothesis proposed by Maisey et al., 2004). This placement of *Tristychius* renders Hybodontiformes paraphyletic without Neoselachii. Eight unambiguous synapomorphies support a clade comprising Neoselachii + hybodonts, to the exclusion of *Tristychius*. Based on these results, it is suggested that Hybodontiformes may need to be restrictively redefined to exclude *Tristychius*. Within the clade *Onychoselache* + Hybodontoidei, several additional monophyletic clades are supported. The monophyly of Hybodontoidei (*Hamiltonichthys* + Mesozoic hybodonts) is strongly supported. A 'Mesozoic hybodont' clade is also supported, as are Lonchidiidae, Hybodontidae, and Hybodontinae. However, *Hybodus medius* resolves outside of other members of *Hybodus* at the base of Hybodontinae, and its placement in a new genus may be necessary.

7. Phylogenetic analysis supports the conclusion that *Tribodus limae* is correctly placed within the clades '*Onychoselache* + Hybodontoidea' (Hybodontiformes exclusive of *Tristychius*), Hybodontoidea, and Hybodontidae. However, its inclusion in a monophyletic subfamily 'Acrodontinae' is not unequivocally supported by the results of the present analysis. *Tribodus limae* resolves as the sister group of *Asteracanthus* in all most parsimonious trees (MPTs) resulting from the analysis, but in the strict consensus of 70 total MPTs *Acrodus* is placed in an unresolved trichotomy with Hybodontinae and a *Tribodus*/*Asteracanthus* clade. *Acrodus* differs from both *Tribodus* and *Asteracanthus* in having anteriorly elongate jaws that reach the ethmoid region and have ethmoidal facets, as in Hybodontinae. Its placement in Acrodontinae is considered questionable. If *Acrodus*

is ultimately removed from Acrodontinae, that subfamily would need to be renamed to reflect only included genera.

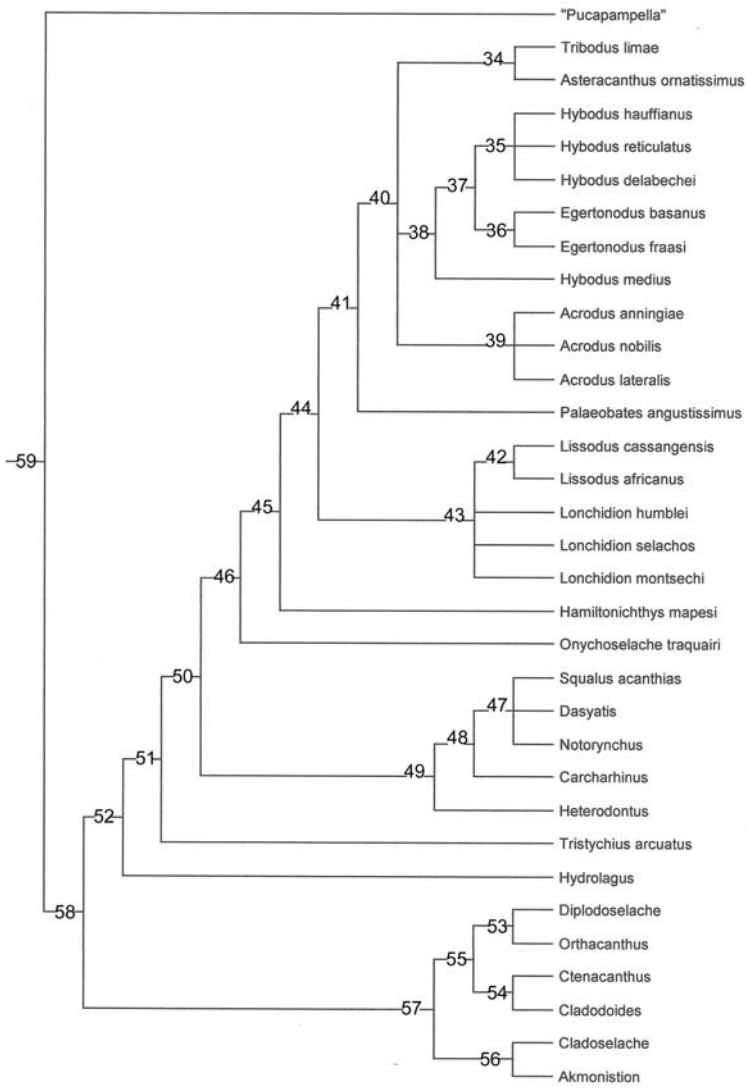



Figure 115: Strict consensus of 70 MPTs resulting from heuristic search in PAUP* 4.0, nodes numbered to correspond to text and Appendix E (list of apomorphies).

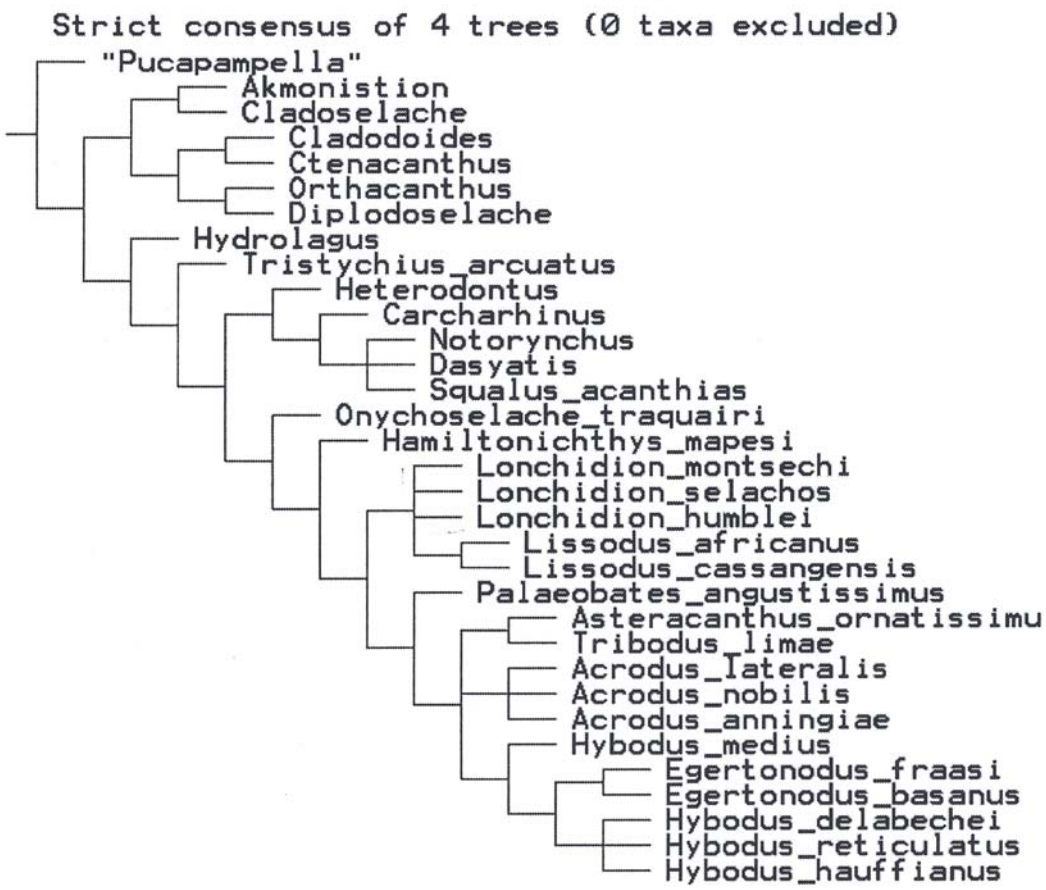



FIGURE 116: Strict consensus of 4 most parsimonious trees generated in T.N.T. (Tree analysis using New Technology: Goloboff, 1998) using identical search parameters to the PAUP search, and resulting in the same topology as in the PAUP analysis.

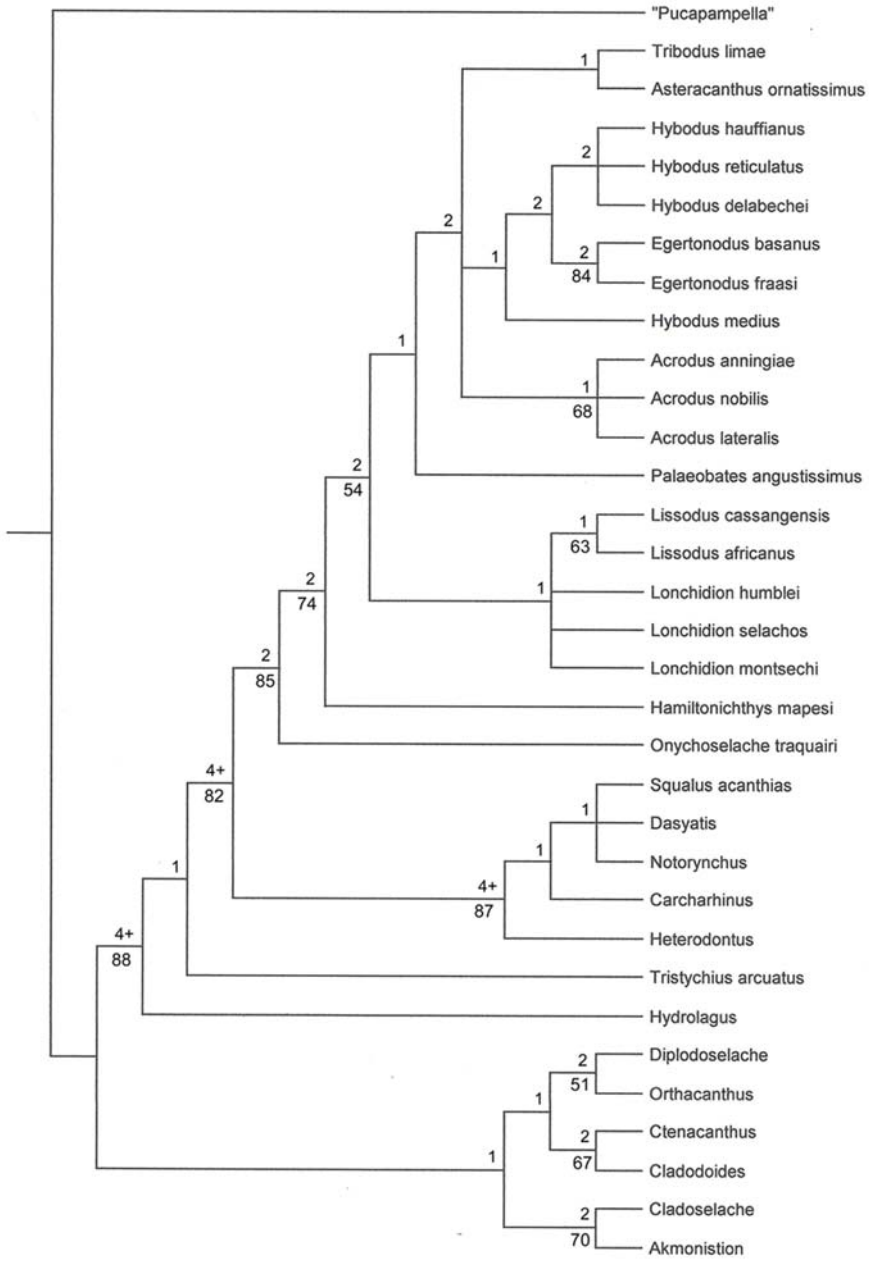



Figure 117: Strict consensus of 70 most parsimonious trees resulting from heuristic search using PAUP version 4.0b. Data matrix shown in Appendix B. Bremer support values are indicated above and Bootstrap values above 50% are indicated below each node. Consistency Index (CI) = 0.5309; Retention Index (RI) = 0.7996; Rescaled Consistency Index (RC) = 0.4245.

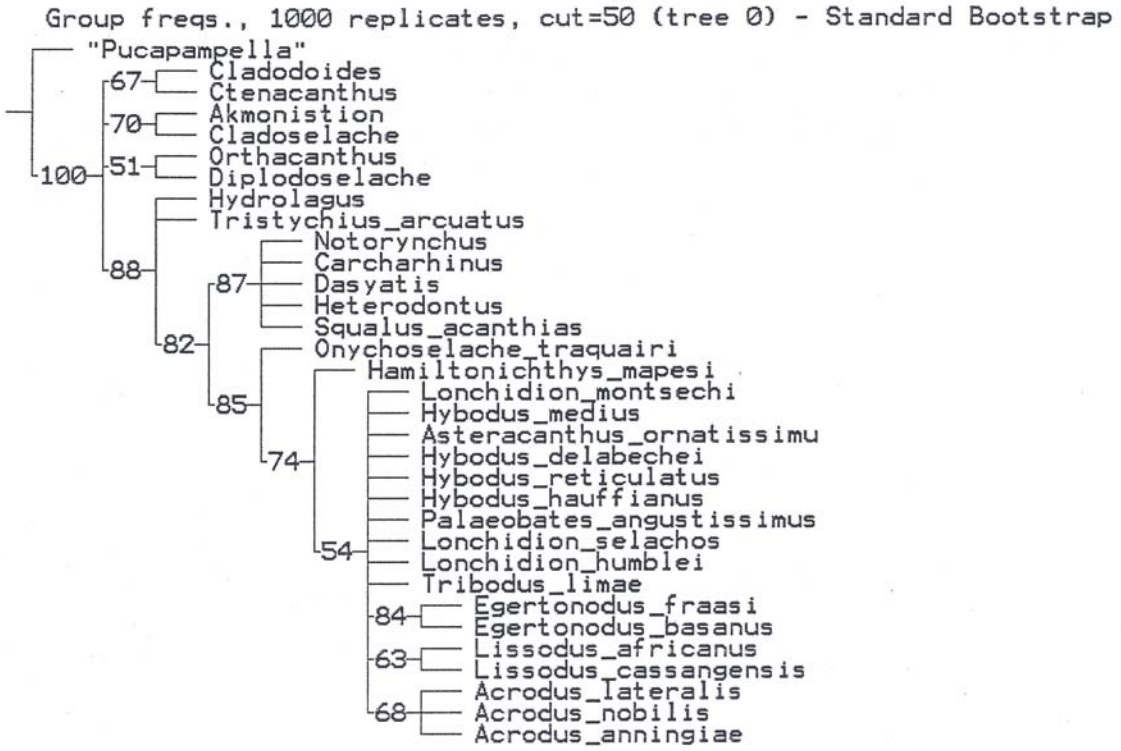



Figure 118: Results of Bootstrap analysis performed on the dataset using TNT (Goloboff, 1998). Bootstrap values are mapped onto the strict consensus tree in Figure 117. Nodes appearing in the strict consensus tree but collapsed here have Bootstrap values less than 50%.

FIGURE 119. Phylogeny of Hybodontiformes proposed by Maisey, 1989. Characters: 1, shoulder-joint with strong propterygial support; 2, pectoral articulation rotated; 3, enlarged pelvic "propterygium"; 4, glossopharyngeal canal; 5, calcified pleural ribs; 6, fin spines possess large retrorse denticles and smooth ribs; 7, low-crowned teeth; 8, otic capsules located between postorbital processes; 9, elongate lateral teeth; 10, postorbital articulation absent; 11, inflated and elongate jugular canal; 12, large, downturned postorbital processes; 13, puboischiadic bar in males; 14, cephalic spines present; 15, fin spines have convex posterior wall denticles adjacent to posterior midline; 16, low number (10–12) of pleural ribs; 17, pattern of pectoral basals and radials; 18, coracoid and scapular regions of subequal length; 19, puboischiadic bar in females; 20, palatoquadrate with separate ethmopalatine and ethmoidal articular surfaces anteriorly; 21, erect hyomandibula with broad upper end passing dorsal to palatoquadrate; 22, "hybodontid-type" growing dermal denticles (sensu Reif); 23, "*Sphenonchus*" cephalic spines; 24, "convict-arrow" shaped cephalic spines; 25, osteodont teeth with anaulacorhize base; 26, cephalic spines with secondarily closed pulp cavity; 27, large labial apparatus; 28, teeth with columnar osteodentine; 29, adjacent tooth-rows; 30, fin-spines with stellate tubercles; 31, cephalic spines lack accessory cusps; 32, elaborate durophagous dentition; 33, high-crowned, multicuspid teeth; 34, all dermal denticles nongrowing; 35, single pair of cephalic spines.

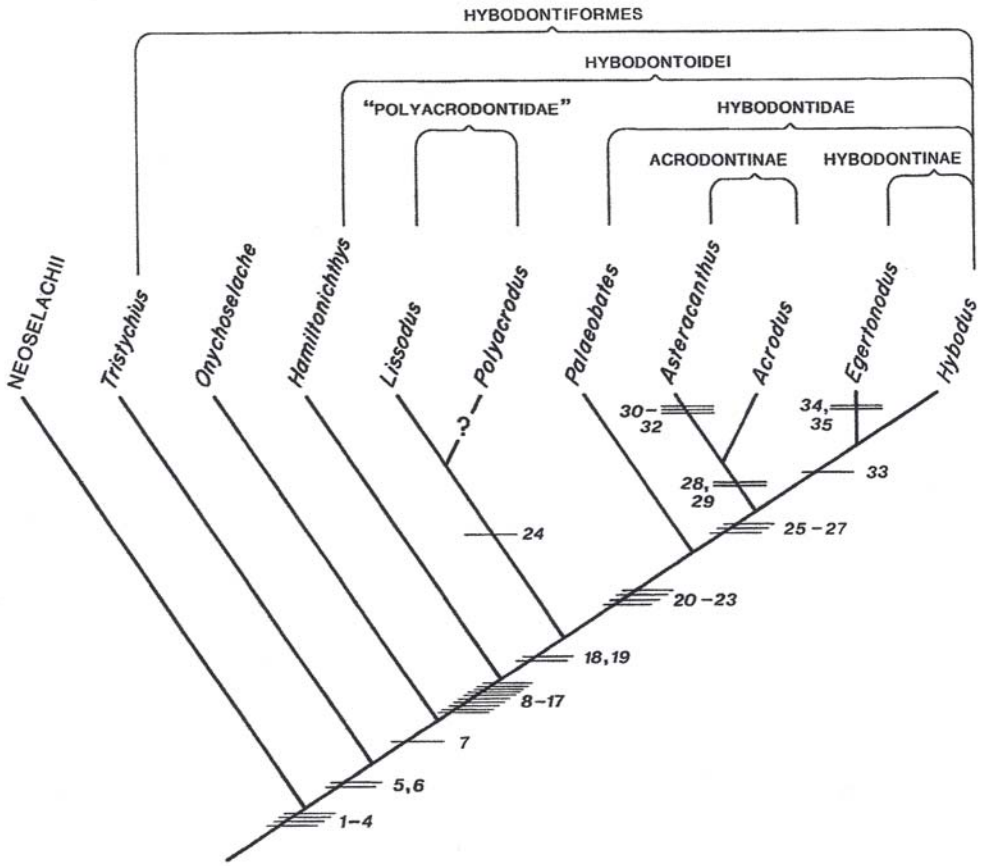

HYBODONTIFORMES
HYBODONTOIDEI
"POLYACRODONTIDAE"
HYBODONTIDAE
ACRODONTINAE
HYBODONTINAE
NEOSELACHII
Tristychius
Onychoselache
Hamiltonichthys
Lissodus
? Polyacrodus
Palaeobates
Asteracanthus
Acrodus
Egertonodus
Hybodus
30–32
34, 35
28, 29
33
24
25–27
20–23
18,19
8–17
7
5,6
1–4

FIGURE 120. Phylogeny of Hybodontoidea proposed by Rees, 2008. Numbers refer to characters used by Rees (2008). 1, cephalic spines present; 2, cephalic spines without large lateral cusplets; 3, T-shaped basal plate of cephalic spines; 4, low-cusped teeth with labial protuberance, low root with row of small foramina on the upper part, arrow-shaped basal plate of cephalic spines; 5, labio-lingually narrow, gracile teeth without ornamentation, strong and narrow labial protuberance; 6, bulky teeth ornamented with granulae; 7, crushing dentition and complex, partly reticulate ornamentation; 8, moderately high cusp and cusplets, labial protuberance rounded, ornamentation with few folds; 9, T-shaped basal plate of cephalic spine with short and rounded posterior lobe; 10, domed teeth with low cusp and cusplets, wide and triangular labial protuberance, ornamentation with numerous weak folds, posterior lobe of basal plate of cephalic spine long and dorso-ventrally flattened, anterior lobes of basal plate thin and having raised anterior edges; 11, high-crowned teeth with cusplets, no differentiated, small circular foramina on root; 12, crushing dentition with enlarged lateral teeth, complex ornamentation; 13, interlocking teeth with flat crown, asymmetrical lateral teeth, reticulate ornamentation, massive root with well-defined foramina; 14, cusps in anterior teeth, symmetrical enlarged lateral teeth, porous root; 15, wide lateral teeth, reduced number of tooth files, fin spines with tubercles on the anterior side; 16, narrow lateral teeth; 17, cutting dentition with wide, flattened cusp, serrated cutting edges; 18, high, narrow, and slender or conical cusps with close to circular cross-section, porous root; 19, stout cusplets, strong ornamentation; 20, sigmoidal curvature of the cusp, slender cusplets, weak ornamentation; 21, diverging cusplets, weak or no ornamentation; 22, high and wide symmetrical teeth, strong, rarely serrated cutting edges, simple ornamentation

with short folds; 23, strongly diverging cusplets, evenly serrated cutting edges, high and massive root; 24, diverging cusplets in anterior teeth, recurved crown in lateral teeth, poorly serrated cutting edges.

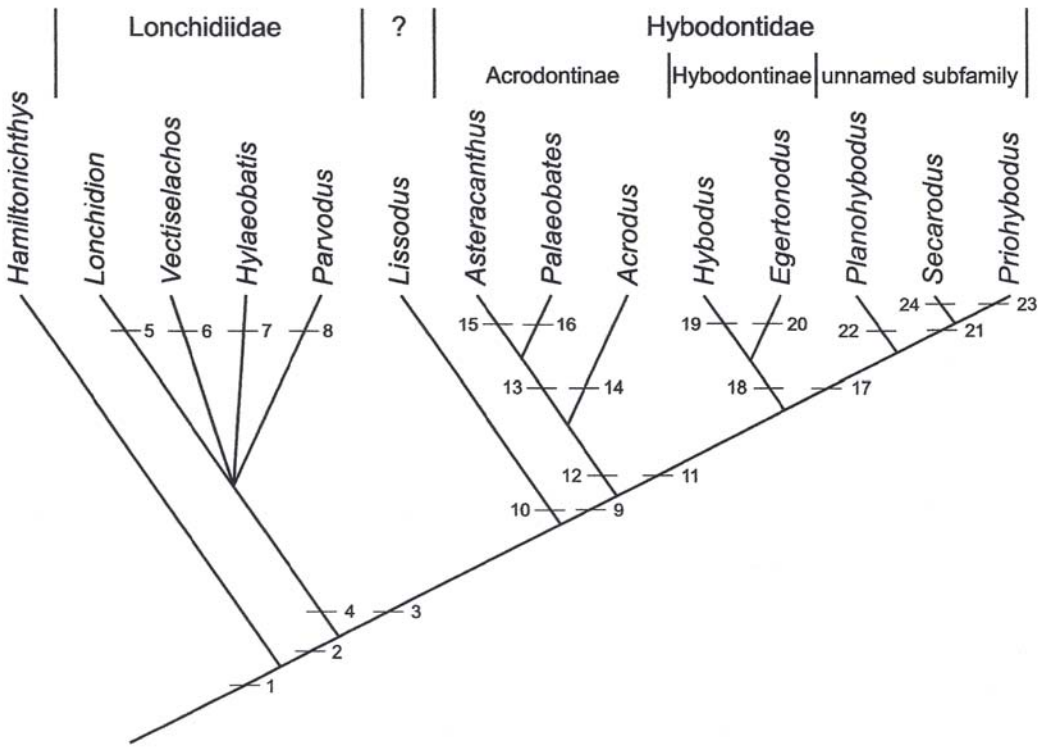

Lonchidiidae
?
Hybodontidae
Acrodontinae
Hybodontinae
unnamed subfamily
Hamiltonichthys
Lonchidion
Vectiselachos
Hylaeobatis
Parvodus
Lissodus
Asteracanthus
Palaeobates
Acrodus
Hybodus
Egertonodus
Planohybodus
Secarodus
Priohybodus
1
2
3
4
5
6
7
8
9
10
11
12
13
14
15
16
17
18
19
20
21
22
23
24

FIGURE 121. Phylogeny of hybodonts proposed by Maisey et al., 2004.

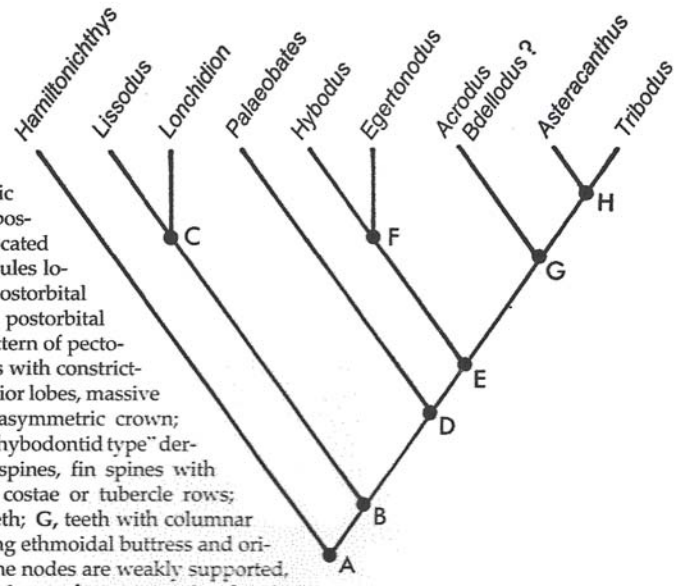



**Fig. 2.**
Hypothesis of phylogenetic relationships among the better-known Mesozoic hybodonts. *Hamiltonichthys* (Pennsylvanian, Kansas) represents the cladistically primitive sister taxon of remaining hybodonts. Characters supporting nodes as follows: **A,** cephalic spines present, fin spines with convex posterior wall and with retrorse denticles located at fin spine posterior midline, otic capsules located between postorbital processes, postorbital articulation absent, large downturned postorbital process, low number of pleural ribs, pattern of pectoral basals and radials; **B,** cephalic spines with constricted basal plate, distinct lateral and posterior lobes, massive central cusp with retrorse barb, and asymmetric crown; **C,** "convict-arrow" cephalic spines; **D,** "hybodontid type" dermal denticles, "*Sphenonchus*" cephalic spines, fin spines with numerous bifurcating or intercalating costae or tubercle rows; **E,** osteodont teeth; **F,** high-crowned teeth; **G,** teeth with columnar osteodentine; **H,** palatoquadrates lacking ethmoidal buttress and oriented transversely. Although some of the nodes are weakly supported, by emphasizing dermal features the phylogeny has some utility for identifying isolated teeth, denticles and spines.

FIGURE 122. Previous hypotheses of neoselachian interrelationships. Adapted from Maisey et al., 2004.

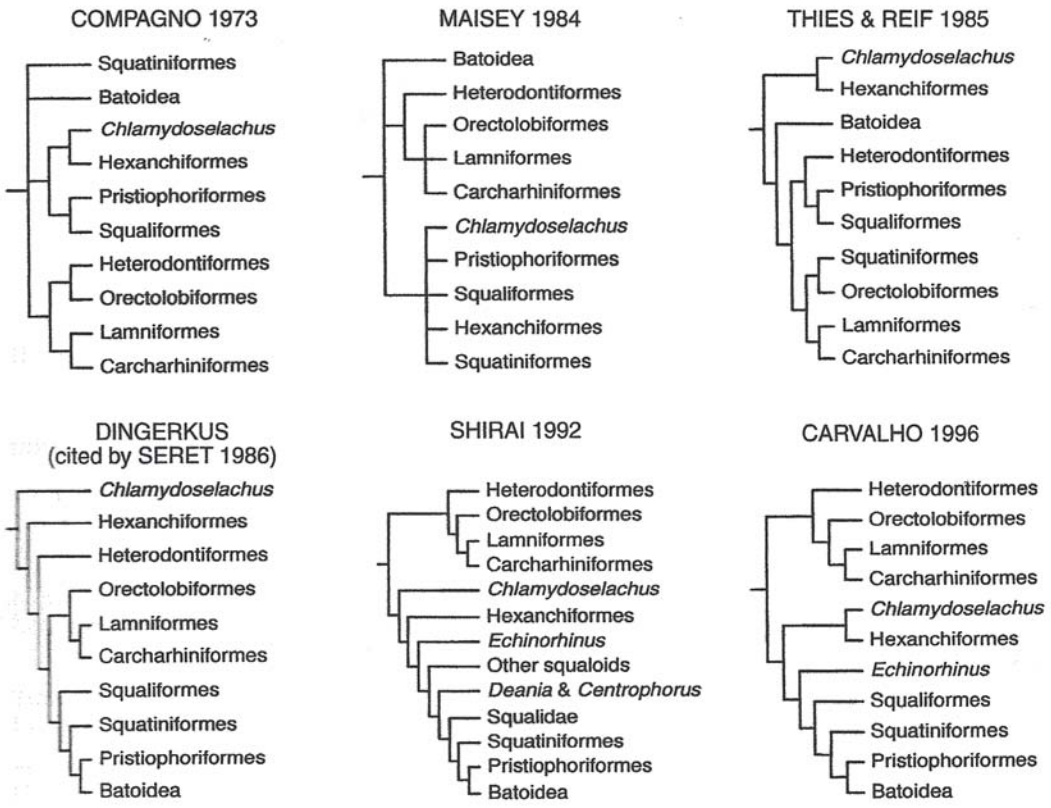
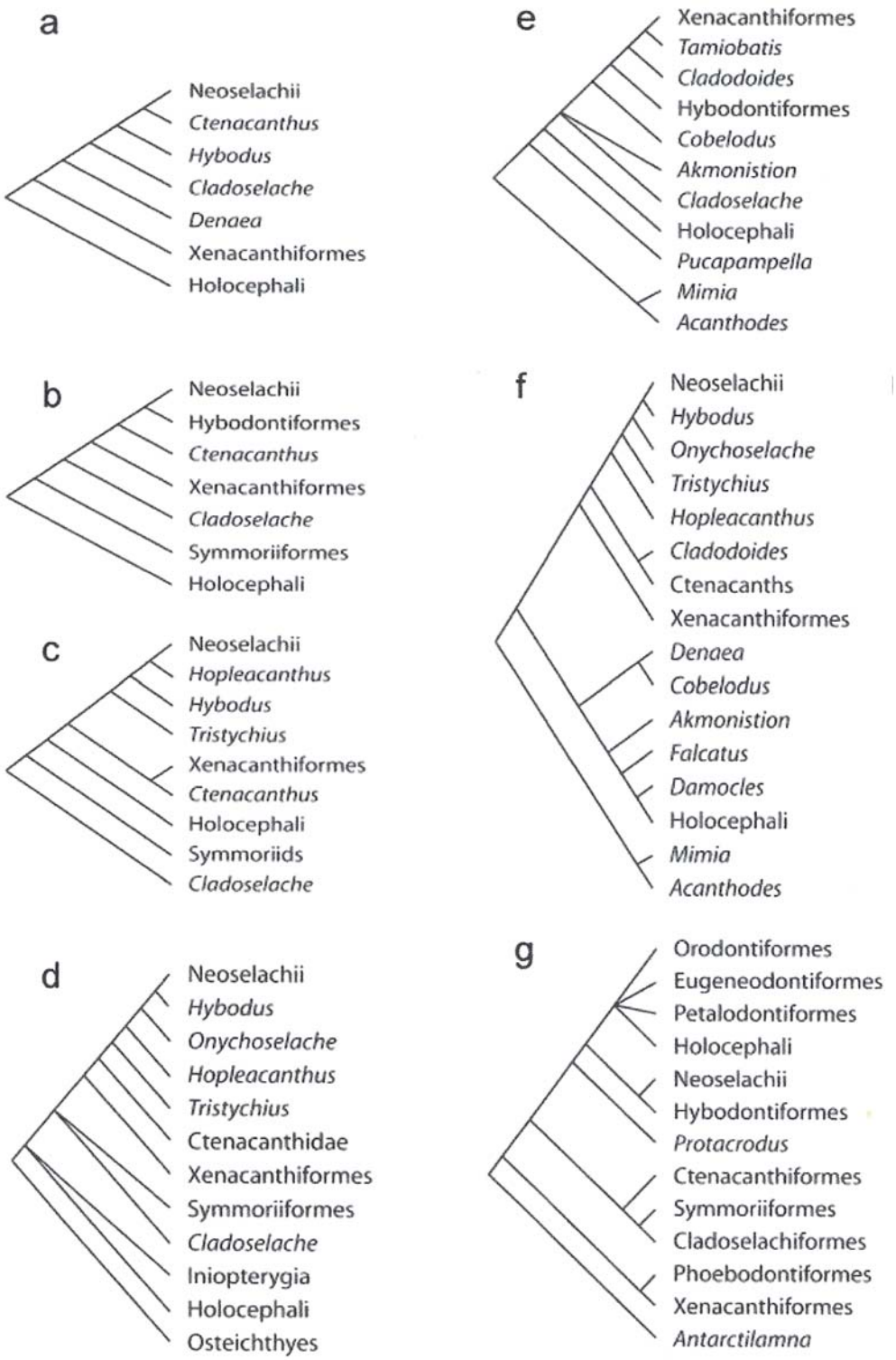

COMPAGNO 1973
Squatiniformes
Batoidea
Chlamydoselachus
Hexanchiformes
Pristiophoriformes
Squaliformes
Heterodontiformes
Orectolobiformes
Lamniformes
Carcharhiniformes
MAISEY 1984
Batoidea
Heterodontiformes
Orectolobiformes
Lamniformes
Carcharhiniformes
Chlamydoselachus
Pristiophoriformes
Squaliformes
Hexanchiformes
Squatiniformes
THIES & REIF 1985
Chlamydoselachus
Hexanchiformes
Batoidea
Heterodontiformes
Pristiophoriformes
Squaliformes
Squatiniformes
Orectolobiformes
Lamniformes
Carcharhiniformes
DINGERKUS
(cited by SERET 1986)
Chlamydoselachus
Hexanchiformes
Heterodontiformes
Orectolobiformes
Lamniformes
Carcharhiniformes
Squaliformes
Squatiniformes
Pristiophoriformes
Batoidea
SHIRAI 1992
Heterodontiformes
Orectolobiformes
Lamniformes
Carcharhiniformes
Chlamydoselachus
Hexanchiformes
Echinorhinus
Other squaloids
Deania & Centrophorus
Squalidae
Squatiniformes
Pristiophoriformes
Batoidea
CARVALHO 1996
Heterodontiformes
Orectolobiformes
Lamniformes
Carcharhiniformes
Chlamydoselachus
Hexanchiformes
Echinorhinus
Squaliformes
Squatiniformes
Pristiophoriformes
Batoidea

FIGURE 123. Previous hypotheses of chondrichthyan interrelationships. A, Schaeffer and Williams, 1977; B, Young, 1982; C, Maisey, 1984; D, Gaudin, 1991; E, Maisey, 2001; F, Coates and Sequeira, 2001a, b; G, Ginter, 2005. Modified from Gillis and Donoghue, 2007.


a
Neoselachii
Ctenacanthus
Hybodus
Cladoselache
Denaea
Xenacanthiformes
Holocephali
b
Neoselachii
Hybodontiformes
Ctenacanthus
Xenacanthiformes
Cladoselache
Symmoriiformes
Holocephali
c
Neoselachii
Hopleacanthus
Hybodus
Tristychius
Xenacanthiformes
Ctenacanthus
Holocephali
Symmoriids
Cladoselache
d
Neoselachii
Hybodus
Onychoselache
Hopleacanthus
Tristychius
Ctenacanthidae
Xenacanthiformes
Symmoriiformes
Cladoselache
Iniopterygia
Holocephali
Osteichthyes
e
Xenacanthiformes
Tamiobatis
Cladodoides
Hybodontiformes
Cobelodus
Akmonistion
Cladoselache
Holocephali
Pucapampella
Mimia
Acanthodes
f
Neoselachii
Hybodus
Onychoselache
Tristychius
Hopleacanthus
Cladodoides
Ctenacanths
Xenacanthiformes
Denaea
Cobelodus
Akmonistion
Falcatus
Damocles
Holocephali
Mimia
Acanthodes
g
Orodontiformes
Eugeneodontiformes
Petalodontiformes
Holocephali
Neoselachii
Hybodontiformes
Protacrodus
Ctenacanthiformes
Symmoriiformes
Cladoselachiformes
Phoebodontiformes
Xenacanthiformes
Antarctilamna

# APPENDIX A: LIST OF CHARACTERS

## Neurocranium

1. Precerebral fontanelle absent=0; present=1

2. glossopharyngeal nerve passes through metotic fissure absent=0; present=1

3. Dorsal otic ridge has horizontal crests=0; dorsal otic ridge lacks horizontal crests=1 (CG)

4. Otico-occipital fissure open behind posterior dorsal fontanelle=0; otico-occipital fissure closed behind posterior dorsal fontanelle=1 (JGM; CG)

5. Metotic fissure open=0; metotic fissure closed=1 (CG)

6. Ventral otic fissure open=0; ventral otic fissure closed=1 (CG)

7. Occipital block not wedged between otic capsules=0; occipital block wedged between otic capsules=1 (CG)

8. Dorsal otic ridge absent=0; present=1

9. Crus between anterior and posterior semicircular canals present=0; absent=1 (JGM; CG)

10. Inner ear adapted for semi-directional low-frequency phonoreception (i.e., Pre-ampullary part of posterior semicircular canal extends dorsally to perilymphatic fenestra, so that the canal forms a complete circuit; separation of utricular and saccular regions; posterior canal duct and perilymphatic openings present; medial chondrified otic capsule wall separating labyrinth and endocranial cavity) absent=0; present=1 (JGM; CG)

11. internasal keel absent=0; present=1

12. rostral bar elongated=0; short=1

13. inflated ethmopalatine processes absent=0; present=1

14. Suborbital shelf present=0; absent=1

15. suborbital shelf broad and laterally flared beneath postnasal wall: absent=0; present=1

16. Trochlear foramen dorsal and anterior to optic foramen
absent=0; present=1 (CG)

17. Proximal part of epihyal/hyomandibula located anteriorly in the otic region: absent=0; present=1.

18. posterior dorsal fontanelle absent=0; present=1

19. Occipital half-centrum absent=0; present=1

20. efferent pseudobranchial foramen dorsal to level of suborbital shelf or base of orbit: absent=0; present=1

21. Hypotic lamina absent=0; present=1

22. Otic capsules located between postorbital processes
absent=0; present=1 (JGM; CG)

23. Large, down-turned postorbital process
absent=0; present=1 (JGM; CG)

24. postorbital process positioned over trigemino-facialis region: absent=0; present=1

25. Lateral commissure chondrified to contain jugular canal: present=0; absent=1

26. Postorbital articulation with the palatoquadrate
present=0; absent=1 (JGM; CG)

27. postorbital articulation with lateral commissure present=0; absent=1

28. Postorbital articulation with primary postorbital process absent=0; present=1

29. Lateral dorsal aortae enter basicranial cartilage prior to junction with efferent hyoidean artery=0; lateral dorsal aortae do not enter basicranial cartilage prior to junction with efferent hyoidean artery=1

30. lateral dorsal aortae enter braincase at level of occipital block through single posterior foramen=0; through paired foramina=1

31. lateral dorsal aortae enter basicranium at level of occipital block present=0; absent=1

32. lateral dorsal aortae extend laterally to meet efferent hyoidean arteries (forming a "Bell-shaped" basicranial arterial circuit) absent=0; present=1

33. inflated and elongate jugular canal (i.e., jugular canal extends posteriorly to midpoint of otic region) absent=0; present=1

34. Ethmoidal articulation present=0; absent=1

35. Palatobasal articulation absent=0; present=1

**Visceral Skeleton**

36. Mandibular joint located behind occiput. present=0; absent=1

37. upper jaw not fused with neurocranium=0; upper jaw fused to neurocranium (holostyly)=1

38. Jaws extend to ethmoid region=0; jaws do not extend to ethmoid region=1

39. Palatoquadrates separated symphysially by ethmoid region=0; palatoquadrates meet or are fused symphysially=1

40. quadrate flange extends anterolaterally to overhang adductor fossa absent=0; present=1

41. palatoquadrate otic process expanded dorsally behind postorbital process present=0; absent=1 (CG)

42. palatoquadrate "cleaver-shaped" present=0; absent=1

43. orbital process of palatoquadrate extends into orbit between optic pedicel and optic nerve foramen. absent=0; present=1

44. labial cartilage complex extends from ethmoid region to postorbital process: absent=0; present=1

45. hyomandibula decoupled from ceratohyal: absent=0; present=1

46. Basihyal forms a wide transverse bar: absent=0; present=1

47. Hyoid rays elongate supporting opercular flap: absent=0; present=1

48. Operculum supported by opercular cartilage absent=0; present=1

49. Branchial arches beneath rear of neurocranium
absent=0; present=1 (CG)

50. Posteriormost pharyngobranchials unfused=0; fused=1

51. Pharyngobranchial blade absent=0; present=1

52. Most hypobranchials directed posteriorly towards the midline absent=0; present=1

53. Basibranchials separated from basihyal by a gap: absent=0; present=1

54. Posteriorly directed median basibranchial copula absent=0; present=1

**Appendicular Skeleton**

55. Scapular process narrow dorsally and lacking posterolateral angle absent=0; present=1 (CG)

56. Scapulocoracoid with a continuously concave anteromedial edge (coracoid anterodorsal shoulder reduced or absent)
absent=0; present=1 (CG)

57. Imperforate scapulocoracoid, foramen for diazonal nerves and blood vessels missing
absent=0; present=1 (CG)

58. Coracobranchial fossa (grooved leading edge) on scapulocoracoid
absent=0; present=1 (CG)

59. Pectoral fin articulation on lateral face of coracoid
absent=0; present=1 (CG)

60. Coracoid and scapular regions of near-equal length
absent=0; present=1 (JGM; CG)

61. Shoulder girdle fused with vertebral column: absent=0; present=1

62. tribasal pectoral fin: absent=0; present=1

63. Dibasal fin, separate mesopterygium missing
absent=0; present=1 (CG)

64. pectoral articular surface oriented horizontally=0; oriented obliquely=1

65. Propterygium with convex leading edge
absent=0; present=1 (CG)

66. Mesopterygium sickle-shaped
absent=0; present=1 (CG)

67. metapterygium connecting with distinct series of distal radials articulating proximodistally to form an axis: absent=0; present=1

68. premetapterygial radials articulate with compound basal cartilages absent=0; present=1

69. Puboischiadic bar in males
absent=0; present=1 (JGM; CG)

70. Puboischiadic bar in females
absent=0; present=1 (JGM; CG)

71. First pelvic radial (propterygium) enlarged relative to other radials.
absent=0; present=1 (JGM; CG)

72. Pelvic propterygium terminal, no distal cartilages
absent=0; present=1 (CG)

73. pelvic metapterygium articulates with all but the first few radials: absent=0; present=1

**Axial skeleton**

74. calcified pleural ribs
absent=0; present=1 (JGM; CG)

75. low number (10-12) of pleural ribs
absent=0; present=1 (JGM; CG)

76. vertebral column includes calcified chordal centra: absent=0; present=1

77. anterior neural and hemal arcualia unfused=0; fused to form synarcual=1

78. anterior dorsal fin absent=0; present=1

79. anterior dorsal fin base plate uncalcified=0; calcified=1

80. posterior dorsal fin absent=0; present=1

81. posterior dorsal fin base plate uncalcified=0; calcified=1

82. complete series of perichondrally calcified radials in anterior dorsal fin: absent=0; present=1

83. single dorsal fin elongate, extending from near pectoral level to anal or pre-anal fin level absent=0; present=1

84. anal fin absent=0; anal fin present=1

85. anal fin with double base-plate absent=0; present=1

86. semilunate tail with well-developed hypaxial endoskeleton present=0; absent=1

**Dermal Skeleton**

87. single-crystallite enameloid (SCE) in teeth absent=0; present=1

88. low-crowned teeth
absent=0; present=1 (JGM; CG)

89. Tooth crowns with a lingual swelling
absent=0; present=1 (JGM; CG)

90. Elongate lateral teeth
absent=0; present=1 (JGM; CG)

91. Tooth histology: orthodont=0; osteodont=1
(modified from JGM; CG)

92. "parallel-fibred" enameloid absent=0; present=1

93. "tangle-fibred" enameloid absent=0; present=1

94. High-crowned multicuspid teeth
absent=0; present=1 (JGM; CG)

95. Teeth with columnar osteodentine
absent=0; present=1 (JGM; CG)

96. Teeth without labial peg=0; labial peg present=1

97. Teeth with sigmoidal curvature of the cusps, slender cusplets, weak ornamentation
absent=0; present=1 [Rees, 2008]

98. Domed teeth with low cusp and cusplets, wide triangular labial protuberance, ornament with numerous weak folds (Rees, 2008): absent=0; present=1

99. Occlusally flattened elongate lateral teeth with reticulate ornamentation and massive root: absent=0; present=1

100. pavement dentition absent=0; present=1

101. Diplodont teeth absent=0; present=1

102. Crushing teeth with rounded cusps, ornament of ridges radiating from cusp apex and bifurcating towards tooth base: absent=0; present=1

103. Fin spines possess large retrorse denticles and smooth ribs
absent=0; present=1 (JGM; CG)

104. Fin spines have convex posterior wall, denticles adjacent to posterior midline:
absent=0; present=1 (JGM; CG)

105. Fin spines with numerous bifurcating or intercalating costae or tubercle rows:
absent=0; present=1 (JGM; CG)

106. Fin spines with few, widely-spaced costae absent=0; present=1

107. Anterior dorsal fin spine absent=0; present=1

108. Posterior dorsal fin spine. absent=0; present=1

109. Dorsal fin spine rounded in cross-section, ornamented only by retrorse denticles:
absent=0; present=1

110. Fin spines with stellate tubercles absent=0; present=1

111. Finspines with mantle of shiny enameloid, lacking posterior denticles: absent=0;
present=1

112. Spine-brush complex absent=0; present=1

113. Male cephalic spines
absent=0; present=1 (JGM; CG)

114. Cephalic spines with constricted basal plate, lateral and posterior lobes, massive central cusp, and retrorse barb
absent=0; present=1 (JGM; CG)

115. 'Convict-arrow' shaped cephalic spines with narrow posterior lobe: absent=0;
present=1 (JGM; CG)

116. 'Sphenonchus' cephalic spines
absent=0; present=1 (JGM; CG)

117. Single (posterior) pair of cephalic spines: absent=0; present=1

118. Two pairs of cephalic spines (anterior and posterior): absent=0; present=1

119. Cephalic spines with accessory cusps present=0; absent=1

120. Cephalic spines with single principal cusp (with or without accessory cusps) absent=0; present=1

121. Cephalic spines lack large lateral cusplets (Rees. 2008) absent=0; present=1

122. Posterior lobe of cephalic spine and spine cusp of near-equal width=0; posterior lobe wider than spine cusp=1

123. Cephalic spines with T-shaped basal plate absent=0; present=1

124. Cephalic spine base plate with gracile lobes=0; with robust lobes=1

125. Synchronomorial (non-growing) denticles absent=0; present=1 (CG)

126. All dermal denticles nongrowing absent=0; present=1

127. Dermal denticles with constricted neck absent=0; present=1

128. Ring or C-shaped scales enclosing sensory canals absent=0; present=1

129. "Cladodont" teeth absent=0; present=1

# APPENDIX B: MATRIX OF TAXA AND CHARACTERS

Boldface type: ingroup tested in the present analysis

| TAXON | 1-10 | 11-20 | 21-30 | 31-40 | 41-50 | 51-60 | 61-70 | 71-80 | 81-90 | 91-100 | 101-110 | 110-120 | 121-129 |
|---|---|---|---|---|---|---|---|---|---|---|---|---|---|
| *"Pucapampella"* | ?010000100 | ???0?00100 | 1000000001 | 0100100000 | 000?0??0?? | ?????????? | ?????????? | ?????0???? | ?????????? | ?????????? | ?????????? | ??000000-0 | --0-????? |
| ***Tribodus limae*** | 1111111011 | 0101010101 | 111001100- | 1001110111 | 1100010000 | 1???110101 | 0101100111 | 1?11100111 | 100??11110 | 1000100001 | 0011101100 | 0011011011 | 101011000 |
| ***Onychoselache traquairi*** | 1?11111??? | ??????010? | ?11??11??? | ??101100?1 | 1100??000? | ????110110 | 0101110?0? | 1011000111 | 100101?110 | 0000000000 | 0010011100 | 00100000-0 | --0-11000 |
| ***Tristychius arcuatus*** | 111111100? | 0-0001110? | 100100001- | 1000110011 | 11000?101? | 11?1011000 | 0011001100 | 0011000111 | 100101?000 | 0000000000 | 0010011100 | 00000000-0 | --0-11100 |
| ***Hamiltonichthys mapesi*** | 1111111??? | 1??00?010? | 111?01101- | 1010110001 | 110???000? | ?111110100 | 0101100110 | 1011000111 | 1001111111 | 0000000000 | 0011011100 | 0010000101 | 0-0-11000 |
| ***Lissodus cassangensis*** | ?????????? | ??????0??? | ?????????? | ?????10??1 | 11??0?0000 | 1???110101 | 0101100111 | 1111100111 | 1001111101 | 0000010100 | 0011011100 | 001110??01 | 101011000 |
| ***Lissodus africanus*** | 1111111??? | ??????010? | 111?0????? | ?????10??1 | 110?0?000? | ????110101 | 0101100111 | 1?11100111 | 1001111101 | 0000010100 | 0011011100 | 0011100101 | 1010???00 |
| ***Lonchidion humblei*** | ?????????? | ?????????? | ?????????? | ?????????? | ?????????? | ?????????? | ?????????? | ???????1?1 | ??0????101 | 0000010000 | 001101?100 | 001110??01 | 1000????0 |
| ***Lonchidion selachos*** | ?????????? | ?????????? | ?????????? | ?????????? | ?????????? | ?????????? | ?????????? | ???????1?1 | ??0????101 | 0000010000 | 001101?100 | 001110???1 | 1000????0 |
| ***Lonchidion montsechi*** | ?????????? | ?????????? | ?????110?? | ?????10??1 | 1101??000? | ????11??01 | 0101100??? | ????1?0?1?? | ??0????101 | 0000010000 | 00????1??? | ?0???????? | ??????000 |
| ***Palaeobates angust.*** | ?????????? | ?????????? | ?????110?? | ??????0??1 | 110???00?? | ????11??01 | 0101??01?? | ????1100?1? | 100???1111 | 0000000010 | 0011101100 | 001101???1 | 1?11????0 |
| ***Hybodus hauffianus*** | 1111111??? | 1010010?10 | 111101101- | 1010110001 | 1101000000 | 11?1110101 | 0101100111 | 1111100111 | 100111?000 | 1001000000 | 0011101100 | 0011010111 | 111110000 |
| ***Hybodus reticulatus*** | 1111111??? | 10100?0100 | 111101101- | 1010110?1 | 1101000000 | ?111110101 | 0101100??? | ????1100111 | 100??11000 | 1001000000 | 0011101100 | 0011010101 | 111110000 |
| ***Hybodus delabechei*** | 1111111??? | 1010?1010? | 111?0110?? | ??10110001 | 1101000000 | ?1??11??01 | 0??1?????? | ?????0?111 | 100???1000 | 1001000000 | 0011101100 | 0011010101 | 111110000 |
| ***Hybodus medius*** | ?????????? | ????????0? | ??10111??? | ??10?10001 | 11010?0000 | ????110101 | 0??1?????? | ????1100111 | ?00????001 | ?000?00000 | 0011101100 | 0011010101 | 11111?000 |
| ***Egertonodus basanus*** | 1111111011 | 1110110101 | 111001101- | 1010110001 | 1101000000 | ??1?1??1?? | 0????????? | ????1100111 | 100????000 | 1001001000 | 0011101100 | 0011011011 | 111111000 |
| ***Egertonodus fraasi*** | 1111111??? | 1110110?10 | 1110011??? | ??10110001 | 11010?0000 | 0???11?101 | 0101100??1 | 1111100111 | 1001?11000 | 1001001000 | 0011101100 | 00????????? | ????110?0 |
| ***Acrodus anningiae*** | 1111111??? | ??1???0?10 | 111?0??0?? | ??101100?1 | 11010?000? | ?????????? | ?????????? | ?????0?111 | ?00???1111 | 1000100000 | 0111101100 | 0011010111 | 111110000 |
| ***Acrodus nobilis*** | ???1111??? | ??1???0?0? | 111?0??01- | 101?110??? | 11?10??00? | ?????????? | ?????????? | ?????0?111 | ?00???1111 | 1000100000 | 0111101100 | 0011010111 | 1111100?0 |
| ***Acrodus lateralis*** | ?????????? | ??1??????? | ???????0?? | ???0110001 | 110???000? | ????1????? | 0????????? | ???110?1?1 | ?00???1111 | 1000100000 | 0111101100 | 0011010111 | 1111100?0 |
| ***Asteracanthus ornatiss.*** | ?????????? | ?????????? | ?????110?? | ???11?0111 | 110??????? | ?????????? | ?????????? | ?????????1 | ??0????111 | 1000100010 | 0011101101 | 001101??11 | 11111?1?0 |
| *Squalus acanthias* | 1111111011 | 0-01000111 | 110011101- | 1101110110 | 1110010001 | 0111110001 | 0101100111 | 1010010111 | 1100010000 | 0110000000 | 0000001100 | 10000000-0 | ----11100 |
| *Notorynchus cepedianus* | 1111111011 | 0-01000111 | 110010111- | 1101100010 | 0110001001 | 0111110001 | 0101000111 | 1010010001 | 1001010000 | 0110000000 | 0000000000 | 00000000-0 | --0-11100 |
| *Heterodontus francisci* | 1111111011 | 0-00001111 | 110011101- | 1100010010 | 1100000001 | 1111110001 | 0101100111 | 1010010111 | 1101011101 | 0110100000 | 0000001100 | 10000000-0 | ----11000 |
| *Carcharhinus brevipinna* | 1111111011 | 0-00001111 | 110011101- | 1100010010 | 1100000001 | 1111110001 | 0101000111 | 1010010111 | 1101010000 | 0110000000 | 00000-0000 | 00000000-0 | --0-11100 |
| *Dasyatis americana* | 1111111011 | 0-01000101 | 110011101- | 1101010110 | 1100110001 | 0111010010 | 1100000111 | 1010011000 | 0000010100 | 0010000000 | 00000-0000 | 00000000-0 | ----11000 |
| *Hydrolagus collei* | 0011110000 | 0-0?001000 | 00001??01- | 100--11--0 | -0-0001111 | 0001000000 | 0011000100 | 0010001110 | -?11010--0 | 1000000000 | 0010011000 | 00000000-0 | ----11010 |
| *Diplodoselache* | ?????????? | ?????????? | ?0???0???? | ??????00?0 | 0000???00? | ????11?010 | 0100001100 | 0100000100 | 0011001000 | 0000000000 | 1000001010 | 00000000-0 | ----00?00 |
| *Orthacanthus* | 1100011100 | 1100000100 | 1000000001 | 0000100000 | 00000?1000 | 1??0000000 | 0101001100 | 0001000100 | 0011001000 | 0000000000 | 1000001010 | 00000000-0 | ----???00 |
| *Cladoselache* | ???0010??? | 0?000?010? | 100?000000 | 0000?000?0 | 00000?100? | ?00?00?010 | 00000-1000 | 0?00000101 | 0000001000 | 0001000000 | 0000001000 | 00000000-0 | ----???01 |
| *Akmonistion* | 110001010? | 00000?010? | 1000000000 | 0000?00000 | 00000?1000 | 0000000010 | 00000-100? | 0000000111 | 0000001000 | 0001000000 | 00000-1000 | 01000000-0 | ----11011 |
| ctenacanths | 1100111100 | ??00000100 | 1001000001 | 0000100000 | 0000????0? | ????000000 | 0101001100 | 0111000111 | 1001001000 | 0001000000 | 0000001100 | 00000000-0 | ----00101 |
| *Cladodoides* | 1100111100 | ???0000100 | 1001000001 | 0000100??? | 0000?????? | ?????????? | ?????????? | ?????0???? | ???????000 | 0001000000 | 00????????? | ??000000-0 | ----????1 |

# APPENDIX C: LIST OF SPECIMENS EXAMINED

| Specimens | Where Reposited |
|---|---|
| ***Tribodus limae*** AMNH 13957; AMNH 13958; AMNH 13959; AMNH 13961 | American Museum of Natural History, New York |
| ***Tribodus limae*** MN 5807V; MN 5808-V | Museu Nacional do Rio de Janeiro, Brazil |
| ***Tribodus limae*** UERJ-PMB-40; UERJ-PMB-114; UERJ-PMB-119 | Universidade do Estado do Rio de Janeiro (UERJ), Brazil |
| ***Tribodus limae*** GP/2T2 IG-USP | Instituto de Geosciencias, Universidade de Sao Paulo, Sao Paulo, Brazil (specimen lost; cast in UERJ paleontology collection). |
| ***Hamiltonichthys mapesi*** AMNH 10807; AMNH 10802 | American Museum of Natural History, New York |
| ***Egertonodus fraasi*** BSPGM 1899-I-2 | The Palaeontological Museum, Munich, Germany |
| ***Egertonodus basanus*** NHM 40718; NHM P60110; NHM 6356; NHM 6357; NHM P11870; NHM P11871; NHM P.11872; NHM P13094; NHM P2082; NHM P. 3172; NHM 40716; NHM 40717 | The Natural History Museum, London, UK |
| ***Egertonodus basanus*** AMNH 4692 | American Museum of Natural History, New York |
| ***Hybodus reticulatus*** NHM P2208; NHM P3168; NHM P2203D; NHM P.3170; NHM P3160; *Hybodus* cf. *reticulatus* NHM P.62349; NHM P.3163; NHM 40335; NHM P. 2198a; NHM P.5876; NHM P. 3156; NHM P. 423 | The Natural History Museum, London, UK |
| ***Hybodus* cf. *reticulatus*** SMNS 51949 | Staatliches Museum für Naturkunde, Stuttgart, Germany |
| ***Hybodus reticulatus*** J3088; J3920 | Oxford University Museum, Oxford, UK |
| ***Hybodus reticulatus*** MCZ 780; MCZ 816 | Museum of Comparative Zoology, Harvard, Cambridge, Massachusetts |
| ***Lissodus africanus*** AMNH 8854 | American Museum of Natural History, New York |
| ***Lissodus africanus*** NHM 16035; NHM 16036; NHM 16037; NHM 16038; NHM 16039; NHM 17530; NHM 17531 | The Natural History Museum, London, UK |
| ***Lissodus africanus*** UCMZ GN 949C; GN 949D; GN 333; GN 966 | University of Cambridge Museum of Zoology, Cambridge, UK |
| ***Lissodus cassangensis*** IICT 69; IICT 70 | Instituto de Investigação Científica Tropical, Lisboa, Portugal (specimen peels available in AMNH collection) |
| ***Hybodus delabechei*** NHM 39880; NHM P.3159; NHM P.3160; NHM P.3161; NHM 40352; NHM P. 3171; NHM P.40352; NHM P.2795 | The Natural History Museum, London, UK |
| ***Hybodus hauffianus*** SMNS 8663; SMNS 8503; SMNS 52458; SMNS 10062; SMNS 15150; SMNS 80594; SMNS 54048; SMNS 52460; SMNS 51136; SMNS 80595; SMNS 51135; SMNS 58749; SMNS 58748; SMNS 52222; SMNS 50804 | Staatliches Museum für Naturkunde, Stuttgart, Germany |
| ***Hybodus hauffianus*** NHM P.16361 | The Natural History Museum, London |

| | |
|---|---|
| ***Hybodus hauffianus*** GPIT uncatalogued specimens | Palaontologische Sammlung Institut fur Geowissenschaften Universitat Tubingen, Tubingen, Germany |
| ***Hybodus medius*** NHM P.41103; NHM 340 | The Natural History Museum, London, UK |
| ***Acrodus anningiae*** NHM P.2731 (holotype); NHM P. 2734; NHM P.3155; NHM P.3152; NHM P.3153; NHM P.38125; NHM P.6332; NHM P.2732; NHM P.32751; NHM P.2146 | The Natural History Museum, London, UK |
| ***Acrodus nobilis*** NHM P50809; NHM P.3154; NHM P.2737; NHM P.2165 | The Natural History Museum, London, UK |
| ***Asteracanthus ornatissimus*** NHM P12614; NHM P.47441; NHM P.41378; NHM P.6867; NHM P.6867-1 | The Natural History Museum, London, UK |
| ***Onychoselache traquairi*** RSM 1885.54.1; RSM 1974.23.14 | Royal Scottish Museum, Edinburgh, Scotland, UK |
| ***Tristychius arcuatus*** RSM 1972.27.449A,B; 1972.27.450B; 1972.27.451A,B; 1972.27.455A; 1972.27.481D; 1972.27.494A–D; 1972.27.497A,B; 1973.24.41; 1973.24.50; 1974.23.19A–D; 1974.23.44A–C; 1974.51.5A; 1974.51.9A,B; | Royal Scottish Museum, Edinburgh, Scotland, UK |
| ***Tristychius arcuatus*** NHM P.11383; NHM P.11384; NHM P.11385; NHM P.60963a, b | The Natural History Museum, London, UK |
| ***Tristychius arcuatus*** HM 131310 | Hunterian Museum, Glasgow, UK |
| ***Orthacanthus texensis*** MCZ 12872; MCZ 13384; MCZ 13388; MCZ 13915; MCZ 13916 | Museum of Comparative Zoology, Harvard University, Cambridge, Massachusetts |
| ***Orthacanthus texensis*** AMNH 7254; AMNH FF 20272; AMNH uncat. (cast of University of Michigan #16194) | American Museum of Natural History, New York |
| ***Tamiobatis*** sp. AMNH 2140 | American Museum of Natural History, New York |
| ***Akmonistion zangerli*** UCMZ GN 1047 | University of Cambridge Museum of Zoology, Cambridge, UK |
| ***Akmonistion zangerli*** HM V8246; HM V8250 | Hunterian Museum, Glasgow, UK |
| ***Squalus acanthias*** AMNH 225783SW; and uncatalogued purchased dissection specimens | AMNH Ichthyology Department |
| ***Carcharhinus brevipinna*** AMNH 93845SD; AMNH 93846SD; AMNH 218152SD | AMNH Ichthyology Department |
| ***Notorhynchus cepedianus*** AMNH uncatalogued specimens | American Museum of Natural History, New York |
| ***Heterodontus francisci*** 38182SW; AMNH 47912SW; AMNH 96795; AMNH 225820SW | AMNH Ichthyology Department |
| ***Dasyatis americana*** AMNH 218289SD | AMNH Ichthyology Department |
| ***Hydrolagus colliei*** AMNH 58237SW | AMNH Ichthyology Department |

## APPENDIX D: TABLE OF HYBODONTIFORM TAXA EXAMINED

| Taxon | Age | Locality | Geological Unit | Selected References |
|---|---|---|---|---|
| *Tribodus limae* Brito & Ferreira, 1989 | Lower Cretaceous (Aptian/Albian) | Chapada do Araripe, Ceara Province, NE Brazil | Santana Formation ('Romualdo Member'), Concretion-bearing strata | Brito and Ferreira, 1989; Brito, 1992; Maisey and Carvalho, 1997 |
| *Egertonodus basanus* (Egerton, 1845) | Lower Cretaceous (Valanginian-lower Aptian) | Isle of Wight and Sussex coast (Bexhill, Cooden, and Pevensey areas), SE England | Wealden and Purbeck series [Ashdown Sand (Valanginian), Weald Clay (Barremian), Atherfield Clay (lower Aptian)] | Maisey, 1983; 1987; Woodward, 1916, Patterson, 1966 |
| *Egertonodus fraasi* (Brown, 1900) | Upper Jurassic | Bavaria, Germany | Solnhofen Limestone | Maisey, 1986; 1987; Brown, 1900 |
| *Hybodus hauffianus* Fraas, 1895 | Lower Jurassic (Toarcian) | Holzmaden, Baden-Württemberg, S. Germany | Schwarzjura: upper part of *semicelatum* Zone to lower part of *fibulatum* Zone | Koken, 1907; Duffin, 1997 |
| *Hybodus reticulatus* Agassiz, 1837 | Lower Jurassic (Sinemurian) | Lyme Regis, Dorset, Southern England | Lower Lias | Agassiz, 1837; Woodward, 1889a; Maisey, 1987 |
| *Hybodus delabechei* Charlesworth, 1839 | Lower Jurassic (Lower Lias) | Lyme Regis, Dorset, Southern England | Lower Lias | Charlesworth, 1839; Agassiz, 1843; Day, 1865; Woodward, 1889a; Maisey, 1982 |
| *Hybodus medius* Agassiz, 1843 | Lower Jurassic (Lower Lias) | Lyme Regis, Dorset, Southern England | Lower Lias | Agassiz, 1843; Woodward 1889a |
| *Acrodus anningiae* Agassiz, 1839 | Lower Jurassic (Lower Lias) | Lyme Regis, Dorset, Southern England | Lower Lias | Agassiz, 1837; Woodward, 1889a |
| *Acrodus nobilis* Agassiz, 1838 | Lower Jurassic (Lower Lias) | Lyme Regis, Dorset, Southern England | Lower Lias | Agassiz, 1838; Woodward, 1889a |
| *Acrodus lateralis* Agassiz, 1837 | Middle Triassic | Monte San Giorgio, Kt. Tessin, Southern Switzerland | Grenzbitumenhorizon | Agassiz, 1837; Rieppel, 1981 |
| *Asteracanthus ornatissimus* Agassiz, 1837 | Upper Jurassic (Lias: Kimmeridgian) | N. France; S. England; W. Switzerland; N. and S.W. Germany | "Lower-Upper Oolite" (Woodward, 1889a) | Agassiz, 1837; Woodward, 1889a; Peyer, 1946; Maisey, 1982 |

| Taxon | Age | Locality | Geological Unit | Selected References |
|---|---|---|---|---|
| *Lissodus cassangensis* (Teixeira, 1954) | Early Triassic | Lutoa, Baixa do Cassange, Angola, Africa | "Camadas com peixes" | Maisey, 1990, Duffin 2001 |
| *Lissodus africanus* (Broom, 1909) | Early Triassic (Scythian) | Bekker's Kraal, District Rouxville, Orange Free State, South Africa | Lower Cynognathus zone, Upper Beaufort Series (Karroo System) | Broom, 1909; Brough, 1935; Duffin, 2001 |
| *Lonchidion humblei* Murry, 1981 | Late Triassic (?Upper Carnian) | "Near the headwaters of Home Creek," S.E. Crosby Co., Texas, USA | Tecovas Formation, Dockum Group | Murry, 1981, 1986; Duffin, 1985, 1989, 1993, 2001; Gomez-Pallerola, 1992 |
| *Lonchidion selachos* Estes, 1964 | Late Cretaceous (Campanian–Maastrichtian) | Type: UC locality V5817, eastern Wyoming, USA | Lance Formation, WY (Maastrichtian), and other localities (see Duffin, 2001) | Estes, 1964; Duffin, 2001 |
| *Lonchidion montsechi* (Gomez-Pallerola, 1979) | Early Cretaceous (Berriasian to Valanginian) | Santa Maria de Meyá Quarry, Montsec (Lérida), Spain | "La caliza litográfica del Montsec" | Gomez-Pallerola, 1979; Duffin, 2001 |
| *Palaeobates angustissimus* (Agassiz, 1838) | Middle Triassic | Monte San Giorgio, Kt. Tessin, Southern Switzerland (Rieppel, 1981); S. Germany/E. France (Woodward, 1889a) | Grenzbitumenhorizon, S. Switzerland (Rieppel, 1981); Muschelkalk: S. Germany, E. France (Woodward, 1889a) | Woodward, 1889A; Rieppel, 1981 |
| *Hamiltonichthys mapesi* Maisey, 1989 | Upper Pennsylvanian (Middle Virgilian) | Hamilton Quarry, near Hamilton, Eastern Kansas (USA) | Hartford Limestone (either uppermost Shawnee Group or Wabaunsee Group) | Maisey, 1989 |
| *Onychoselache traquairi* Dick, 1978 | Upper Mississippian (Viséan: Holkerian) | Glencartholm fish beds and Mumbie Quarry (Glencartholm, Dumfries District); and Wardie Shales (Wardie, Edinburgh); both Scotland, UK | Glencartholm Volcanic Beds (Upper Border Group of Calciferous Sandstone); Wardie Shales, Scottish (Lower Lothian) Oil Shale Group | Dick, 1978; Dick and Maisey, 1980; Coates and Gess, 2007; Moy-Thomas, 1936; Traquair, 1888; Woodward, 1924 |
| *Tristychius arcuatus* Agassiz, 1837 | Lower Carboniferous (Viséan) to Upper Carboniferous (Namurian) | Woodside Pits, West Glasgow, Scotland; and Scottish Midland Valley | Base of Lower Scottish Oil Shale Group (Granton Sandstones) to Upper Limestone Group (South Parrot Coal-Shale) | Agassiz, 1837; Dick, 1978 |

# APPENDIX E: APOMORPHY LIST

(Numbered nodes refer to nodes on strict consensus tree)

Apomorphy lists:

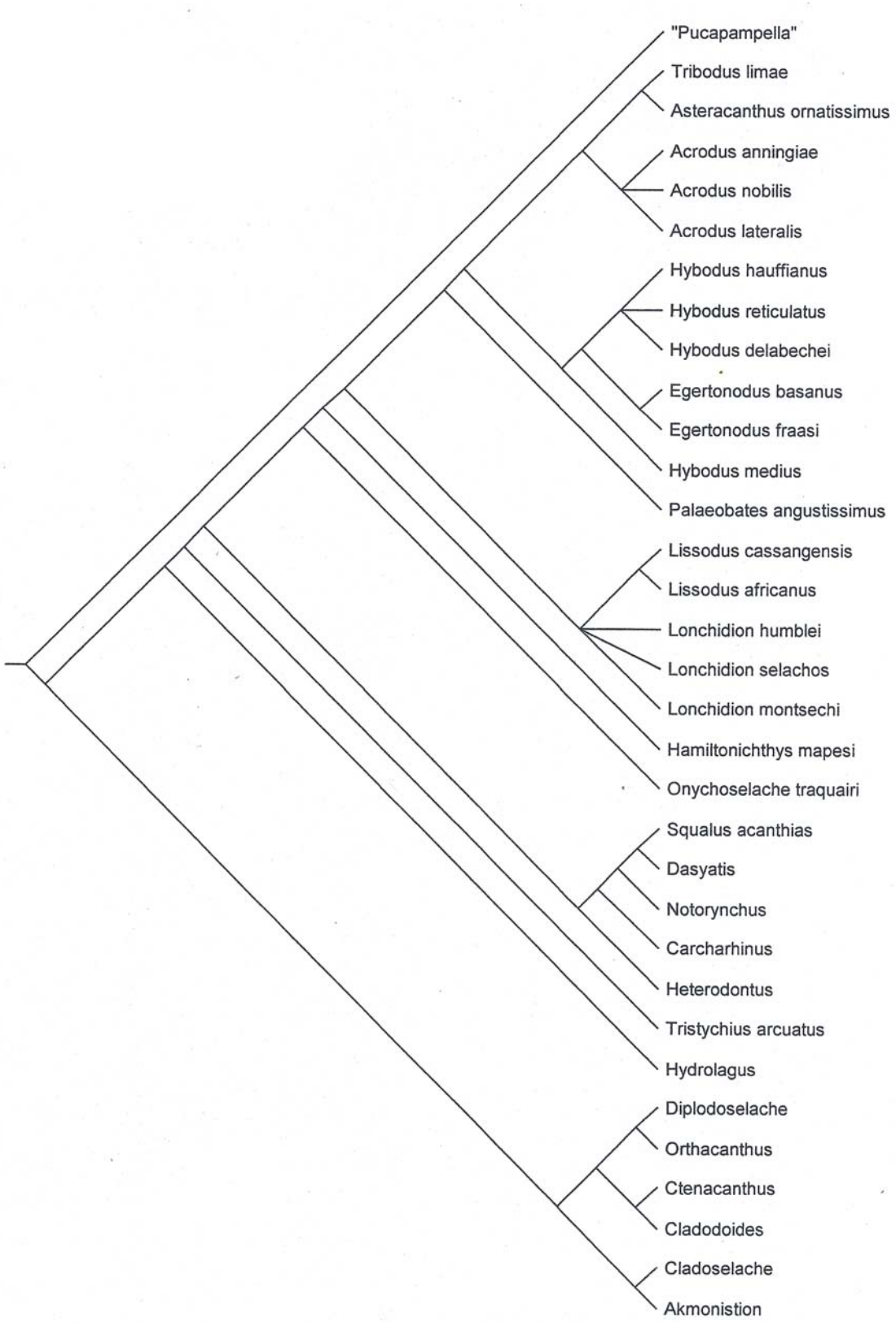
| Branch | Character | Steps | CI | Change |
|---|---|---|---|---|
| node_59 --> "Pucapampella" | 32 (lateral dorsal ) | 1 | 0.500 | 0 --> 1 |
| node_59 --> node_58 | 2 (glossopharyngeal) | 1 | 0.500 | 0 --> 1 |
| | 6 (ventral otic fis) | 1 | 1.000 | 0 --> 1 |
| node_58 --> node_52 | 4 (otico-occipital ) | 1 | 1.000 | 0 ==> 1 |
| | 5 (metotic fissure ) | 1 | 0.500 | 0 ==> 1 |
| | 8 (dorsal otic ridg) | 1 | 1.000 | 1 ==> 0 |
| | 17 (hyomandibular f) | 1 | 0.333 | 0 ==> 1 |
| | 29 (lateral dorsal ) | 1 | 0.500 | 0 ==> 1 |
| | 31 (lateral dorsal ) | 1 | 1.000 | 0 ==> 1 |
| | 36 (mandibular join) | 1 | 0.500 | 0 ==> 1 |
| | 39 (palatoquadrates) | 1 | 0.333 | 0 --> 1 |
| | 41 (palatoquadrate ) | 1 | 0.500 | 0 --> 1 |
| | 49 (branchial arche) | 1 | 0.500 | 0 --> 1 |
| | 50 (posteriormost p) | 1 | 0.500 | 0 --> 1 |
| | 54 (posteriorly dir) | 1 | 1.000 | 0 --> 1 |
| | 63 (dibasal fin, se) | 1 | 0.500 | 0 --> 1 |
| | 73 (pelvic metapter) | 1 | 0.500 | 0 --> 1 |
| | 81 (posterior dorsa) | 1 | 0.333 | 0 --> 1 |
| | 86 (semilunate tail) | 1 | 1.000 | 0 --> 1 |
| | 103 (fin spines pos) | 1 | 0.500 | 0 --> 1 |
| | 106 (fin spines wit) | 1 | 0.333 | 0 --> 1 |
| node_52 --> node_51 | 7 (occipital block ) | 1 | 0.500 | 0 ==> 1 |
| | 10 (inner ear adapt) | 1 | 1.000 | 0 --> 1 |
| | 16 (trochlear foram) | 1 | 0.500 | 0 --> 1 |
| | 20 (efferent pseudo) | 1 | 0.500 | 0 --> 1 |
| | 40 (quadrate flange) | 1 | 0.500 | 0 --> 1 |
| | 42 (palatoquadrate ) | 1 | 1.000 | 0 ==> 1 |
| | 51 (pharyngobranchi) | 1 | 0.250 | 0 --> 1 |
| | 52 (most hypobranch) | 1 | 1.000 | 0 ==> 1 |
| | 53 (basibranchials ) | 1 | 1.000 | 0 --> 1 |
| | 56 (scapulocoracoid) | 1 | 0.500 | 0 ==> 1 |
| | 74 (calcified pleur) | 1 | 0.250 | 0 --> 1 |
| | 108 (posterior dors) | 1 | 0.250 | 0 ==> 1 |
| node_51 --> node_50 | 9 (crus between ant) | 1 | 1.000 | 0 ==> 1 |
| | 22 (otic capsules l) | 1 | 1.000 | 0 ==> 1 |
| | 26 (postorbital art) | 1 | 0.500 | 0 ==> 1 |
| | 27 (postorbital art) | 1 | 1.000 | 0 ==> 1 |
| | 47 (hyoid rays elon) | 1 | 0.500 | 1 ==> 0 |
| | 49 (branchial arche) | 1 | 0.500 | 1 --> 0 |
| | 55 (scapular proces) | 1 | 0.333 | 0 ==> 1 |
| | 62 (tribasal pector) | 1 | 0.500 | 0 ==> 1 |
| | 63 (dibasal fin, se) | 1 | 0.500 | 1 --> 0 |
| | 65 (propterygium wi) | 1 | 0.333 | 0 --> 1 |
| | 69 (Puboischiadic b) | 1 | 0.500 | 0 --> 1 |
| | 70 (puboischiadic b) | 1 | 0.500 | 0 --> 1 |
| | 71 (first pelvic ra) | 1 | 1.000 | 0 ==> 1 |
| | 88 (low-crowned tee) | 1 | 0.250 | 0 --> 1 |
| node_50 --> node_46 | 11 (internasal keel) | 1 | 0.333 | 0 --> 1 |
| | 13 (inflated ethmop) | 1 | 0.500 | 0 --> 1 |
| | 17 (hyomandibular f) | 1 | 0.333 | 1 ==> 0 |

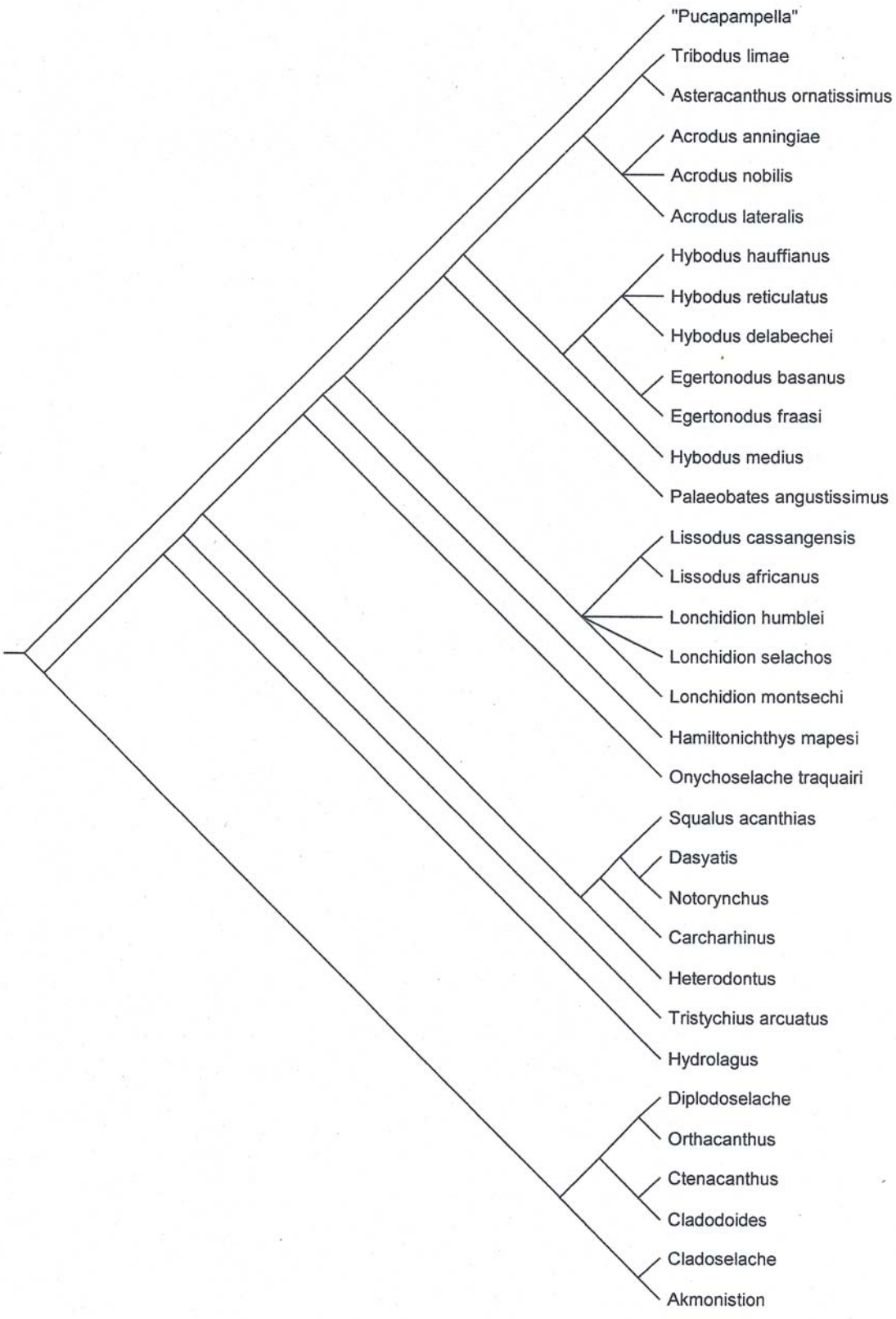
| | | | | | |
|---|---|---|---|---|---|
| | 23 (large, down-tur) | 1 | 1.000 | 0 | ==> 1 |
| | 33 (inflated and el) | 1 | 0.500 | 0 | ==> 1 |
| | 39 (palatoquadrates) | 1 | 0.333 | 1 | --> 0 |
| | 50 (posteriormost p) | 1 | 0.500 | 1 | --> 0 |
| | 58 (coracobranchial) | 1 | 1.000 | 0 | ==> 1 |
| | 89 (tooth crowns wi) | 1 | 0.333 | 0 | ==> 1 |
| | 113 (male cephalic ) | 1 | 1.000 | 0 | ==> 1 |
| node_46 --> node_45 | 44 (labial complex ) | 1 | 0.500 | 0 | --> 1 |
| | 85 (anal fin with d) | 1 | 1.000 | 0 | ==> 1 |
| | 90 (elongate latera) | 1 | 0.250 | 0 | ==> 1 |
| | 104 (Fin spines hav) | 1 | 1.000 | 0 | ==> 1 |
| | 118 (two pairs of c) | 1 | 0.333 | 0 | ==> 1 |
| | 120 (cephalic spine) | 1 | 1.000 | 0 | ==> 1 |
| node_45 --> node_44 | 60 (coracoid and sc) | 1 | 0.333 | 0 | ==> 1 |
| | 72 (pelvic proptery) | 1 | 0.333 | 0 | ==> 1 |
| | 75 (low number (10-) | 1 | 1.000 | 0 | ==> 1 |
| | 114 (cephalic spine) | 1 | 1.000 | 0 | ==> 1 |
| | 121 (cephalic spine) | 1 | 1.000 | 0 | --> 1 |
| node_44 --> node_41 | 105 (fin spines wit) | 1 | 1.000 | 0 | ==> 1 |
| | 106 (fin spines wit) | 1 | 0.333 | 1 | ==> 0 |
| | 116 ('Sphenonchus' ) | 1 | 1.000 | 0 | ==> 1 |
| | 119 (cephalic spine) | 1 | 0.250 | 0 | --> 1 |
| | 122 (posterior lobe) | 1 | 0.500 | 0 | --> 1 |
| | 123 (cephalic spine) | 1 | 0.500 | 0 | ==> 1 |
| | 124 (cephalic spine) | 1 | 0.500 | 0 | --> 1 |
| node_41 --> node_40 | 91 (tooth histology) | 1 | 0.500 | 0 | ==> 1 |
| | 95 (teeth with colu) | 1 | 0.333 | 0 | --> 1 |
| node_40 --> node_34 | 11 (internasal keel) | 1 | 0.333 | 1 | --> 0 |
| | 13 (inflated ethmop) | 1 | 0.500 | 1 | --> 0 |
| | 14 (suborbital shel) | 1 | 0.500 | 0 | --> 1 |
| | 29 (lateral dorsal ) | 1 | 0.500 | 1 | --> 0 |
| | 33 (inflated and el) | 1 | 0.500 | 1 | --> 0 |
| | 34 (ethmopalatine a) | 1 | 0.500 | 0 | ==> 1 |
| | 38 (jaws extend to ) | 1 | 0.333 | 0 | ==> 1 |
| | 39 (palatoquadrates) | 1 | 0.333 | 0 | ==> 1 |
| | 44 (labial complex ) | 1 | 0.500 | 1 | --> 0 |
| | 46 (basihyal forms ) | 1 | 0.333 | 0 | --> 1 |
| | 117 (single (poster) | 1 | 0.500 | 0 | --> 1 |
| | 118 (two pairs of c) | 1 | 0.333 | 1 | --> 0 |
| node_34 --> Tribodus limae | 90 (elongate latera) | 1 | 0.250 | 1 | ==> 0 |
| | 100 (pavement denti) | 1 | 1.000 | 0 | ==> 1 |
| | 122 (posterior lobe) | 1 | 0.500 | 1 | ==> 0 |
| | 124 (cephalic spine) | 1 | 0.500 | 1 | ==> 0 |
| node_34 --> Asteracanthus or | 99 (occlusally flat) | 1 | 0.500 | 0 | ==> 1 |
| | 110 (fin spines wit) | 1 | 1.000 | 0 | ==> 1 |
| | 127 (dermal denticl) | 1 | 0.200 | 0 | ==> 1 |
| node_40 --> node_38 | 88 (low-crowned tee) | 1 | 0.250 | 1 | ==> 0 |
| | 89 (tooth crowns wi) | 1 | 0.333 | 1 | ==> 0 |
| | 95 (teeth with colu) | 1 | 0.333 | 1 | --> 0 |
| | 119 (cephalic spine) | 1 | 0.250 | 1 | --> 0 |
| node_38 --> node_37 | 90 (elongate latera) | 1 | 0.250 | 1 | ==> 0 |
| | 94 (high-crowned mu) | 1 | 0.333 | 0 | ==> 1 |
| node_37 --> node_35 | 12 (rostral bar abo) | 1 | 0.500 | 1 | ==> 0 |
| | 20 (efferent pseudo) | 1 | 0.500 | 1 | --> 0 |
| | 24 (postorbital pro) | 1 | 0.333 | 0 | ==> 1 |
| | 126 (all dermal den) | 1 | 0.333 | 1 | ==> 0 |
| node_35 --> Hybodus hauffian | 119 (cephalic spine) | 1 | 0.250 | 0 | --> 1 |
| node_37 --> node_36 | 15 (suborbital shel) | 1 | 1.000 | 0 | ==> 1 |
| | 51 (pharyngobranchi) | 1 | 0.250 | 1 | --> 0 |
| | 97 (teeth with sigm) | 1 | 1.000 | 0 | ==> 1 |
| | 117 (single (poster) | 1 | 0.500 | 0 | --> 1 |
| | 118 (two pairs of c) | 1 | 0.333 | 1 | --> 0 |
| | 119 (cephalic spine) | 1 | 0.250 | 0 | --> 1 |
| node_38 --> Hybodus medius | 25 (lateral commiss) | 1 | 0.333 | 0 | ==> 1 |
| node_40 --> node_39 | 102 (crushing teeth) | 1 | 1.000 | 0 | ==> 1 |
| | 126 (all dermal den) | 1 | 0.333 | 1 | ==> 0 |
| node_41 --> Palaeobates angu | 99 (occlusally flat) | 1 | 0.500 | 0 | ==> 1 |

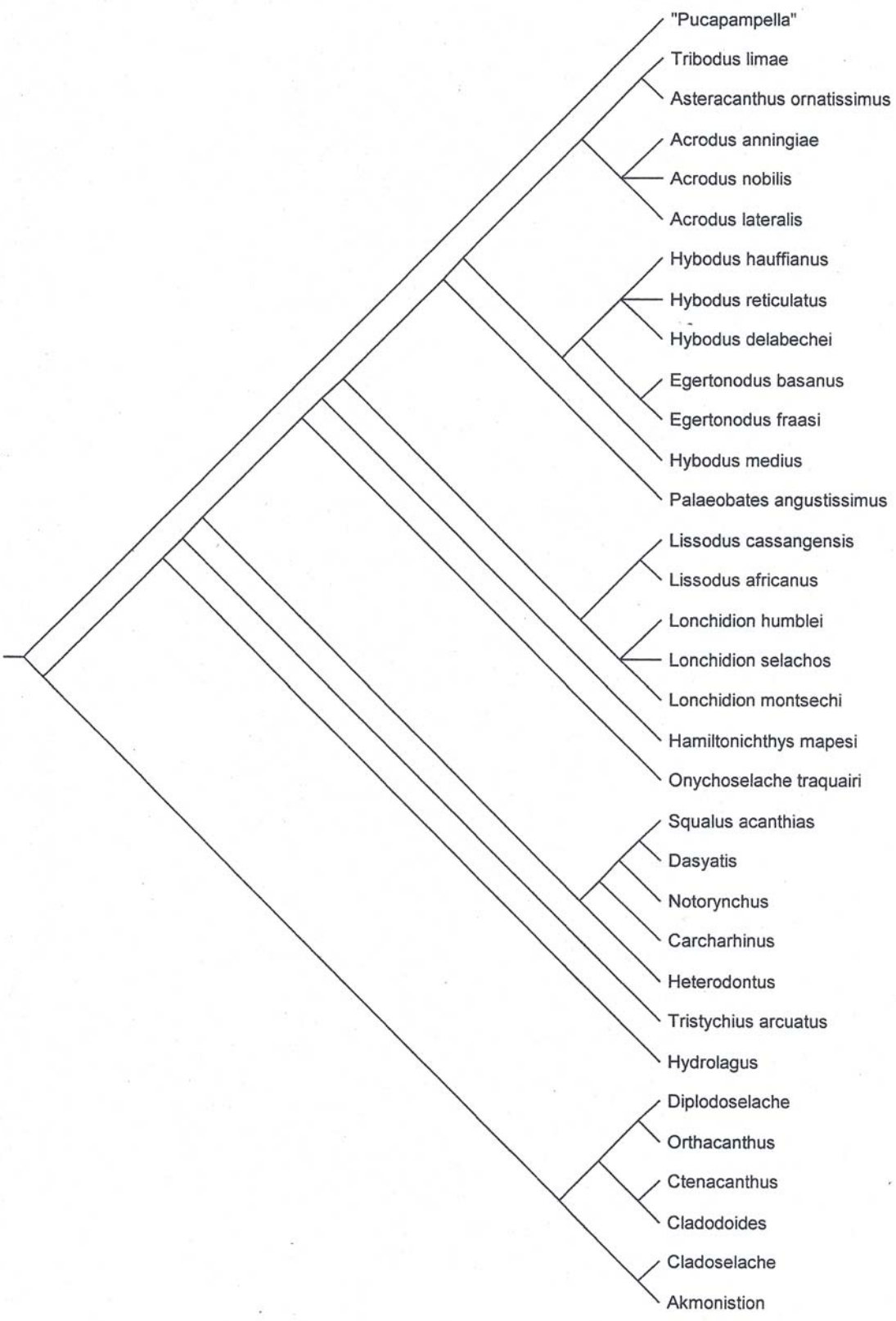
| | | | | | |
|---|---|---|---|---|---|
| node_44 --> node_43 | 89 (tooth crowns wi) | 1 | 0.333 | 1 | ==> 0 |
| | 96 (teeth without l) | 1 | 1.000 | 0 | ==> 1 |
| | 115 ('convict-arrow) | 1 | 1.000 | 0 | ==> 1 |
| node_43 --> node_42 | 98 (domed teeth wit) | 1 | 1.000 | 0 | ==> 1 |
| | 123 (cephalic spine) | 1 | 0.500 | 0 | ==> 1 |
| node_45 --> Hamiltonichthys | 70 (puboischiadic b) | 1 | 0.500 | 1 | --> 0 |
| node_46 --> Onychoselache tr | 59 (pectoral fin ar) | 1 | 0.250 | 0 | ==> 1 |
| | 66 (mesopterygium s) | 1 | 1.000 | 0 | ==> 1 |
| | 69 (Puboischiadic b) | 1 | 0.500 | 1 | --> 0 |
| node_50 --> node_49 | 16 (trochlear foram) | 1 | 0.500 | 1 | --> 0 |
| | 19 (occipital half-) | 1 | 0.500 | 0 | ==> 1 |
| | 25 (lateral commiss) | 1 | 0.333 | 0 | ==> 1 |
| | 32 (lateral dorsal ) | 1 | 0.500 | 0 | ==> 1 |
| | 35 (palatobasal art) | 1 | 0.333 | 1 | --> 0 |
| | 40 (quadrate flange) | 1 | 0.500 | 1 | --> 0 |
| | 60 (coracoid and sc) | 1 | 0.333 | 0 | ==> 1 |
| | 74 (calcified pleur) | 1 | 0.250 | 1 | --> 0 |
| | 76 (vertebral colum) | 1 | 1.000 | 0 | ==> 1 |
| | 82 (complete series) | 1 | 0.333 | 0 | --> 1 |
| | 92 ("parallel-fibre) | 1 | 0.500 | 0 | ==> 1 |
| | 93 ("tangle-fibred") | 1 | 1.000 | 0 | ==> 1 |
| | 103 (fin spines pos) | 1 | 0.500 | 1 | ==> 0 |
| | 106 (fin spines wit) | 1 | 0.333 | 1 | ==> 0 |
| node_49 --> node_48 | 65 (propterygium wi) | 1 | 0.333 | 1 | --> 0 |
| | 87 (SCE in teeth) | 1 | 0.500 | 1 | ==> 0 |
| | 88 (low-crowned tee) | 1 | 0.250 | 1 | --> 0 |
| | 107 (anterior dorsa) | 1 | 0.500 | 1 | ==> 0 |
| | 108 (posterior dors) | 1 | 0.250 | 1 | ==> 0 |
| | 127 (dermal denticl) | 1 | 0.200 | 0 | ==> 1 |
| node_48 --> node_47 | 14 (suborbital shel) | 1 | 0.500 | 0 | ==> 1 |
| | 17 (hyomandibular f) | 1 | 0.333 | 1 | ==> 0 |
| | 34 (ethmopalatine a) | 1 | 0.500 | 0 | ==> 1 |
| | 35 (palatobasal art) | 1 | 0.333 | 0 | --> 1 |
| | 38 (jaws extend to ) | 1 | 0.333 | 0 | --> 1 |
| | 43 (orbital process) | 1 | 0.500 | 0 | --> 1 |
| | 46 (basihyal forms ) | 1 | 0.333 | 0 | --> 1 |
| | 51 (pharyngobranchi) | 1 | 0.250 | 1 | ==> 0 |
| | 78 (anterior dorsal) | 1 | 0.500 | 1 | --> 0 |
| | 79 (anterior dorsal) | 1 | 0.250 | 1 | --> 0 |
| | 82 (complete series) | 1 | 0.333 | 1 | --> 0 |
| | 84 (anal fin) | 1 | 0.333 | 1 | --> 0 |
| node_47 --> Squalus acanthia | 65 (propterygium wi) | 1 | 0.333 | 0 | ==> 1 |
| | 78 (anterior dorsal) | 1 | 0.500 | 0 | --> 1 |
| | 79 (anterior dorsal) | 1 | 0.250 | 0 | --> 1 |
| | 82 (complete series) | 1 | 0.333 | 0 | --> 1 |
| | 107 (anterior dorsa) | 1 | 0.500 | 0 | ==> 1 |
| | 108 (posterior dors) | 1 | 0.250 | 0 | ==> 1 |
| | 111 (finspines with) | 1 | 0.500 | 0 | ==> 1 |
| node_47 --> Dasyatis | 19 (occipital half-) | 1 | 0.500 | 1 | ==> 0 |
| | 35 (palatobasal art) | 1 | 0.333 | 1 | --> 0 |
| | 43 (orbital process) | 1 | 0.500 | 1 | --> 0 |
| | 45 (hyomandibula an) | 1 | 1.000 | 0 | ==> 1 |
| | 55 (scapular proces) | 1 | 0.333 | 1 | ==> 0 |
| | 59 (pectoral fin ar) | 1 | 0.250 | 0 | ==> 1 |
| | 60 (coracoid and sc) | 1 | 0.333 | 1 | ==> 0 |
| | 61 (shoulder girdle) | 1 | 1.000 | 0 | ==> 1 |
| | 64 (pectoral articu) | 1 | 0.333 | 1 | ==> 0 |
| | 77 (anterior neural) | 1 | 0.500 | 0 | ==> 1 |
| | 80 (posterior dorsa) | 1 | 0.333 | 1 | ==> 0 |
| | 81 (posterior dorsa) | 1 | 0.333 | 1 | ==> 0 |
| | 88 (low-crowned tee) | 1 | 0.250 | 0 | ==> 1 |
| | 92 ("parallel-fibre) | 1 | 0.500 | 1 | ==> 0 |
| | 127 (dermal denticl) | 1 | 0.200 | 1 | ==> 0 |
| node_47 --> Notorynchus | 26 (postorbital art) | 1 | 0.500 | 1 | ==> 0 |
| | 28 (postorbital art) | 1 | 1.000 | 0 | ==> 1 |
| | 36 (mandibular join) | 1 | 0.500 | 1 | ==> 0 |
| | 38 (jaws extend to ) | 1 | 0.333 | 1 | --> 0 |

| | | | | | |
|---|---|---|---|---|---|
| | 41 (palatoquadrate ) | 1 | 0.500 | 1 | ==> 0 |
| | 46 (basihyal forms ) | 1 | 0.333 | 1 | --> 0 |
| | 47 (hyoid rays elon) | 1 | 0.500 | 0 | ==> 1 |
| | 84 (anal fin) | 1 | 0.333 | 0 | --> 1 |
| node_49 --> Heterodontus | 90 (elongate latera) | 1 | 0.250 | 0 | ==> 1 |
| | 95 (teeth with colu) | 1 | 0.333 | 0 | ==> 1 |
| | 111 (finspines with) | 1 | 0.500 | 0 | ==> 1 |
| node_51 --> Tristychius arcu | 24 (postorbital pro) | 1 | 0.333 | 0 | ==> 1 |
| | 57 (imperforate sca) | 1 | 1.000 | 0 | ==> 1 |
| | 67 (metapterygium c) | 1 | 0.500 | 0 | --> 1 |
| | 127 (dermal denticl) | 1 | 0.200 | 0 | ==> 1 |
| node_52 --> Hydrolagus | 1 (precerebral font) | 1 | 1.000 | 1 | ==> 0 |
| | 2 (glossopharyngeal) | 1 | 0.500 | 1 | --> 0 |
| | 18 (posterior dorsa) | 1 | 1.000 | 1 | ==> 0 |
| | 21 (hypotic lamina) | 1 | 1.000 | 1 | ==> 0 |
| | 25 (lateral commiss) | 1 | 0.333 | 0 | ==> 1 |
| | 37 (upper jaw not f) | 1 | 1.000 | 0 | ==> 1 |
| | 48 (operculum suppo) | 1 | 1.000 | 0 | ==> 1 |
| | 77 (anterior neural) | 1 | 0.500 | 0 | ==> 1 |
| | 80 (posterior dorsa) | 1 | 0.333 | 1 | ==> 0 |
| | 83 (single dorsal f) | 1 | 0.500 | 0 | ==> 1 |
| | 87 (SCE in teeth) | 1 | 0.500 | 1 | ==> 0 |
| | 91 (tooth histology) | 1 | 0.500 | 0 | ==> 1 |
| | 128 (ring or C-shap) | 1 | 0.500 | 0 | ==> 1 |
| node_58 --> node_57 | 3 (dorsal otic ridg) | 1 | 1.000 | 1 | ==> 0 |
| | 67 (metapterygium c) | 1 | 0.500 | 0 | --> 1 |
| | 94 (high-crowned mu) | 1 | 0.333 | 0 | --> 1 |
| | 129 ("Cladodont" te) | 1 | 0.500 | 0 | --> 1 |
| node_57 --> node_55 | 7 (occipital block ) | 1 | 0.500 | 0 | ==> 1 |
| | 11 (internasal keel) | 1 | 0.333 | 0 | --> 1 |
| | 51 (pharyngobranchi) | 1 | 0.250 | 0 | --> 1 |
| | 62 (tribasal pector) | 1 | 0.500 | 0 | ==> 1 |
| | 72 (pelvic proptery) | 1 | 0.333 | 0 | --> 1 |
| | 74 (calcified pleur) | 1 | 0.250 | 0 | --> 1 |
| | 125 (synchronomoria) | 1 | 1.000 | 1 | ==> 0 |
| | 126 (all dermal den) | 1 | 0.333 | 1 | ==> 0 |
| | 127 (dermal denticl) | 1 | 0.200 | 0 | --> 1 |
| node_55 --> node_53 | 79 (anterior dorsal) | 1 | 0.250 | 1 | ==> 0 |
| | 80 (posterior dorsa) | 1 | 0.333 | 1 | ==> 0 |
| | 83 (single dorsal f) | 1 | 0.500 | 0 | ==> 1 |
| | 94 (high-crowned mu) | 1 | 0.333 | 1 | --> 0 |
| | 101 (diplodont teet) | 1 | 1.000 | 0 | ==> 1 |
| | 109 (dorsal fin spi) | 1 | 1.000 | 0 | ==> 1 |
| | 129 ("Cladodont" te) | 1 | 0.500 | 1 | --> 0 |
| node_53 --> Diplodoselache | 55 (scapular proces) | 1 | 0.333 | 0 | ==> 1 |
| | 56 (scapulocoracoid) | 1 | 0.500 | 0 | ==> 1 |
| | 59 (pectoral fin ar) | 1 | 0.250 | 0 | ==> 1 |
| | 64 (pectoral articu) | 1 | 0.333 | 1 | ==> 0 |
| | 74 (calcified pleur) | 1 | 0.250 | 1 | --> 0 |
| node_53 --> Orthacanthus | 72 (pelvic proptery) | 1 | 0.333 | 1 | --> 0 |
| node_55 --> node_54 | 5 (metotic fissure ) | 1 | 0.500 | 0 | ==> 1 |
| | 24 (postorbital pro) | 1 | 0.333 | 0 | ==> 1 |
| | 73 (pelvic metapter) | 1 | 0.500 | 0 | --> 1 |
| | 81 (posterior dorsa) | 1 | 0.333 | 0 | --> 1 |
| | 108 (posterior dors) | 1 | 0.250 | 0 | --> 1 |
| node_57 --> node_56 | 12 (rostral bar abo) | 1 | 0.500 | 1 | --> 0 |
| | 30 (lateral dorsal ) | 1 | 1.000 | 1 | ==> 0 |
| | 59 (pectoral fin ar) | 1 | 0.250 | 0 | ==> 1 |
| | 64 (pectoral articu) | 1 | 0.333 | 1 | ==> 0 |
| | 68 (premetapterygia) | 1 | 1.000 | 1 | ==> 0 |
| | 84 (anal fin) | 1 | 0.333 | 1 | ==> 0 |
| node_56 --> Cladoselache | 79 (anterior dorsal) | 1 | 0.250 | 1 | ==> 0 |
| node_56 --> Akmonistion | 112 (spine-brush co) | 1 | 1.000 | 0 | ==> 1 |
| | 128 (ring or C-shap) | 1 | 0.500 | 0 | ==> 1 |

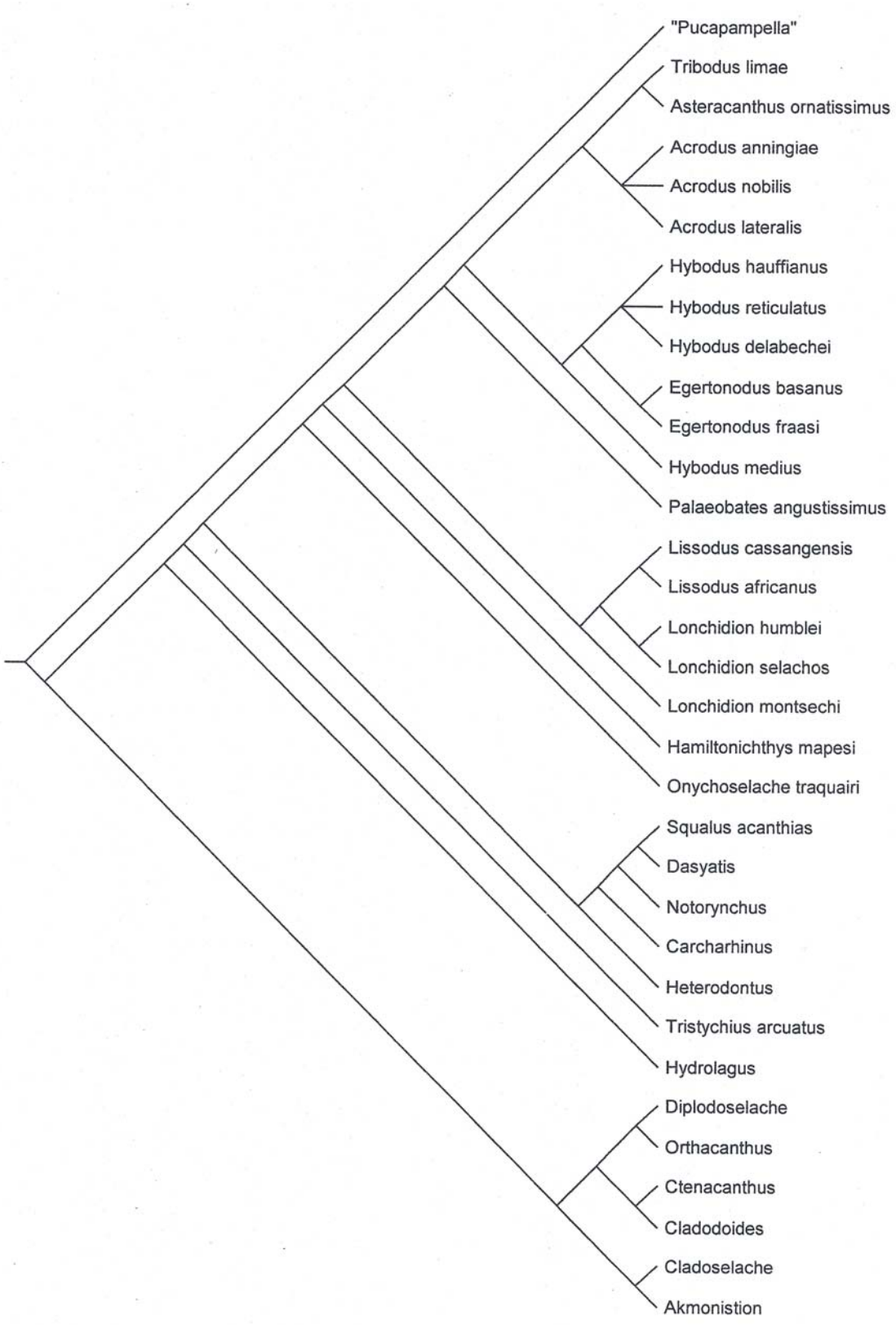
# APPENDIX F: PRINCIPAL TREES

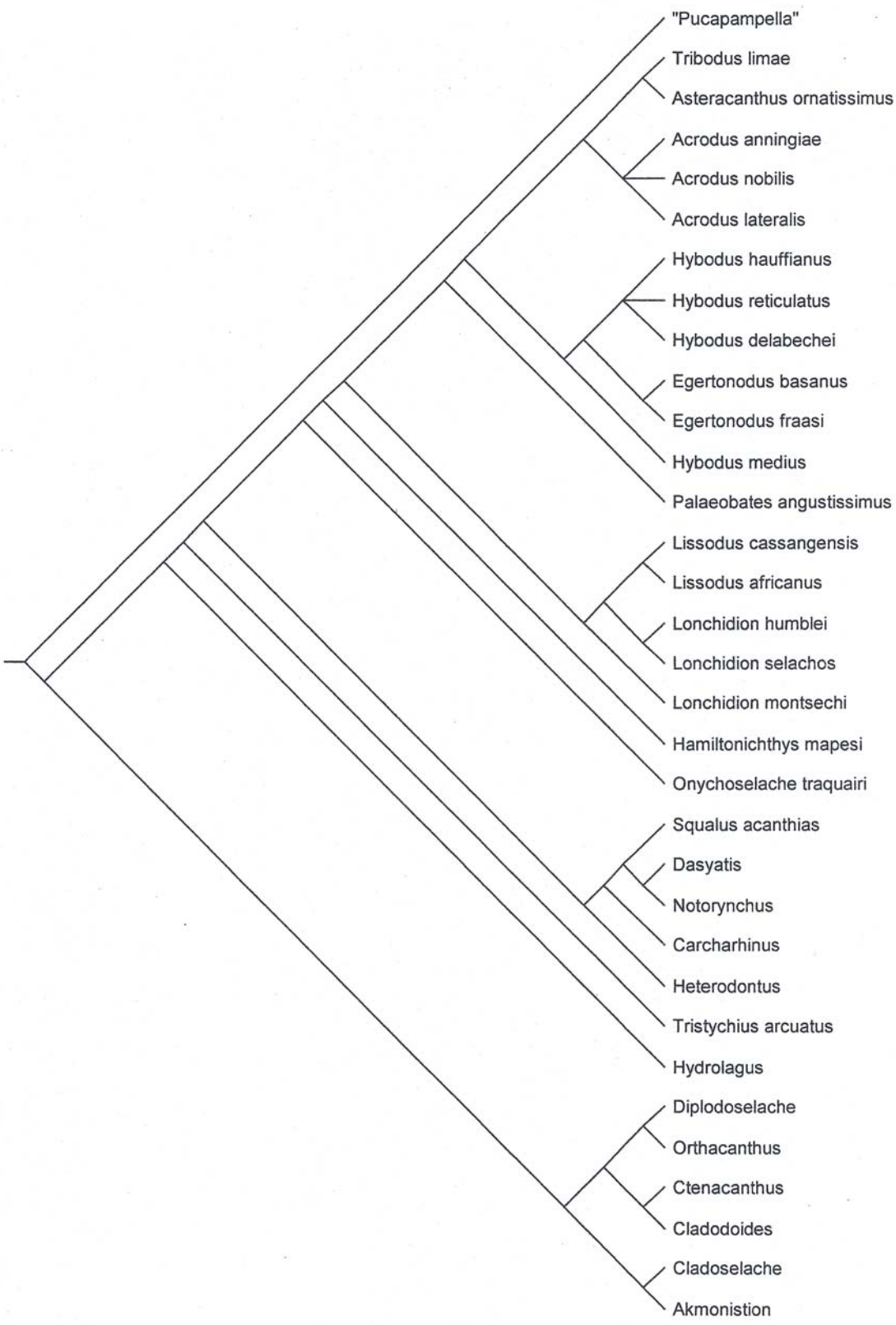


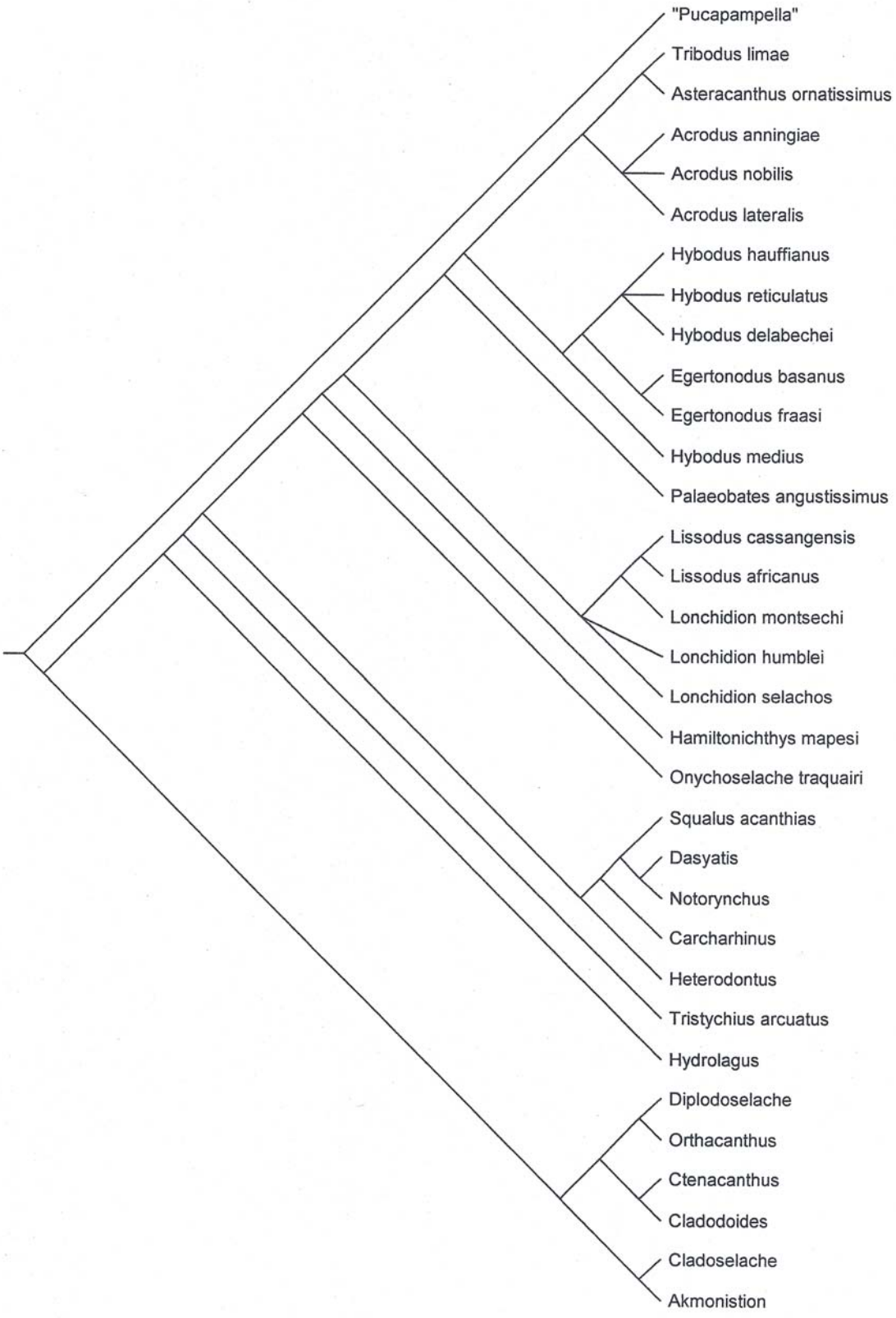

"Pucapampella"
Tribodus limae
Asteracanthus ornatissimus
Acrodus anningiae
Acrodus nobilis
Acrodus lateralis
Hybodus hauffianus
Hybodus reticulatus
Hybodus delabechei
Egertonodus basanus
Egertonodus fraasi
Hybodus medius
Palaeobates angustissimus
Lissodus cassangensis
Lissodus africanus
Lonchidion humblei
Lonchidion selachos
Lonchidion montsechi
Hamiltonichthys mapesi
Onychoselache traquairi
Squalus acanthias
Dasyatis
Notorynchus
Carcharhinus
Heterodontus
Tristychius arcuatus
Hydrolagus
Diplodoselache
Orthacanthus
Ctenacanthus
Cladodoides
Cladoselache
Akmonistion

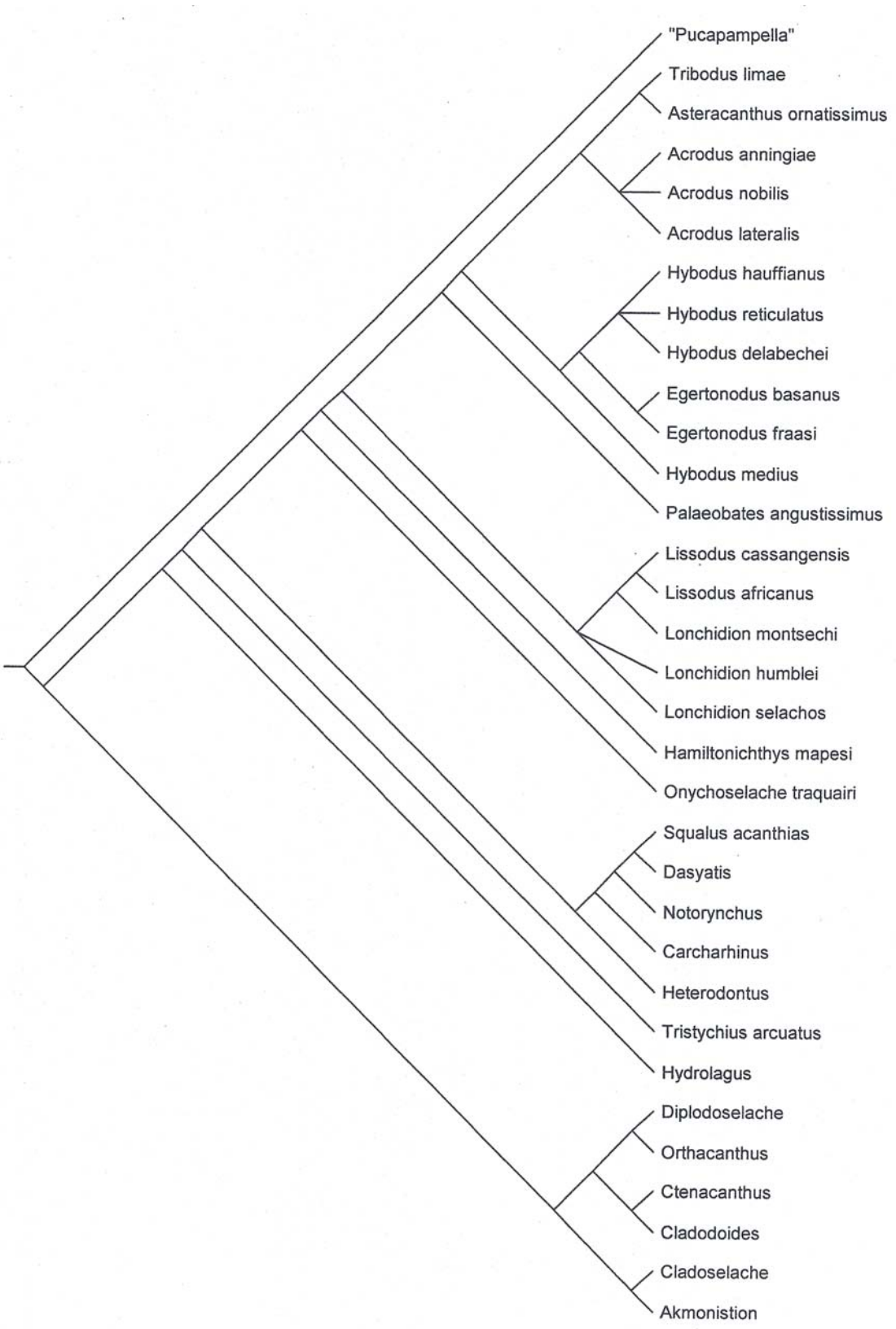

"Pucapampella"
Tribodus limae
Asteracanthus ornatissimus
Acrodus anningiae
Acrodus nobilis
Acrodus lateralis
Hybodus hauffianus
Hybodus reticulatus
Hybodus delabechei
Egertonodus basanus
Egertonodus fraasi
Hybodus medius
Palaeobates angustissimus
Lissodus cassangensis
Lissodus africanus
Lonchidion humblei
Lonchidion selachos
Lonchidion montsechi
Hamiltonichthys mapesi
Onychoselache traquairi
Squalus acanthias
Dasyatis
Notorynchus
Carcharhinus
Heterodontus
Tristychius arcuatus
Hydrolagus
Diplodoselache
Orthacanthus
Ctenacanthus
Cladodoides
Cladoselache
Akmonistion

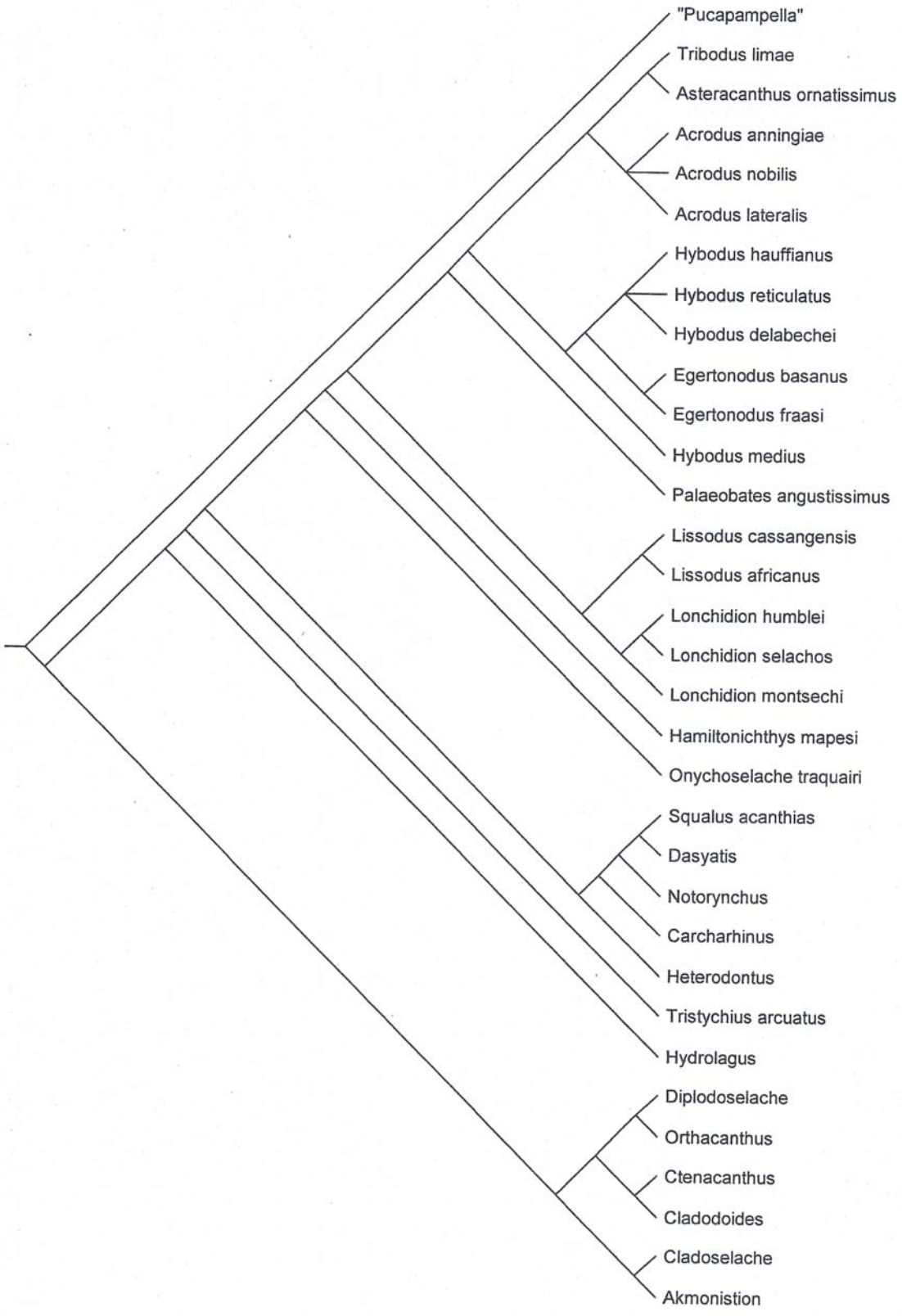

"Pucapampella"
Tribodus limae
Asteracanthus ornatissimus
Acrodus anningiae
Acrodus nobilis
Acrodus lateralis
Hybodus hauffianus
Hybodus reticulatus
Hybodus delabechei
Egertonodus basanus
Egertonodus fraasi
Hybodus medius
Palaeobates angustissimus
Lissodus cassangensis
Lissodus africanus
Lonchidion humblei
Lonchidion selachos
Lonchidion montsechi
Hamiltonichthys mapesi
Onychoselache traquairi
Squalus acanthias
Dasyatis
Notorynchus
Carcharhinus
Heterodontus
Tristychius arcuatus
Hydrolagus
Diplodoselache
Orthacanthus
Ctenacanthus
Cladodoides
Cladoselache
Akmonistion

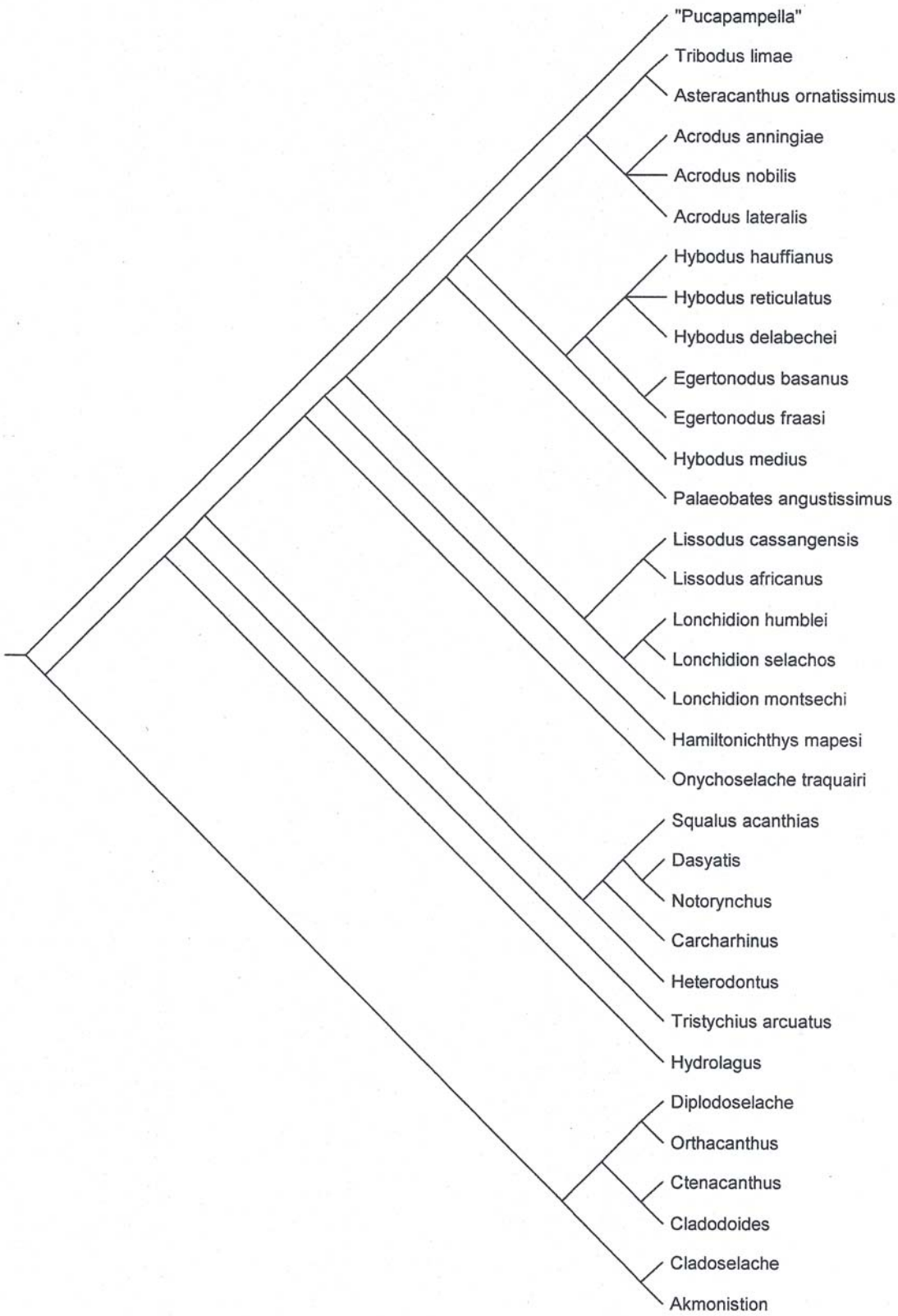

"Pucapampella"
Tribodus limae
Asteracanthus ornatissimus
Acrodus anningiae
Acrodus nobilis
Acrodus lateralis
Hybodus hauffianus
Hybodus reticulatus
Hybodus delabechei
Egertonodus basanus
Egertonodus fraasi
Hybodus medius
Palaeobates angustissimus
Lissodus cassangensis
Lissodus africanus
Lonchidion humblei
Lonchidion selachos
Lonchidion montsechi
Hamiltonichthys mapesi
Onychoselache traquairi
Squalus acanthias
Dasyatis
Notorynchus
Carcharhinus
Heterodontus
Tristychius arcuatus
Hydrolagus
Diplodoselache
Orthacanthus
Ctenacanthus
Cladodoides
Cladoselache
Akmonistion

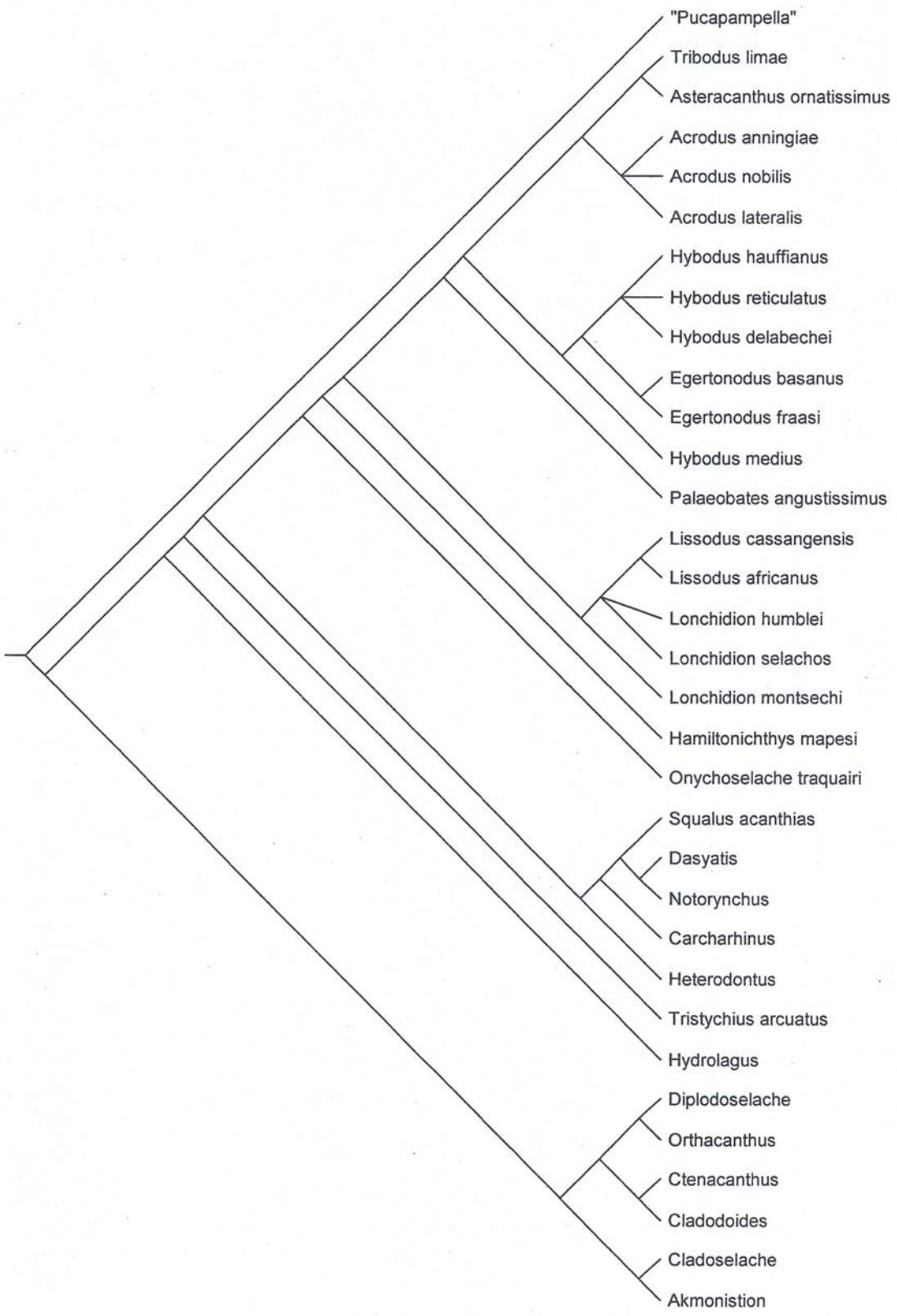

"Pucapampella"
Tribodus limae
Asteracanthus ornatissimus
Acrodus anningiae
Acrodus nobilis
Acrodus lateralis
Hybodus hauffianus
Hybodus reticulatus
Hybodus delabechei
Egertonodus basanus
Egertonodus fraasi
Hybodus medius
Palaeobates angustissimus
Lissodus cassangensis
Lissodus africanus
Lonchidion humblei
Lonchidion selachos
Lonchidion montsechi
Hamiltonichthys mapesi
Onychoselache traquairi
Squalus acanthias
Dasyatis
Notorynchus
Carcharhinus
Heterodontus
Tristychius arcuatus
Hydrolagus
Diplodoselache
Orthacanthus
Ctenacanthus
Cladodoides
Cladoselache
Akmonistion

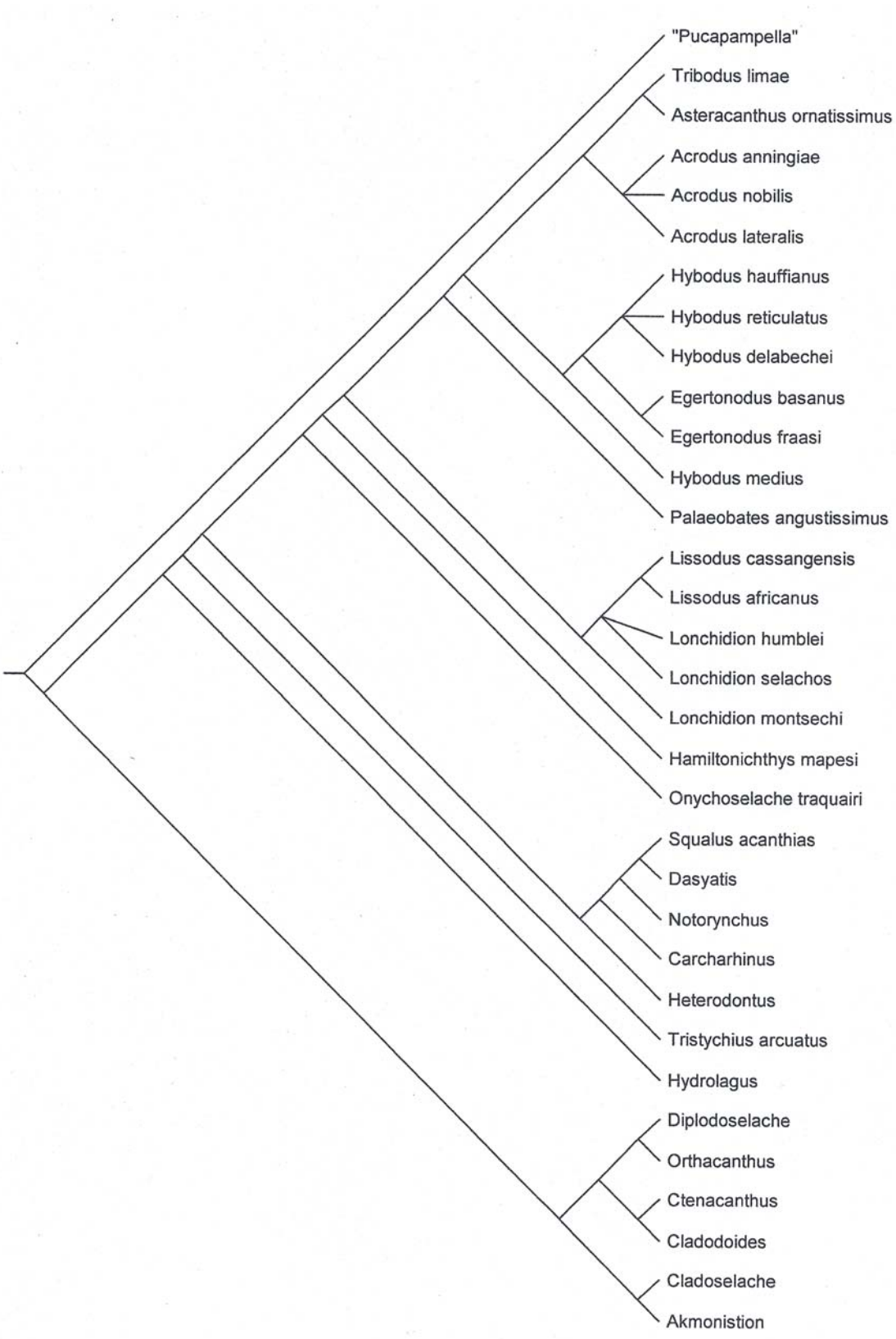

"Pucapampella"
Tribodus limae
Asteracanthus ornatissimus
Acrodus anningiae
Acrodus nobilis
Acrodus lateralis
Hybodus hauffianus
Hybodus reticulatus
Hybodus delabechei
Egertonodus basanus
Egertonodus fraasi
Hybodus medius
Palaeobates angustissimus
Lissodus cassangensis
Lissodus africanus
Lonchidion montsechi
Lonchidion humblei
Lonchidion selachos
Hamiltonichthys mapesi
Onychoselache traquairi
Squalus acanthias
Dasyatis
Notorynchus
Carcharhinus
Heterodontus
Tristychius arcuatus
Hydrolagus
Diplodoselache
Orthacanthus
Ctenacanthus
Cladodoides
Cladoselache
Akmonistion


"Pucapampella"
Tribodus limae
Asteracanthus ornatissimus
Acrodus anningiae
Acrodus nobilis
Acrodus lateralis
Hybodus hauffianus
Hybodus reticulatus
Hybodus delabechei
Egertonodus basanus
Egertonodus fraasi
Hybodus medius
Palaeobates angustissimus
Lissodus cassangensis
Lissodus africanus
Lonchidion montsechi
Lonchidion humblei
Lonchidion selachos
Hamiltonichthys mapesi
Onychoselache traquairi
Squalus acanthias
Dasyatis
Notorynchus
Carcharhinus
Heterodontus
Tristychius arcuatus
Hydrolagus
Diplodoselache
Orthacanthus
Ctenacanthus
Cladodoides
Cladoselache
Akmonistion

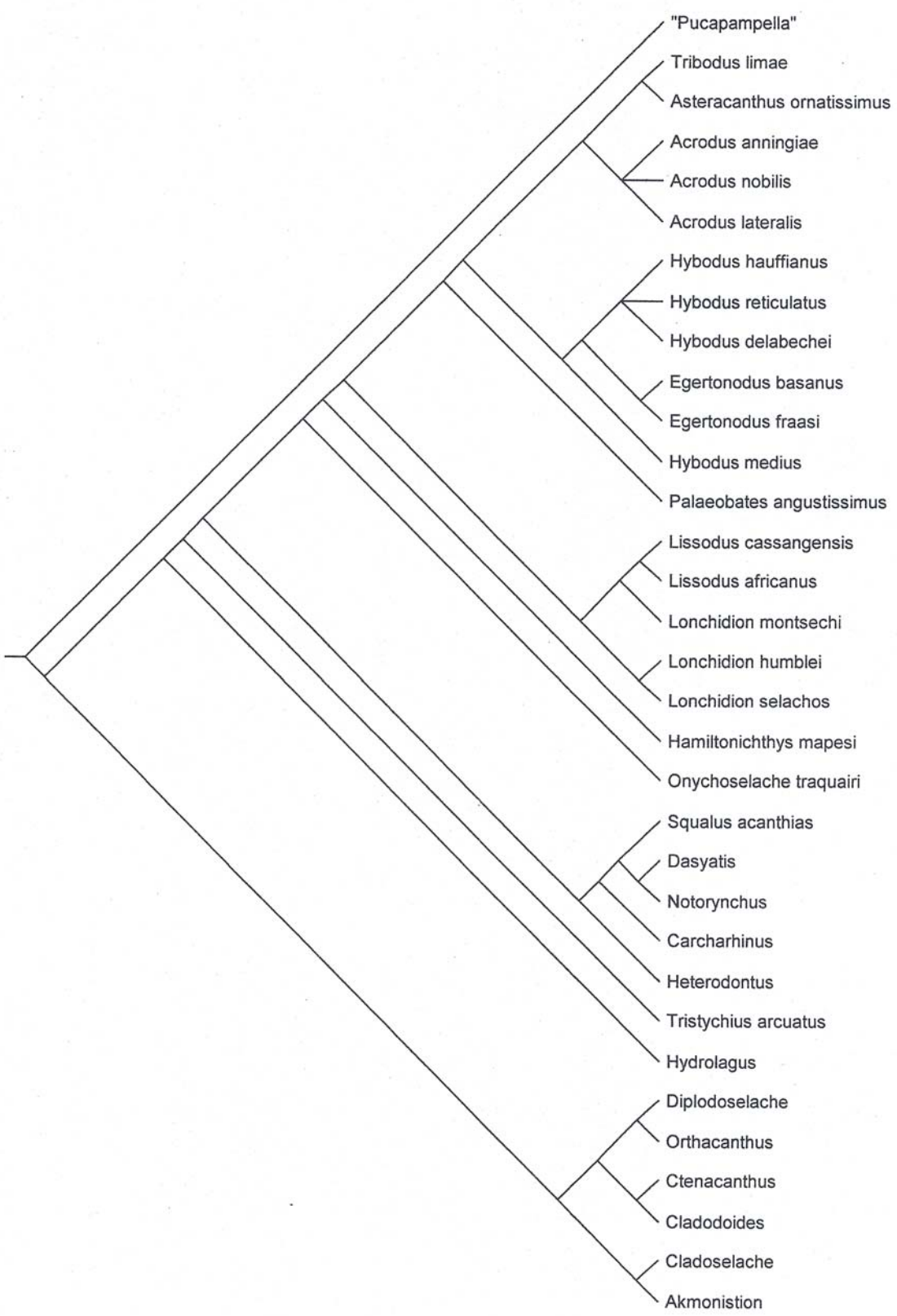

"Pucapampella"
Tribodus limae
Asteracanthus ornatissimus
Acrodus anningiae
Acrodus nobilis
Acrodus lateralis
Hybodus hauffianus
Hybodus reticulatus
Hybodus delabechei
Egertonodus basanus
Egertonodus fraasi
Hybodus medius
Palaeobates angustissimus
Lissodus cassangensis
Lissodus africanus
Lonchidion humblei
Lonchidion selachos
Lonchidion montsechi
Hamiltonichthys mapesi
Onychoselache traquairi
Squalus acanthias
Dasyatis
Notorynchus
Carcharhinus
Heterodontus
Tristychius arcuatus
Hydrolagus
Diplodoselache
Orthacanthus
Ctenacanthus
Cladodoides
Cladoselache
Akmonistion


"Pucapampella"
Tribodus limae
Asteracanthus ornatissimus
Acrodus anningiae
Acrodus nobilis
Acrodus lateralis
Hybodus hauffianus
Hybodus reticulatus
Hybodus delabechei
Egertonodus basanus
Egertonodus fraasi
Hybodus medius
Palaeobates angustissimus
Lissodus cassangensis
Lissodus africanus
Lonchidion humblei
Lonchidion selachos
Lonchidion montsechi
Hamiltonichthys mapesi
Onychoselache traquairi
Squalus acanthias
Dasyatis
Notorynchus
Carcharhinus
Heterodontus
Tristychius arcuatus
Hydrolagus
Diplodoselache
Orthacanthus
Ctenacanthus
Cladodoides
Cladoselache
Akmonistion

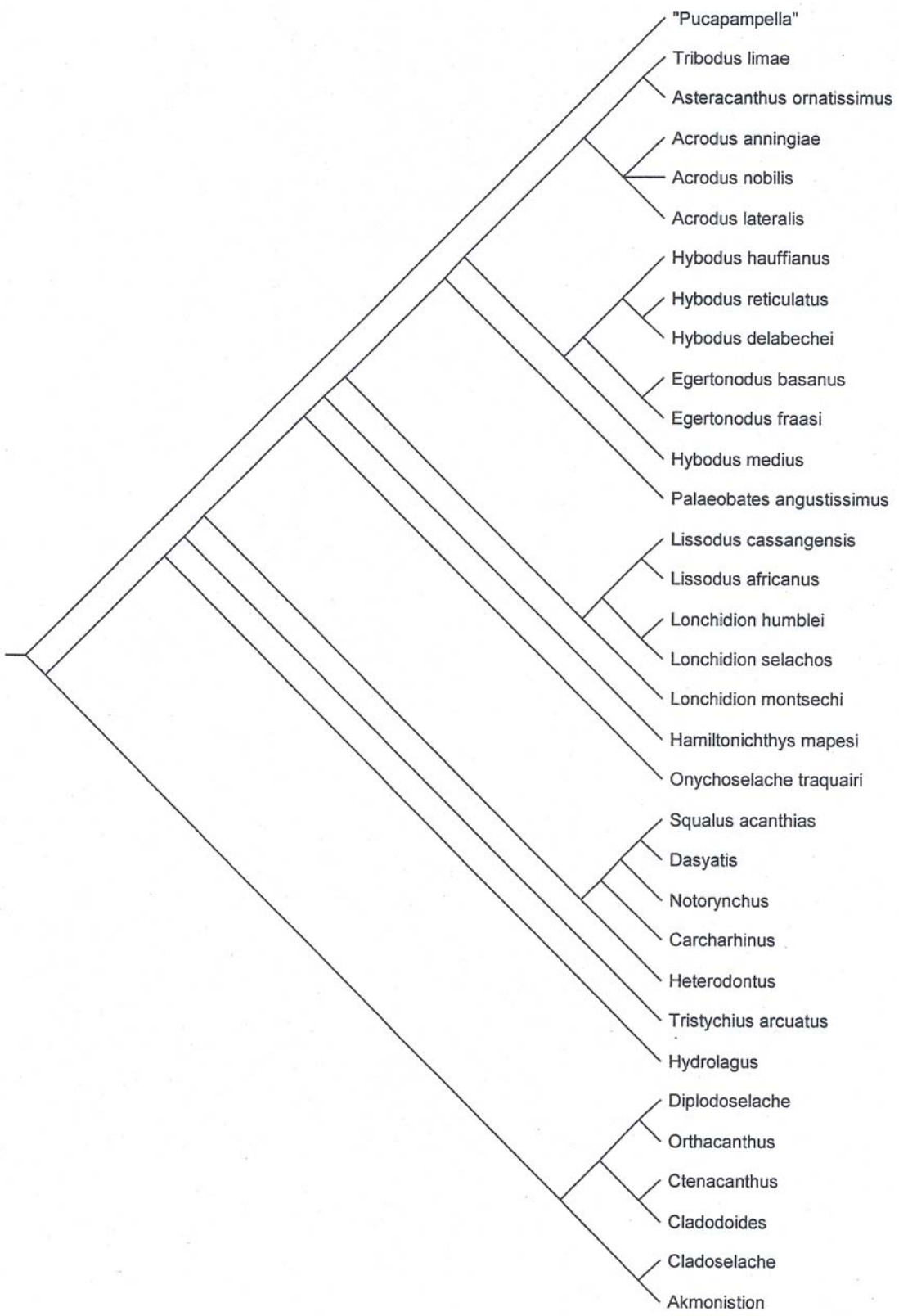

"Pucapampella"
Tribodus limae
Asteracanthus ornatissimus
Acrodus anningiae
Acrodus nobilis
Acrodus lateralis
Hybodus hauffianus
Hybodus reticulatus
Hybodus delabechei
Egertonodus basanus
Egertonodus fraasi
Hybodus medius
Palaeobates angustissimus
Lissodus cassangensis
Lissodus africanus
Lonchidion humblei
Lonchidion selachos
Lonchidion montsechi
Hamiltonichthys mapesi
Onychoselache traquairi
Squalus acanthias
Dasyatis
Notorynchus
Carcharhinus
Heterodontus
Tristychius arcuatus
Hydrolagus
Diplodoselache
Orthacanthus
Ctenacanthus
Cladodoides
Cladoselache
Akmonistion

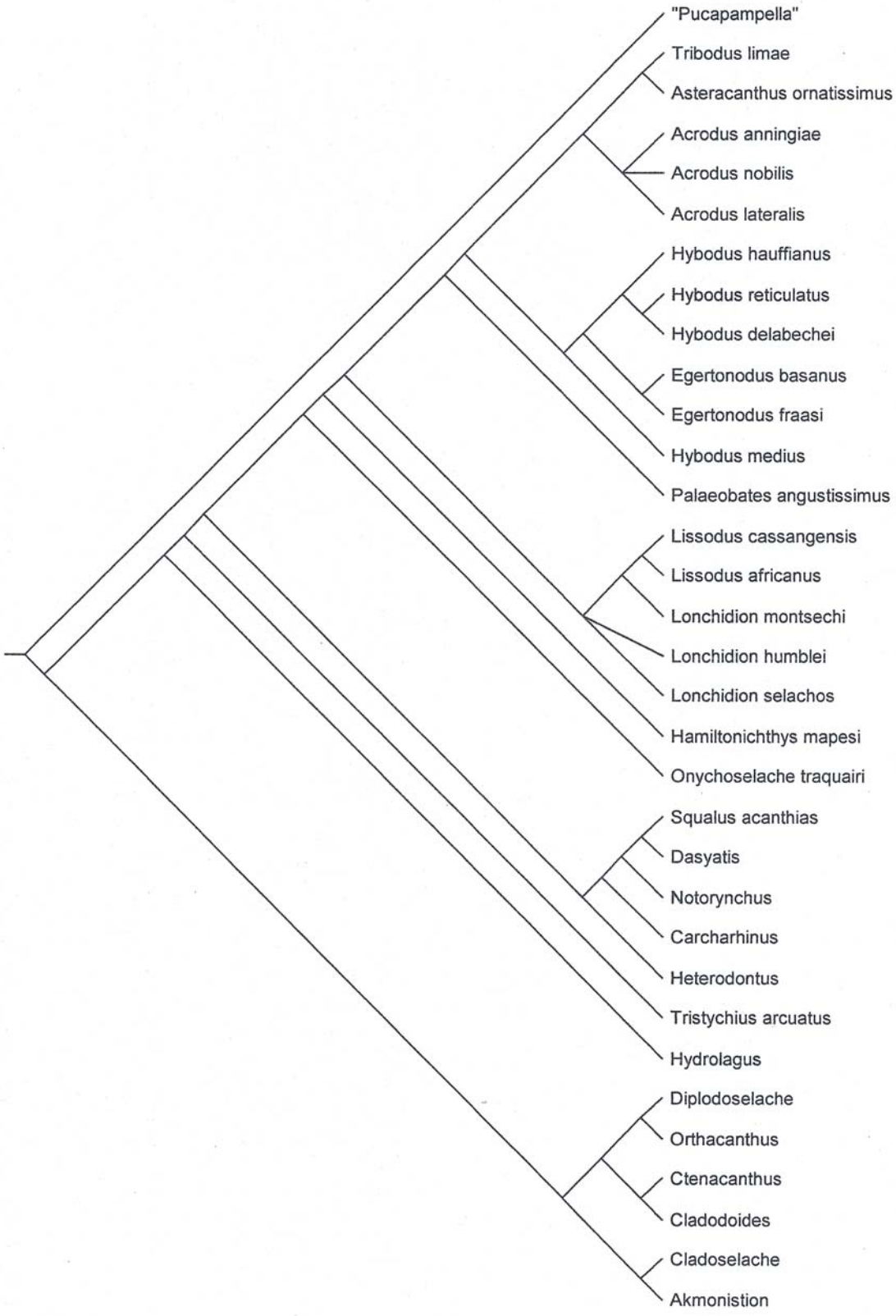

"Pucapampella"
Tribodus limae
Asteracanthus ornatissimus
Acrodus anningiae
Acrodus nobilis
Acrodus lateralis
Hybodus hauffianus
Hybodus reticulatus
Hybodus delabechei
Egertonodus basanus
Egertonodus fraasi
Hybodus medius
Palaeobates angustissimus
Lissodus cassangensis
Lissodus africanus
Lonchidion humblei
Lonchidion selachos
Lonchidion montsechi
Hamiltonichthys mapesi
Onychoselache traquairi
Squalus acanthias
Dasyatis
Notorynchus
Carcharhinus
Heterodontus
Tristychius arcuatus
Hydrolagus
Diplodoselache
Orthacanthus
Ctenacanthus
Cladodoides
Cladoselache
Akmonistion

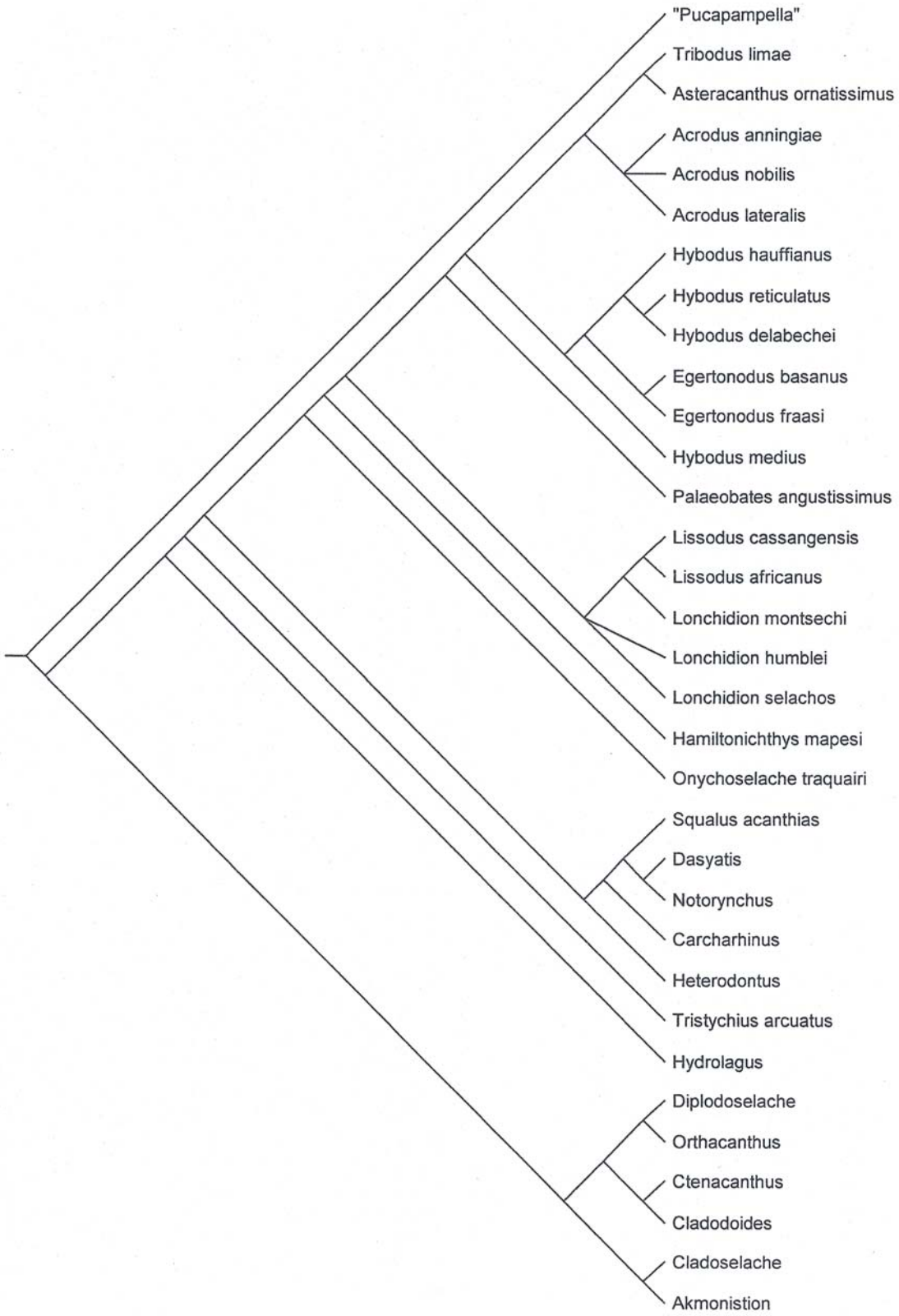

"Pucapampella"
Tribodus limae
Asteracanthus ornatissimus
Acrodus anningiae
Acrodus nobilis
Acrodus lateralis
Hybodus hauffianus
Hybodus reticulatus
Hybodus delabechei
Egertonodus basanus
Egertonodus fraasi
Hybodus medius
Palaeobates angustissimus
Lissodus cassangensis
Lissodus africanus
Lonchidion montsechi
Lonchidion humblei
Lonchidion selachos
Hamiltonichthys mapesi
Onychoselache traquairi
Squalus acanthias
Dasyatis
Notorynchus
Carcharhinus
Heterodontus
Tristychius arcuatus
Hydrolagus
Diplodoselache
Orthacanthus
Ctenacanthus
Cladodoides
Cladoselache
Akmonistion

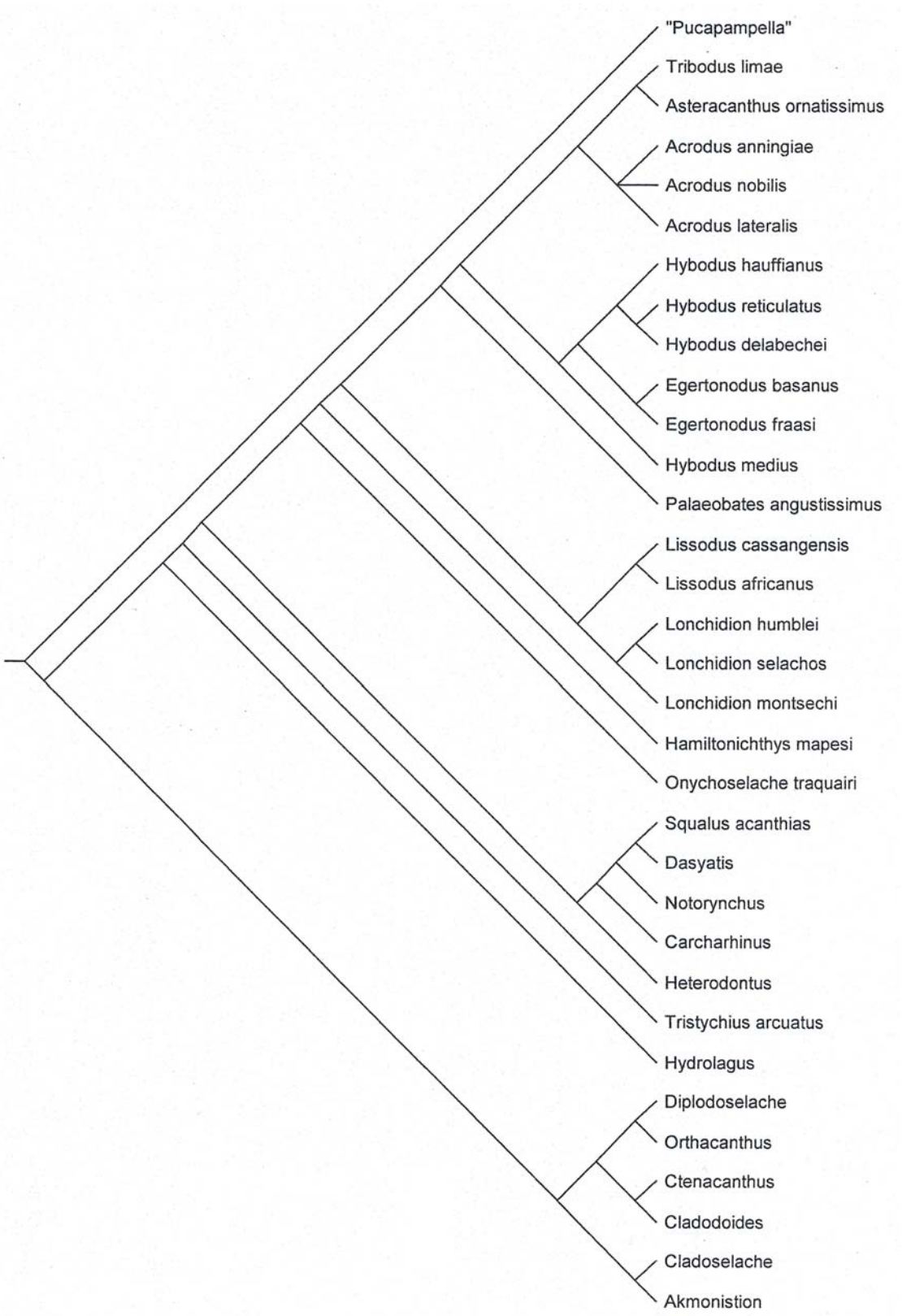

"Pucapampella"
Tribodus limae
Asteracanthus ornatissimus
Acrodus anningiae
Acrodus nobilis
Acrodus lateralis
Hybodus hauffianus
Hybodus reticulatus
Hybodus delabechei
Egertonodus basanus
Egertonodus fraasi
Hybodus medius
Palaeobates angustissimus
Lissodus cassangensis
Lissodus africanus
Lonchidion montsechi
Lonchidion humblei
Lonchidion selachos
Hamiltonichthys mapesi
Onychoselache traquairi
Squalus acanthias
Dasyatis
Notorynchus
Carcharhinus
Heterodontus
Tristychius arcuatus
Hydrolagus
Diplodoselache
Orthacanthus
Ctenacanthus
Cladodoides
Cladoselache
Akmonistion

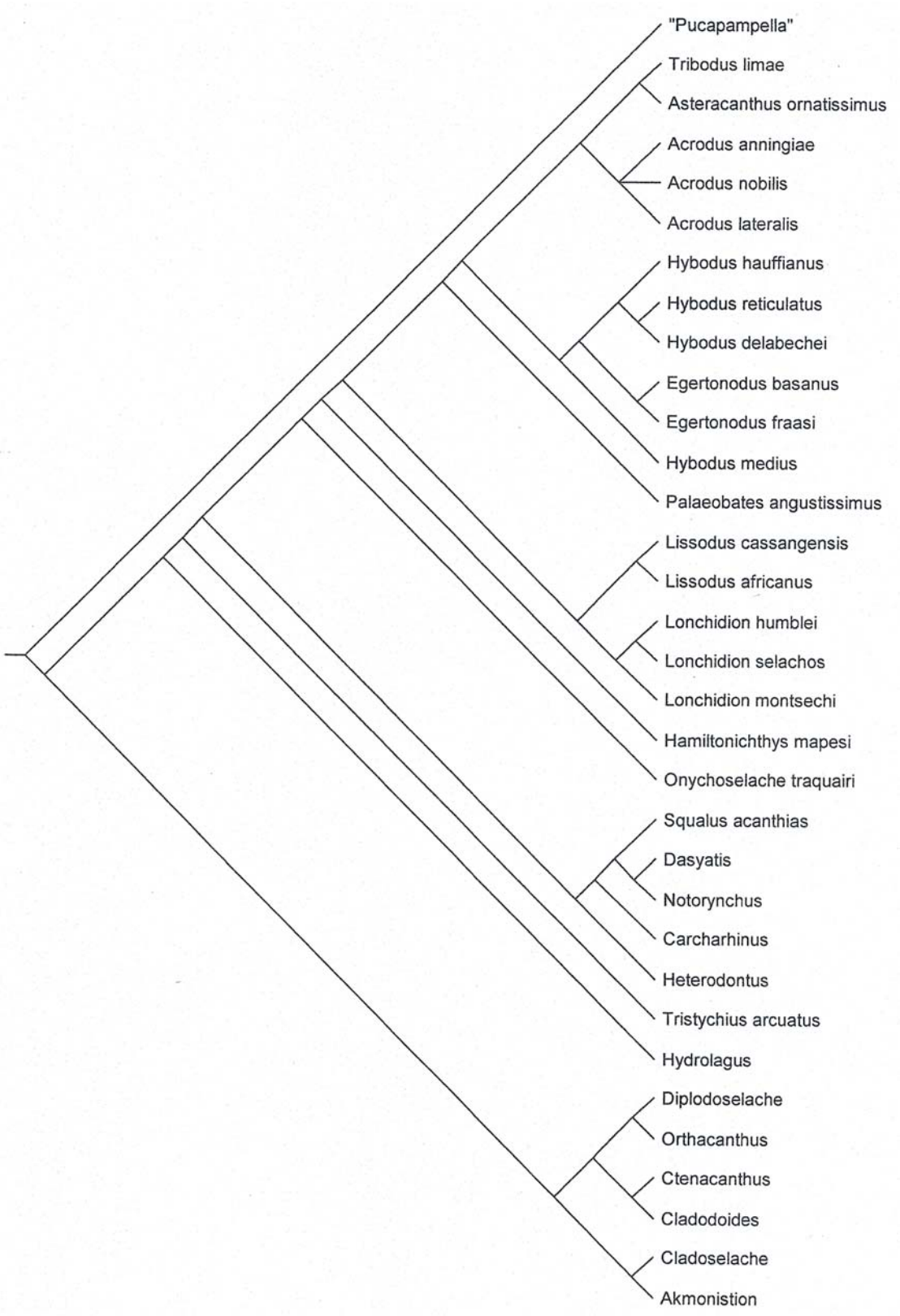

"Pucapampella"
Tribodus limae
Asteracanthus ornatissimus
Acrodus anningiae
Acrodus nobilis
Acrodus lateralis
Hybodus hauffianus
Hybodus reticulatus
Hybodus delabechei
Egertonodus basanus
Egertonodus fraasi
Hybodus medius
Palaeobates angustissimus
Lissodus cassangensis
Lissodus africanus
Lonchidion humblei
Lonchidion selachos
Lonchidion montsechi
Hamiltonichthys mapesi
Onychoselache traquairi
Squalus acanthias
Dasyatis
Notorynchus
Carcharhinus
Heterodontus
Tristychius arcuatus
Hydrolagus
Diplodoselache
Orthacanthus
Ctenacanthus
Cladodoides
Cladoselache
Akmonistion

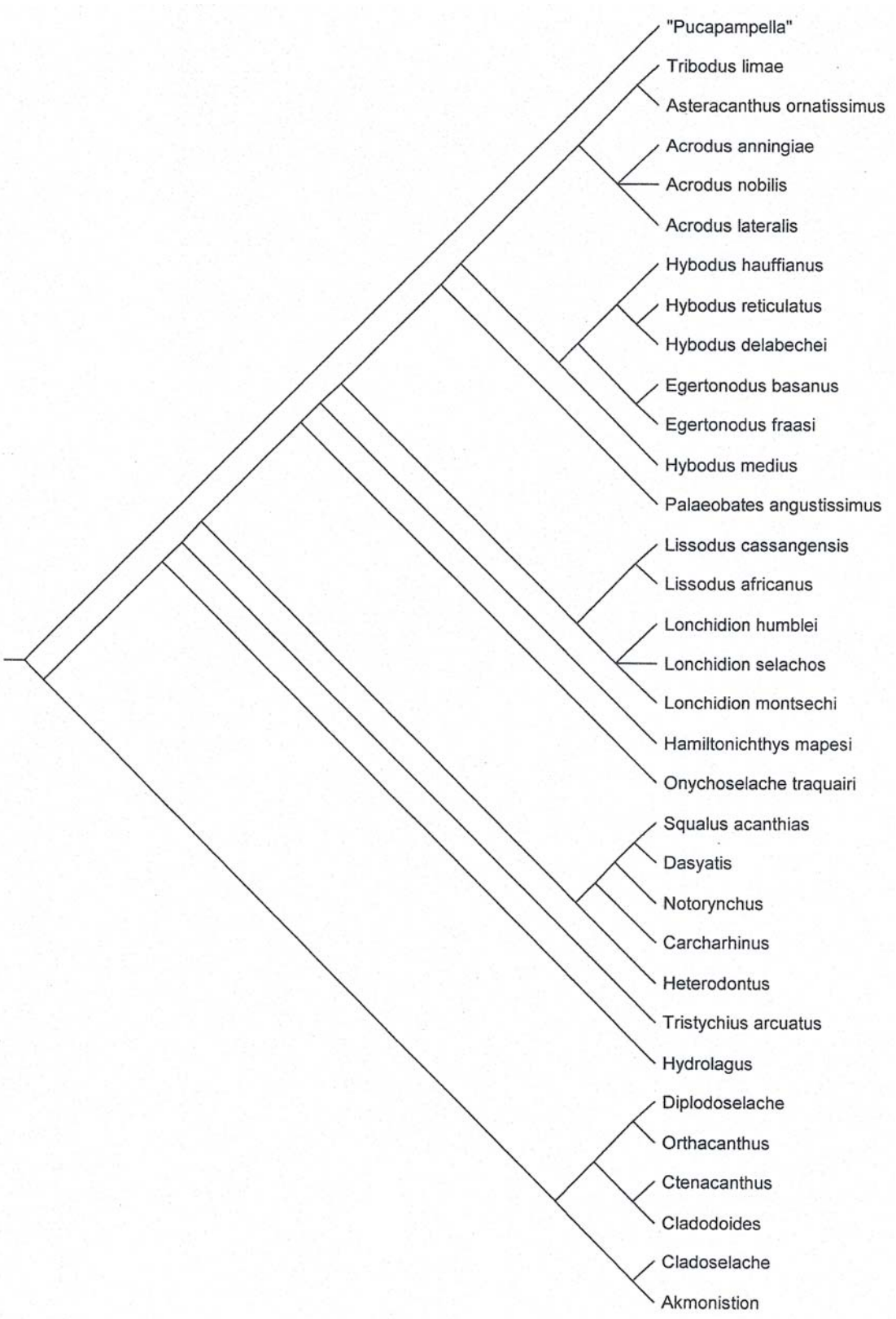

"Pucapampella"
Tribodus limae
Asteracanthus ornatissimus
Acrodus anningiae
Acrodus nobilis
Acrodus lateralis
Hybodus hauffianus
Hybodus reticulatus
Hybodus delabechei
Egertonodus basanus
Egertonodus fraasi
Hybodus medius
Palaeobates angustissimus
Lissodus cassangensis
Lissodus africanus
Lonchidion humblei
Lonchidion selachos
Lonchidion montsechi
Hamiltonichthys mapesi
Onychoselache traquairi
Squalus acanthias
Dasyatis
Notorynchus
Carcharhinus
Heterodontus
Tristychius arcuatus
Hydrolagus
Diplodoselache
Orthacanthus
Ctenacanthus
Cladodoides
Cladoselache
Akmonistion

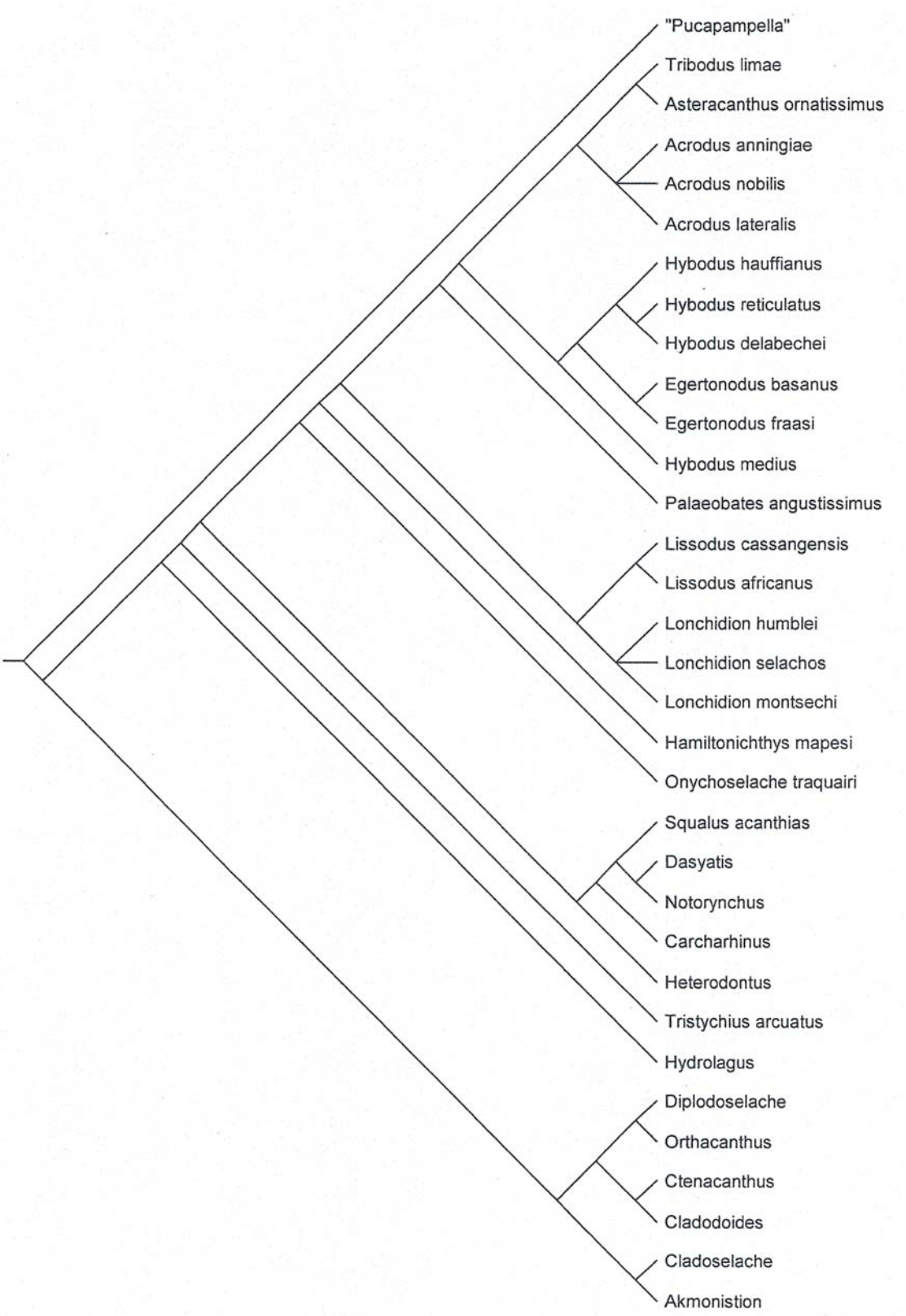

"Pucapampella"
Tribodus limae
Asteracanthus ornatissimus
Acrodus anningiae
Acrodus nobilis
Acrodus lateralis
Hybodus hauffianus
Hybodus reticulatus
Hybodus delabechei
Egertonodus basanus
Egertonodus fraasi
Hybodus medius
Palaeobates angustissimus
Lissodus cassangensis
Lissodus africanus
Lonchidion montsechi
Lonchidion humblei
Lonchidion selachos
Hamiltonichthys mapesi
Onychoselache traquairi
Squalus acanthias
Dasyatis
Notorynchus
Carcharhinus
Heterodontus
Tristychius arcuatus
Hydrolagus
Diplodoselache
Orthacanthus
Ctenacanthus
Cladodoides
Cladoselache
Akmonistion

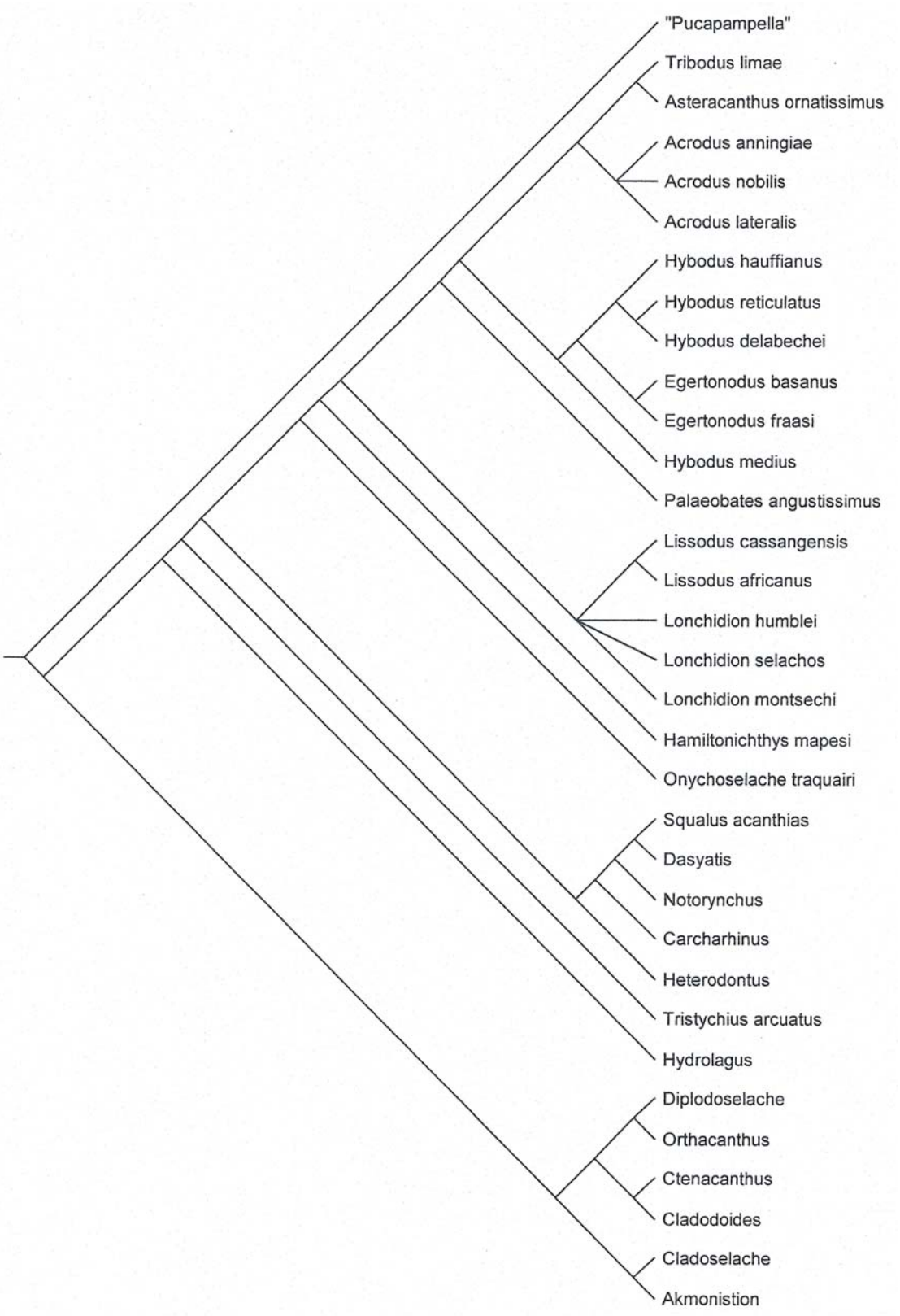

"Pucapampella"
Tribodus limae
Asteracanthus ornatissimus
Acrodus anningiae
Acrodus nobilis
Acrodus lateralis
Hybodus hauffianus
Hybodus reticulatus
Hybodus delabechei
Egertonodus basanus
Egertonodus fraasi
Hybodus medius
Palaeobates angustissimus
Lissodus cassangensis
Lissodus africanus
Lonchidion montsechi
Lonchidion humblei
Lonchidion selachos
Hamiltonichthys mapesi
Onychoselache traquairi
Squalus acanthias
Dasyatis
Notorynchus
Carcharhinus
Heterodontus
Tristychius arcuatus
Hydrolagus
Diplodoselache
Orthacanthus
Ctenacanthus
Cladodoides
Cladoselache
Akmonistion

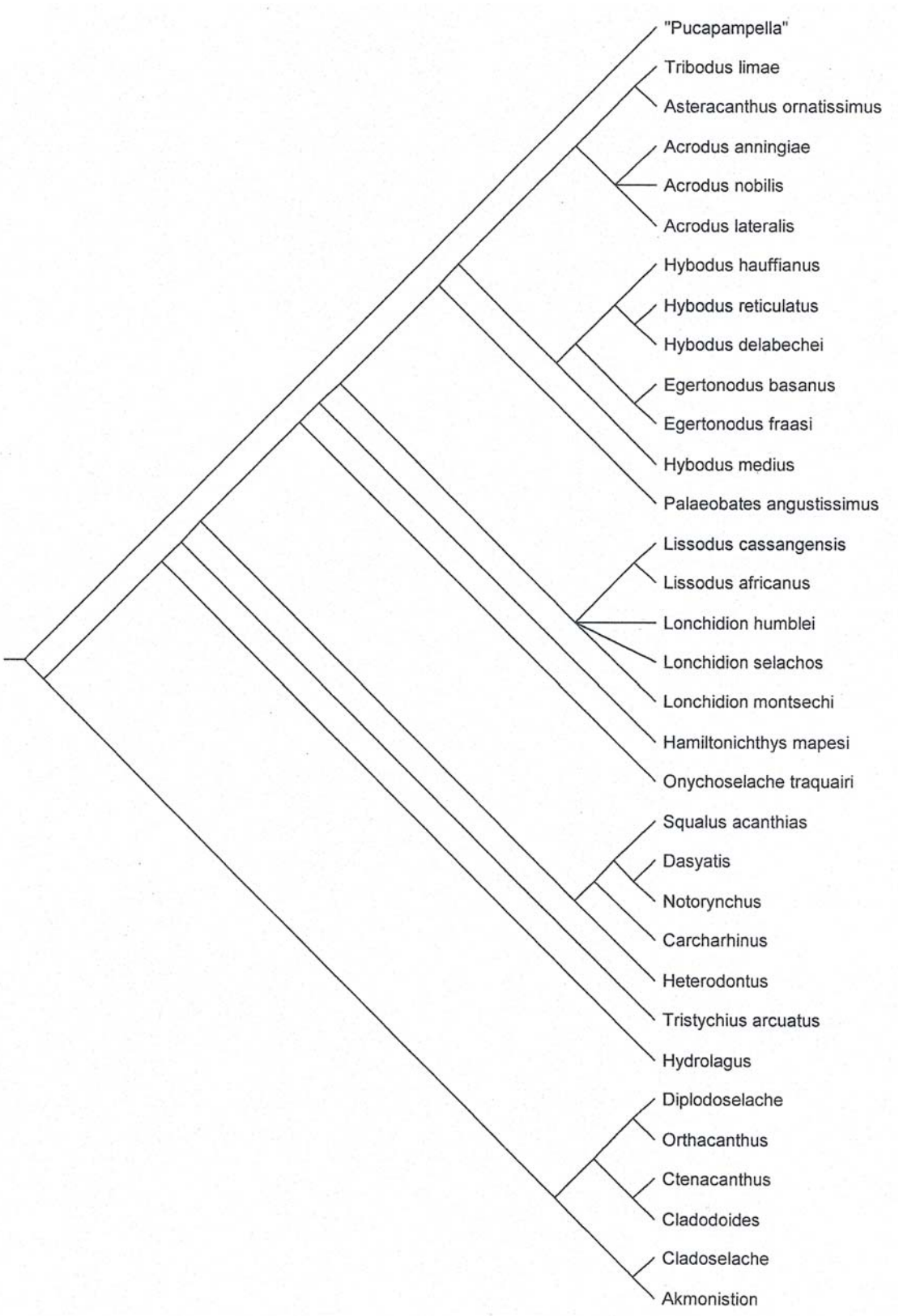

"Pucapampella"
Tribodus limae
Asteracanthus ornatissimus
Acrodus anningiae
Acrodus nobilis
Acrodus lateralis
Hybodus hauffianus
Hybodus reticulatus
Hybodus delabechei
Egertonodus basanus
Egertonodus fraasi
Hybodus medius
Palaeobates angustissimus
Lissodus cassangensis
Lissodus africanus
Lonchidion humblei
Lonchidion selachos
Lonchidion montsechi
Hamiltonichthys mapesi
Onychoselache traquairi
Squalus acanthias
Dasyatis
Notorynchus
Carcharhinus
Heterodontus
Tristychius arcuatus
Hydrolagus
Diplodoselache
Orthacanthus
Ctenacanthus
Cladodoides
Cladoselache
Akmonistion

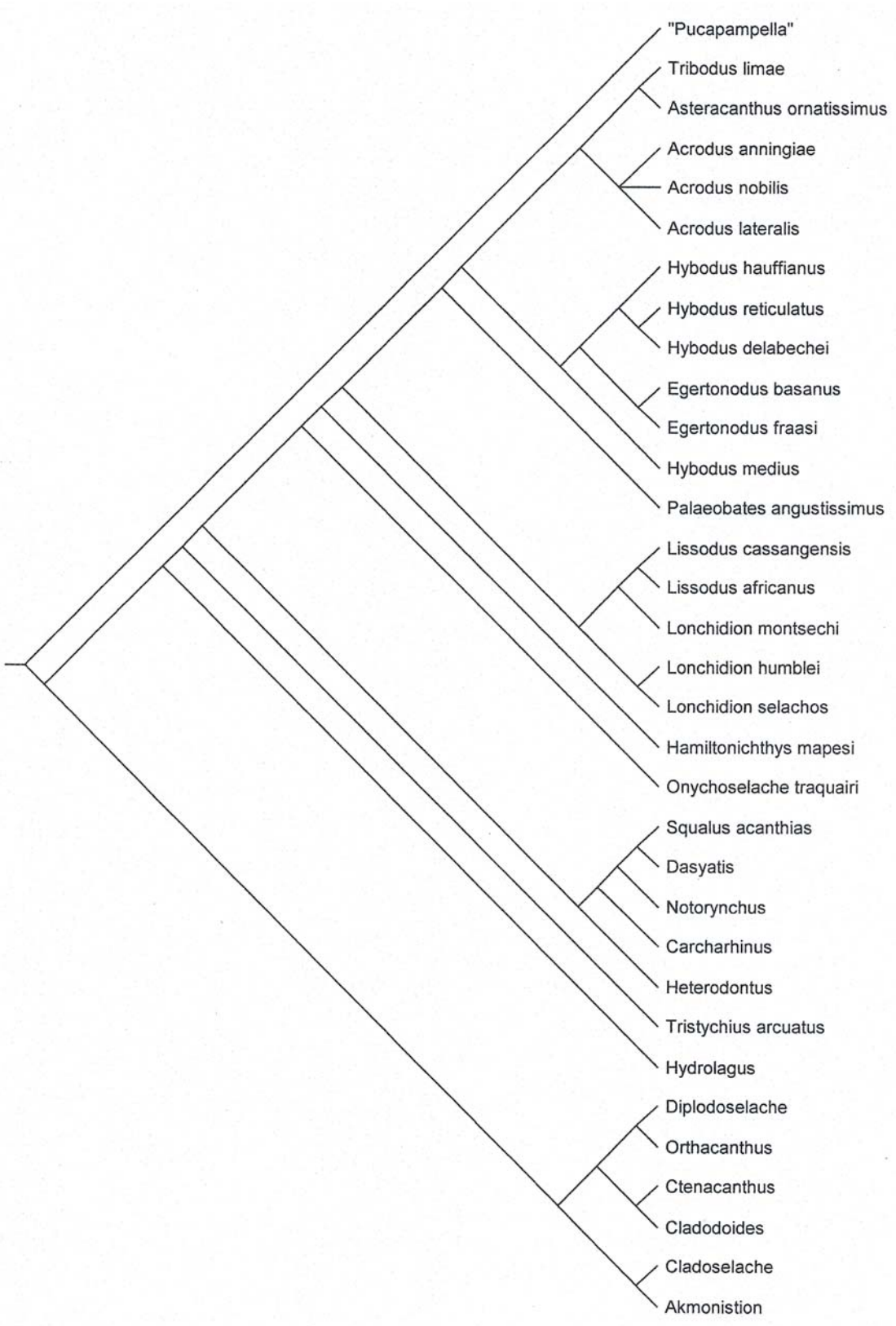

"Pucapampella"
Tribodus limae
Asteracanthus ornatissimus
Acrodus anningiae
Acrodus nobilis
Acrodus lateralis
Hybodus hauffianus
Hybodus reticulatus
Hybodus delabechei
Egertonodus basanus
Egertonodus fraasi
Hybodus medius
Palaeobates angustissimus
Lissodus cassangensis
Lissodus africanus
Lonchidion humblei
Lonchidion selachos
Lonchidion montsechi
Hamiltonichthys mapesi
Onychoselache traquairi
Squalus acanthias
Dasyatis
Notorynchus
Carcharhinus
Heterodontus
Tristychius arcuatus
Hydrolagus
Diplodoselache
Orthacanthus
Ctenacanthus
Cladodoides
Cladoselache
Akmonistion

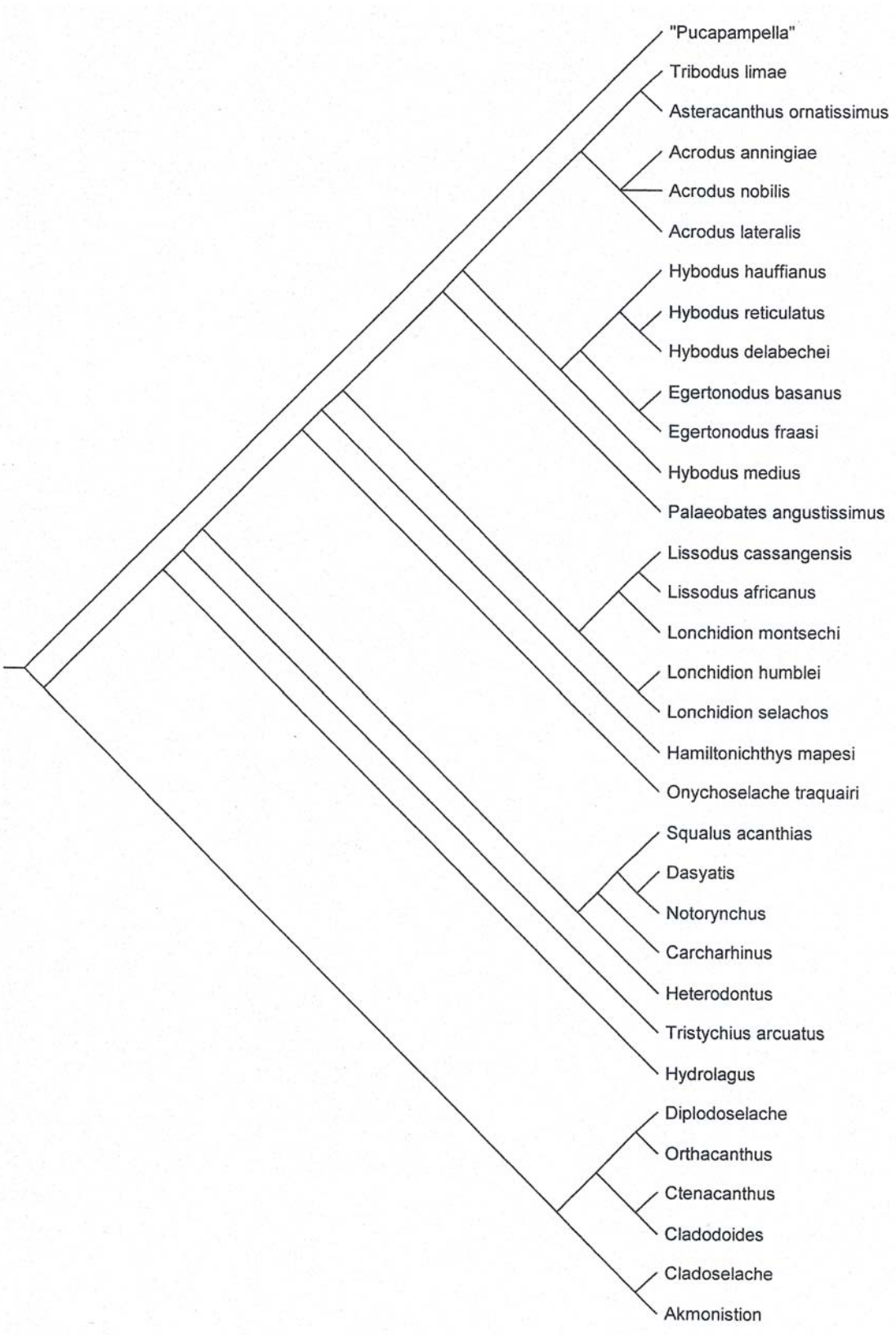

"Pucapampella"
Tribodus limae
Asteracanthus ornatissimus
Acrodus anningiae
Acrodus nobilis
Acrodus lateralis
Hybodus hauffianus
Hybodus reticulatus
Hybodus delabechei
Egertonodus basanus
Egertonodus fraasi
Hybodus medius
Palaeobates angustissimus
Lissodus cassangensis
Lissodus africanus
Lonchidion humblei
Lonchidion selachos
Lonchidion montsechi
Hamiltonichthys mapesi
Onychoselache traquairi
Squalus acanthias
Dasyatis
Notorynchus
Carcharhinus
Heterodontus
Tristychius arcuatus
Hydrolagus
Diplodoselache
Orthacanthus
Ctenacanthus
Cladodoides
Cladoselache
Akmonistion

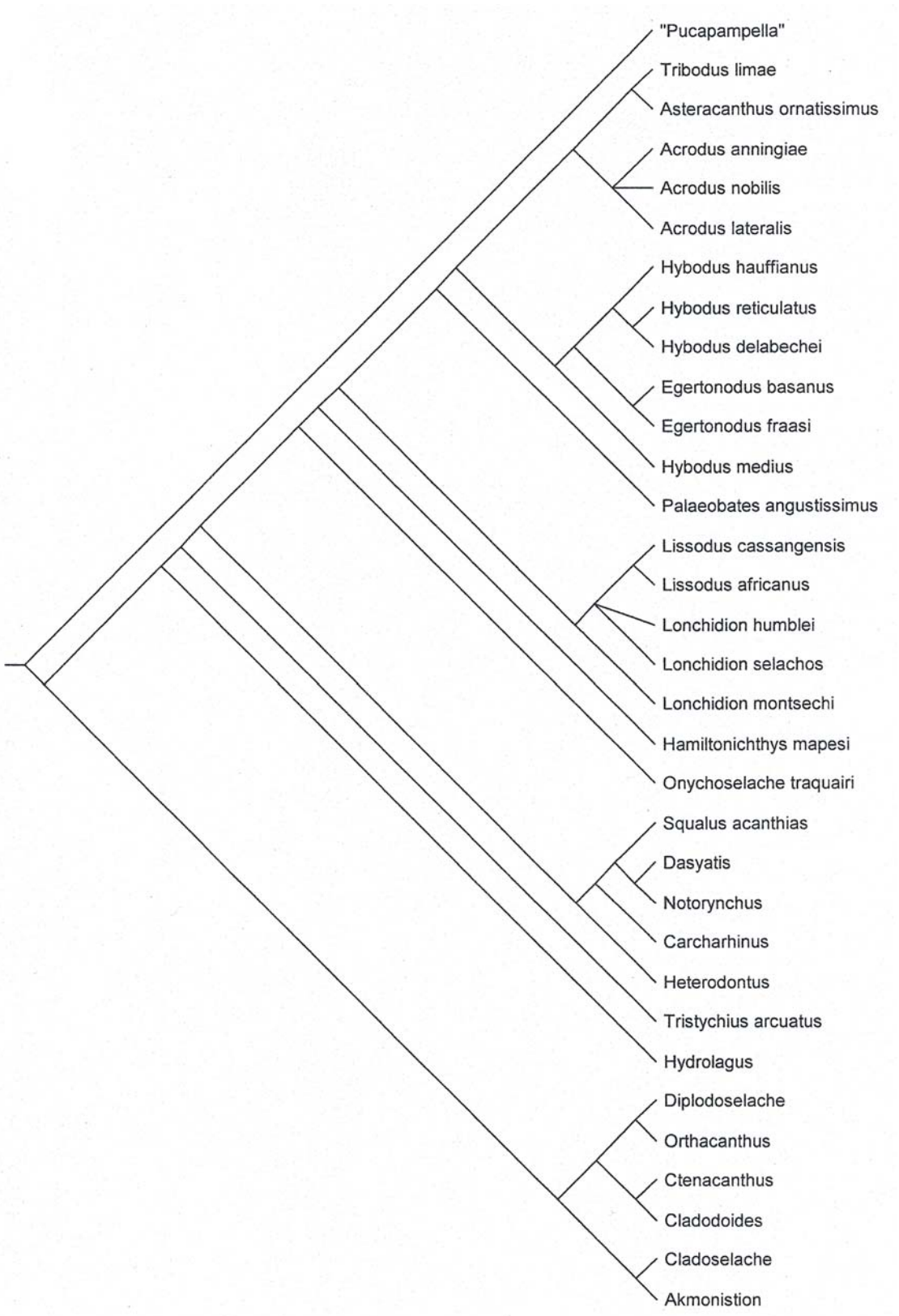

"Pucapampella"
Tribodus limae
Asteracanthus ornatissimus
Acrodus anningiae
Acrodus nobilis
Acrodus lateralis
Hybodus hauffianus
Hybodus reticulatus
Hybodus delabechei
Egertonodus basanus
Egertonodus fraasi
Hybodus medius
Palaeobates angustissimus
Lissodus cassangensis
Lissodus africanus
Lonchidion humblei
Lonchidion selachos
Lonchidion montsechi
Hamiltonichthys mapesi
Onychoselache traquairi
Squalus acanthias
Dasyatis
Notorynchus
Carcharhinus
Heterodontus
Tristychius arcuatus
Hydrolagus
Diplodoselache
Orthacanthus
Ctenacanthus
Cladodoides
Cladoselache
Akmonistion

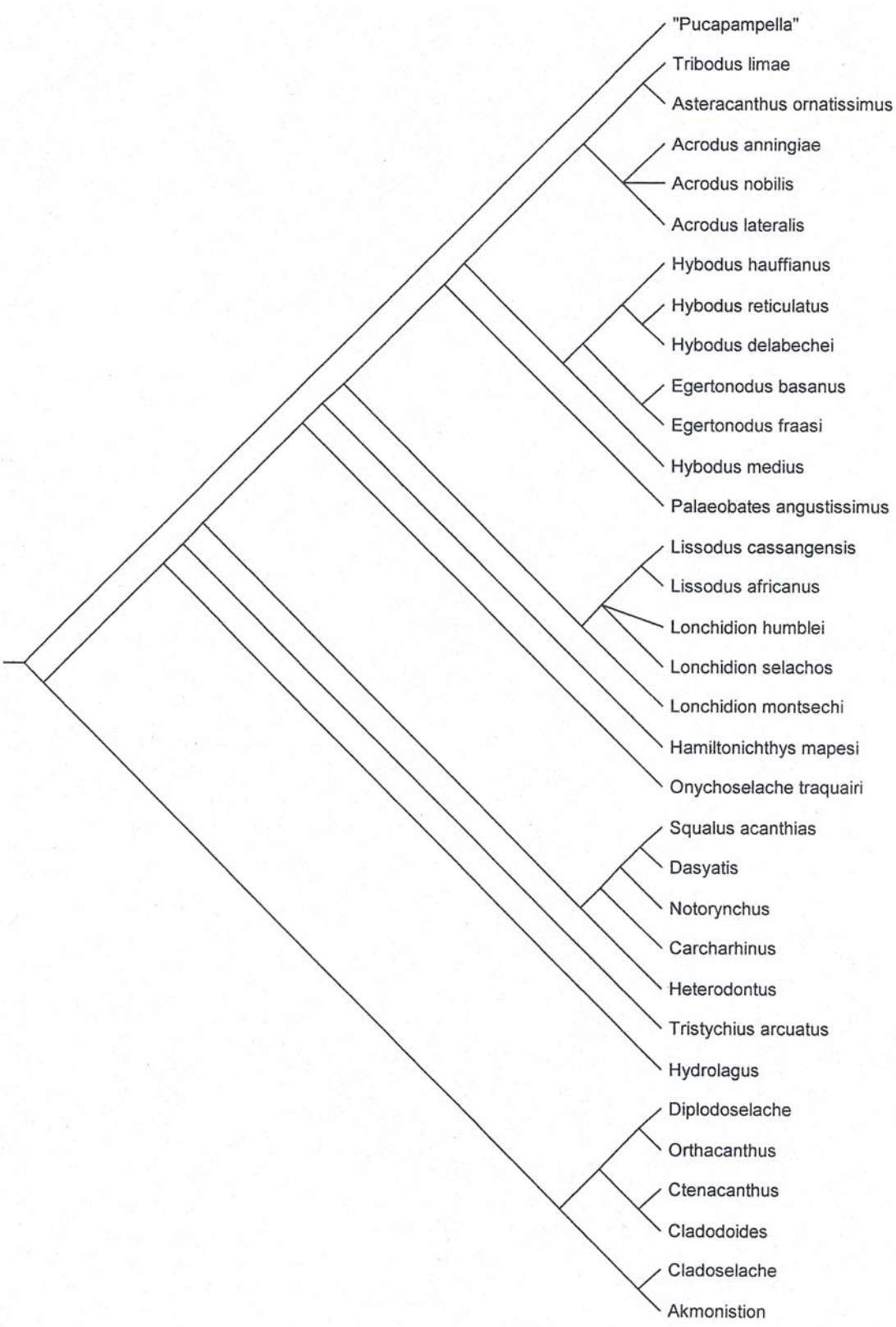

"Pucapampella"
Tribodus limae
Asteracanthus ornatissimus
Acrodus anningiae
Acrodus nobilis
Acrodus lateralis
Hybodus hauffianus
Hybodus reticulatus
Hybodus delabechei
Egertonodus basanus
Egertonodus fraasi
Hybodus medius
Palaeobates angustissimus
Lissodus cassangensis
Lissodus africanus
Lonchidion humblei
Lonchidion selachos
Lonchidion montsechi
Hamiltonichthys mapesi
Onychoselache traquairi
Squalus acanthias
Dasyatis
Notorynchus
Carcharhinus
Heterodontus
Tristychius arcuatus
Hydrolagus
Diplodoselache
Orthacanthus
Ctenacanthus
Cladodoides
Cladoselache
Akmonistion

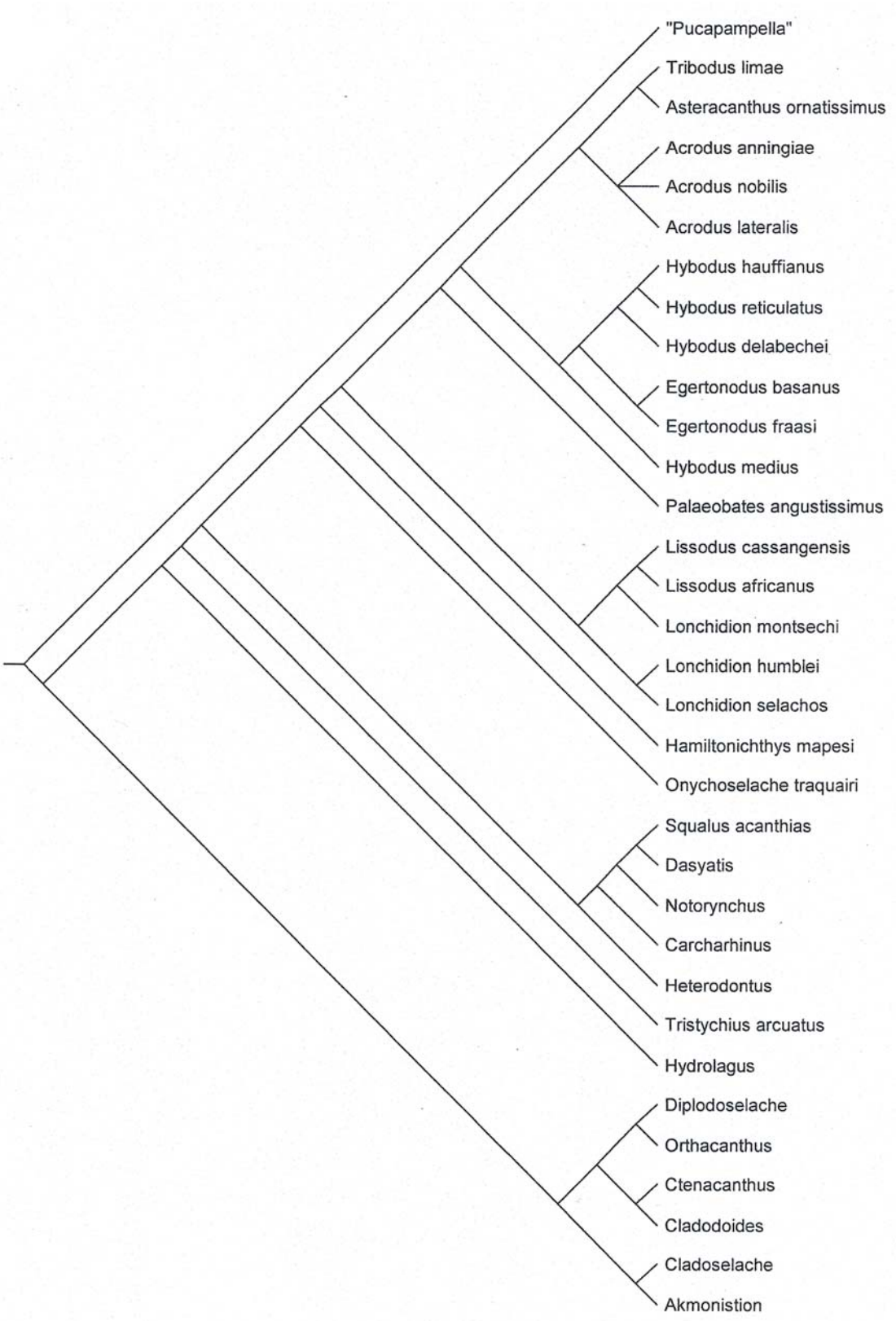

"Pucapampella"
Tribodus limae
Asteracanthus ornatissimus
Acrodus anningiae
Acrodus nobilis
Acrodus lateralis
Hybodus hauffianus
Hybodus reticulatus
Hybodus delabechei
Egertonodus basanus
Egertonodus fraasi
Hybodus medius
Palaeobates angustissimus
Lissodus cassangensis
Lissodus africanus
Lonchidion humblei
Lonchidion selachos
Lonchidion montsechi
Hamiltonichthys mapesi
Onychoselache traquairi
Squalus acanthias
Dasyatis
Notorynchus
Carcharhinus
Heterodontus
Tristychius arcuatus
Hydrolagus
Diplodoselache
Orthacanthus
Ctenacanthus
Cladodoides
Cladoselache
Akmonistion

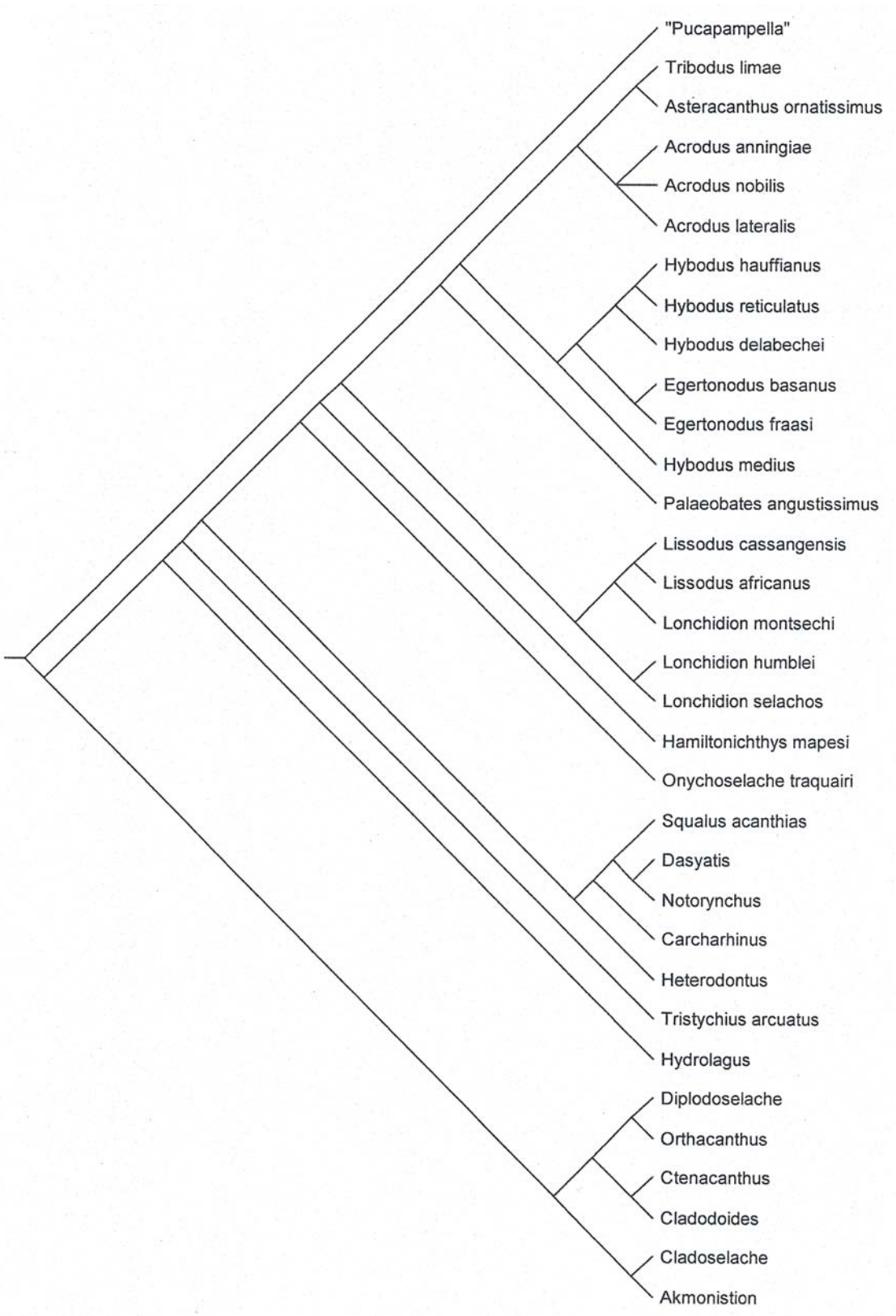

"Pucapampella"
Tribodus limae
Asteracanthus ornatissimus
Acrodus anningiae
Acrodus nobilis
Acrodus lateralis
Hybodus hauffianus
Hybodus reticulatus
Hybodus delabechei
Egertonodus basanus
Egertonodus fraasi
Hybodus medius
Palaeobates angustissimus
Lissodus cassangensis
Lissodus africanus
Lonchidion montsechi
Lonchidion humblei
Lonchidion selachos
Hamiltonichthys mapesi
Onychoselache traquairi
Squalus acanthias
Dasyatis
Notorynchus
Carcharhinus
Heterodontus
Tristychius arcuatus
Hydrolagus
Diplodoselache
Orthacanthus
Ctenacanthus
Cladodoides
Cladoselache
Akmonistion

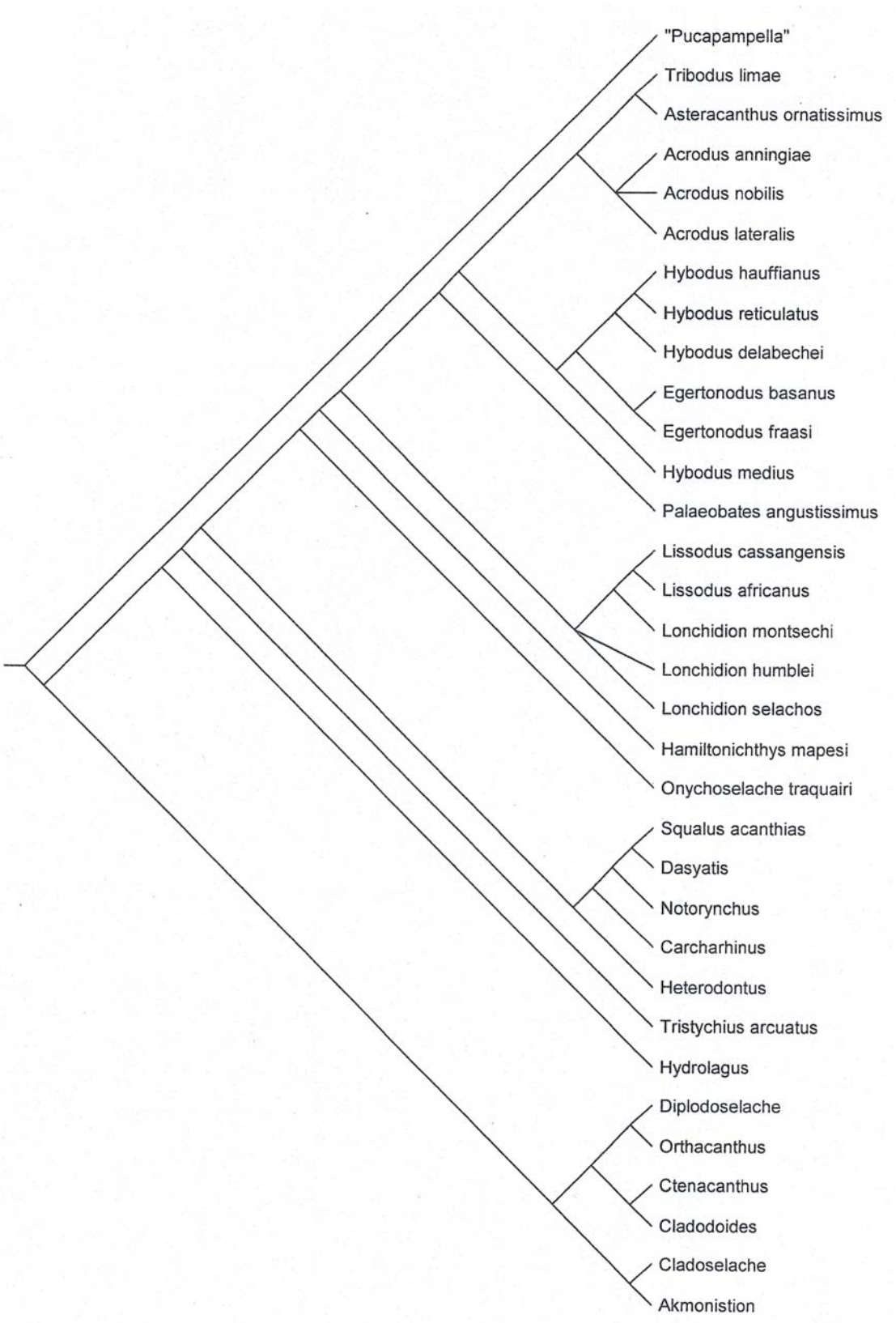

"Pucapampella"
Tribodus limae
Asteracanthus ornatissimus
Acrodus anningiae
Acrodus nobilis
Acrodus lateralis
Hybodus hauffianus
Hybodus reticulatus
Hybodus delabechei
Egertonodus basanus
Egertonodus fraasi
Hybodus medius
Palaeobates angustissimus
Lissodus cassangensis
Lissodus africanus
Lonchidion montsechi
Lonchidion humblei
Lonchidion selachos
Hamiltonichthys mapesi
Onychoselache traquairi
Squalus acanthias
Dasyatis
Notorynchus
Carcharhinus
Heterodontus
Tristychius arcuatus
Hydrolagus
Diplodoselache
Orthacanthus
Ctenacanthus
Cladodoides
Cladoselache
Akmonistion

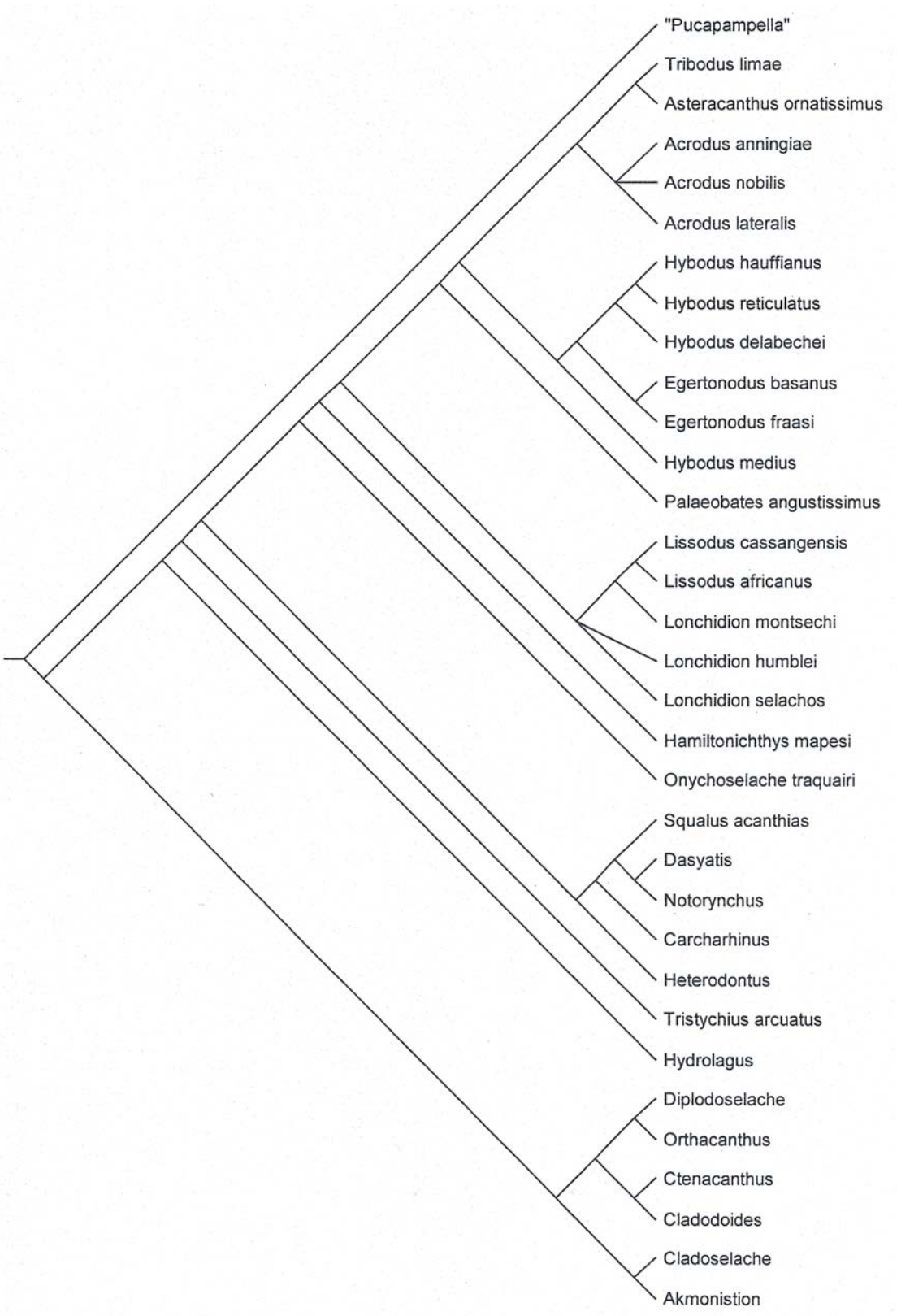

"Pucapampella"
Tribodus limae
Asteracanthus ornatissimus
Acrodus anningiae
Acrodus nobilis
Acrodus lateralis
Hybodus hauffianus
Hybodus reticulatus
Hybodus delabechei
Egertonodus basanus
Egertonodus fraasi
Hybodus medius
Palaeobates angustissimus
Lissodus cassangensis
Lissodus africanus
Lonchidion humblei
Lonchidion selachos
Lonchidion montsechi
Hamiltonichthys mapesi
Onychoselache traquairi
Squalus acanthias
Dasyatis
Notorynchus
Carcharhinus
Heterodontus
Tristychius arcuatus
Hydrolagus
Diplodoselache
Orthacanthus
Ctenacanthus
Cladodoides
Cladoselache
Akmonistion


"Pucapampella"
Tribodus limae
Asteracanthus ornatissimus
Acrodus anningiae
Acrodus nobilis
Acrodus lateralis
Hybodus hauffianus
Hybodus reticulatus
Hybodus delabechei
Egertonodus basanus
Egertonodus fraasi
Hybodus medius
Palaeobates angustissimus
Lissodus cassangensis
Lissodus africanus
Lonchidion humblei
Lonchidion selachos
Lonchidion montsechi
Hamiltonichthys mapesi
Onychoselache traquairi
Squalus acanthias
Dasyatis
Notorynchus
Carcharhinus
Heterodontus
Tristychius arcuatus
Hydrolagus
Diplodoselache
Orthacanthus
Ctenacanthus
Cladodoides
Cladoselache
Akmonistion

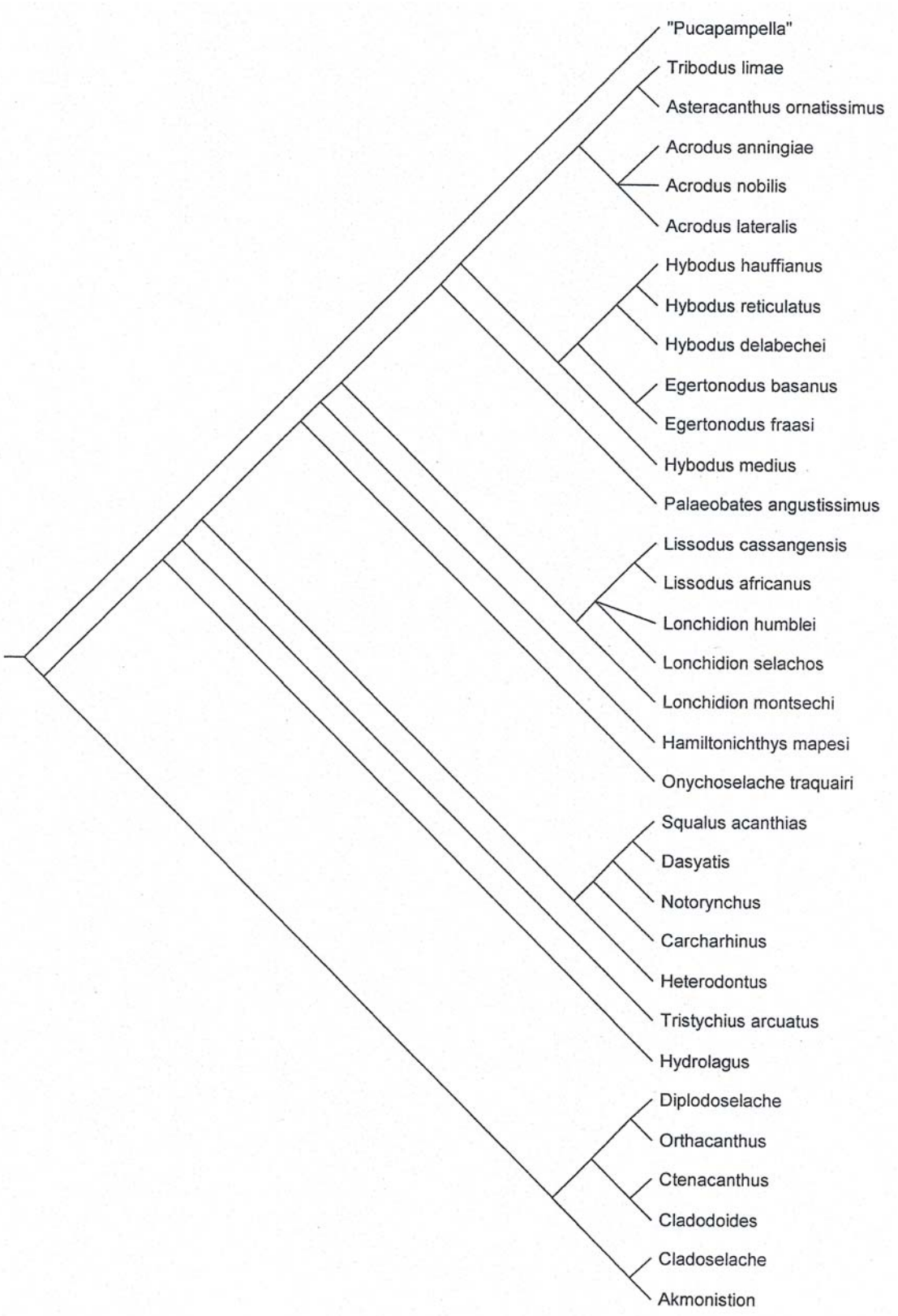

"Pucapampella"
Tribodus limae
Asteracanthus ornatissimus
Acrodus anningiae
Acrodus nobilis
Acrodus lateralis
Hybodus hauffianus
Hybodus reticulatus
Hybodus delabechei
Egertonodus basanus
Egertonodus fraasi
Hybodus medius
Palaeobates angustissimus
Lissodus cassangensis
Lissodus africanus
Lonchidion montsechi
Lonchidion humblei
Lonchidion selachos
Hamiltonichthys mapesi
Onychoselache traquairi
Squalus acanthias
Dasyatis
Notorynchus
Carcharhinus
Heterodontus
Tristychius arcuatus
Hydrolagus
Diplodoselache
Orthacanthus
Ctenacanthus
Cladodoides
Cladoselache
Akmonistion

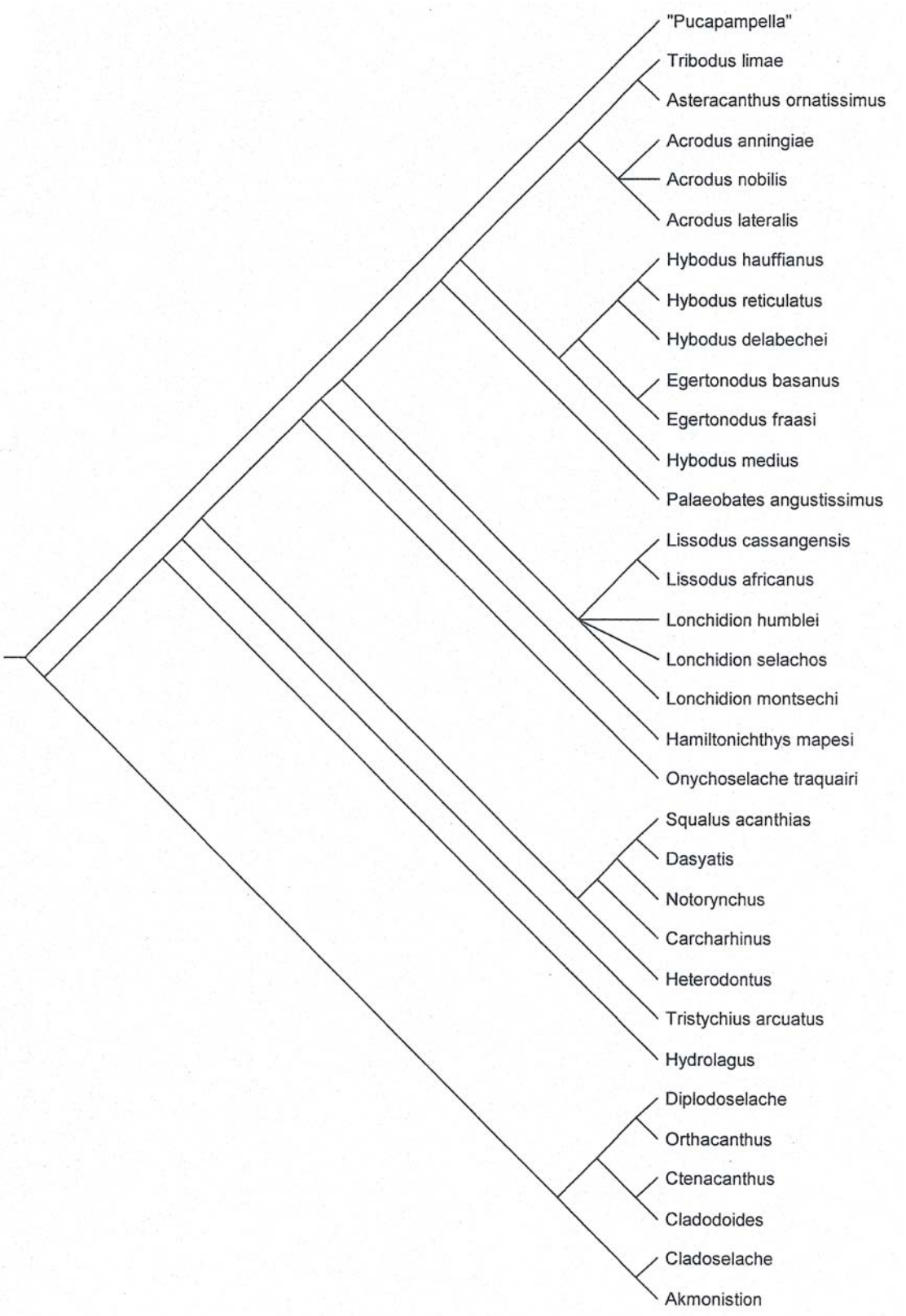

"Pucapampella"
Tribodus limae
Asteracanthus ornatissimus
Acrodus anningiae
Acrodus nobilis
Acrodus lateralis
Hybodus hauffianus
Hybodus reticulatus
Hybodus delabechei
Egertonodus basanus
Egertonodus fraasi
Hybodus medius
Palaeobates angustissimus
Lissodus cassangensis
Lissodus africanus
Lonchidion montsechi
Lonchidion humblei
Lonchidion selachos
Hamiltonichthys mapesi
Onychoselache traquairi
Squalus acanthias
Dasyatis
Notorynchus
Carcharhinus
Heterodontus
Tristychius arcuatus
Hydrolagus
Diplodoselache
Orthacanthus
Ctenacanthus
Cladodoides
Cladoselache
Akmonistion

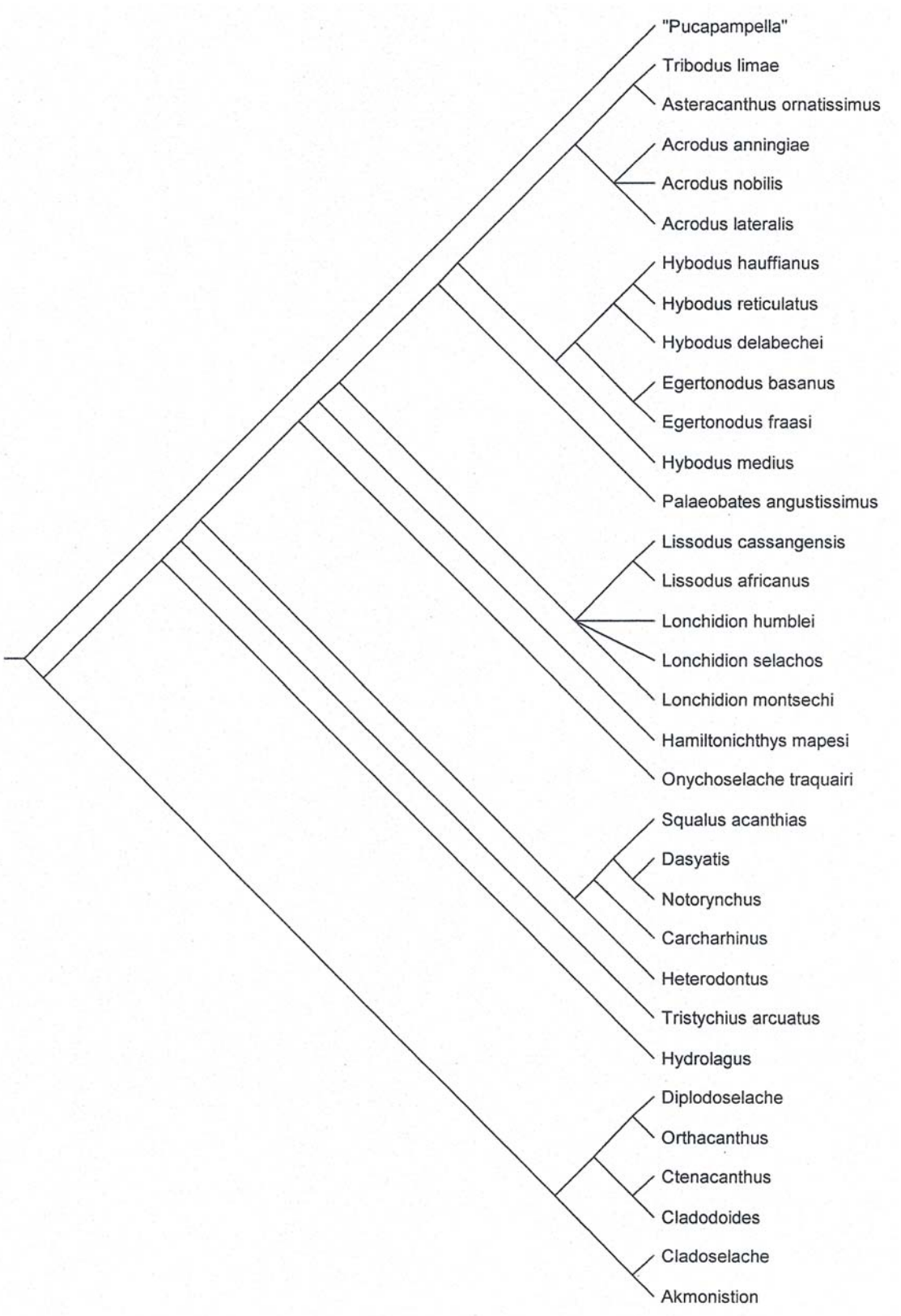

"Pucapampella"
Tribodus limae
Asteracanthus ornatissimus
Acrodus anningiae
Acrodus nobilis
Acrodus lateralis
Hybodus hauffianus
Hybodus reticulatus
Hybodus delabechei
Egertonodus basanus
Egertonodus fraasi
Hybodus medius
Palaeobates angustissimus
Lissodus cassangensis
Lissodus africanus
Lonchidion montsechi
Lonchidion humblei
Lonchidion selachos
Hamiltonichthys mapesi
Onychoselache traquairi
Squalus acanthias
Dasyatis
Notorynchus
Carcharhinus
Heterodontus
Tristychius arcuatus
Hydrolagus
Diplodoselache
Orthacanthus
Ctenacanthus
Cladodoides
Cladoselache
Akmonistion


"Pucapampella"
Tribodus limae
Asteracanthus ornatissimus
Acrodus anningiae
Acrodus nobilis
Acrodus lateralis
Hybodus hauffianus
Hybodus reticulatus
Hybodus delabechei
Egertonodus basanus
Egertonodus fraasi
Hybodus medius
Palaeobates angustissimus
Lissodus cassangensis
Lissodus africanus
Lonchidion montsechi
Lonchidion humblei
Lonchidion selachos
Hamiltonichthys mapesi
Onychoselache traquairi
Squalus acanthias
Dasyatis
Notorynchus
Carcharhinus
Heterodontus
Tristychius arcuatus
Hydrolagus
Diplodoselache
Orthacanthus
Ctenacanthus
Cladodoides
Cladoselache
Akmonistion

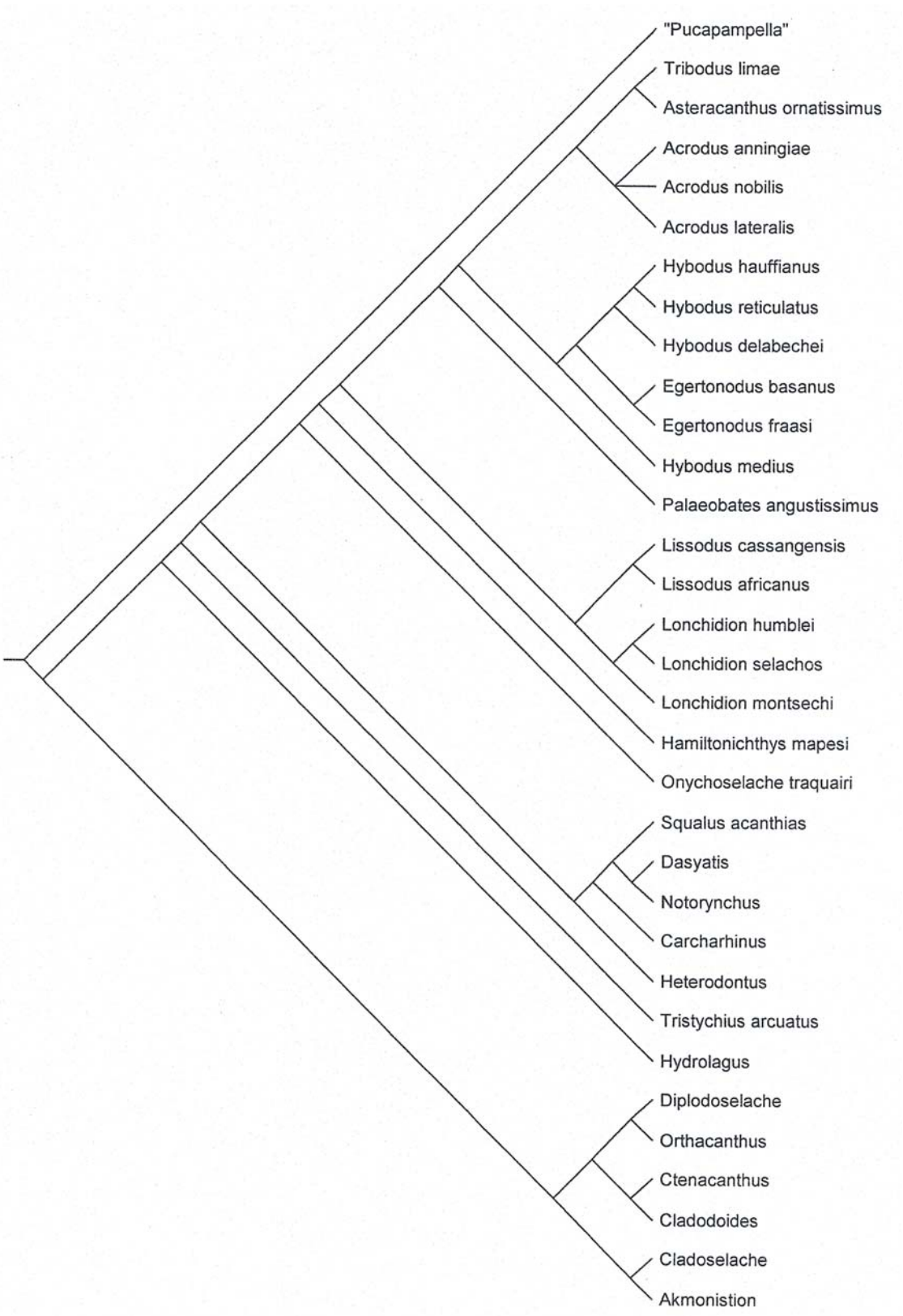

"Pucapampella"
Tribodus limae
Asteracanthus ornatissimus
Acrodus anningiae
Acrodus nobilis
Acrodus lateralis
Hybodus hauffianus
Hybodus reticulatus
Hybodus delabechei
Egertonodus basanus
Egertonodus fraasi
Hybodus medius
Palaeobates angustissimus
Lissodus cassangensis
Lissodus africanus
Lonchidion humblei
Lonchidion selachos
Lonchidion montsechi
Hamiltonichthys mapesi
Onychoselache traquairi
Squalus acanthias
Dasyatis
Notorynchus
Carcharhinus
Heterodontus
Tristychius arcuatus
Hydrolagus
Diplodoselache
Orthacanthus
Ctenacanthus
Cladodoides
Cladoselache
Akmonistion

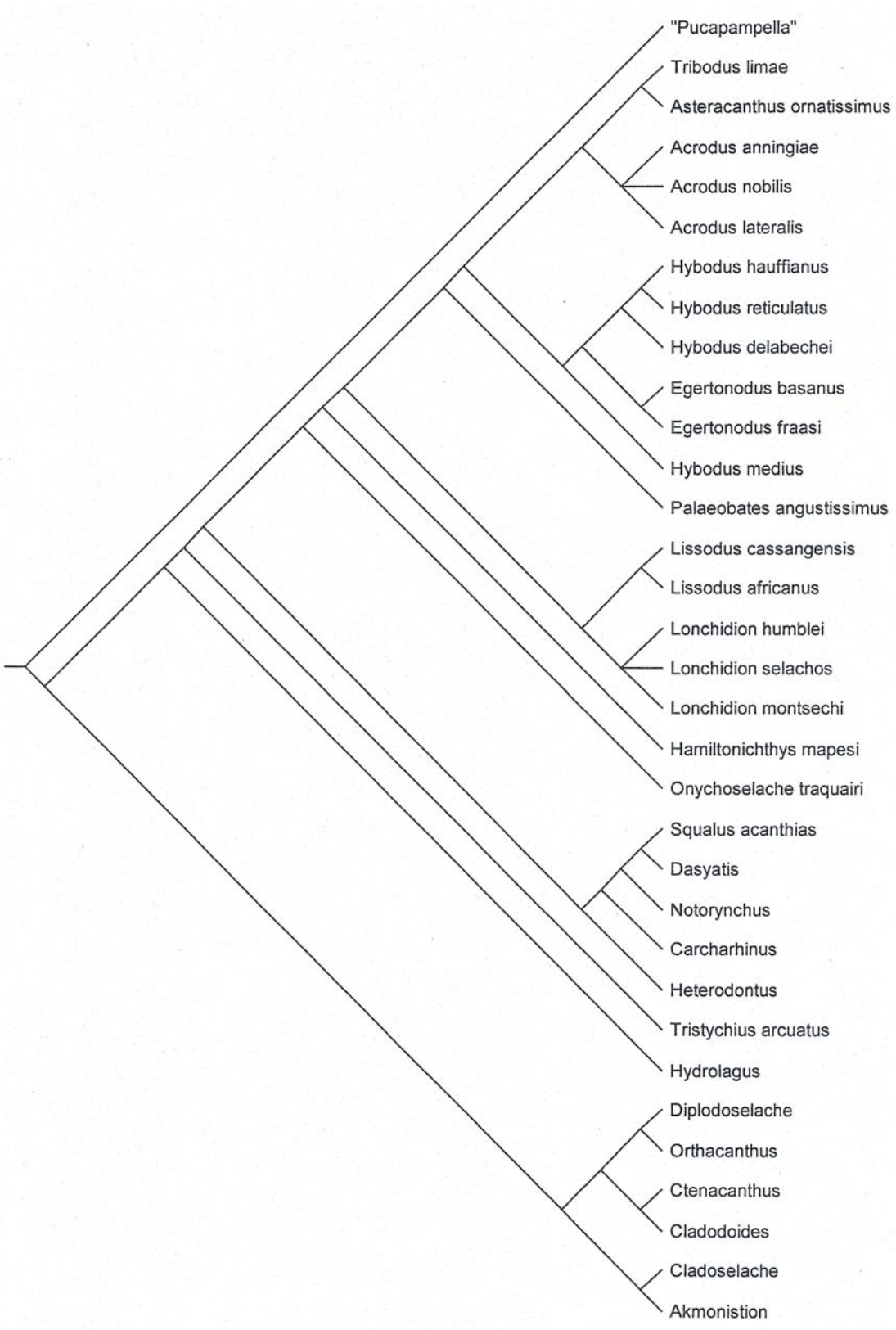

"Pucapampella"
Tribodus limae
Asteracanthus ornatissimus
Acrodus anningiae
Acrodus nobilis
Acrodus lateralis
Hybodus hauffianus
Hybodus reticulatus
Hybodus delabechei
Egertonodus basanus
Egertonodus fraasi
Hybodus medius
Palaeobates angustissimus
Lissodus cassangensis
Lissodus africanus
Lonchidion humblei
Lonchidion selachos
Lonchidion montsechi
Hamiltonichthys mapesi
Onychoselache traquairi
Squalus acanthias
Dasyatis
Notorynchus
Carcharhinus
Heterodontus
Tristychius arcuatus
Hydrolagus
Diplodoselache
Orthacanthus
Ctenacanthus
Cladodoides
Cladoselache
Akmonistion

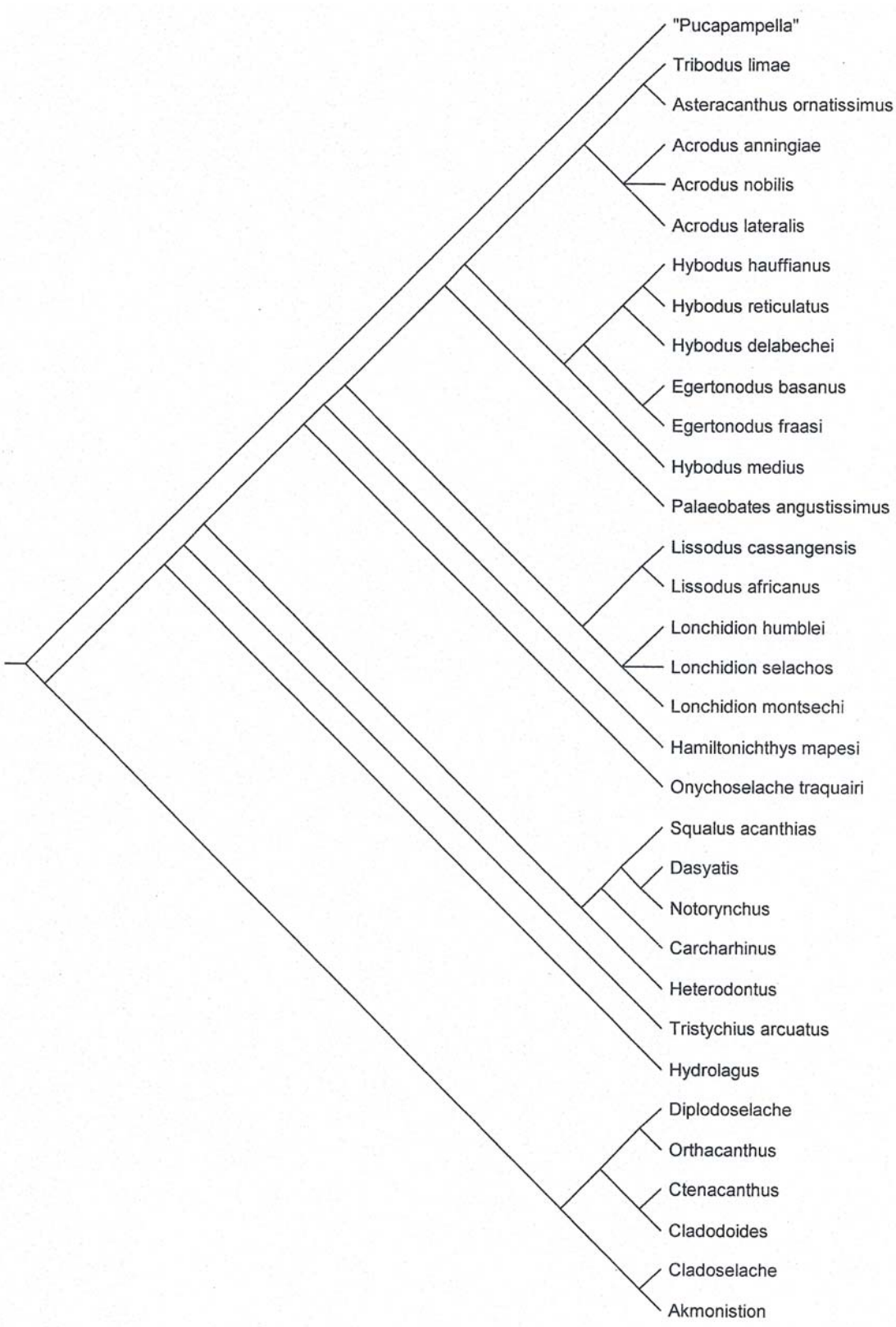

"Pucapampella"
Tribodus limae
Asteracanthus ornatissimus
Acrodus anningiae
Acrodus nobilis
Acrodus lateralis
Hybodus hauffianus
Hybodus reticulatus
Hybodus delabechei
Egertonodus basanus
Egertonodus fraasi
Hybodus medius
Palaeobates angustissimus
Lissodus cassangensis
Lissodus africanus
Lonchidion humblei
Lonchidion selachos
Lonchidion montsechi
Hamiltonichthys mapesi
Onychoselache traquairi
Squalus acanthias
Dasyatis
Notorynchus
Carcharhinus
Heterodontus
Tristychius arcuatus
Hydrolagus
Diplodoselache
Orthacanthus
Ctenacanthus
Cladodoides
Cladoselache
Akmonistion

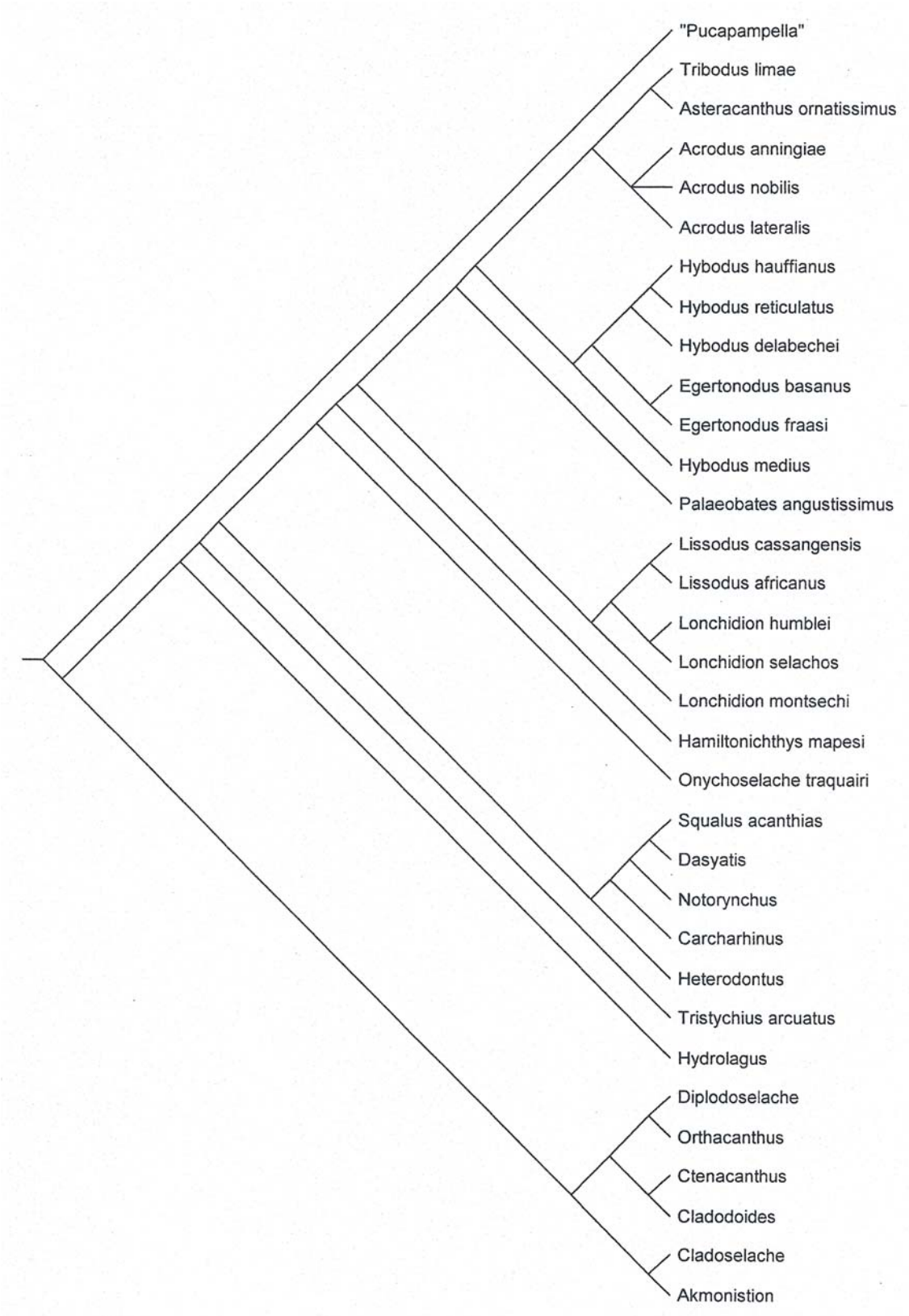

"Pucapampella"
Tribodus limae
Asteracanthus ornatissimus
Acrodus anningiae
Acrodus nobilis
Acrodus lateralis
Hybodus hauffianus
Hybodus reticulatus
Hybodus delabechei
Egertonodus basanus
Egertonodus fraasi
Hybodus medius
Palaeobates angustissimus
Lissodus cassangensis
Lissodus africanus
Lonchidion humblei
Lonchidion selachos
Lonchidion montsechi
Hamiltonichthys mapesi
Onychoselache traquairi
Squalus acanthias
Dasyatis
Notorynchus
Carcharhinus
Heterodontus
Tristychius arcuatus
Hydrolagus
Diplodoselache
Orthacanthus
Ctenacanthus
Cladodoides
Cladoselache
Akmonistion

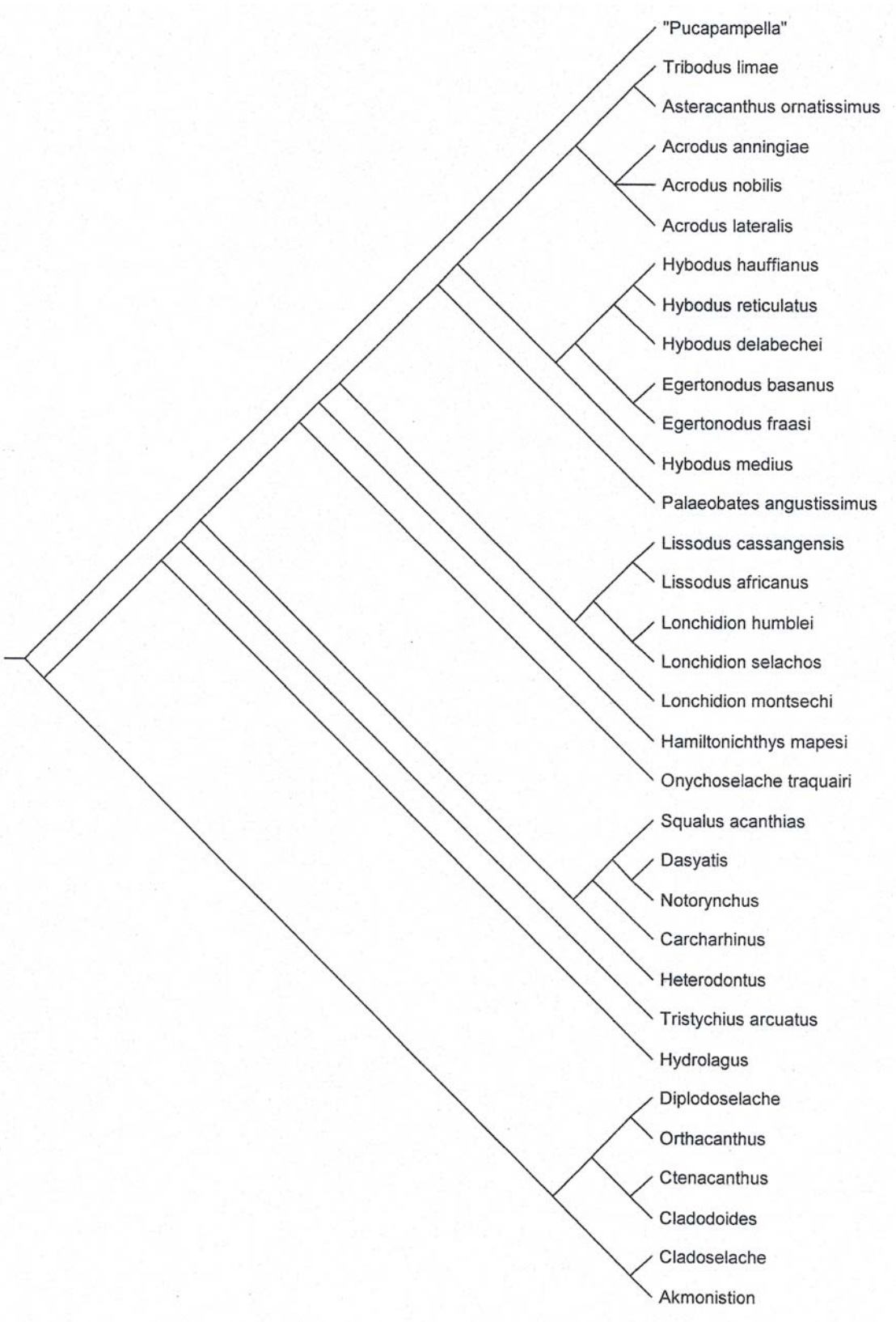

"Pucapampella"
Tribodus limae
Asteracanthus ornatissimus
Acrodus anningiae
Acrodus nobilis
Acrodus lateralis
Hybodus hauffianus
Hybodus reticulatus
Hybodus delabechei
Egertonodus basanus
Egertonodus fraasi
Hybodus medius
Palaeobates angustissimus
Lissodus cassangensis
Lissodus africanus
Lonchidion humblei
Lonchidion selachos
Lonchidion montsechi
Hamiltonichthys mapesi
Onychoselache traquairi
Squalus acanthias
Dasyatis
Notorynchus
Carcharhinus
Heterodontus
Tristychius arcuatus
Hydrolagus
Diplodoselache
Orthacanthus
Ctenacanthus
Cladodoides
Cladoselache
Akmonistion

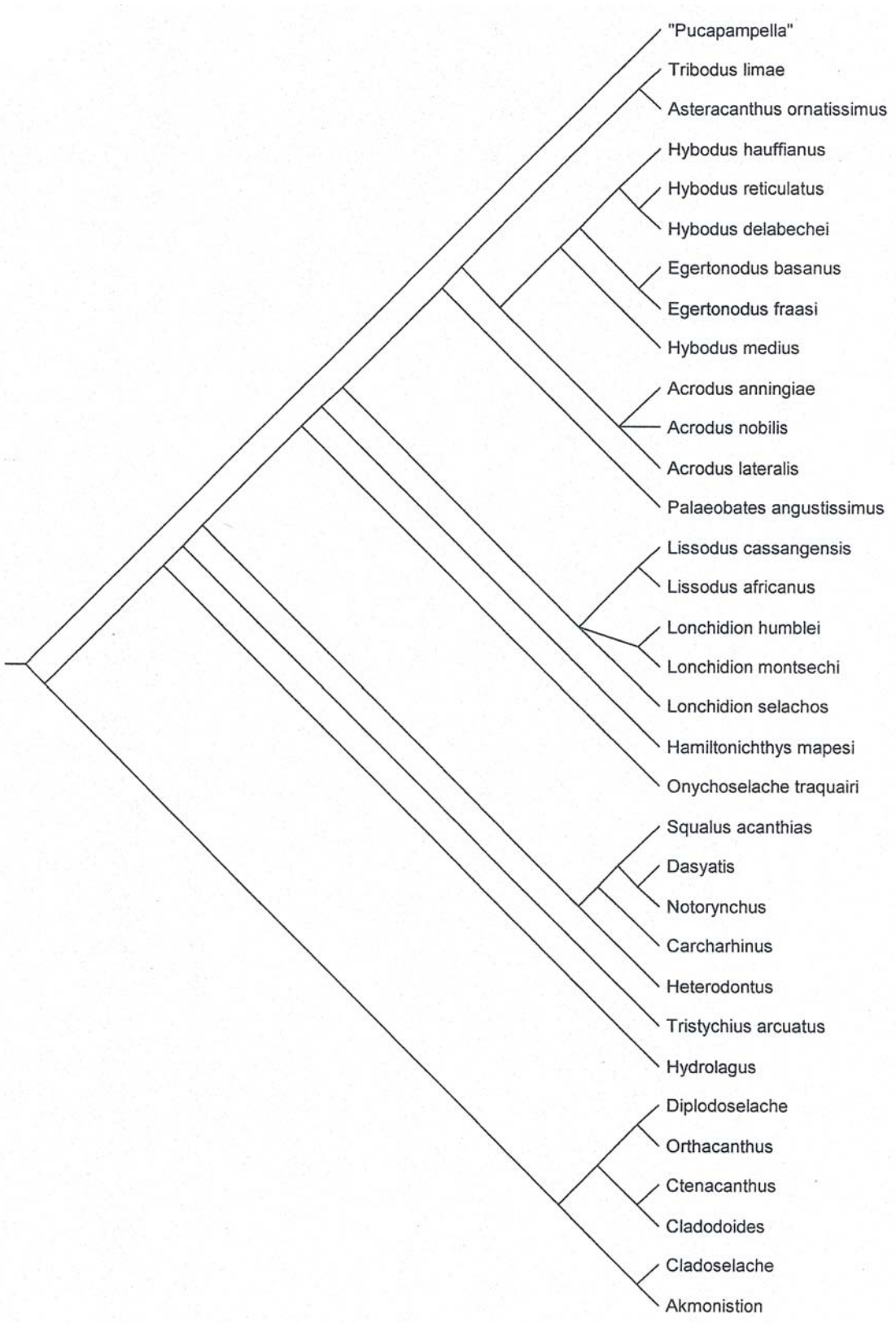

"Pucapampella"
Tribodus limae
Asteracanthus ornatissimus
Acrodus anningiae
Acrodus nobilis
Acrodus lateralis
Hybodus hauffianus
Hybodus reticulatus
Hybodus delabechei
Egertonodus basanus
Egertonodus fraasi
Hybodus medius
Palaeobates angustissimus
Lissodus cassangensis
Lissodus africanus
Lonchidion humblei
Lonchidion selachos
Lonchidion montsechi
Hamiltonichthys mapesi
Onychoselache traquairi
Squalus acanthias
Dasyatis
Notorynchus
Carcharhinus
Heterodontus
Tristychius arcuatus
Hydrolagus
Diplodoselache
Orthacanthus
Ctenacanthus
Cladodoides
Cladoselache
Akmonistion

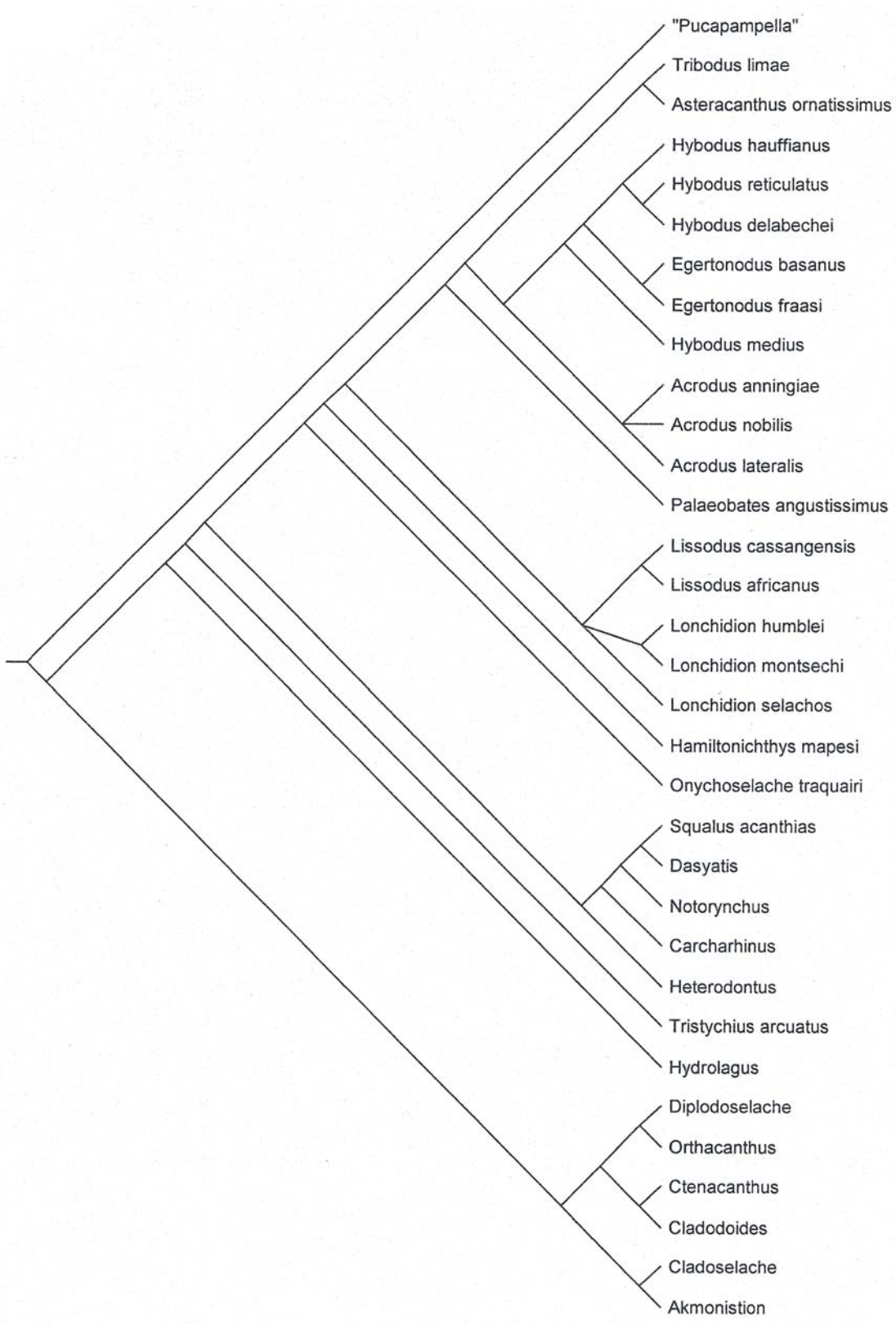

"Pucapampella"
Tribodus limae
Asteracanthus ornatissimus
Acrodus anningiae
Acrodus nobilis
Acrodus lateralis
Hybodus hauffianus
Hybodus reticulatus
Hybodus delabechei
Egertonodus basanus
Egertonodus fraasi
Hybodus medius
Palaeobates angustissimus
Lissodus cassangensis
Lissodus africanus
Lonchidion humblei
Lonchidion selachos
Lonchidion montsechi
Hamiltonichthys mapesi
Onychoselache traquairi
Squalus acanthias
Dasyatis
Notorynchus
Carcharhinus
Heterodontus
Tristychius arcuatus
Hydrolagus
Diplodoselache
Orthacanthus
Ctenacanthus
Cladodoides
Cladoselache
Akmonistion

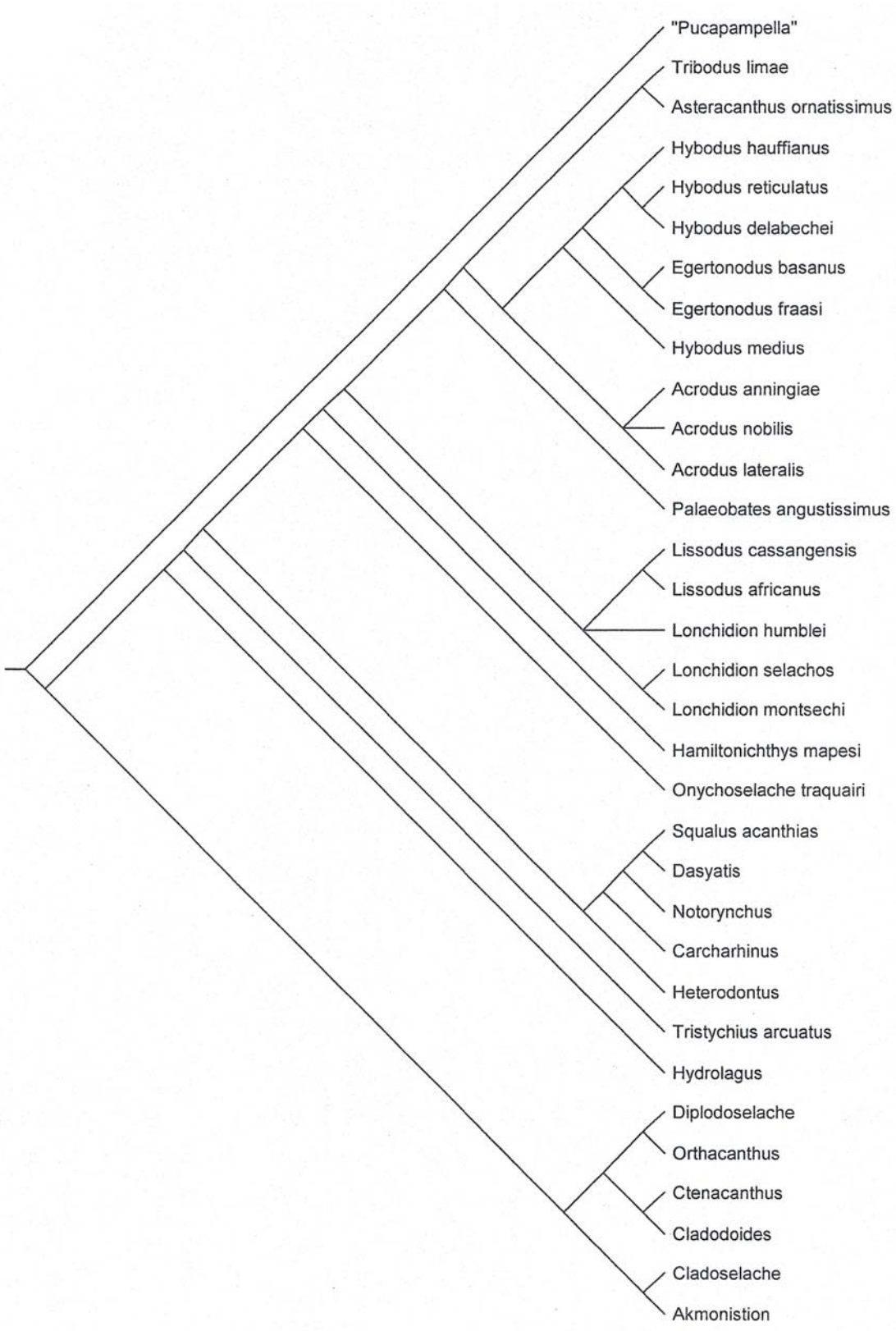

"Pucapampella"
Tribodus limae
Asteracanthus ornatissimus
Acrodus anningiae
Acrodus nobilis
Acrodus lateralis
Hybodus hauffianus
Hybodus reticulatus
Hybodus delabechei
Egertonodus basanus
Egertonodus fraasi
Hybodus medius
Palaeobates angustissimus
Lissodus cassangensis
Lissodus africanus
Lonchidion humblei
Lonchidion selachos
Lonchidion montsechi
Hamiltonichthys mapesi
Onychoselache traquairi
Squalus acanthias
Dasyatis
Notorynchus
Carcharhinus
Heterodontus
Tristychius arcuatus
Hydrolagus
Diplodoselache
Orthacanthus
Ctenacanthus
Cladodoides
Cladoselache
Akmonistion

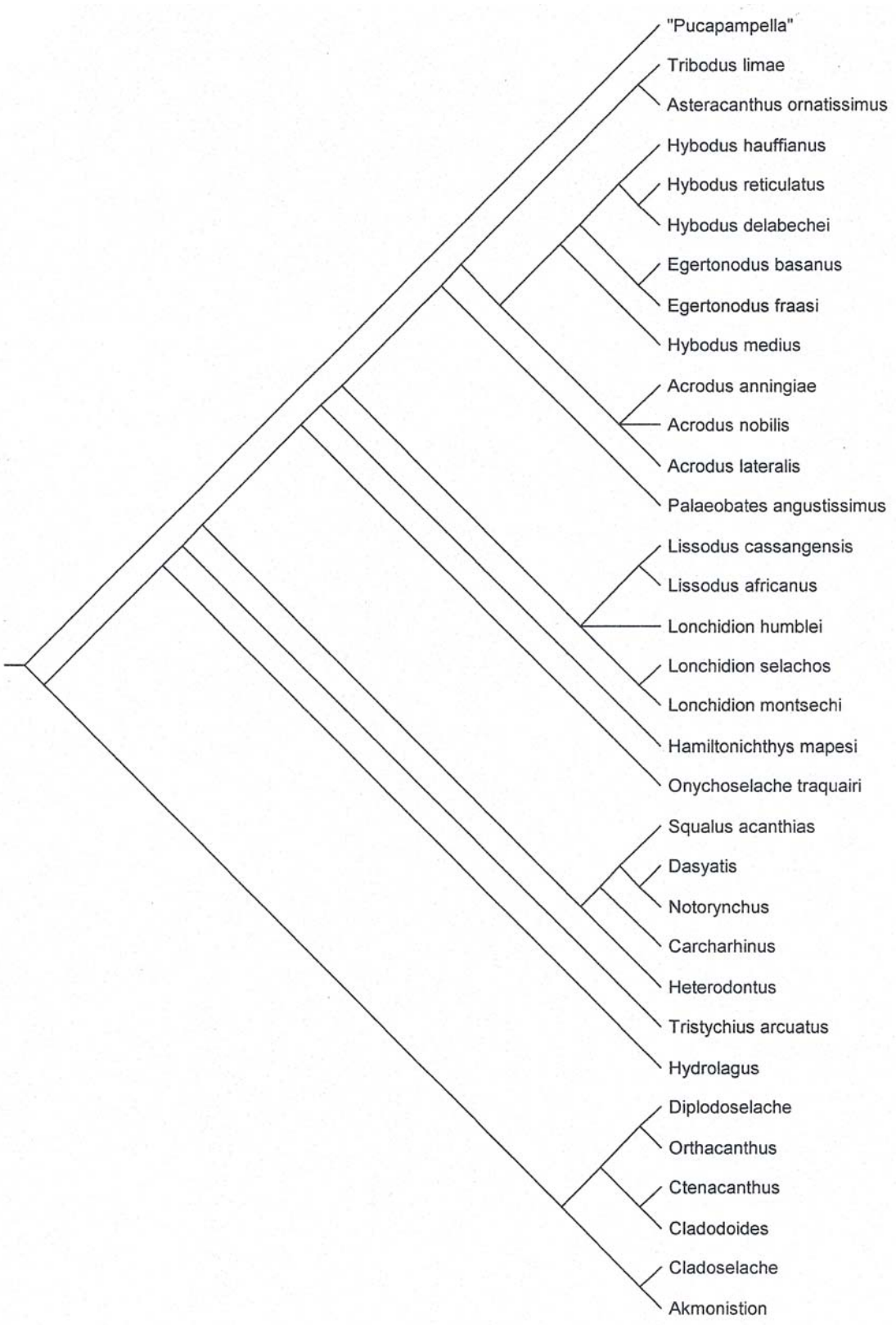

"Pucapampella"
Tribodus limae
Asteracanthus ornatissimus
Acrodus anningiae
Acrodus nobilis
Acrodus lateralis
Hybodus hauffianus
Hybodus reticulatus
Hybodus delabechei
Egertonodus basanus
Egertonodus fraasi
Hybodus medius
Palaeobates angustissimus
Lissodus cassangensis
Lissodus africanus
Lonchidion humblei
Lonchidion selachos
Lonchidion montsechi
Hamiltonichthys mapesi
Onychoselache traquairi
Squalus acanthias
Dasyatis
Notorynchus
Carcharhinus
Heterodontus
Tristychius arcuatus
Hydrolagus
Diplodoselache
Orthacanthus
Ctenacanthus
Cladodoides
Cladoselache
Akmonistion

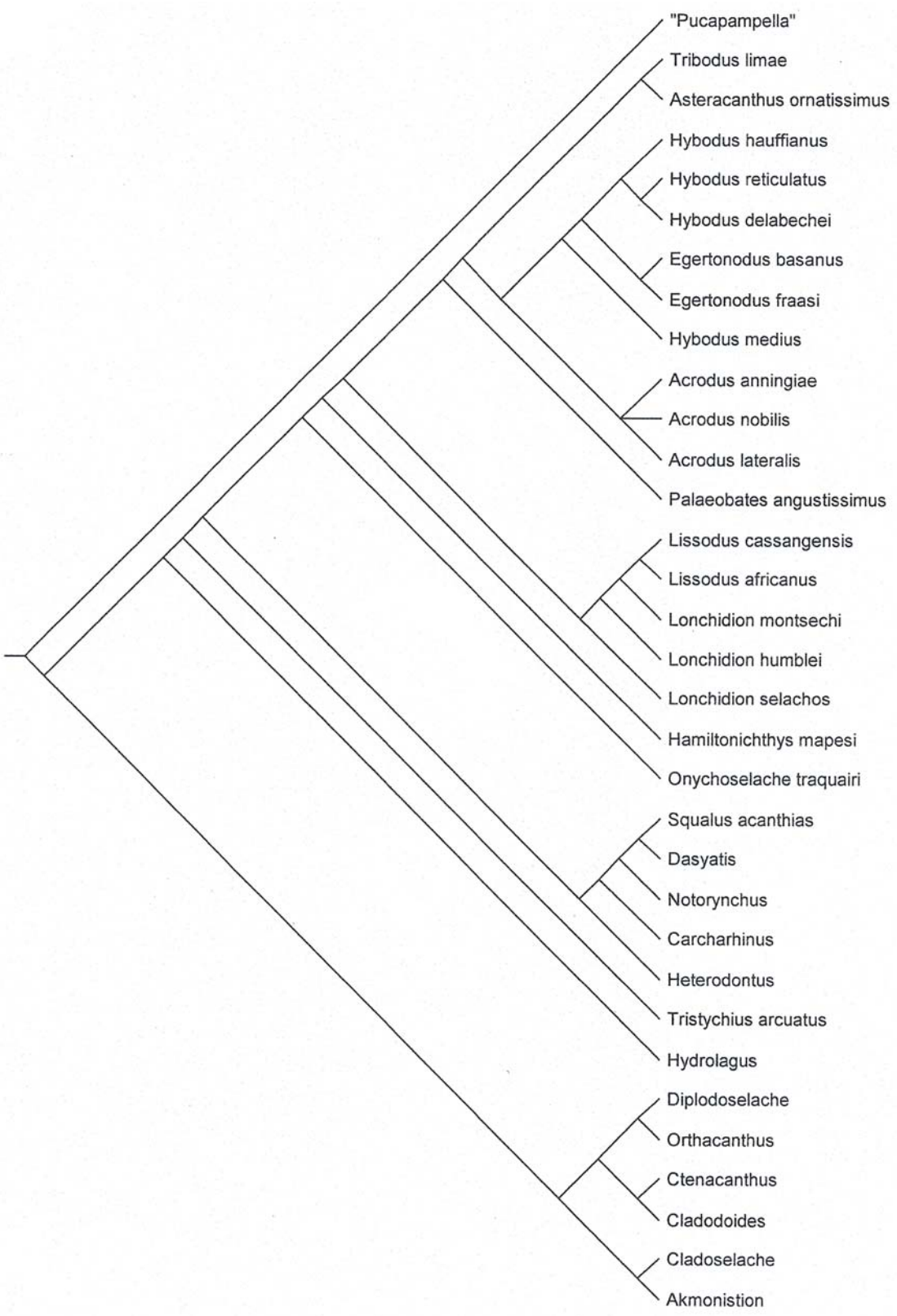

"Pucapampella"
Tribodus limae
Asteracanthus ornatissimus
Acrodus anningiae
Acrodus nobilis
Acrodus lateralis
Hybodus hauffianus
Hybodus reticulatus
Hybodus delabechei
Egertonodus basanus
Egertonodus fraasi
Hybodus medius
Palaeobates angustissimus
Lissodus cassangensis
Lissodus africanus
Lonchidion humblei
Lonchidion selachos
Lonchidion montsechi
Hamiltonichthys mapesi
Onychoselache traquairi
Squalus acanthias
Dasyatis
Notorynchus
Carcharhinus
Heterodontus
Tristychius arcuatus
Hydrolagus
Diplodoselache
Orthacanthus
Ctenacanthus
Cladodoides
Cladoselache
Akmonistion

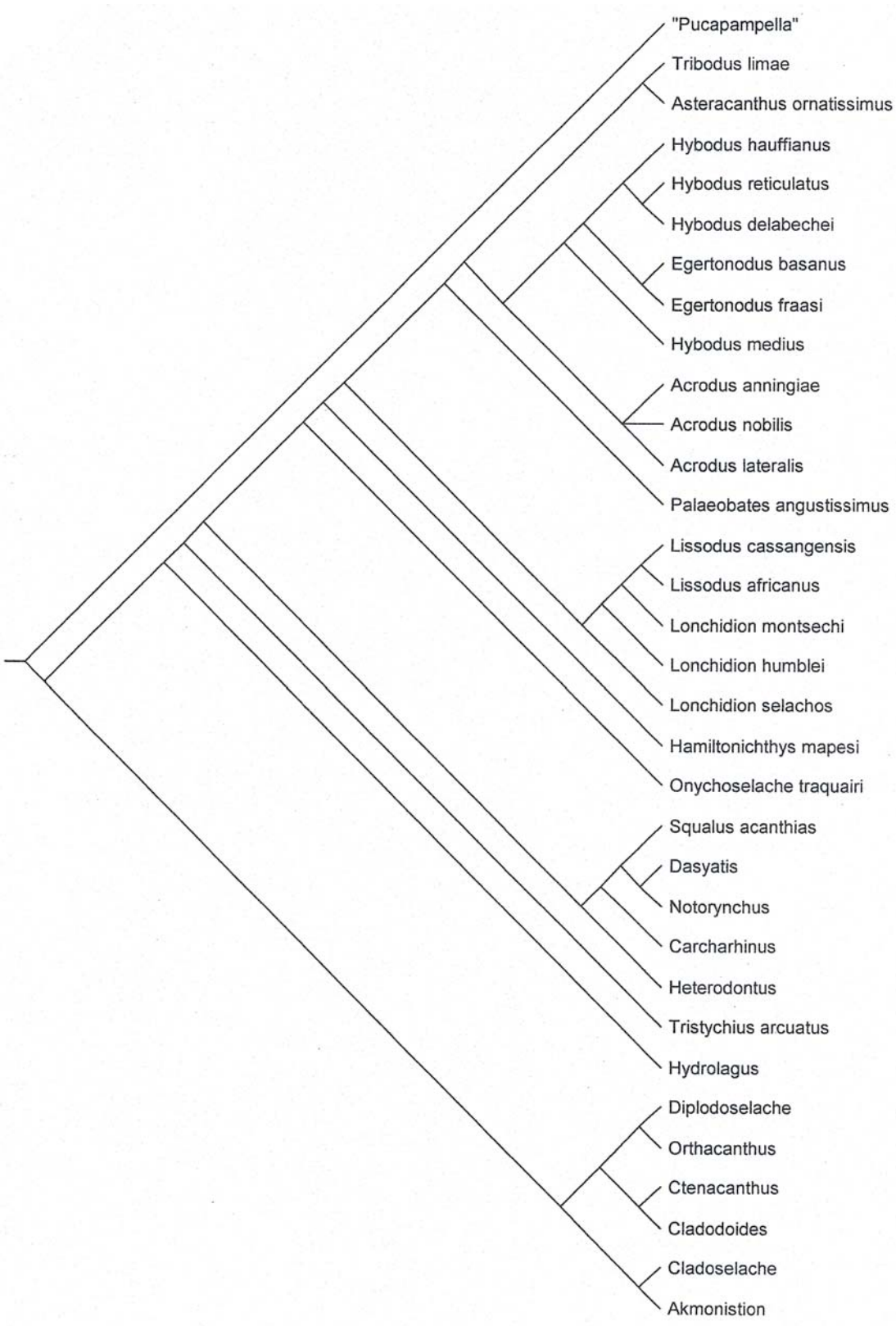

"Pucapampella"
Tribodus limae
Asteracanthus ornatissimus
Hybodus hauffianus
Hybodus reticulatus
Hybodus delabechei
Egertonodus basanus
Egertonodus fraasi
Hybodus medius
Acrodus anningiae
Acrodus nobilis
Acrodus lateralis
Palaeobates angustissimus
Lissodus cassangensis
Lissodus africanus
Lonchidion humblei
Lonchidion montsechi
Lonchidion selachos
Hamiltonichthys mapesi
Onychoselache traquairi
Squalus acanthias
Dasyatis
Notorynchus
Carcharhinus
Heterodontus
Tristychius arcuatus
Hydrolagus
Diplodoselache
Orthacanthus
Ctenacanthus
Cladodoides
Cladoselache
Akmonistion

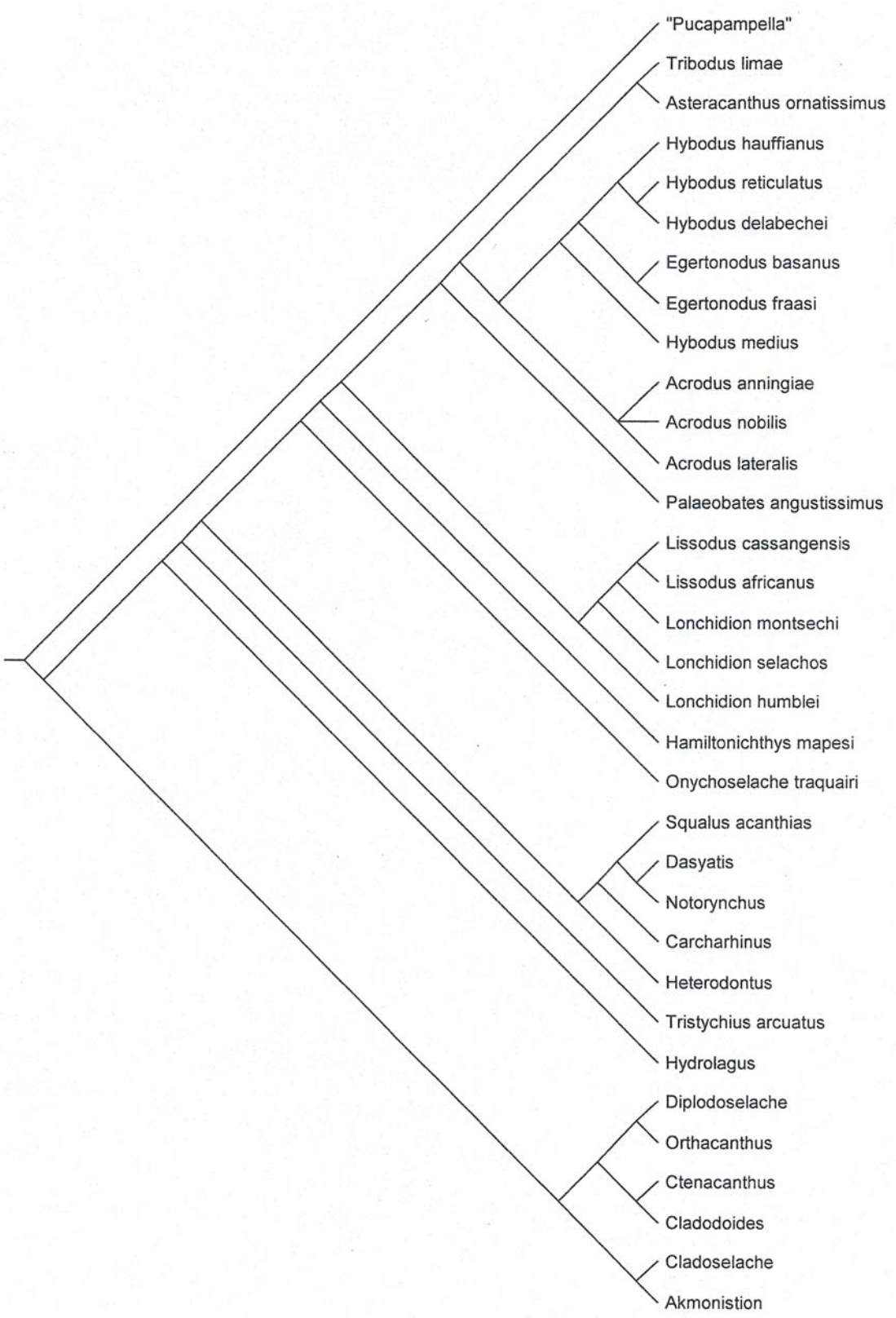

"Pucapampella"
Tribodus limae
Asteracanthus ornatissimus
Hybodus hauffianus
Hybodus reticulatus
Hybodus delabechei
Egertonodus basanus
Egertonodus fraasi
Hybodus medius
Acrodus anningiae
Acrodus nobilis
Acrodus lateralis
Palaeobates angustissimus
Lissodus cassangensis
Lissodus africanus
Lonchidion humblei
Lonchidion montsechi
Lonchidion selachos
Hamiltonichthys mapesi
Onychoselache traquairi
Squalus acanthias
Dasyatis
Notorynchus
Carcharhinus
Heterodontus
Tristychius arcuatus
Hydrolagus
Diplodoselache
Orthacanthus
Ctenacanthus
Cladodoides
Cladoselache
Akmonistion

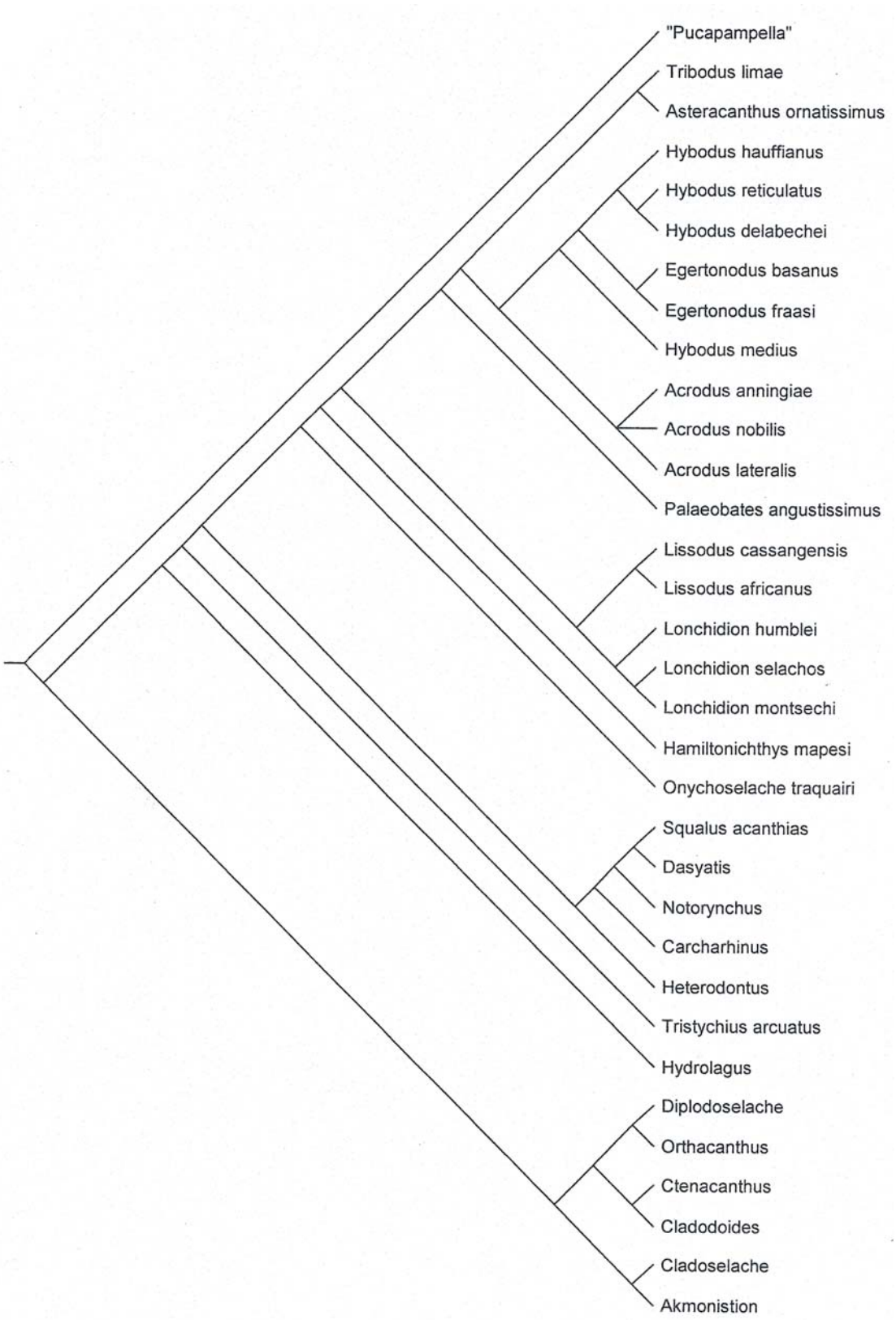

"Pucapampella"
Tribodus limae
Asteracanthus ornatissimus
Hybodus hauffianus
Hybodus reticulatus
Hybodus delabechei
Egertonodus basanus
Egertonodus fraasi
Hybodus medius
Acrodus anningiae
Acrodus nobilis
Acrodus lateralis
Palaeobates angustissimus
Lissodus cassangensis
Lissodus africanus
Lonchidion humblei
Lonchidion selachos
Lonchidion montsechi
Hamiltonichthys mapesi
Onychoselache traquairi
Squalus acanthias
Dasyatis
Notorynchus
Carcharhinus
Heterodontus
Tristychius arcuatus
Hydrolagus
Diplodoselache
Orthacanthus
Ctenacanthus
Cladodoides
Cladoselache
Akmonistion

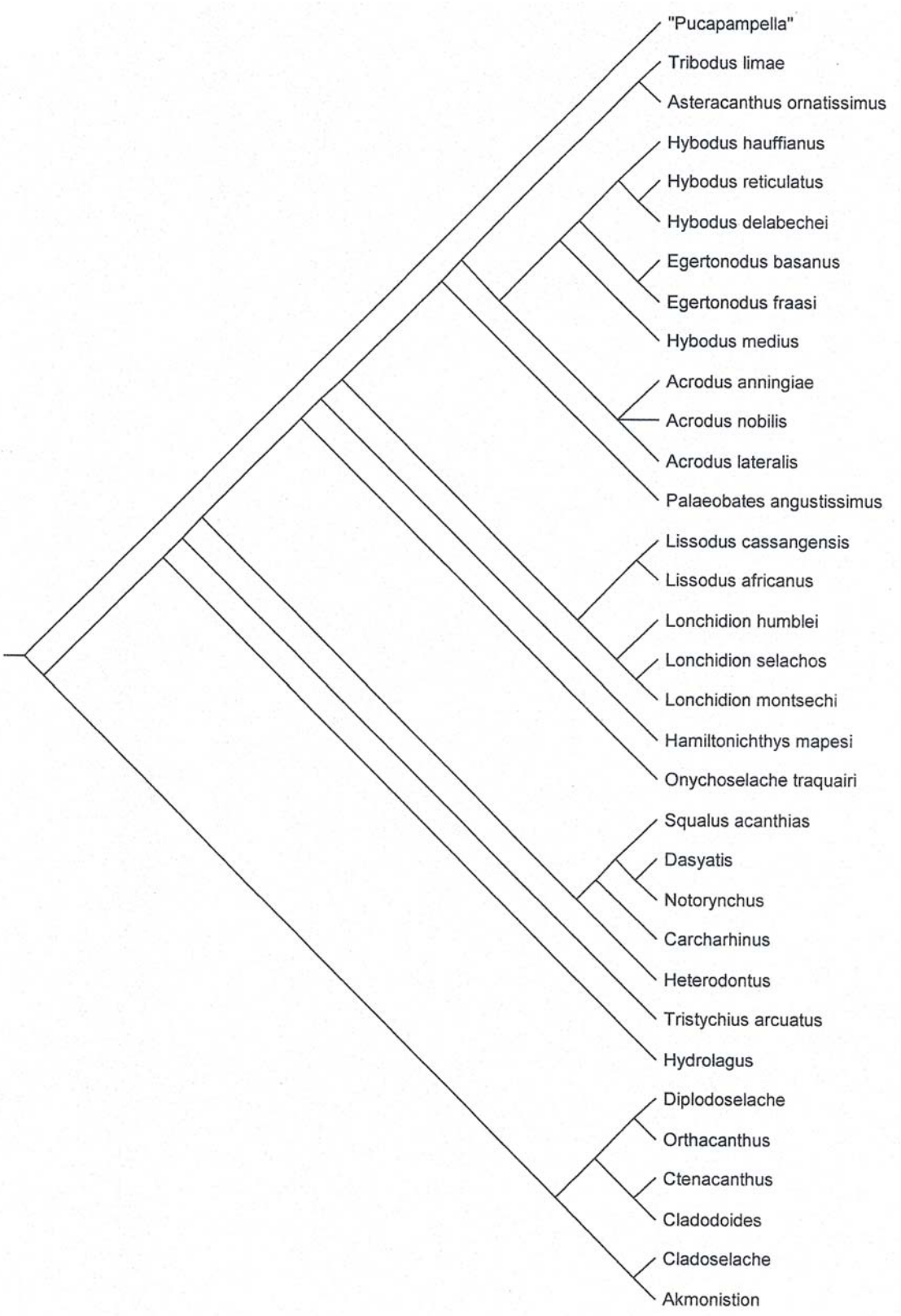

"Pucapampella"
Tribodus limae
Asteracanthus ornatissimus
Hybodus hauffianus
Hybodus reticulatus
Hybodus delabechei
Egertonodus basanus
Egertonodus fraasi
Hybodus medius
Acrodus anningiae
Acrodus nobilis
Acrodus lateralis
Palaeobates angustissimus
Lissodus cassangensis
Lissodus africanus
Lonchidion humblei
Lonchidion selachos
Lonchidion montsechi
Hamiltonichthys mapesi
Onychoselache traquairi
Squalus acanthias
Dasyatis
Notorynchus
Carcharhinus
Heterodontus
Tristychius arcuatus
Hydrolagus
Diplodoselache
Orthacanthus
Ctenacanthus
Cladodoides
Cladoselache
Akmonistion

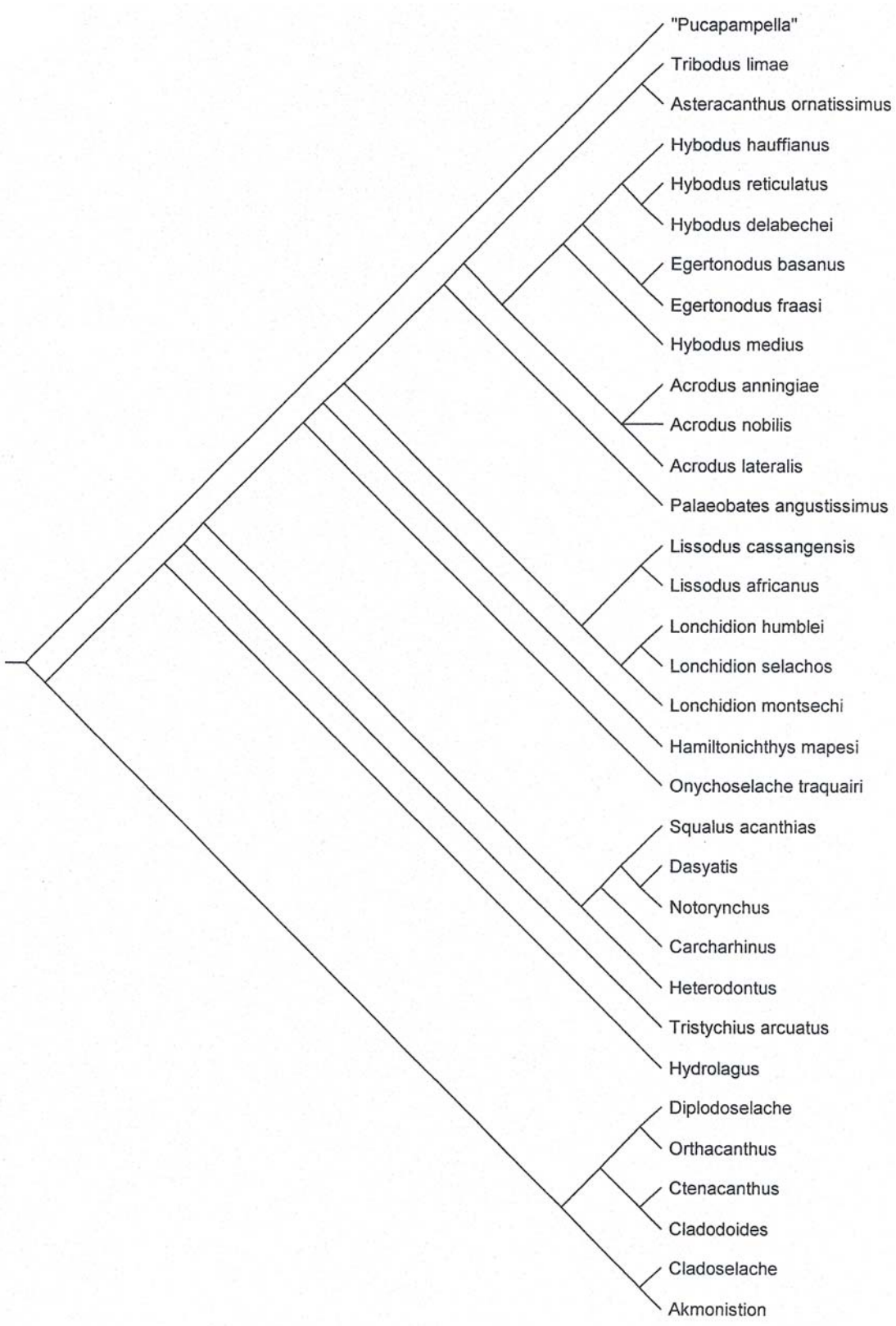

"Pucapampella"
Tribodus limae
Asteracanthus ornatissimus
Hybodus hauffianus
Hybodus reticulatus
Hybodus delabechei
Egertonodus basanus
Egertonodus fraasi
Hybodus medius
Acrodus anningiae
Acrodus nobilis
Acrodus lateralis
Palaeobates angustissimus
Lissodus cassangensis
Lissodus africanus
Lonchidion montsechi
Lonchidion humblei
Lonchidion selachos
Hamiltonichthys mapesi
Onychoselache traquairi
Squalus acanthias
Dasyatis
Notorynchus
Carcharhinus
Heterodontus
Tristychius arcuatus
Hydrolagus
Diplodoselache
Orthacanthus
Ctenacanthus
Cladodoides
Cladoselache
Akmonistion

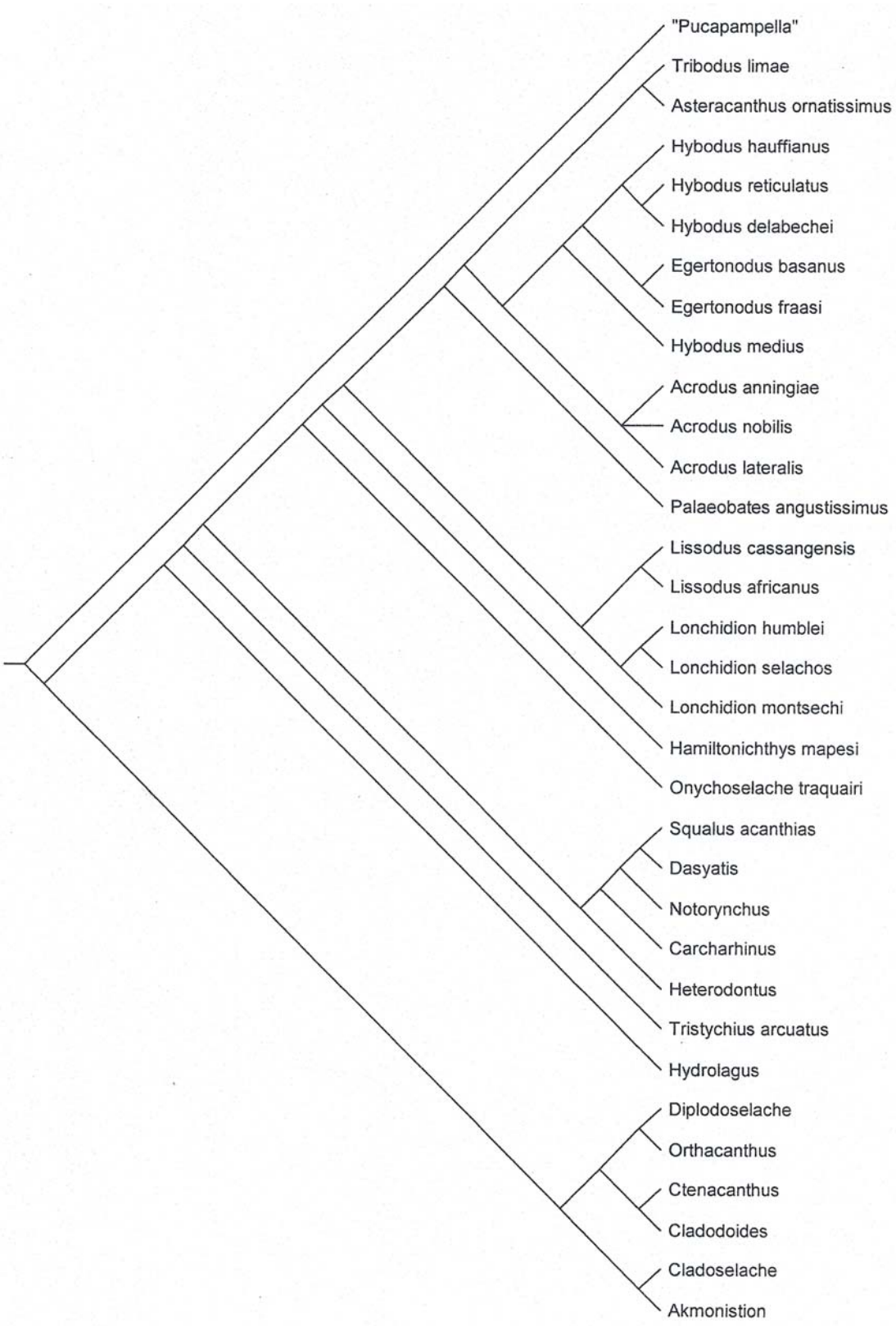

"Pucapampella"
Tribodus limae
Asteracanthus ornatissimus
Hybodus hauffianus
Hybodus reticulatus
Hybodus delabechei
Egertonodus basanus
Egertonodus fraasi
Hybodus medius
Acrodus anningiae
Acrodus nobilis
Acrodus lateralis
Palaeobates angustissimus
Lissodus cassangensis
Lissodus africanus
Lonchidion montsechi
Lonchidion humblei
Lonchidion selachos
Hamiltonichthys mapesi
Onychoselache traquairi
Squalus acanthias
Dasyatis
Notorynchus
Carcharhinus
Heterodontus
Tristychius arcuatus
Hydrolagus
Diplodoselache
Orthacanthus
Ctenacanthus
Cladodoides
Cladoselache
Akmonistion

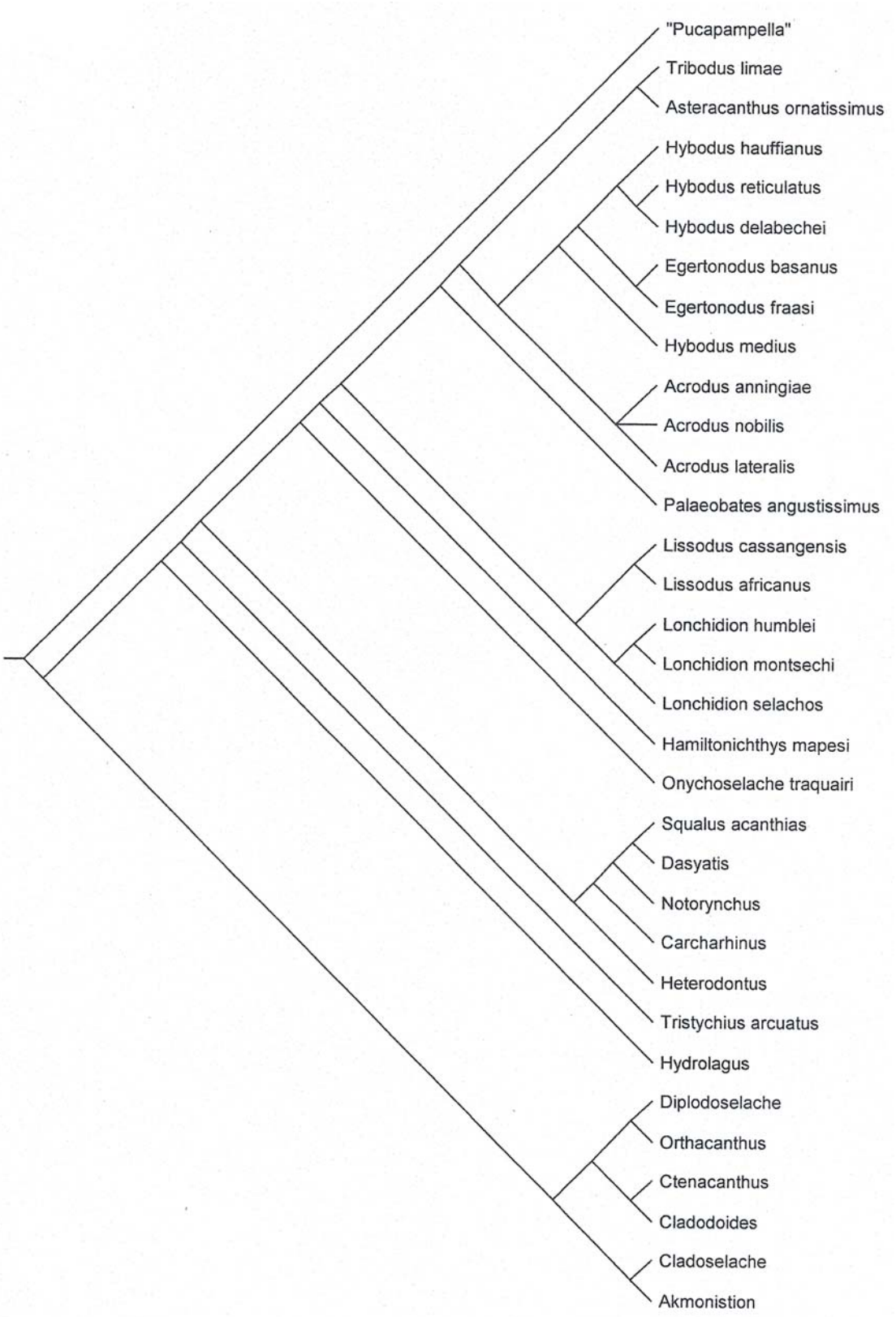

"Pucapampella"
Tribodus limae
Asteracanthus ornatissimus
Hybodus hauffianus
Hybodus reticulatus
Hybodus delabechei
Egertonodus basanus
Egertonodus fraasi
Hybodus medius
Acrodus anningiae
Acrodus nobilis
Acrodus lateralis
Palaeobates angustissimus
Lissodus cassangensis
Lissodus africanus
Lonchidion montsechi
Lonchidion selachos
Lonchidion humblei
Hamiltonichthys mapesi
Onychoselache traquairi
Squalus acanthias
Dasyatis
Notorynchus
Carcharhinus
Heterodontus
Tristychius arcuatus
Hydrolagus
Diplodoselache
Orthacanthus
Ctenacanthus
Cladodoides
Cladoselache
Akmonistion

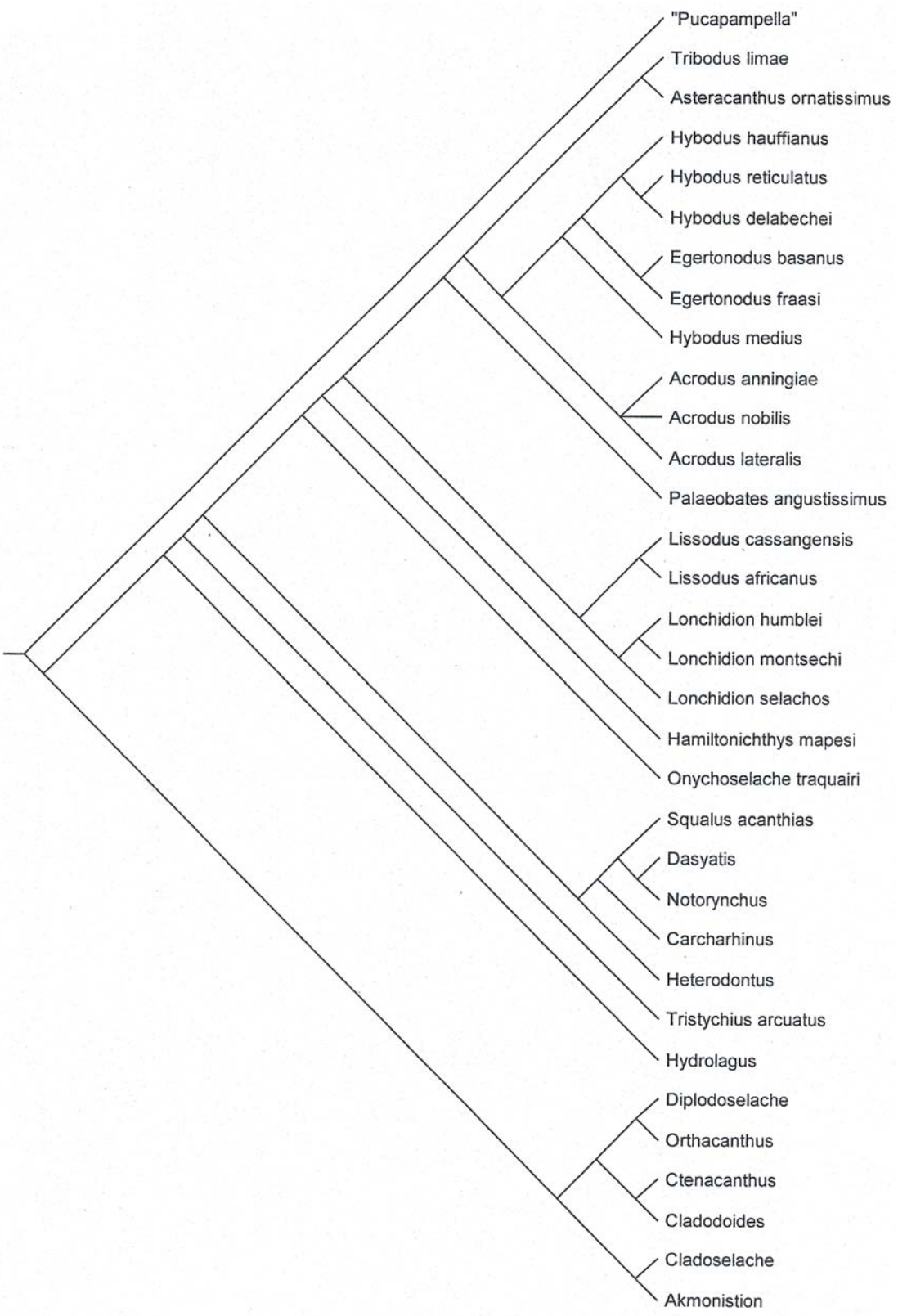

"Pucapampella"
Tribodus limae
Asteracanthus ornatissimus
Hybodus hauffianus
Hybodus reticulatus
Hybodus delabechei
Egertonodus basanus
Egertonodus fraasi
Hybodus medius
Acrodus anningiae
Acrodus nobilis
Acrodus lateralis
Palaeobates angustissimus
Lissodus cassangensis
Lissodus africanus
Lonchidion humblei
Lonchidion selachos
Lonchidion montsechi
Hamiltonichthys mapesi
Onychoselache traquairi
Squalus acanthias
Dasyatis
Notorynchus
Carcharhinus
Heterodontus
Tristychius arcuatus
Hydrolagus
Diplodoselache
Orthacanthus
Ctenacanthus
Cladodoides
Cladoselache
Akmonistion

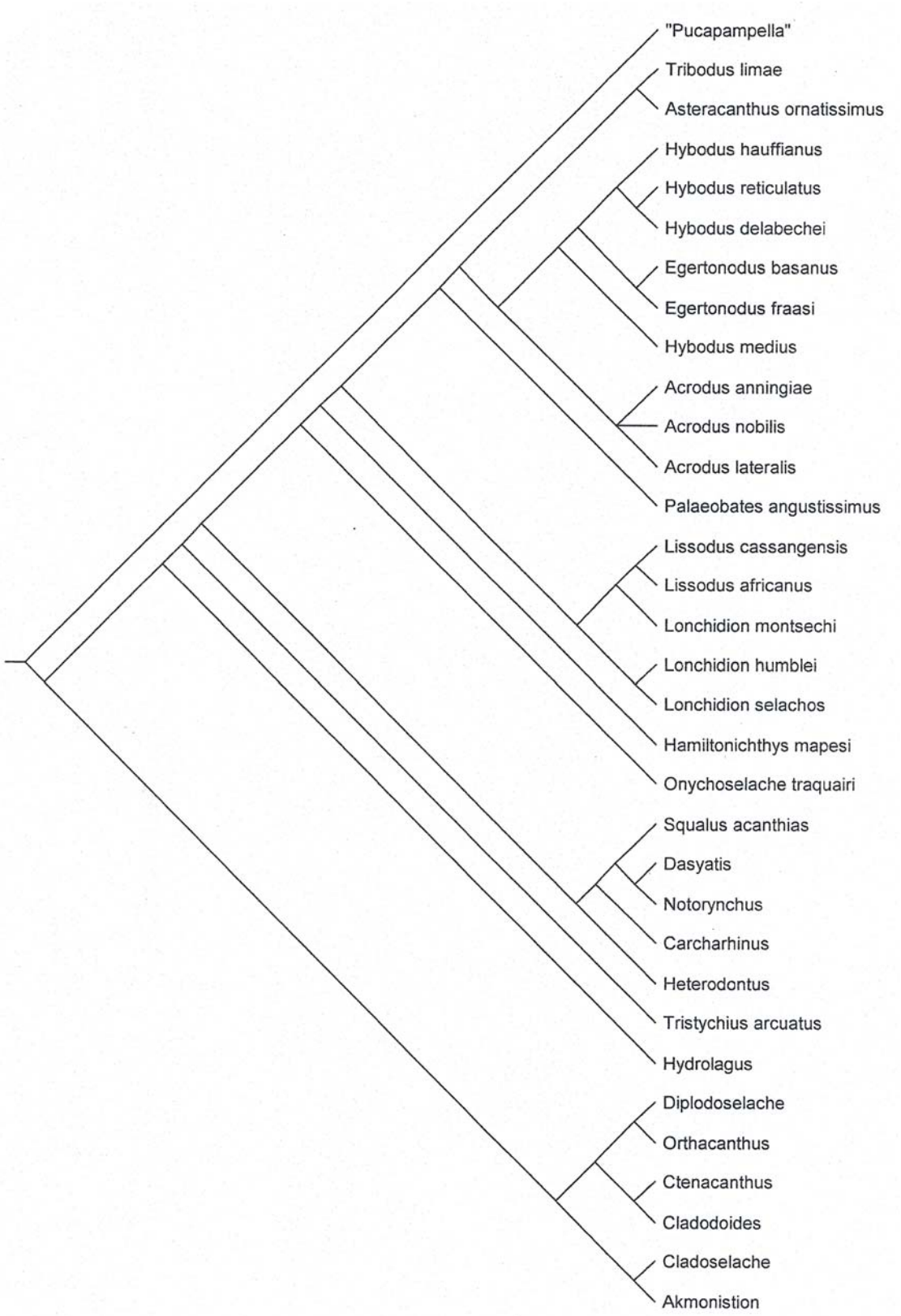

"Pucapampella"
Tribodus limae
Asteracanthus ornatissimus
Hybodus hauffianus
Hybodus reticulatus
Hybodus delabechei
Egertonodus basanus
Egertonodus fraasi
Hybodus medius
Acrodus anningiae
Acrodus nobilis
Acrodus lateralis
Palaeobates angustissimus
Lissodus cassangensis
Lissodus africanus
Lonchidion humblei
Lonchidion selachos
Lonchidion montsechi
Hamiltonichthys mapesi
Onychoselache traquairi
Squalus acanthias
Dasyatis
Notorynchus
Carcharhinus
Heterodontus
Tristychius arcuatus
Hydrolagus
Diplodoselache
Orthacanthus
Ctenacanthus
Cladodoides
Cladoselache
Akmonistion


"Pucapampella"
Tribodus limae
Asteracanthus ornatissimus
Hybodus hauffianus
Hybodus reticulatus
Hybodus delabechei
Egertonodus basanus
Egertonodus fraasi
Hybodus medius
Acrodus anningiae
Acrodus nobilis
Acrodus lateralis
Palaeobates angustissimus
Lissodus cassangensis
Lissodus africanus
Lonchidion humblei
Lonchidion selachos
Lonchidion montsechi
Hamiltonichthys mapesi
Onychoselache traquairi
Squalus acanthias
Dasyatis
Notorynchus
Carcharhinus
Heterodontus
Tristychius arcuatus
Hydrolagus
Diplodoselache
Orthacanthus
Ctenacanthus
Cladodoides
Cladoselache
Akmonistion

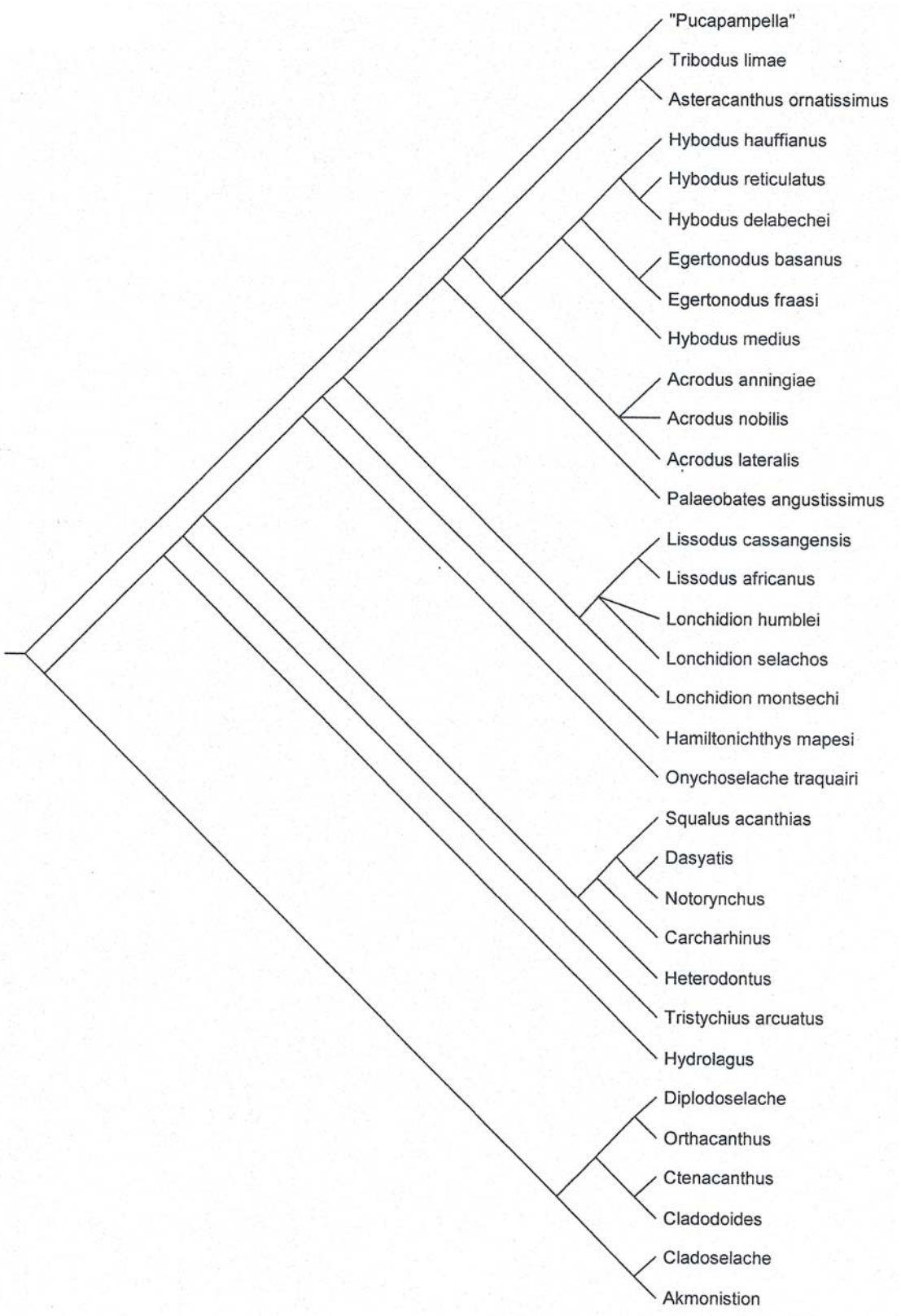

"Pucapampella"
Tribodus limae
Asteracanthus ornatissimus
Hybodus hauffianus
Hybodus reticulatus
Hybodus delabechei
Egertonodus basanus
Egertonodus fraasi
Hybodus medius
Acrodus anningiae
Acrodus nobilis
Acrodus lateralis
Palaeobates angustissimus
Lissodus cassangensis
Lissodus africanus
Lonchidion humblei
Lonchidion selachos
Lonchidion montsechi
Hamiltonichthys mapesi
Onychoselache traquairi
Squalus acanthias
Dasyatis
Notorynchus
Carcharhinus
Heterodontus
Tristychius arcuatus
Hydrolagus
Diplodoselache
Orthacanthus
Ctenacanthus
Cladodoides
Cladoselache
Akmonistion

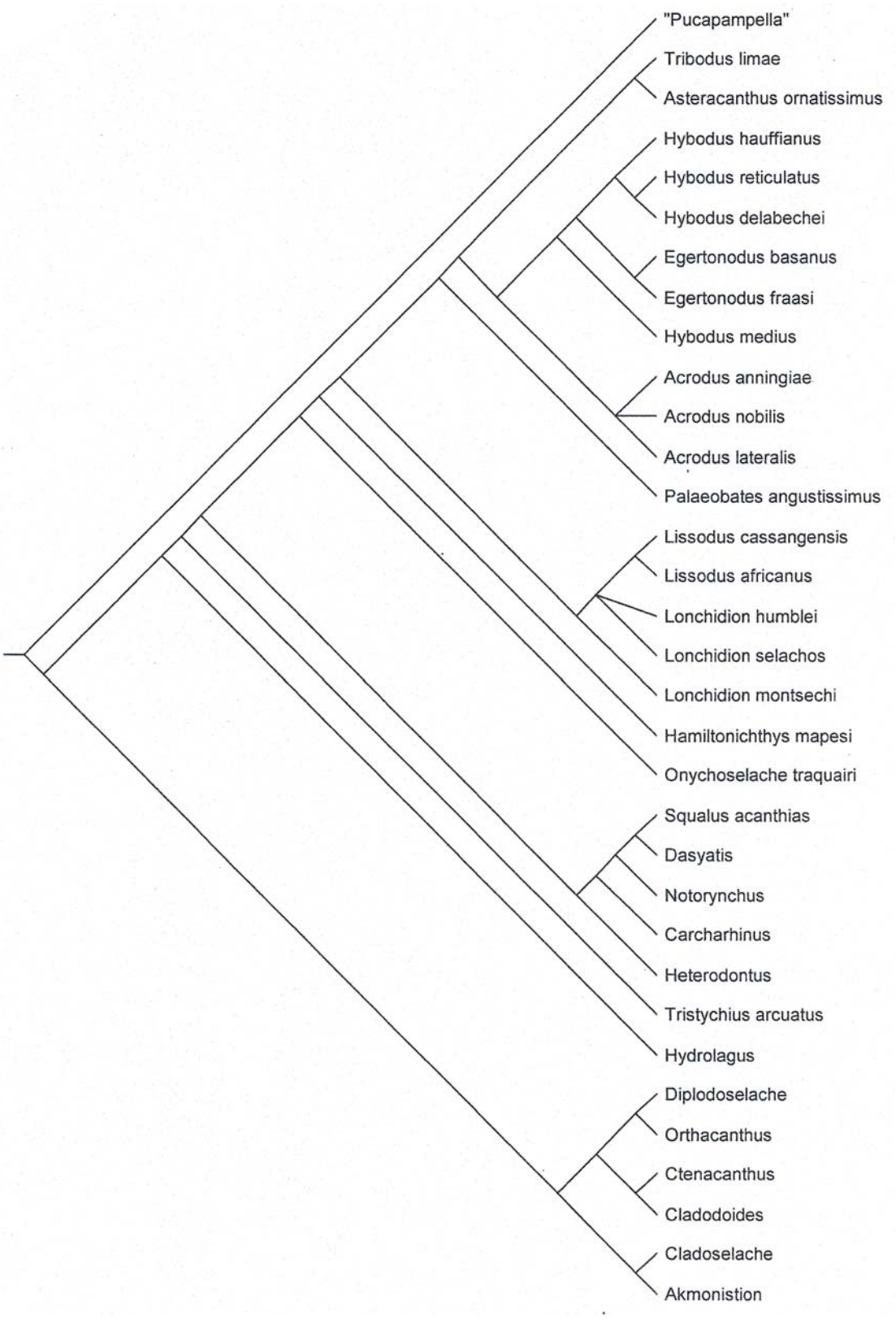

"Pucapampella"
Tribodus limae
Asteracanthus ornatissimus
Hybodus hauffianus
Hybodus reticulatus
Hybodus delabechei
Egertonodus basanus
Egertonodus fraasi
Hybodus medius
Acrodus anningiae
Acrodus nobilis
Acrodus lateralis
Palaeobates angustissimus
Lissodus cassangensis
Lissodus africanus
Lonchidion humblei
Lonchidion montsechi
Lonchidion selachos
Hamiltonichthys mapesi
Onychoselache traquairi
Squalus acanthias
Dasyatis
Notorynchus
Carcharhinus
Heterodontus
Tristychius arcuatus
Hydrolagus
Diplodoselache
Orthacanthus
Ctenacanthus
Cladodoides
Cladoselache
Akmonistion

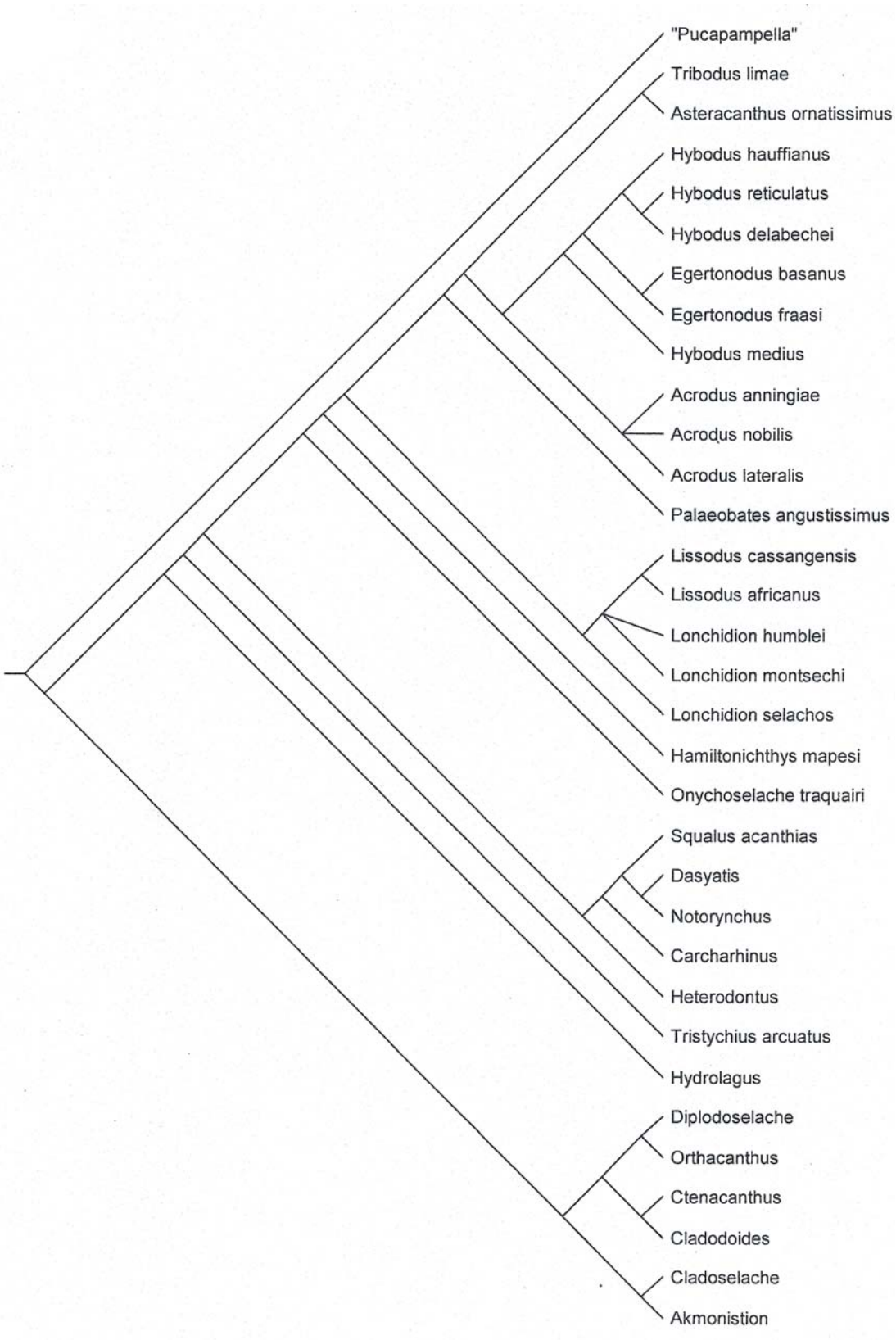

"Pucapampella"
Tribodus limae
Asteracanthus ornatissimus
Hybodus hauffianus
Hybodus reticulatus
Hybodus delabechei
Egertonodus basanus
Egertonodus fraasi
Hybodus medius
Acrodus anningiae
Acrodus nobilis
Acrodus lateralis
Palaeobates angustissimus
Lissodus cassangensis
Lissodus africanus
Lonchidion humblei
Lonchidion montsechi
Lonchidion selachos
Hamiltonichthys mapesi
Onychoselache traquairi
Squalus acanthias
Dasyatis
Notorynchus
Carcharhinus
Heterodontus
Tristychius arcuatus
Hydrolagus
Diplodoselache
Orthacanthus
Ctenacanthus
Cladodoides
Cladoselache
Akmonistion

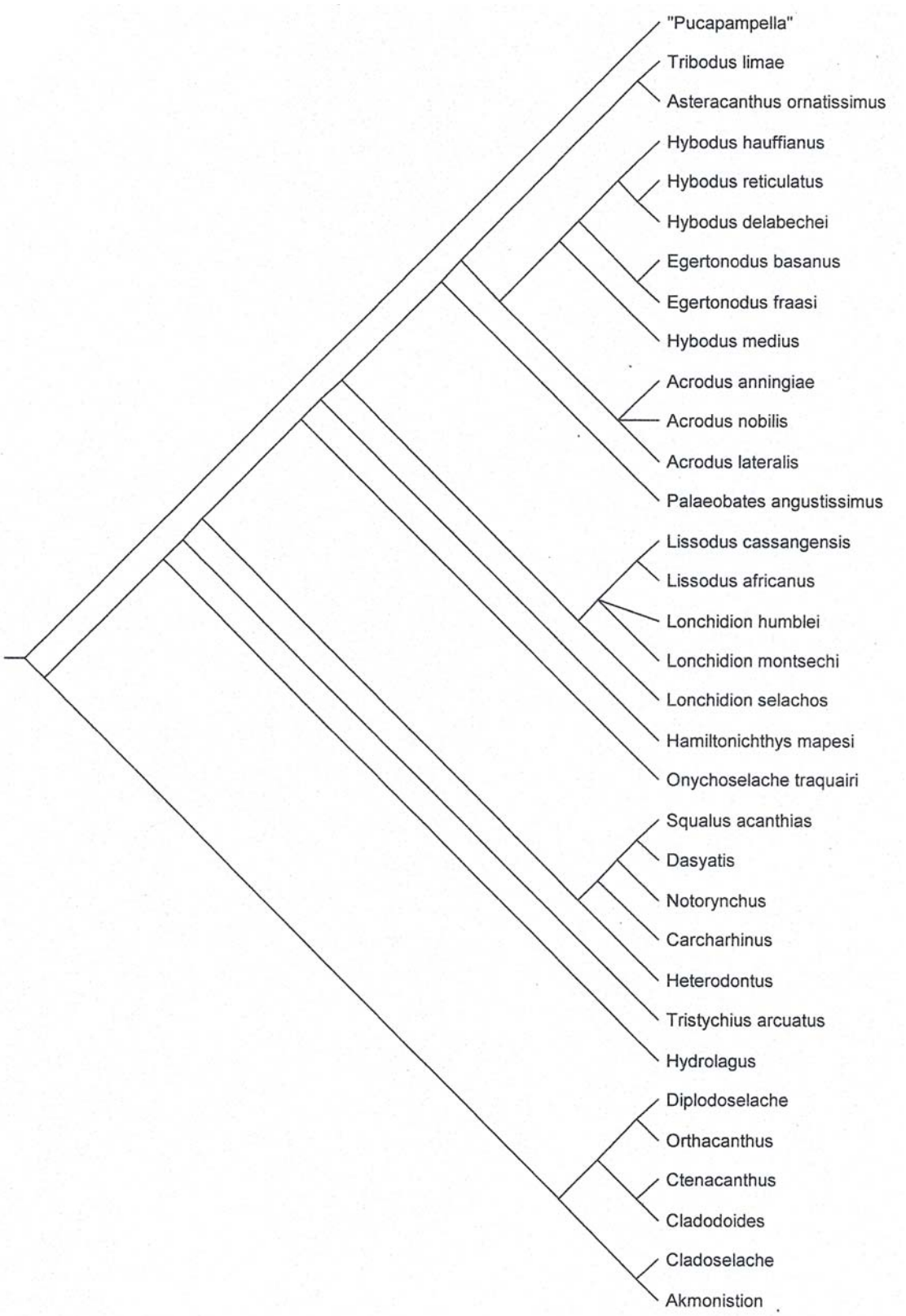

"Pucapampella"
Tribodus limae
Asteracanthus ornatissimus
Hybodus hauffianus
Hybodus reticulatus
Hybodus delabechei
Egertonodus basanus
Egertonodus fraasi
Hybodus medius
Acrodus anningiae
Acrodus nobilis
Acrodus lateralis
Palaeobates angustissimus
Lissodus cassangensis
Lissodus africanus
Lonchidion montsechi
Lonchidion humblei
Lonchidion selachos
Hamiltonichthys mapesi
Onychoselache traquairi
Squalus acanthias
Dasyatis
Notorynchus
Carcharhinus
Heterodontus
Tristychius arcuatus
Hydrolagus
Diplodoselache
Orthacanthus
Ctenacanthus
Cladodoides
Cladoselache
Akmonistion

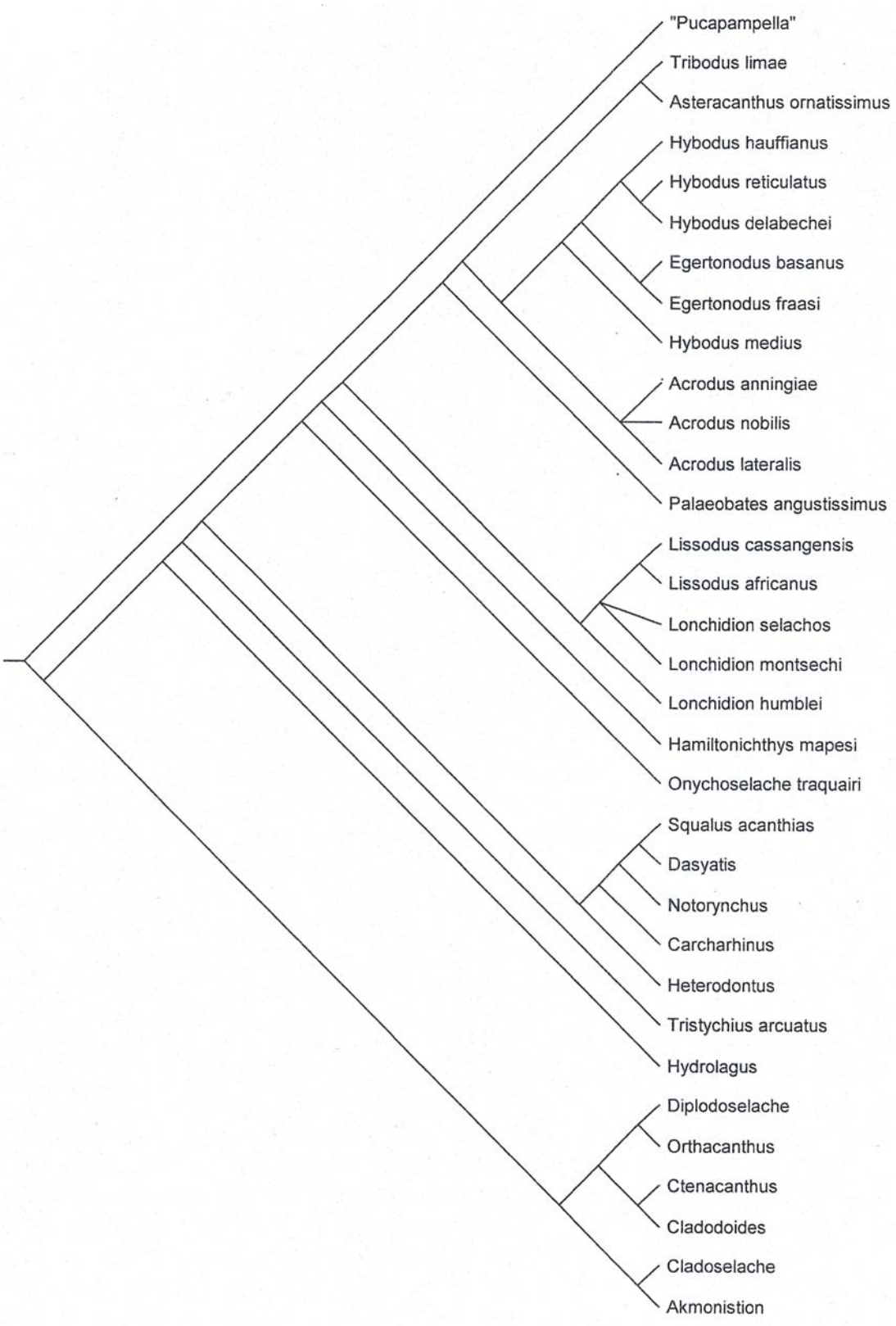

"Pucapampella"
Tribodus limae
Asteracanthus ornatissimus
Hybodus hauffianus
Hybodus reticulatus
Hybodus delabechei
Egertonodus basanus
Egertonodus fraasi
Hybodus medius
Acrodus anningiae
Acrodus nobilis
Acrodus lateralis
Palaeobates angustissimus
Lissodus cassangensis
Lissodus africanus
Lonchidion montsechi
Lonchidion humblei
Lonchidion selachos
Hamiltonichthys mapesi
Onychoselache traquairi
Squalus acanthias
Dasyatis
Notorynchus
Carcharhinus
Heterodontus
Tristychius arcuatus
Hydrolagus
Diplodoselache
Orthacanthus
Ctenacanthus
Cladodoides
Cladoselache
Akmonistion

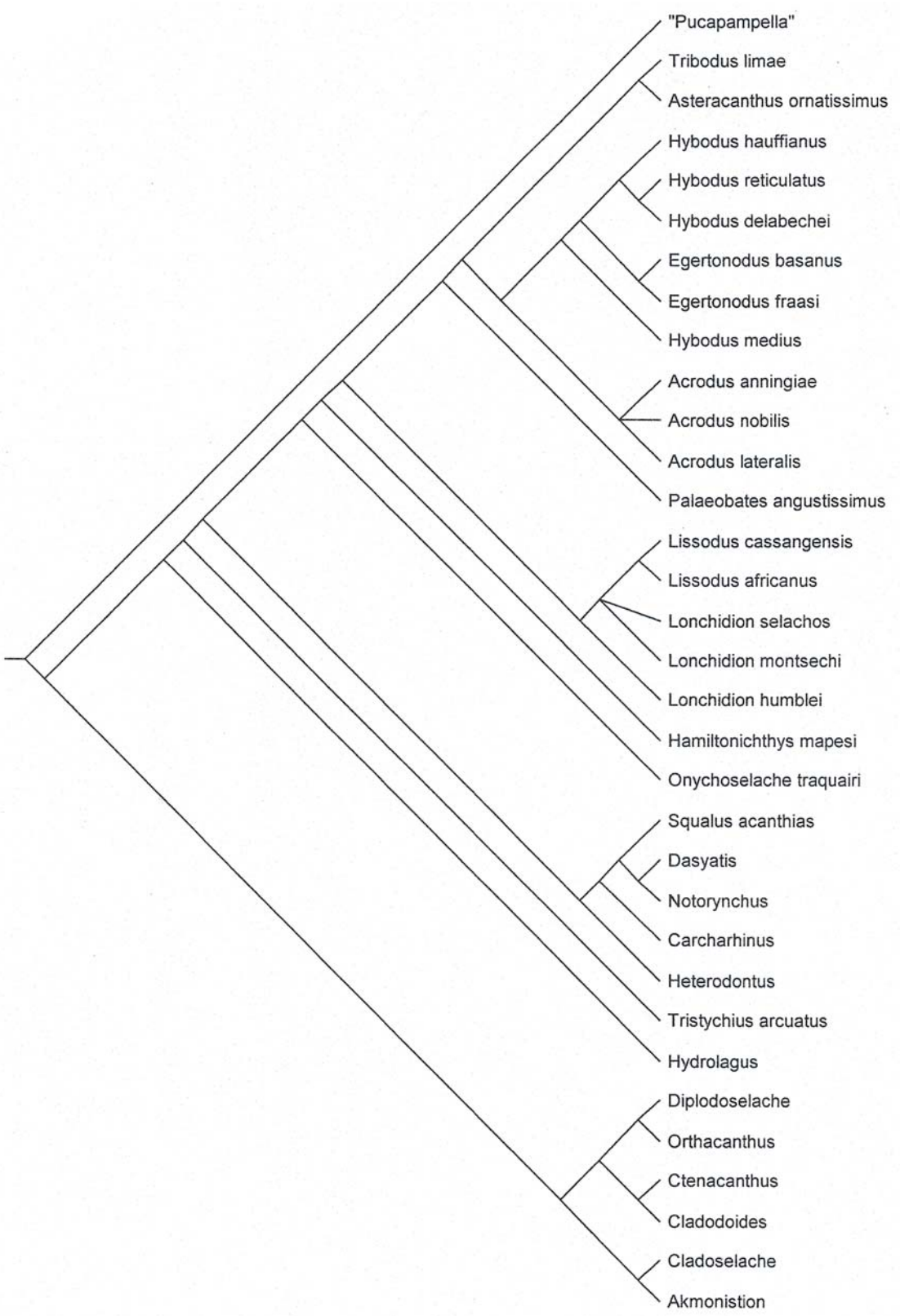

"Pucapampella"
Tribodus limae
Asteracanthus ornatissimus
Hybodus hauffianus
Hybodus reticulatus
Hybodus delabechei
Egertonodus basanus
Egertonodus fraasi
Hybodus medius
Acrodus anningiae
Acrodus nobilis
Acrodus lateralis
Palaeobates angustissimus
Lissodus cassangensis
Lissodus africanus
Lonchidion humblei
Lonchidion selachos
Lonchidion montsechi
Hamiltonichthys mapesi
Onychoselache traquairi
Squalus acanthias
Dasyatis
Notorynchus
Carcharhinus
Heterodontus
Tristychius arcuatus
Hydrolagus
Diplodoselache
Orthacanthus
Ctenacanthus
Cladodoides
Cladoselache
Akmonistion

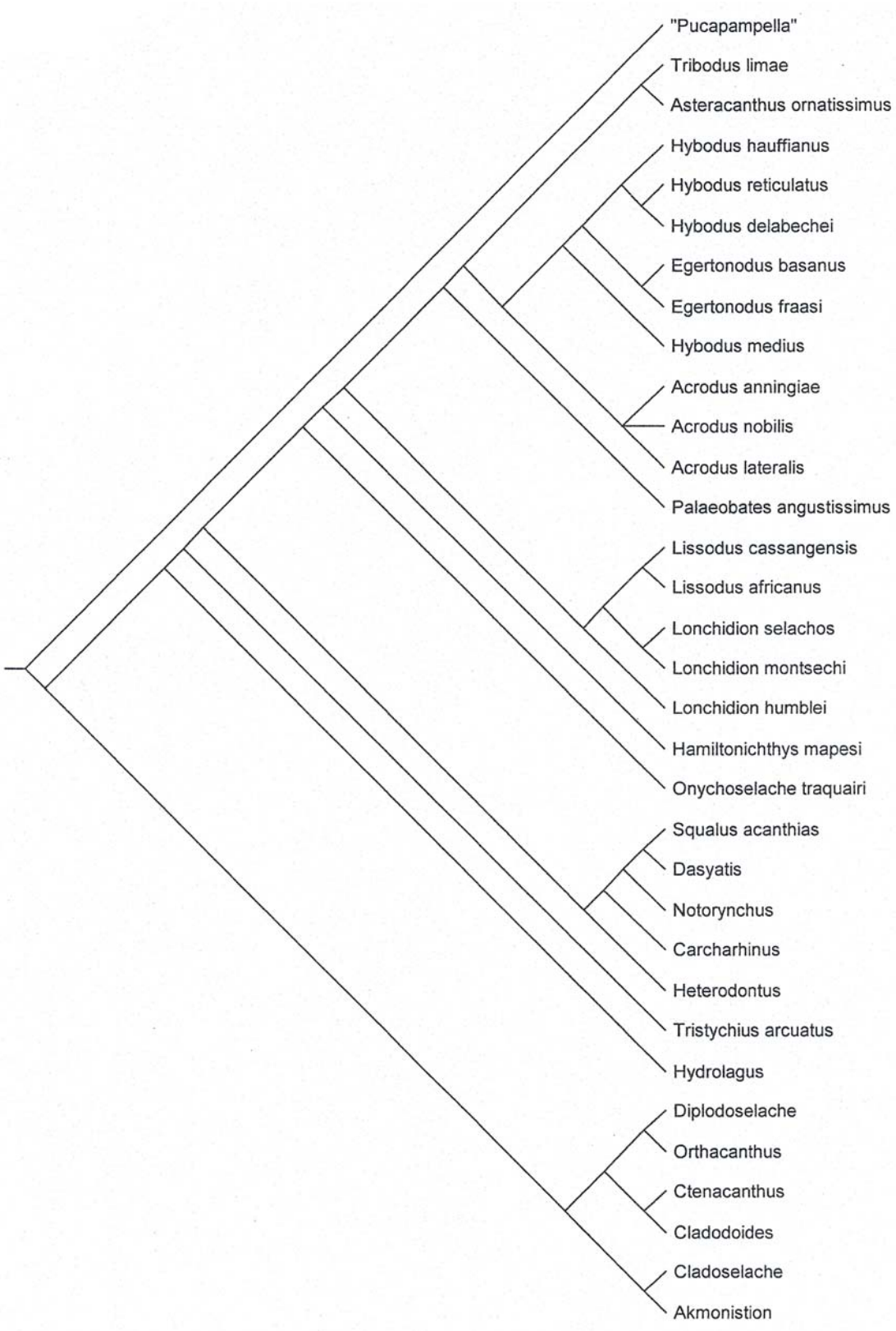

"Pucapampella"
Tribodus limae
Asteracanthus ornatissimus
Hybodus hauffianus
Hybodus reticulatus
Hybodus delabechei
Egertonodus basanus
Egertonodus fraasi
Hybodus medius
Acrodus anningiae
Acrodus nobilis
Acrodus lateralis
Palaeobates angustissimus
Lissodus cassangensis
Lissodus africanus
Lonchidion humblei
Lonchidion selachos
Lonchidion montsechi
Hamiltonichthys mapesi
Onychoselache traquairi
Squalus acanthias
Dasyatis
Notorynchus
Carcharhinus
Heterodontus
Tristychius arcuatus
Hydrolagus
Diplodoselache
Orthacanthus
Ctenacanthus
Cladodoides
Cladoselache
Akmonistion

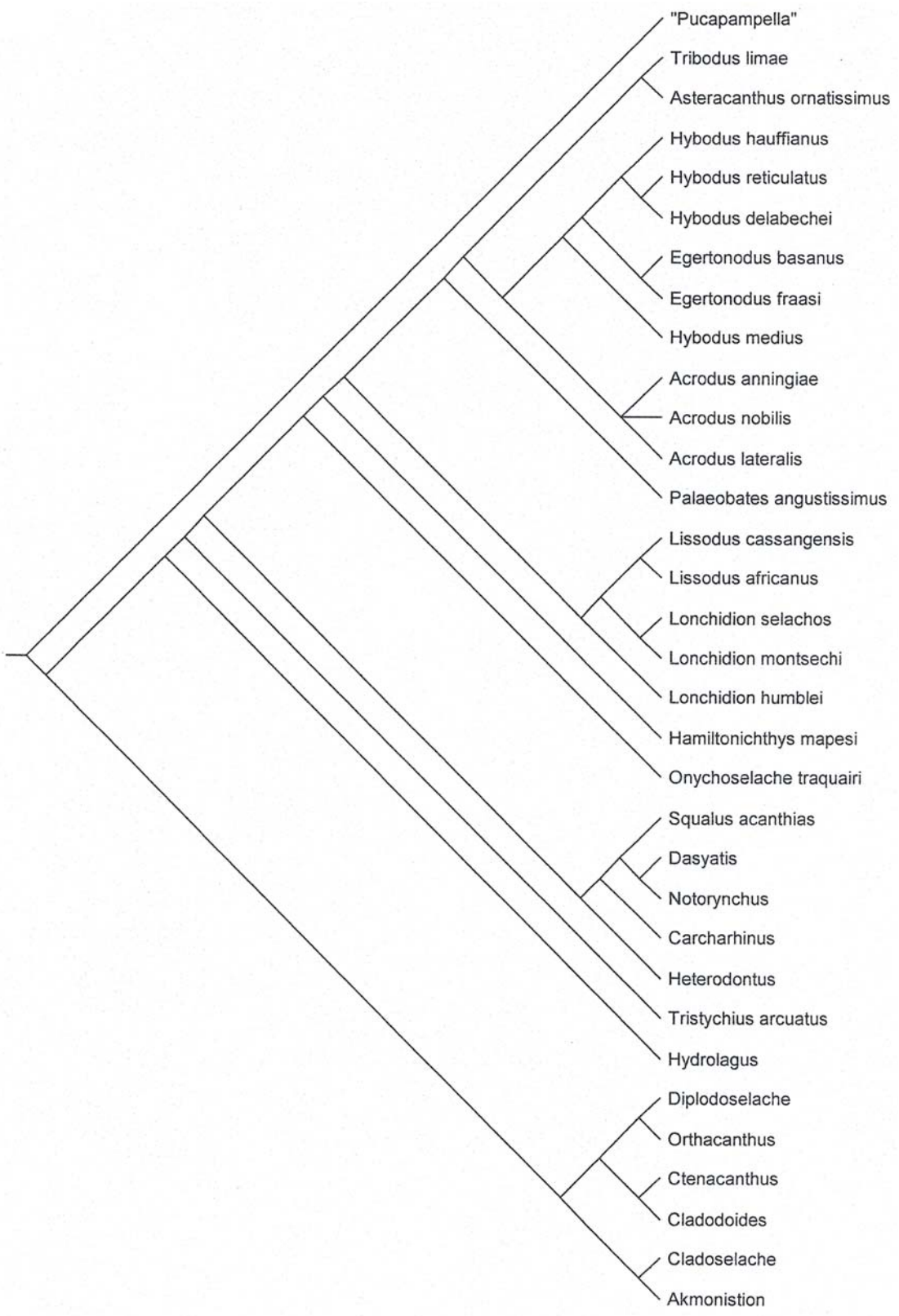

"Pucapampella"
Tribodus limae
Asteracanthus ornatissimus
Hybodus hauffianus
Hybodus reticulatus
Hybodus delabechei
Egertonodus basanus
Egertonodus fraasi
Hybodus medius
Acrodus anningiae
Acrodus nobilis
Acrodus lateralis
Palaeobates angustissimus
Lissodus cassangensis
Lissodus africanus
Lonchidion humblei
Lonchidion montsechi
Lonchidion selachos
Hamiltonichthys mapesi
Onychoselache traquairi
Squalus acanthias
Dasyatis
Notorynchus
Carcharhinus
Heterodontus
Tristychius arcuatus
Hydrolagus
Diplodoselache
Orthacanthus
Ctenacanthus
Cladodoides
Cladoselache
Akmonistion

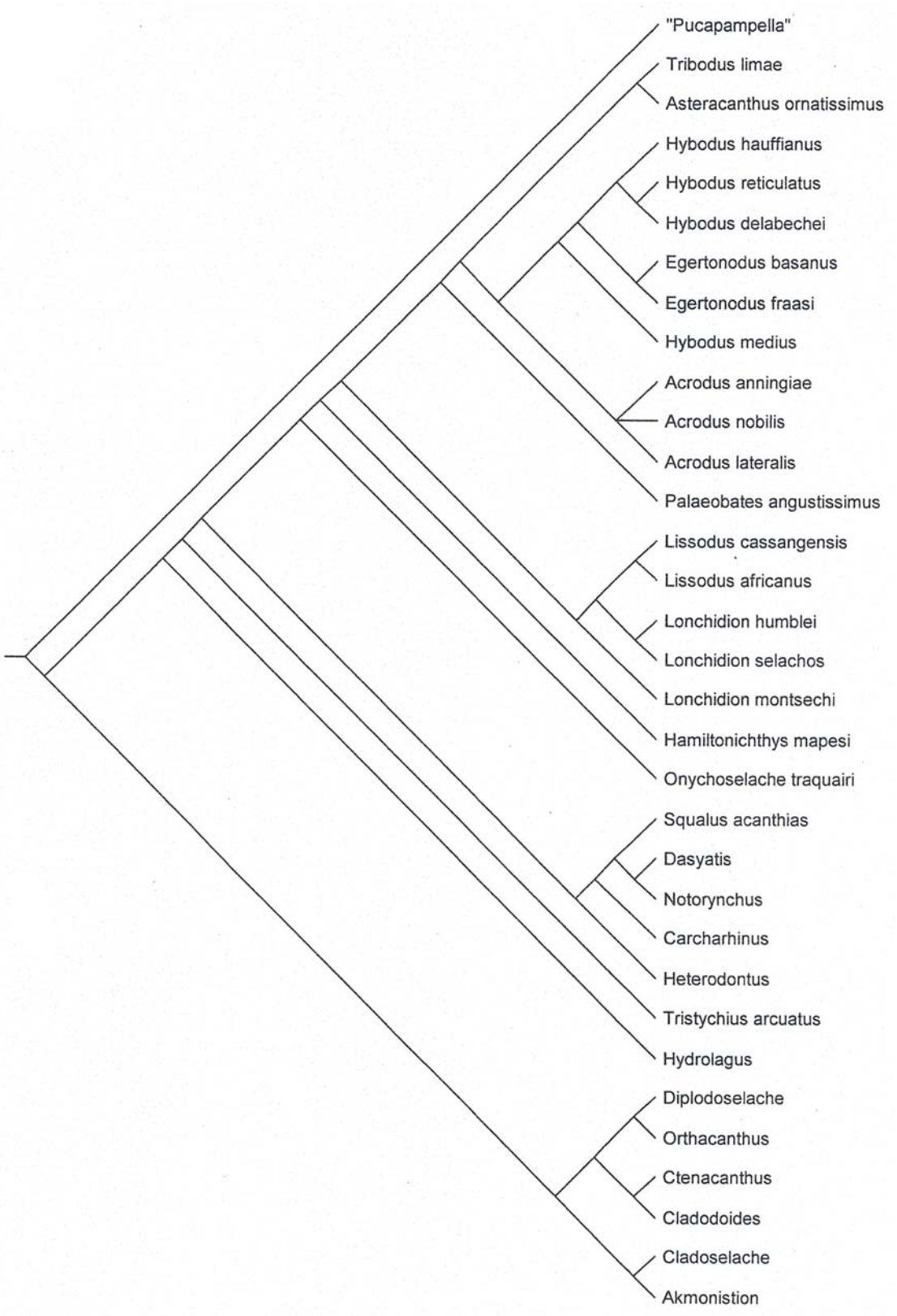

"Pucapampella"
Tribodus limae
Asteracanthus ornatissimus
Hybodus hauffianus
Hybodus reticulatus
Hybodus delabechei
Egertonodus basanus
Egertonodus fraasi
Hybodus medius
Acrodus anningiae
Acrodus nobilis
Acrodus lateralis
Palaeobates angustissimus
Lissodus cassangensis
Lissodus africanus
Lonchidion humblei
Lonchidion montsechi
Lonchidion selachos
Hamiltonichthys mapesi
Onychoselache traquairi
Squalus acanthias
Dasyatis
Notorynchus
Carcharhinus
Heterodontus
Tristychius arcuatus
Hydrolagus
Diplodoselache
Orthacanthus
Ctenacanthus
Cladodoides
Cladoselache
Akmonistion


"Pucapampella"
Tribodus limae
Asteracanthus ornatissimus
Hybodus hauffianus
Hybodus reticulatus
Hybodus delabechei
Egertonodus basanus
Egertonodus fraasi
Hybodus medius
Acrodus anningiae
Acrodus nobilis
Acrodus lateralis
Palaeobates angustissimus
Lissodus cassangensis
Lissodus africanus
Lonchidion selachos
Lonchidion montsechi
Lonchidion humblei
Hamiltonichthys mapesi
Onychoselache traquairi
Squalus acanthias
Dasyatis
Notorynchus
Carcharhinus
Heterodontus
Tristychius arcuatus
Hydrolagus
Diplodoselache
Orthacanthus
Ctenacanthus
Cladodoides
Cladoselache
Akmonistion

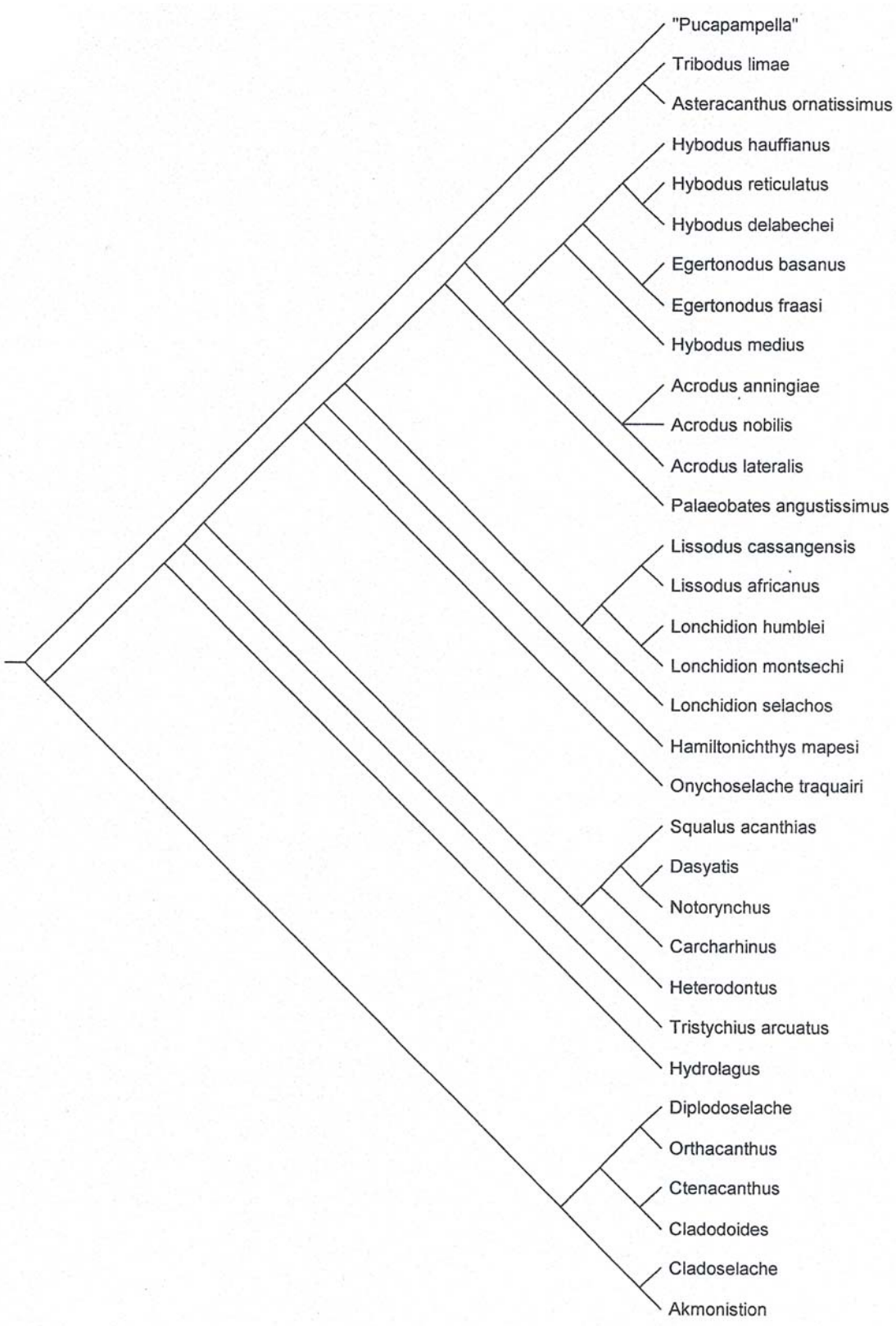

"Pucapampella"
Tribodus limae
Asteracanthus ornatissimus
Hybodus hauffianus
Hybodus reticulatus
Hybodus delabechei
Egertonodus basanus
Egertonodus fraasi
Hybodus medius
Acrodus anningiae
Acrodus nobilis
Acrodus lateralis
Palaeobates angustissimus
Lissodus cassangensis
Lissodus africanus
Lonchidion selachos
Lonchidion montsechi
Lonchidion humblei
Hamiltonichthys mapesi
Onychoselache traquairi
Squalus acanthias
Dasyatis
Notorynchus
Carcharhinus
Heterodontus
Tristychius arcuatus
Hydrolagus
Diplodoselache
Orthacanthus
Ctenacanthus
Cladodoides
Cladoselache
Akmonistion


"Pucapampella"
Tribodus limae
Asteracanthus ornatissimus
Hybodus hauffianus
Hybodus reticulatus
Hybodus delabechei
Egertonodus basanus
Egertonodus fraasi
Hybodus medius
Acrodus anningiae
Acrodus nobilis
Acrodus lateralis
Palaeobates angustissimus
Lissodus cassangensis
Lissodus africanus
Lonchidion selachos
Lonchidion montsechi
Lonchidion humblei
Hamiltonichthys mapesi
Onychoselache traquairi
Squalus acanthias
Dasyatis
Notorynchus
Carcharhinus
Heterodontus
Tristychius arcuatus
Hydrolagus
Diplodoselache
Orthacanthus
Ctenacanthus
Cladodoides
Cladoselache
Akmonistion


"Pucapampella"
Tribodus limae
Asteracanthus ornatissimus
Hybodus hauffianus
Hybodus reticulatus
Hybodus delabechei
Egertonodus basanus
Egertonodus fraasi
Hybodus medius
Acrodus anningiae
Acrodus nobilis
Acrodus lateralis
Palaeobates angustissimus
Lissodus cassangensis
Lissodus africanus
Lonchidion selachos
Lonchidion montsechi
Lonchidion humblei
Hamiltonichthys mapesi
Onychoselache traquairi
Squalus acanthias
Dasyatis
Notorynchus
Carcharhinus
Heterodontus
Tristychius arcuatus
Hydrolagus
Diplodoselache
Orthacanthus
Ctenacanthus
Cladodoides
Cladoselache
Akmonistion


"Pucapampella"
Tribodus limae
Asteracanthus ornatissimus
Hybodus hauffianus
Hybodus reticulatus
Hybodus delabechei
Egertonodus basanus
Egertonodus fraasi
Hybodus medius
Acrodus anningiae
Acrodus nobilis
Acrodus lateralis
Palaeobates angustissimus
Lissodus cassangensis
Lissodus africanus
Lonchidion humblei
Lonchidion selachos
Lonchidion montsechi
Hamiltonichthys mapesi
Onychoselache traquairi
Squalus acanthias
Dasyatis
Notorynchus
Carcharhinus
Heterodontus
Tristychius arcuatus
Hydrolagus
Diplodoselache
Orthacanthus
Ctenacanthus
Cladodoides
Cladoselache
Akmonistion


"Pucapampella"
Tribodus limae
Asteracanthus ornatissimus
Hybodus hauffianus
Hybodus reticulatus
Hybodus delabechei
Egertonodus basanus
Egertonodus fraasi
Hybodus medius
Acrodus anningiae
Acrodus nobilis
Acrodus lateralis
Palaeobates angustissimus
Lissodus cassangensis
Lissodus africanus
Lonchidion humblei
Lonchidion selachos
Lonchidion montsechi
Hamiltonichthys mapesi
Onychoselache traquairi
Squalus acanthias
Dasyatis
Notorynchus
Carcharhinus
Heterodontus
Tristychius arcuatus
Hydrolagus
Diplodoselache
Orthacanthus
Ctenacanthus
Cladodoides
Cladoselache
Akmonistion


"Pucapampella"
Tribodus limae
Asteracanthus ornatissimus
Hybodus hauffianus
Hybodus reticulatus
Hybodus delabechei
Egertonodus basanus
Egertonodus fraasi
Hybodus medius
Acrodus anningiae
Acrodus nobilis
Acrodus lateralis
Palaeobates angustissimus
Lissodus cassangensis
Lissodus africanus
Lonchidion humblei
Lonchidion montsechi
Lonchidion selachos
Hamiltonichthys mapesi
Onychoselache traquairi
Squalus acanthias
Dasyatis
Notorynchus
Carcharhinus
Heterodontus
Tristychius arcuatus
Hydrolagus
Diplodoselache
Orthacanthus
Ctenacanthus
Cladodoides
Cladoselache
Akmonistion


"Pucapampella"
Tribodus limae
Asteracanthus ornatissimus
Hybodus hauffianus
Hybodus reticulatus
Hybodus delabechei
Egertonodus basanus
Egertonodus fraasi
Hybodus medius
Acrodus anningiae
Acrodus nobilis
Acrodus lateralis
Palaeobates angustissimus
Lissodus cassangensis
Lissodus africanus
Lonchidion humblei
Lonchidion montsechi
Lonchidion selachos
Hamiltonichthys mapesi
Onychoselache traquairi
Squalus acanthias
Dasyatis
Notorynchus
Carcharhinus
Heterodontus
Tristychius arcuatus
Hydrolagus
Diplodoselache
Orthacanthus
Ctenacanthus
Cladodoides
Cladoselache
Akmonistion


"Pucapampella"
Tribodus limae
Asteracanthus ornatissimus
Acrodus anningiae
Acrodus nobilis
Acrodus lateralis
Hybodus hauffianus
Hybodus reticulatus
Hybodus delabechei
Egertonodus basanus
Egertonodus fraasi
Hybodus medius
Palaeobates angustissimus
Lissodus cassangensis
Lissodus africanus
Lonchidion montsechi
Lonchidion humblei
Lonchidion selachos
Hamiltonichthys mapesi
Onychoselache traquairi
Squalus acanthias
Dasyatis
Notorynchus
Carcharhinus
Heterodontus
Tristychius arcuatus
Hydrolagus
Diplodoselache
Orthacanthus
Ctenacanthus
Cladodoides
Cladoselache
Akmonistion

# REFERENCES

Adams, E.N., III. 1972. Consensus techniques and the comparison of taxonomic trees. Systematic Zoology 21:390–397.

Agassiz, J. L. R. 1833–1844. Recherches sur les poissons fossils, 5 volumes and atlas. Imprimerie Petitpierre, Neuchâtel and Soleure, 1420 pp.

Agassiz, L. 1841. On the fossil fishes found by Mr. Gardner in the Province of Ceará, in the north of Brazil. Edin. New Phil. J. 30:82–84.

Allis, E.P. 1911. The pseudobranchial and carotid arteries in *Chlamydoselachus anguineus*. Anatomischer Anzeiger 39: 511.

Allis, E.P. 1912. The branchial, pseudobranchial and carotid arteries in *Raja radiata*. Anatomischer Anzeiger 41: 579.

Allis, E.P. 1914. The pituitary fossa and trigemino-facialis chamber in selachians. Anatomischer Anzeiger 46: 225–253.

Allis, E. P. 1923. The cranial anatomy of *Chlamydoselachus anguineus*. Acta Zoologica 4:123–221

Anderson, M. E., Long, J. A., Gess, R. W., and Hiller, N. 1999. An unusual new fossil shark (Pisces: Chondrichthyes) from the Late Devonian of South Africa. Records of the Western Australia Museum, Supplement, 57:151–156.

Anderson, P.S.L. 2008. Cranial muscle homology across modern gnathostomes. Biological Journal of the Linnaean Society 94:195–216.

Antunes, M.T., Maisey, J.G., Marques, M.M., Schaeffer, B., and K.S. Thomson. 1990. Triassic Fishes from the Cassange Depression (R.P. de Angola). Ciências da Terra (UNL), Número Especial:1–64.

Ashley, L. M., and R. B. Chiasson. 1988. Laboratory Anatomy of the Shark, 5th ed. McGraw-Hill, New York, 84 pp.

Balfour, F. M. 1881. On the development of the skeleton of the paired fins of Elasmobranchii, considered in relation to its bearings on the nature of the limbs of the Vertebrata. Proceedings of the Zoological Society of London 1881:656–671.

Basden, A.M., Young, G.C., Coates, M., and A. Ritchie. 2000. The most primitive osteichthyan braincase? Nature 403:185–188.

Baudin, F., Berthou, P.-Y., Herbin, J.P., and D.A. Campos. 1990. Matière organique et sédimentation argileuse dans le Crétacé du Bassin d'Araripe. Comparaison avec les données du Crétacé d'autres bassins brésiliens. In Campos, D.A., Viana, M.S.S., Brito, P.M., and G. Beurlen (eds.). Atas do I Simposio sobre a Bacia do Araripe e Bacias Interiores do Nordeste. URCA, Crato. pp. 83–93.

Bendix-Almgreen, S. E. 1975. The paired fins and shoulder girdle in *Cladoselache*, their morphology and phyletic significance; pp. 111–123 in J. P. Lehman (ed.), Problèmes Actuels de Paléontologie: Évolution des Vertébrés. Colloque international du Centre National de la Recherche Scientifique, 218, Paris.

Berg, L.S. 1955. Classification of fishes and fish-like vertebrates, living and fossils. 2nd ed., corrected and enlarged (in Russian). Trav. Inst. Zool., Acad. Sci., USSR, Leningrad, pp. 1–286.

Beurlen, K. 1962. A geologia da Chapada do Araripe. An. Acad. brasil Ciênc. 34(3):365–370.

Beurlen, K. 1963. Geologia e Estratigrafia da Chapada do Araripe. XVII Congr. Brasil. Geol. Publ. SUDENE:1–47.

Beurlen, K. 1971. As condições ecológicas e faciológicas da Formação Santana na Chapada do Araripe (Nordeste do Brasil). Anais da Academia Brasileira de Ciências 43:411–415.

Blot, J. 1969. Holocéphales et élasmobranches. Systematique. *In* Piveteau, J. (ed.), Traité de Paleontologie, vol. 4, pp. 702–776. Masson et Cie, Paris.

Bonaparte, C.L. 1832. Selachorum tabula analytica. Nuovi Annali Scienze Naturali (Bologna) 1: 195–214.

Braun, O. P. G. 1966. Estratigrafia dos sedimentos da parte interior da regiao Nordeste do Brasil (Bacias de Tucano—Jatoba, Mirandiba e Araripe). D. N. P. M./Div. Geol. Miner., Bol. 236:1–15.

Bremer, K. 1988. The limits of amino acid sequence data in angiosperm phylogenetic reconstruction. Evolution 42:795–803.

Bremer, K. 1994. Branch support and tree stability. Cladistics 10:295–304.

Brito, P.M. 1991. Systematic atlas: *Tribodus* Brito and Ferreira, 1989**.** *In* J.G. Maisey (editor), Santana fossils: an illustrated atlas. Neptune City, New Jersey: T. F. H. Publications. pp. 108–109.

Brito, P. M. 1992. Nouvelles données sur l'anatomie et la position systématique de *Tribodus limae* Brito and Ferreira, 1989 (Chondrichthyes, Elasmobranchii) du Crétacé Inférieur de la Chapada do Araripe (N-E Brésil). Géobios 14:143–150.

Brito, P. M., and P. L. N. Ferreira. 1989. The first hybodont shark, *Tribodus limae* n.g., n.sp., from the Lower Cretaceous of Chapada do Araripe (North-East Brazil). Anais da Academia Brasileira de Ciências 61(1):53–57.

Broom, R. 1909. Fossil fishes of the upper Karroo Beds of South Africa. Ann. S. African Mus., vol. 7, pp. 251–269.

Brough, J. 1935. On the structure and relationships of the hybodont sharks. Memoirs and Proceedings of the Manchester Literary and Philosophical Society 79:35–50.

Brown, C. 1900. Über das Genus *Hybodus* und seine systematische Stellung. Palaeontographica 46:149–174.

Cappetta, H. 1987. Chondrichthyes II: Mesozoic and Cenozoic Elasmobranchii. In Handbook of Paleoichthyology, Vol. 3B. H.–P. Schultze (ed.). Gustav Fischer Verlag, Stuttgart, Germany, 193 pp.

Cappetta, H. 1992. Nouveaux Rhinobatoidei (Neoselachii, Rajiformes) à denture spécialisée du Maastrichtian du Maroc. Remarques sur l'évolution dentaire des Rajiformes et des Myliobatiformes. Neues Jahrbuch fur Geologie und Palaontologie, Abhandlungen 187:31–52.

Cappetta, H, and G. R. Case. 1999. Additions aux faunes de sélaciens du Crétacé du Texas (Albien supérieur-Campanien). Palaeo Ichthyologica 9:5–111.

Cappetta, H., Buffetaut, E., Cuny, G., and V. Suteethorn. 2006. A new elasmobranch assemblage from the Lower Cretaceous of Thailand. Palaeontology 49:547–555.

Carroll, R. L. 1988. Vertebrate Paleontology and Evolution. W. H. Freeman and Co, New York, 698 pp.

Carvalho, M. R. 1996. Higher-level elasmobranch phylogeny, basal squaleans, and paraphyly; pp. 35–62 in M. L. J. Stiassny, L. R. Parenti, and G. D. Johnson (eds.), Interrelationships of Fishes. Academic Press, San Diego.

Carvalho, M. R., & J.G. Maisey. 1996. Phylogenetic relationships of the Late Jurassic Shark *Protospinax* Woodward 1919 (Chondrichthyes: Elasmobranchii). In Mesozoic Fishes: Systematics and Paleoecology. G. Arratia & G. Viohl (eds.). Verlag Dr. Friedrich Pfeil, Munchen, Germany, pp. 9–46.

Carvalho, M.R., Maisey, J.G., and L. Grande. 2004. Freshwater stingrays of the Green River Formation of Wyoming (Early Eocene), with the description of a new genus and species and an analysis of its phylogenetic relationships (Chondrichthyes: Myliobatiformes). Bulletin of the American Museum of Natural History 284:1–136.

Casier, E. 1961. Matériaux pour la faune ichthyologique Eocrétacique du Congo. Annales, Musée royal de l'Afrique centrale, Tervuren, (8), 39:1–96.

Cavin, L., Boudad, L., Duffaud, S., Kabiri, L., Le Lœuff, J., Rouget, I., and H. Tong. 2001. L'évolution paléoenvironnementale des faunes de poisons du Crétacé supérieur du basin du Tafilalt et des régions avoisinantes (Sud-Est du Maroc): implications paléobiogéographiques. Comptes Rendus de l'Académie des Sciences de Paris, Sciences de la Terre et des Planètes 333:677–683.

Cerny, R., Lwigale, P., Ericsson, R., Meulemans, D., Epperlein, H.-H., and M. Bronner-Fraser. 2004. Developmental origins and evolution of jaws: new interpretation of "maxillary" and "mandibular." Developmental Biology 276:225–236.

Charlesworth, E. 1839. Illustrated zoological notices—on the remains of a species of *Hybodus* from Lyme Regis. Mag. Nat. Hist., n.s., vol. 3, pp. 242–248.

Charlesworth, E. 1945. On the fossil bodies regarded by M. Agassiz as the teeth of a fish, and upon which he has founded his supposed genus *Sphenonchus*. Report of the British Association for the Advancement of Science, 15th meeting, part 2, p. 56.

Coates, M. I. 2003. The evolution of paired fins. Theory in Biosciences 122:266–287.

Coates, M. I., and R. W. Gess. 2007. A new reconstruction of *Onychoselache traquairi*, comments on early chondrichthyan pectoral girdles and hybodontiform phylogeny. Palaeontology 50:1–26.

Coates, M.I., and S. E. Sequeira. 1998. The braincase of a primitive shark. Transactions of the Royal Society of Edinburgh: Earth Sciences 89: 63–85.

Coates, M. I., and S. E. K. Sequeira. 2001A. Early sharks and primitive gnathostome interrelationships; pp. 241–262 in P. E. Ahlberg (ed.), Major Events in Early Vertebrate Evolution: Paleontology, Phylogeny, Genetics and Development. Systematics Association Special Volume Series 61. Taylor and Francis, New York.

Coates, M.I., and S. E. Sequeira. 2001B. A new stethacanthid chondrichthyan from the Lower Carboniferous of Bearsden, Scotland. Journal of Vertebrate Paleontology 21(3):438–459.

Compagno, L.J.V. 1973. Interrelationships of living elasmobranchs. In Greenwood, P.H., R.S. Miles, and C. Patterson (eds.), Interrelationships of fishes. Lin. Soc. London, vol. 53, pp. 15–61. Academic Press, London.

Compagno, L.J.V. 1988. Sharks of the order Carcharhiniformes. Princeton: Princeton University Press. 486 pp.

Compagno, L. J. V. 1999. Endoskeleton; pp. 69–92 in W. C. Hamlett (ed.), Sharks, Skates, and Rays: The Biology of Elasmobranch Fishes. The Johns Hopkins University Press, Baltimore, Maryland.

Cope, E. D. 1884. On the structure of the skull in the elasmobranch genus *Didymodus*. Proceedings of the American Philosophical Society 21: 572–590.

Cope, E. D. 1893. On *Symmorium*, and the position of the cladodont sharks. American Naturalist 27:999–1001.

Cordier, R. 1954. Le système nerveux central et les nerfs cérébro-spinaux. pp. 202–332 In Grassé, P.-P. (ed.), Traité de zoologie: Anatomie, systématique, biologie, Tome XII, Vertébrés. Paris: Masson et Cie, Éditeurs, 1145 pp.

Cressey, R., and C. Patterson. 1973. Fossil parasitic copepods from a Lower Cretaceous fish. Science, N. Y. 180:1283–1285.

Cuny, G., Rieppel, O., and P.M. Sander. 2001. The shark fauna from the Middle Triassic (Anisian) of North-Western Nevada. Zoological Journal of the Linnean Society 133:285–301.

Cuny, G., Suteethorn, V., Buffetaut, E., and Ouaja, M. 2001. Freshwater hybodont sharks in the Aptian-Albian of Tunisia and Thailand. In Ferre, B., Fouray, M., and J. Tabouelle (eds.), Colloque sur le Cénomanien, Bulletin de la Société d'étude des Sciences naturelles d'Elbeuf, pp. 27–29.

Cuny, G., Ouaja, M., Srarff, D., Schmitz, L., Buffetaut, E., and M. J. Benton. 2004. Fossil sharks from the Early Cretaceous of Tunisia. Revue de Paleobiologie, Geneve, 9:127–142.

Cuny, G., Suteethorn, V., Kamha, S., Buffetaut, E., and M. Philippe. 2006. A new hybodont shark assemblage from the Lower Cretaceous of Thailand. Historical Biology 18(1):21–31.

Cuny, G., Suteethorn, V., Kamha, S., and E. Buffetaut. 2008. Hybodont sharks from the lower Cretaceous Khok Kruat Formation of Thailand, and hybodont diversity during the early Cretaceous. In Cavin, L., Longbottom, A., and M. Richter (eds.), Fishes and the break-up of Pangaea. Geological Society, London, Special Publication 295:93–107.

Daniel, J. F. 1934. The Elasmobranch Fishes, 3rd ed. University of California Press, Berkeley, California, 332 pp.

Davis, M. C., N. H. Shubin, and A. Force. 2004. Pectoral fin and girdle development in the basal actinopterygians *Polyodon spathula* and *Acipenser transmontanus*. Journal of Morphology 262:608–628.

Day, E.C.H. 1864. On *Acrodus anningiae*; with remarks upon the affinities of the genera *Acrodus* and *Hybodus*. Geological Magazine 1:57–65.

Dean, B. 1894. Contributions to the morphology of Cladoselache (Cladodus). Journal of Morphology 9:87–114.

Dean, M.N., Huber, D.R., and H.A. Nance. 2004. Functional morphology of jaw trabeculation in the lesser electric ray *Narcine brasiliensis*, with comments on the evolution of structural support in the Batoidea. Journal of Morphology 267(10): 1137–1146.

Dean, M.N., and P.J. Motta. 2004. Anatomy and functional morphology of the feeding apparatus of the Lesser Electric Ray, *Narcine brasiliensis* (Elasmobranchii: Batoidea). Journal of Morphology 262:462–483.

De Beer, G. R. 1931. The development of the skull of *Scyllium* (*Scyliorhinus*) *canicula*. London Quarterly Journal of Microscopic Science, n.s., 74:591–645.

De Beer, G. R. 1937. The development of the vertebrate skull. Oxford University Press, xxiv + 552 pp.

Devillers, C. 1954. Les cotes. In Grasse, P.P. (ed.), Traite de zoologie. Paris, Masson et Cie, volume 12:673–697.

Dick, J.R.F. 1978. On the Carboniferous Shark *Tristychius arcuatus* Agassiz from Scotland. Transactions of the Royal Society of Edinburgh 70(4): 63–109.

Dick, J.R.F. 1981. *Diplodoselache woodi* gen. et sp. nov., an early Carboniferous shark from the Midland Valley of Scotland. Transactions of the Royal Society of Edinburgh 72:99–113.

Dick, J. R. F., and J. G. Maisey. 1980. The Scottish Lower Carboniferous shark *Onychoselache traquairi*. Palaeontology 23(2):363–374.

Didier, D.A. 1995. Phylogenetic systematics of extant chimaeroid fishes (Holocephali, Chimaeroidei). American Museum Novitates 3119:1–86.

Duarte, L. 1969. Paleoflórula da Formação Santana. Soc. Brasil. Geol. Nucl. Bahia, Spec. Bull., 1:59 (summary).

Duffin, C.J. 1985. Revision of the hybodont selachian genus *Lissodus* Brough (1935). Palaeontographica, Abt. A, 188: 105–152.

Duffin, C.J. 1997. The dentition of *Hybodus hauffianus* Fraas, 1895 (Toarcian, Early Jurassic). Stuttgarter Beitrage zur Naturkunde Ser. B 256:1–20.

Duffin, C. J. 2001. Synopsis of the selachian genus *Lissodus* Brough, 1935. Neues Jahrbuch für Geologie und Paläontologie Abhandlungen 221:145–218.

Duffin, C.J., and G. Cuny. 2008. *Carcharopsis prototypus* and the adaptations of single crystallite enameloid in cutting dentitions. Acta Geologica Polonica 58(2):181–184.

Dutheil, D. 1999. An overview of the freshwater fish fauna from the Kem Kem beds (Late Cretaceous: Cenomanian) of southeastern Morocco. In Arratia, G., and H.-P. Schultze (eds.), Mesozoic Fishes 2–Systematics and the Fossil Record, Verlag Dr. Friedrich Pfeil, Munich, Germany, pp. 553–563.

Dutheil, D. 2001. New freshwater fish from the Late Cretaceous (Cenomanian) of Niger. Journal of Vertebrate Paleontology, 21(3), supplement:46A.

Dutra, M.F.A., and Malabarba, M.C.S.L. 2001. Peixes do Albiano-Cenomaniano do Grupo Itapecuru, Estado do Maranhão, Brasil. In D.F. Rossetti, A.M. Góes, and W. Truckenbrodt (eds.), O Cretáceo na Bacia São Luís-Grajaú. Belém: Museu Paraense Emilio Goeldi. pp. 191–208.

Eastman, C.R. 1897. *Tamiobatis vetustus*: a new form of fossil skate. Amer. Jour. Sci., 4th ser., vol. 4, pp. 85–90.

El-Toubi, M.R. 1949. The development of the chondrocranium of the spiny dogfish, *Acanthias vulgaris* (*Squalus acanthias*). Part I. Neurocranium, mandibular and hyoid arches. Journal of Morphology 84:227–280.

Estes, R. 1964. Fossil vertebrates from the late Cretaceous Lance Formation, eastern Wyoming. University of California Publications in Geological Sciences 49:1–187.

Fanton, J. C. M., Ricardi Branco, F., Dilcher, D., Bernardes de Oliveira, M. 2006. New Gymnosperm related with Gnetales from the Crato palaeoflora (Lower Cretaceous, Santana Formation, Araripe Basin, northeastern Brazil); preliminary study. Geociencias (Sao Paulo) 25(2):205–210.

Felsenstein, J. 1985. Confidence limits on phylogenies: an approach using the bootstrap. Evolution 39:783–791.

Fischer, J. 2008. Brief synopsis of the hybodont form taxon *Lissodus* Brough, 1935, with remarks on the environment and associated fauna. Freiberger Forschungshefte, C 528:1–23.

Forey, P. Cladistics for palaeontologists. Newsletter of the Palaeontological Association 60:26–37.

Forey, P. Cladistic characters. Newsletter of the Palaeontological Association 61:33–42.

Forey, P. Tree building. Newsletter of the Palaeontological Association 62:43–59.

Forey, P. Cladistics: optimisation. Newsletter of the Palaeontological Association 63:26–35.

Forey, P. Consensus trees and tree support. Newsletter of the Palaeontological Association 64:28–34.

Forey, P. Missing values and stratigraphy. Newsletter of the Palaeontological Association 65:29–35.

Fraas, E. 1889. Kopfstacheln von *Hybodus* und *Acrodus*, sogenannte *Ceratodus heteromorphus* Ag. Jahreshefte Ver. Vaterl. Naturk. Württemberg, vol. 45, pp. 233–240.

Fraas, E. 1896. Neue Selachier-Reste aus dem oberen Lias von Holzmaden in Württemberg. Jahreshefte des Vereins für vaterländische Naturkunde in Württemberg 52:1–25.

Fritsch, A. 1889. Fauna der Gaskohle und der Kalksteine der Permformation Böhmens. Z. (Stegocephali, Dipnoi, Selachii). Prague, vol. II, 114 pp.

Fritsch, A. 1895. Fauna der Gaskohle und der Kalksteine der Permformation Böhmens. Prague, vol. III, 132 pp.

Gaffney, E. S., Campos, D. A., and R. Hirayama. 2001. Cearachelys, a new side-necked turtle (Pelomedusoides; Bothremydidae) from the Early Cretaceous of Brazil. American Museum Novitates 3319, 20 pp.

Gans, C., and T. S. Parsons. 1981. A Photographic Atlas of Shark Anatomy: the Gross Morphology of *Squalus acanthias*. University of Chicago Press, Chicago, Illinois, 106 pp.

Gardiner, B.G. 1984. The relationships of the palaeoniscid fishes, a review based on new specimens of *Mimia* and *Moythomasia* from the Upper Devonian of Western Australia. Bulletin of the British Museum (Natural History) 37(4):173–428.

Gardner, G. 1849. Travels in the Interior of Brazil, principally through the Northern Provinces. Reeve, Benham, and Reeve, London. 428 pp.

Gaudin, T.J. 1991. A re-examination of elasmobranch monophyly and chondrichthyan phylogeny. Neues Jahrbuch für Geologie und Paläontologie, Abhandlungen 182: 133–160.

Gauthier, J., Kluge, A.G., & Rowe, T. 1988. Amniote phylogeny and the importance of fossils. Cladistics 4(2): 105–210.

Gegenbaur, C. 1872. Untersuchungen zur vergleichenden Anatomie der Wirbelthiere. III. Das Kopfskelet der Selachier, ein Beitrag zur Erkenntniss der Genese des Kopfskeletes der Wirbelthiere. Leipzig, Wilhelm Engelmann. 316 pp.

Gillis, J.A., and P.C.J. Donoghue. 2007. The homology and phylogeny of chondrichthyan tooth enameloid. Journal of Morphology 268:33–49.

Ginter, M. 2005. The euselachian type of tooth-bases in Palaeozoic chondrichthyans. In: Hairapetian, V., Ginter, M. (eds.), Devonian Vertebrates of the Continental Margins. pp. 11–12. Ichthyolith Issues, Special Publication 8, Yerevin, Armenia.

Glikman, L.S. 1964. Subclass Elasmobranchii (sharks). In Obruchev, D.V. (ed.), Fundamentals of Paleontology, Israel Program for Scientific Translations, Jerusalem.

Goloboff, P., Farris, J., and K. Nixon. 2003. T.N.T.: Tree Analysis Using New Technology. Program and Documentation, available at http:// www.zmuc.dk/public/phylogeny/tnt.

Goloboff, P.A., Farris, J.S., and K.C. Nixon. 2008. TNT, a free program for phylogenetic analysis. Cladistics 24 (2008):1–13.

Gomez-Pallerola, J.E. 1985. Nuevos hybodontidos del Cretácio Inferior de Santa María de Meyá (Lérida). Boletin Geologico y Minero 96(4):372–380.

Gomez-Pallerola, J.E. 1992. Nota sobre los tiburones hybodontos de las calizas litográficas del Cretácio Inferior del Montsec (Lérida). Boletin Geologico y Minero 103:3–33.

Gomez-Pallerola, J.E. 1979. Un ave y otras especies fósiles nuevas de la biofacies de Santa María de Meyá (Lérida). Boln. Geol. Min. 90(4):333–346.

Goodrich, E. S. 1909. Vertebrata Craniata, First Fascicle: Cyclostomes and Fishes. In E. R. Lankester (ed.), A Treatise on Zoology, Volume 9, Vertebrata Craniata. A+C Black, London, 518 pp.

Goodrich, E. S. 1930. Studies on the Structure and Development of Vertebrates. MacMillan and Co., London, xxx + 837 pp.

Goodrich, E. S. 1958. Studies on the Structure and Development of Vertebrates, Volume 1. Dover Publications, New York, 485 pp.

Goujet, D. 2001. Placoderms and Basal Gnathostome Apomorphies; pp. 209–222 in P. E. Ahlberg (ed.), Major Events in Early Vertebrate Evolution. Taylor and Francis, New York.

Goujet, D., and G. C. Young. 2004. Placoderm Anatomy and Phylogeny: New Insights; pp. 109–126 in G. Arratia, M. V. H. Wilson, and R. Cloutier (eds.), Recent Advances in the Origin and Early Radiation of Vertebrates (H.-P. Schultze, Festschrift). Verlag Dr. Friedrich Pfeil, München.

Gregory, W.K. 1904. The relations of the anterior visceral arches to the chondrocranium. Biol. Bull. 7:55–69.

Grimaldi, D. 2003. A revision of Cretaceous mantises and their relationships, including new taxa (Insecta, Dictyoptera, Mantodea). American Museum Novitates 3412, 47 pp.

Grogan, E.D., Lund, R., and D. Didier. 1999. Description of the chimaerid jaw and its phyletic origins. Journal of Morphology 239:45–59.

Hampe, O. 1988. Uber die Bezahnung des *Orthacanthus* (Chondrichthyes: Xenacanthida; Oberkarbon–Unterperm). Palaontologische Zeitschrift 62:285–296.

Harris, J.E. 1938. The neurocranium and jaws of Cladoselache. Sci. Publ. Cleveland Mus. Nat. Hist. vol. 8, no. 1, pp. 7–12.

Heidtke, U. 1982. Der Xenacanthide *Orthacanthus senckenbergianus* aus dem pfälzischen Rotliegenden (Unter-Perm). Pollichia 70:65–86.

Heidtke, U.H.J. 1999. *Orthacanthus* (*Lebachacanthus*) *senckenbergensis* Fritsch 1889 (Xenacanthida: Chondrichthyes): revision, organisation und phylogenie. Freiburger Forschung-sheft C481: 63–106.

Helbing, H. 1904. Beiträge zur Anatomie und Systematik der Laemargiden. Nova Acta: Abhandlungen der Kaiserlich Leopoldinisch-Carolinisch Deutschen Akademie der Naturforscher 82:335–524.

Holmgren, N. 1940. Studies on the head in fishes. Part I. Development of the skull in sharks and rays. Acta Zoologica (Stockholm) 21: 51–267.

Holmgren, N. 1941. Studies on the head in fishes. Part II. Comparative anatomy of the adult selachian skull with remarks on the dorsal fins in sharks. Acta Zoologica (Stockholm) 22: 1–100.

Holmgren, N. 1942. Studies on the head in fishes. Part III. The phylogeny of elasmobranch fishes. Acta Zoologica (Stockholm) 23: 129–261.

Holmgren, N. 1943. Studies on the head in fishes. Part IV. General morphology of the head in fish. Acta Zoologica (Stockholm) 23: 1–188.

Hotton, N. 1952. Jaws and teeth of American xenacanth sharks. Journal of Paleontology 26(3): 489–500.

Huber, D.R., Dean, M.N., and A.P. Summers. 2008. Hard prey, soft jaws and the ontogeny of feeding mechanics in the spotted ratfish *Hydrolagus colliei*. Journal of the Royal Society Interface 5:941–952.

Huxley, T.H. 1876. On Ceratodus fosteri, with observations on the classification of fishes. Proceedings of the Zoological Society of London 1876:24–59.

Huxley, T.H. 1880. On the application of the laws of evolution to the arrangement of the Vertebrata and more particularly of the Mammalia. Proceedings of the Zoological Society of London 1880: 649–662.

Jaekel, O. M. J. 1889. Die Selachier aus dem oberen Muschelkalk Lothringens. Abhandl. Geol. Specialk. Elsass-Lothringen, vol. 3, pp. 273–332.

Jaekel, O. M. J. 1906. Neue Rekonstruktionen von *Pleuracanthus sessilis* und von *Polyacrodus* (*Hybodus*) *hauffianus*. Sitzungs-berichte der Gesellschaft Naturforschender Freunde zu Berlin 1906:155–159.

Janvier, P. 1998. Early Vertebrates. Clarendon Press, Oxford, United Kingdom, 393 pp.

Janvier, P., M. Arsenault, and S. Desbiens. 2004. Calcified cartilage in the paired fins of the osteostracan *Escuminaspis laticeps* (Traquair, 1890), from the late Devonian of Miguasha (Quebec, Canada), with a consideration of the early evolution of the pectoral fin endoskeleton in vertebrates. Journal of Vertebrate Paleontology 24: 773–779.

Jarvik, E. 1942. On the structure of the snout of crossopterygians and lower gnathostomes in general. Zoologiska Bidrag från Uppsala 21: 235–675.

Jarvik, E. 1980. Basic structure and evolution of vertebrates, Vol. 1. Academic Press, London. 575 pp.

Jordan, D.S. 1919. New genera of fossil fishes from Brazil. Proceedings of the Academy of Natural Sciences of Philadelphia 71:208–210.

Kearney, M., and J.M. Clark. 2003. Problems due to missing data in phylogenetic analysis including fossils: a critical review. Journal of Vertebrate Paleontology 23(2):263–274.

Kellner, A. W. A. 2004. The ankle structure of two pterodactyloid pterosaurs from the Santana Formation (Lower Cretaceous), Brazil. Bulletin of the American Museum of Natural History 285:25–35.

Kellner, A. W. A. 1987. Ocorrência de um Novo Crocodiliano no Cretáceo Inferior da Bacia do Araripe, Nordeste do Brasil. Anais da Academia Brasileira de Ciências 59(3):219–232.

Kellner, A. W. A., and D. A. Campos. 1986. Primerio registro de amphibian (Anura) no Cretáceo Inferior da bacia do Araripe, nordeste do brasil. Anais da Academia Brasileiras de Ciências 58(4):610.

Kellner, A. W. A., Campos, D. A. 2002. The function of the cranial crest and jaws of a unique pterosaur from the Early Cretaceous of Brazil. Science 297(5580):389–392.

Kitching, I.J., Forey, P.L., Humphries, C.J., and D.M. Williams. 1998. Cladistics, 2nd edition: the theory and practice of parsimony analysis. The Systematics Association Publication No. II. New York: Oxford Science Publications, 228 pp.

Kluge, A. 1984. The relevance of parsimony to phylogenetic inference. In. Duncan T, Stuessy, T.F., eds. Cladistics: Perspectives on the Reconstruction of Evolutionary History. New York: Columbia University Press, 24-38.

Kluge, A.G., Wolf, A.J. 1993. Cladistics: What's in a word? Cladistics 9: 183-199.

Koken, E. 1907. Über *Hybodus*. Geologische und Paläontologische Abhandlungen 5(4):261–276.

Kuhn, E. 1945. Ueber *Acrodus*-Funde aus dem Grenzbitumenhorizont der anisischen Stufe der Trias des Monte San Giorgio (Kt. Tessin). Eclogae geol. Helvetiae 38(2):662–673.

Landemaine, O. 1991. Sélaciens nouveaux du Crétacé supérieur du sud-ouest de la France. Quelques apports à la systématique des élasmobranches. Société Amicale des Géologues Amateurs (MNHN, Paris). SAGA information, hors-série 1:1–45.

Lane, J.A., and J.G. Maisey. 2009. Pectoral anatomy of *Tribodus limae* (Elasmobranchii: Hybodontiformes) from the Lower Cretaceous of northeastern Brazil. Journal of Vertebrate Paleontology 29(1):25–38.

Liem, K.F., and A. P. Summers. 1999. Muscular system: gross anatomy and functional morphology of muscles; pp. 93–114 in W. C. Hamlett (ed.), Sharks, Skates, and Rays: The Biology of Elasmobranch Fishes. The Johns Hopkins University Press, Baltimore, Maryland.

Liem, K.F., Bemis, W.E., Walker, W.F., Jr., and Grande, L., eds. 2001. Functional anatomy of the vertebrates: an evolutionary perspective, third edition. New York: Harcourt College Publishers. 703 pp.

Lima, M. R. 1979a. Paleontologia da formação Santana (Cretáceo do Nordeste do Brasil): Estágio atual de conhecimentos. Anais da Academia Brasileira de Ciências 51(3):545–556.

Lima, M. R. 1979b. Palinologia da Formação Exu, Cretáceo do Nordeste Brasil. Ameghiniana 16:27–63.

Mabee, P. M., and M. Noordsy. 2004. Development of the paired fins in the paddlefish, *Polyodon spathula*. Journal of Morphology 261:334–344.

Mabesoone, J. M., and I. M. Tinoco. 1973. Paleoecology of the Aptian Santana Formation (Northeastern Brazil). Paleogeography, Paleoclimatology, Paleoecology 14(2).

Maddison, W. P., Donoghue, M. J., & Maddison, D. R. 1984. Outgroup analysis and parsimony. Systematic Zoology 83: 83-103.

Maisey, J.G. 1978. Growth and form of finspines in hybodont sharks. Palaeontology 21(3):657–666.

Maisey, J.G. 1980. An evaluation of jaw suspension in sharks. American Museum Novitates 2706:1–17.

Maisey, J. G. 1982. The anatomy and interrelationships of Mesozoic hybodont sharks. American Museum Novitates 2724:1–48.

Maisey, J.G. 1983. Cranial anatomy of *Hybodus basanus* Egerton from the Lower Cretaceous of England. American Museum Novitates 2758:1–64.

Maisey, J. G. 1984. Chondrichthyan phylogeny: a look at the evidence. Journal of Vertebrate Paleontology 4:359–371.

Maisey, J.G. 1985. Cranial morphology of the fossil elasmobranch *Synechodus dubrisiensis*. American Museum Novitates 2804:1–28.

Maisey, J.G. 1986A. Heads and tails: a chordate phylogeny. Cladistics 2:201–256.

Maisey, J. G. 1986B. Anatomical revision of the fossil shark *Hybodus fraasi* (Chondrichthyes: Elasmobranchii). American Museum Novitates 2857:1–16.

Maisey, J.G. 1986C. Coelacanths from the Lower Cretaceous of Brazil. American Museum Novitates 2866:1–30.

Maisey, J.G. 1987. Cranial anatomy of the Lower Jurassic shark *Hybodus reticulatus* (Chondrichthyes: Elasmobranchii), with comments on hybodontid systematics. American Museum Novitates 2878:1–39.

Maisey, J. G. 1989A. *Hamiltonichthys mapesi*, g. and sp. nov. (Chondrichthyes; Elasmobranchii), from the Upper Pennsylvanian of Kansas. American Museum Novitates 2931:1–42.

Maisey, J.G. 1989B. Visceral skeleton and musculature of a Late Devonian shark. Journal of Vertebrate Paleontology 9(2):174–190.

Maisey, J.G. 1990. Selachii (III.2.1). In Antunes et al. (eds.), Triassic fishes from the Cassange depression (R.P. de Angola). Ciências da Terra (UNL), Número Especial: 1–16; Lisbon, Portugal.

Maisey, J.G. (ed.). 1991. Santana Fossils, an Illustrated Atlas. T.F.H. Publications, Neptune City, NJ.

Maisey, J. G. 2000. Continental break-up and the distribution of fishes of Western Gondwana during the Early Cretaceous. Cretaceous Research, Amsterdam, 21:281–314.

Maisey, J.G. 2001A. Remarks on the Inner Ear of Elasmobranchs and its Interpretation from Skeletal Labyrinth Morphology. Journal of Morphology 250: 236–264.

Maisey, J.G. 2001B. A primitive chondrichthyan braincase from the Middle Devonian of Bolivia. pp. 263–288 *In* P. E. Ahlberg (ed.), Major Events in Early Vertebrate Evolution: Palaeontology, Phylogeny and Development. Taylor and Francis, for the Systematics Association, London.

Maisey, J.G. 2001C. CT-scan reveals new cranial features in Devonian chondrichthyan "*Cladodus*" *wildungensis*. Journal of Vertebrate Paleontology 21(4):807–810.

Maisey, J.G. 2004A. Endocranial morphology in fossil and recent chondrichthyans. *In* Recent Advances in the Origin and Early Radiation of Vertebrates, G. Arratia & R. Cloutier (eds.), Verlag Dr. Friedrich Pfeil, Munchen, Germany, pp. 139-170.

Maisey, J. G. 2004B. Morphology of the Braincase in the Broadnose Sevengill Shark *Notorynchus* (Elasmobranchii: Hexanchiformes) Based on CT Scanning. American Museum Novitates 3351:1–52.

Maisey, J.G. 2005. Braincase of the Upper Devonian Shark *Cladodoides wildungensis* (Chondrichthyes, Elasmobranchii), with Observations on the Braincase in Early Chondrichthyans. Bulletin of the American Museum of Natural History 228: 1–103.

Maisey, J.G. 2007. The braincase in Paleozoic symmoriiform and cladoselachian sharks. Bulletin of the American Museum of Natural History 307: 1–122.

Maisey, J.G. 2008. The Postorbital Palatoquadrate Articulation in Elasmobranchs. Journal of Morphology 269:1022–1040.

Maisey, J.G., and M.E. Anderson. 2001. A primitive chondrichthyan braincase from the Early Devonian of South Africa. Journal of Vertebrate Paleontology 21(4):702–713.

Maisey, J. G., and M. R. de Carvalho. 1997. A new look at old sharks. Nature 385:779–780.

Maisey, J. G., Naylor, G. J. P., and D. J. Ward. 2004. Mesozoic elasmobranchs, neoselachian phylogeny and the rise of modern elasmobranch diversity; pp. 17-56 in G. Arratia and A. Tintori (eds.), Mesozoic Fishes 3: Systematics, paleoenvironments and biodiversity. Verlag Dr. Friedrich Pfeil, Munchen, Germany.

Maisey, J., Miller, R., and S. Turner. 2009. The braincase of the chondrichthyan *Doliodus* from the Lower Devonian Campbellton Formation of New Brunswick, Canada. Acta Zoologica (Stockholm) 90 (Suppl. 1):109–122.

Marinelli, W., and A. Strenger. 1959. Vergleichende Anatomie und Morphologie der Wirbeltiere 3: *Squalus acanthias*. Vienna: Franz Deuticke, 308 pp.

Martill, D.M. 1993. Fossils of the Santana and Crato Formations, Brazil. Palaeontological Association Field Guides Fossils 5:1–159.

Martill, D. M. 2007. The age of the Cretaceous Santana Formation fossil Konservat Lagerstätte of north-east Brazil: a historical review and an appraisal of the biochronostratigraphic utility of its paleobiota. Cretaceous Research 28:895–920.

Martill, D. M. 1988. Preservation of fishes in the Cretaceous Santana Formation of Brazil. Paleontology 31:1–18.

Martill, D. M., Loveridge, R., and U. Heimhofer. 2007. Halite pseudomorphs in the Crato Formation (Early Cretaceous, late Aptian-early Albian), Araripe Basin, northeast Brazil; further evidence for hypersalinity. Cretaceous Research 28(4):613–620.

Martins-Neto, R. G., and A. W. A. Kellner. 1988. Premeiro registro de pena na Formação Santana (Cretáceo Inférior), Bacia do Araripe, Nordeste do Brasil. Anais da Academia Brasileira de Ciências 60(1):61–67.

Meyer, H. von. 1849–1851. Fische, Crustaceen, Echinodermen und andere Versteinerungen aus dem Muschelkalk Oberschlesiens. Palaeontographica 1:216–242.

Miles, R.S. 1969. Features of placoderm diversification and the evolution of the arthrodire feeding mechanism. Transactions of the Royal Society of Scotland 68: 123–170.

Miles, R. S. 1973. Articulated acanthodian fishes from the Old Red Sandstone of England, with a review of the structure and evolution of the acanthodian shoulder-girdle. Bulletin of the British Museum (Natural History), Geology 24:113–213.

Moraes, L. J., Barros, F. C., and E. Ramos. 1963. Reconhecimento Fotogeológico da Região Nordeste do Brasil. Div. Fom. Prod. Mineral., D. N. P. M. Fôlha Crato SB240, Esc. 1:250,000. Rio de Janeiro.

Moy-Thomas, J. A. 1936. The structure and affinities of the fossil elasmobranch fishes from the Lower Carboniferous rocks of Glencartholm, Eskdale. Proceedings of the Zoological Society of London 1936:761–788.

Moy-Thomas, J. A. 1939a. The early evolution and relationships of the elasmobranchs. Biol. Rev., vol. 14, pp. 1–26.

Moy-Thomas, J. A. 1939b. Palaeozoic fishes. Chemical Publ. Co., Inc., New York, 149 pp.

Moy-Thomas, J. A. 1951. On the name of the fossil shark *Goodrichia*. Annals and Magazine of Natural History 4:304.

Murry, P.A. 1981. A new species of freshwater hybodont from the Dockum Group (Triassic) of Texas. Journal of Paleontology 55:603–607.

Murry, P.A. 1986. Vertebrate paleontology of the Dockum Group, western Texas and eastern New Mexico. Pages 109–137 in Padian, K. (ed.), The beginning of the age of dinosaurs. Faunal change across the Triassic-Jurassic boundary. Cambridge: Cambridge University Press, 378 pp.

Nelson, G. 1979. Cladistic analysis and synthesis: principles and definitions, with a historical note on Adanson's Familles des Plantes (1763–1764). Systematic Zoology 28:1–21.

Nessov, L.A., Zhelago, V.I., and A.O. Averianov. 1998. A new locality of Late Cretaceous snakes, mammals and other vertebrates in Africa (western Libya). Annales de Paléontologie 84:265–274.

Newberry, J. S. 1889. The Paleozoic fishes of North America. Monograph of the United States Geological Survey 16:1–340.

Nielsen, E. 1932. Permo-Carboniferous fishes from East Greenland. Meddelelser om Grønland 86:1–63.

Northcutt, R.G., and W.E. Bemis. 1993. Cranial nerves of the coelacanth *Latimeria chalumnae* (Osteichthyes: Sarcopterygii: Actinistia) and comparisons with other craniata. Brain, Behavior and Evolution 42 (suppl. 1):1–76.

Owen, R. 1840-1845. Odontography; or a treatise on the comparative anatomy of teeth, etc. (2 vols.). London, lxxiv + 655 pp.

Owen, R. 1846. Lectures on the comparative anatomy and physiology of the vertebrate animals. Pt. I: Fishes. 8 volumes, xi + 304 pp.

Page, R.D.M. 2001. Nexus Data Editor, version 0.5.0. r.page@bio.gla.ac.uk.

Page, R.D.M. 2004. TreeViewX, version 0.4, v. 0.4. r.page@bio.gla.ac.uk.

Patterson, C. 1966. British Wealden sharks. British Museum (Natural History) Bulletin of Geology 11(7):281–350.

Patterson, C. 1967. Elasmobranchii (Chondrichthyes). In Harland, W.B. et al. (eds.), The fossil record. Geological Society of London.

Patterson, C. 1982. Morphological characters and homology. In: Joysey, K.A., Friday, A.E., eds. Problems of Phylogenetic Reconstruction. New York: Academic Press, 21-74.

Peyer, B. 1946. Die schweizerischen Funde von *Asteracanthus* (*Strophodus*). Schweiz. Palaont. Abh. 64:1–101.

Pons, D., Berthou, P. Y., and D. Campos. 1990. Quelques observations sur la palynologie de l'Aptien supérieur et de l'Albien du Bassin d'Araripe (N-E Brésil). I Simpósio sobre a bacia do Araripe e bacias interiors do nordeste. DNPM:245–252.

Poplin, C., and Ricqlès, A. de. 1970. A technique of serial sectioning for the study of undecalcified fossils. Curator 13:7–20.

Price, L. I. 1959. Sôbre um crocodilídeo notosúquio do Cretácico Brasilèiro. Bolm. Div. Geol. Mineral. 188:1–155.

Pruvost, P. 1922. Description de *Denaea fournieri*, selacien nouveau du marbre noir de Denée. Part 2 in G. Fournier and P. Pruvost, Decouverte d'un poisson nouveau dans le marbre noir de Denee. Bulletin de la Classe des sciences, Academie royale de Belgique, Bruxelles 5(8):210–218.

Rage, J.-C., and H. Cappetta. 2002. Vertebrates from the Cenomanian, and the geological age of the Draa Ubari fauna (Libya). Annales de Paléontologie 88:79–84.

Ramsay, J.B., and C.D. Wilga. 2007. Morphology and mechanics of the teeth and jaws of White-Spotted Bamboo Sharks (Chiloscyllium plagiosum). Journal of Morphology 268:664–682.

Rees, J. 2008. Interrelationships of Mesozoic hybodont sharks as indicated by dental morphology—preliminary results. Acta Geologica Polonica, Vol. 58(2):217–221.

Rees, J., and C.J. Underwood. 2002. The status of the shark genus *Lissodus* Brough, 1935, and the position of nominal *Lissodus* species within the Hybodontoidea (Selachii). Journal of Vertebrate Paleontology 22(3):471–479.

Rees, J., and C.J. Underwood. 2008. Hybodont sharks of the English Bathonian and Callovian (Middle Jurassic). Palaeontology 51(1):117–147.

Regan, C.T. 1906. A classification of the selachian fishes. Proceedings of the Zoological Society of London, 1906, pp. 115–124.

Reif, W.-E. 1973. Morphologie und Ultrastruktur des Hai-"Schmelzes." Zoologica Scripta 2:231–250.

Reif, W.-E. 1977. Tooth enameloid as a taxonomic criterion: 1. A new euselachian shark from the Rhaetic-Liassic boundary. Neues Jahrbuch Geol. Palaont. Mh. 1977, H. 9:565–576.

Reif, W.-E. 1978A. Tooth enameloid as a taxonomic criterion 2. Is "*Dalatias*" *barnstonensis* Sykes, 1971 (Triassic, England) a squalomorphic shark? Neues Jahrbuch Geol. Paläont. Mh. 1978, H. 1:42–58.

Reif, W.-E. 1978B. Types of morphogenesis of the dermal skeleton in fossil sharks. Paläontologische Zeitschrift 52: 110–128.

Reif, W.-E. 1979. Morphogenesis and history of large scales of batoids (Elasmobranchii). Paläontologische Zeitschrift 53:26–37.

Rieppel, O. 1981. The hybodontiform sharks from the Middle Triassic of Mte. San Giorgio, Switzerland. Neues Jahrbuch Geol. Paläont. Abh. 161(3):324–353.

Romer, A.S. 1945. Vertebrate paleontology. 2nd ed., vii + 687 pp. Univ. Chicago Press.

Romer, A.S. 1964. The braincase of the Paleozoic elasmobranch *Tamiobatis*. Bull. Mus. Comp. Zool., vol. 131, pp. 87 –105.

Rosen, D.E., Forey, P.E., Gardiner, B.G., and C. Patterson. 1981. Lungfishes, tetrapods, paleontologyand parsimony. Bulletin of the American Museum of Natural History 167:159–276.

Schaeffer, B. 1967. Comments on elasmobranch evolution. *In* Gilbert, P.W., R.F. Mathewson, and D.P. Rall (eds.), Sharks, skates and rays. Baltimore, Johns Hopkins University Press, pp. 3–35.

Schaeffer, B. 1981. The xenacanth shark neurocranium, with comments on elasmobranch monophyly. Bulletin of the American Museum of Natural History 169: Article 1, pp. 1–66.

Schaeffer, B., and M. Mangus. 1976. An Early Triassic fish assemblage from British Colombia. Bulletin of the American Museum of Natural History 156:517–563.

Schobbenhaus, C., and D. A. Campos. 1984. A evolucao da plataforma Sul-Americana no Brasil a suas principais concentracoes minerais. In: Schobbenhaus, C., et al. (eds.), Geologia do Brasil, DNPM:9–53.

Schuh, R.T. 2000. Biological systematics: principles and applications. Ithaca: Cornell University Press, 239 pp.

Schuh, R.T., and J.T. Polhemus. 1980. Analysis of taxonomic congruence among morphological, ecological, and biogeographic data sets for the Leptopodomorpha (Hemiptera). Systematic Zoology 29:1–26.

Sequeira, S. E. K., and M. I. Coates. 2000. Reassessment of "*Cladodus*" *neilsoni* Traquair; a primitive shark from the Lower Carboniferous of East Kilbride, Scotland. Palaeontology 43:153–172.

Shirai, S. 1992. Squalean phylogeny. Hokkaido University Press, Sapporo, Japan, 151 pp.

Shirai, S. 1996. Phylogenetic interrelationships of neoselachians (Chondrichthyes: Euselachii). pp. 9–34 in M. L. Stiassny, L. R. Parenti, and G. D. Johnson (eds.), Interrelationships of Fishes. Academic Press, San Diego, California.

Silva, M. A. M. 1983. The Araripe Basin, Northeastern Brazil: Regional Geology and Facies Analysis of a Lower Cretaceous Evaporitic Depositional Complex. Unpublished PhD. Thesis, Columbia University, New York. 290 pp.

Silva, M. A. M. 1986A. Lower Cretaceous unconformity truncating evaporate-carbonate sequence, Araripe basin, Northeastern Brazil. Revista Brasileira de Geociências 16(3):301–310.

Silva, M. A. M. 1986B. Lower Cretaceous sedimentary sequences in the Araripe basin, Northeastern Brazil: A revision. Revista Brasileira de Geociências 16(3):311–319.

Silva Santos, R. da. 1947. Uma rediscrição de *Dastilbe elongatus*, com algumas considerações sobre o genero Dastilbe. D. G. M./D. N. P. M., Notas Prelim. Estudos 42:1–7.

Silva Santos, R. da.1991. Paleogeography of the Araripe Basin; pp. 40-41 in J. G. Maisey (ed.), Santana Fossils: An Illustrated Atlas. TFH Publications, Neptune, New Jersey.

Silva Santos, R. da, and L. G. Valença. 1968. A formação Santana e sua paleoictiofauna. Anais da Academia Brasileira de Ciências 40(3):339–360.

Small, H. 1913. Geologia e suprimento de água subterrânea no Ceará e parte do Píaui. Insp. Obras Contra Secas., Series Geol. 25:1–180.

Smith, B. G. 1937. The anatomy of the frilled shark *Chlamydoselachus anguineus* Garman; pp. 331–505 in E. W. Gudger (ed.), The Bashford Dean Memorial Volume: Archaic Fishes, Article VI. American Museum of Natural History, New York.

Sokal, R.R., and F.J. Rohlf. 1981. Taxonomic congruence in the Leptopodomorpha re-examined. Systematic Zoology 30:309–325.

Spix, J.B., and C.F.P. Martius. 1823–1831. Reise im Brasilien. 3 vols. and Atlas. Munich.

Stahl, B. J. 1999. Chondrichthyes III: Holocephali; in H.-P. Schultze (ed.), Handbook of Paleoichthyology, Volume 4. Verlag Dr. Friedrich Pfeil, München, 164 pp.

Stensio, E.A. 1927. The Devonian and Downtonian vertebrates of Spitsbergen. 1. Family Cephalaspidae. Skrifter om Svalbard og Ishavet, 12, 1–391.

Stensiö, E. A. 1959. On the pectoral fin and shoulder girdle of the arthrodires. Kungliga Svenska Vetenskapsakacademiens Handlingar Series 4:1–229.

Stensiö, E. A.1969. Elasmobranchiomorphi, Placodermata, Arthrodires; pp. 71–692 in J. Piveteau (ed.), Traité de paléontologie, Volume 4(2). Masson, Paris.

Stromer, E. 1927. Ergebnisse der Forschungsreisen Prof. E. Stromers in den Wüsten Ägyptens. II. Wirbeltier-Reste der Baharîje-Stufe (unterstes Cenoman). 9. Die Plagiostomen, mit Anhang über käno- und mesozoische Rückenflossenstacheln von Elasmobranchiern. Abh. bayer. Akad. Wiss., München 31(5):1–64.

Sues, H.-D., Frey, E., Martill, D. M., and D. M. Scott. 2002. *Irritator challengeri*, a spinosaurid (Dinosauria, Theropoda) from the Lower Cretaceous of Brazil. Journal of Vertebrate Paleontology 22(3):535–547.

Summers, A.P., Koob, T.J., and E.L. Brainerd. 1998. Stingray jaws strut their stuff. Nature 395:450–451.

Summers, A. 2000. Stiffening the stingray skeleton—an investigation of durophagy in myliobatid stingrays (Chondrichthyes, Batoidea, Myliobatidae). Journal of Morphology 243:113–126.

Swofford, D.L. 2001. Phylogenetic Analysis Using Parsimony (and other methods). Version 4.0b10 for 32-bit Microsoft Windows. Sinauer Associates, Inc., Sunderland, Massachusetts.

Teixeira, C. 1954. Sur un hybodontidé du Karroo de l'Angola. Garcia de Orta, vol. 2, no. 2, pp. 205–207.

Teixeira, C. 1956. Sur un hybodontidé du Karroo de l'Angola. Revista da Faculdade de Ciências de Lisboa, ser. C., vol. 5, pp. 135–136.

Teixeira, C. 1978. Les poissons fossiles du Karroo du Lutoa et de Iongo en Angola. Centenario da Academia das Ciências de Lisboa, no. II, pp. 275–300.

Thomson, K.S. 1982. An Early Triassic hybodont shark from northern Madagascar. Postilla 186:1–16.

Thomson, K. S. and D. E. Simanek. 1977. Body form and locomotion in sharks. American Zoologist 17:343–354.

Traquair, R. H. 1888. Notes on Carboniferous Selachii. Geological Magazine 5:81–86.

Traquair, R. H. 1890. Notes on the Devonian fishes of Scaumenac Bay and Campbellton in Canada. Geological Magazine 7:12–17.

Vullo, R., Néraudeau, D., and B. Videt. 2003. Un faciès de type falun dans le Cénomanien basal de Charente-Maritime (France). Annales de Paléontologie 89:171–189.

Vullo, R, Néraudeau, D., Allain, R., and H. Cappetta. 2005. Un nouveau gisement à microrestes de vertébrés continentaux et littoraux dans le Cénomanien inférieur de Fouras (Charente-Maritime, Sud-Ouest de la France). Comptes Rendus Palevol 4:95–107.

Vullo, R., Cappetta, H., and Néraudeau, D. 2007. New sharks and rays from the Cenomanian and Turonian of Charentes, France. Acta Palaeontologica Polonica 52:99–116.

Vullo, R., and D. Néraudeau. 2008. When the "primitive" shark *Tribodus* (Hybodontiformes) meets the "modern" ray *Pseudohypolophus* (Rajiformes): the unique co-occurrence of these two durophagous Cretaceous selachians in Charentes (SW France). Acta Geologica Polonica 58(2):249–255.

Wang, N.-Z., Zhang, X., Zhu, M., and W.-J. Zhao. 2009. A new articulated hybodontoid from Late Permian of northwestern China. Acta Zoologica (Stockholm) 90 (Suppl.1):159–170.

Werner, C. 1989. Die elasmobranchier-fauna des Gebel Dist Member der Bahariya Formation (Obercenoman) der Oase Bahariya, Ägypten. Palaeo Ichthyologica 5:5-112.

Werner, C. 1990. Biostratigraphical results of investigations on the Cenomanian elasmobranchian fauna of Bahariya Oasis, Egypt. Berliner geowissenschaftliche Abhandlungen (A) 120.2:943–956.

Werner, C. 1994. Die kontinentale Wirbeltierfauna aus der unteren Oberkreide des Sudan (Wadi Milk Formation). Berliner Geowissenschaftliche Abhandlungen E (B. Krebs-Festschrift), 13:221–249.

White, E.G. 1937. Interrelationships of the elasmobranchs with a key to the Order Galea. Bull. Amer. Mus. Nat. Hist., vol. 75, pp. 1–138.

Wilga, C. 2000. Durophagy in sharks: feeding mechanics of the Hammerhead *Sphyrna tiburo*. Journal of Experimental Biology 203:2781–2796.

Wilga, C. 2002. A functional analysis of jaw suspension in elasmobranchs. Biological Journal of the Linnean Society 75(4):483–502.

Wilga, C. 2005. Morphology and Evolution of the jaw suspension in lamniform sharks. Journal of Morphology 265:102–119.

Wilga, C.A.D. and G. V. Lauder. 2004. Biomechanics of Locomotion in Sharks, Rays, and Chimeras. pp. 139–202, in J.C. Carrier, J.A. Musick and M.R. Heithaus (eds.) Biology of sharks and their relatives. Marine Biology. Boca Raton (Florida): CRC Press.

Wilga, C.D., and P.J. Motta. 1998. Feeding mechanism of the Atlantic Guitarfish *Rhinobatos lentiginosus*: modulation of kinematic and motor activity. Journal of Experimental Biology 201:3167–3184.

Wilga, C.D., Motta, P.J., and C.P. Sanford. 2007. Evolution and ecology of feeding in elasmobranchs. Integrative and Comparative Biology 47(1):55–69.

Wilga, C.D., Wainwright, P.C., and P.J. Motta. 2000. Evolution of jaw depression mechanics in aquatic vertebrates: insights from Chondrichthyes. Biological Journal of the Linnean Society 71:165–185.

Williams, M.E. 1998. A new specimen of *Tamiobatis vetustus* (Chondrichthyes, Ctenacanthoidea) from the late Devonian Cleveland Shale of Ohio. Journal of Vertebrate Paleontology 18(2):251–260.

Winchell, C. J., A. P. Martin, and J. Mallatt. 2004. Phylogeny of elasmobranchs based on LSU and SSU ribosomal RNA genes. Molecular Phylogenetics and Evolution 31(2004):214–224.

Wischnitzer, S. 1993. Atlas and dissection guide for comparative anatomy, 5th ed. W. H. Freeman and Company, New York, 295 pp.

Witmer, L.M. 1995. The Extant Phylogenetic Bracket and the importance of reconstructing soft tissues in fossils. pp. 19–33 in J. Thomason (ed.), Functional Morphology in Vertebrate Paleontology. Cambridge University Press, Cambridge.

Woodward, A. S. 1886. On the palaeontology of the selachian genus Notidanus, Cuvier. Geol. Mag., n.s., vol. 3, pp. 205–217, 253–259.

Woodward, A. S. 1889A. Catalogue of the fossil fishes in the British Museum (Natural History). Part I. London, British Museum (Natural History), xivii + 474 pp.

Woodward, A. S. 1889B. On the head of Hybodus delabechei, associated with dorsal fin spines, from the Lower Lias of Lyme Regis, Dorsetshire. Ann. Rept. Com. Yorks. Phil. Soc., 1889, pp. 58–61.

Woodward, A. S. 1916. The fossil fishes of the English Wealden and Purbeck formations. Part 1. Palaeontographical Society Monograph for 1915:1–48.

Woodward, A.S. 1919. The fossil fishes of the English Wealden and Purbeck formations. Part III. Palaeontographical Society Monograph for 1917:105–148.

Woodward, A. S. 1924. On a hybodont shark (*Tristychius*) from the Calciferous Sandstone Series of Eskdale (Dumfriesshire). Quarterly Journal of the Geological Society of London 80:338–342.

Young, G.C. 1982. Devonian sharks from South-Eastern Australia and Antarctica. Palaeontology 25:817–843.

Young, G.C. 1986. The relationships of placoderm fishes. Zoological Journal of the Linnean Society 88:1–57.

Young, J.Z. 1962. The life of vertebrates, 2nd ed. Oxford Univ. Press, xvi + 820 pp.

Zangerl, R. 1981. Chondrichthyes I: Paleozoic Elasmobranchii; in H.-P. Schultze (ed.), Handbook of Paleoichthyology, Volume 3A. Verlag Dr. Friedrich Pfeil, München, 115 pp.

Zangerl, R., and G. R. Case. 1973. Iniopterygia, a new order of chondrichthyan fishes from the Pennsylvanian of North America. Fieldiana, Geological Memoirs 6:1–67.

Zangerl, R., & G.R. Case. 1976. *Cobelodus aculeatus* (Cope), an anacanthous shark from Pennsylvanian black shales of North America. Palaeontogr., vol. 154, pp. 107–157.

Zhu, M., Yu, X., and P. Ahlberg. 2001. A primitive sarcopterygian fish with an eyestalk. Nature 410:81–84.

Zittel, K. von. 1911. Grundzuege der Palaontologie, 2nd ed. II. Abt. Vertebrata, vii + 598 pp. R. Oldenburg Verlag, Munchen, Berlin.